SPIE. Fellow

OPTICA SENIOR MEMBER

IEEE Senior Member

Implementation of Digital Optical Switches and Signal Routers for High-Speed Communication

Prof. (Dr.) Santosh Kumar
Liaocheng University, China
Associate Editor, Biomedical Optics Express
Chair, Optical Biosensors Optica Technical Group
Email Id: santosh@lcu.edu.cn

Introduction

- Photonics has settled its effectiveness in various switching functions due to its key features of large bandwidth, EMI immunity, integrability and high speed.
- The use of light offers the possibility of high-speed operation around 10^4 times faster than that conceivable employing electronic circuits.
- Lightwaves of different frequencies (or wavelengths) can be used within the same guided wave channel or device.
- Linear electro-optic effect (Pockels Effect) can be efficiently used to obtain switching phenomena based on integrated MZIs.
- The integrated MZIs are used to design various WDM components such as combinational and sequential logic devices, signal routers, wavelength selectors etc.

Motivation of work

- In the switching context of WDM components, integrated photonic devices have a distinct advantage of high speed and low signal degradation over their electronic counterparts in this area.

- To fulfill the growing demand of high speed communication, the WDM systems are acquiring popularity worldwide.

- Successful demonstrations and development have been seen on the component level (switches, routing devices), system level (large photonic switch architectures), and the network level (wavelength-switched networks).

Motivation cont….

- Till date, several combinational and sequential circuits have been proposed utilizing various technologies such as periodically poled $LiNbO_3$ (PPLN), Erbium doped optical amplifier (EDFA) and Fabryperot laser diodes (FP-LDs).

<u>The following problem occurs in the previous work:</u>

- ✓ PPLN based logic circuits require numerous light sources and so, they are costly.
- ✓ Erbium doped fiber amplifier operates exclusively at low speeds upto 1 Gbps.
- ✓ Devices implemented with FP-LDs are complex in the sense that more number of FP- LDs and some external devices are required to implement even a simple logic circuit.

Motivation cont….

- ✓ SOAs based logic circuits need interferometric structure that requires numerous devices with matching characteristics and proper control.

Electro-optic modulator (EOM) seems to be an interesting substitute because of its distinct features of being:

  - ✓ lightweight,
  - ✓ miniature,
  - ✓ immune to electromagnetic interference,
  - ✓ wider bandwidth (faster switching times),
  - ✓ lower drive power,
  - ✓ and inherently compatible with optical fiber.

Motivation cont….

- $LiNbO_3$ possess a combination of unique electro-optical, acoustic, piezoelectric, and non-linear optical properties making it a suitable material for implementation of integrated photonic devices.

- Beam propagation method (BPM) is one of the popular numerical methods. The mathematical details of the mode concept satisfying mode solution are reviewed.

WDM System

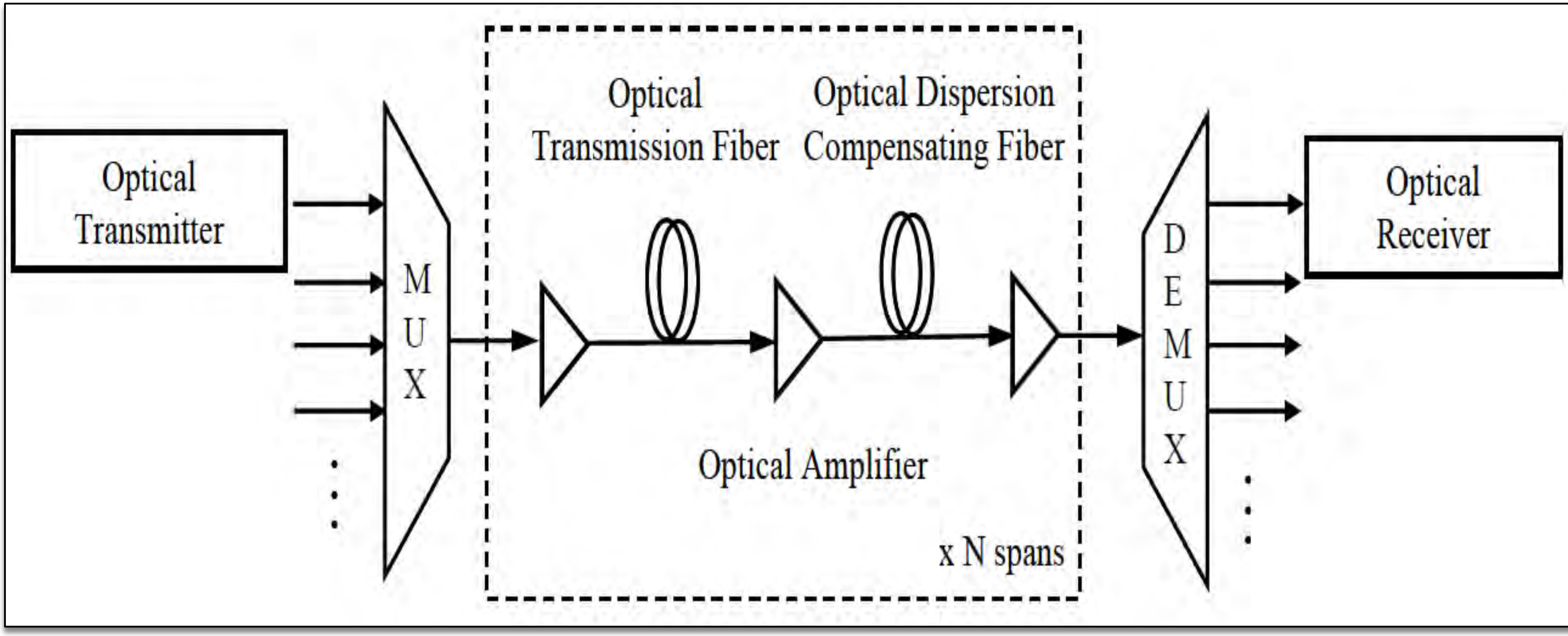

Figure: General block diagram of Wavelength Division Multiplexed System

- Wavelength-division multiplexing (WDM) is a technology which multiplexes a number of optical carrier signals onto a single optical fiber by using different wavelengths.

- Some of the optical WDM network components are: multiplexers (MUX), de-multiplexers (De-MUX), Single mode DFB laser, power divider, power splitters, Optical add-drop multiplexers (OADM), WDM Couplers etc.

Pockels Effect

Figure: (a) Cross section of the optical indicatrix with no applied field, $n_1 = n_2 = n_o$
(b) Applied field along y in $LiNbO_3$ modifies the indicatrix and changes n_1 and n_2 change to n'_1 and n'_2.

$$n_1' \approx n_1 + \frac{1}{2} n_1^3 r E_a \quad \text{and} \quad n_2' \approx n_2 - \frac{1}{2} n_1^3 r E_a \qquad (1)$$

$$\varphi_1 = \frac{2\pi n_1'}{\lambda} L = \frac{2\pi L}{\lambda}\left(n_0 + \frac{1}{2} n_0^3 \, r \, \frac{V}{d}\right) \qquad (2)$$

$$\varphi_2 = \frac{2\pi n_1'}{\lambda} L = \frac{2\pi L}{\lambda}\left(n_0 - \frac{1}{2} n_0^3 \, r \, \frac{V}{d}\right) \qquad (3)$$

$$\Delta\varphi = \varphi_1 - \varphi_2 = \frac{2\pi}{\lambda} \, n_0^3 \, r \frac{L}{d} V \qquad (4)$$

where,

$\lambda \rightarrow$ *Wavelength of the signal.*

$n_0 \rightarrow$ *Refractive index of the material.*

$d \rightarrow$ *Separation between the electrodes.*

$r \rightarrow$ *Electro − optic coefficients (m/V).*

$V \rightarrow$ *Voltage applied across the waveguide.*

$L \rightarrow$ *Length of the waveguide.*

Cont …

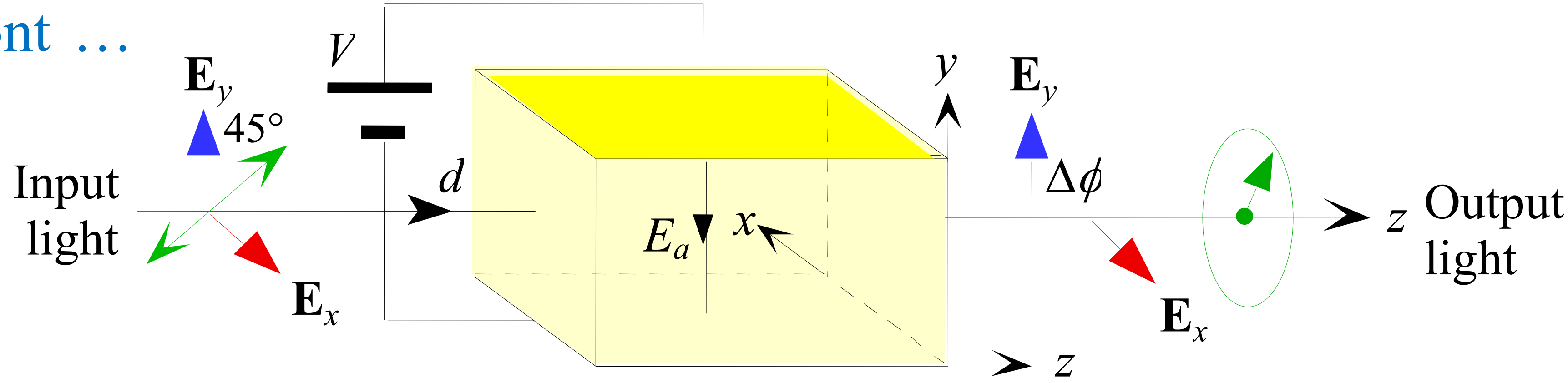

Figure: Tranverse Pockels cell phase modulator. A linearly polarized input light into an electro-optic crystal emerges as a circularly polarized light.

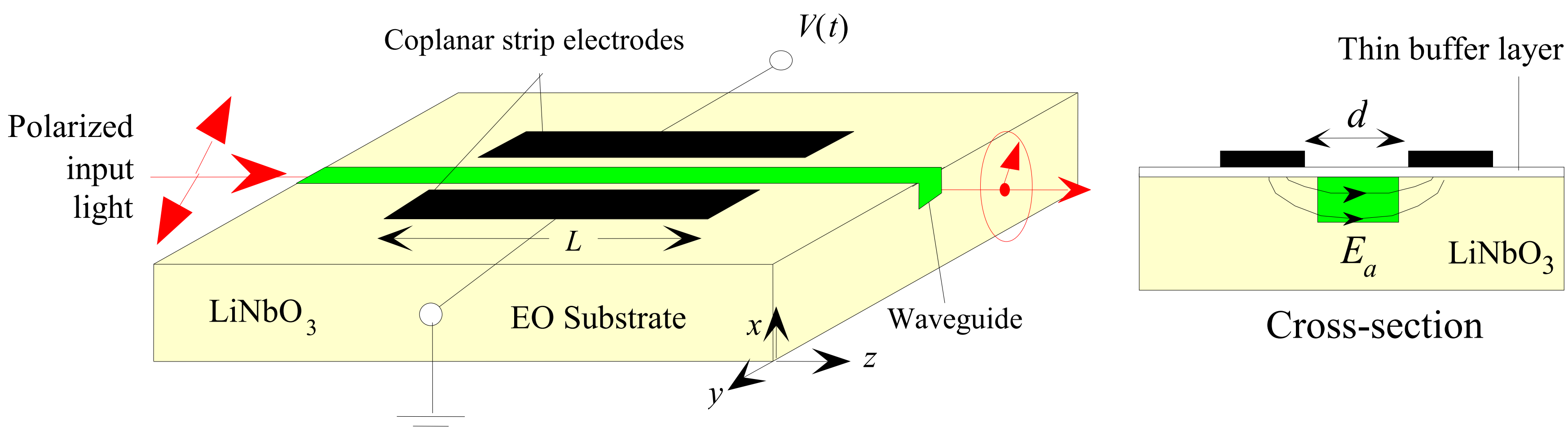

Figure: Integrated transverse Pockels cell phase modulator in which a waveguide is diffused into an electro-optic (EO) substrate of $LiNbO_3$. Coplanar strip electrodes apply a transverse field E_a through the waveguide.

Interferometric Modulator

Table: Different parameters to obtain particular voltage Vπ

.

Parameters	Value of Parameters
Wavelengths (λ)	1.33 μm
Separation between the electrodes (d)	6 μm
Refractive index	1.47
Electro-optic coefficients	$36.6 \times 10^{-12}\ m/V$
Substantial Length (L)	10000 μm

$$V_\pi = \frac{\lambda}{n^3}\frac{1}{r}\frac{d}{L} = 6.75\ V$$

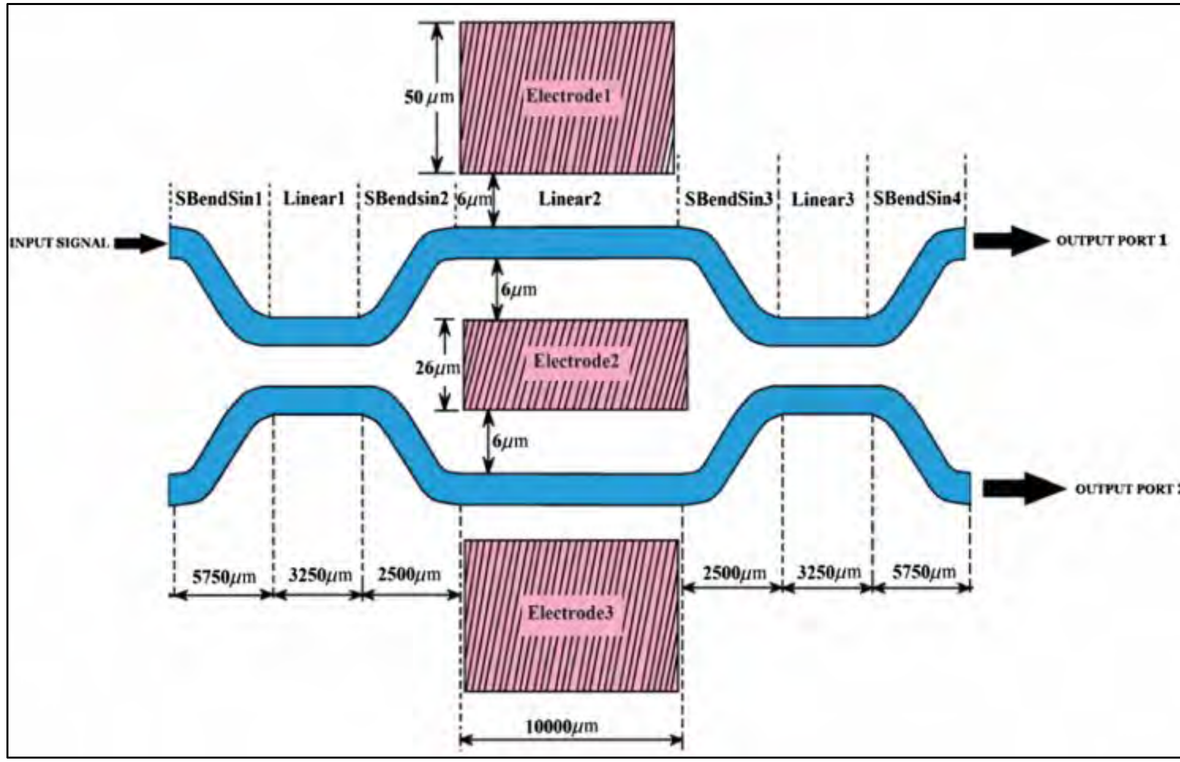

Figure: Schematic view of Mach Zehnder interferometer

- In matrix form, we can obtain the following relation between the input, output and intermediate signals.

$$\begin{bmatrix} A \\ B \end{bmatrix} = \begin{bmatrix} \sqrt{1-\alpha_1} & j\sqrt{\alpha_1} \\ j\sqrt{\alpha_1} & \sqrt{1-\alpha_1} \end{bmatrix} \begin{bmatrix} E_{in} \\ 0 \end{bmatrix} \quad (5)$$

$$\begin{bmatrix} C \\ D \end{bmatrix} = \begin{bmatrix} e^{-j\varphi_1} & 0 \\ 0 & e^{-j\varphi_2} \end{bmatrix} \begin{bmatrix} A \\ B \end{bmatrix} \quad (6)$$

$$\begin{bmatrix} OUT_1 \\ OUT_2 \end{bmatrix} = \begin{bmatrix} \sqrt{1-\alpha_2} & j\sqrt{\alpha_2} \\ j\sqrt{\alpha_2} & \sqrt{1-\alpha_2} \end{bmatrix} \begin{bmatrix} C \\ D \end{bmatrix} \quad (7)$$

Where,
α_1 and α_2 →
Attenuation constant of first and second directional coupler

φ_1 and φ_2 → Phase arises due to application of voltage

Cont …

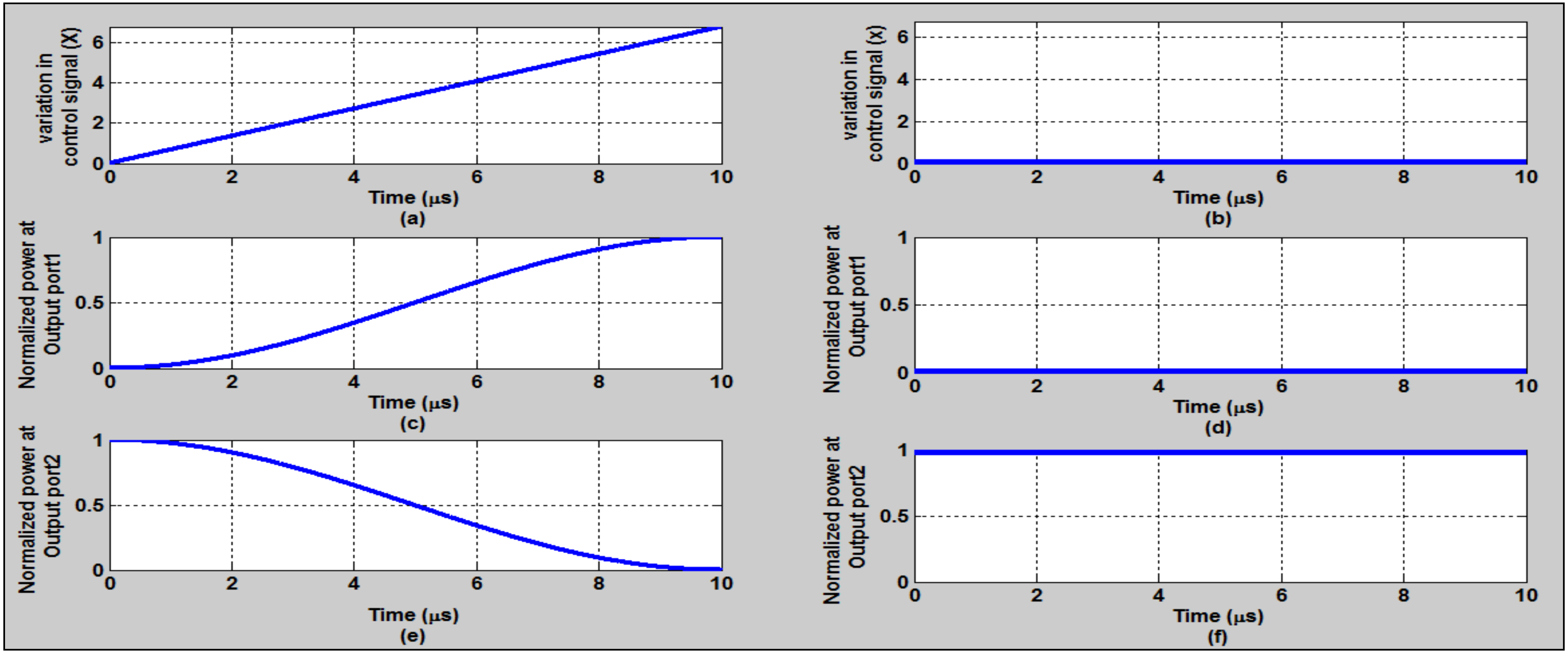

Figure: Simulation of MZI due to the variation of the control signal X.

$$P_{out\,1} = \left|\frac{OUT_1}{E_{in}}\right|^2 = \left|je^{-j(\varphi_0)}sin\left(\frac{\Delta\varphi}{2}\right)\right|^2 = sin^2\left(\frac{\Delta\varphi}{2}\right) \qquad (8)$$

$$P_{out\,2} = \left|\frac{OUT_2}{E_{in}}\right|^2 = \left|je^{-j(\varphi_0)}cos\left(\frac{\Delta\varphi}{2}\right)\right|^2 = cos^2\left(\frac{\Delta\varphi}{2}\right) \qquad (9)$$

Cont…

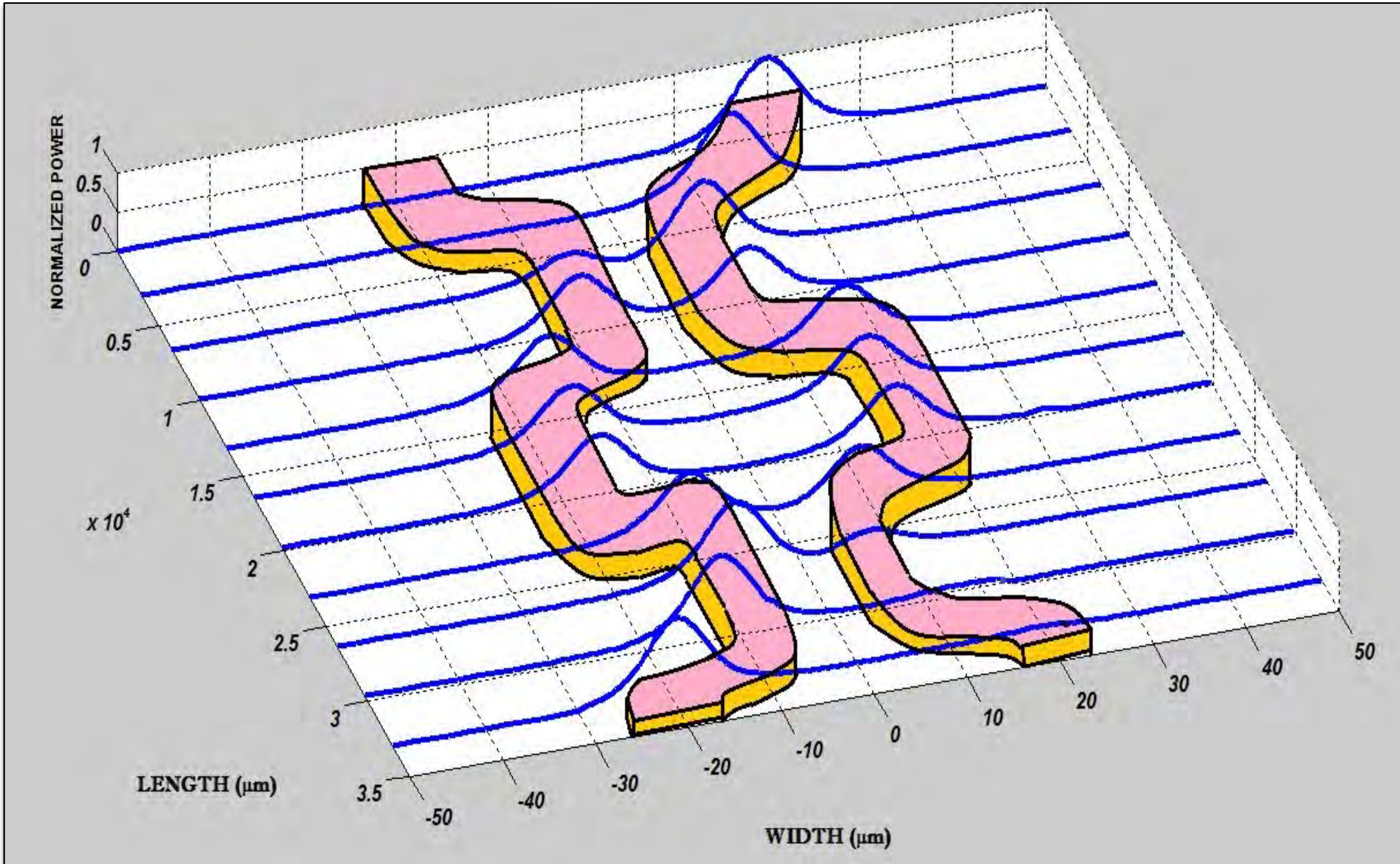

Figure: Optical field propagation through 2x2 coupler part of MZI

Design of NOT gate using MZI

Santosh Kumar et. al., *Optical Engineering (SPIE)*, Vol. 52, No. 9, PP. 097106 (Sep. 20, 2013)

Design of NOT gate using MZI

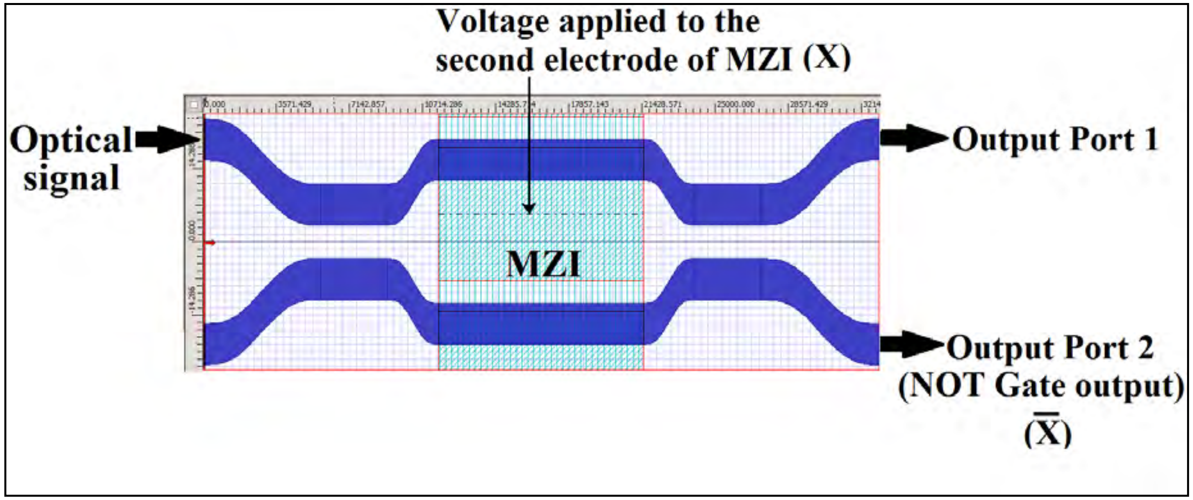

Figure: Design of NOT gate using Mach-Zehnder Interferometers.

$$\left|\frac{OUT2}{E_{in}}\right|^2 = \cos^2\left(\frac{\Delta\varphi}{2}\right)$$

For calculation, it has been assumed that,

$$\varphi_0 = \left.\frac{\varphi_1 + \varphi_2}{2}\right\} \quad \text{and} \quad \Delta\varphi = \varphi_1 - \varphi_2 = \left.\frac{\pi}{V_\pi}X\right\}$$

φ_1 and φ_2 are the phase angle generated at the upper arm and the lower arm of MZI respectively.

Contd…

Table: Optical signal at the two ports due to different combination of control signal.

Control signals	Signal output at different ports	
X	**Port 1**	**Port 2 ($\bar{X}$)**
0	**0**	**1**
1	**1**	**0**

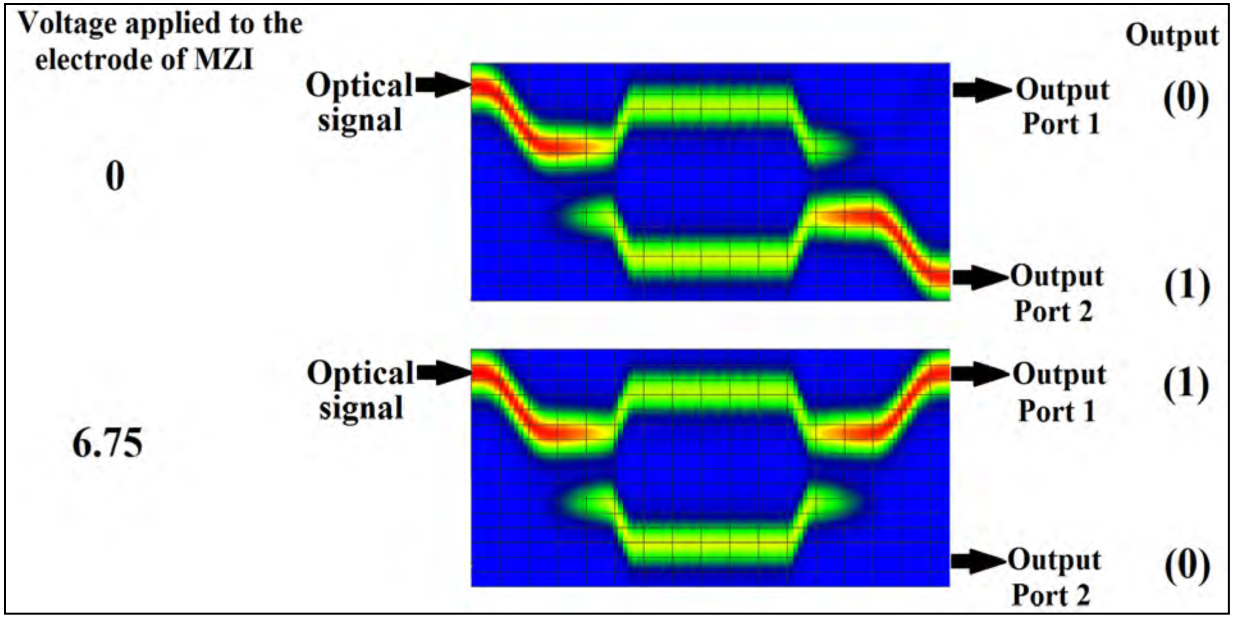

Figure: Simulation result of the NOT logic gate operation at different combination of the control signals.

Design of AND Gate using MZIs

Santosh Kumar et. al., *Proc. SPIE 9131, Optical Modelling and Design III*, SPIE Photonics Europe 2014, Brussels, **Belgium**, PP. 913120 (May 1, 2014).

AND Gate

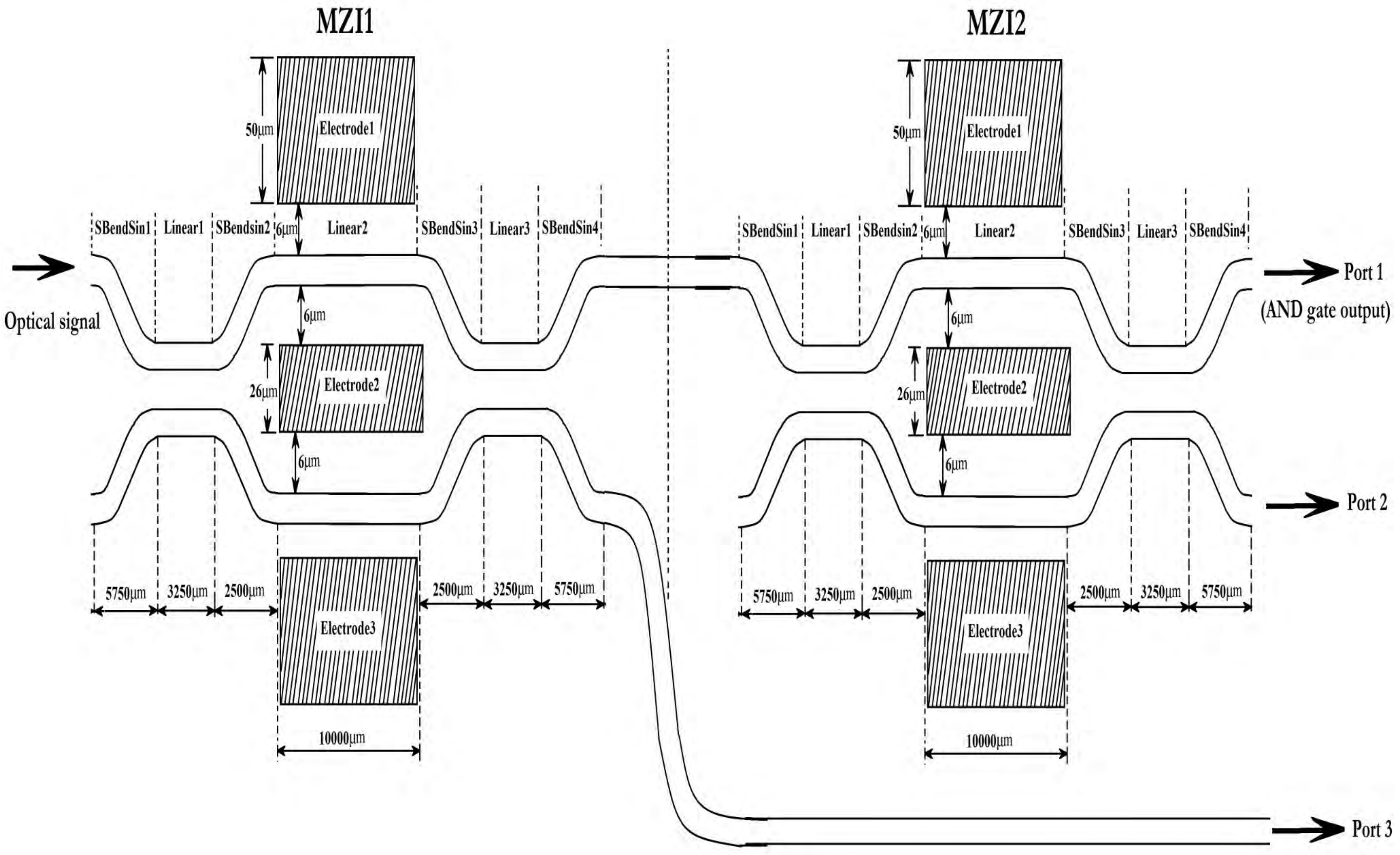
MZI1
MZI2
Electrode1
Electrode2
Electrode3
50μm
26μm
6μm
SBendSin1
Linear1
SBendsin2
Linear2
SBendSin3
Linear3
SBendSin4
Optical signal
5750μm
3250μm
2500μm
10000μm
Port 1
(AND gate output)
Port 2
Port 3

Matlab result of AND Gate

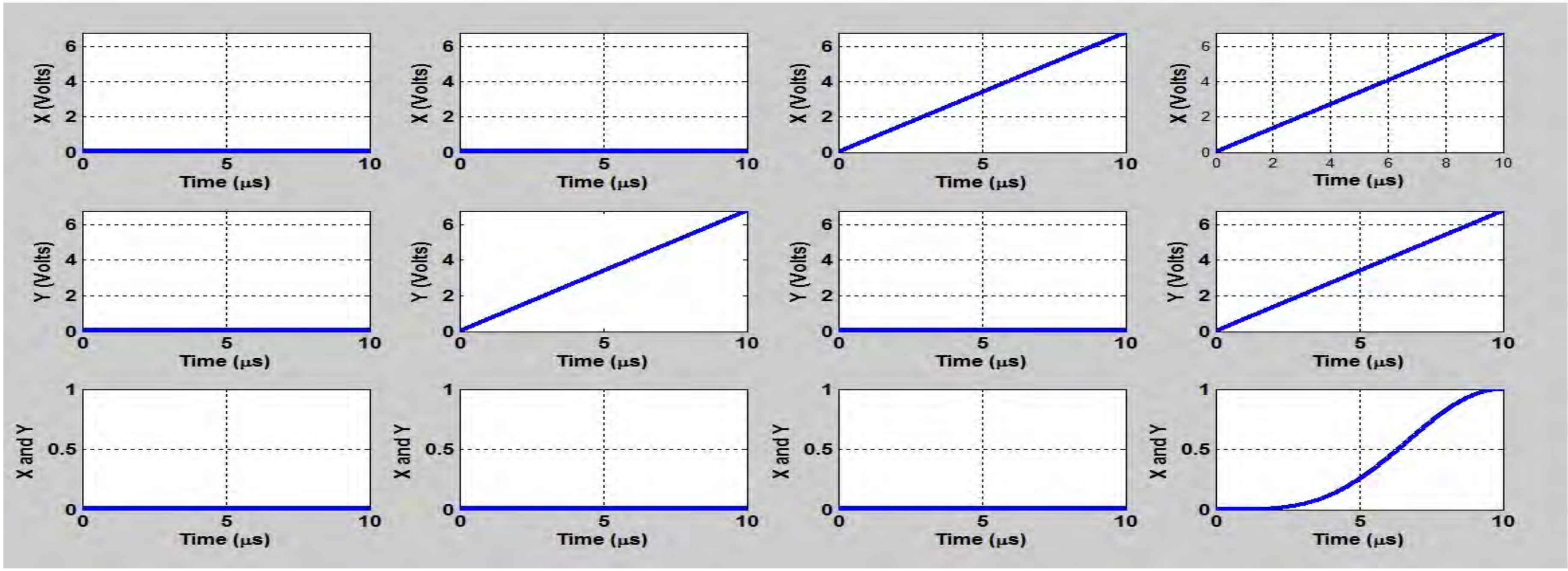

$$\left|\frac{OUT1_{MZI2}}{E_{in}}\right|^2 = \sin^2\left(\frac{\Delta\varphi_{MZI1}}{2}\right)\sin^2\left(\frac{\Delta\varphi_{MZI2}}{2}\right)$$

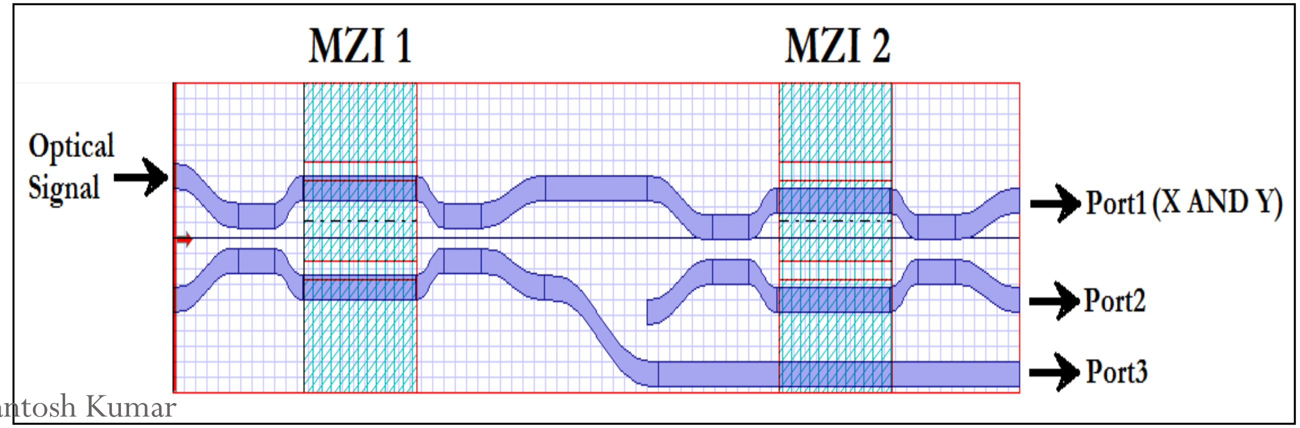

Figure: Layout to design AND logic gate.

BPM result of AND Gate

X	Y	Representation of AND Logic	X AND Y
0	0	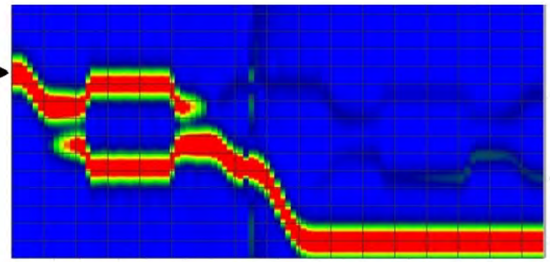	0
0	1	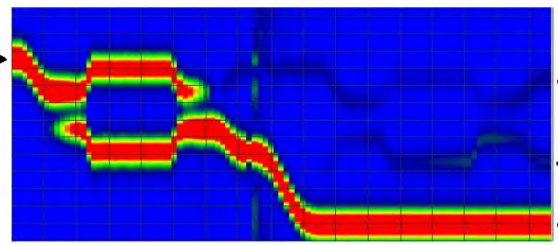	0
1	0	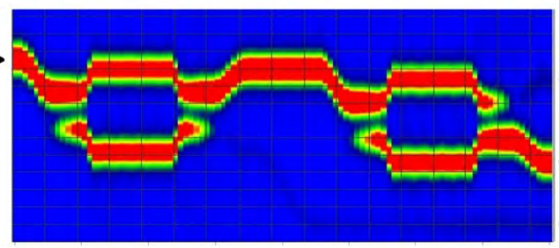	0
1	1	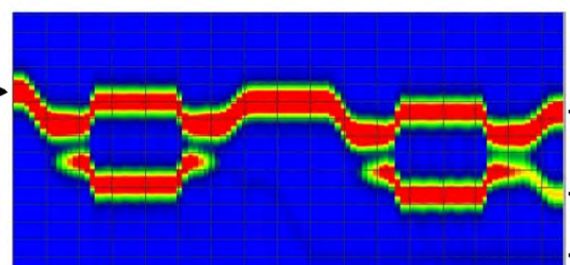	1

Design of OR gate using MZIs

Santosh Kumar et. al., Journal of Optical Communications (Degruyter), Dec. 2016.

OR gate

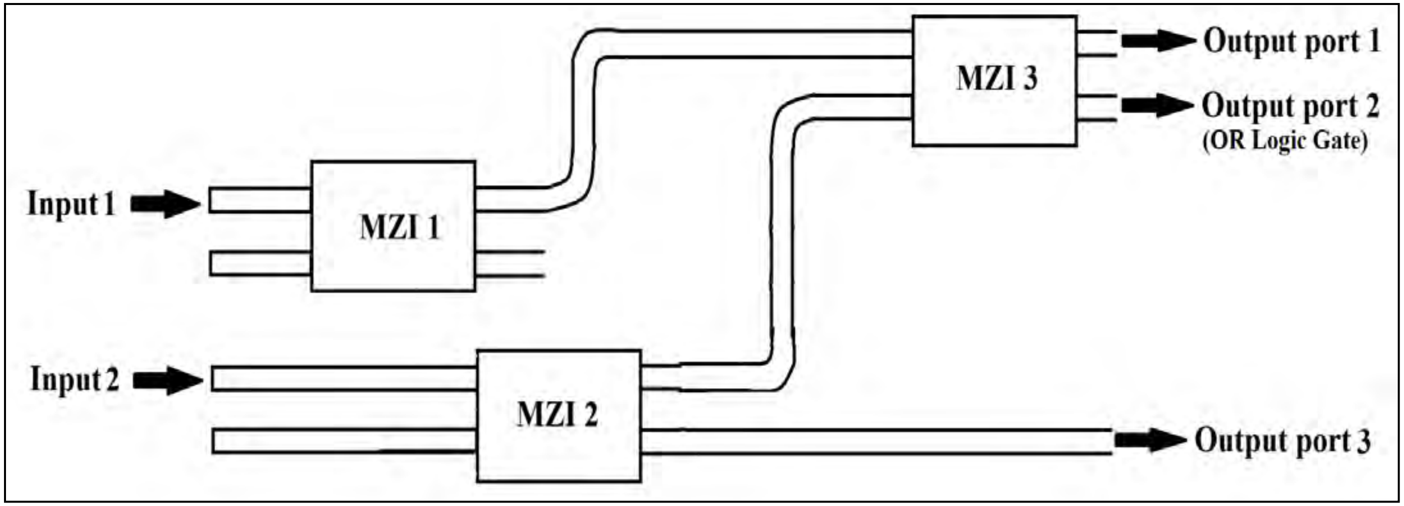

Output port 2 (OR Logic Gate) = $m_1 + m_2 + m_3$

$$= \cos^2\left(\frac{\Delta\varphi_{MZI1}}{2}\right)\sin^2\left(\frac{\Delta\varphi_{MZI2}}{2}\right)\sin^2\left(\frac{\Delta\varphi_{MZI3}}{2}\right) + \sin^2\left(\frac{\Delta\varphi_{MZI1}}{2}\right)\cos^2\left(\frac{\Delta\varphi_{MZI2}}{2}\right)\cos^2\left(\frac{\Delta\varphi_{MZI3}}{2}\right) + \sin^2\left(\frac{\Delta\varphi_{MZI1}}{2}\right)\sin^2\left(\frac{\Delta\varphi_{MZI2}}{2}\right)\sin^2\left(\frac{\Delta\varphi_{MZI3}}{2}\right)$$

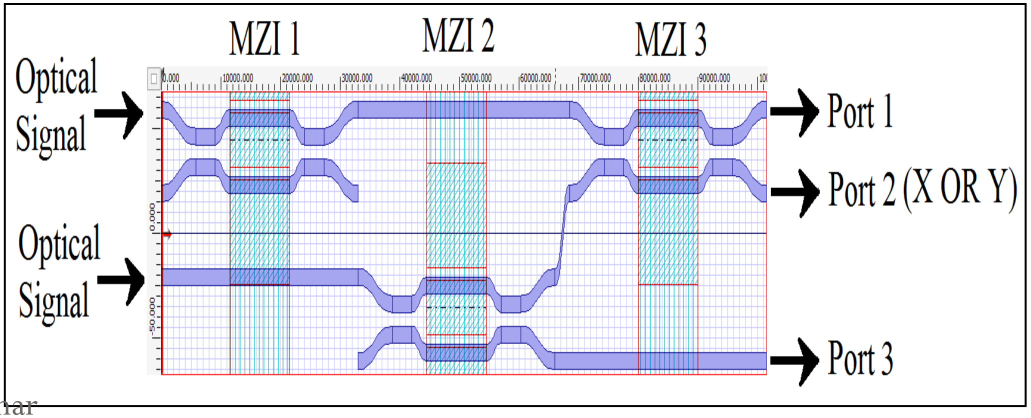

Figure: Layout of implementation of OR logic gate.

BPM result of OR Gate

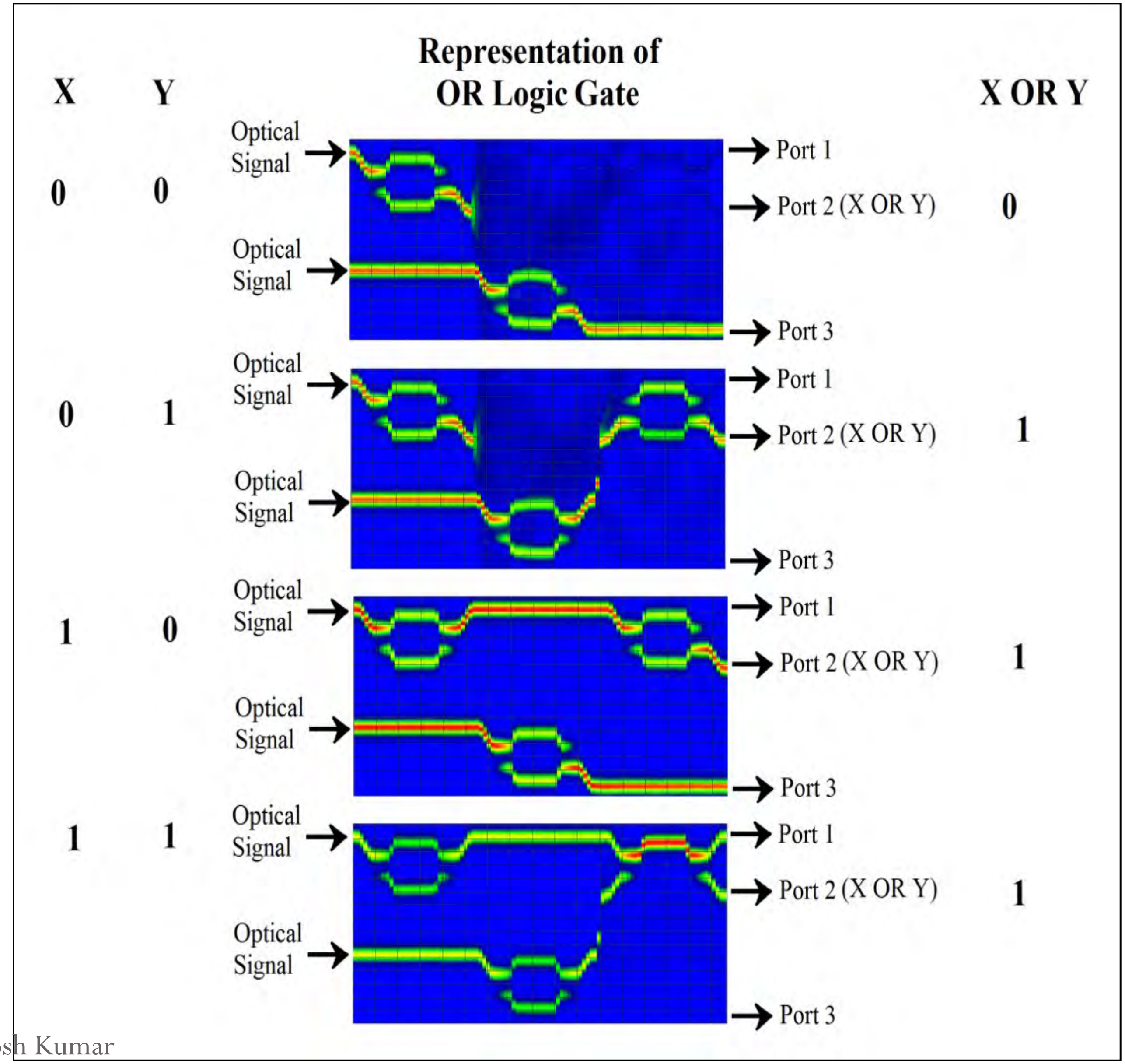

Design of Universal Logic Gates using MZIs

<u>Santosh Kumar</u> et. al., Applied Optics (OSA), Vol. 54, Issue 28, pp. 8479-8484 (Sept. 30, 2015).

Design of universal logic gates

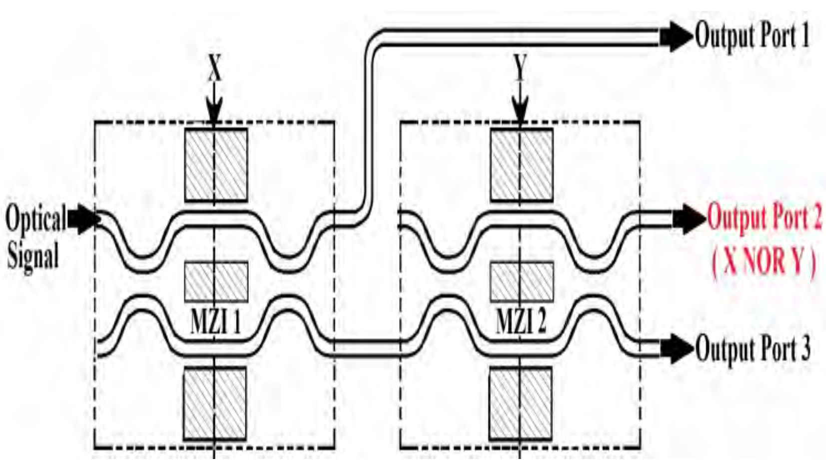

Figure: Schematic diagram of NOR gate using the MZIs.

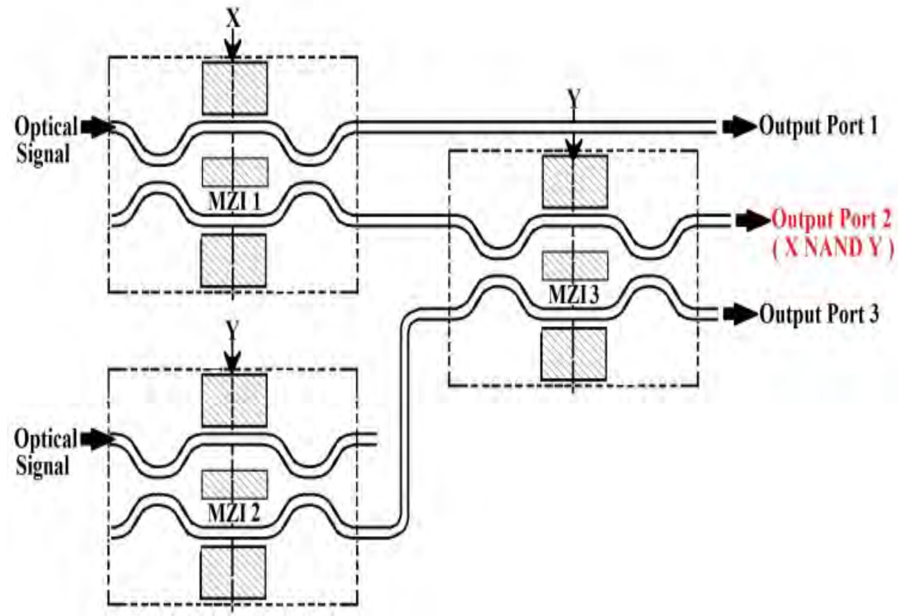

Figure: Schematic diagram of NAND gate using the MZIs.

Table: Optical signal at the different ports due to different combination of control signals.

Control signals		Signal output at different ports		
X	Y	Port 1	Port 2 (X NOR Y)	Port3
0	0	0	1	0
0	1	0	0	1
1	0	1	0	0
1	1	1	0	0

Table: Optical signal at the different ports due to different combination of control signals.

Control signals		Signal output at different ports		
X	Y	Port 1	Port 2 (X NAND Y)	Port 3
0	0	0	1	1
0	1	0	1	0
1	0	1	1	0
1	1	1	0	0

Cont …

$$\text{Output port 2 (NOR logic gate)} = \left|\frac{\text{OUT1}_{\text{MZI2}}}{E_{in}}\right|^2$$

$$= \cos^2\left(\frac{\Delta\varphi_{\text{MZI1}}}{2}\right)\cos^2\left(\frac{\Delta\varphi_{\text{MZI2}}}{2}\right)$$

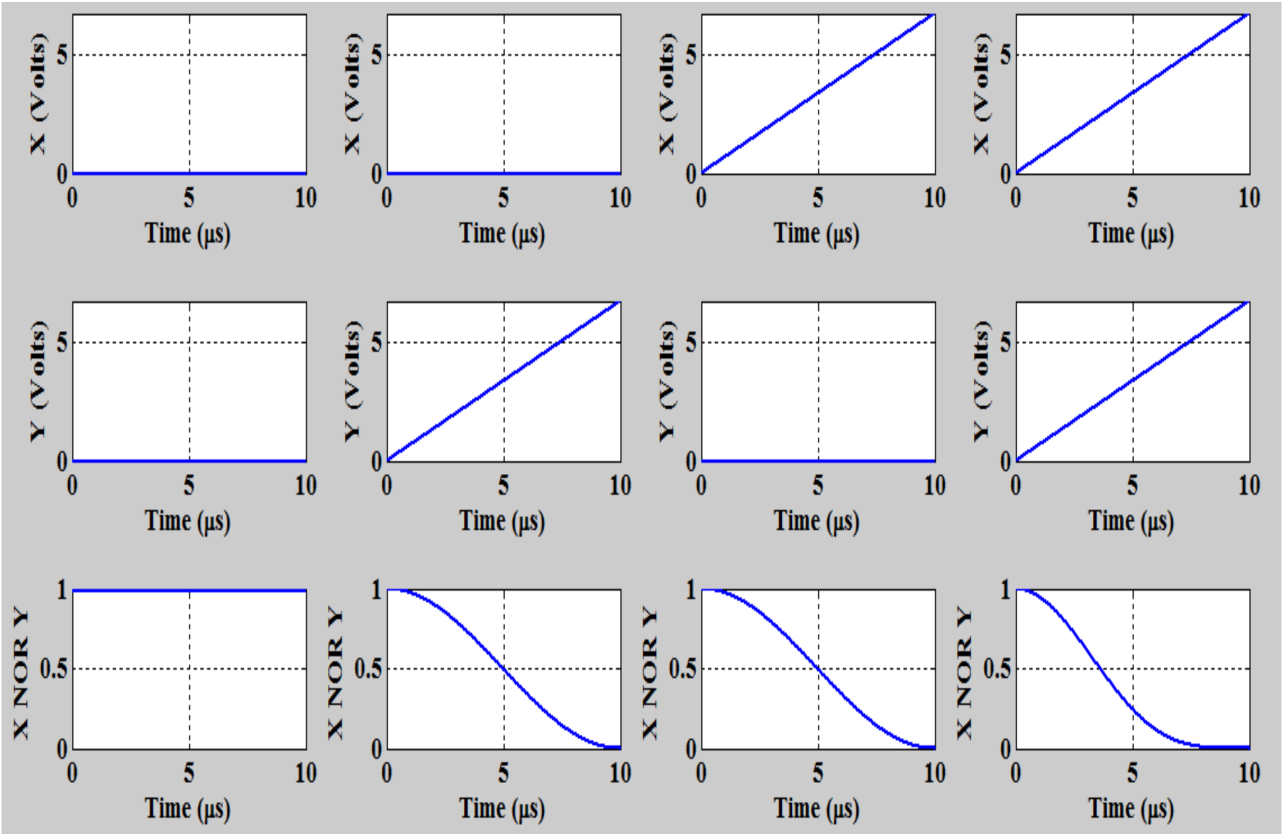

Figure: MATLAB simulation result of the NOR gate.

Cont …

$$\text{Output port 2 (NAND Logic Gate)} = \left|\frac{OUT1_{MZI3}}{E_{in}}\right|^2 =$$

$$= \cos^2\left(\frac{\Delta\varphi_{MZI1}}{2}\right)\cos^2\left(\frac{\Delta\varphi_{MZI2}}{2}\right)\cos^2\left(\frac{\Delta\varphi_{MZI3}}{2}\right) + \cos^2\left(\frac{\Delta\varphi_{MZI1}}{2}\right)\sin^2\left(\frac{\Delta\varphi_{MZI2}}{2}\right)\sin^2\left(\frac{\Delta\varphi_{MZI3}}{2}\right) + \sin^2\left(\frac{\Delta\varphi_{MZI1}}{2}\right)\cos^2\left(\frac{\Delta\varphi_{MZI2}}{2}\right)$$

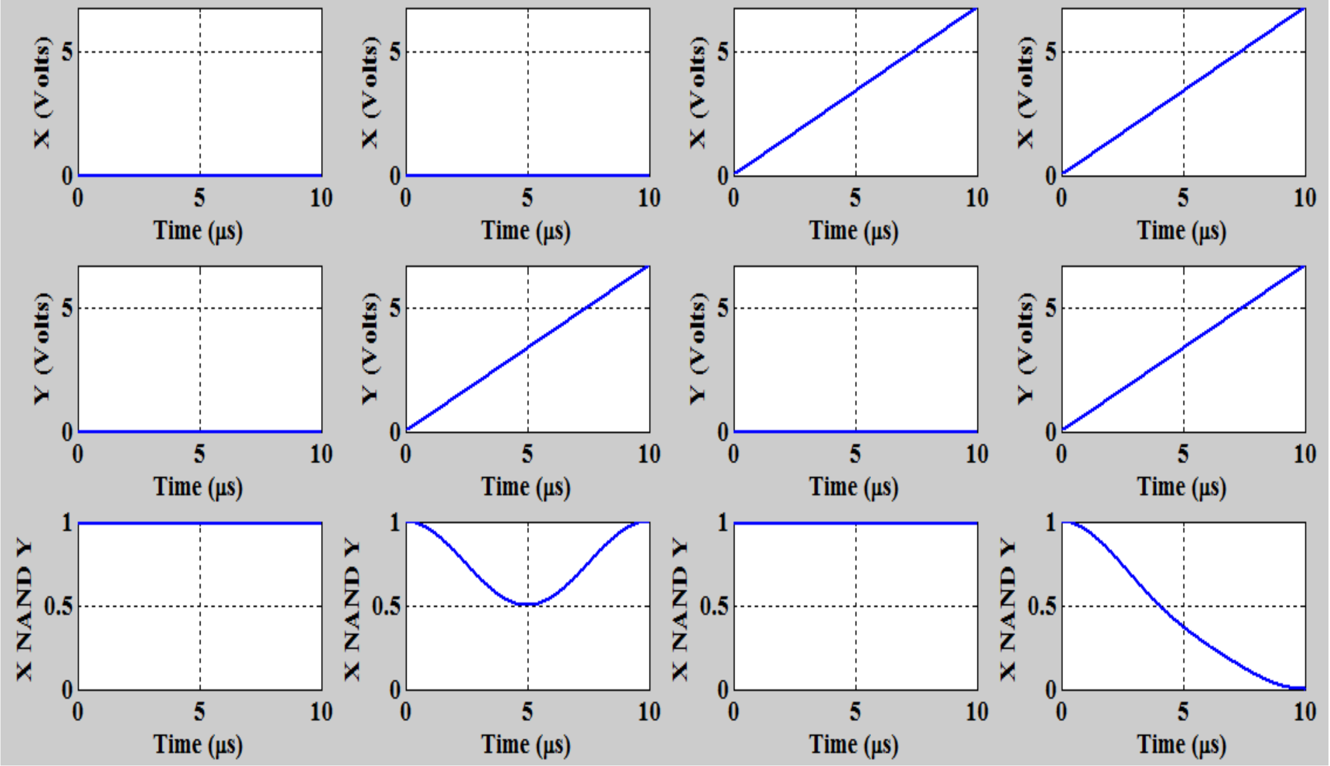

Figure: MATLAB simulation result of the NAND gate.

Cont …

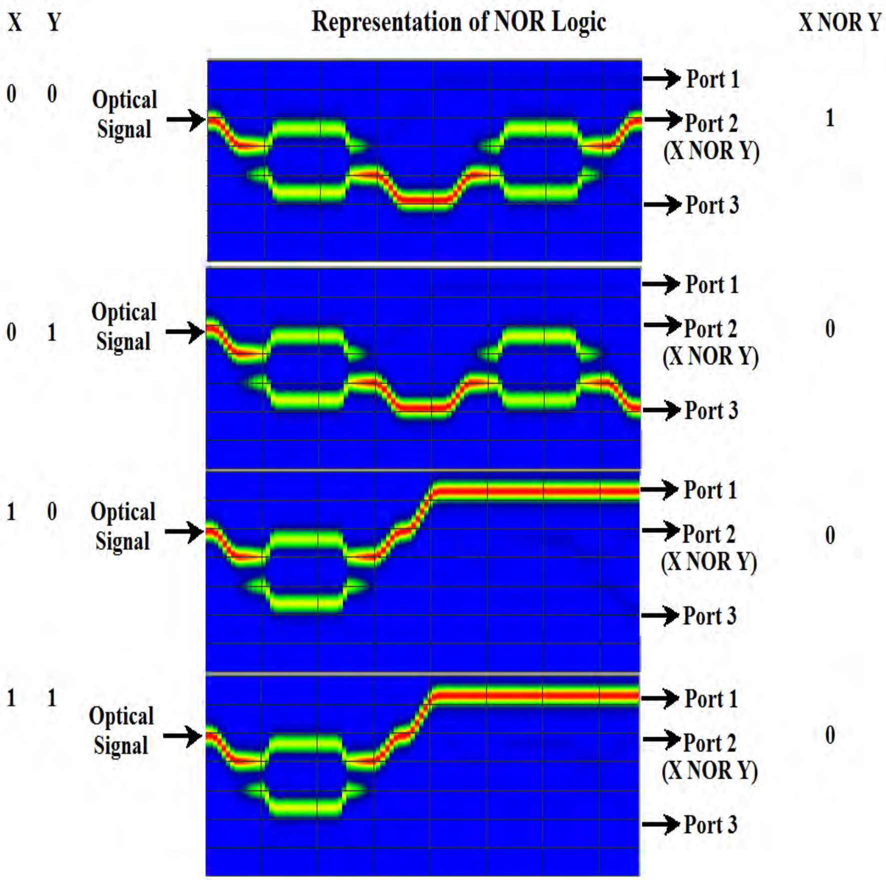

Figure: Results of NOR logic operation for different combination of control signals (X and Y) obtained through Beam propagation method.

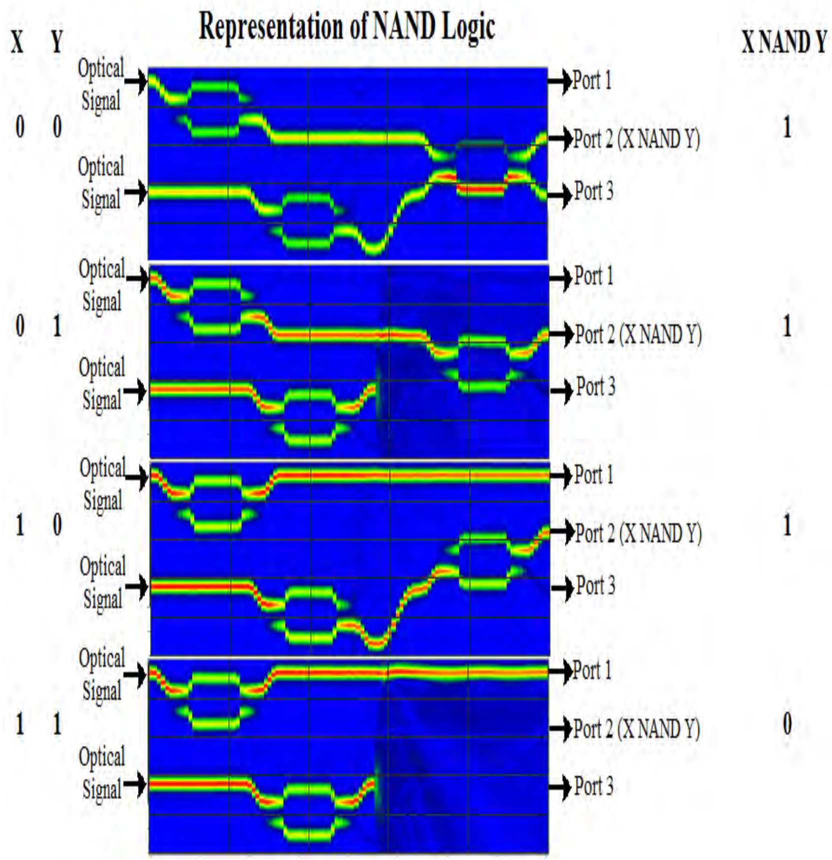

Figure: Results of NAND logic operation for different combination of control signals (X and Y) obtained through Beam propagation method.

Design of XOR/XNOR Gates using MZIs

Santosh Kumar et. al., Optik (Elsevier), Vol. 125, pp. 5764 - 5767 (August 27, 2014).

XOR/XNOR Gates

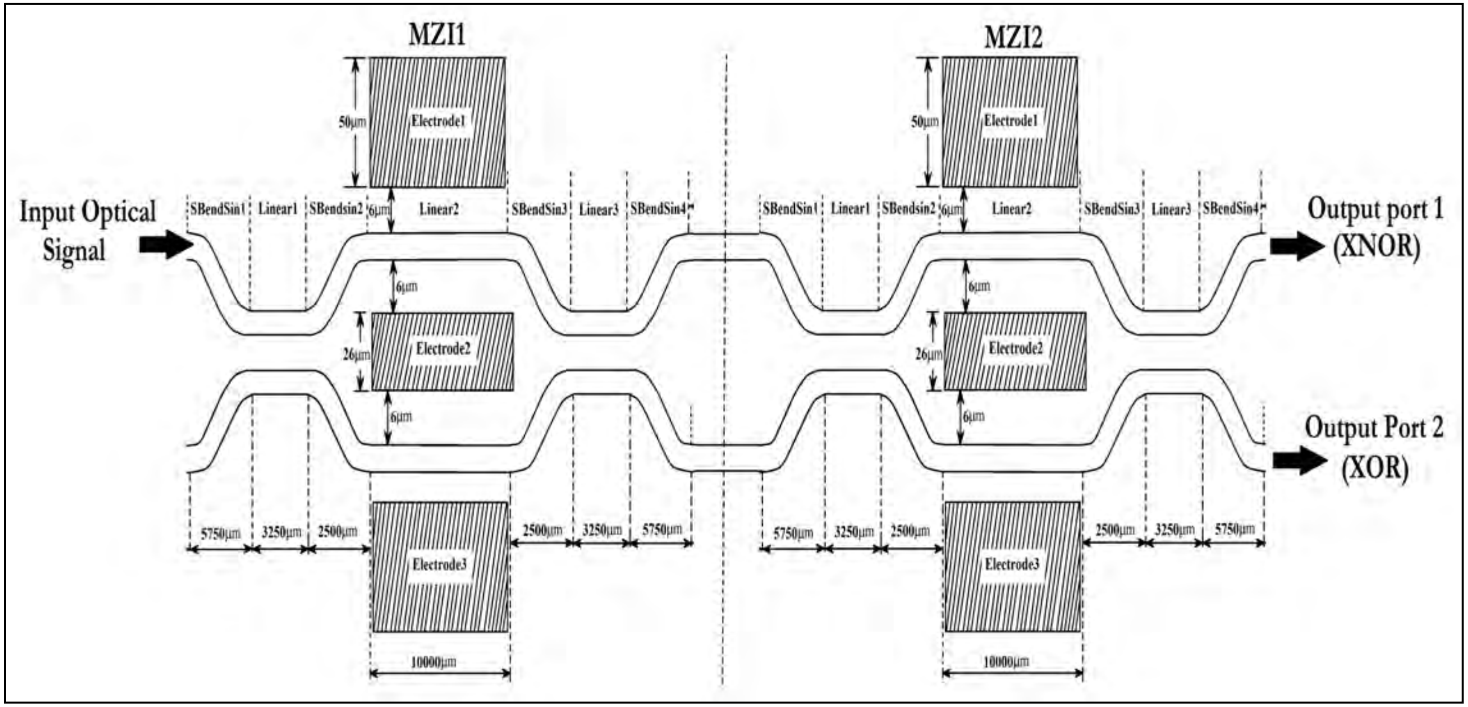

Output port 2 (XOR Logic Gate) = $m_1 + m_2$

$$= \cos^2\left(\frac{\Delta\varphi_{MZI1}}{2}\right)\sin^2\left(\frac{\Delta\varphi_{MZI2}}{2}\right) + \sin^2\left(\frac{\Delta\varphi_{MZI1}}{2}\right)\cos^2\left(\frac{\Delta\varphi_{MZI2}}{2}\right)$$

Output port 1 (XNOR Logic Gate) = $m_3 + m_4$

$$= \cos^2\left(\frac{\Delta\varphi_{MZI1}}{2}\right)\cos^2\left(\frac{\Delta\varphi_{MZI2}}{2}\right) + \sin^2\left(\frac{\Delta\varphi_{MZI1}}{2}\right)\sin^2\left(\frac{\Delta\varphi_{MZI2}}{2}\right)$$

BPM layout and Results

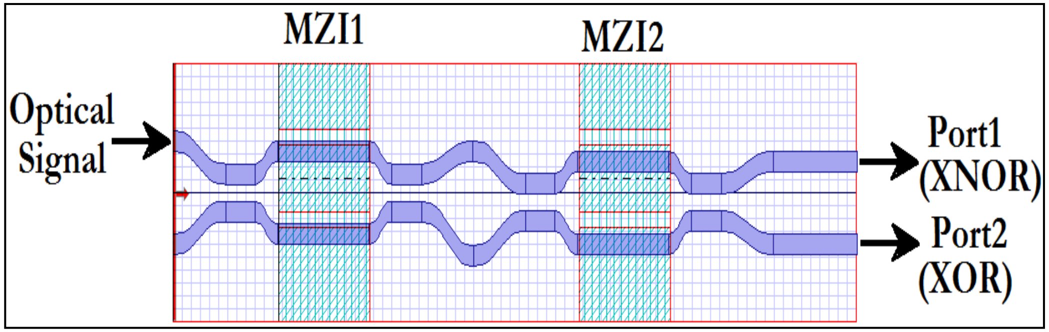

X	Y	Representation of XOR and XNOR logic	XOR	XNOR
0	0	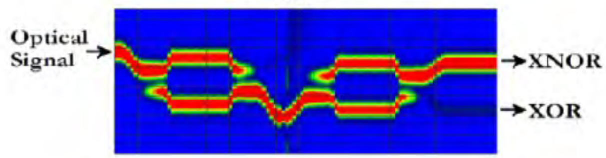	0	1
0	1	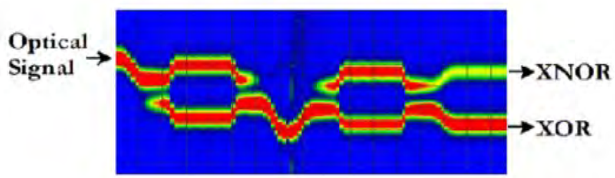	1	0
1	0	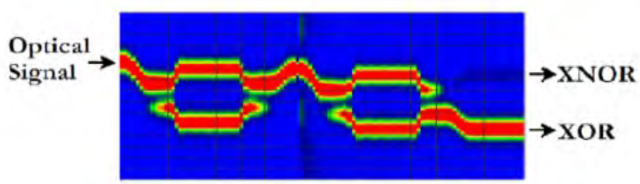	1	0
1	1	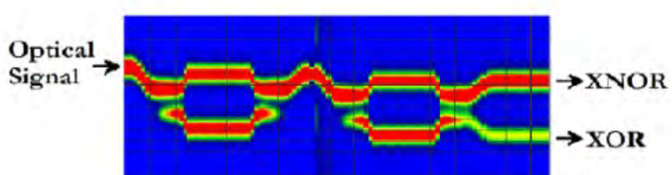	0	1

Design of Full-Adder/Subtractor using the MZIs

<u>**Santosh Kumar**</u> et. al., Optics Communication (Elsevier), Vol. 324, PP. 93-107 (August 15, 2014).

Design of Full-Adder/Subtractor using the MZIs

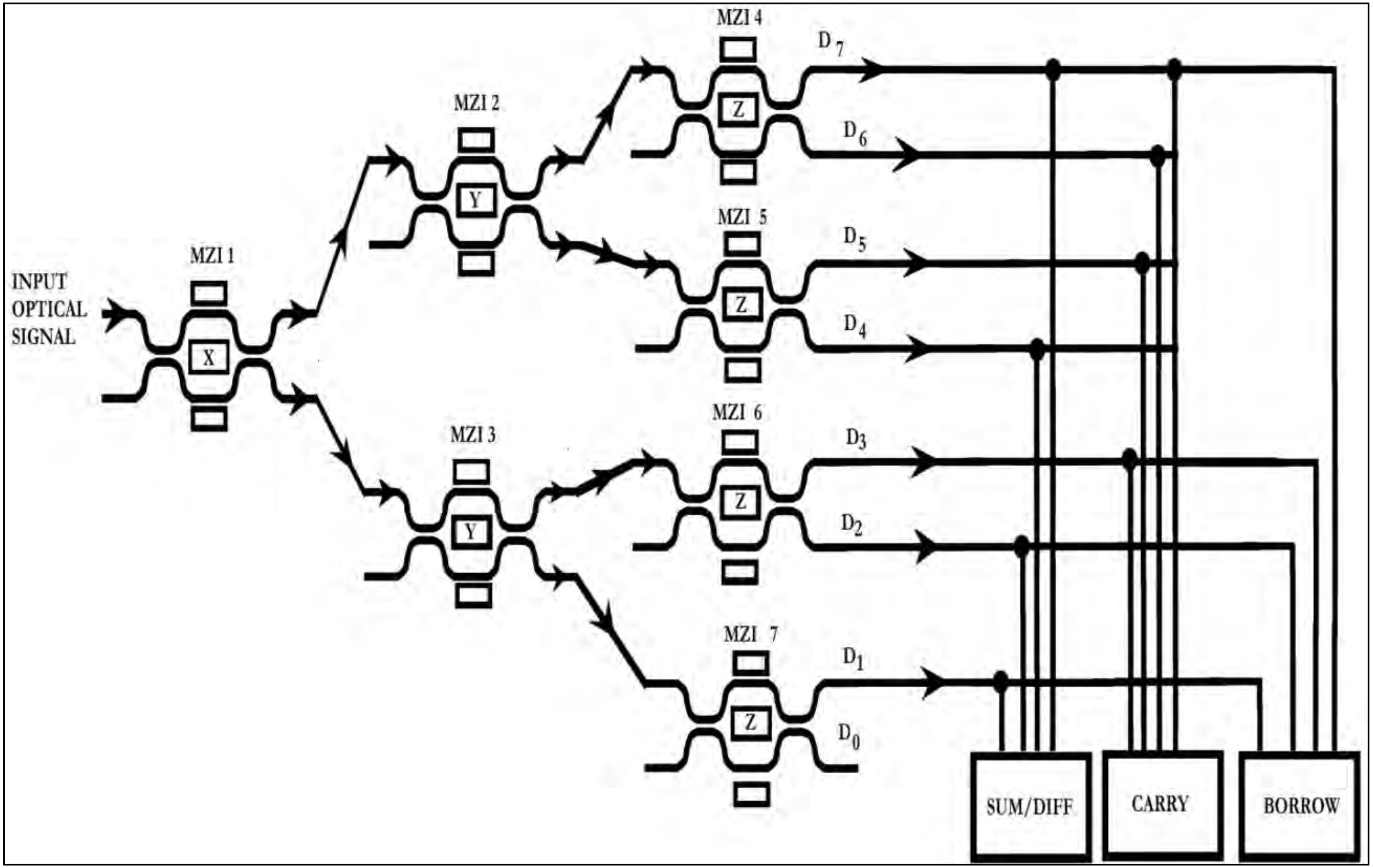

Mathematical Expressions:

$$D_7 = \left|\frac{OUT1_{MZI4}}{E_{in}}\right|^2 = \sin^2\left(\frac{\Delta\varphi_{MZI1}}{2}\right)\sin^2\left(\frac{\Delta\varphi_{MZI2}}{2}\right)\sin^2\left(\frac{\Delta\varphi_{MZI4}}{2}\right)$$

$$D_6 = \left|\frac{OUT2_{MZI4}}{E_{in}}\right|^2 = \sin^2\left(\frac{\Delta\varphi_{MZI1}}{2}\right)\sin^2\left(\frac{\Delta\varphi_{MZI2}}{2}\right)\cos^2\left(\frac{\Delta\varphi_{MZI4}}{2}\right)$$

$$D_5 = \left|\frac{OUT1_{MZI5}}{E_{in}}\right|^2 = \sin^2\left(\frac{\Delta\varphi_{MZI1}}{2}\right)\cos^2\left(\frac{\Delta\varphi_{MZI2}}{2}\right)\sin^2\left(\frac{\Delta\varphi_{MZI5}}{2}\right)$$

$$D_4 = \left|\frac{OUT2_{MZI5}}{E_{in}}\right|^2 = \sin^2\left(\frac{\Delta\varphi_{MZI1}}{2}\right)\cos^2\left(\frac{\Delta\varphi_{MZI2}}{2}\right)\cos^2\left(\frac{\Delta\varphi_{MZI5}}{2}\right)$$

$$D_3 = \left|\frac{OUT1_{MZI6}}{E_{in}}\right|^2 = \cos^2\left(\frac{\Delta\varphi_{MZI1}}{2}\right)\sin^2\left(\frac{\Delta\varphi_{MZI3}}{2}\right)\sin^2\left(\frac{\Delta\varphi_{MZI6}}{2}\right)$$

$$D_2 = \left|\frac{OUT2_{MZI6}}{E_{in}}\right|^2 = \cos^2\left(\frac{\Delta\varphi_{MZI1}}{2}\right)\sin^2\left(\frac{\Delta\varphi_{MZI3}}{2}\right)\cos^2\left(\frac{\Delta\varphi_{MZI6}}{2}\right)$$

$$D_1 = \left|\frac{OUT1_{MZI7}}{E_{in}}\right|^2 = \cos^2\left(\frac{\Delta\varphi_{MZI1}}{2}\right)\cos^2\left(\frac{\Delta\varphi_{MZI3}}{2}\right)\sin^2\left(\frac{\Delta\varphi_{MZI7}}{2}\right)$$

$$D_0 = \left|\frac{OUT1_{MZI7}}{E_{in}}\right|^2 = \cos^2\left(\frac{\Delta\varphi_{MZI1}}{2}\right)\cos^2\left(\frac{\Delta\varphi_{MZI3}}{2}\right)\cos^2\left(\frac{\Delta\varphi_{MZI7}}{2}\right)$$

BPM Layout of Full Adder

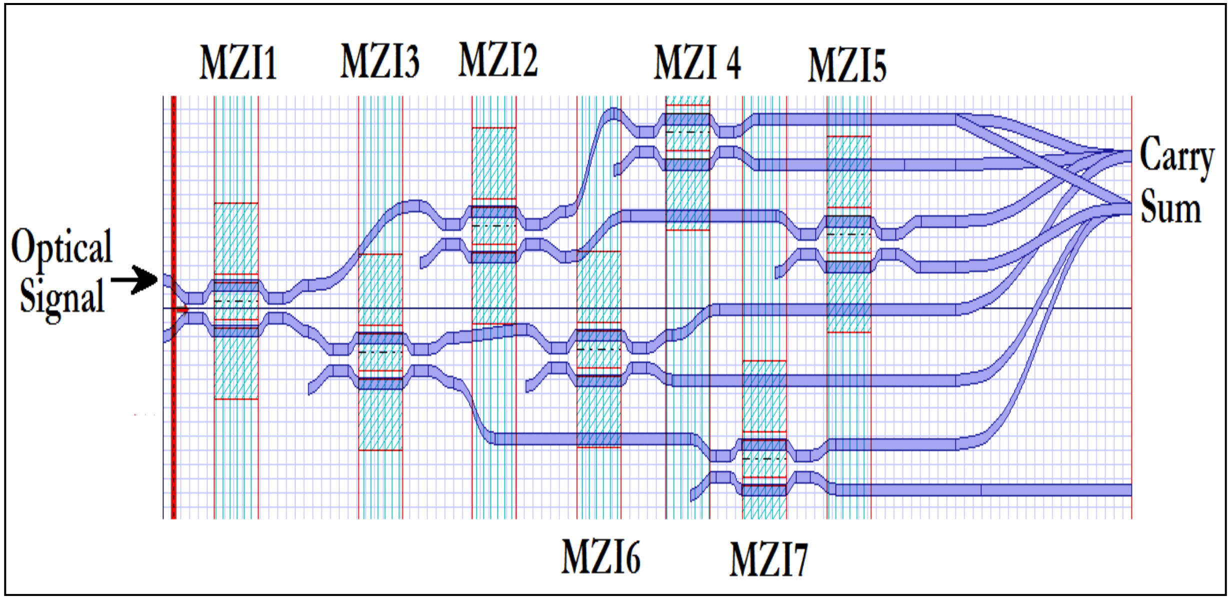

SUM

$$= \cos^2\left(\frac{\Delta\varphi_{MZI1}}{2}\right)\cos^2\left(\frac{\Delta\varphi_{MZI3}}{2}\right)\sin^2\left(\frac{\Delta\varphi_{MZI7}}{2}\right) + \cos^2\left(\frac{\Delta\varphi_{MZI1}}{2}\right)\sin^2\left(\frac{\Delta\varphi_{MZI3}}{2}\right)\cos^2\left(\frac{\Delta\varphi_{MZI6}}{2}\right) + \sin^2\left(\frac{\Delta\varphi_{MZI1}}{2}\right)\cos^2\left(\frac{\Delta\varphi_{MZI2}}{2}\right)\cos^2\left(\frac{\Delta\varphi_{MZI5}}{2}\right) + \sin^2\left(\frac{\Delta\varphi_{MZI1}}{2}\right)\sin^2\left(\frac{\Delta\varphi_{MZI2}}{2}\right)\sin^2\left(\frac{\Delta\varphi_{MZI4}}{2}\right)$$

CARRY

$$= cos^2\left(\frac{\Delta\varphi_{MZI1}}{2}\right)sin^2\left(\frac{\Delta\varphi_{MZI3}}{2}\right)sin^2\left(\frac{\Delta\varphi_{MZI6}}{2}\right) + sin^2\left(\frac{\Delta\varphi_{MZI1}}{2}\right)cos^2\left(\frac{\Delta\varphi_{MZI2}}{2}\right)sin^2\left(\frac{\Delta\varphi_{MZI5}}{2}\right) + sin^2\left(\frac{\Delta\varphi_{MZI1}}{2}\right)sin^2\left(\frac{\Delta\varphi_{MZI2}}{2}\right)cos^2\left(\frac{\Delta\varphi_{MZI4}}{2}\right) + sin^2\left(\frac{\Delta\varphi_{MZI1}}{2}\right)sin^2\left(\frac{\Delta\varphi_{MZI2}}{2}\right)sin^2\left(\frac{\Delta\varphi_{MZI4}}{2}\right)$$

BPM Results of Full Adder

X	Y	Z	Representation of Full-Adder logic	Sum	Carry
0	0	0	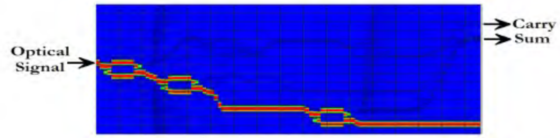	0	0
0	0	1	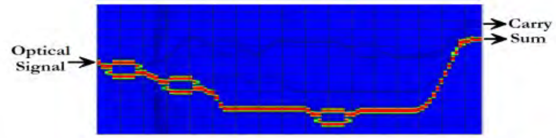	1	0
0	1	0	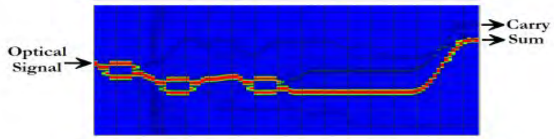	1	0
0	1	1	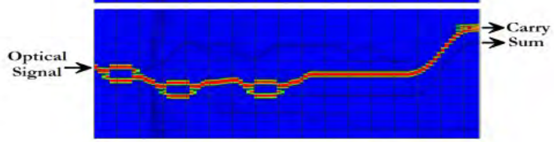	0	1
1	0	0	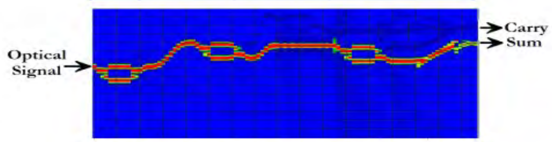	1	0
1	0	1	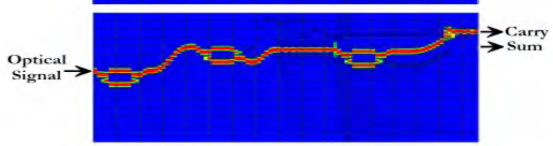	0	1
1	1	0	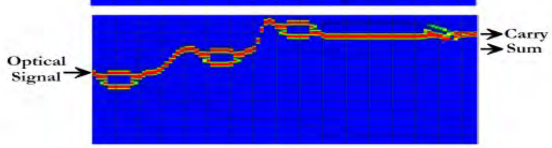	0	1
1	1	1	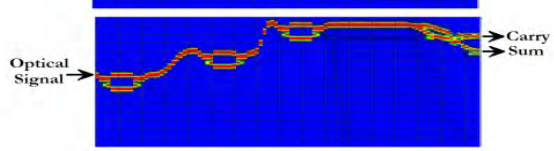	1	1

BPM Layout of Full Subtractor

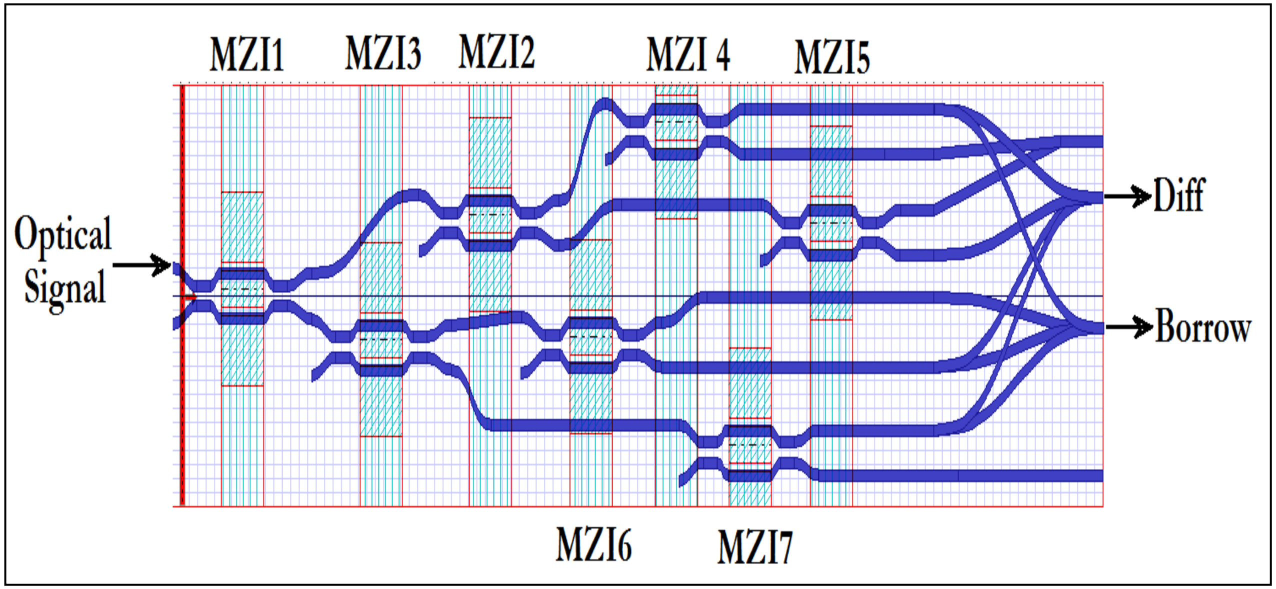

$$DIFFERENCE = cos^2\left(\frac{\Delta\varphi_{MZI1}}{2}\right) cos^2\left(\frac{\Delta\varphi_{MZI3}}{2}\right) sin^2\left(\frac{\Delta\varphi_{MZI7}}{2}\right) + cos^2\left(\frac{\Delta\varphi_{MZI1}}{2}\right) sin^2\left(\frac{\Delta\varphi_{MZI3}}{2}\right) cos^2\left(\frac{\Delta\varphi_{MZI6}}{2}\right) + sin^2\left(\frac{\Delta\varphi_{MZI1}}{2}\right) cos^2\left(\frac{\Delta\varphi_{MZI2}}{2}\right) cos^2\left(\frac{\Delta\varphi_{MZI5}}{2}\right) + sin^2\left(\frac{\Delta\varphi_{MZI1}}{2}\right) sin^2\left(\frac{\Delta\varphi_{MZI2}}{2}\right) sin^2\left(\frac{\Delta\varphi_{MZI4}}{2}\right)$$

BORROW

$$= cos^2\left(\frac{\Delta\varphi_{MZI1}}{2}\right) cos^2\left(\frac{\Delta\varphi_{MZI3}}{2}\right) sin^2\left(\frac{\Delta\varphi_{MZI7}}{2}\right) + cos^2\left(\frac{\Delta\varphi_{MZI1}}{2}\right) sin^2\left(\frac{\Delta\varphi_{MZI3}}{2}\right) cos^2\left(\frac{\Delta\varphi_{MZI6}}{2}\right) + cos^2\left(\frac{\Delta\varphi_{MZI1}}{2}\right) sin^2\left(\frac{\Delta\varphi_{MZI3}}{2}\right) sin^2\left(\frac{\Delta\varphi_{MZI6}}{2}\right) + sin^2\left(\frac{\Delta\varphi_{MZI1}}{2}\right) sin^2\left(\frac{\Delta\varphi_{MZI2}}{2}\right) sin^2\left(\frac{\Delta\varphi_{MZI4}}{2}\right)$$

BPM Results of Full Subtractor

X	Y	Z	Representation of Full- Subtractor logic	Diff	Borrow
0	0	0		0	0
0	0	1		1	1
0	1	0		1	1
0	1	1		0	1
1	0	0		1	0
1	0	1		0	0
1	1	0		0	0
1	1	1		1	1

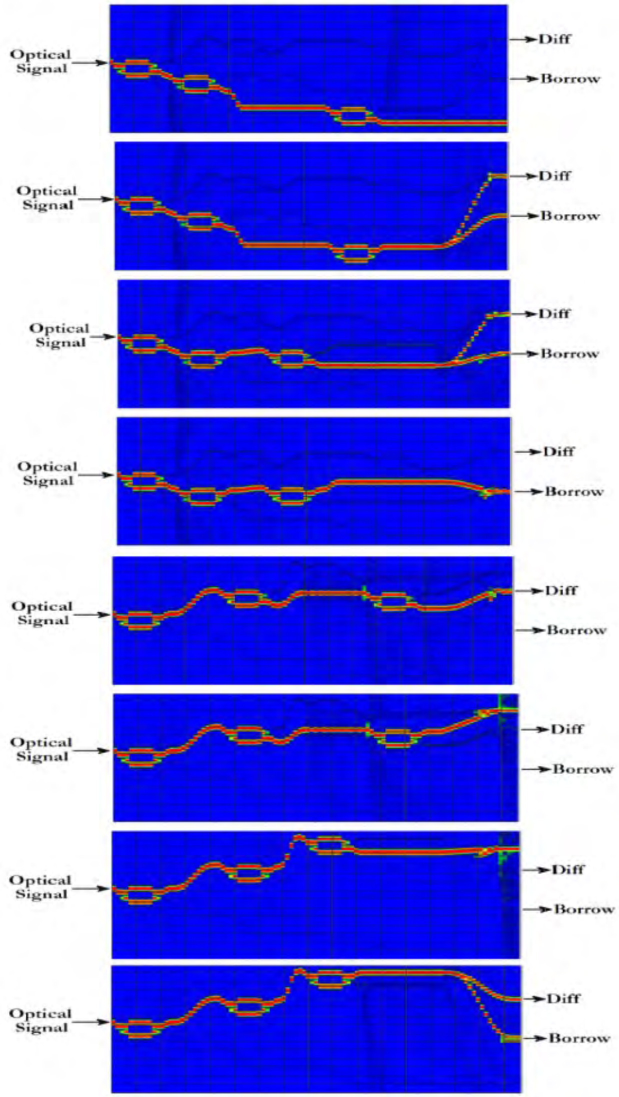

Design of an optical N-bit reversible ripple carry adder

Santosh Kumar et. al., IEEE Workshop on Recent Advances in Photonics, Indian Institute of Science, Bangalore, 2015.

Design of an optical N-bit reversible ripple carry adder

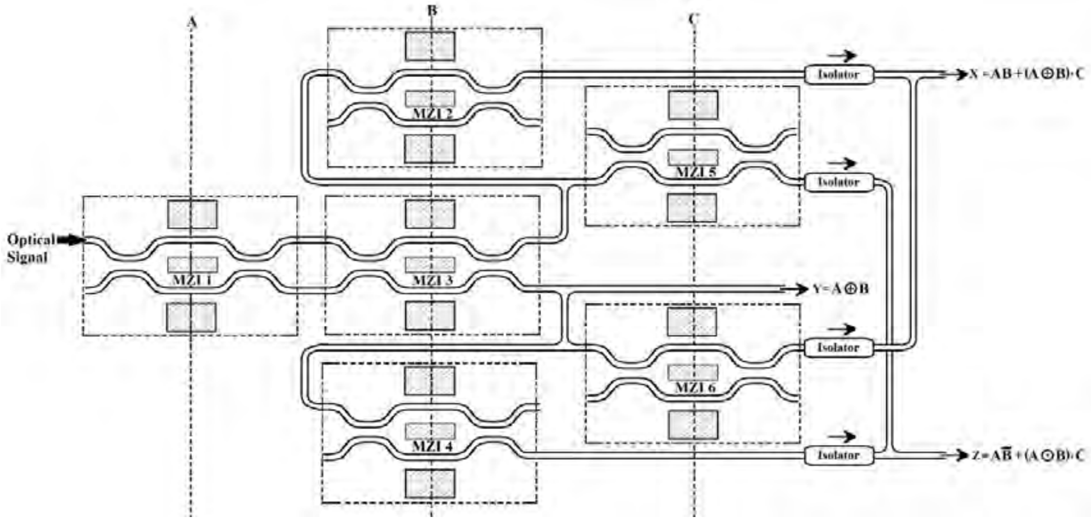

Fig. 23: Schematic diagram of optical reversible gate-I (ORG-I).

Table 6: State table for optical reversible gate-I (ORG-I)

S. No.	Control signal 'A' (V)	Control signal 'B' (V)	Control signal 'C' (V)	$AB + (A \oplus B)C$	$(A \oplus B)$	$A\overline{B} + (\overline{A \oplus B})C$
1	0	0	0	0	0	0
2	0	0	6.75	0	0	1
3	0	6.75	0	0	1	0
4	0	6.75	6.75	1	1	0
5	6.75	0	0	0	1	1
6	6.75	0	6.75	1	1	1
7	6.75	6.75	0	1	0	0
8	6.75	6.75	6.75	1	0	1

Cont …

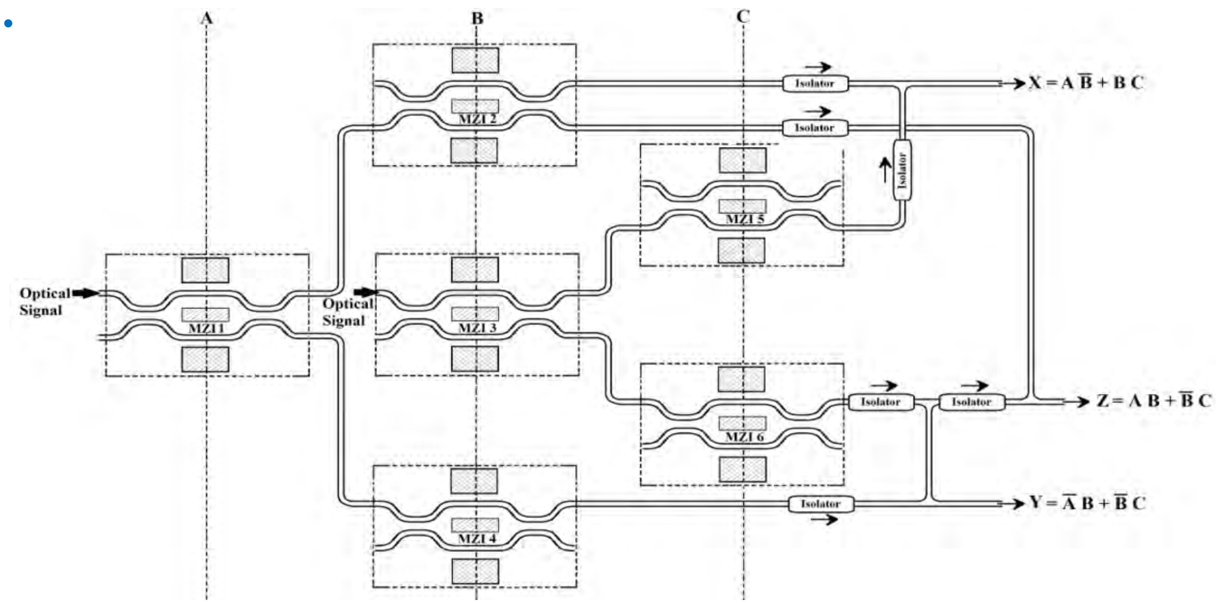

Fig. 24: Schematic diagram of optical reversible gate-I (ORG-I).

Table 7: State table for optical reversible gate-II (ORG-II)

S. No.	Control signal 'A' (V)	Control signal 'B' (V)	Control signal 'C' (V)	$X = A\overline{B} + BC$	$Y = \overline{B}C + \overline{A}B$	$Z = AB + \overline{B}C$
1	0	0	0	0	0	0
2	0	0	6.75	0	1	1
3	0	6.75	0	0	1	0
4	0	6.75	6.75	1	1	0
5	6.75	0	0	1	0	0
6	6.75	0	6.75	1	1	1
7	6.75	6.75	0	0	0	1
8	6.75	6.75	6.75	1	0	1

Cont …

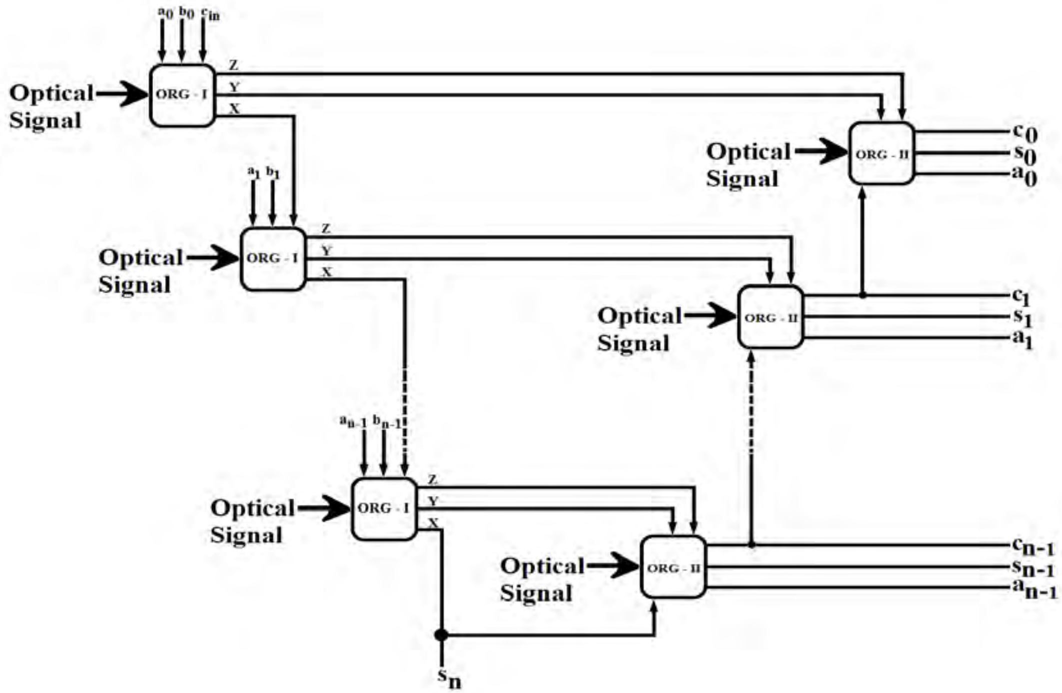

Figure: Schematic diagram of an n-bit reversible ripple carry adder using ORG-I and ORG-II.

Sum, 's' and carry C_j are given as

$$s_j = \begin{cases} a_j \oplus b_j \oplus c_j & for \quad 0 \le j \le n-1 \\ C_n & for \quad j = n \end{cases}$$

$$C_j = \begin{cases} C_0 & ; \quad j = 0 \\ a_{j-1}b_{j-1} + (a_{j-1} \oplus b_{j-1})C_{j-1} & ; \quad 1 \le j \le n \end{cases}$$

Cont …

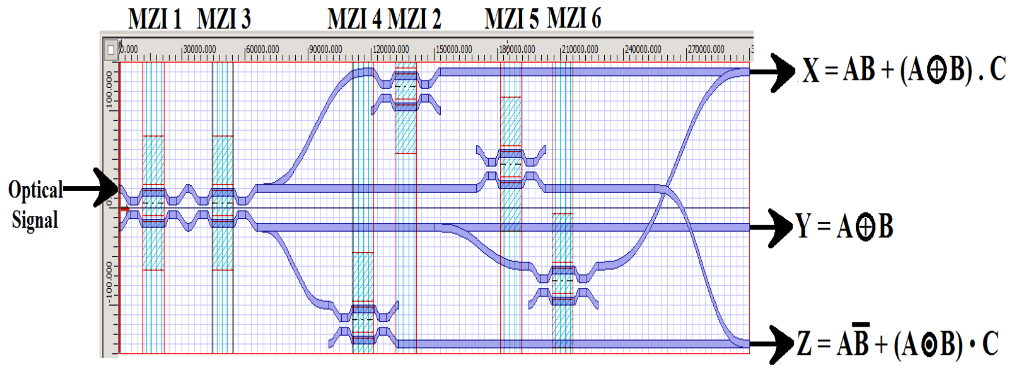

Figure OptiBPM layout for optical reversible gate-I (ORG-I).

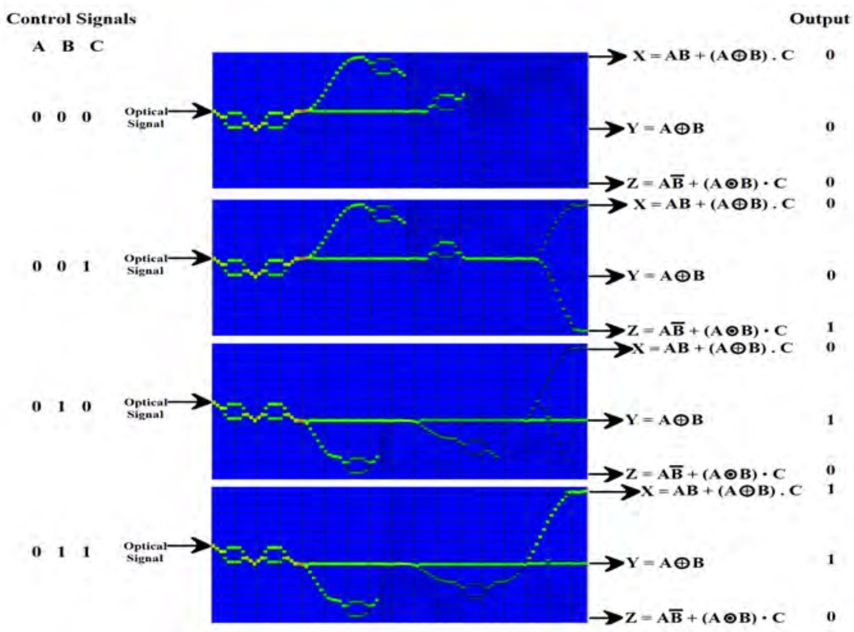

Figure: OptiBPM simulation results for ORG-I, when control signals A, B and C are varied from 000 to 011.

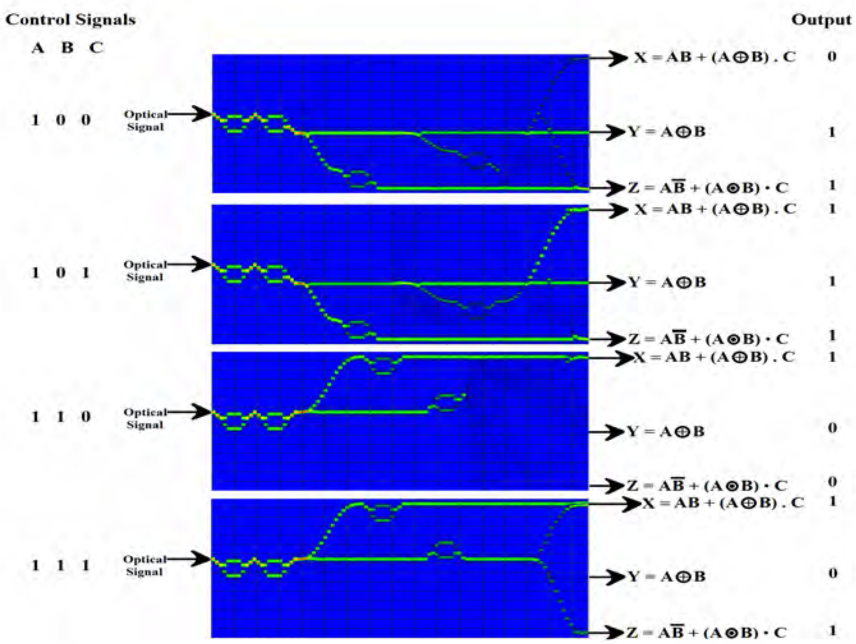

Figure: OptiBPM simulation results for ORG-I, when control signals A, B and C are varied from 100 to 111.

Cont …

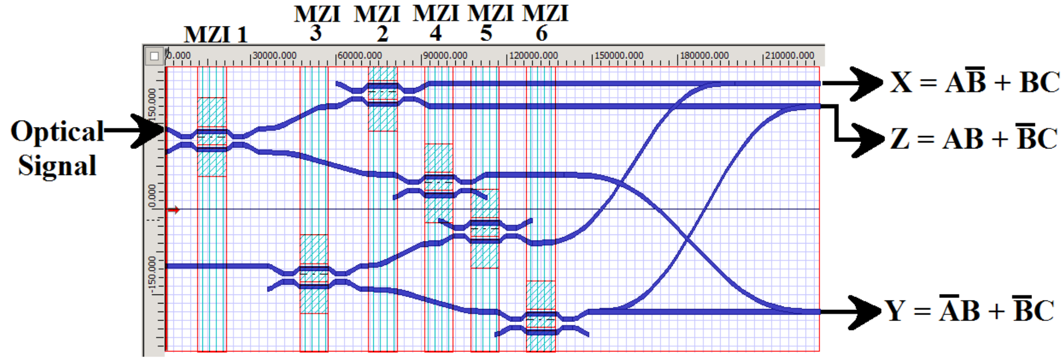

Fig.: OptiBPM layout for optical reversible gate-II (ORG-II).

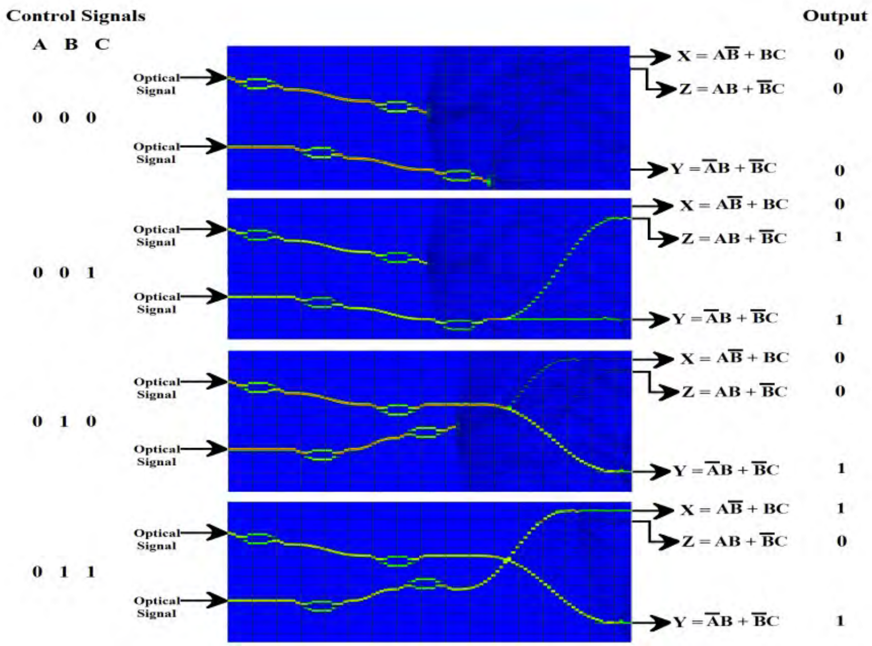

Fig.: OptiBPM simulation results for ORG-II, when control signals A, B and C are varied from 000 to 011.

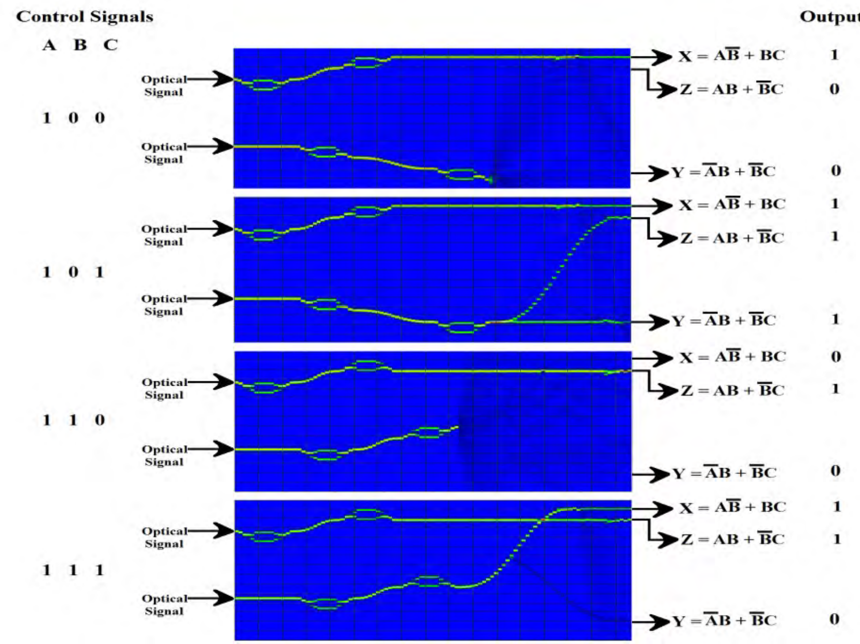

Fig.: OptiBPM simulation results for ORG-II, when control signals A, B and C are varied from 100 to 111.

Design of 2-bit Multiplier using MZIs

Santosh Kumar et. al., Optical and Quantum Electronics (Springer), Vol. 47, Issue 12, pp 3667-3688 (August 20, 2015).

Design of 2-bit Multiplier using MZIs

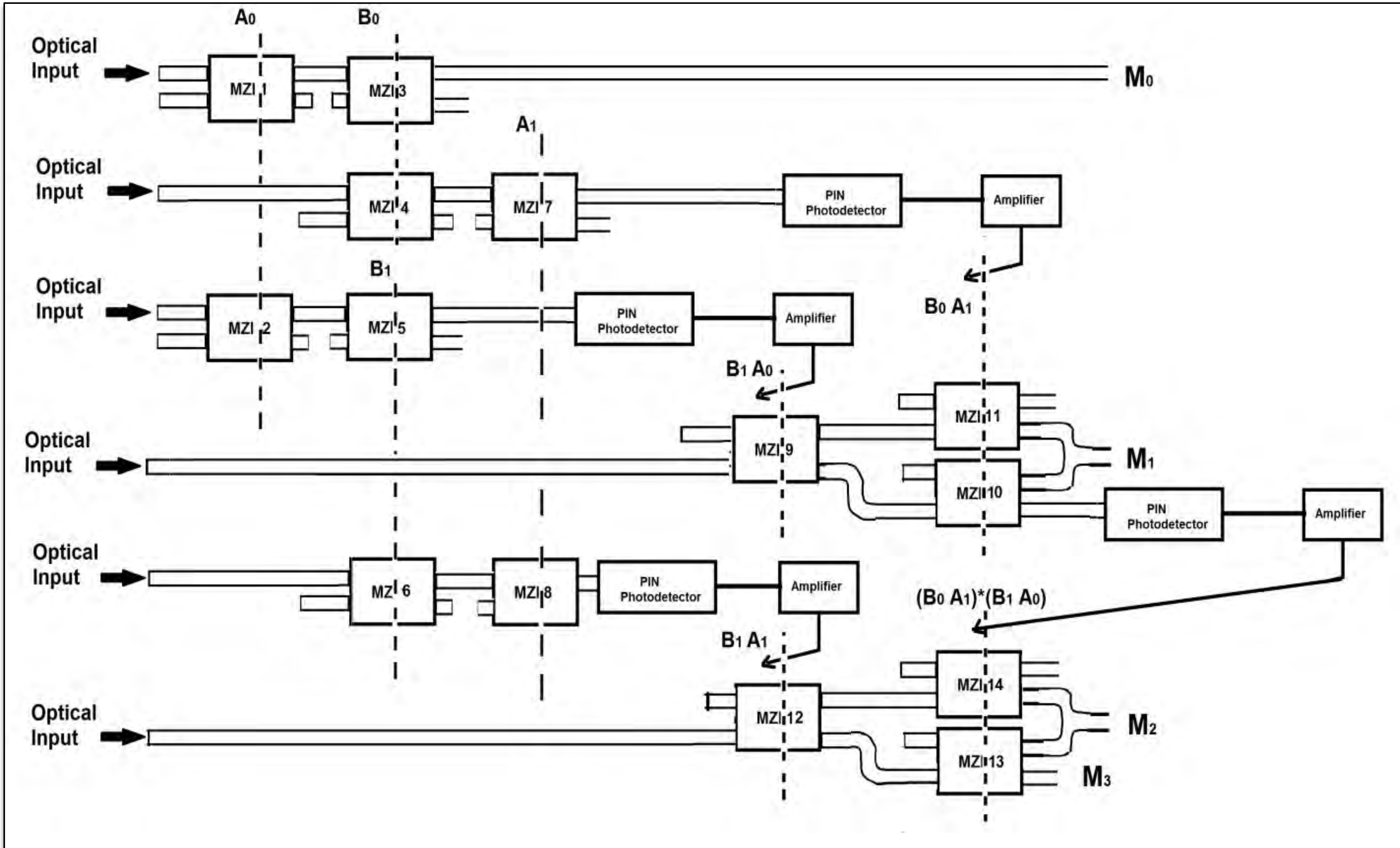

Figure: Schematic diagram of two-bit multiplier using MZIs.

Mathematical expression of 2-bit Multiplier

The normalized output power at different output ports can be represented by the following equations;

At Port M_0;

$$M_0 = \left|\frac{OUT1_{MZI3}}{E_{in}}\right|^2 = \left\{ \sin^2\left(\frac{\Delta\varphi_{MZI1}}{2}\right)\ \sin^2\left(\frac{\Delta\varphi_{MZI3}}{2}\right)\right\}$$

At Port M_1;

$$M_1 = \left\{ \sin^2\left(\frac{\Delta\varphi_{MZI9}}{2}\right)\cos^2\left(\frac{\Delta\varphi_{MZI10}}{2}\right)\right\} + \left\{\cos^2\left(\frac{\Delta\varphi_{MZI9}}{2}\right)\sin^2\left(\frac{\Delta\varphi_{MZI11}}{2}\right)\right\}$$

At Port M_2;

$$M_2 = \left\{ \sin^2\left(\frac{\Delta\varphi_{MZI12}}{2}\right)\cos^2\left(\frac{\Delta\varphi_{MZI13}}{2}\right)\right\} + \left\{\cos^2\left(\frac{\Delta\varphi_{MZI12}}{2}\right)\sin^2\left(\frac{\Delta\varphi_{MZI14}}{2}\right)\right\}$$

At Port M_3;

$$M_3 = \left|\frac{OUT1_{MZI3}}{E_{in}}\right|^2 = \left\{ \sin^2\left(\frac{\Delta\varphi_{MZI12}}{2}\right)\ \sin^2\left(\frac{\Delta\varphi_{MZI13}}{2}\right)\right\}$$

MATLAB Result of 2-bit Multiplier

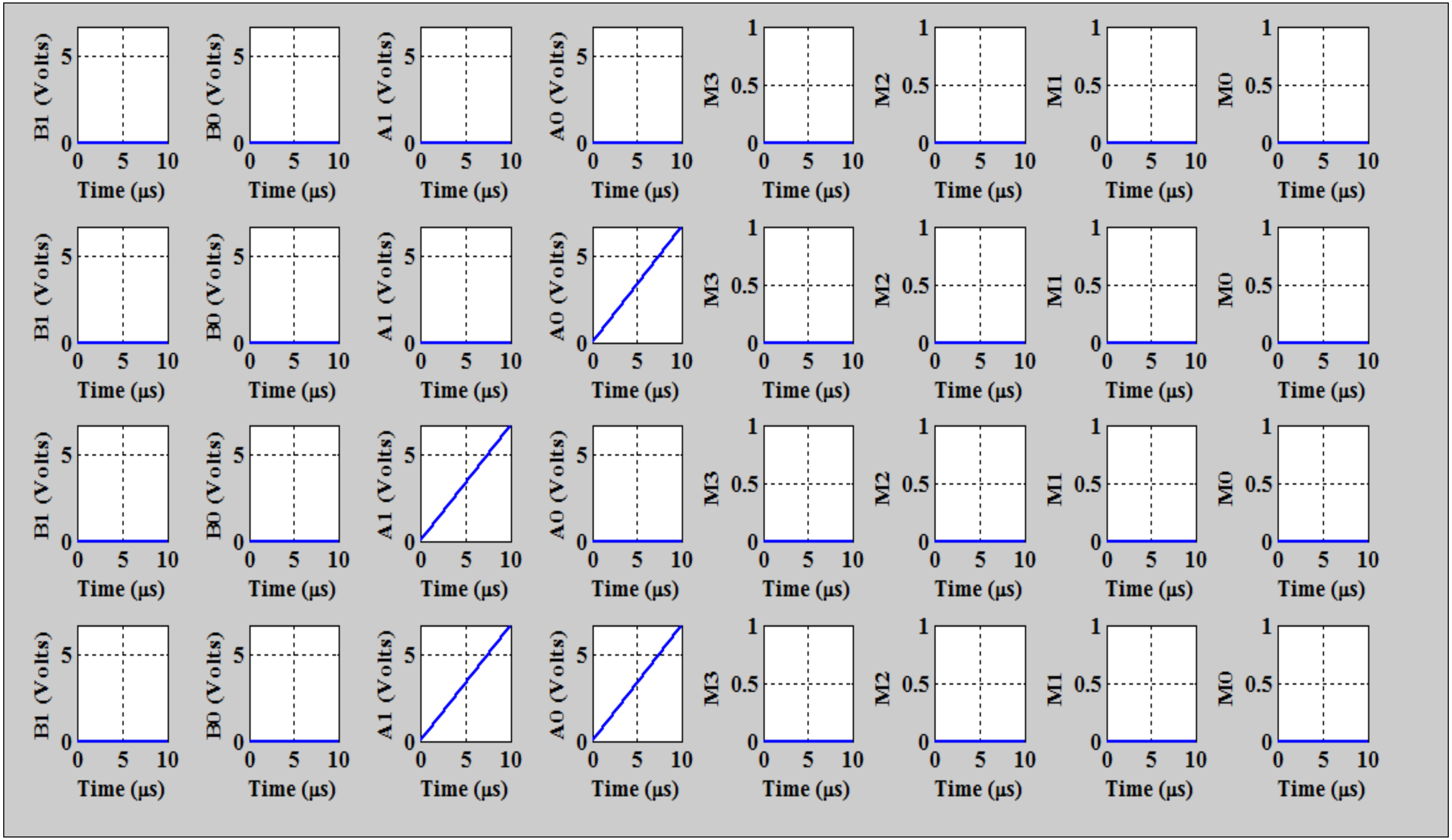

Figure: MATLAB simulation results of 2-bit multiplier, when the magnitude of B is 0 and magnitude of A changes from 0 to 3.

Cont …

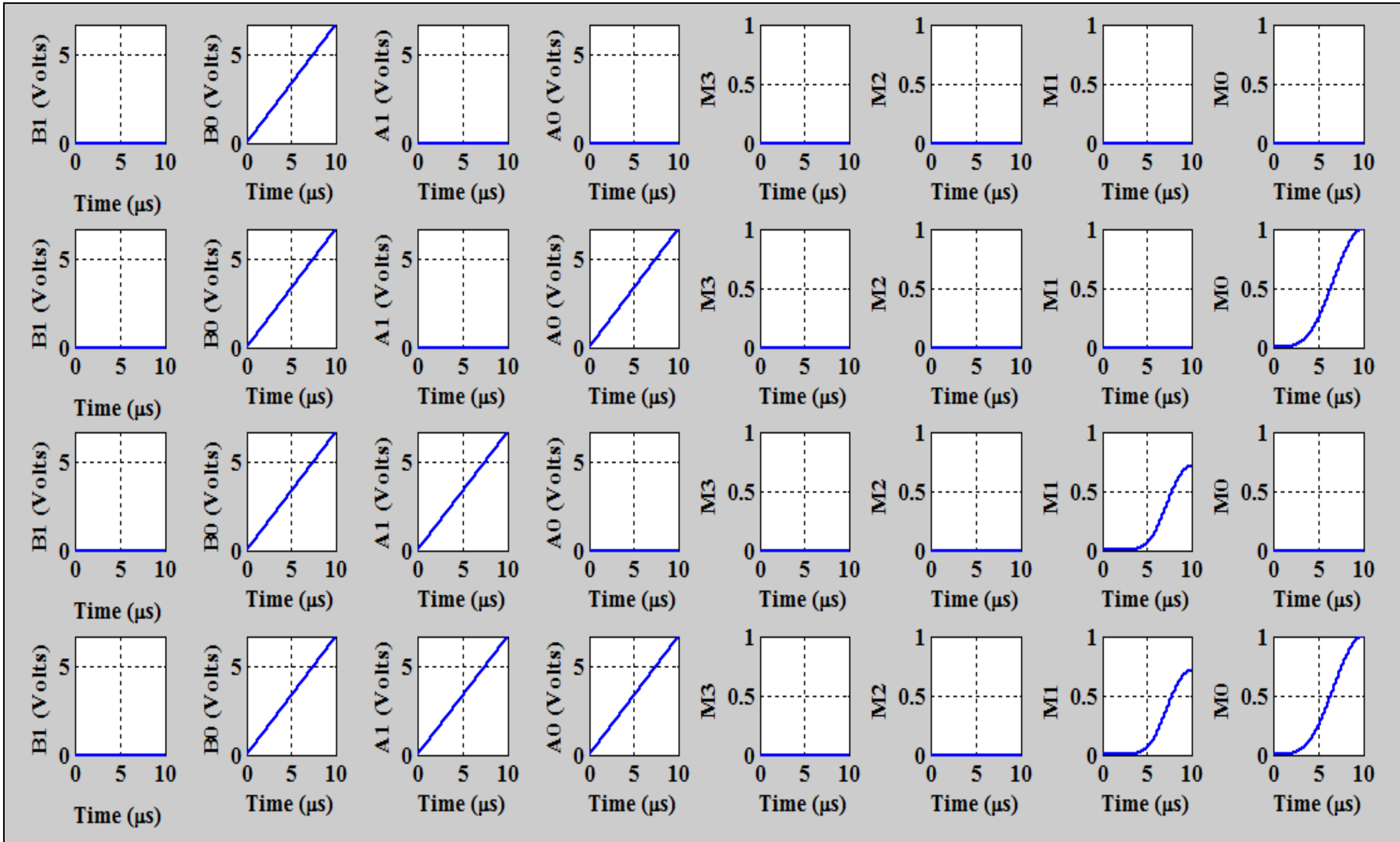

Figure: MATLAB simulation results of 2-bit multiplier, when magnitude of B is 1 and magnitude of A changes from 0 to 3.

Cont …

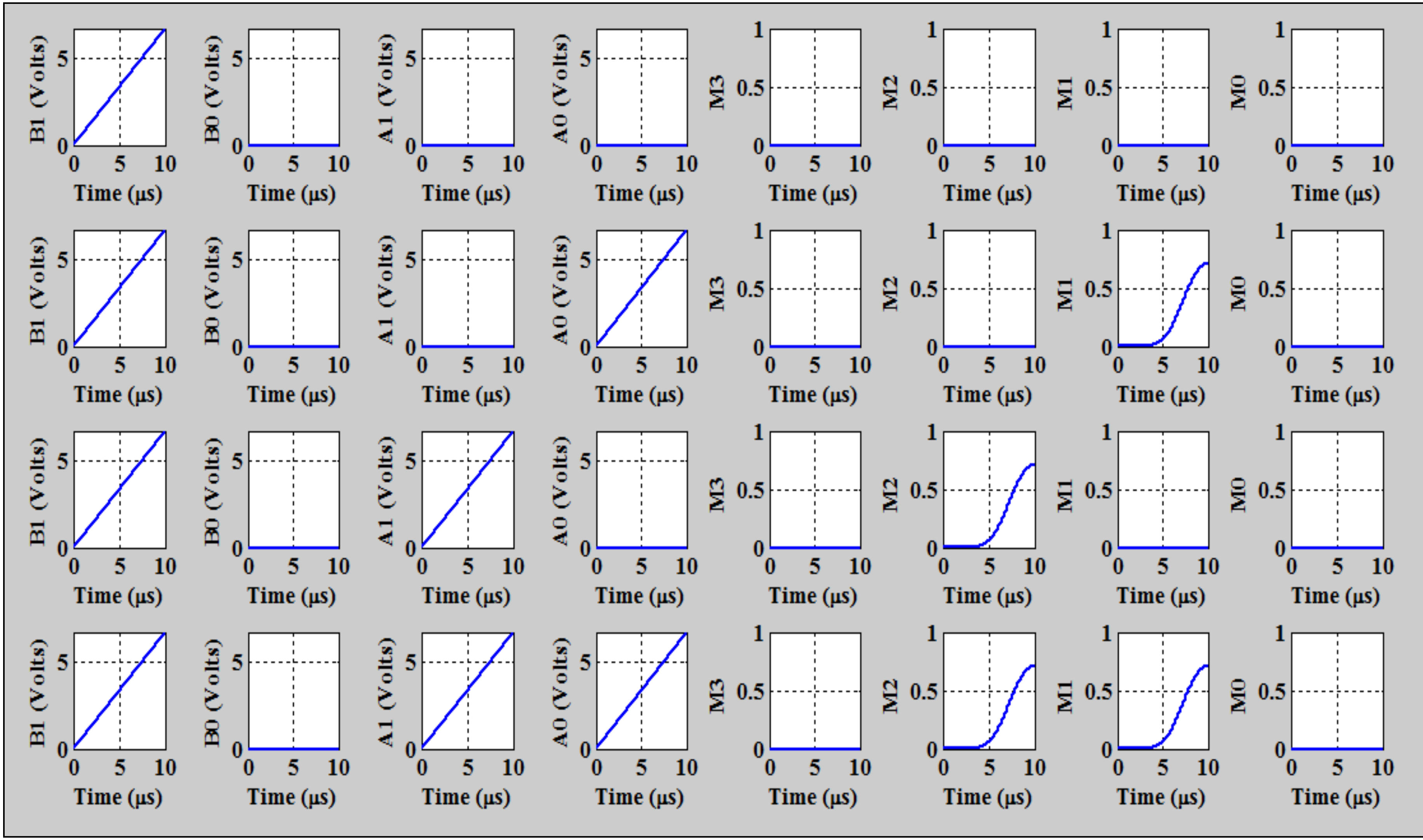

Figure: MATLAB simulation results of 2-bit multiplier, when magnitude of B is 2 and magnitude of A changes from 0 to 3.

Cont …

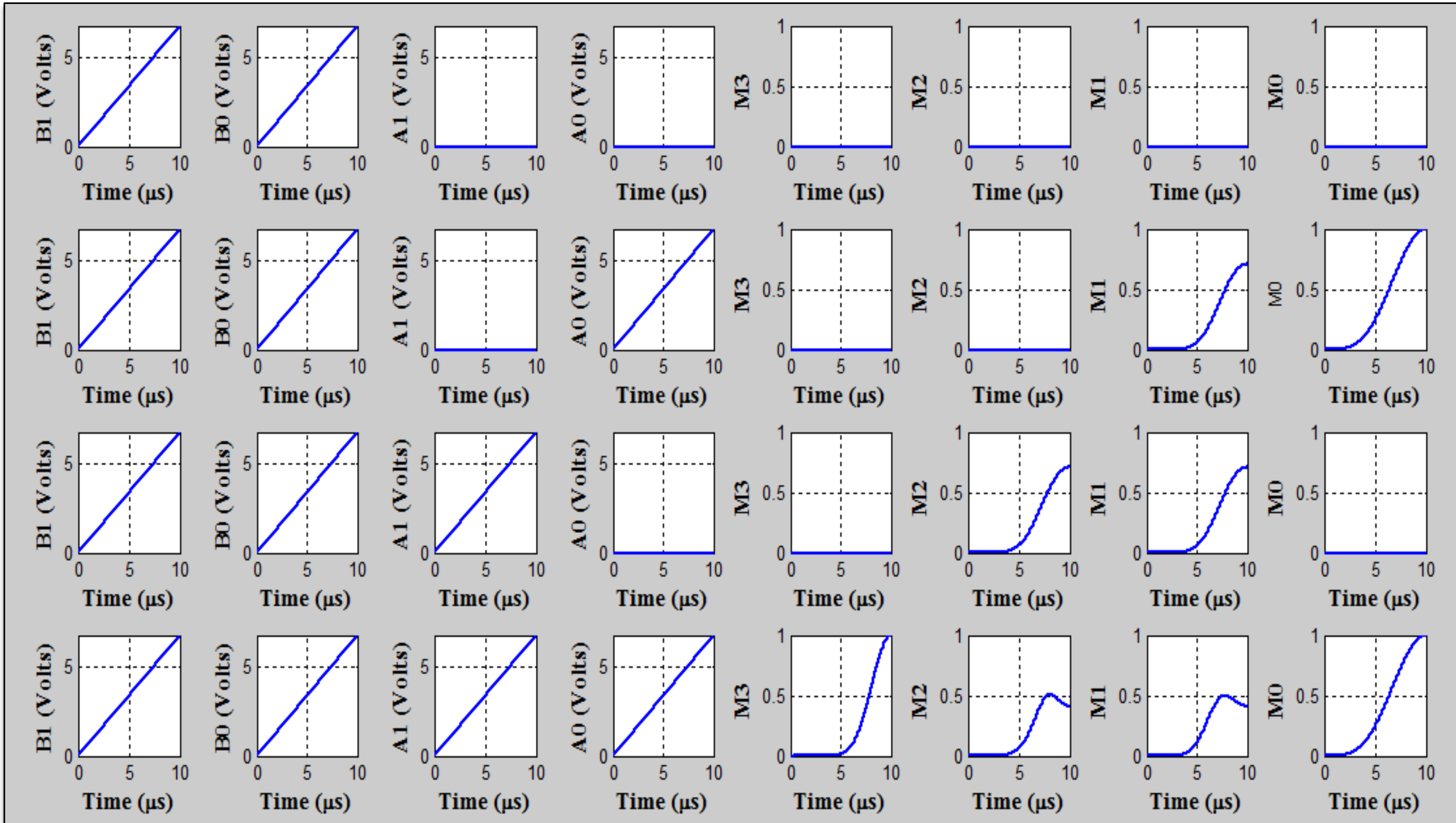

Figure: MATLAB simulation results of 2-bit multiplier, when the magnitude of B is 3 and magnitude of A changes from 0 to 3.

BPM Result of 2-bit Multiplier

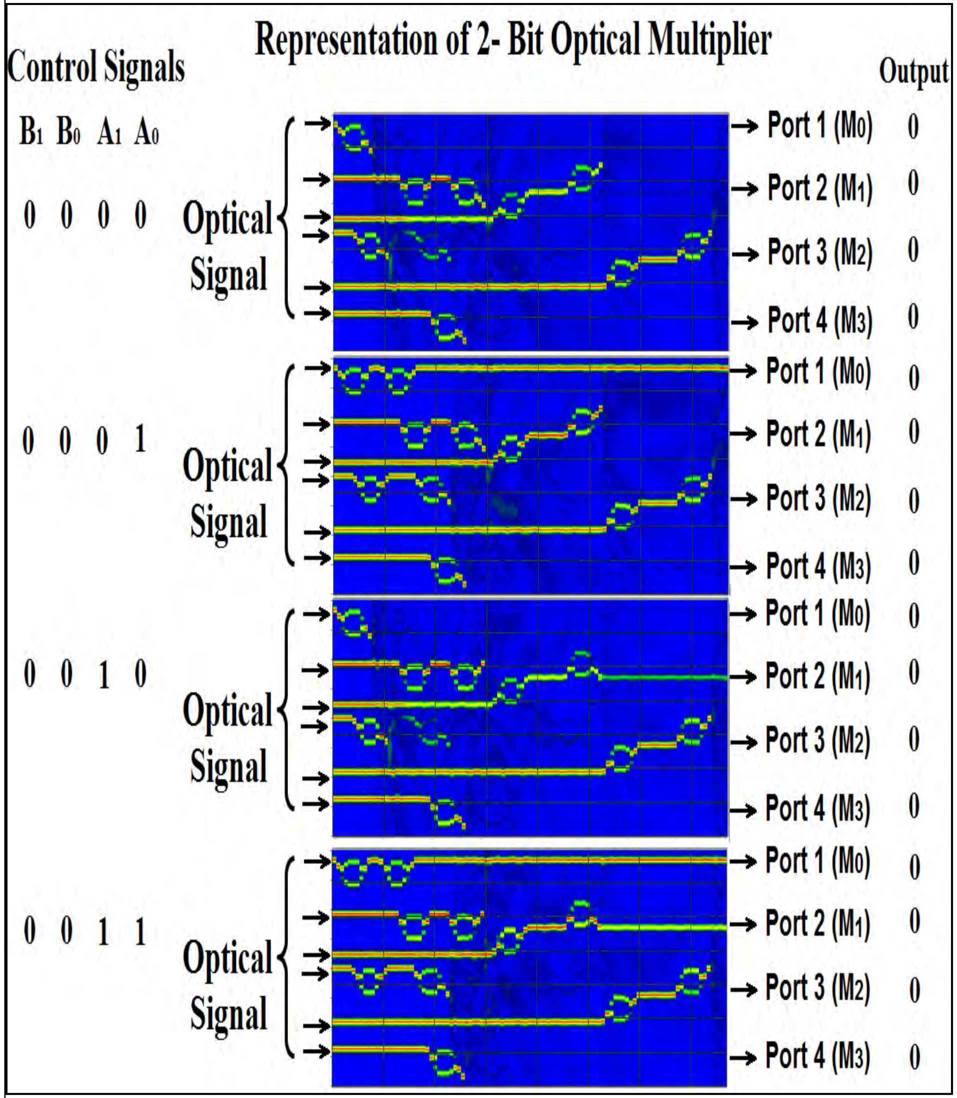

Figure: The results of 2–bit multiplier operation, when magnitude of B is 0 and magnitudes A changes from 0 to 3.

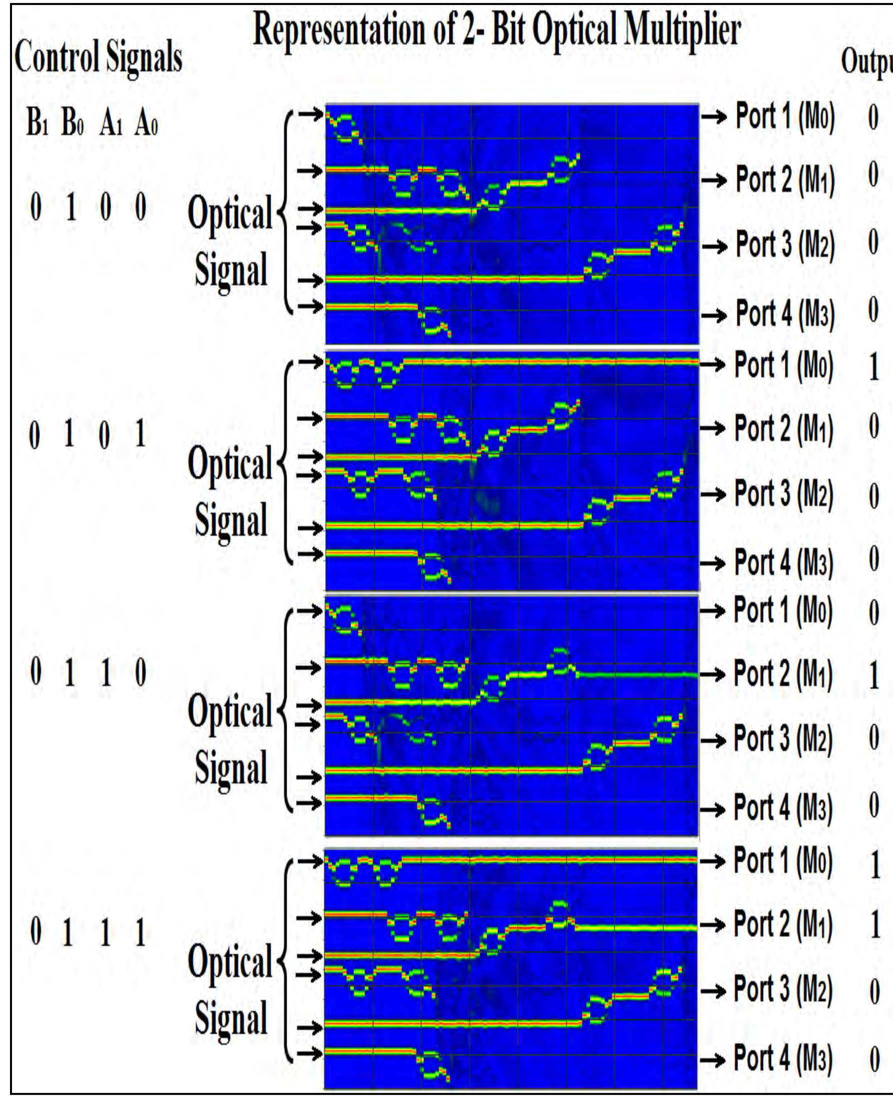

Figure: The results of 2–bit multiplier operation, when magnitude of B is 1 and magnitudes A changes from 0 to 3.

Cont …

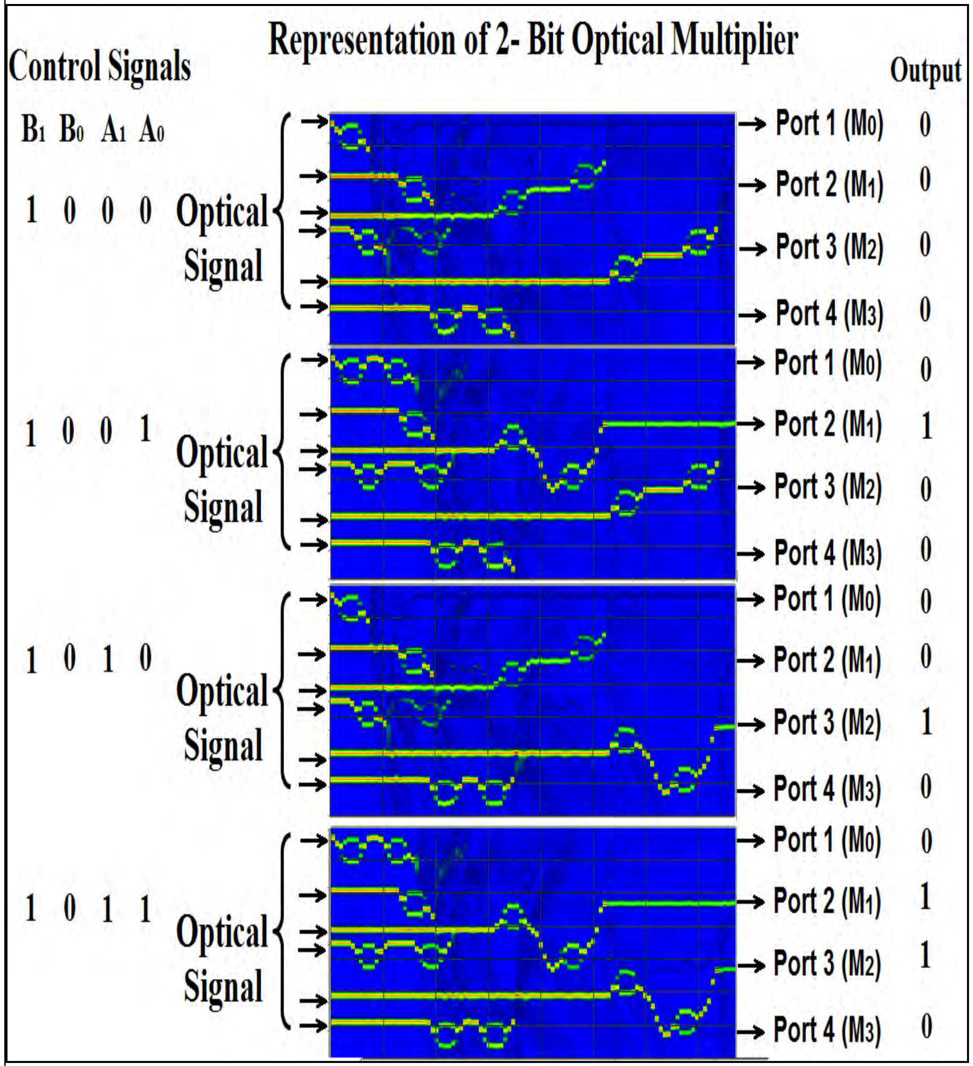

Figure: The results of 2–bit multiplier operation, when magnitude of B is 2 and magnitudes A changes from 0 to 3.

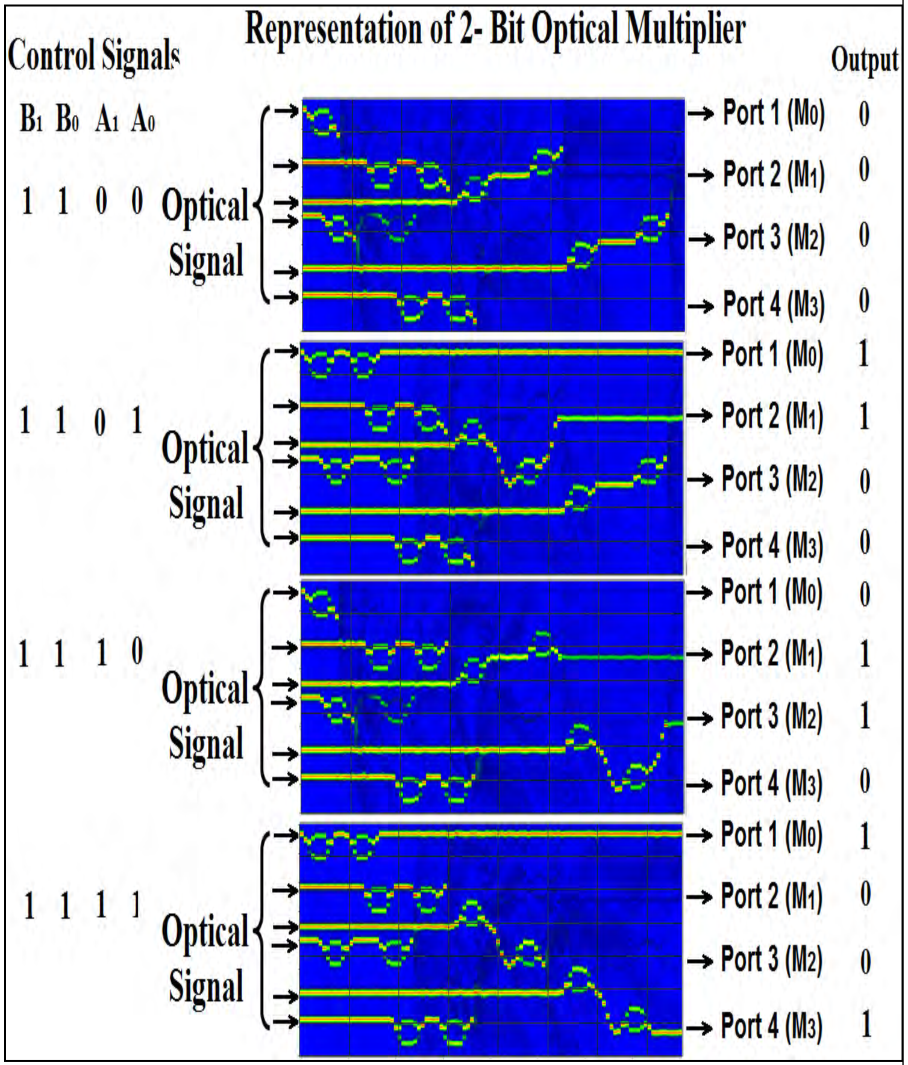

Figure: The results of 2–bit multiplier operation, when magnitude of B is 3 and magnitudes A changes from 0 to 3.

Design of 1-bit and 2-bit magnitude comparators

<u>Santosh Kumar</u> et. al., Optics Communications (Elsevier), Vol. 357, PP. 127-147 (Sept. 09, 2015).

Design of 1-bit and 2-bit magnitude comparators

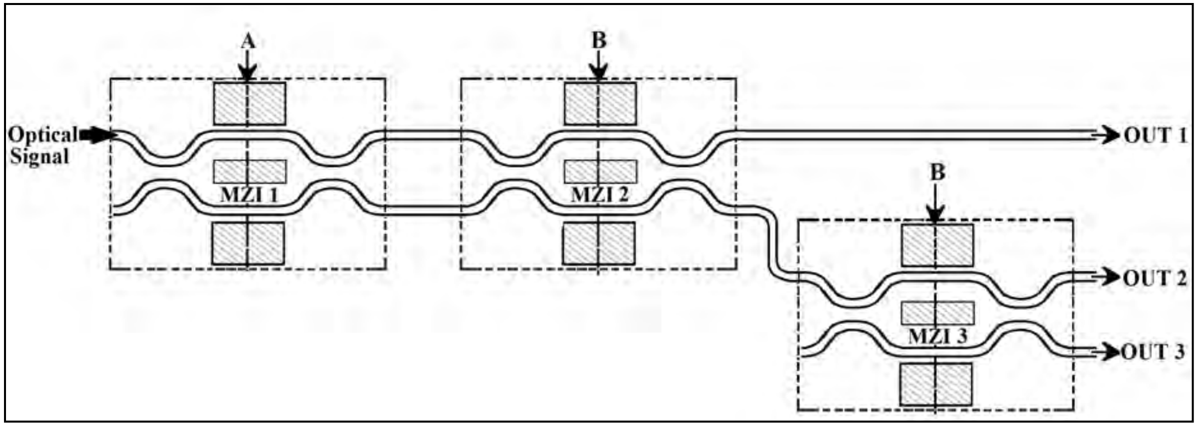

Figure: Schematic diagram of 1-bit comparator using the MZIs.

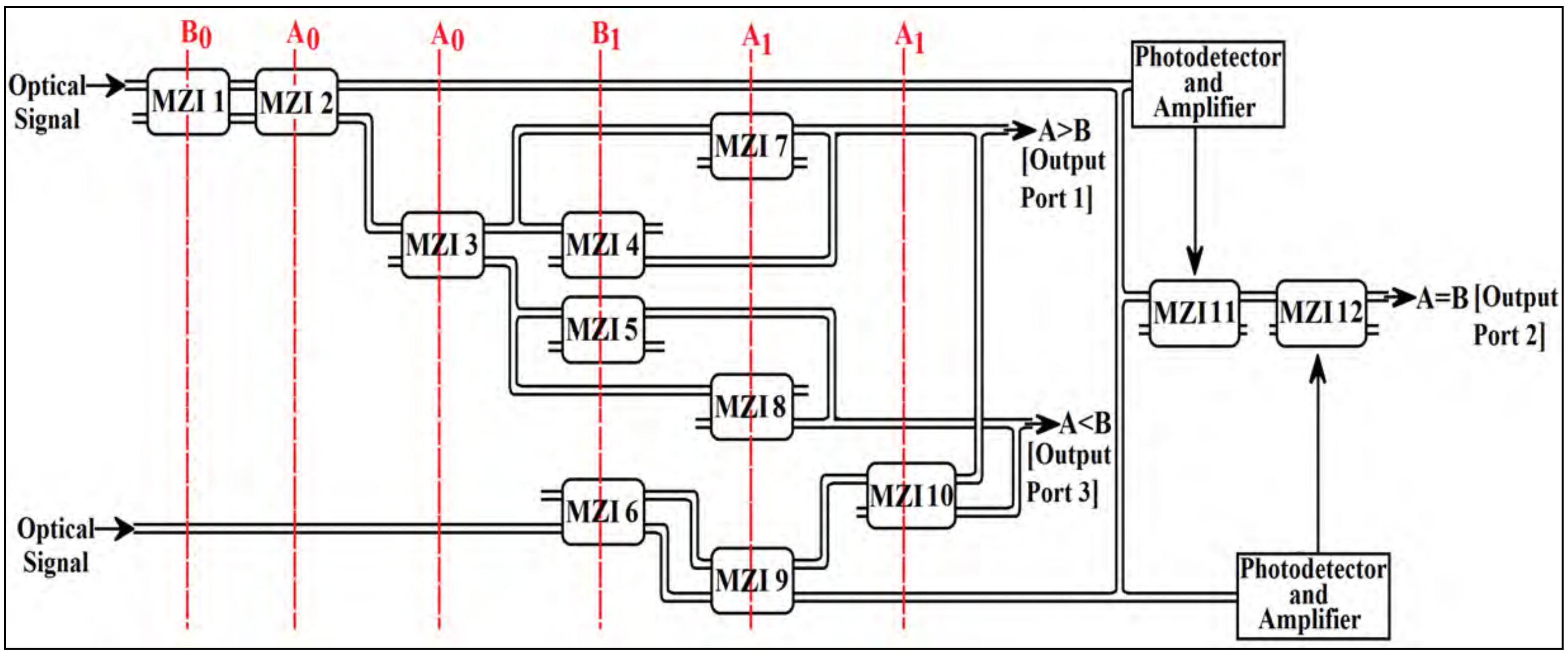

Figure: Schematic diagram of 2-bit comparator using the MZIs.

Cont …

For case 1 ($A = B$);

$$\mathrm{OUT1} = \left|\frac{\mathrm{OUT1_{MZI2}}}{\mathrm{E_{in}}}\right|^2 = \left\{\cos^2\left(\frac{\Delta\varphi_{\mathrm{MZI1}}}{2}\right)\ \cos^2\left(\frac{\Delta\varphi_{\mathrm{MZI2}}}{2}\right)\right\} + \left\{\sin^2\left(\frac{\Delta\varphi_{\mathrm{MZI1}}}{2}\right)\ \sin^2\left(\frac{\Delta\varphi_{\mathrm{MZI2}}}{2}\right)\right\}$$

For case 2 ($A < B$);

$$\mathrm{OUT2} = \left|\frac{\mathrm{OUT1_{MZI3}}}{E_{in}}\right|^2 = \cos^2\left(\frac{\Delta\varphi_{\mathrm{MZI1}}}{2}\right)\ \sin^2\left(\frac{\Delta\varphi_{\mathrm{MZI2}}}{2}\right)\ \sin^2\left(\frac{\Delta\varphi_{\mathrm{MZI3}}}{2}\right)$$

For case 3 ($A > B$);

$$\mathrm{OUT3} = \left|\frac{\mathrm{OUT2_{MZI3}}}{\mathrm{E_{in}}}\right|^2 = \cos^2\left(\frac{\Delta\varphi_{\mathrm{MZI1}}}{2}\right) \sin^2\left(\frac{\Delta\varphi_{\mathrm{MZI2}}}{2}\right)\ \cos^2\left(\frac{\Delta\varphi_{\mathrm{MZI3}}}{2}\right)$$

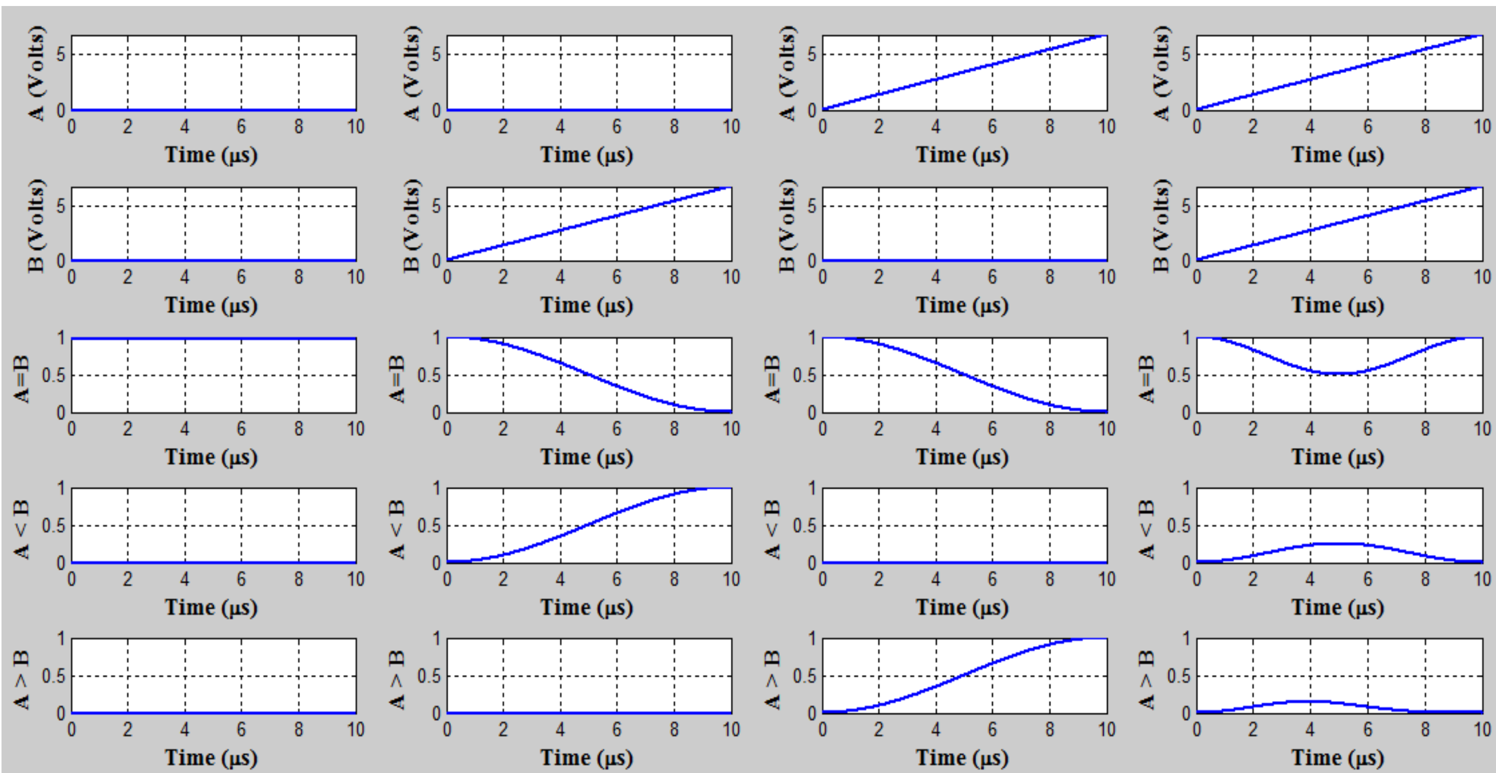

Figure: Simulation result of 1-bit magnitude comparator.

Cont …

For Case 1 ($A = B$):

$$\mathrm{OUT1} = \left|\frac{\mathrm{OUT1_{MZI12}}}{\mathrm{E_{in}}}\right|^2$$

$$= \left\{\cos^2\left(\frac{\Delta\varphi_{\mathrm{MZI1}}}{2}\right)\cos^2\left(\frac{\Delta\varphi_{\mathrm{MZI2}}}{2}\right)\cos^2\left(\frac{\Delta\varphi_{\mathrm{MZI6}}}{2}\right)\cos^2\left(\frac{\Delta\varphi_{\mathrm{MZI9}}}{2}\right)\right\} + \left\{\cos^2\left(\frac{\Delta\varphi_{\mathrm{MZI6}}}{2}\right)\cos^2\left(\frac{\Delta\varphi_{\mathrm{MZI9}}}{2}\right)\sin^2\left(\frac{\Delta\varphi_{\mathrm{MZI1}}}{2}\right)\sin^2\left(\frac{\Delta\varphi_{\mathrm{MZI2}}}{2}\right)\right\}$$
$$+ \left\{\cos^2\left(\frac{\Delta\varphi_{\mathrm{MZI1}}}{2}\right)\cos^2\left(\frac{\Delta\varphi_{\mathrm{MZI2}}}{2}\right)\sin^2\left(\frac{\Delta\varphi_{\mathrm{MZI6}}}{2}\right)\sin^2\left(\frac{\Delta\varphi_{\mathrm{MZI9}}}{2}\right)\right\}$$
$$+ \left\{\sin^2\left(\frac{\Delta\varphi_{\mathrm{MZI6}}}{2}\right)\sin^2\left(\frac{\Delta\varphi_{\mathrm{MZI9}}}{2}\right)\sin^2\left(\frac{\Delta\varphi_{\mathrm{MZI1}}}{2}\right)\sin^2\left(\frac{\Delta\varphi_{\mathrm{MZI2}}}{2}\right)\right\}$$

For Case 2 ($A < B$):

$$\mathrm{OUT2} = \left|\frac{\mathrm{OUT2_{MZI10}}}{E_{in}}\right|^2$$

$$= \sin^2\left(\frac{\Delta\varphi_{\mathrm{MZI1}}}{2}\right)\cos^2\left(\frac{\Delta\varphi_{\mathrm{MZI2}}}{2}\right)\cos^2\left(\frac{\Delta\varphi_{\mathrm{MZI3}}}{2}\right)\cos^2\left(\frac{\Delta\varphi_{\mathrm{MZI8}}}{2}\right) + \sin^2\left(\frac{\Delta\varphi_{\mathrm{MZI6}}}{2}\right)\cos^2\left(\frac{\Delta\varphi_{\mathrm{MZI9}}}{2}\right)\cos^2\left(\frac{\Delta\varphi_{\mathrm{MZI10}}}{2}\right)$$
$$+ \sin^2\left(\frac{\Delta\varphi_{\mathrm{MZI1}}}{2}\right)\sin^2\left(\frac{\Delta\varphi_{\mathrm{MZI5}}}{2}\right)\cos^2\left(\frac{\Delta\varphi_{\mathrm{MZI2}}}{2}\right)\cos^2\left(\frac{\Delta\varphi_{\mathrm{MZI3}}}{2}\right)$$
$$+ \sin^2\left(\frac{\Delta\varphi_{\mathrm{MZI1}}}{2}\right)\cos^2\left(\frac{\Delta\varphi_{\mathrm{MZI8}}}{2}\right)\cos^2\left(\frac{\Delta\varphi_{\mathrm{MZI2}}}{2}\right)\cos^2\left(\frac{\Delta\varphi_{\mathrm{MZI3}}}{2}\right)$$

For Case 3 ($A > B$):

$$\mathrm{OUT3} = \left|\frac{\mathrm{OUT1_{MZI7}}}{\mathrm{E_{in}}}\right|^2$$

$$= \sin^2\left(\frac{\Delta\varphi_{\mathrm{MZI2}}}{2}\right)\sin^2\left(\frac{\Delta\varphi_{\mathrm{MZI3}}}{2}\right)\cos^2\left(\frac{\Delta\varphi_{\mathrm{MZI1}}}{2}\right)\cos^2\left(\frac{\Delta\varphi_{\mathrm{MZ4}}}{2}\right) + \sin^2\left(\frac{\Delta\varphi_{\mathrm{MZI9}}}{2}\right)\sin^2\left(\frac{\Delta\varphi_{\mathrm{MZI10}}}{2}\right)\cos^2\left(\frac{\Delta\varphi_{\mathrm{MZI6}}}{2}\right)$$
$$+ \sin^2\left(\frac{\Delta\varphi_{\mathrm{MZI2}}}{2}\right)\sin^2\left(\frac{\Delta\varphi_{\mathrm{MZI3}}}{2}\right)\cos^2\left(\frac{\Delta\varphi_{\mathrm{MZI1}}}{2}\right)\cos^2\left(\frac{\Delta\varphi_{\mathrm{MZI4}}}{2}\right)$$
$$+ \sin^2\left(\frac{\Delta\varphi_{\mathrm{MZI2}}}{2}\right)\sin^2\left(\frac{\Delta\varphi_{\mathrm{MZI3}}}{2}\right)\cos^2\left(\frac{\Delta\varphi_{\mathrm{MZI1}}}{2}\right)\sin^2\left(\frac{\Delta\varphi_{\mathrm{MZI7}}}{2}\right)$$

Cont …

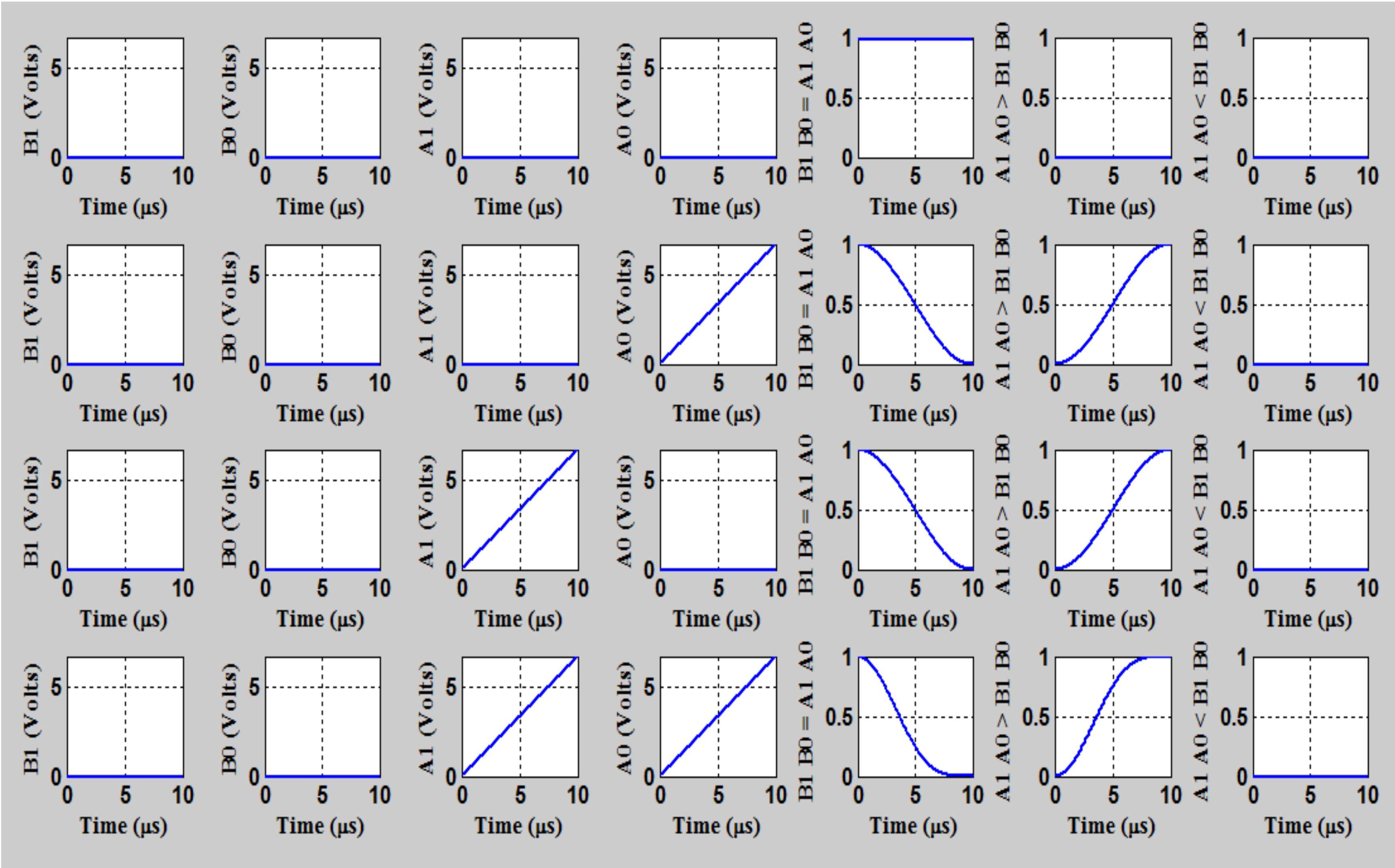

Figure: Simulation result of 1-bit magnitude comparator.

Design of 1-bit and 2-bit magnitude comparators

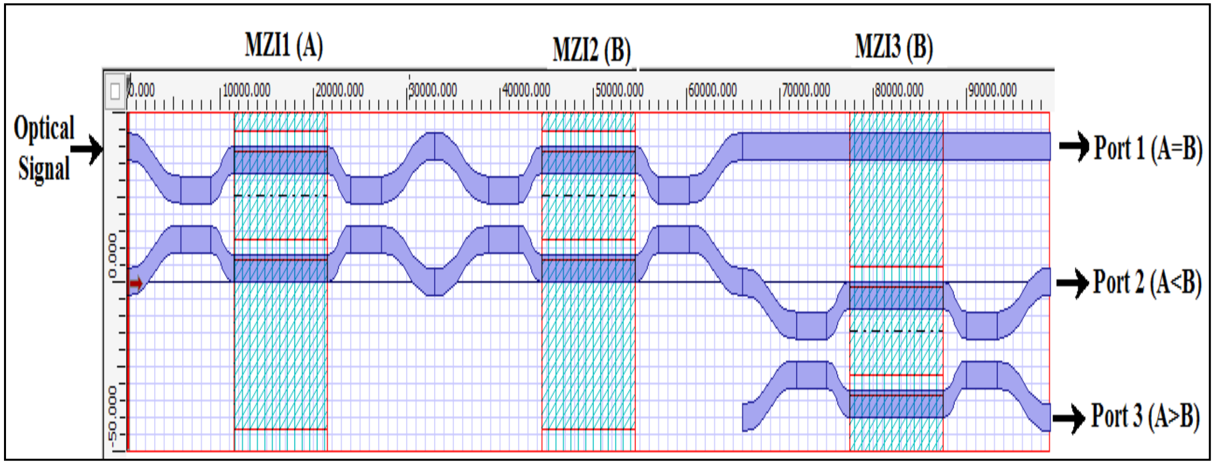

Figure: Layout of 1-bit comparator using the MZIs.

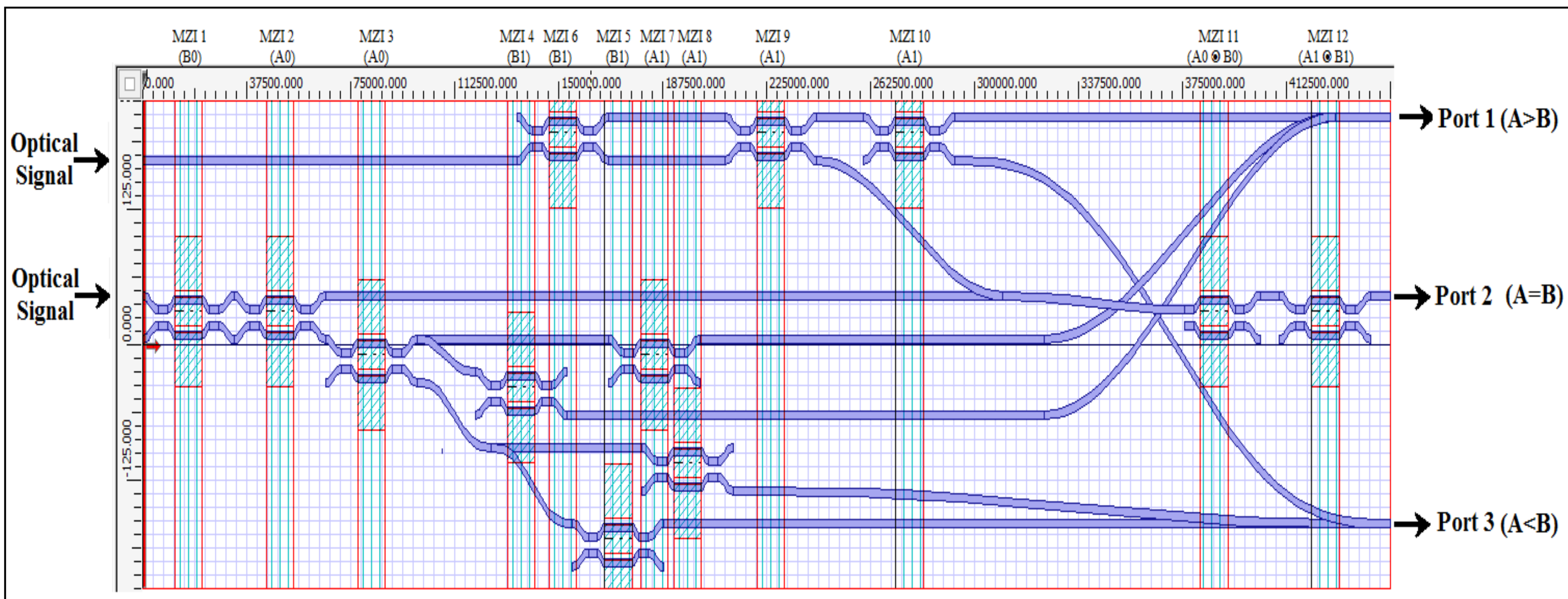

Dr. Santosh Kumar

Figure: Layout of 2-bit comparator using the MZIs.

Cont …

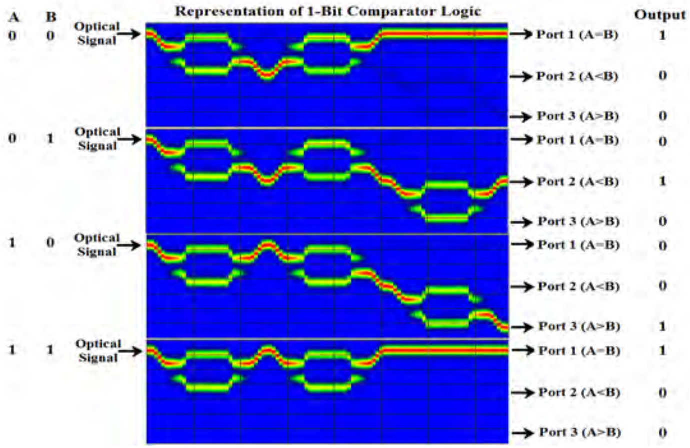

Fig.: Results of 1- bit comparator.

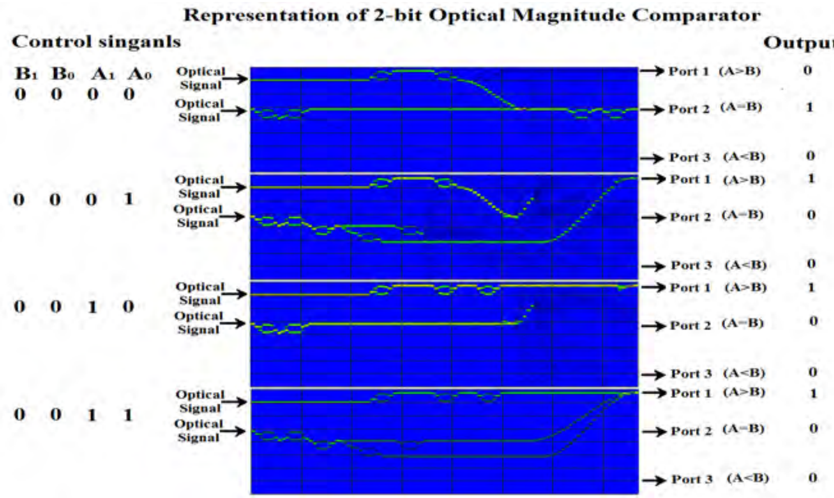

(a)

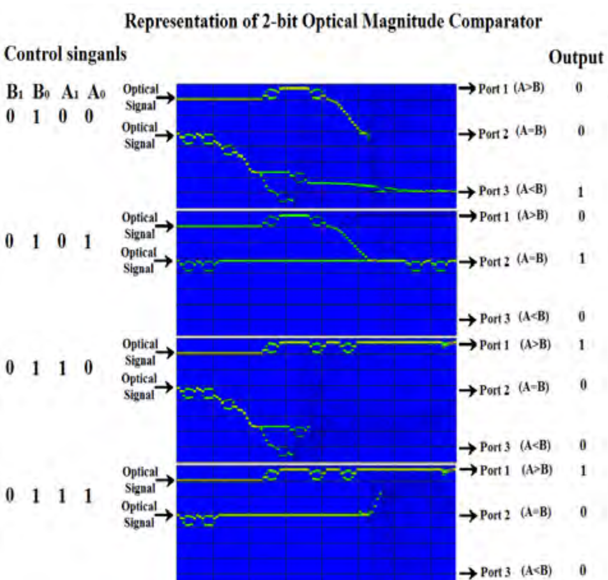

(b)

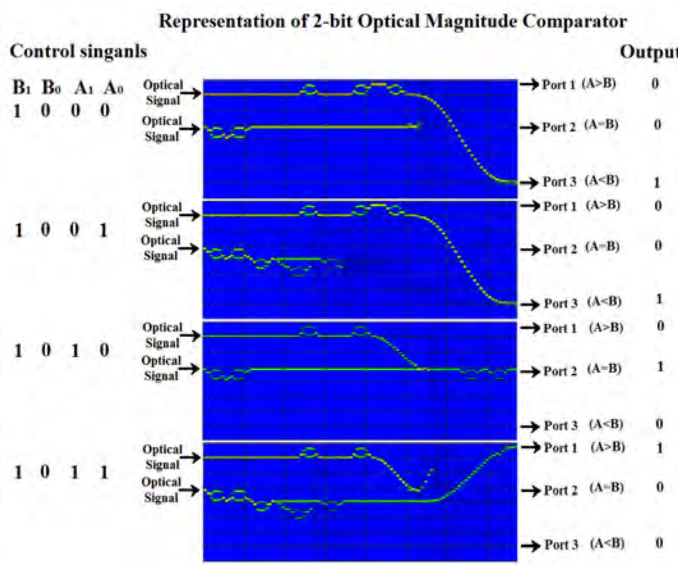

(c)

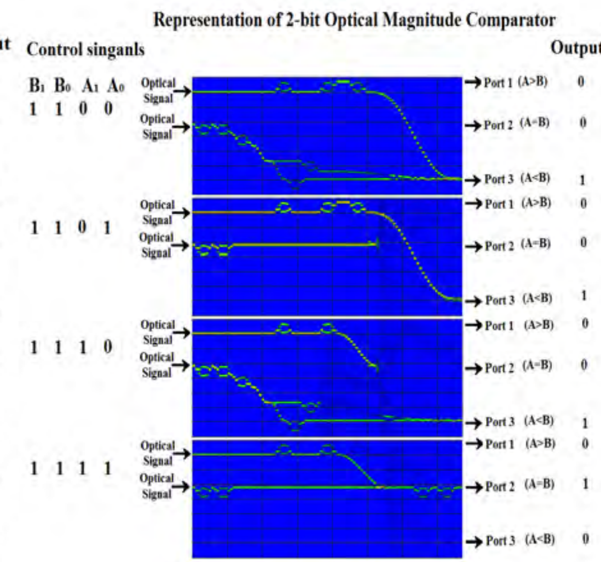

(d)

Figure: Results of the 2–bit magnitude comparator, when magnitude of B is (a) 0, (b) 1 (c) 2 and (d) 3 and magnitude of A changes from 0 to 3.

Design of Parity Generator and Checker Circuit

<u>Santosh Kumar</u> et. al., Optics Communications (Elsevier), Vol. 364, PP. 195–224 (Dec. 07, 2015).

Even Parity Generator

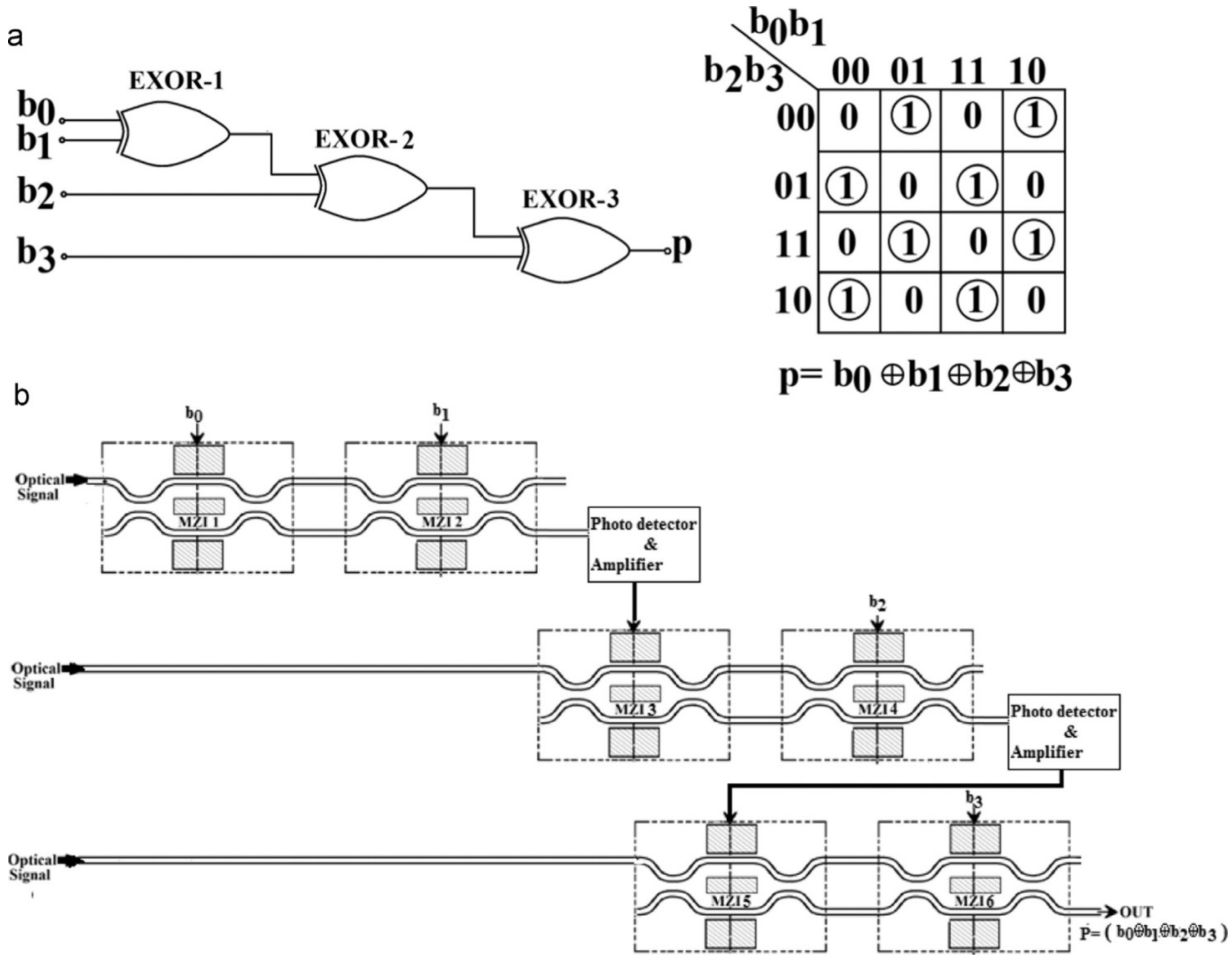

Figure: (a) Digital circuit and K-map of even parity generator. (b) Schematic diagram of even parity generator using MZIs

Mathematical Expression for Even Parity

For Even Parity:

$$p = \left[sin^2\left(\frac{\Delta\emptyset_1}{2}\right)cos^2\left(\frac{\Delta\emptyset_2}{2}\right) + cos^2\left(\frac{\Delta\emptyset_1}{2}\right)sin^2\left(\frac{\Delta\emptyset_2}{2}\right)\right]$$
$$+ \left[sin^2\left(\frac{\Delta\emptyset_3}{2}\right)cos^2\left(\frac{\Delta\emptyset_4}{2}\right) + cos^2\left(\frac{\Delta\emptyset_3}{2}\right)sin^2\left(\frac{\Delta\emptyset_4}{2}\right)\right]$$
$$+ \left[sin^2\left(\frac{\Delta\emptyset_5}{2}\right)cos^2\left(\frac{\Delta\emptyset_6}{2}\right) + cos^2\left(\frac{\Delta\emptyset_5}{2}\right)sin^2\left(\frac{\Delta\emptyset_6}{2}\right)\right]$$

MATLAB Results (Even Parity Generator)

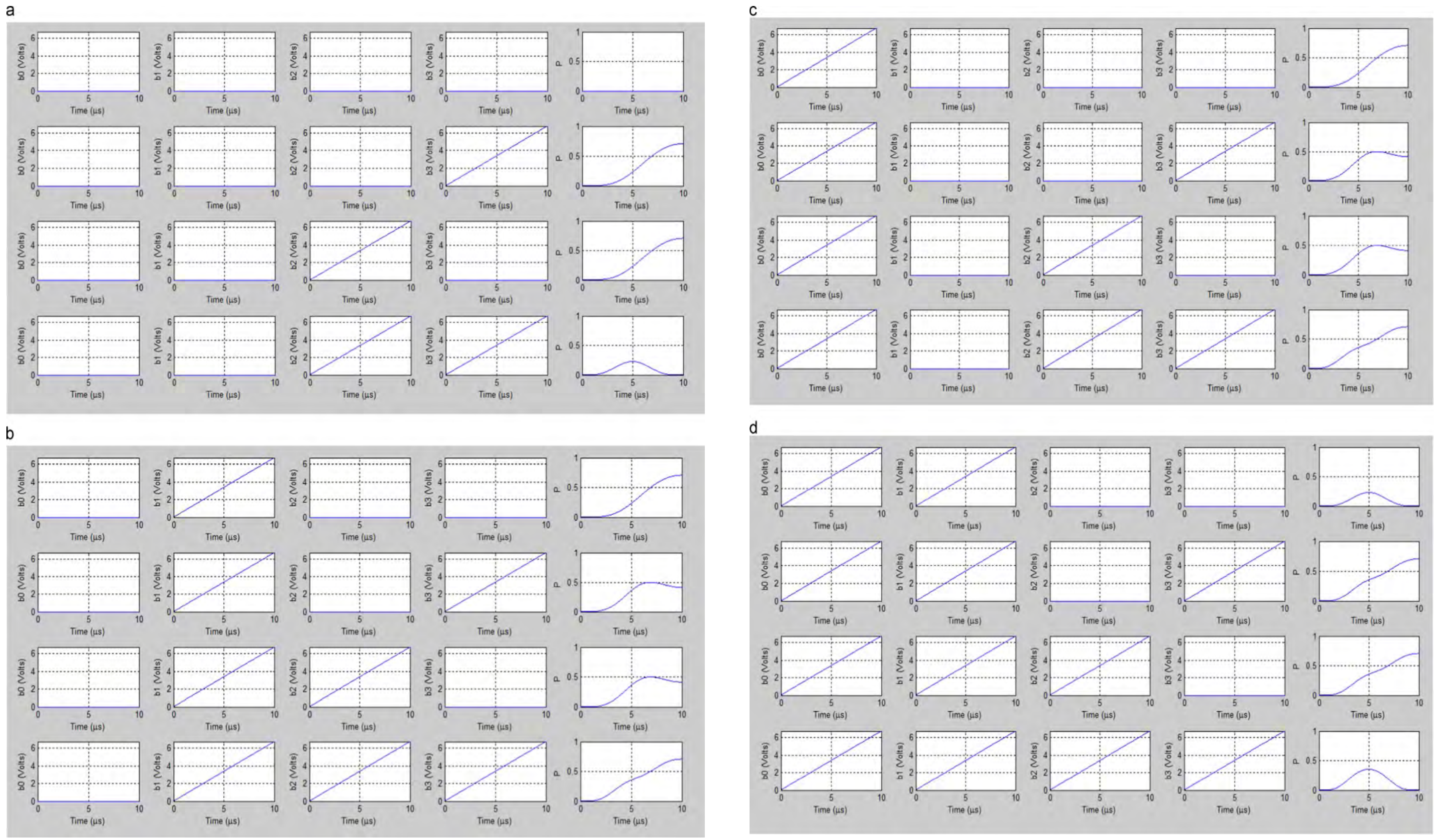

Figure: MATLAB simulation result of Even Parity generator where $B_3\ B_2\ B_1\ B_0$ varies from 0000 to 1111

BPM Layout of Even Parity Generator

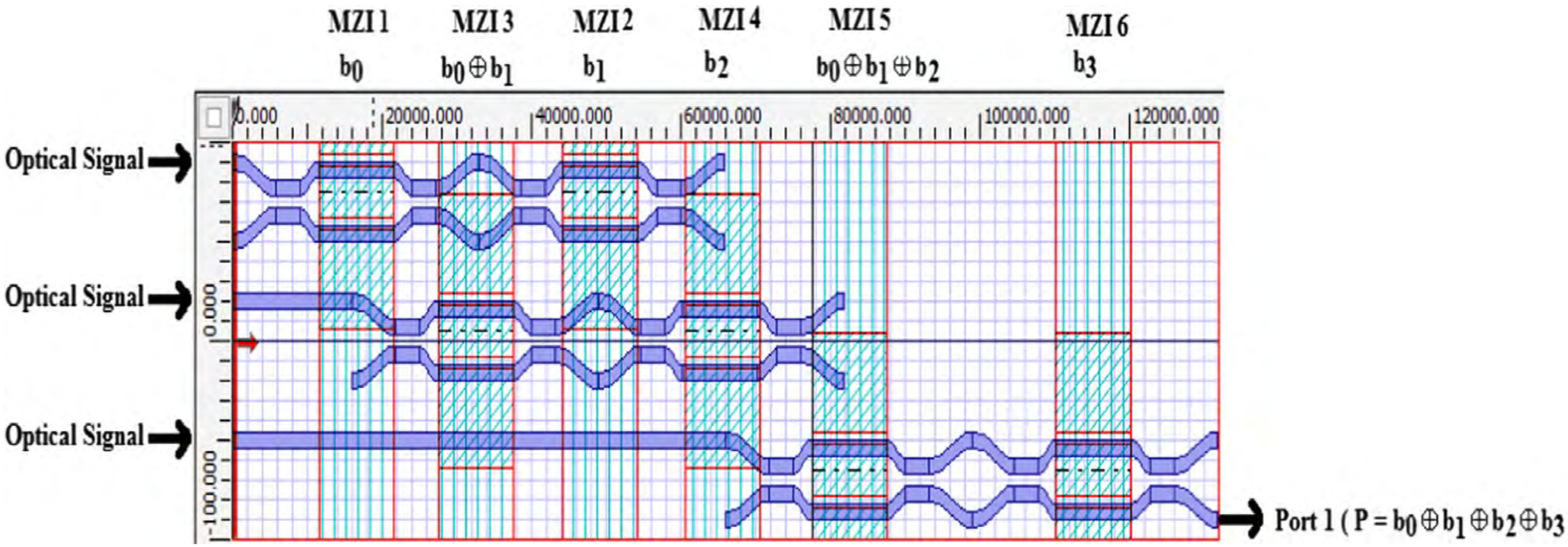

Figure: BPM layout of even parity generator.

Simulation Result from BPM (Even Parity Generator)

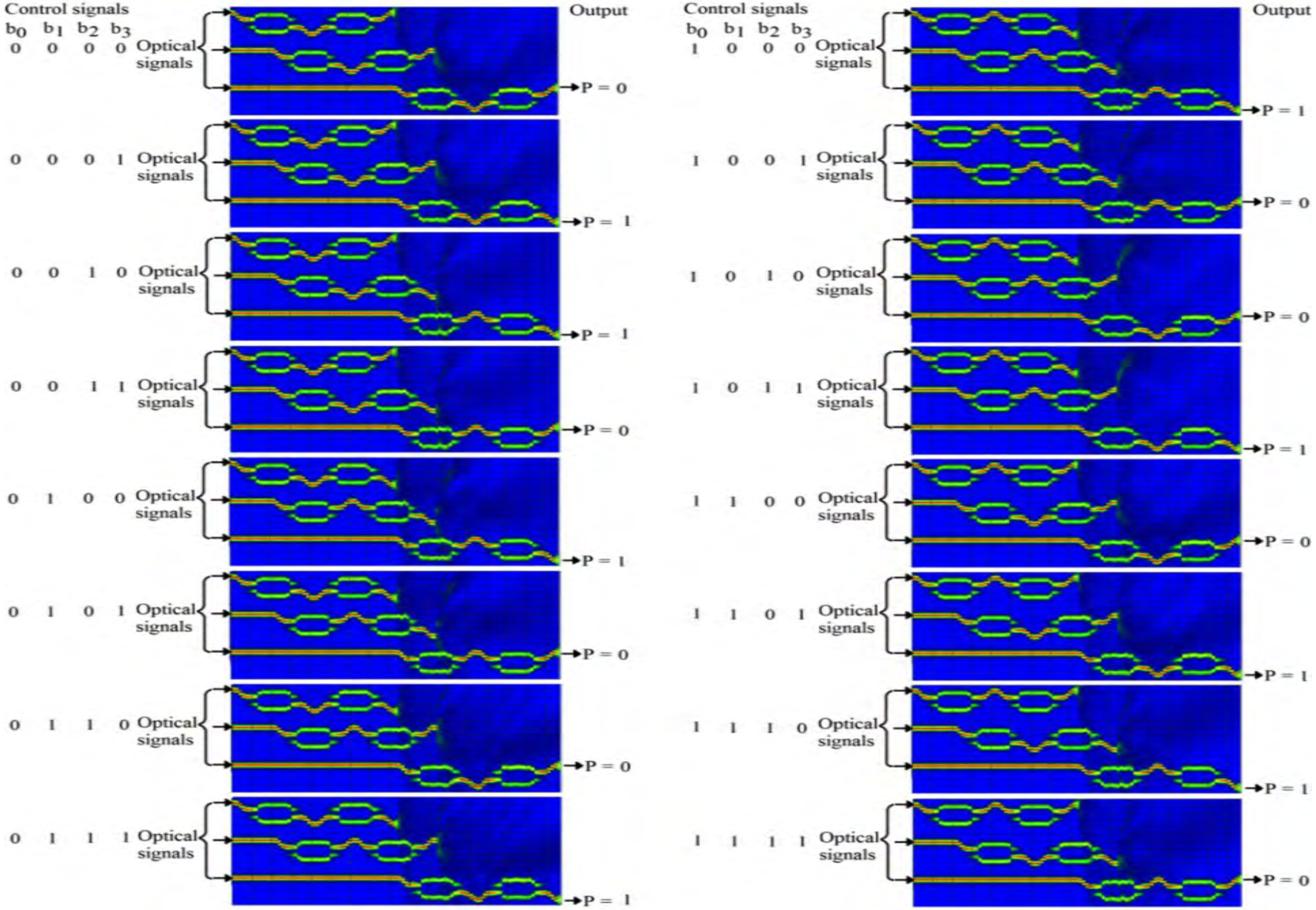

Figure: BPM result to even parity generator where b_0 b_1 b_2 b_3 varies from 0000 to1111 .

Odd Parity Generator

a

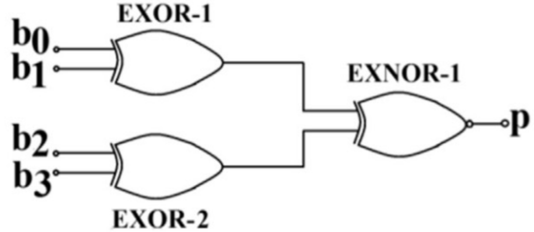

$b_2b_3 \backslash b_0b_1$	00	01	11	10
00	1	0	1	0
01	0	1	0	1
11	1	0	1	0
10	0	1	0	1

$$p = (b_0 \oplus b_1) \odot (b_2 \oplus b_3)$$

b

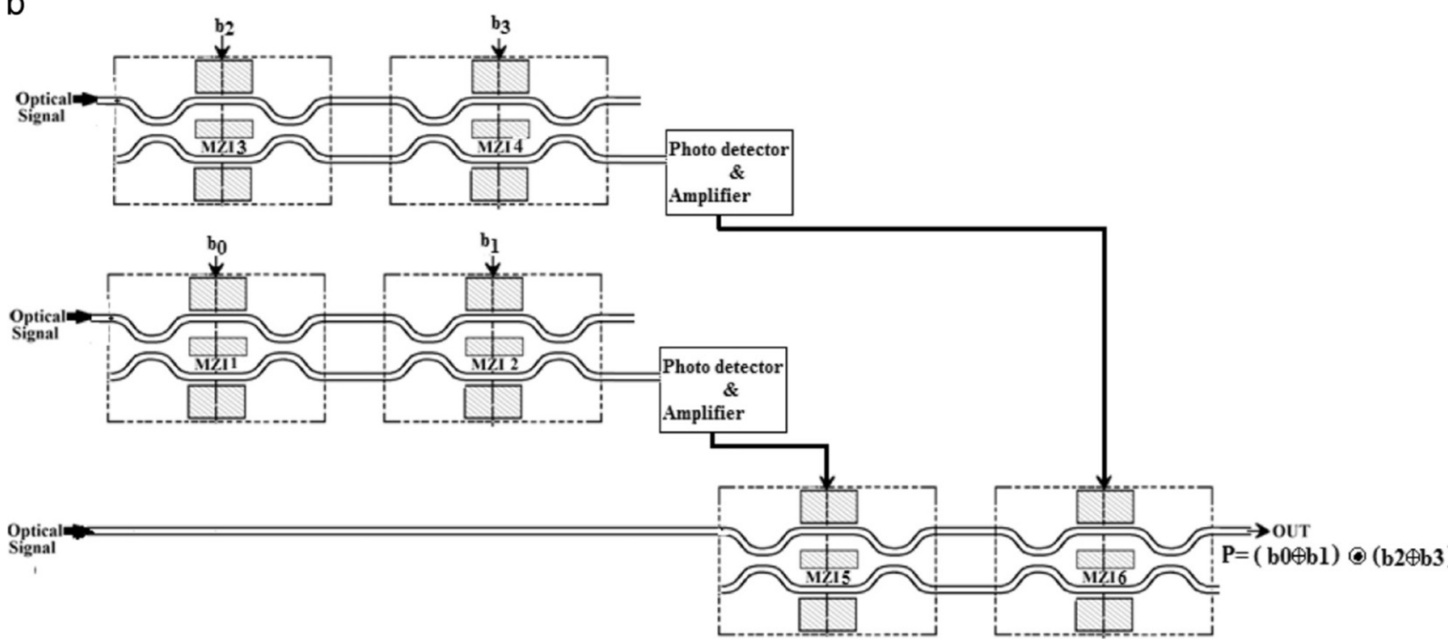

Figure: (a) Digital circuit and K-map of odd parity generator. (b) Schematic diagram of odd parity generator using MZIs.

Mathematical Expression for Odd Parity Generator

For Odd Parity:

$$p = \left[sin^2\left(\frac{\Delta\emptyset_1}{2}\right)cos^2\left(\frac{\Delta\emptyset_2}{2}\right) + cos^2\left(\frac{\Delta\emptyset_1}{2}\right)sin^2\left(\frac{\Delta\emptyset_2}{2}\right)\right]$$
$$+\left[sin^2\left(\frac{\Delta\emptyset_3}{2}\right)cos^2\left(\frac{\Delta\emptyset_4}{2}\right) + cos^2\left(\frac{\Delta\emptyset_3}{2}\right)sin^2\left(\frac{\Delta\emptyset_4}{2}\right)\right]$$
$$+\left[sin^2\left(\frac{\Delta\emptyset_5}{2}\right)sin^2\left(\frac{\Delta\emptyset_6}{2}\right) + cos^2\left(\frac{\Delta\emptyset_5}{2}\right)cos^2\left(\frac{\Delta\emptyset_6}{2}\right)\right]$$

MATLAB Results (Odd Parity Generator)

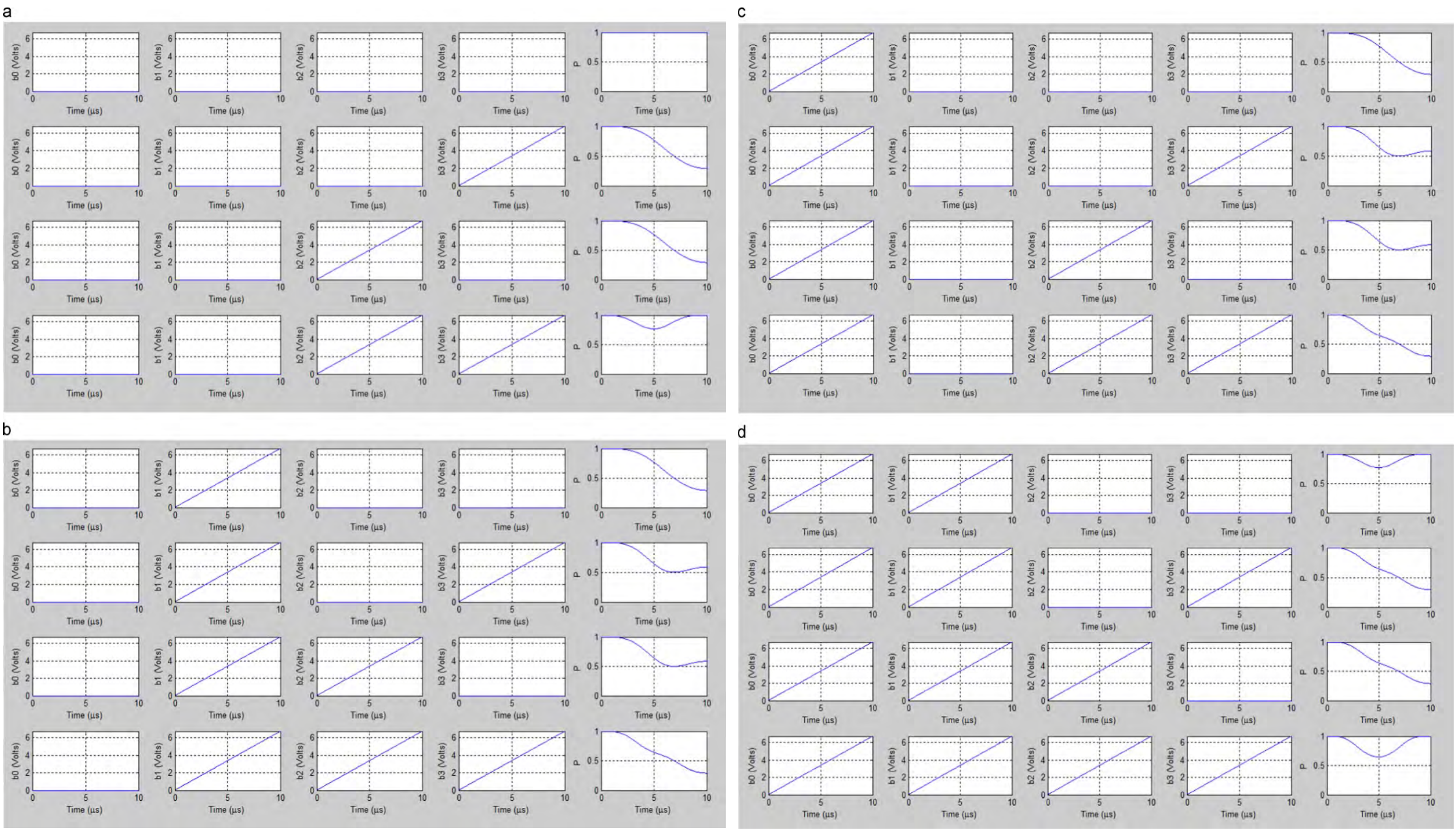

Figure: MATLAB simulation result of odd Parity generator where B_3 B_2 B_1 B_0 varies from 0000 to 1111

BPM Layout of Odd Parity Generator

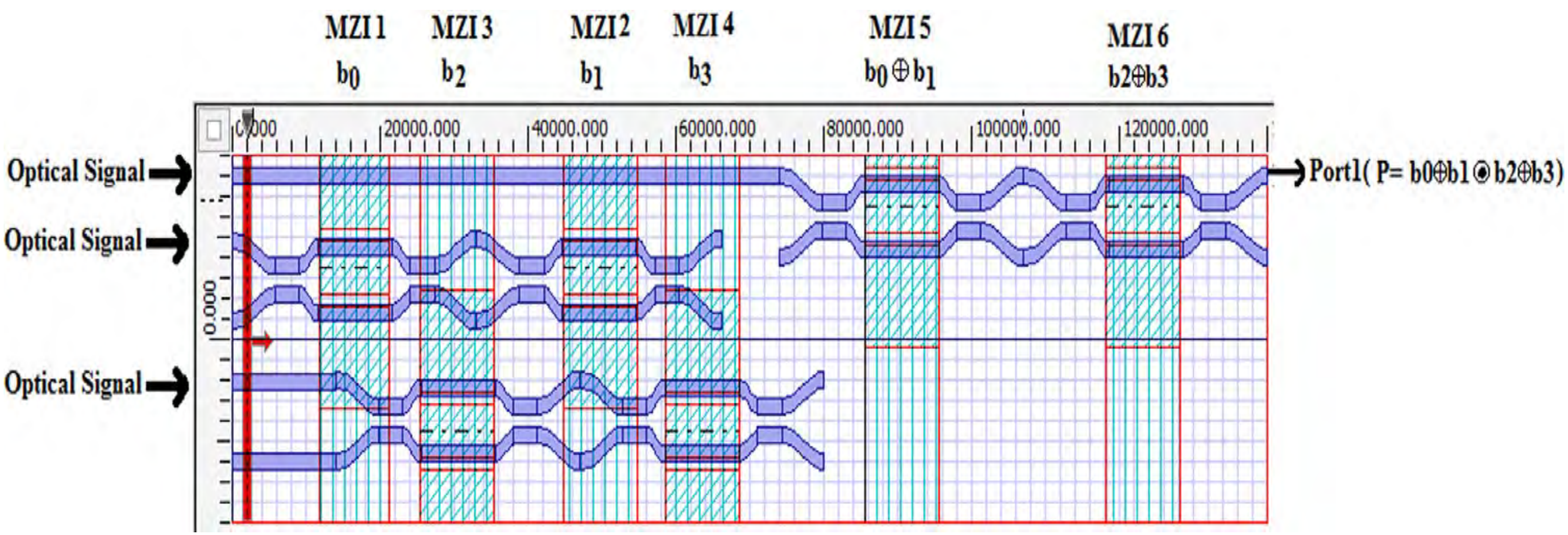

Figure: BPM layout of odd parity generator.

Simulation Result from BPM (Odd Parity Generator)

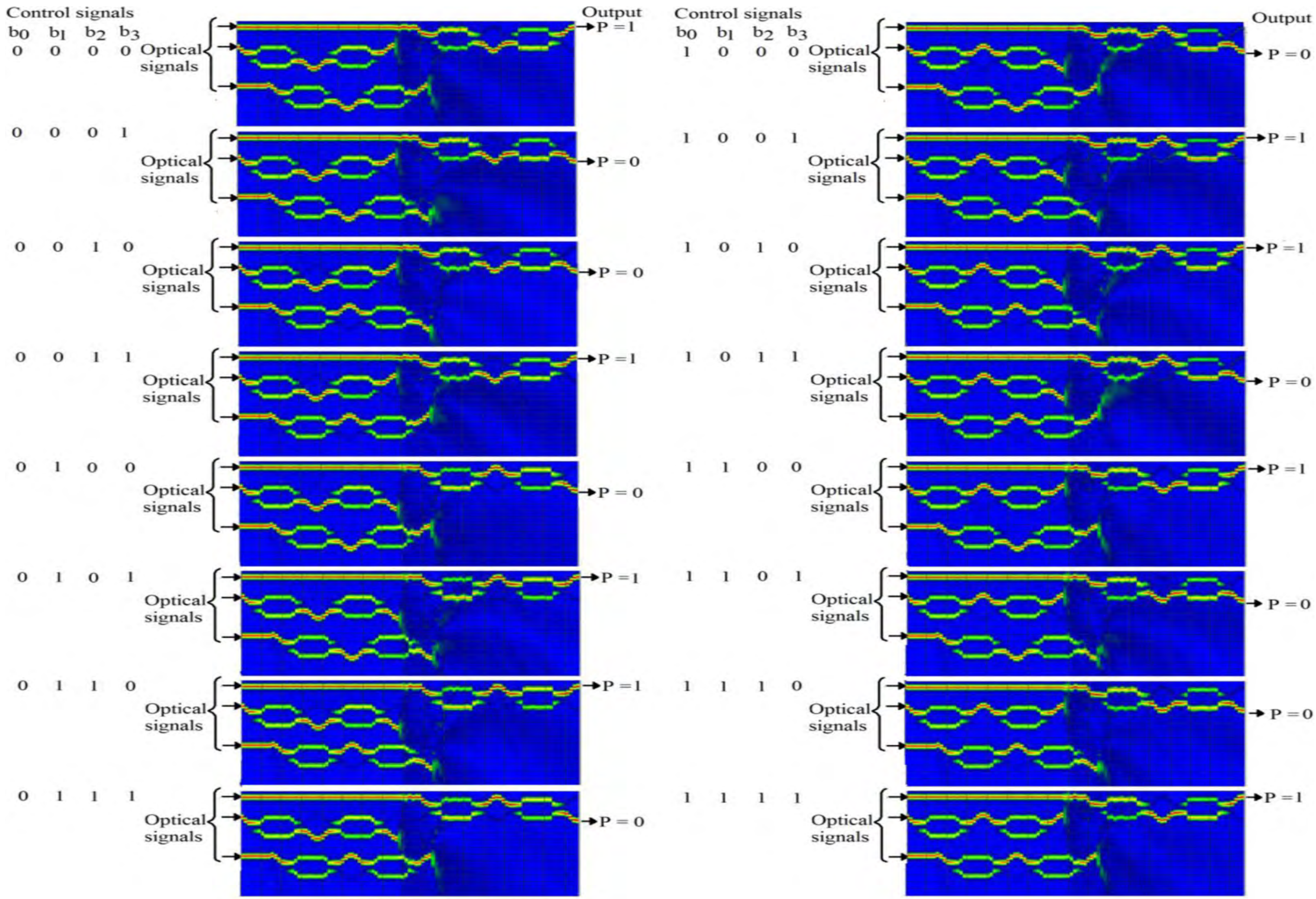

Figure: BPM result to even parity generator where b_0 b_1 b_2 b_3 varies from 0000 to1111 .

Even Parity Checker

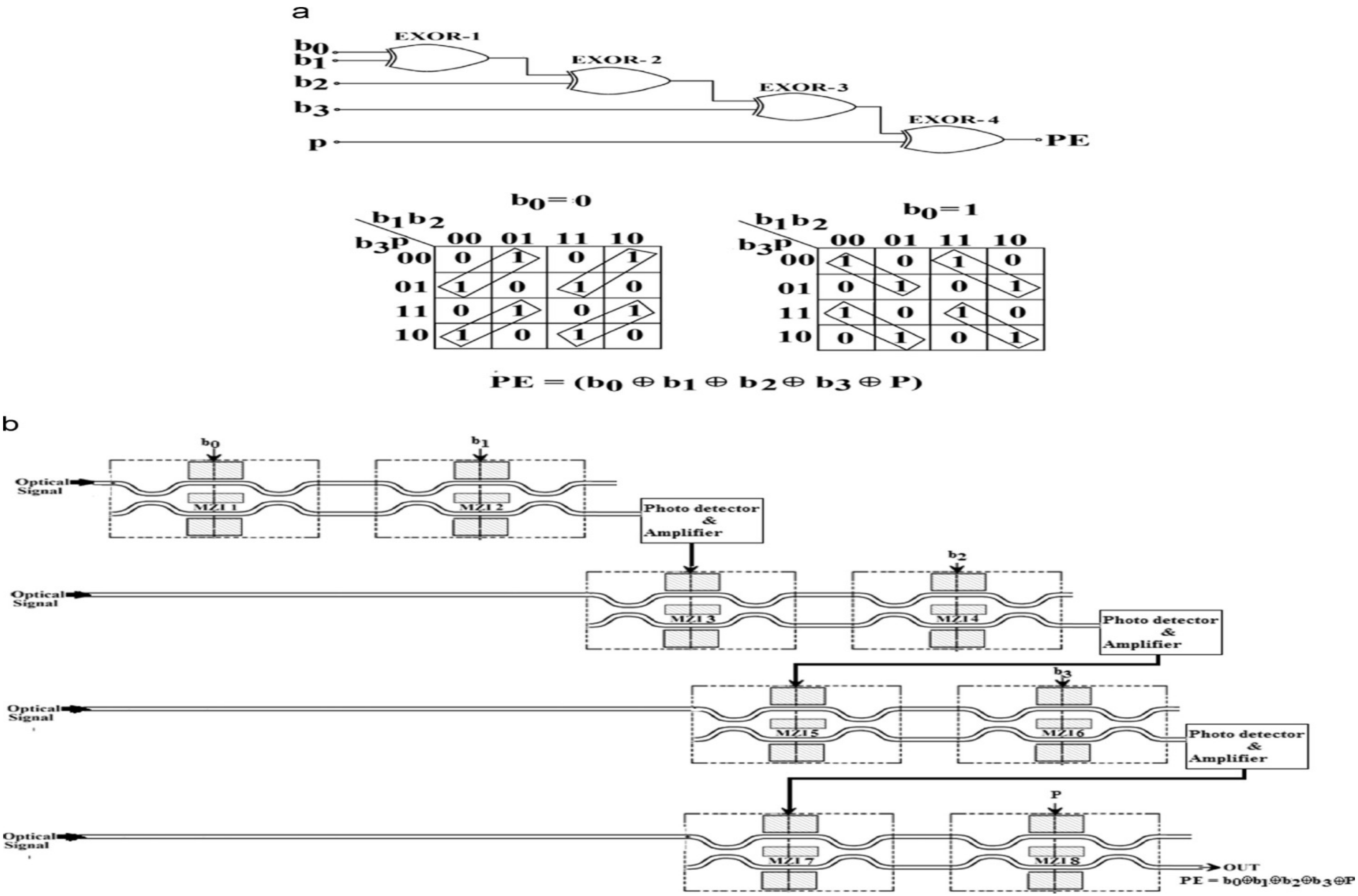

Figure: (a) Digital circuit and K-map of even parity checker (b) Schematic diagram of even parity checker using MZIs

Mathematical Expression for Even Parity Checker

For Even Parity:

$$p = \left[sin^2\left(\frac{\Delta\emptyset_1}{2}\right)cos^2\left(\frac{\Delta\emptyset_2}{2}\right) + cos^2\left(\frac{\Delta\emptyset_1}{2}\right)sin^2\left(\frac{\Delta\emptyset_2}{2}\right)\right]$$
$$+ \left[sin^2\left(\frac{\Delta\emptyset_3}{2}\right)cos^2\left(\frac{\Delta\emptyset_4}{2}\right) + cos^2\left(\frac{\Delta\emptyset_3}{2}\right)sin^2\left(\frac{\Delta\emptyset_4}{2}\right)\right]$$
$$+ \left[sin^2\left(\frac{\Delta\emptyset_5}{2}\right)sin^2\left(\frac{\Delta\emptyset_6}{2}\right) + cos^2\left(\frac{\Delta\emptyset_5}{2}\right)cos^2\left(\frac{\Delta\emptyset_6}{2}\right)\right]$$
$$+ \left[sin^2\left(\frac{\Delta\emptyset_7}{2}\right)cos^2\left(\frac{\Delta\emptyset_8}{2}\right) + cos^2\left(\frac{\Delta\emptyset_7}{2}\right)sin^2\left(\frac{\Delta\emptyset_8}{2}\right)\right]$$

MATLAB Results (Even Parity Checker)

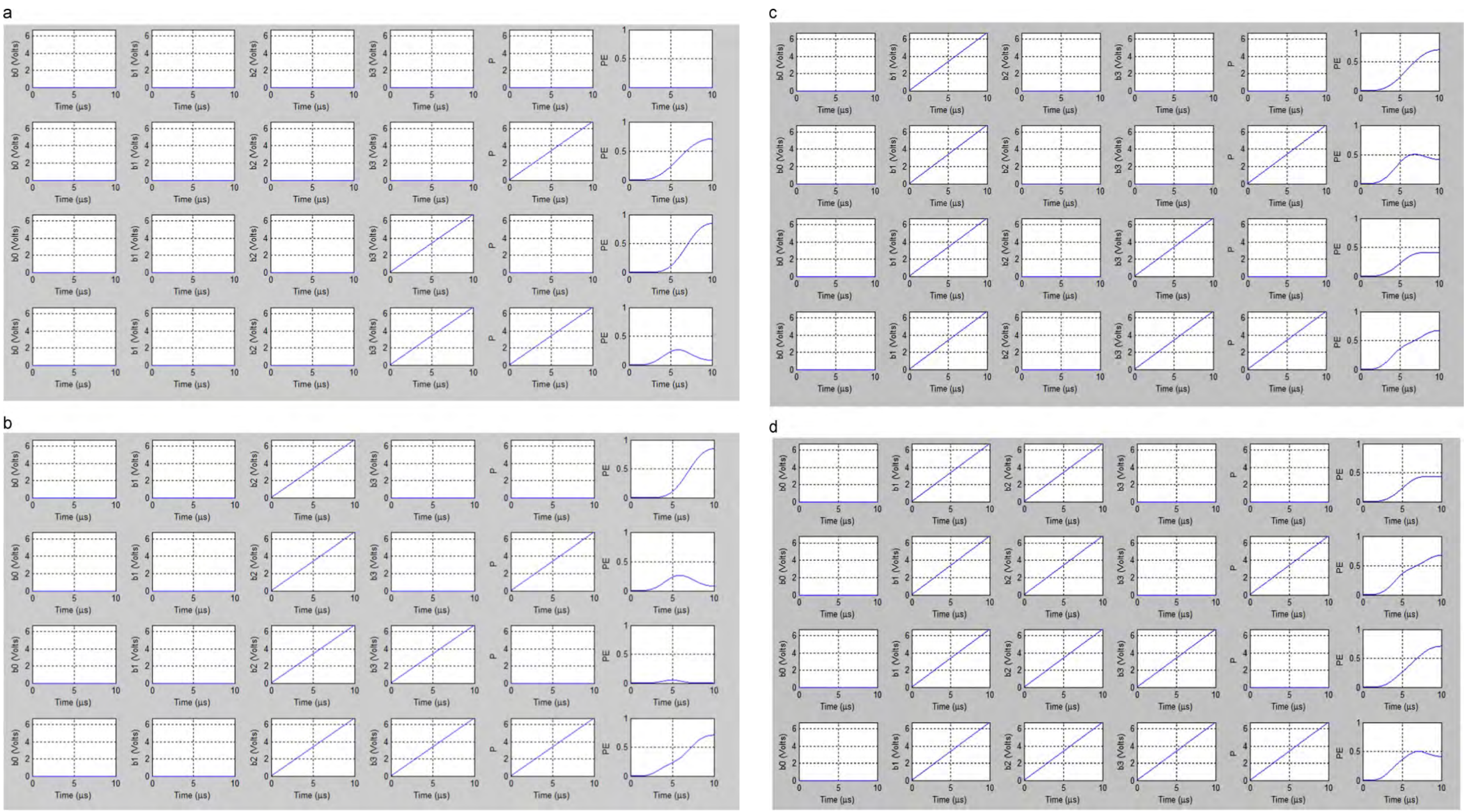

Figure: MATLAB simulation result of Even Parity Checker where B_3 B_2 B_1 B_0 P varies from 00000 to 01111

Contd..

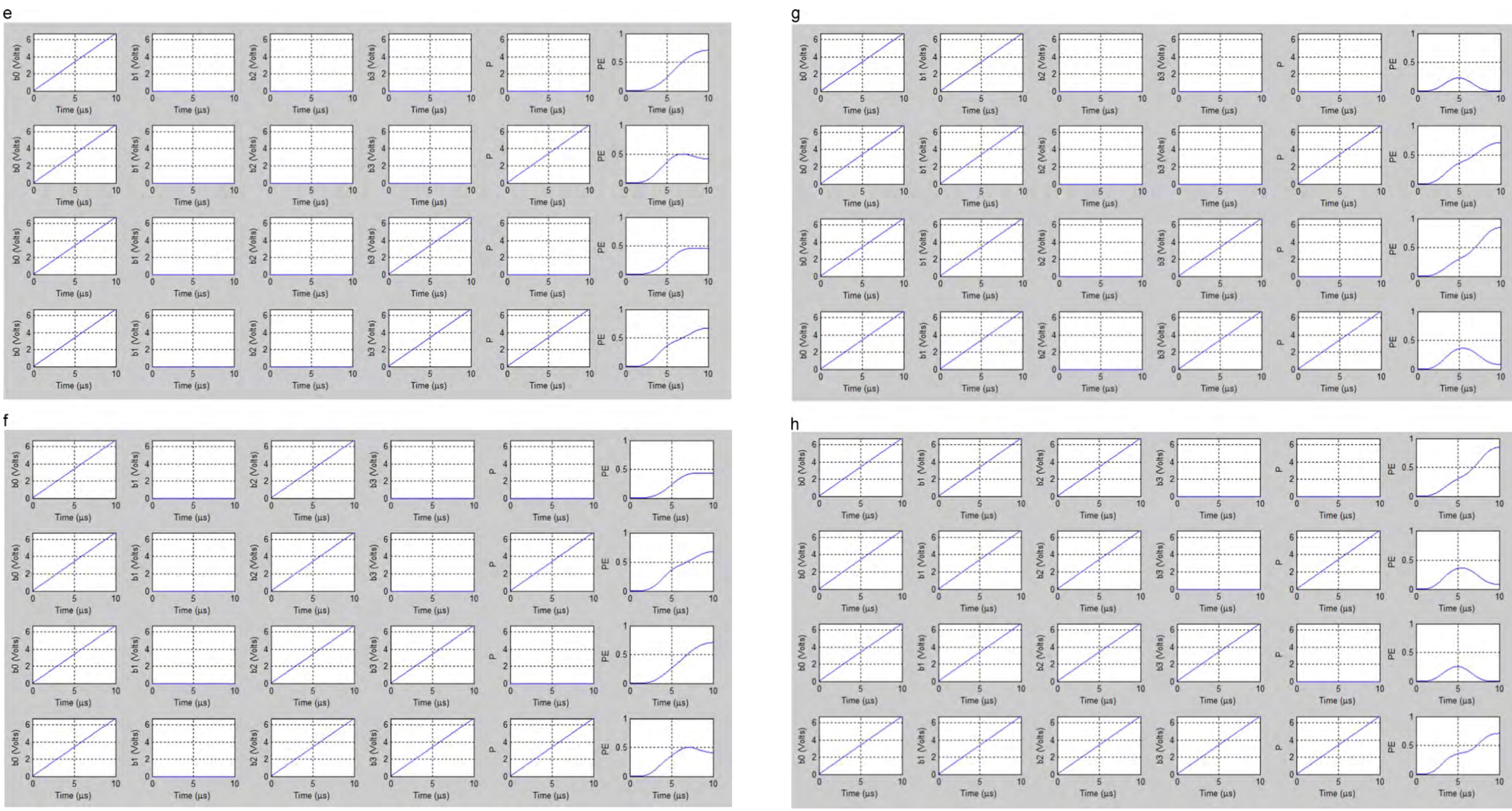

Figure: MATLAB simulation result of Even Parity Checker where B_3 B_2 B_1 B_0 P varies from 10000 to 11111

BPM Layout of Even Parity Checker

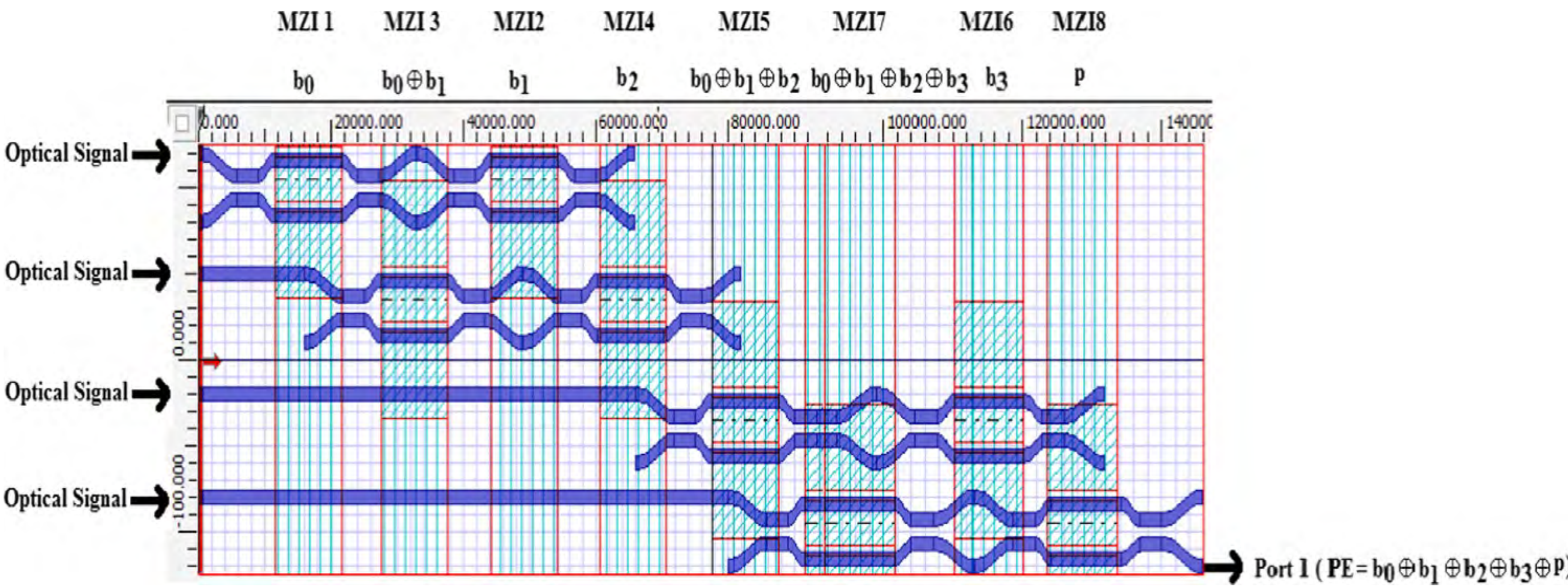

Figure: BPM layout of even parity checker.

Simulation Result from BPM (Even Parity Checker)

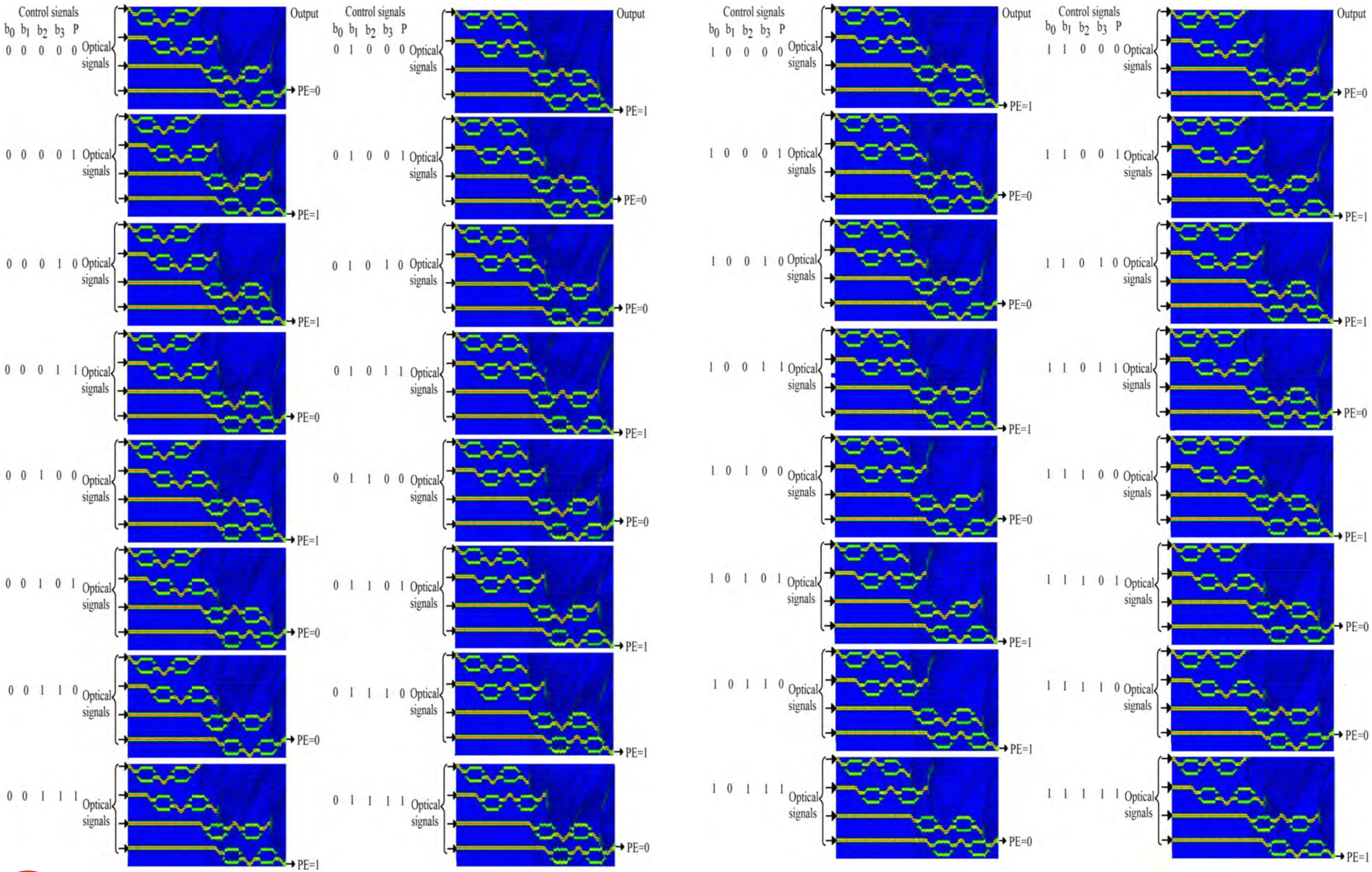

Figure: BPM result to even parity checker where b_0 b_1 b_2 b_3 P varies from 00000 to11111

Odd Parity Checker

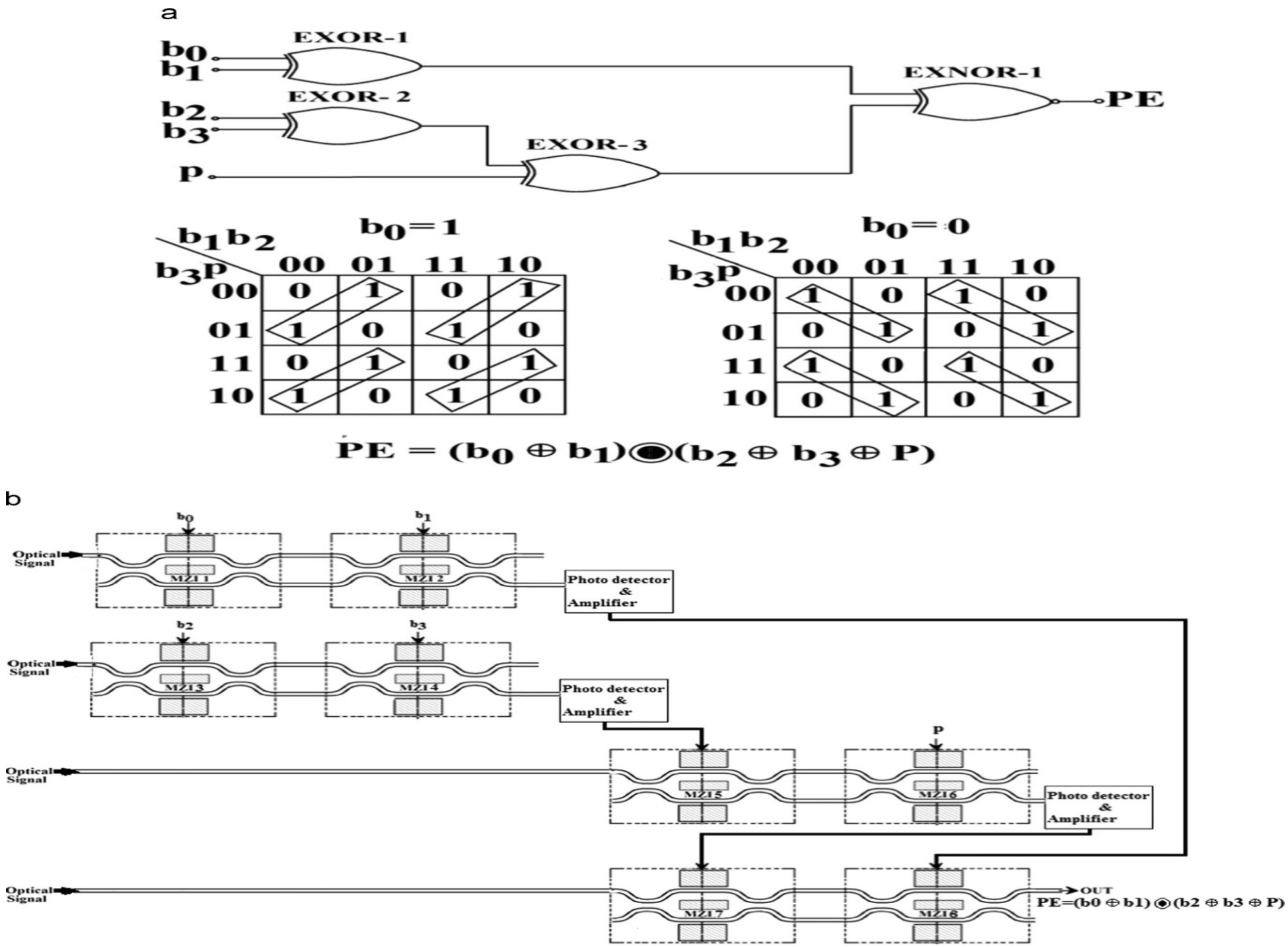

Figure: (a) Digital circuit and K-map of odd parity checker (b) Schematic diagram of odd parity checker using MZIs

Mathematical Expression for Odd parity Checker

For Odd Parity:

$$p = \left[sin^2\left(\frac{\Delta\emptyset_1}{2}\right)cos^2\left(\frac{\Delta\emptyset_2}{2}\right) + cos^2\left(\frac{\Delta\emptyset_1}{2}\right)sin^2\left(\frac{\Delta\emptyset_2}{2}\right)\right]$$

$$+\left[sin^2\left(\frac{\Delta\emptyset_3}{2}\right)cos^2\left(\frac{\Delta\emptyset_4}{2}\right) + cos^2\left(\frac{\Delta\emptyset_3}{2}\right)sin^2\left(\frac{\Delta\emptyset_4}{2}\right)\right]$$

$$+\left[sin^2\left(\frac{\Delta\emptyset_5}{2}\right)cos^2\left(\frac{\Delta\emptyset_6}{2}\right) + cos^2\left(\frac{\Delta\emptyset_5}{2}\right)sin^2\left(\frac{\Delta\emptyset_6}{2}\right)\right]$$

$$+\left[sin^2\left(\frac{\Delta\emptyset_7}{2}\right)sin^2\left(\frac{\Delta\emptyset_8}{2}\right) + cos^2\left(\frac{\Delta\emptyset_7}{2}\right)cos^2\left(\frac{\Delta\emptyset_8}{2}\right)\right]$$

MATLAB Results (Odd Parity Checker)

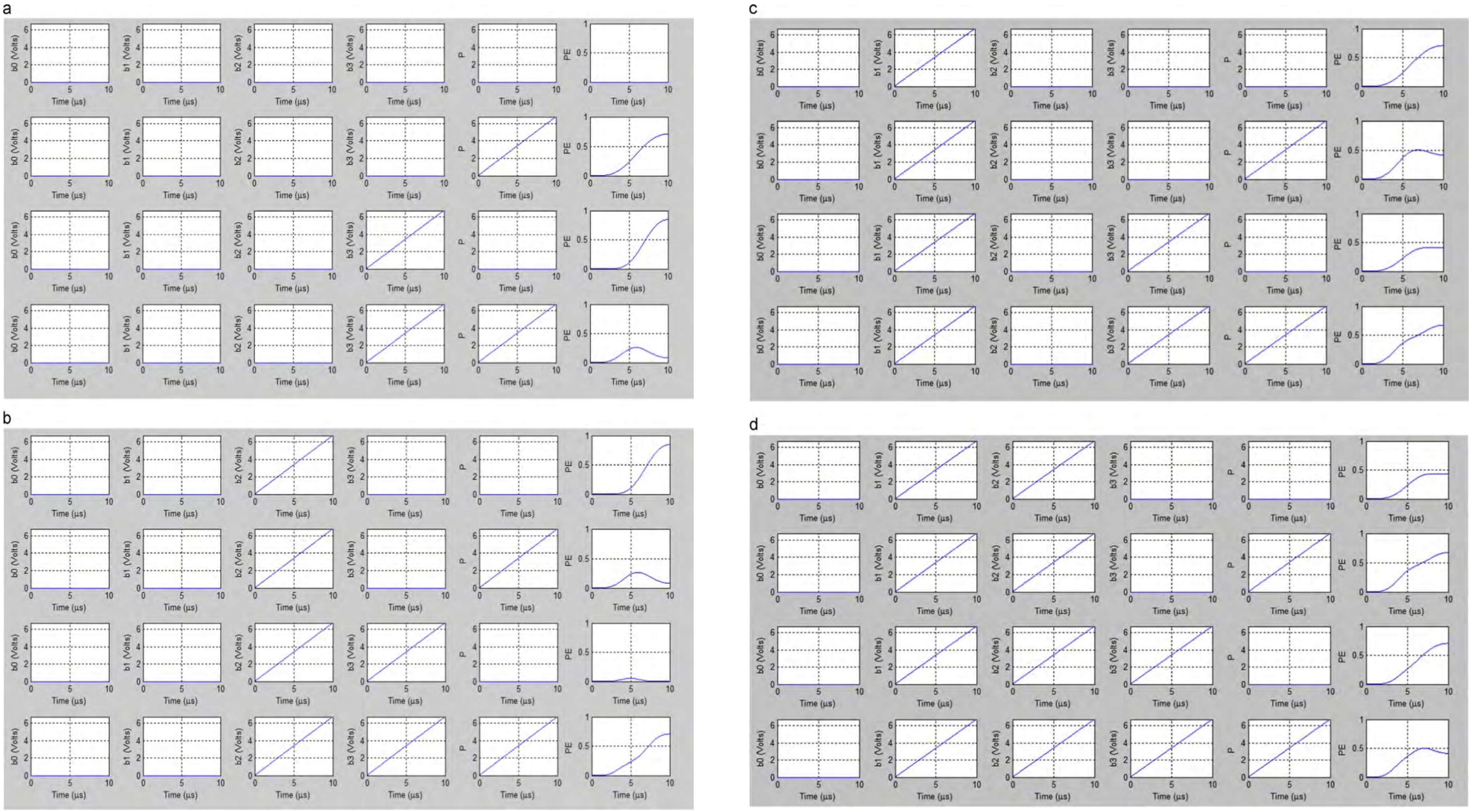

Figure: MATLAB simulation result of Odd Parity Checker where B_3 B_2 B_1 B_0 P varies from 00000 to 01111

Contd..

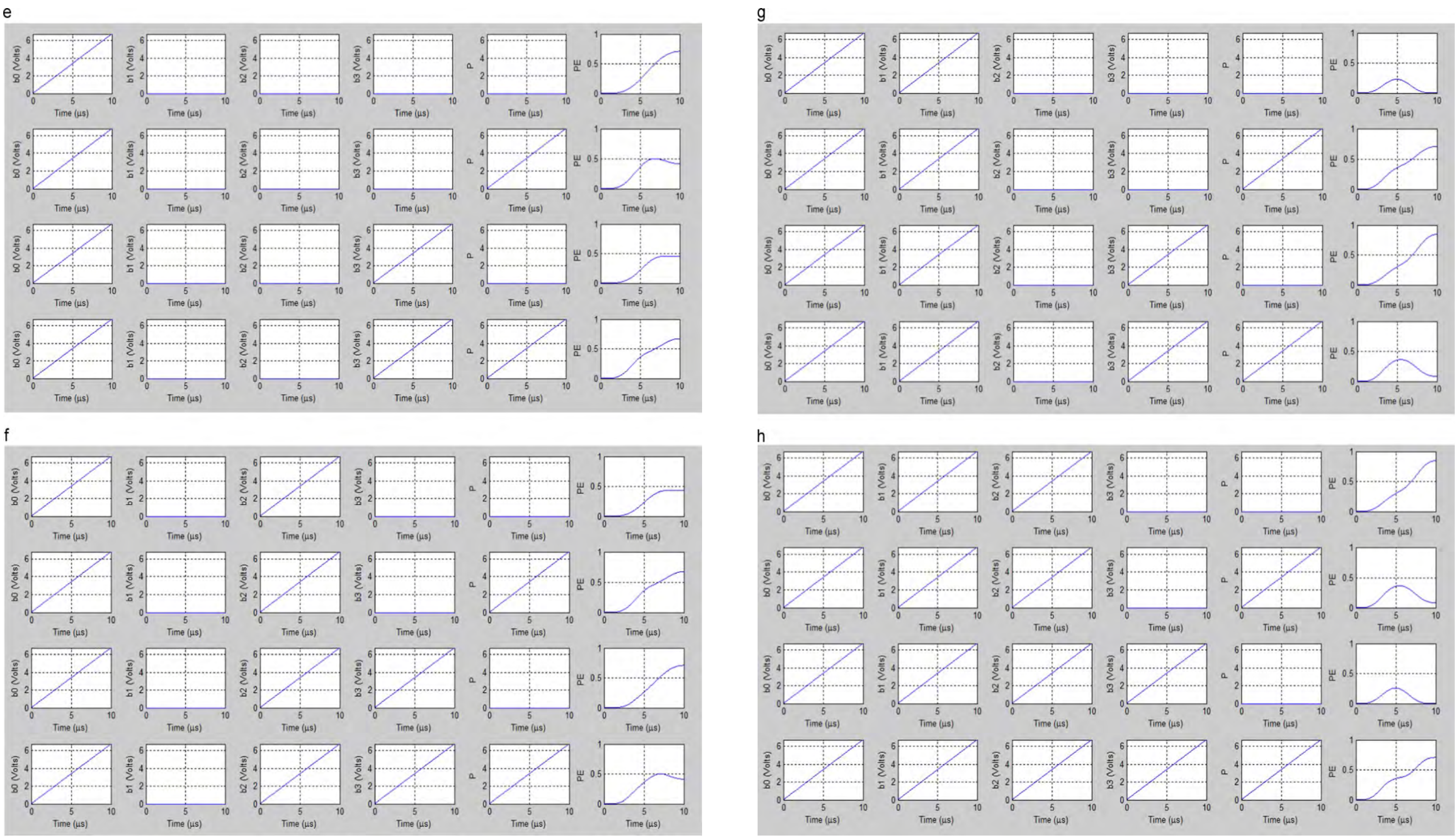

Figure: MATLAB simulation result of Odd Parity Checker where B_3 B_2 B_1 B_0 P varies from 10000 to 11111

BPM Layout of Odd Parity Checker

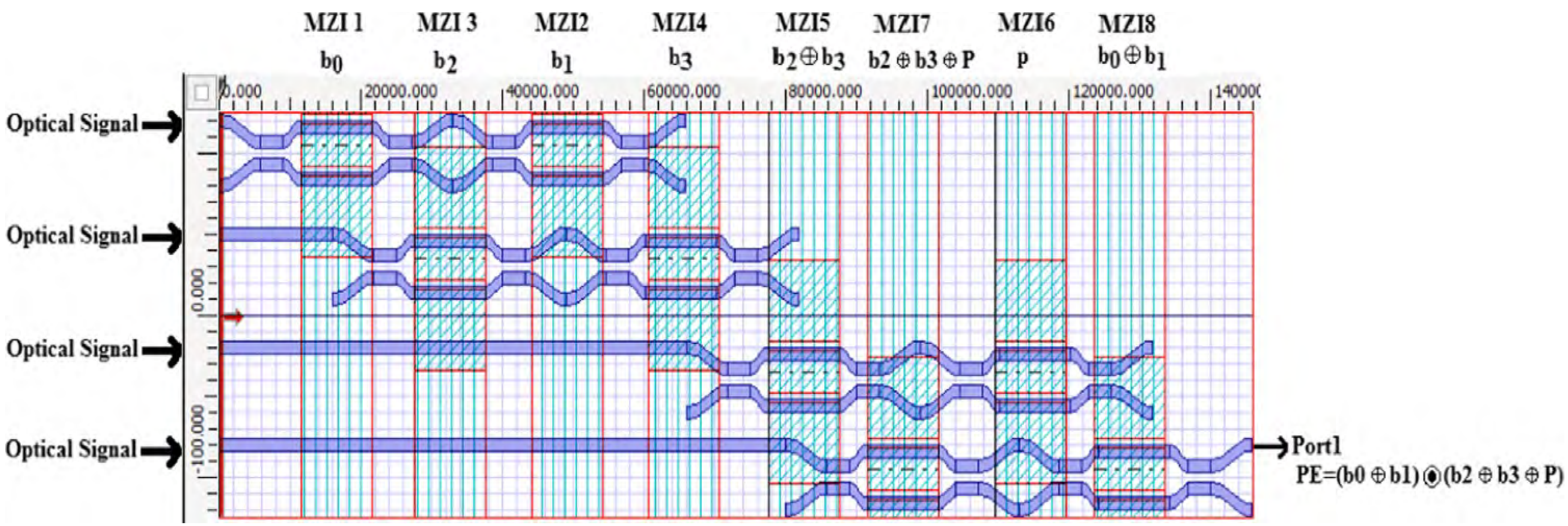

Figure: BPM layout of odd parity checker.

Simulation Result from BPM (Odd Parity Checker)

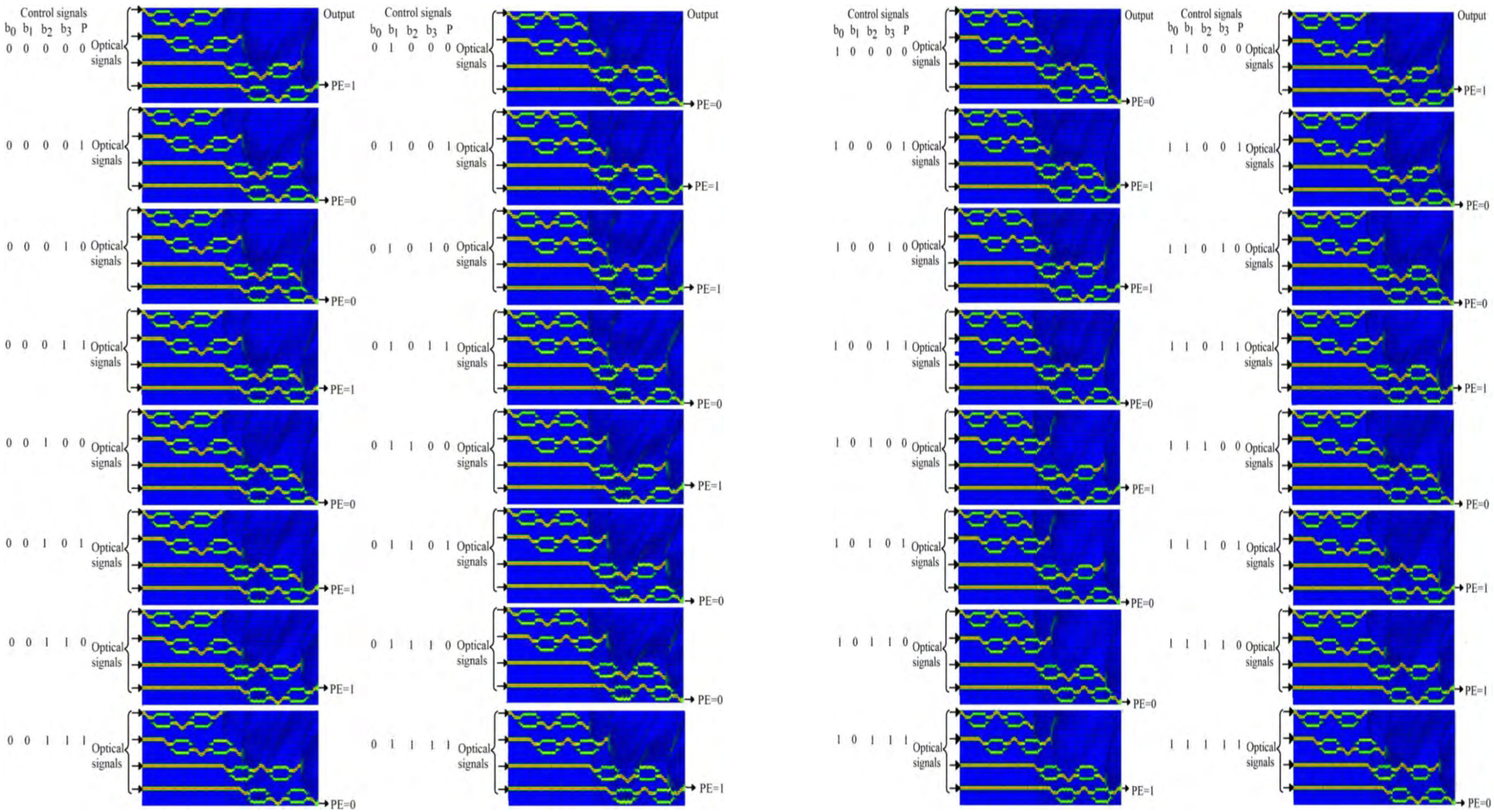

Figure: MATLAB simulation result of Odd Parity Checker where B_3 B_2 B_1 B_0 P varies from 10000 to 11111

Design of BCD to Excess-3 code converter

<u>Santosh Kumar</u> et. al., Frontier in Optics/Laser sources (FiO/LS-2016), paper JW4A.33, Rochester, New York, United States, 17-21 October 2016.

BCD to Excess-3 code converter

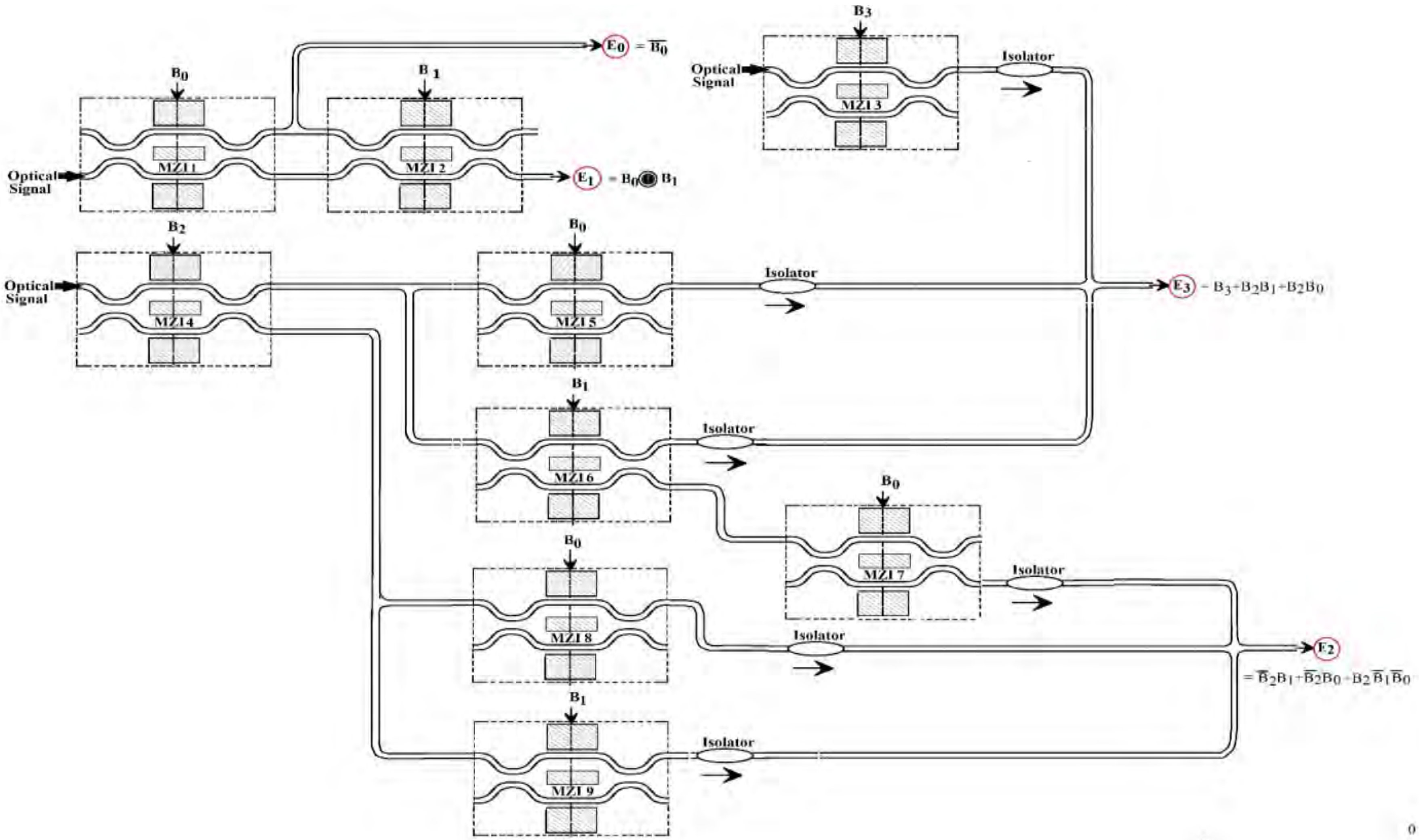

Figure: Schematic diagram of BCD to excess 3 code converter

MATLAB Results for BCD to Excess 3 code converter

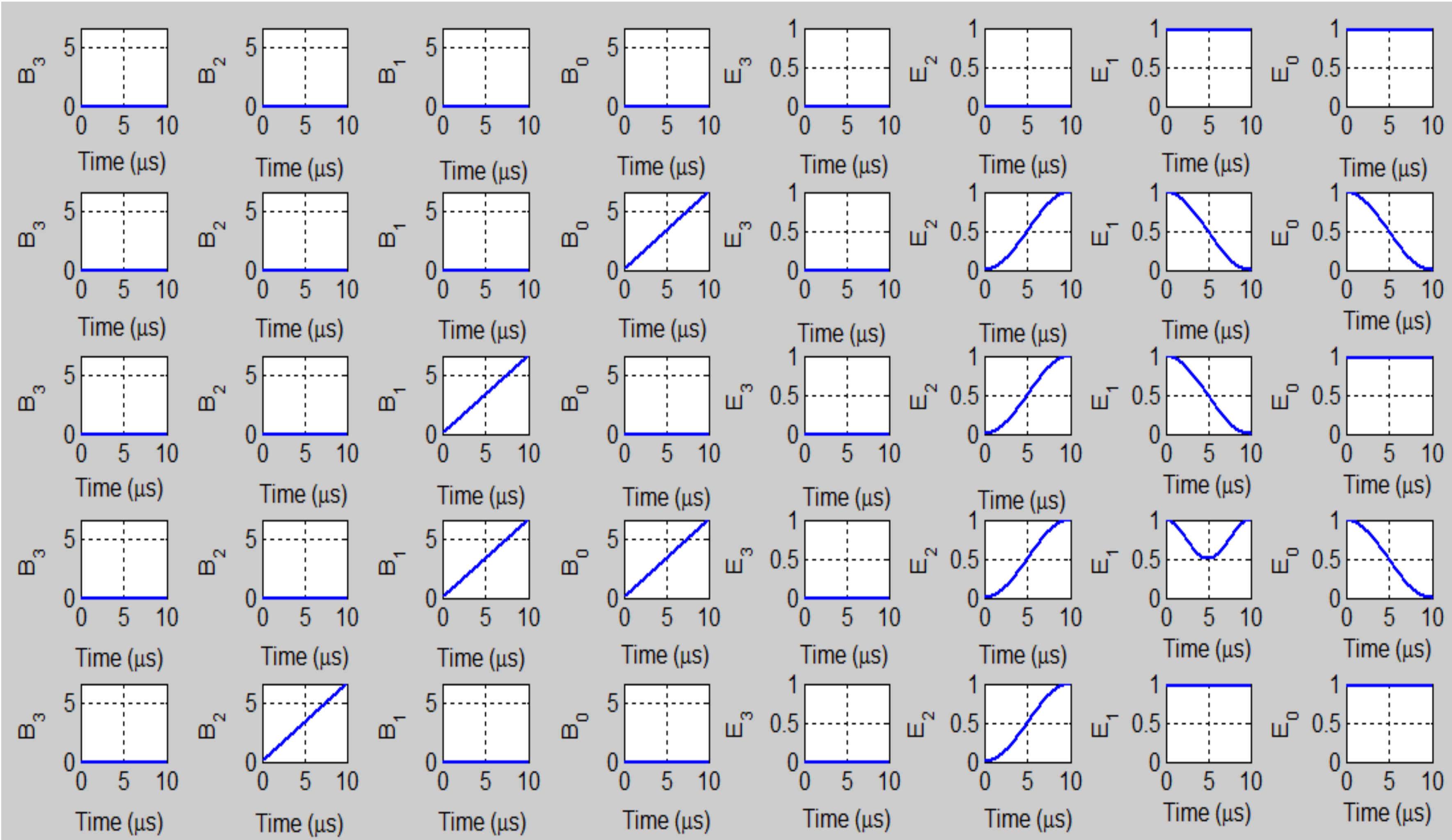

Figure: MATLAB simulation result of BCD to Excess-3 code converter where B_3 B_2 B_1 B_0 varies from 0000 to 0100

BPM Simulation Result

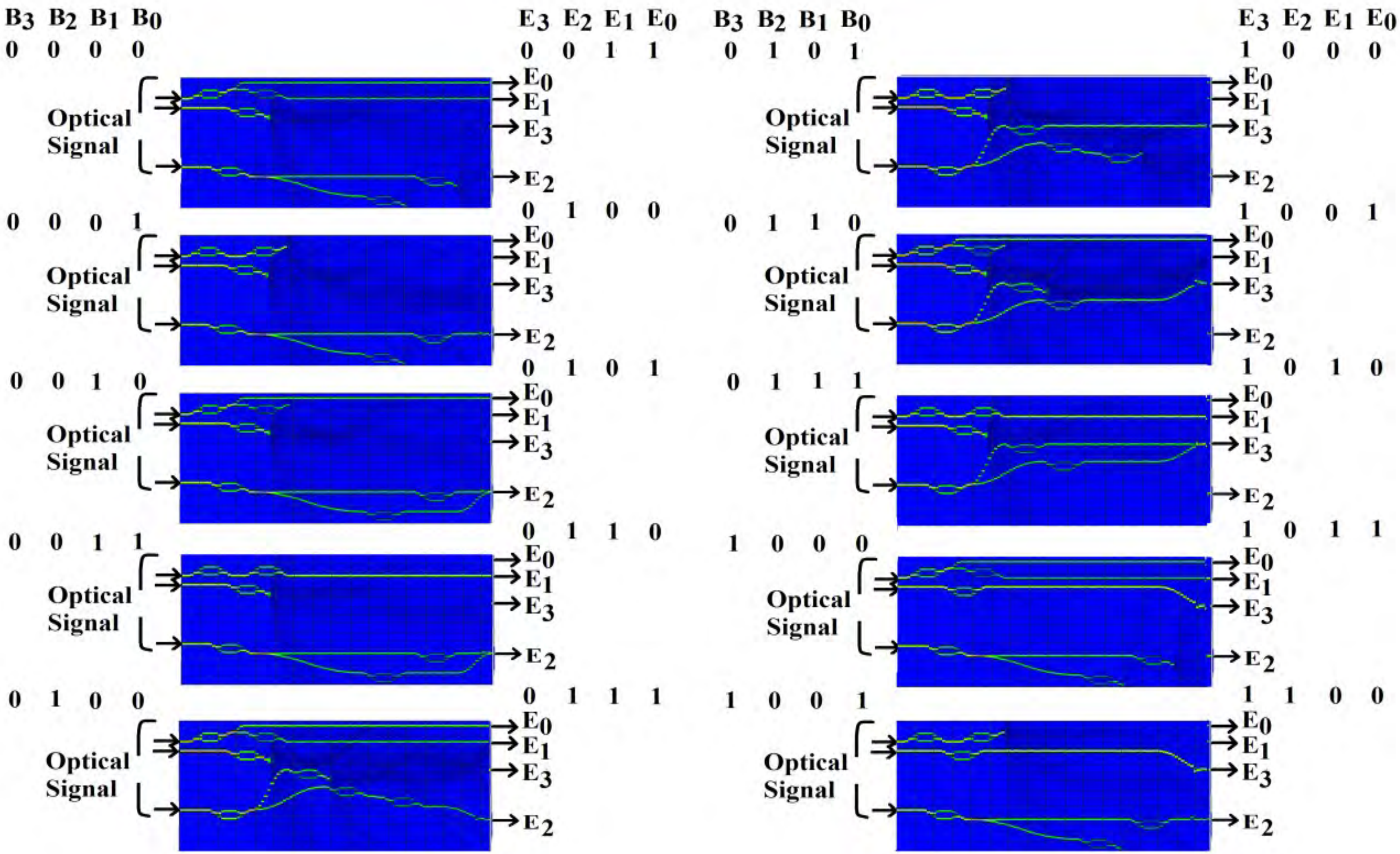

Figure: BPM result of BCD to Excess-3 code converter where B_3 B_2 B_1 B_0 varies from 0000 to 1001

Design of Excess 3 to BCD code converter

Santosh Kumar et. al., Proc. SPIE 9889, Optical Modelling and Design IV, SPIE Photonics Europe 2016, **Brussels, Belgium**, PP. 98890E (April 4-7, 2016).

Excess-3 to BCD code converter

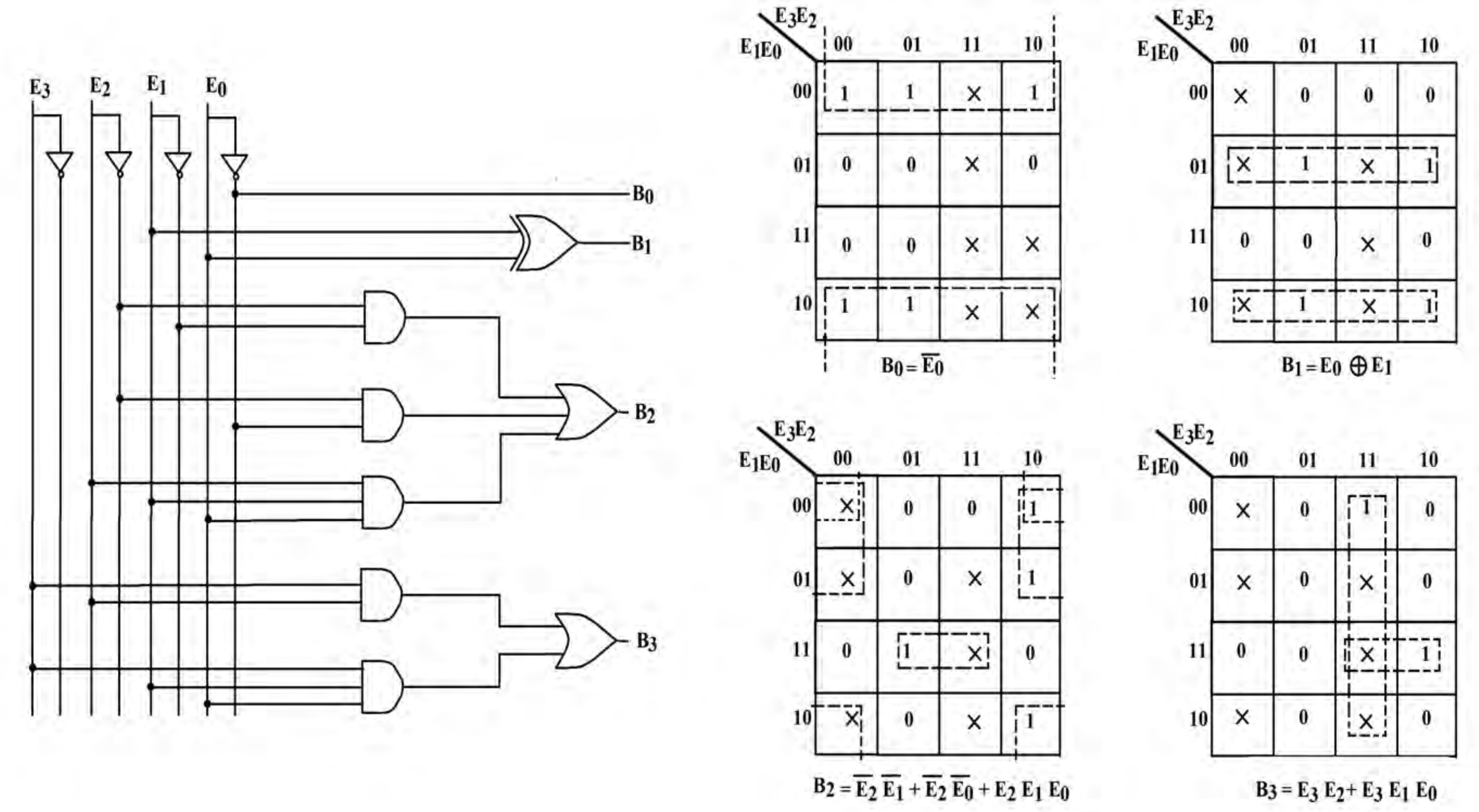

Figure: Digital circuits and Schematic diagram of K-map of excess 3 to BCD code converter.

Excess-3 to BCD code converter

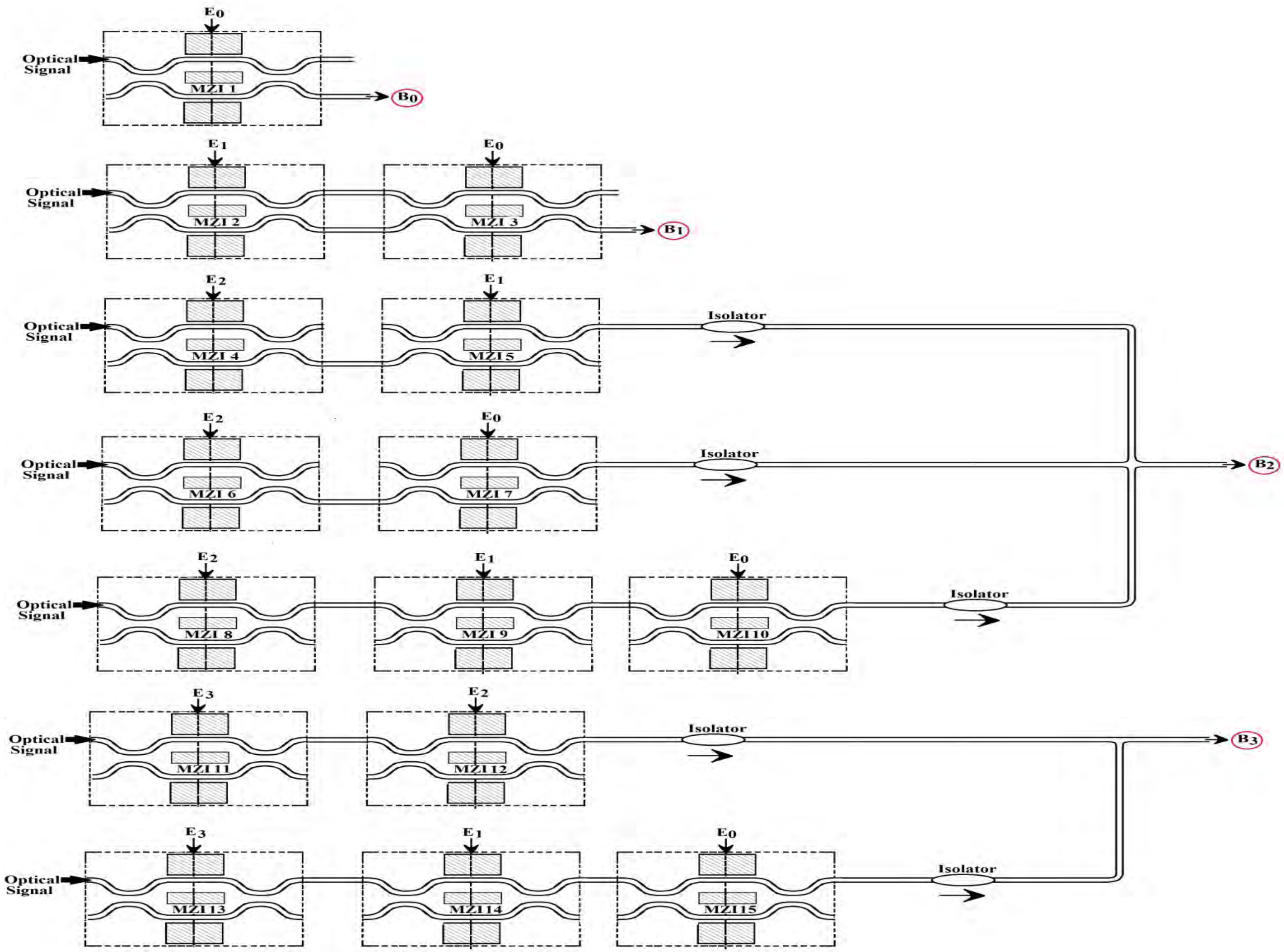

Figure: Schematic diagram of excess 3 to BCD code converter.using MZIs

Mathematical Expression for Excess 3 to BCD code converter

P_0, P_1, P_2, P_3 is output power calculated for B_0, B_1, B_2, B_3 respectively.

$$P_0 = cos^2\left(\frac{\Delta\phi_{MZI1}}{2}\right)$$

$$P_1 = sin^2\left(\frac{\Delta\phi_{MZI2}}{2}\right)cos^2\left(\frac{\Delta\phi_{MZI3}}{2}\right) + cos^2\left(\frac{\Delta\phi_{MZI2}}{2}\right)sin^2\left(\frac{\Delta\phi_{MZI3}}{2}\right)$$

$$P_2 = cos^2\left(\frac{\Delta\phi_{MZI4}}{2}\right)cos^2\left(\frac{\Delta\phi_{MZI5}}{2}\right) + cos^2\left(\frac{\Delta\phi_{MZI6}}{2}\right)cos^2\left(\frac{\Delta\phi_{MZI7}}{2}\right) + sin^2\left(\frac{\Delta\phi_{MZI8}}{2}\right)sin^2\left(\frac{\Delta\phi_{MZI9}}{2}\right)sin^2\left(\frac{\Delta\phi_{MZI10}}{2}\right)$$

$$P_3 = sin^2\left(\frac{\Delta\phi_{MZI11}}{2}\right)sin^2\left(\frac{\Delta\phi_{MZI12}}{2}\right) + sin^2\left(\frac{\Delta\phi_{MZI13}}{2}\right)sin^2\left(\frac{\Delta\phi_{MZI14}}{2}\right)sin^2\left(\frac{\Delta\phi_{MZI15}}{2}\right)$$

MATLAB Results for Excess 3 to BCD code converter

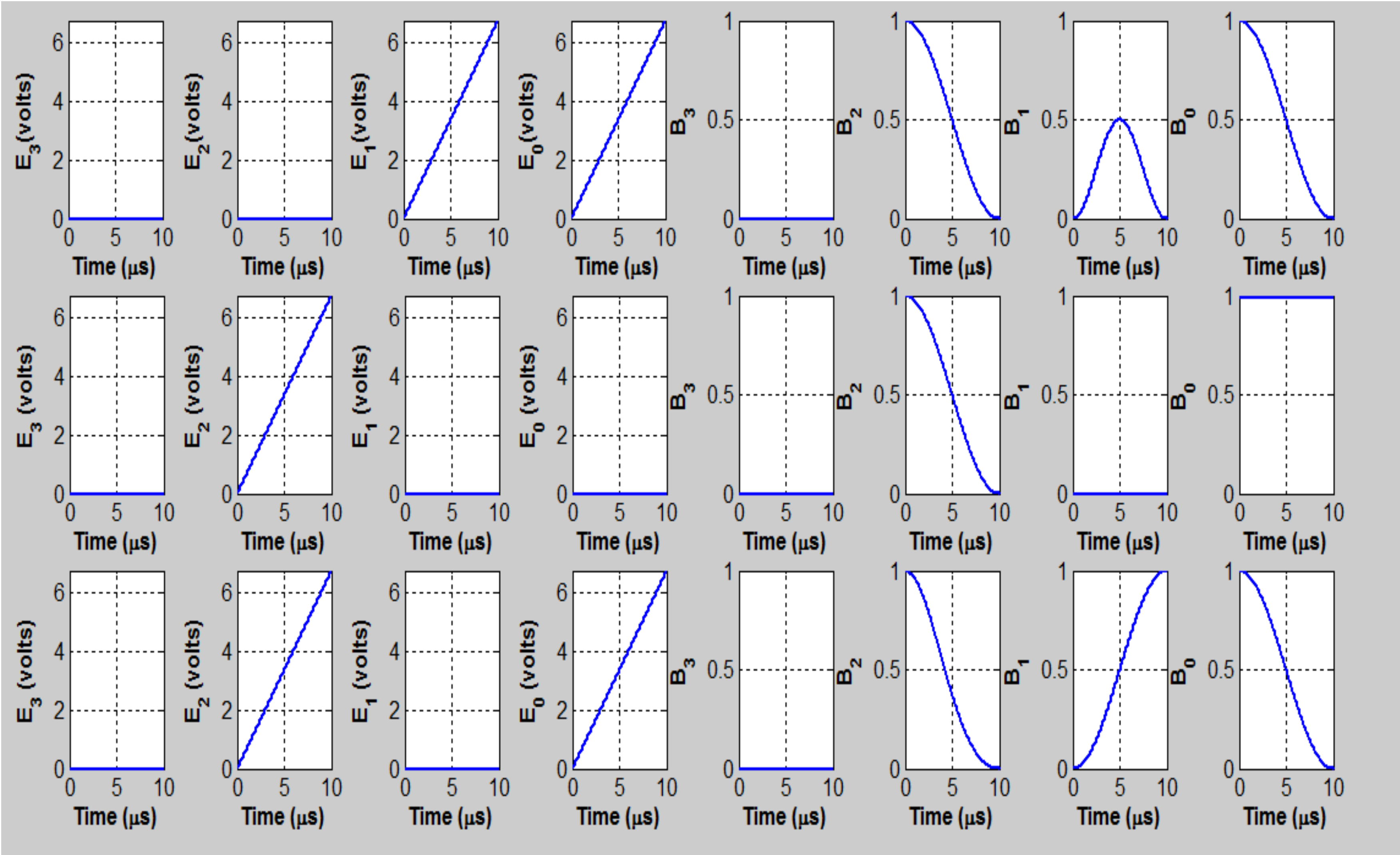

Figure: MATLAB simulation result of Excess 3 to BCD code converter where E_3 E_2 E_1 E_0 varies from 0011 to 0101

Contd..

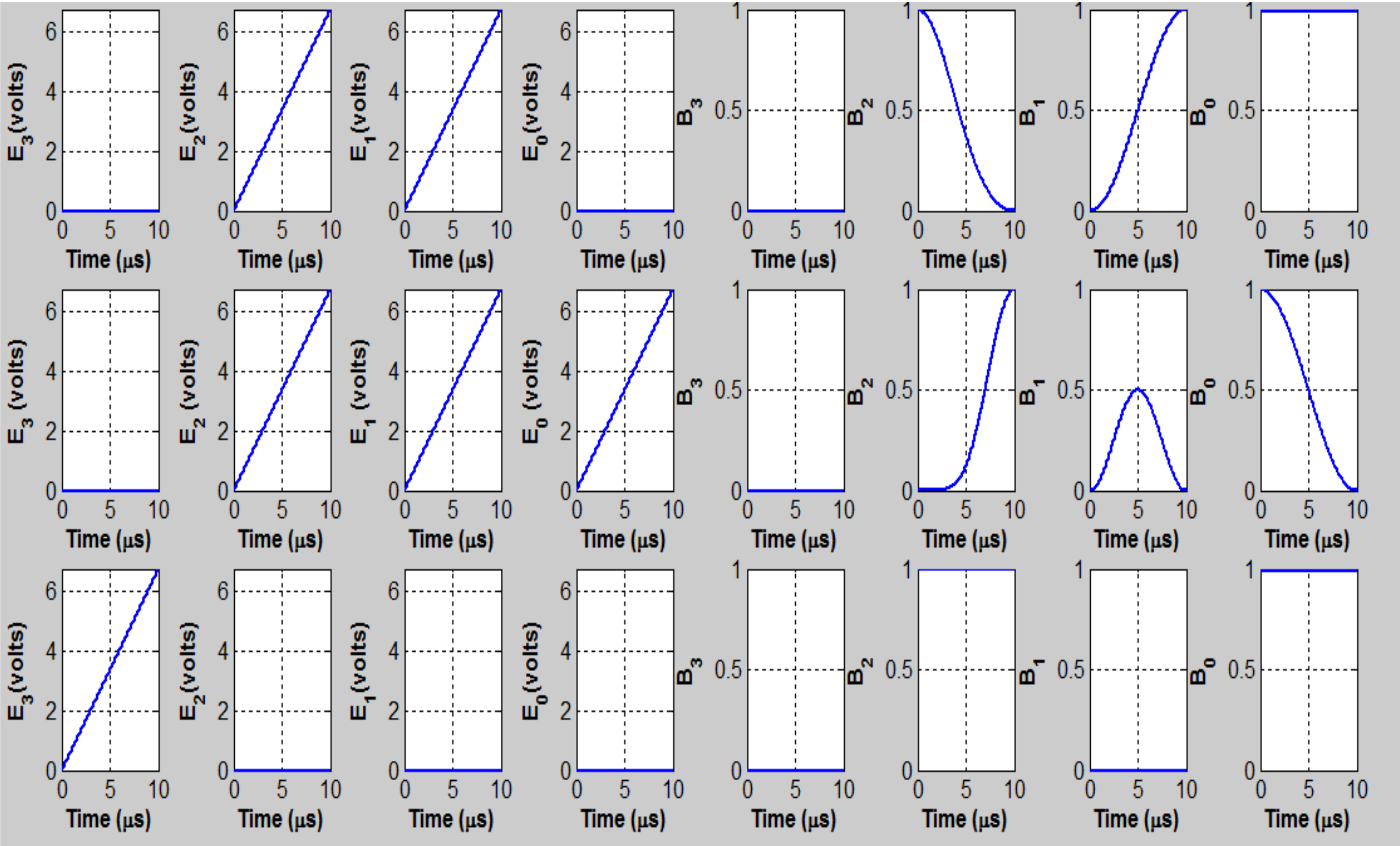

Figure: MATLAB simulation result of Excess 3 to BCD code converter where E_3 E_2 E_1 E_0 varies from 0110 to 1000

Contd..

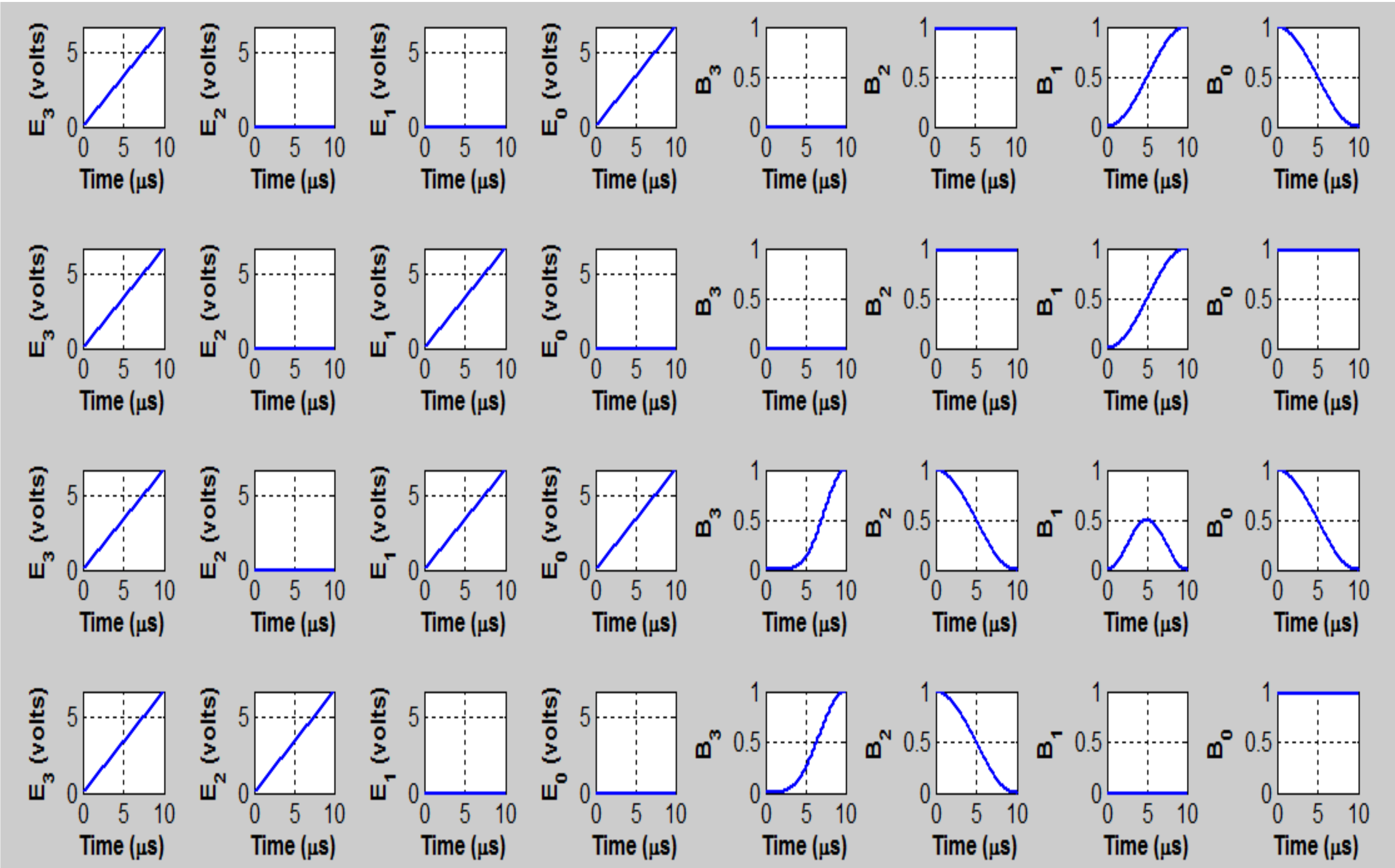

Figure: MATLAB simulation result of Excess 3 to BCD code converter where E_3 E_2 E_1 E_0 varies from 1001 to 1100

BPM Layout of Excess 3 to code converter

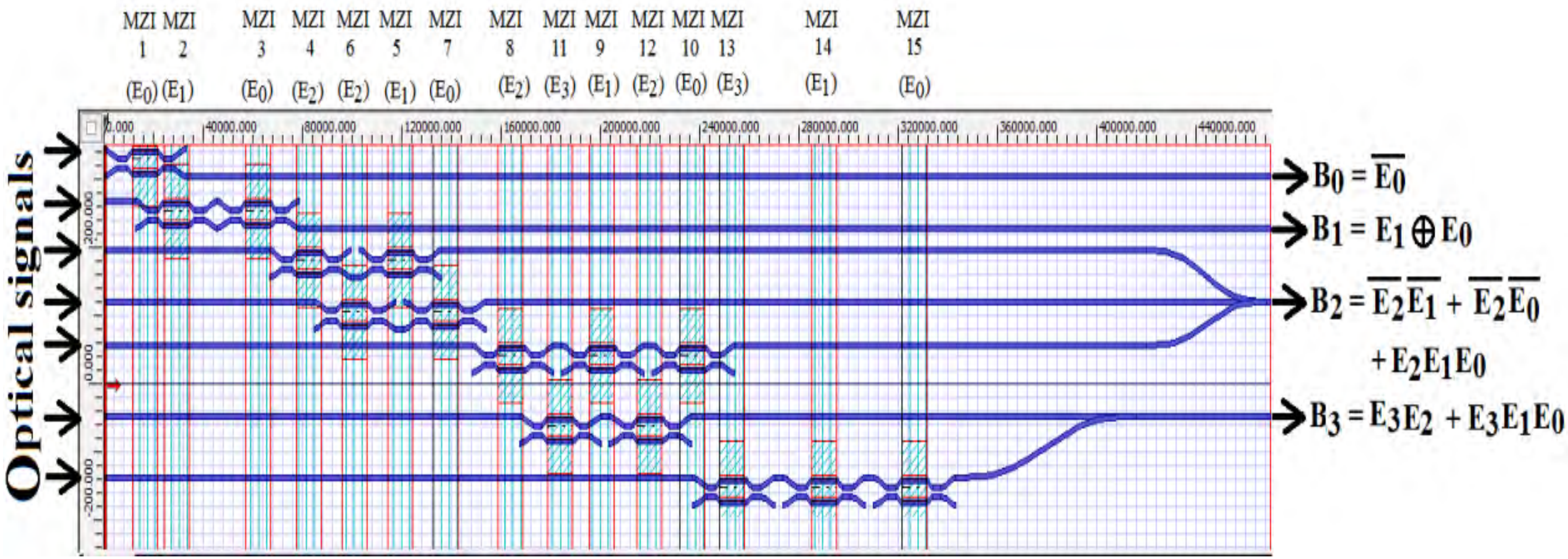

Figure: BPM layout of Excess-3 to BCD code converter

BPM Simulation Result

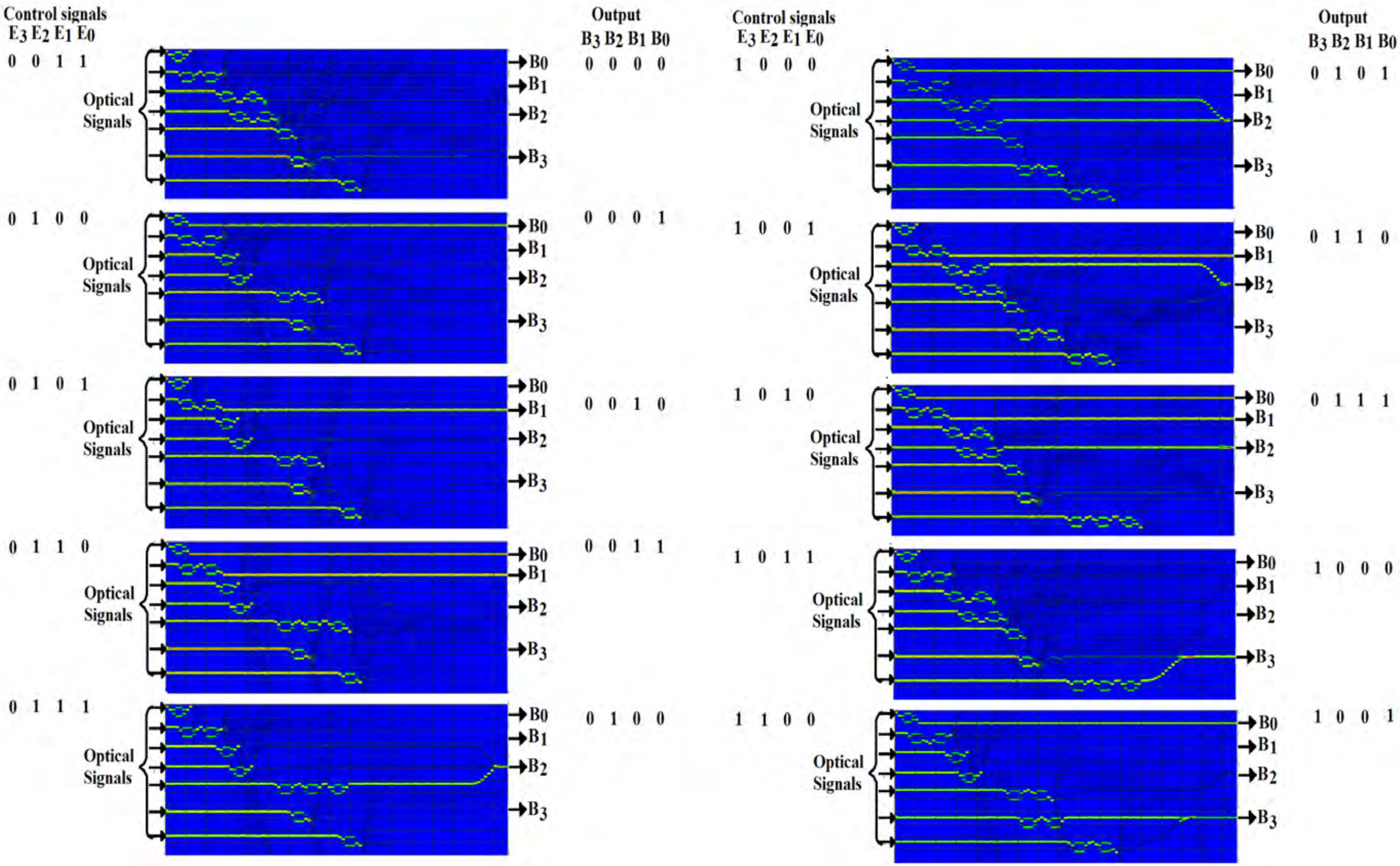

Figure: BPM result of Excess 3 to BCD code converter where E_3 E_2 E_1 E_0 varies from 0011 to 1100

Design of Transmission gate

<u>Santosh Kumar</u> et. al., Photonic Network communications (Springer), Vol. 33, PP. 1-9, (Mar. 24, 2017).

Transmission gate

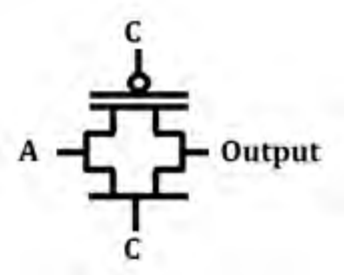

Figure: Digital circuit of transmission gate

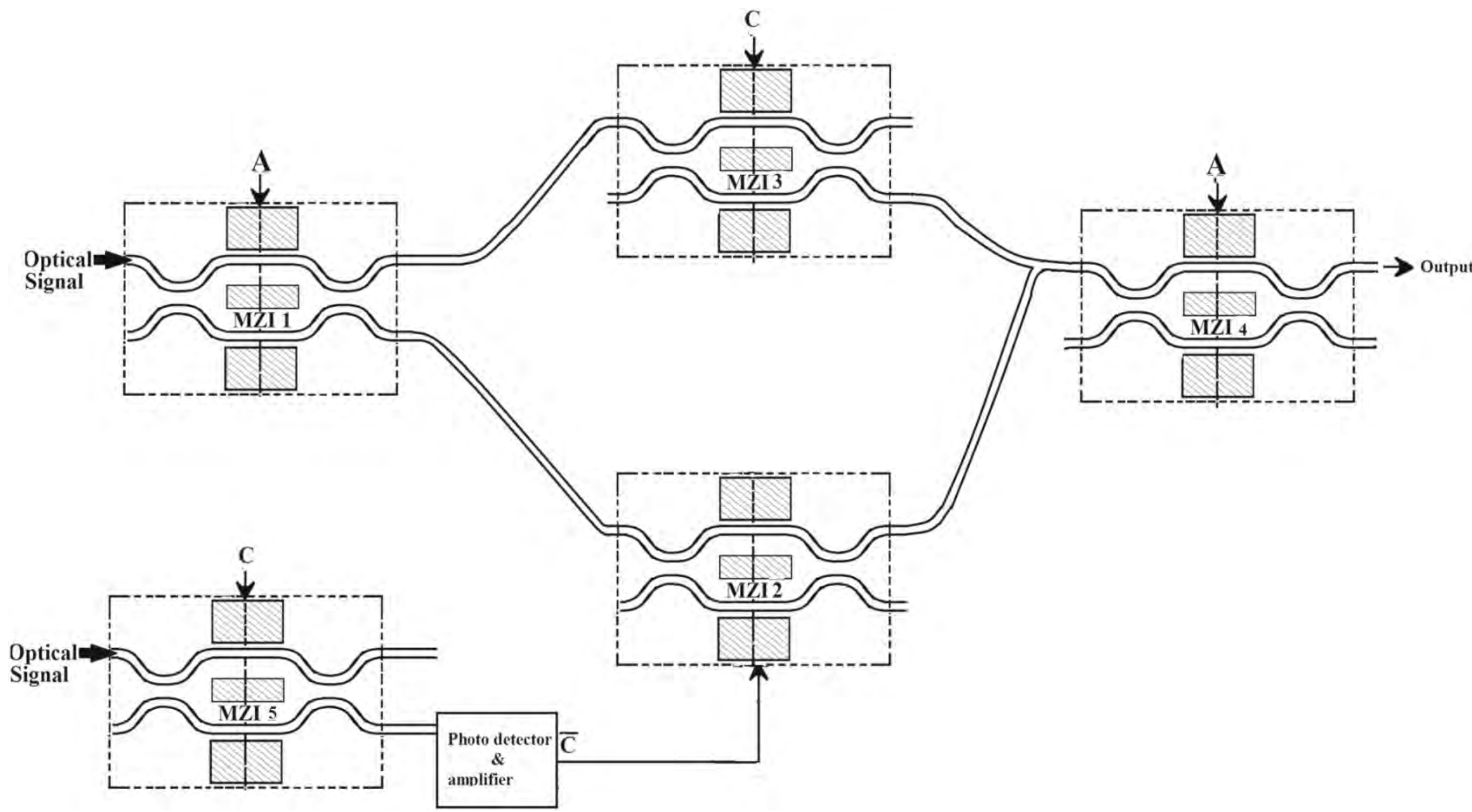

Figure: Schematic diagram of transmission gate using MZIs

Truth table and mathematical expression for Transmission gate

$$output = \left[\sin^2\left(\frac{\Delta\emptyset_{MZI1}}{2}\right)\ \cos^2\left(\frac{\Delta\emptyset_{MZI3}}{2}\right) + \cos^2\left(\frac{\Delta\emptyset_{MZI1}}{2}\right)\ \sin^2\left(\frac{\Delta\emptyset_{MZI2}}{2}\right)\right] \sin^2\left(\frac{\Delta\emptyset_{MZI4}}{2}\right)$$

Control Signal	Input signal	Output Signal
$\bar{C}$	**A**	**Output**
0	0	0
0	1	0
1	0	0
1	1	1

MATLAB Simulation Results

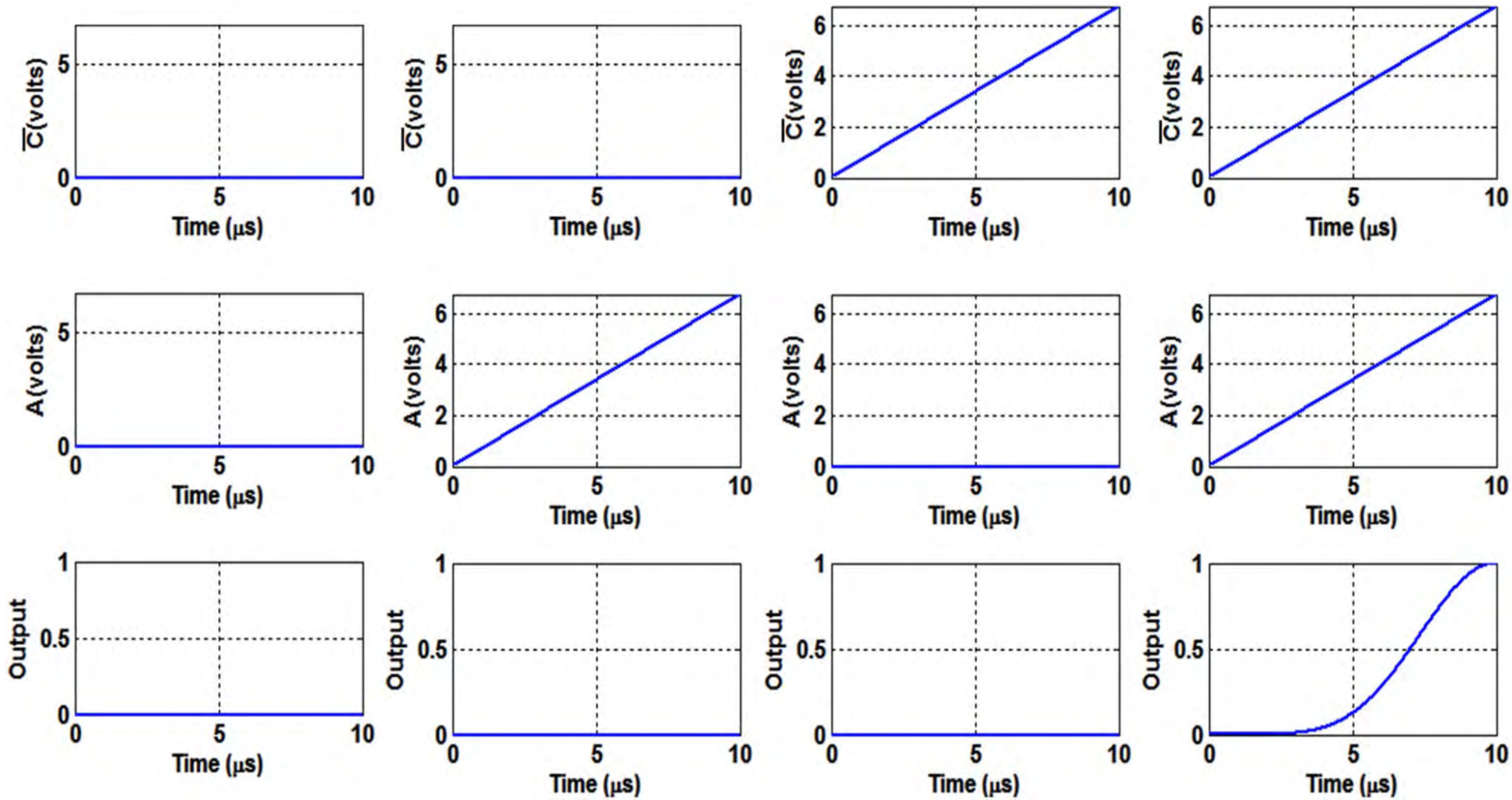

Figure: MATLAB simulation result of transmission gate where C, A varies from 00 to 11

2x1 multiplexer using Transmission gate

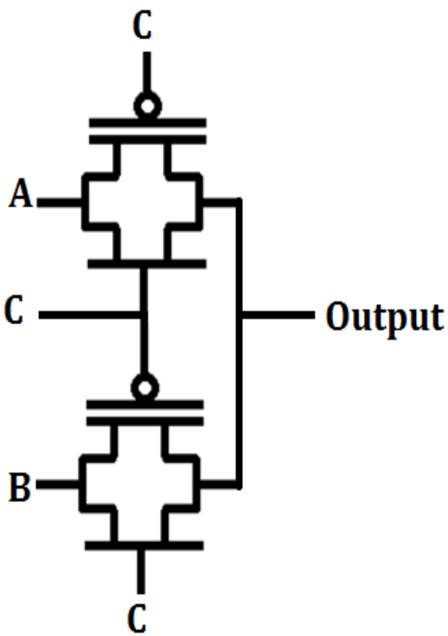

Figure: Digital circuit of 2x1 multiplexer using transmission gate.

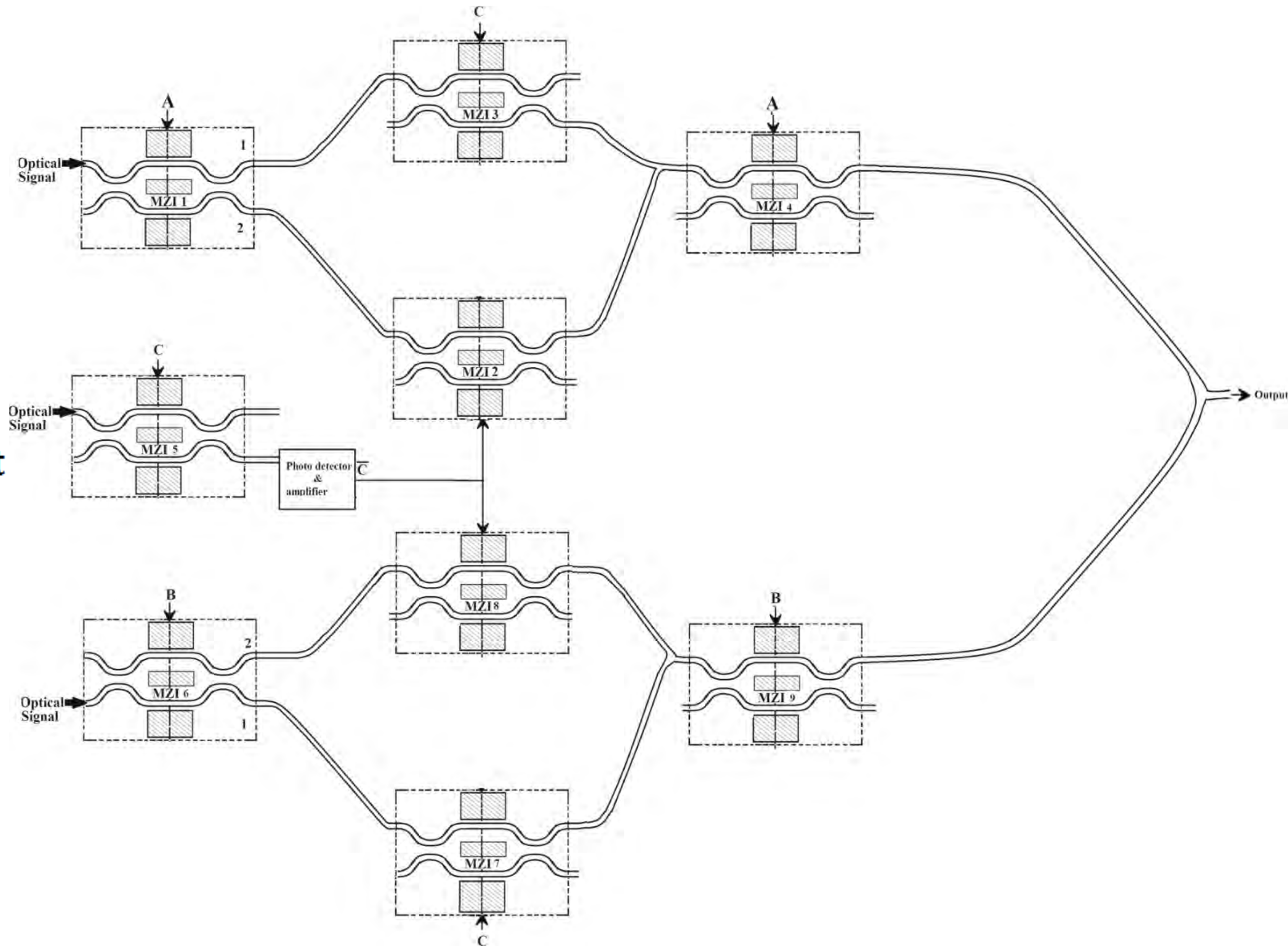

Figure: Schematic diagram of 2 x 1 multiplexer using transmission gate

Truth table and mathematical expression for 2x1 multiplexer using Transmission gate

$$\text{output} = \left[\sin^2\left(\frac{\Delta\emptyset_{MZI1}}{2}\right)\ \cos^2\left(\frac{\Delta\emptyset_{MZI3}}{2}\right) + \cos^2\left(\frac{\Delta\emptyset_{MZI1}}{2}\right)\ \sin^2\left(\frac{\Delta\emptyset_{MZI2}}{2}\right)\right] \sin^2\left(\frac{\Delta\emptyset_{MZI4}}{2}\right) + \left[\sin^2\left(\frac{\Delta\emptyset_{MZI6}}{2}\right)\ \sin^2\left(\frac{\Delta\emptyset_{MZI7}}{2}\right) + \cos^2\left(\frac{\Delta\emptyset_{MZI6}}{2}\right)\ \cos^2\left(\frac{\Delta\emptyset_{MZI8}}{2}\right)\right] \sin^2\left(\frac{\Delta\emptyset_{MZI9}}{2}\right)$$

Control signal	Input signal		Output signal
$\overline{C}$	**B**	**A**	**Output**
0	0	0	0
0	0	1	1
0	1	0	0
0	1	1	1
1	0	0	0
1	0	1	0
1	1	0	1
1	1	1	1

MATLAB Simulation Results of 2x1 multiplexer

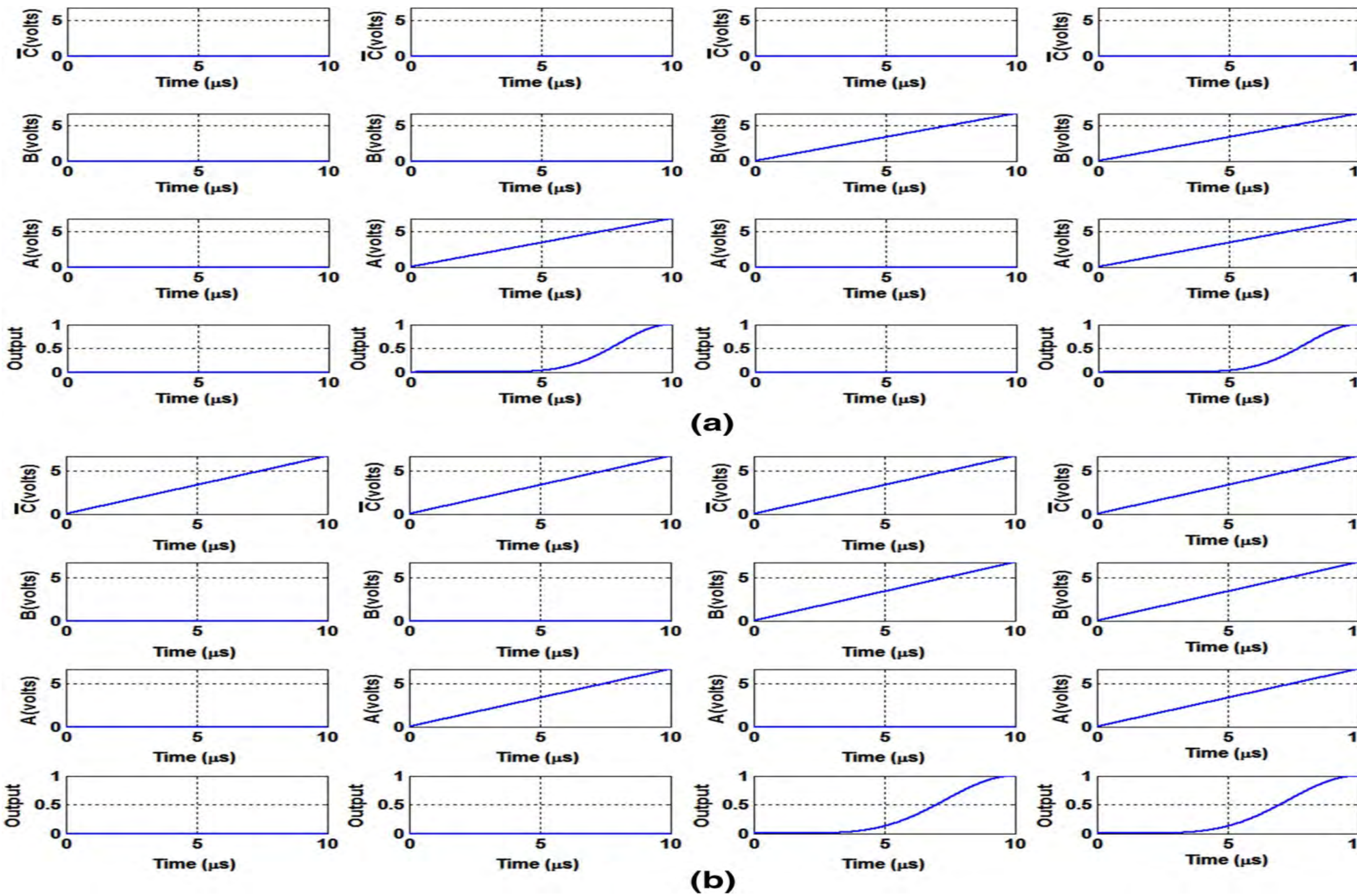

Figure: MATLAB simulation result of 2 × 1 multiplexer using transmission gate where $\bar{C}$, B, A varies from a 000 to 01. b 100 to 111

BPM layout of transmission gate

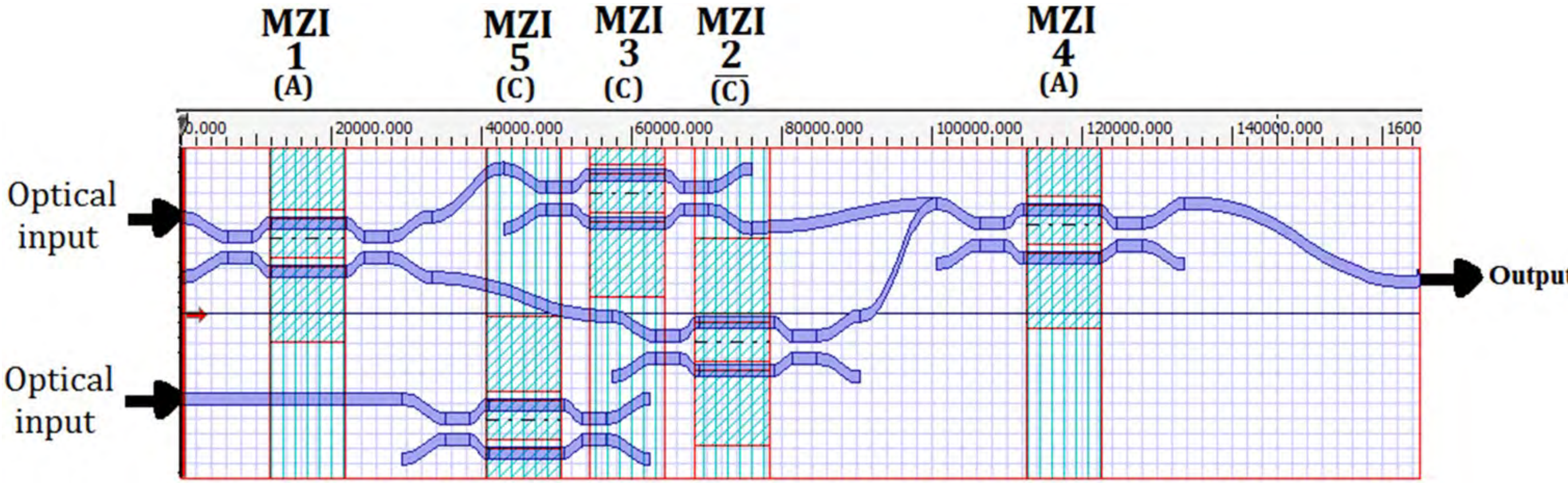

Figure: BPM layout of transmission gate using MZI

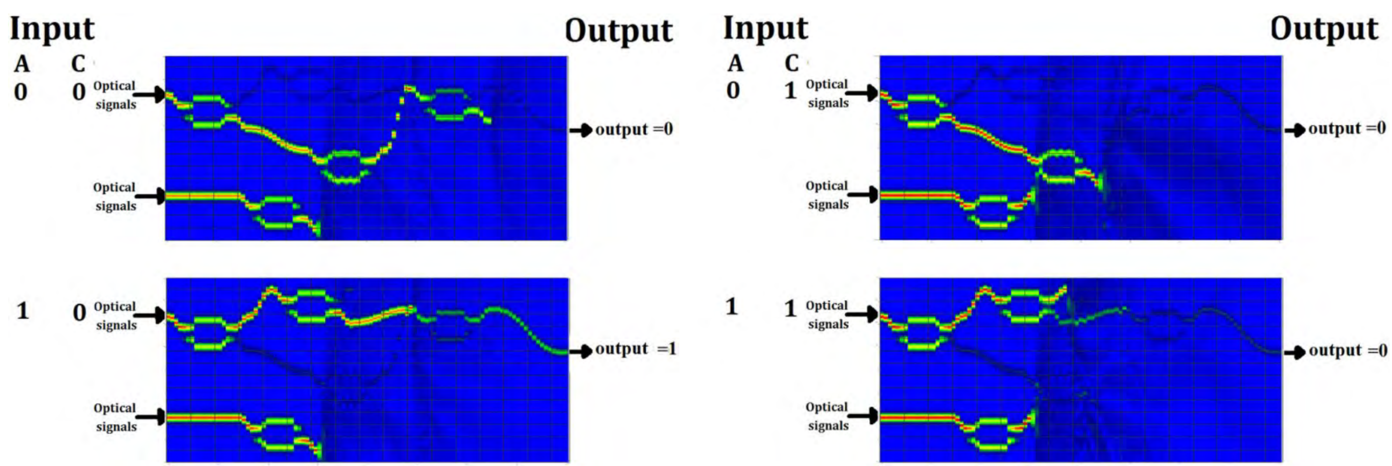

Figure: Simulation results of transmission gate where C, A varies from 00 to 11 obtained through beam propagation method.

BPM layout of 2x1 multiplexer using transmission gate

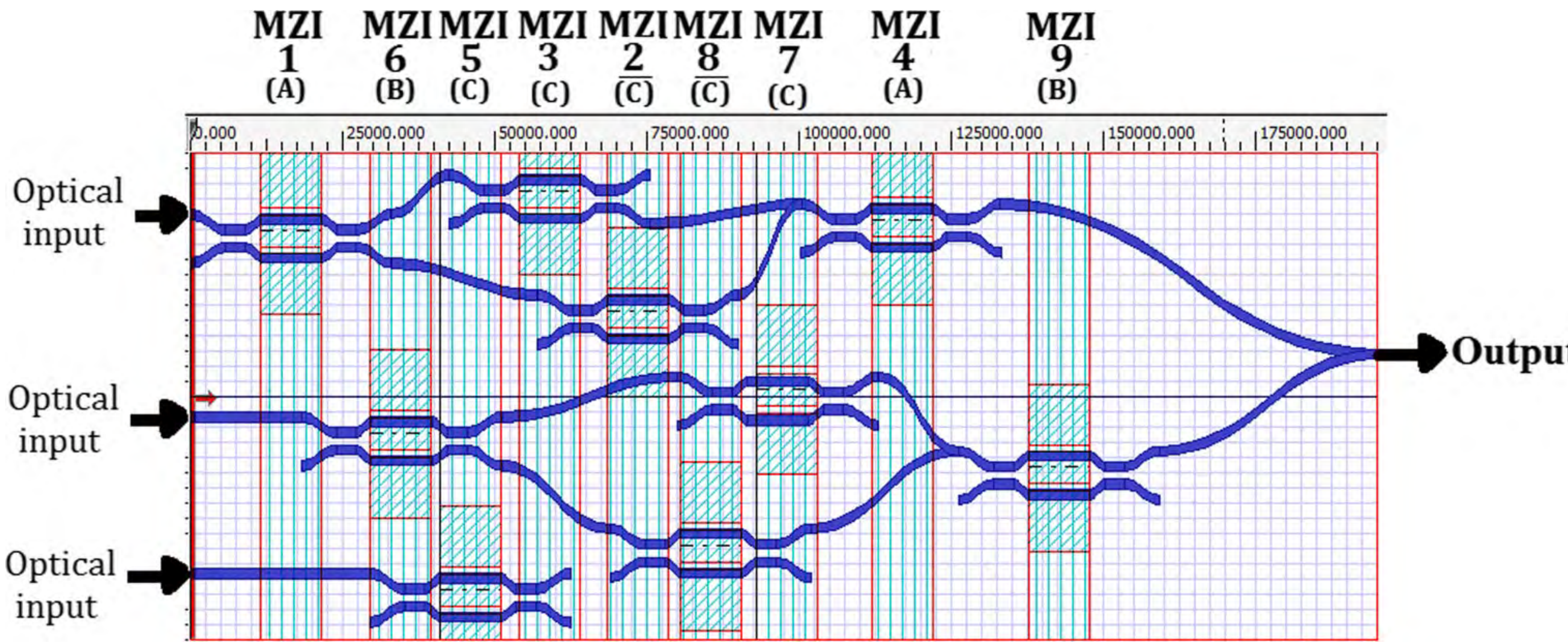

Figure: BPM layout of 2×1 multiplexer using MZI

Simulation Result of 2x1 multiplexer

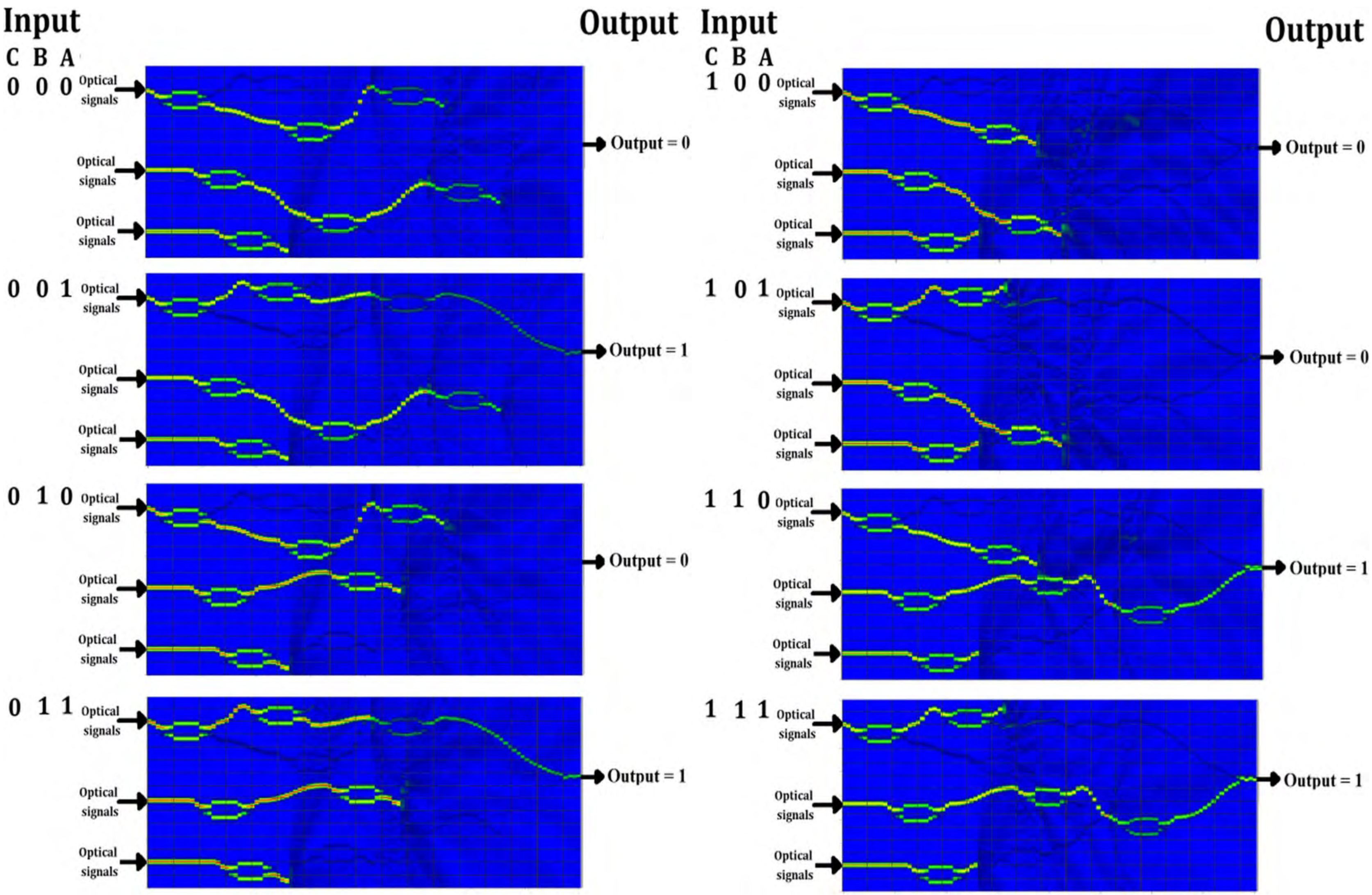

Figure: Simulation result of transmission gate where C, B, A varies from 000 to 111 obtained through beam propagation method

Design of binary to octal and octal to binary code converter

Santosh Kumar et al., Journal of Optical Communications (Degruyter), DOI: 10.1515/joc-2016-N055, August 2016.

Design of binary to octal and octal to binary code converter

- Binary to octal and octal to binary code converter is a device that allows placing digital information from many inputs to many outputs.
- Binary to octal code converter accepts three binary inputs (A, B and C) and produces eight octal outputs ($O_0, O_1, O_2, O_3, O_4, O_5, O_6,$ and O_7).
- Octal to binary code converter accepts eight inputs ($I_0, I_1, I_2, I_3, I_4, I_5, I_6,$ and I_7) and produces three binary outputs (B_0, B_1 and B_2).

Cont….

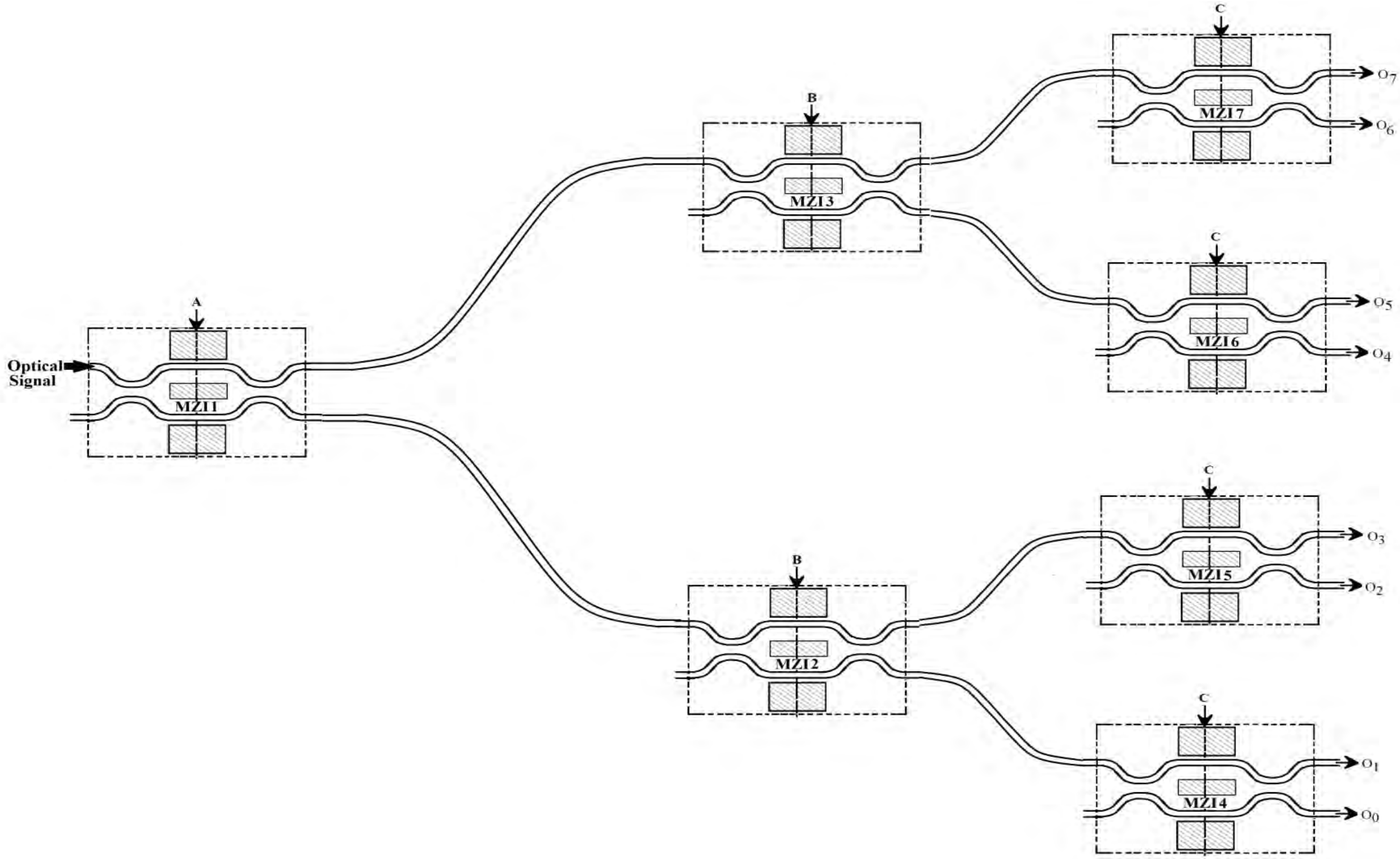

Figure: Schematic diagram of binary to octal code converter using MZIs

Mathematical Expression for binary to octal code converter

Normalizedpower at the output ports ($O_0, O_1, O_2, O_3, O_4, O_5, O_6,$ and O_7) are calculated using the mathematical expression as:

The output O_0 at second output port of MZI4 as

$$O_0 = \ cos^2\left(\frac{\Delta\varphi_{MZI1}}{2}\right) cos^2\left(\frac{\Delta\varphi_{MZI2}}{2}\right) cos^2\left(\frac{\Delta\varphi_{MZI4}}{2}\right)$$

The output O_1 at first output port of MZI4 as;

$$O_1 = \ cos^2\left(\frac{\Delta\varphi_{MZI1}}{2}\right) cos^2\left(\frac{\Delta\varphi_{MZI2}}{2}\right) sin^2\left(\frac{\Delta\varphi_{MZI4}}{2}\right)$$

The output O_2 at second output port of MZI5 as;

$$O_2 = \ cos^2\left(\frac{\Delta\varphi_{MZI1}}{2}\right) sin^2\left(\frac{\Delta\varphi_{MZI2}}{2}\right) cos^2\left(\frac{\Delta\varphi_{MZI5}}{2}\right)$$

Cont….

The output O_3 at first output port of MZI5 as;

$$O_3 = \cos^2\left(\frac{\Delta\varphi_{MZI1}}{2}\right)\sin^2\left(\frac{\Delta\varphi_{MZI2}}{2}\right)\sin^2\left(\frac{\Delta\varphi_{MZI5}}{2}\right)$$

The output O_4 at second output port of MZI6 as;

$$O_4 = \sin^2\left(\frac{\Delta\varphi_{MZI1}}{2}\right)\cos^2\left(\frac{\Delta\varphi_{MZI3}}{2}\right)\cos^2\left(\frac{\Delta\varphi_{MZI6}}{2}\right)$$

The output O_5 at first output port of MZI6 as;

$$O_5 = \sin^2\left(\frac{\Delta\varphi_{MZI1}}{2}\right)\cos^2\left(\frac{\Delta\varphi_{MZI3}}{2}\right)\sin^2\left(\frac{\Delta\varphi_{MZI6}}{2}\right)$$

The output O_6 at second output port of MZI7 as;

$$O_6 = \sin^2\left(\frac{\Delta\varphi_{MZI1}}{2}\right)\sin^2\left(\frac{\Delta\varphi_{MZI3}}{2}\right)\cos^2\left(\frac{\Delta\varphi_{MZI7}}{2}\right)$$

The output O_7 at first output port of MZI7 as;

$$O_7 = \sin^2\left(\frac{\Delta\varphi_{MZI1}}{2}\right)\sin^2\left(\frac{\Delta\varphi_{MZI3}}{2}\right)\sin^2\left(\frac{\Delta\varphi_{MZI7}}{2}\right)$$

MATLAB simulation Results of binary to octal code converter

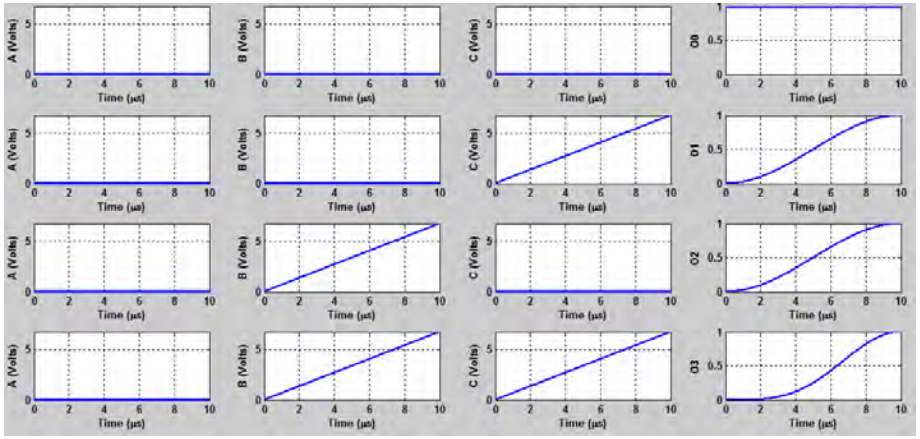

(a)

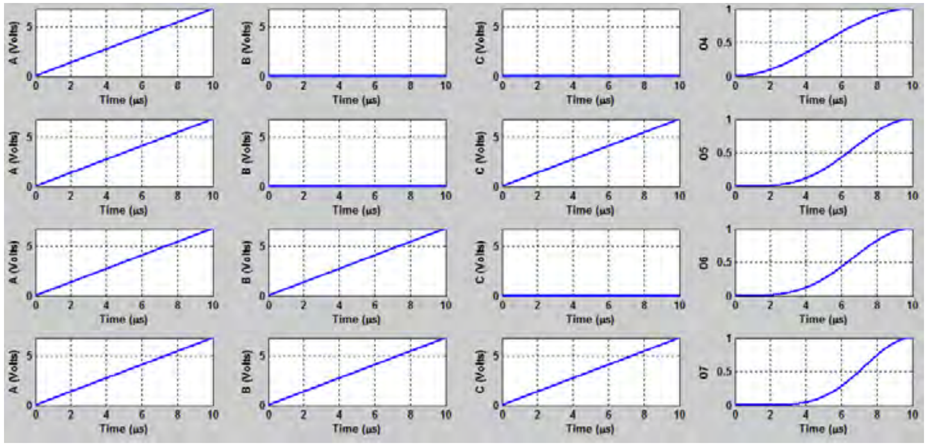

(b)

Figure: MATLAB simulation result for (a) ABC=000 to 011 of B-O code converter
(b) ABC=100 to 111 of B-O code converter

Cont….

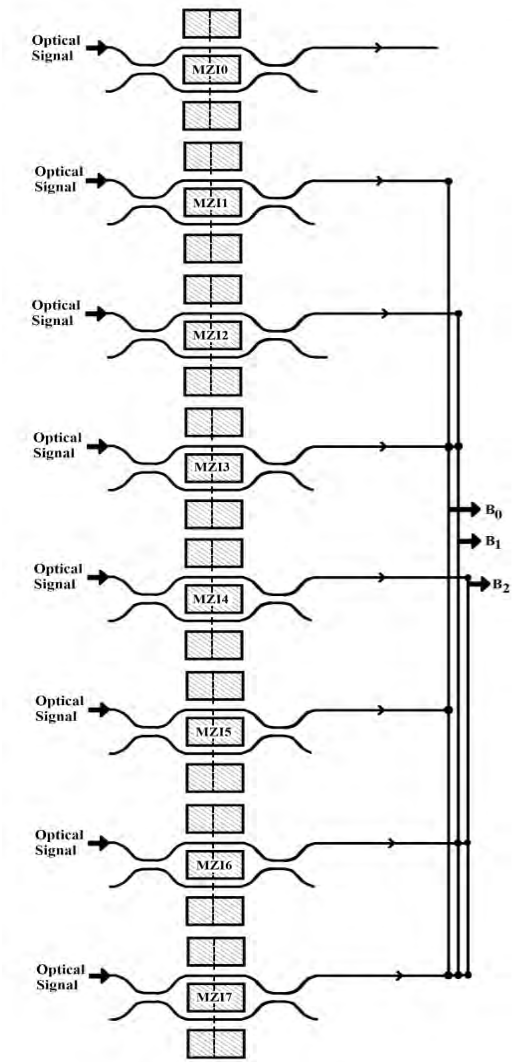

Figure: Schematic diagram of ctal to binary code converter

Table: Truth table of binary to octal code converter

Binary input			**Octal Output**							
A	B	C	O_0	O_1	O_2	O_3	O_4	O_5	O_6	O_7
0	0	0	1	0	0	0	0	0	0	0
0	0	1	0	1	0	0	0	0	0	0
0	1	0	0	0	1	0	0	0	0	0
0	1	1	0	0	0	1	0	0	0	0
1	0	0	0	0	0	0	1	0	0	0
1	0	1	0	0	0	0	0	1	0	0
1	1	0	0	0	0	0	0	0	1	0
1	1	1	0	0	0	0	0	0	0	1

Table: Truth table of octal to binary code converter

Octal Input								**Binary output**		
I_0	I_1	I_2	I_3	I_4	I_5	I_6	I_7	B_2	B_1	B_0
1	0	0	0	0	0	0	0	0	0	0
0	1	0	0	0	0	0	0	0	0	1
0	0	1	0	0	0	0	0	0	1	0
0	0	0	1	0	0	0	0	0	1	1
0	0	0	0	1	0	0	0	1	0	0
0	0	0	0	0	1	0	0	1	0	1
0	0	0	0	0	0	1	0	1	1	0
0	0	0	0	0	0	0	1	1	1	1

Mathematical Expression for octal to binary code converter

Normalized power at output ports are computed using the mathematical expression as:

$$B_0 = sin^2\left(\frac{\Delta\varphi_{MZI1}}{2}\right) + sin^2\left(\frac{\Delta\varphi_{MZI3}}{2}\right) + sin^2\left(\frac{\Delta\varphi_{MZI5}}{2}\right) + sin^2\left(\frac{\Delta\varphi_{MZI7}}{2}\right)$$

$$B_1 = sin^2\left(\frac{\Delta\varphi_{MZI2}}{2}\right) + sin^2\left(\frac{\Delta\varphi_{MZI3}}{2}\right) + sin^2\left(\frac{\Delta\varphi_{MZI6}}{2}\right) + sin^2\left(\frac{\Delta\varphi_{MZI7}}{2}\right)$$

$$B_2 = sin^2\left(\frac{\Delta\varphi_{MZI4}}{2}\right) + sin^2\left(\frac{\Delta\varphi_{MZI5}}{2}\right) + sin^2\left(\frac{\Delta\varphi_{MZI6}}{2}\right) + sin^2\left(\frac{\Delta\varphi_{MZI7}}{2}\right)$$

Cont….

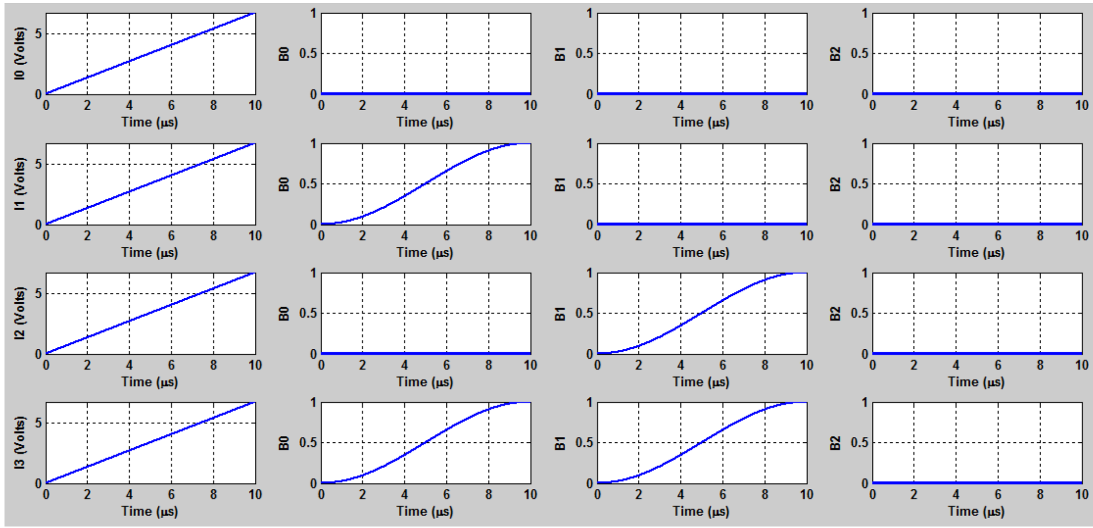

(a)

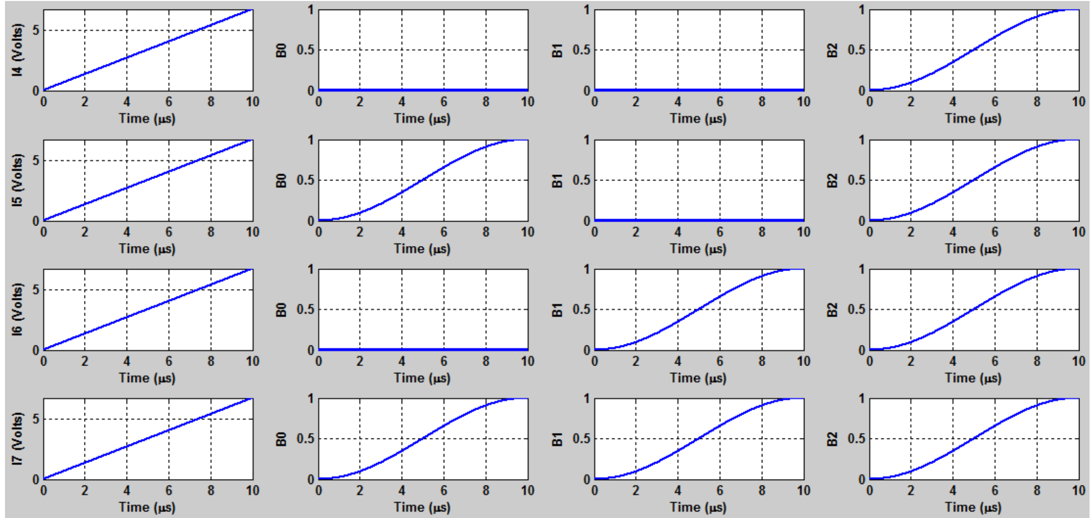

(b)

Figure: MATLAB simulation result for (a) input I_0 to I_3 (b) input I_4 to I_7

BPM layout

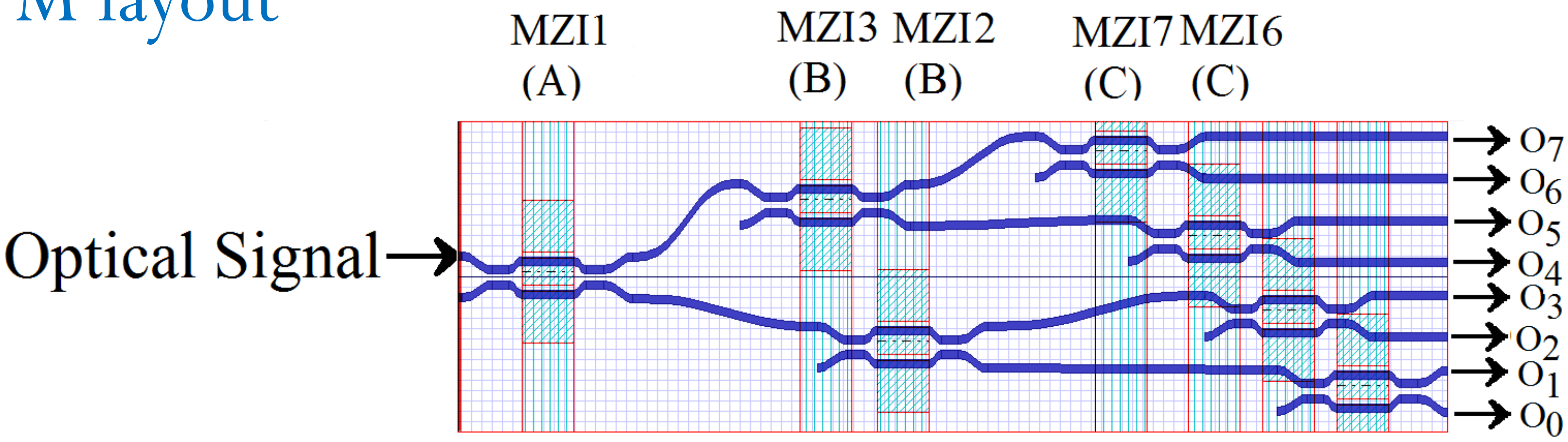

Figure: Layout of binary to octal code converter

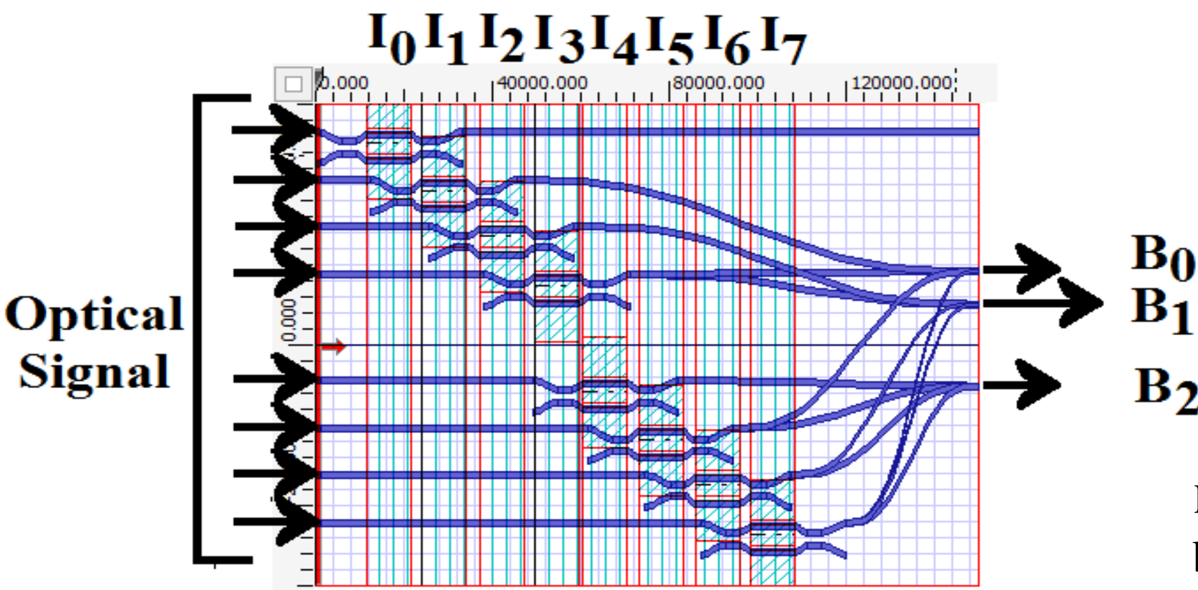

Figure: layout of octal to binary code converter

BPM results of binary to octal code converter

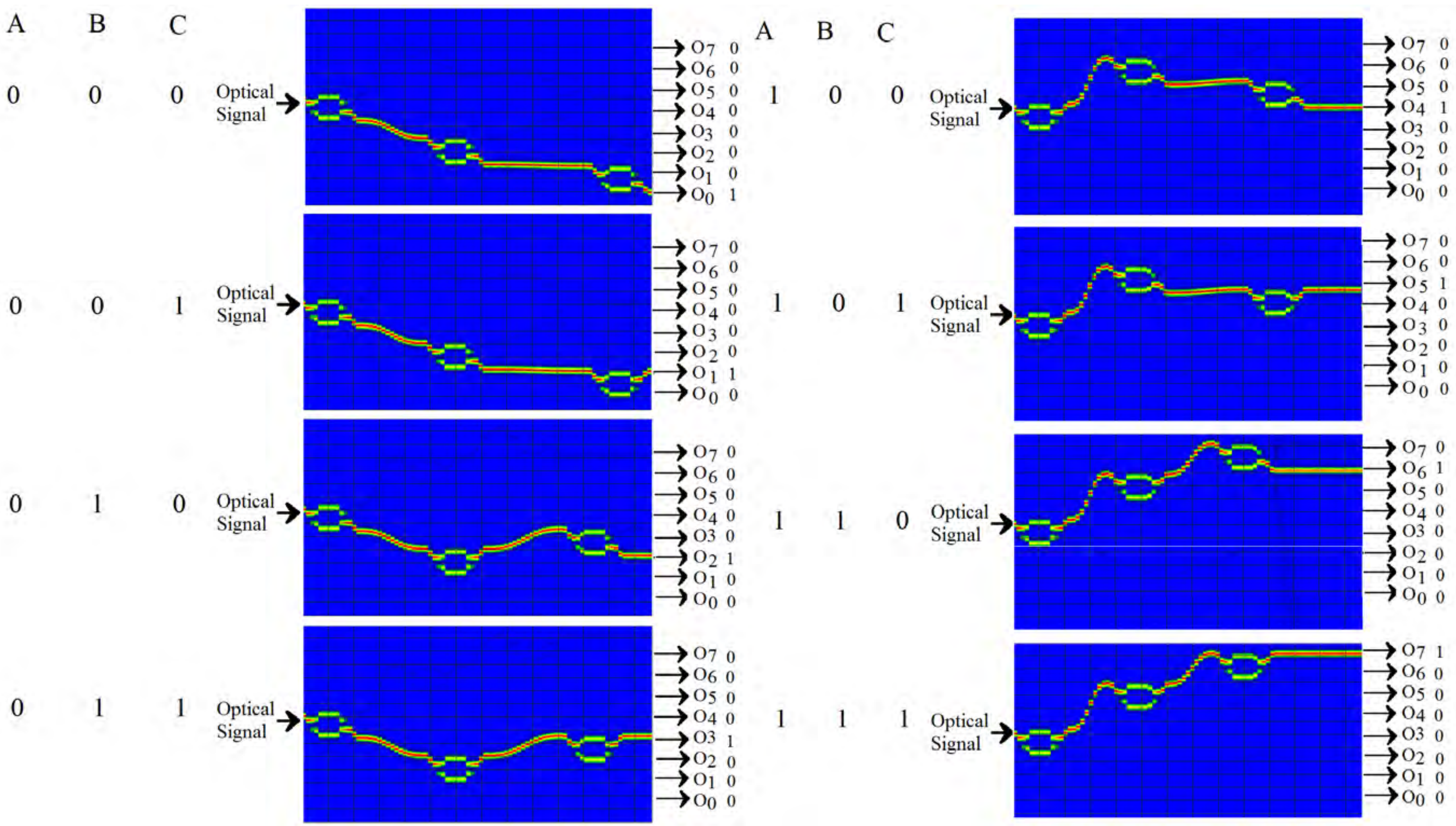

Figure: Results of binary to octal code converter for different combinations of control signals obtained through beam propagation method

BPM results of octal to binary code converter

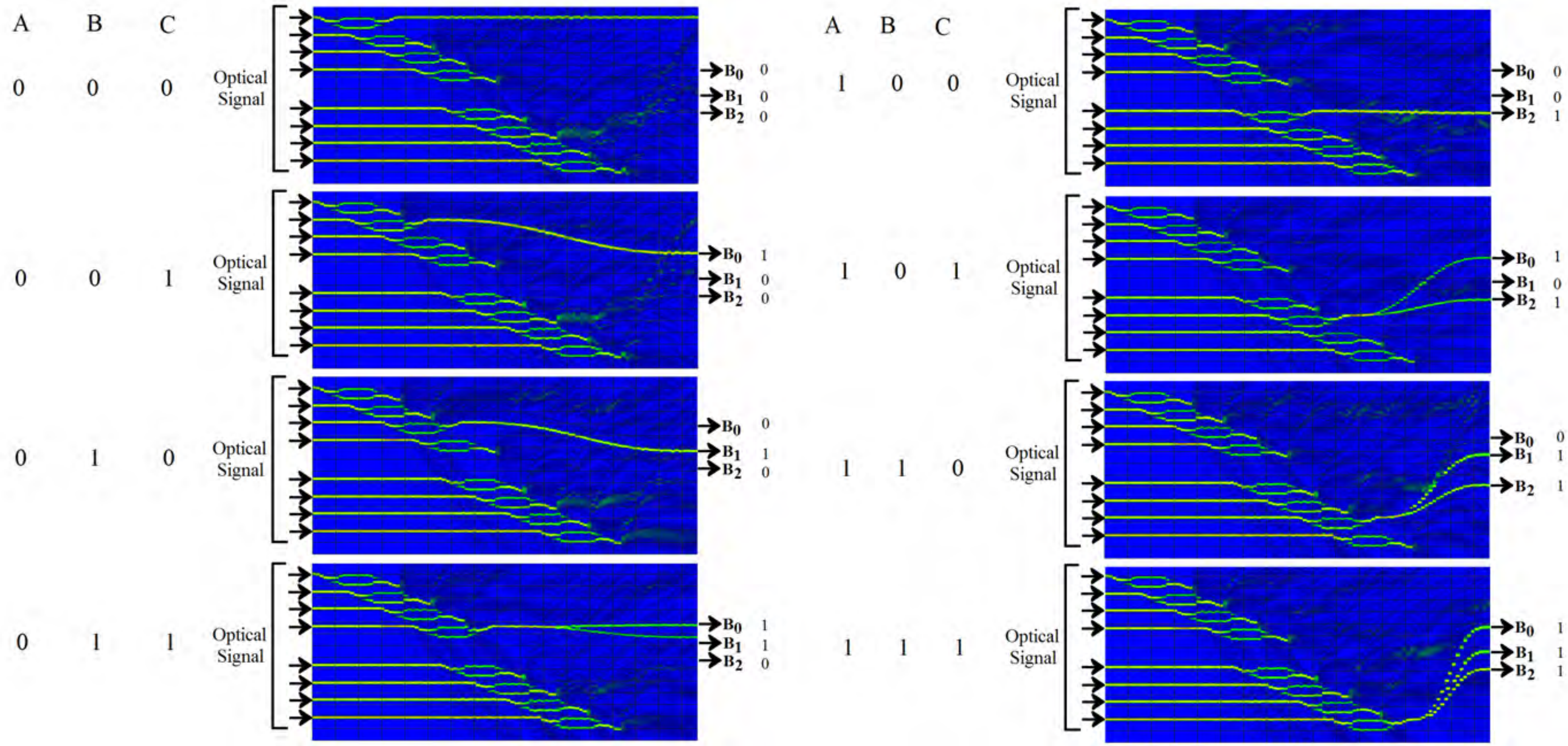

Figure: BPM simulation results for octal to binary code conversion from I_0 to I_7

Design of Optical Boolean function generator

Santosh Kumar et. al., Journal of Optical Communications (Degruyter), DOI: 10.1515/joc-2016-0080, July 2016.

Design of optical Boolean function generator

- Optical Boolean function generator unit can generates multiple logical operations.
- This design have two parts: one part is decoder circuit and other part is logic selection unit.
- A continuous wave (CW) optical signal is applied at second input port of MZI1.

Cont…

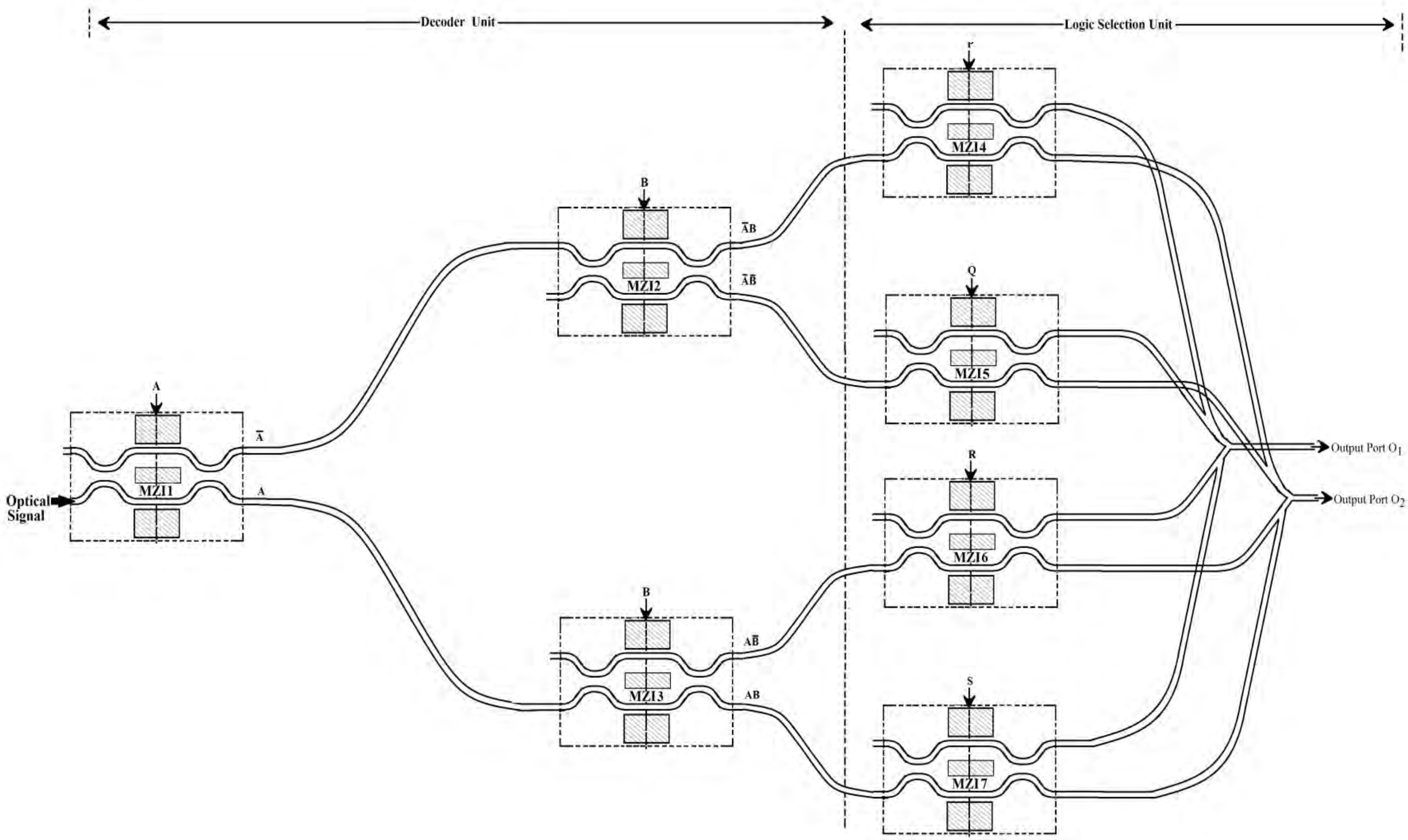

Figure: Schematic diagram of Boolean function generator unit

Cont…

Table: Generation of Boolean logical operation using generator unit for different control signal ($P, Q, R,$ and S)

S No.	Select Control Signal				Output of the function generator unit	
	P	**Q**	**R**	**S**	$\boldsymbol{O_1}$	$\boldsymbol{O_2}$
1	0	0	0	0	1 (High Logic)	0 (Low Logic)
2	0	0	0	1	$(\bar{A}\bar{B} + \bar{A}B + A\bar{B}) = \bar{A} + \bar{B}$	AB
3	0	0	1	0	$(\bar{A}\bar{B} + \bar{A}B + AB) = \bar{A} + B$	$A\bar{B}$
4	0	0	1	1	$(\bar{A}\bar{B} + \bar{A}B) = \bar{A}$	$(A\bar{B} + AB) = A$
5	0	1	0	0	$(\bar{A}B + A\bar{B} + AB) = A + B$	$\bar{A}\bar{B}$
6	0	1	0	1	$(\bar{A}B + A\bar{B}) = A \oplus B$	$(\bar{A}\bar{B} + AB) = A \odot B$
7	0	1	1	0	$(\bar{A}B + AB) = B$	$(\bar{A}\bar{B} + A\bar{B}) = \bar{B}$
8	0	1	1	1	$\bar{A}B$	$(\bar{A}\bar{B} + A\bar{B} + AB) = A + \bar{B}$
9	1	0	0	0	$(\bar{A}\bar{B} + A\bar{B} + AB) = A + \bar{B}$	$\bar{A}B$
10	1	0	0	1	$(\bar{A}\bar{B} + A\bar{B}) = \bar{B}$	$(\bar{A}B + AB) = B$
11	1	0	1	0	$(\bar{A}\bar{B} + AB) = A \odot B$	$(\bar{A}B + A\bar{B}) = A \oplus B$
12	1	0	1	1	$\bar{A}\bar{B}$	$(\bar{A}B + A\bar{B} + AB) = A + B$
13	1	1	0	0	$(A\bar{B} + AB) = A$	$(\bar{A}\bar{B} + \bar{A}B) = \bar{A}$
14	1	1	0	1	$A\bar{B}$	$(\bar{A}\bar{B} + \bar{A}B + AB) = \bar{A} + B$
15	1	1	1	0	AB	$(\bar{A}\bar{B} + \bar{A}B + A\bar{B}) = \bar{A} + \bar{B}$
16	1	1	1	1	0 (Low Logic)	1 (High Logic)

Mathematical Expression for optical Boolean function generator

Using output at single stage MZI, we can write the mathematical expression to obtain optical signal at the output ports O_1, O_2

$$O_1 = \begin{bmatrix} cos^2\left(\frac{\Delta\emptyset_{MZI1}}{2}\right) sin^2\left(\frac{\Delta\emptyset_{MZI2}}{2}\right) cos^2\left(\frac{\Delta\emptyset_{MZI4}}{2}\right) \\ +cos^2\left(\frac{\Delta\emptyset_{MZI1}}{2}\right) cos^2\left(\frac{\Delta\emptyset_{MZI2}}{2}\right) cos^2\left(\frac{\Delta\emptyset_{MZI5}}{2}\right) \\ +sin^2\left(\frac{\Delta\emptyset_{MZI1}}{2}\right) cos^2\left(\frac{\Delta\emptyset_{MZI3}}{2}\right) cos^2\left(\frac{\Delta\emptyset_{MZI6}}{2}\right) \\ +sin^2\left(\frac{\Delta\emptyset_{MZI1}}{2}\right) sin^2\left(\frac{\Delta\emptyset_{MZI3}}{2}\right) cos^2\left(\frac{\Delta\emptyset_{MZI7}}{2}\right) \end{bmatrix}$$

Cont…

$$O_2 = \begin{bmatrix} \cos^2\left(\frac{\Delta\phi_{MZI1}}{2}\right)\sin^2\left(\frac{\Delta\phi_{MZI2}}{2}\right)\sin^2\left(\frac{\Delta\phi_{MZI4}}{2}\right) \\ +\cos^2\left(\frac{\Delta\phi_{MZI1}}{2}\right)\cos^2\left(\frac{\Delta\phi_{MZI2}}{2}\right)\sin^2\left(\frac{\Delta\phi_{MZI5}}{2}\right) \\ +\sin^2\left(\frac{\Delta\phi_{MZI1}}{2}\right)\cos^2\left(\frac{\Delta\phi_{MZI3}}{2}\right)\sin^2\left(\frac{\Delta\phi_{MZI6}}{2}\right) \\ +\sin^2\left(\frac{\Delta\phi_{MZI1}}{2}\right)\sin^2\left(\frac{\Delta\phi_{MZI3}}{2}\right)\sin^2\left(\frac{\Delta\phi_{MZI7}}{2}\right) \end{bmatrix}$$

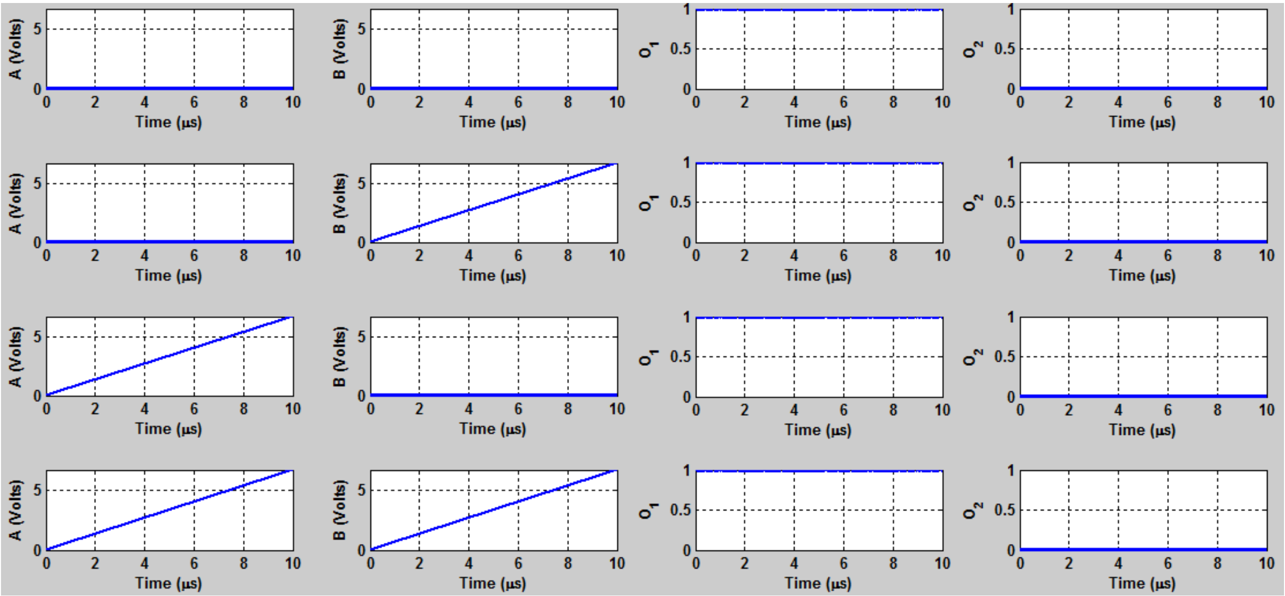

Figure: MATLAB simulation results for different combinations of AB at PQRS=0000

BPM Layout and simulation result

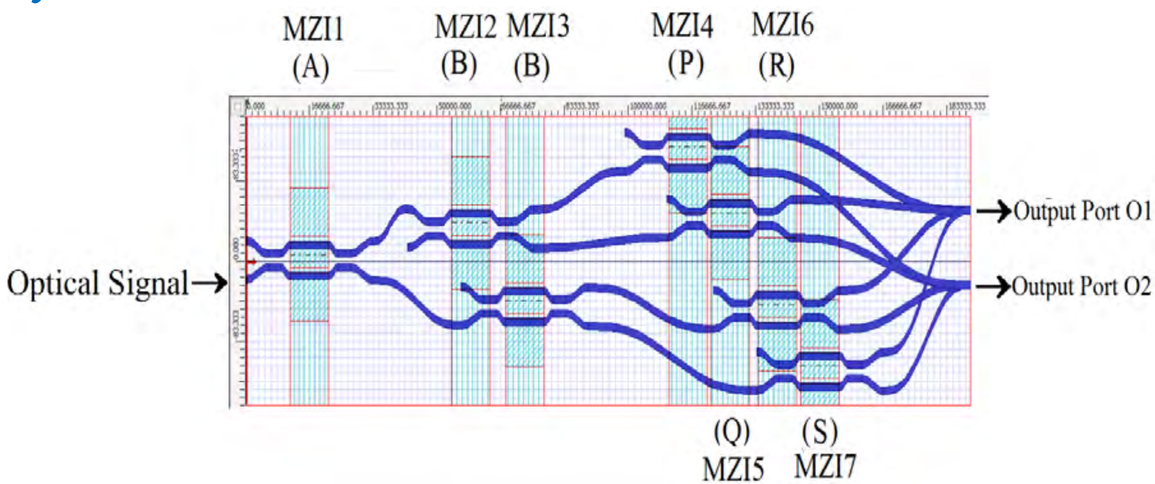

Figure: BPM layout of Boolean function generator unit

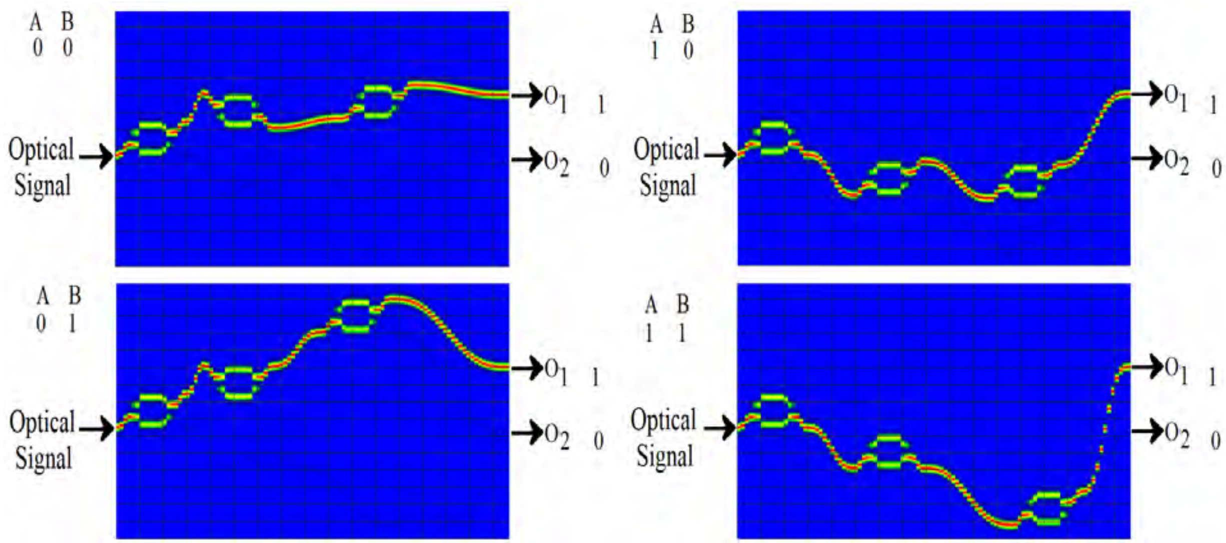

Figure: Optical field propagation for different combinations of decoder unit (AB) and fixed logical unit (PQRS=0000)

Design of 1's and 2's complement device

<u>Santosh Kumar</u> et. al., Optical Engineering (SPIE), Vol. 55, Issue 12, pp. 125104 (Dec 20, 2016).

Optical 1's and 2's complement device

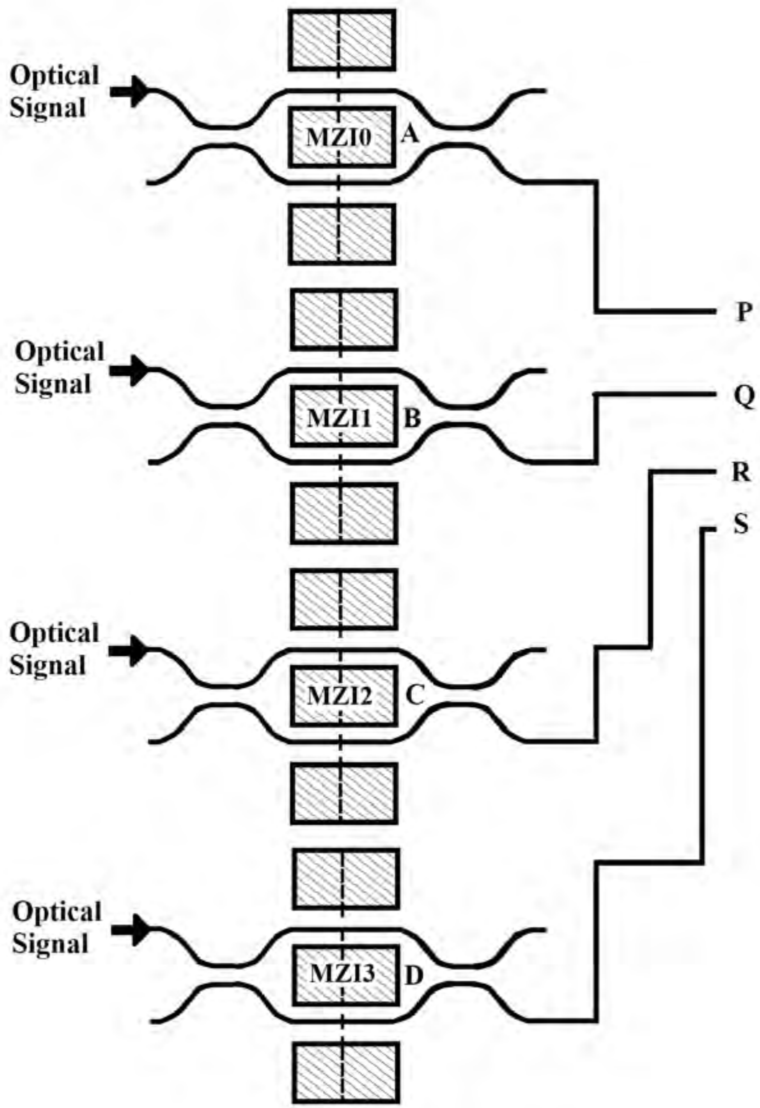

Table: Truth table of 1's complement device

Binary input (4 bit number)				1's complement			
A	B	C	D	P	Q	R	S
0	0	0	0	1	1	1	1
0	0	0	1	1	1	1	0
0	0	1	0	1	1	0	1
0	0	1	1	1	1	0	0
0	1	0	0	1	0	1	1
0	1	0	1	1	0	1	0
0	1	1	0	1	0	0	1
0	1	1	1	1	0	0	0
1	0	0	0	0	1	1	1
1	0	0	1	0	1	1	0
1	0	1	0	0	1	0	1
1	0	1	1	0	1	0	0
1	1	0	0	0	0	1	1
1	1	0	1	0	0	1	0
1	1	1	0	0	0	0	1
1	1	1	1	0	0	0	0

Figure: Schematic diagram of 1's complement using MZIs

Mathematical Expression for 1's complement device

Normalized power at second output port of MZI1 is written as;

$$P = cos^2\left(\frac{\Delta\varphi_{MZI1}}{2}\right)$$

Normalized power at second output port of MZI2

$$Q = cos^2\left(\frac{\Delta\varphi_{MZI2}}{2}\right)$$

Normalized power at second output port of MZI3

$$R = cos^2\left(\frac{\Delta\varphi_{MZI3}}{2}\right)$$

Normalized power at second output port of MZI4

$$S = cos^2\left(\frac{\Delta\varphi_{MZI4}}{2}\right)$$

MATLAB simulation Results of 1's complement device

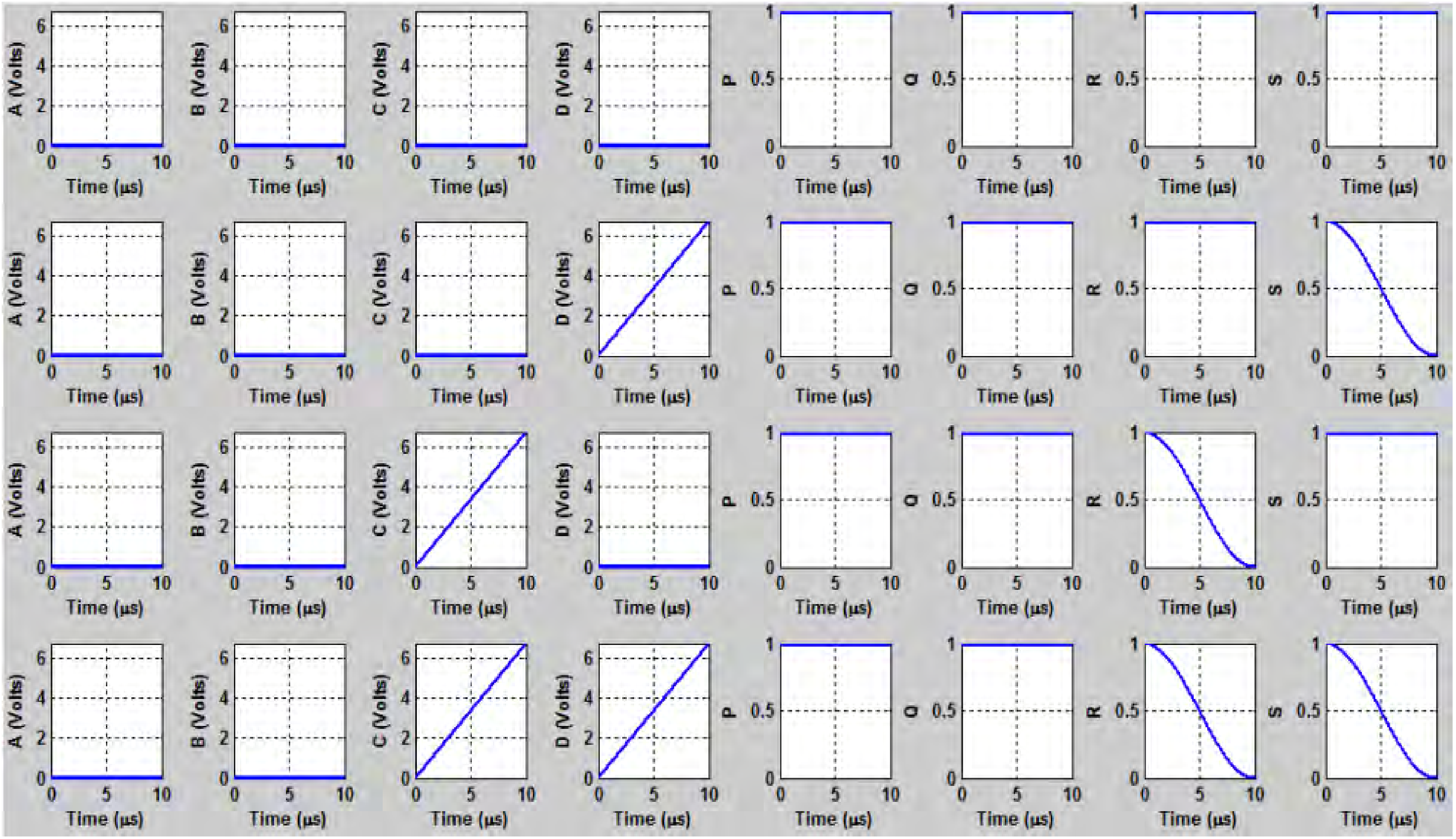

Figure: MATLAB simulation result of 1's complement for different $ABCD$ (0000 – 0011)

BPM Layout of 1's complement device

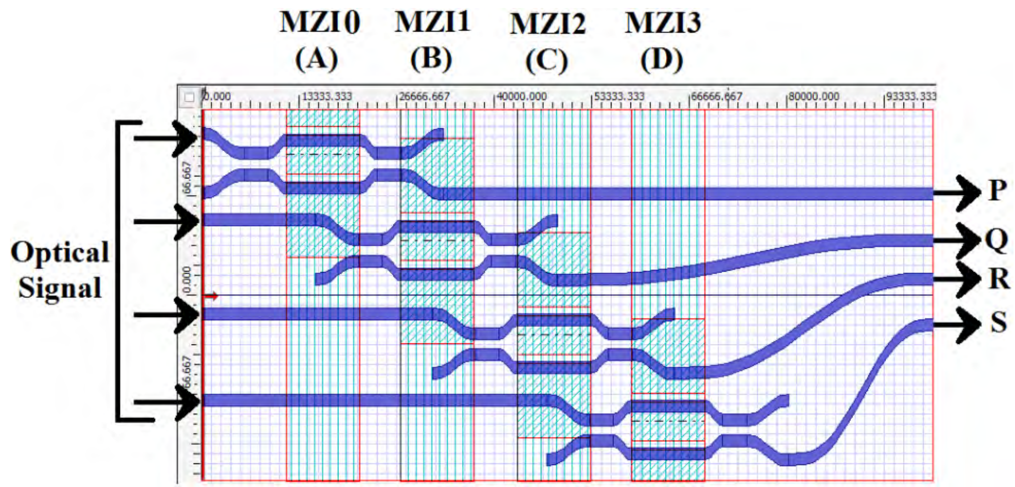

Figure: BPM layout of 1's complement device

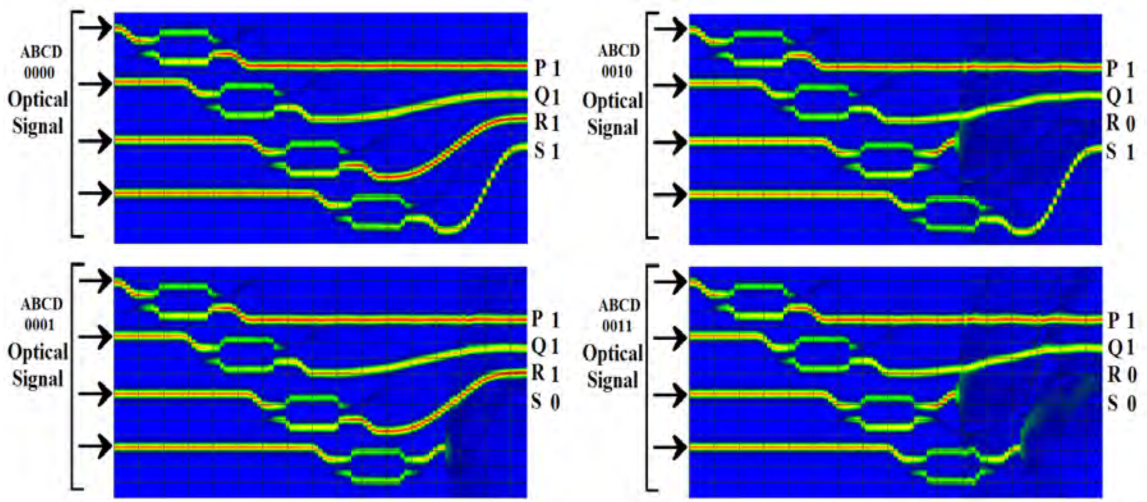

Figure: BPM simulation result of 1's complement device for different control signal $ABCD\ (0000 - 0011)$

2's complement device

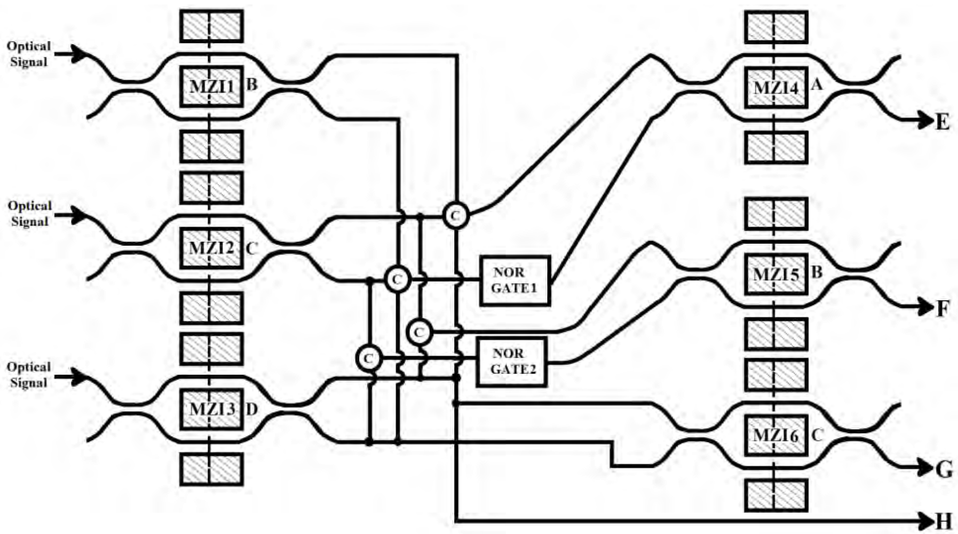

Figure: Schematic layout of 2's complement device

Table: Truth table of 2's complement device

Binary input (4 bit number)				2's complement			
A	**B**	**C**	**D**	**E**	**F**	**G**	**H**
0	0	0	0	0	0	0	0
0	0	0	1	1	1	1	1
0	0	1	0	1	1	1	0
0	0	1	1	1	1	0	1
0	1	0	0	1	1	0	0
0	1	0	1	1	0	1	1
0	1	1	0	1	0	1	0
0	1	1	1	1	0	0	1
1	0	0	0	1	0	0	0
1	0	0	1	0	1	1	1
1	0	1	0	0	1	1	0
1	0	1	1	0	1	0	1
1	1	0	0	0	1	0	0
1	1	0	1	0	0	1	1
1	1	1	0	0	0	1	0
1	1	1	1	0	0	0	1

Mathematical Expression for 2's complement device

Normalized power at second output port of MZI4 is given as

$$E = \begin{bmatrix} \left\{sin^2\left(\frac{\Delta\varphi_{MZI1}}{2}\right) + sin^2\left(\frac{\Delta\varphi_{MZI2}}{2}\right) + sin^2\left(\frac{\Delta\varphi_{MZI3}}{2}\right)\right\} cos^2\left(\frac{\Delta\varphi_{MZI4}}{2}\right) + \\ \left\{cos^2\left(\frac{\Delta\varphi_{MZI1}}{2}\right) + cos^2\left(\frac{\Delta\varphi_{MZI2}}{2}\right) + cos^2\left(\frac{\Delta\varphi_{MZI3}}{2}\right)\right\} \\ \left\{cos^2\left(\frac{\Delta\varphi_{MZI1}}{2}\right) cos^2\left(\frac{\Delta\varphi_{MZI2}}{2}\right) cos^2\left(\frac{\Delta\varphi_{MZI3}}{2}\right)\right\} sin^2\left(\frac{\Delta\varphi_{MZI4}}{2}\right) \end{bmatrix}$$

Cont….

Normalized power at second output port of MZI5 is given as

$$F = \begin{bmatrix} \left\{sin^2\left(\frac{\Delta\varphi_{MZI2}}{2}\right) + sin^2\left(\frac{\Delta\varphi_{MZI3}}{2}\right)\right\} cos^2\left(\frac{\Delta\varphi_{MZI5}}{2}\right) + \\ \left\{cos^2\left(\frac{\Delta\varphi_{MZI2}}{2}\right) + cos^2\left(\frac{\Delta\varphi_{MZI3}}{2}\right)\right\} \\ \left\{cos^2\left(\frac{\Delta\varphi_{MZI2}}{2}\right) cos^2\left(\frac{\Delta\varphi_{MZI3}}{2}\right)\right\} sin^2\left(\frac{\Delta\varphi_{MZI5}}{2}\right) \end{bmatrix}$$

Normalized power at second output port of MZI6 is given as

$$G = \begin{bmatrix} \left\{sin^2\left(\frac{\Delta\varphi_{MZI3}}{2}\right)\right\} cos^2\left(\frac{\Delta\varphi_{MZI6}}{2}\right) + \\ \left\{cos^2\left(\frac{\Delta\varphi_{MZI3}}{2}\right)\right\} sin^2\left(\frac{\Delta\varphi_{MZI6}}{2}\right) \end{bmatrix}$$

Normalized power at first output port of MZI7 is given as

$$H = sin^2\left(\frac{\Delta\varphi_{MZI3}}{2}\right)$$

MATLAB simulation Results of 2's complement device

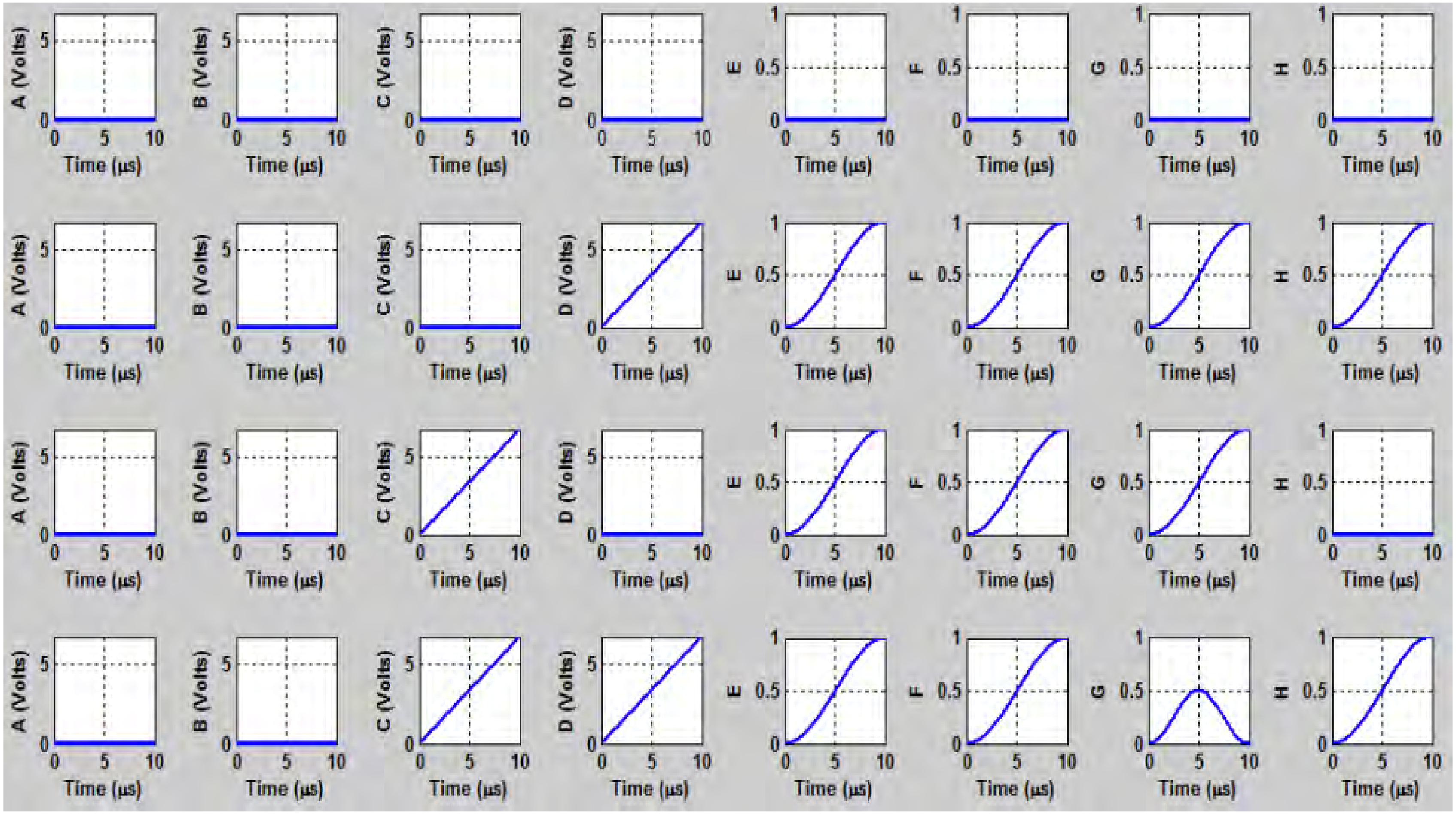

Figure: MATLAB simulation result of 2's complement for differentABCD (0000 – 0011)

BPM Layout of 2's complement device

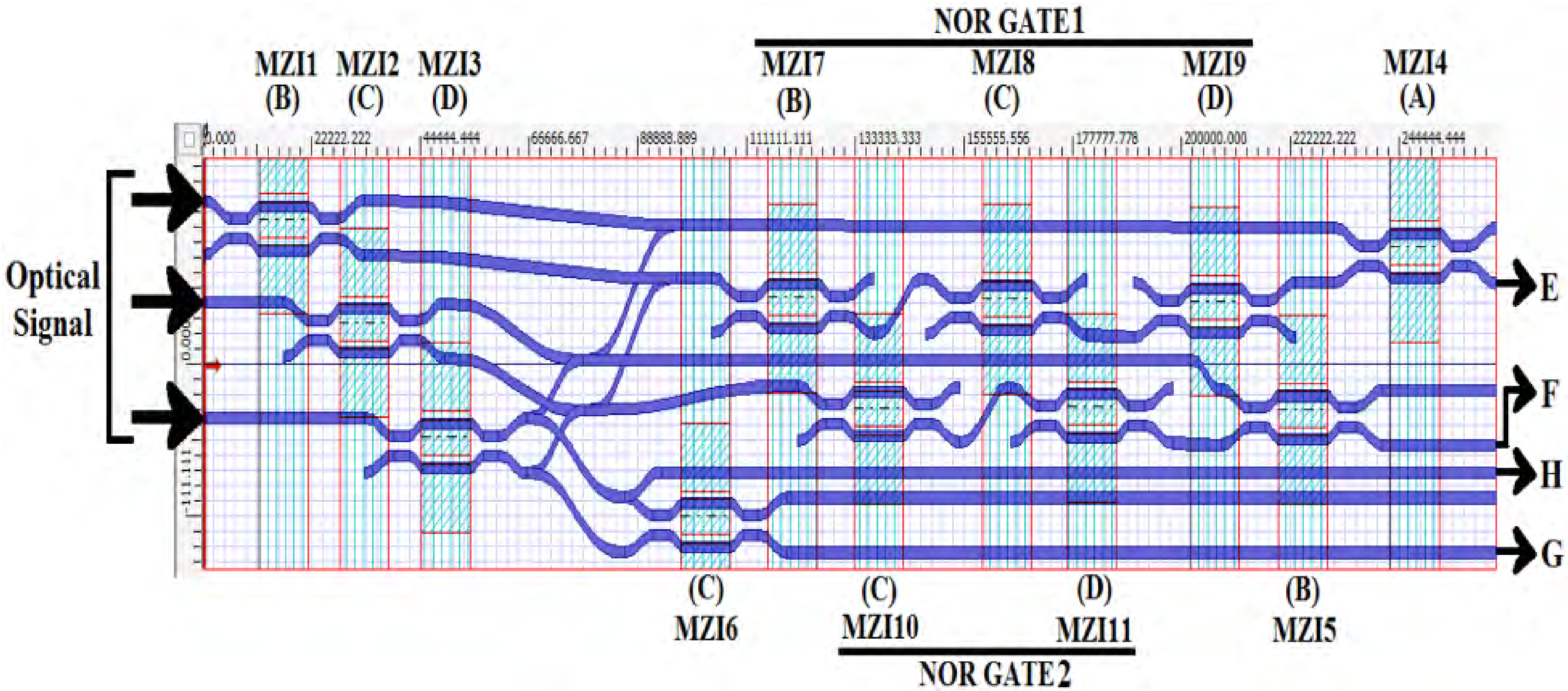

Figure 33: BPM layout of 2's complement device

BPM results of 2's complement device

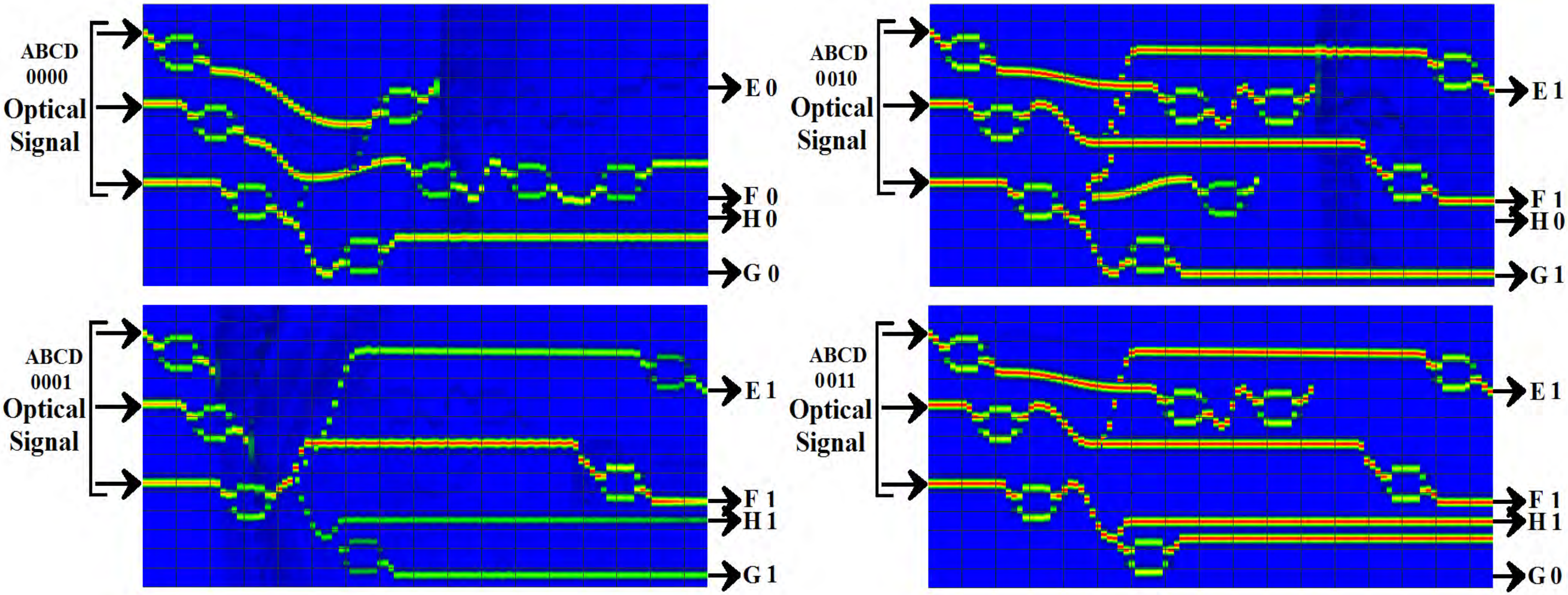

Figure 34: BPM simulation result of 2's complement device for different control signal $ABCD$ (0000 – 0011)

Design of Decoder and Encoder Device

Santosh Kumar et. al., Photonics Network Communication (Springer), (2017) DOI: 10.1007/s11107-017-0718-8

Design of 2 to 4 line Decoder

- Decoder is a device that allows placing digital information from many inputs to many outputs.
- Any application of combinational logic circuit can be implemented by using decoder and external gates.

Cont….

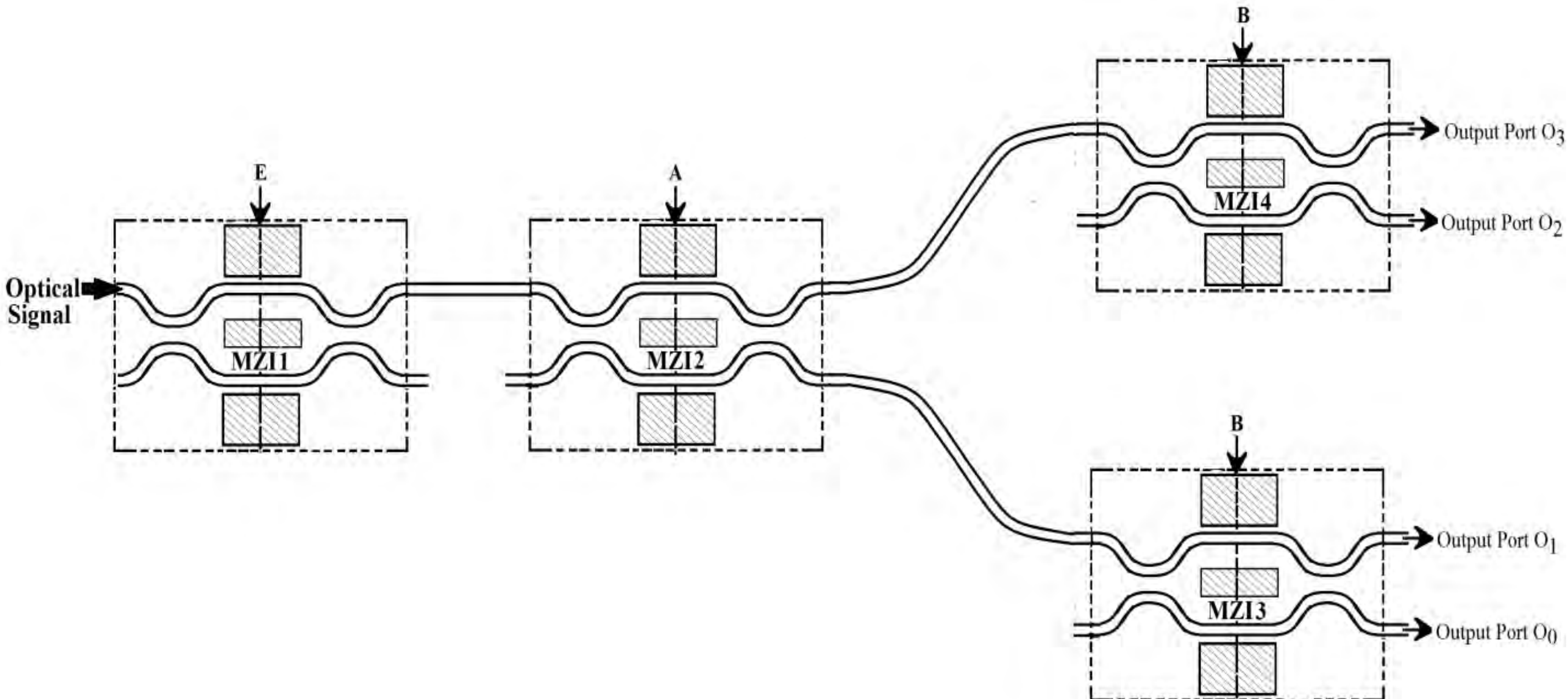

Figure 5: Schematic diagram of 2 to 4 line optical decoder

Table 2: Truth table of 2 to 4 line decoder

Control Signals			Optical propagation at output ports			
E	**A**	**B**	**Output O_0**	**Output O_1**	**Output O_2**	**Output O_3**
0	X	X	0	0	0	0
1	0	0	1	0	0	0
1	0	1	0	1	0	0
1	1	0	0	0	1	0
1	1	1	0	0	0	1

Mathematical Expression for 2 to 4 line decoder

We can write the output O_0 at second output port of MZI3 as;

$$O_0 = \left|\frac{O_{0\,\mathrm{MZI\,3}}}{\mathrm{E_{in}}}\right|^2 = sin^2\left(\frac{\Delta\phi_{MZI1}}{2}\right)cos^2\left(\frac{\Delta\phi_{MZI2}}{2}\right)cos^2\left(\frac{\Delta\phi_{MZI3}}{2}\right) \quad (8)$$

$$O_1 = \left|\frac{O_{1\,\mathrm{MZI\,3}}}{\mathrm{E_{in}}}\right|^2 = sin^2\left(\frac{\Delta\phi_{MZI1}}{2}\right)cos^2\left(\frac{\Delta\phi_{MZI2}}{2}\right)sin^2\left(\frac{\Delta\phi_{MZI3}}{2}\right) \quad (9)$$

$$O_2 = \left|\frac{O_{2\,\mathrm{MZI\,4}}}{\mathrm{E_{in}}}\right|^2 = sin^2\left(\frac{\Delta\phi_{MZI1}}{2}\right)sin^2\left(\frac{\Delta\phi_{MZI2}}{2}\right)cos^2\left(\frac{\Delta\phi_{MZI4}}{2}\right) \quad (10)$$

$$O_3 = \left|\frac{O_{3\,\mathrm{MZI\,4}}}{\mathrm{E_{in}}}\right|^2 = sin^2\left(\frac{\Delta\phi_{MZI1}}{2}\right)sin^2\left(\frac{\Delta\phi_{MZI2}}{2}\right)sin^2\left(\frac{\Delta\phi_{MZI4}}{2}\right) \quad (11)$$

MATLAB simulation Results of 2 to 4 line decoder

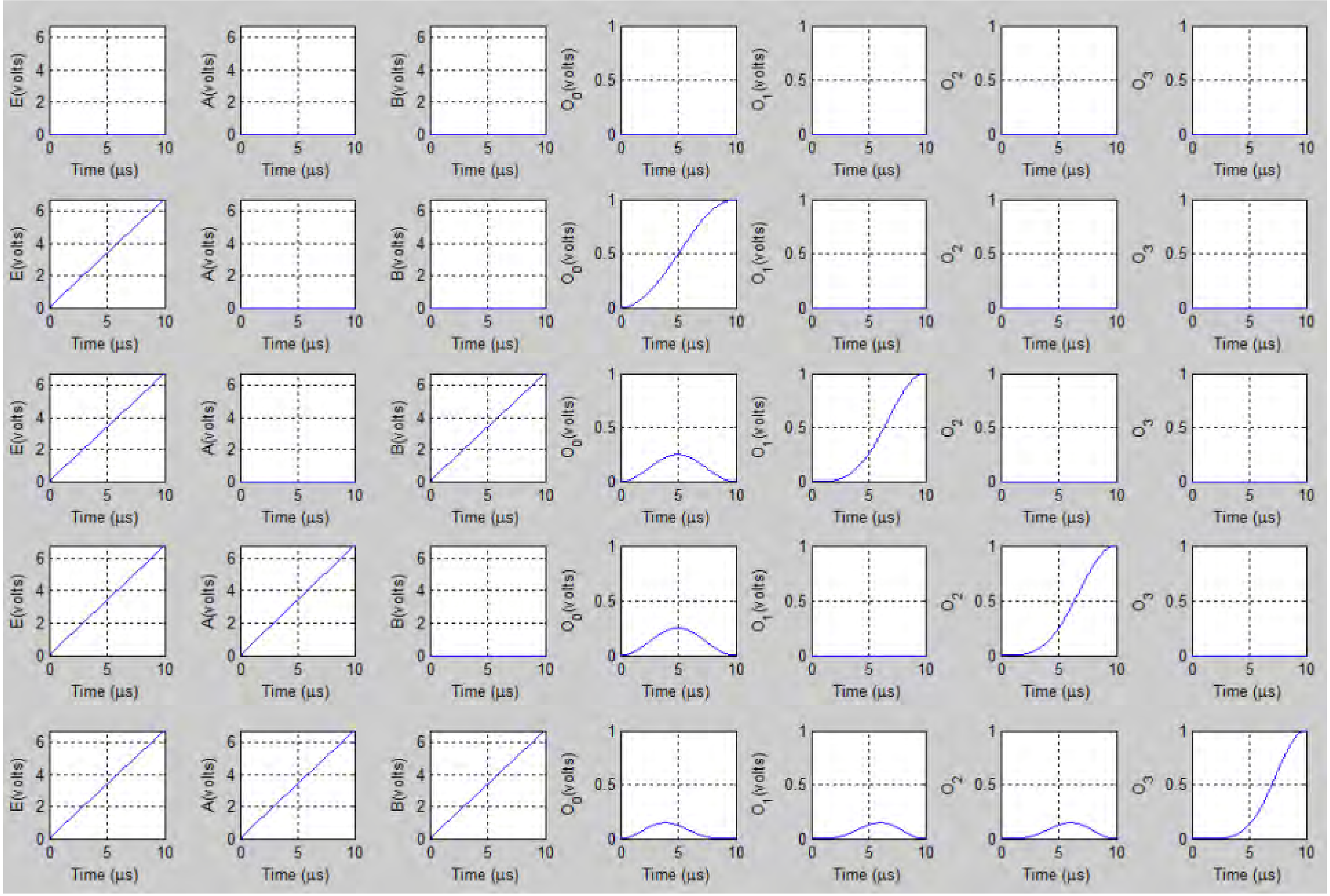

Figure 6: MATLAB simulation result of 2 to 4 line decoder

BPM Layout of 2 to 4 line decoder

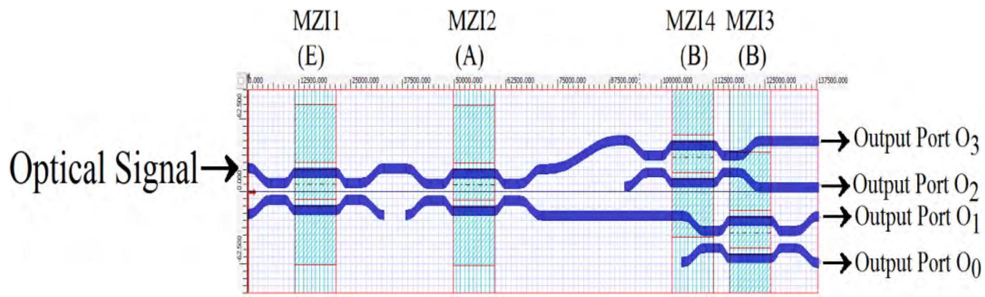

Figure 7: Layout of 2 to 4 line decoder

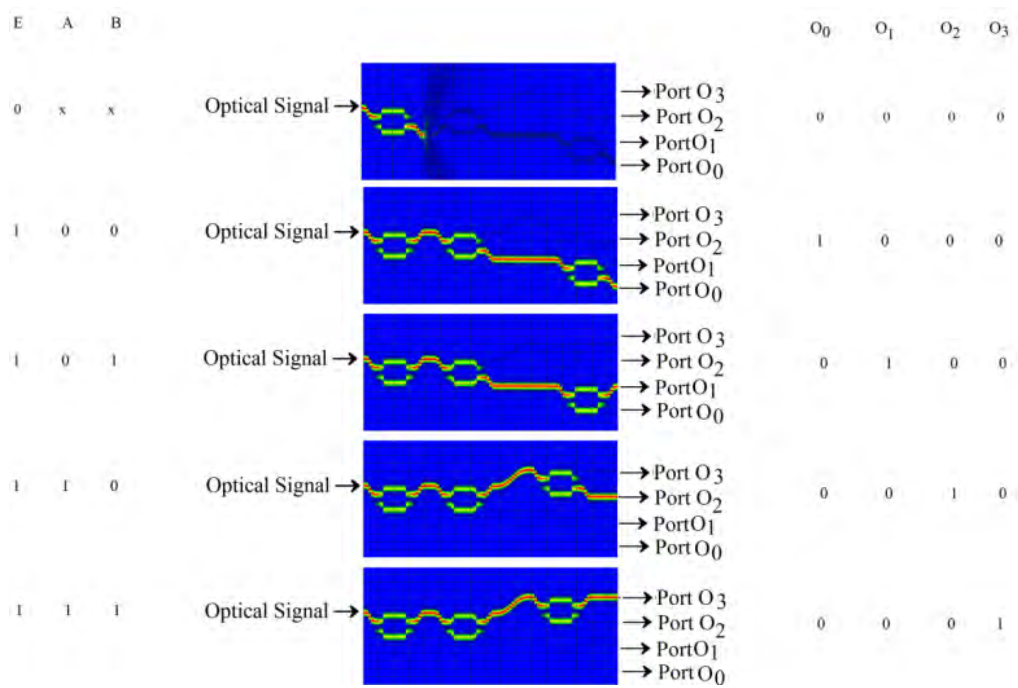

Figure 8: Results of 2 to 4 line decoder for different combinations of control signals (E, A and B) obtained through beam propagation method

Design of 3 to 8 line decoder

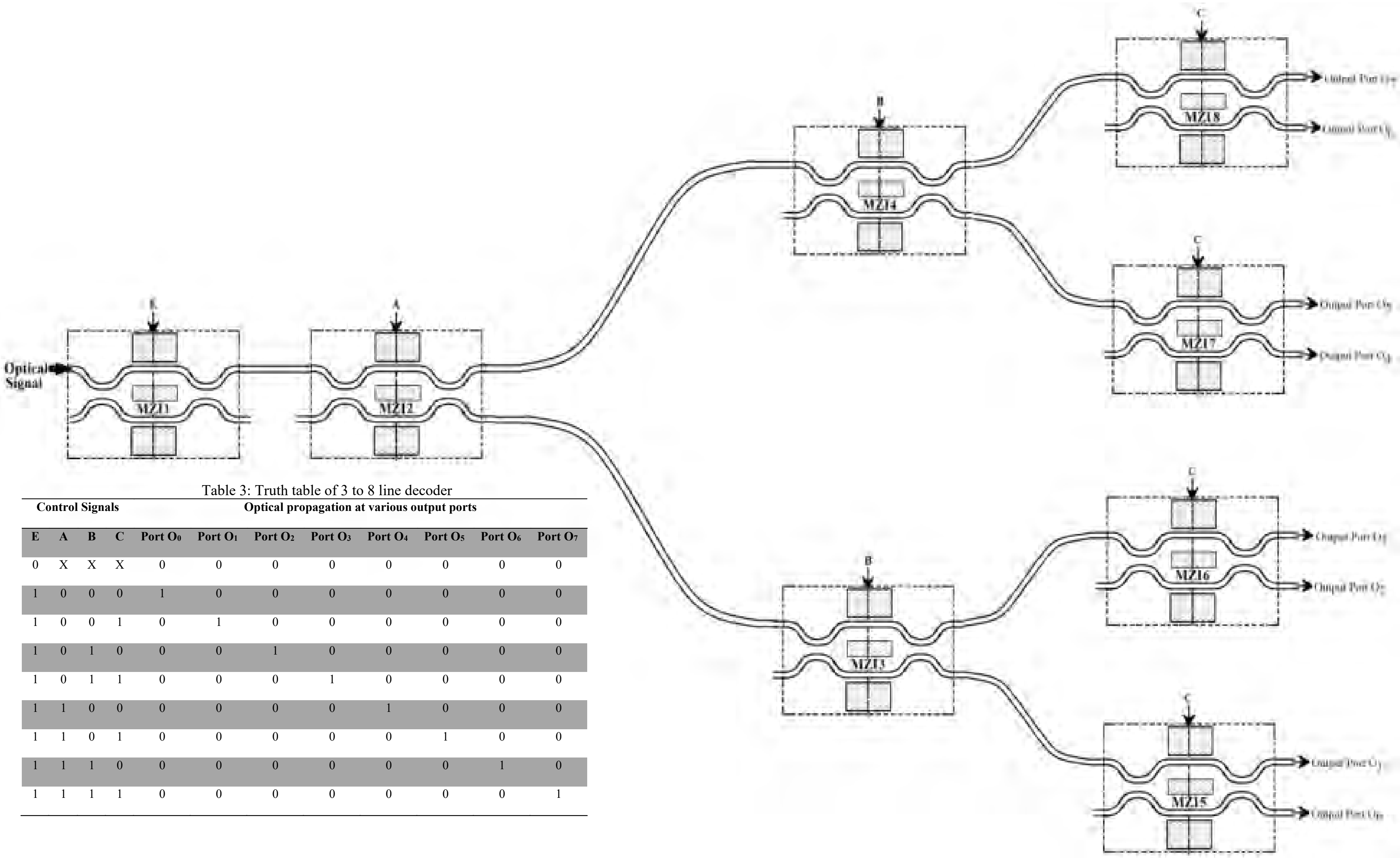

Table 3: Truth table of 3 to 8 line decoder

Control Signals				Optical propagation at various output ports							
E	A	B	C	Port O_0	Port O_1	Port O_2	Port O_3	Port O_4	Port O_5	Port O_6	Port O_7
0	X	X	X	0	0	0	0	0	0	0	0
1	0	0	0	1	0	0	0	0	0	0	0
1	0	0	1	0	1	0	0	0	0	0	0
1	0	1	0	0	0	1	0	0	0	0	0
1	0	1	1	0	0	0	1	0	0	0	0
1	1	0	0	0	0	0	0	1	0	0	0
1	1	0	1	0	0	0	0	0	1	0	0
1	1	1	0	0	0	0	0	0	0	1	0
1	1	1	1	0	0	0	0	0	0	0	1

Figure 9: Schematic digram of 3 to 8 lineoptical decoder

Mathematical Expression for 3 to 8 Line Decoder

The output O_0 at second output port of MZI5 as;

$$O_0 = \left|\frac{O_{0\,\mathrm{MZI\,5}}}{\mathrm{E_{in}}}\right|^2 = sin^2\left(\frac{\Delta\emptyset_{MZI\,1}}{2}\right) cos^2\left(\frac{\Delta\emptyset_{MZI\,2}}{2}\right) cos^2\left(\frac{\Delta\emptyset_{MZI\,3}}{2}\right) cos^2\left(\frac{\Delta\emptyset_{MZI\,5}}{2}\right) \tag{12}$$

The output O_1 at first output port of MZI5 as;

$$O_1 = \left|\frac{O_{1\,\mathrm{MZI\,5}}}{\mathrm{E_{in}}}\right|^2 = sin^2\left(\frac{\Delta\emptyset_{MZI\,1}}{2}\right) cos^2\left(\frac{\Delta\emptyset_{MZI\,2}}{2}\right) cos^2\left(\frac{\Delta\emptyset_{MZI\,3}}{2}\right) sin^2\left(\frac{\Delta\emptyset_{MZI\,5}}{2}\right) \tag{13}$$

The output O_2 at second output port of MZI6 as;

$$O_2 = \left|\frac{O_{2\,\mathrm{MZI\,6}}}{\mathrm{E_{in}}}\right|^2 = sin^2\left(\frac{\Delta\emptyset_{MZI\,1}}{2}\right) cos^2\left(\frac{\Delta\emptyset_{MZI\,2}}{2}\right) sin^2\left(\frac{\Delta\emptyset_{MZI\,3}}{2}\right) cos^2\left(\frac{\Delta\emptyset_{MZI\,6}}{2}\right) \tag{14}$$

The output O_3 at first output port of MZI6 as;

$$O_3 = \left|\frac{O_{3\,\mathrm{MZI\,6}}}{\mathrm{E_{in}}}\right|^2 = sin^2\left(\frac{\Delta\emptyset_{MZI\,1}}{2}\right) cos^2\left(\frac{\Delta\emptyset_{MZI\,2}}{2}\right) sin^2\left(\frac{\Delta\emptyset_{MZI\,3}}{2}\right) \mathrm{sin}^2\left(\frac{\Delta\emptyset_{MZI\,6}}{2}\right) \tag{15}$$

Cont….

The output O_4 at second output port of MZI7 as

$$O_4 = \left|\frac{O_{4\,\mathrm{MZI}\,7}}{\mathrm{E_{in}}}\right|^2 = sin^2\left(\frac{\Delta\emptyset_{MZI1}}{2}\right) sin^2\left(\frac{\Delta\emptyset_{MZI2}}{2}\right) cos^2\left(\frac{\Delta\emptyset_{MZI4}}{2}\right) cos^2\left(\frac{\Delta\emptyset_{MZI7}}{2}\right) \qquad (16)$$

The output O_5 at first output port of MZI7 as

$$O_5 = \left|\frac{O_{5\,\mathrm{MZI}\,7}}{\mathrm{E_{in}}}\right|^2 = sin^2\left(\frac{\Delta\emptyset_{MZI1}}{2}\right) sin^2\left(\frac{\Delta\emptyset_{MZI2}}{2}\right) cos^2\left(\frac{\Delta\emptyset_{MZI4}}{2}\right) sin\left(\frac{\Delta\emptyset_{MZI7}}{2}\right) \qquad (17)$$

The output O_6 at second output port of MZI8 as

$$O_6 = \left|\frac{O_{6\,\mathrm{MZI}\,8}}{\mathrm{E_{in}}}\right|^2 = sin^2\left(\frac{\Delta\emptyset_{MZI1}}{2}\right) sin^2\left(\frac{\Delta\emptyset_{MZI2}}{2}\right) sin^2\left(\frac{\Delta\emptyset_{MZI4}}{2}\right) cos^2\left(\frac{\Delta\emptyset_{MZI8}}{2}\right) \qquad (18)$$

The output O_7 at first output port of MZI8 as

$$O_7 = \left|\frac{O_{7\,\mathrm{MZI}\,8}}{\mathrm{E_{in}}}\right|^2 = sin^2\left(\frac{\Delta\emptyset_{MZI1}}{2}\right) sin^2\left(\frac{\Delta\emptyset_{MZI2}}{2}\right) sin^2\left(\frac{\Delta\emptyset_{MZI4}}{2}\right) sin^2\left(\frac{\Delta\emptyset_{MZI8}}{2}\right) \qquad (19)$$

BPM Layout of 3 to 8 Line Decoder

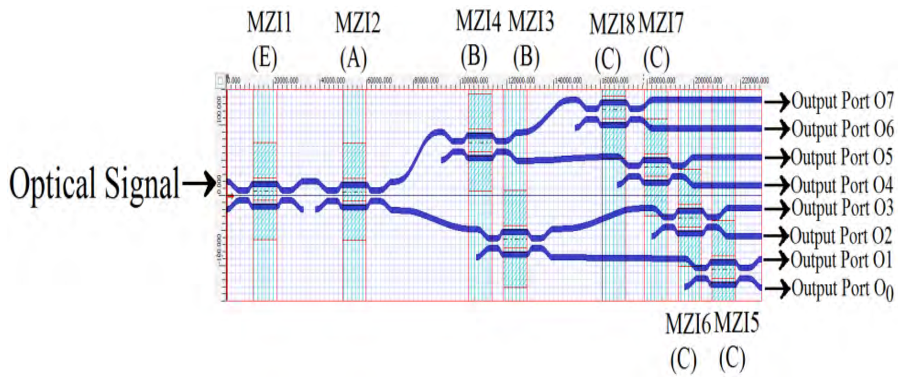

Figure 10: Layout diagram of 3 to 8 line decoder

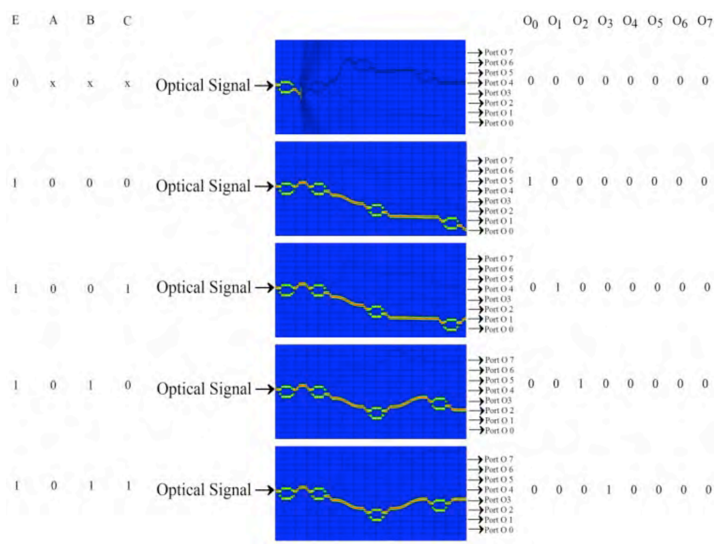

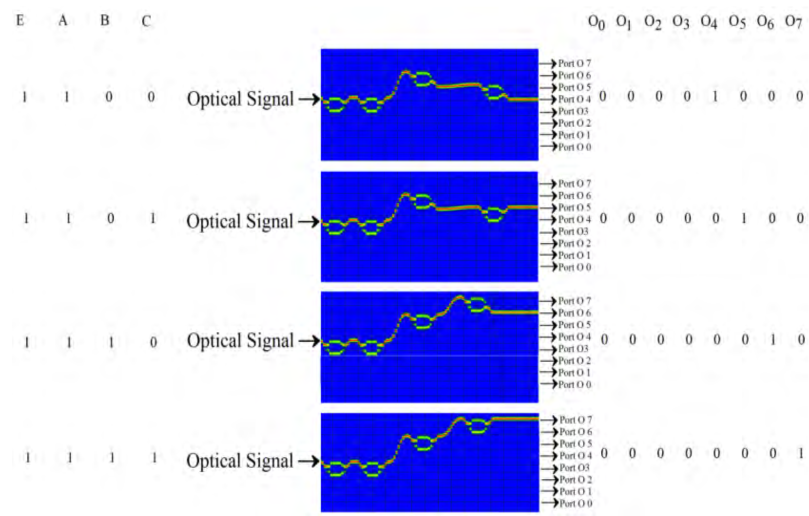

Figure 11 (a): Simulation results of 3 to 8 line decoder forcontrol signals E, A, B and $C$is 1000 to 1011 obtained through beam propagation method

Figure 11 (b): Simulation results of 3 to 8 line decoder forcontrol signals E, A, B and $C$is 1100 to 1111 obtained through beam propagation method

Design of 4 to 2 line Encoder

Santosh Kumar et. al., Proc. SPIE 9889, Optical Modelling and Design IV, 98890H Brussels, Belgium 2016.

Design of 4 to 2 line Encoder

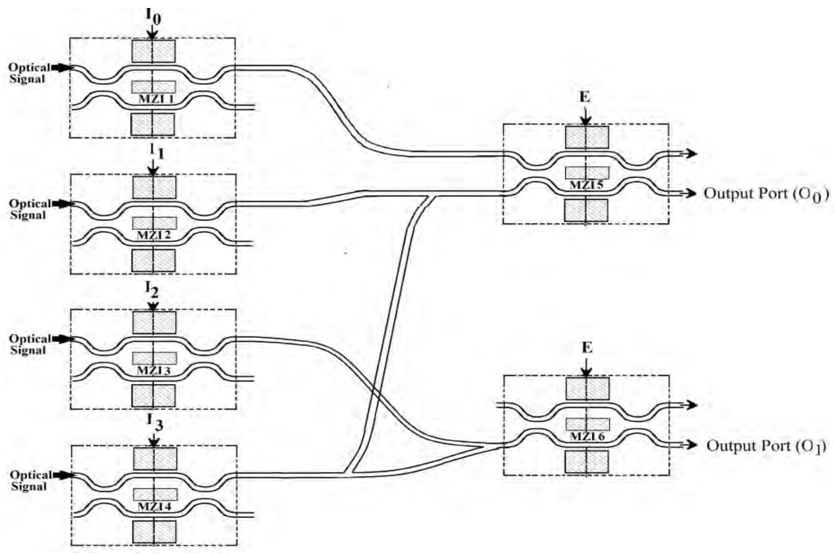

Figure 12: Schematic diagram of 4 to 2 Line Encoder using MZIs

Table 4: Truth table of 4 to 2 line Encoder

Control Signals					Output at different Ports	
E	**I_0**	**I_1**	**I_2**	**I_3**	**Output (O_1)**	**Output (O_0)**
1	1	0	0	0	0	0
1	0	1	0	0	0	1
1	0	0	1	0	1	0
1	0	0	0	1	1	1

Mathematical Expression for 4 to 2 Line Encoder

To operate 4 to 2 line encoder, the power appears at second output port of MZI5 and MZI6. So the normalized power at the second output port is computed as follows:

$$O_0 = sin^2\left(\frac{\Delta\emptyset_{MZI1}}{2}\right)cos^2\left(\frac{\Delta\emptyset_{MZI5}}{2}\right) + sin^2\left(\frac{\Delta\emptyset_{MZI2}}{2}\right)sin^2\left(\frac{\Delta\emptyset_{MZI5}}{2}\right) + sin^2\left(\frac{\Delta\emptyset_{MZI4}}{2}\right)sin^2\left(\frac{\Delta\emptyset_{MZI5}}{2}\right) \quad (20)$$

$$O_1 = sin^2\left(\frac{\Delta\emptyset_{MZI3}}{2}\right)sin^2\left(\frac{\Delta\emptyset_{MZI6}}{2}\right) + sin^2\left(\frac{\Delta\emptyset_{MZI4}}{2}\right)sin^2\left(\frac{\Delta\emptyset_{MZI6}}{2}\right) \quad (21)$$

MATLAB simulation Results of 4 to 2 Line Encoder

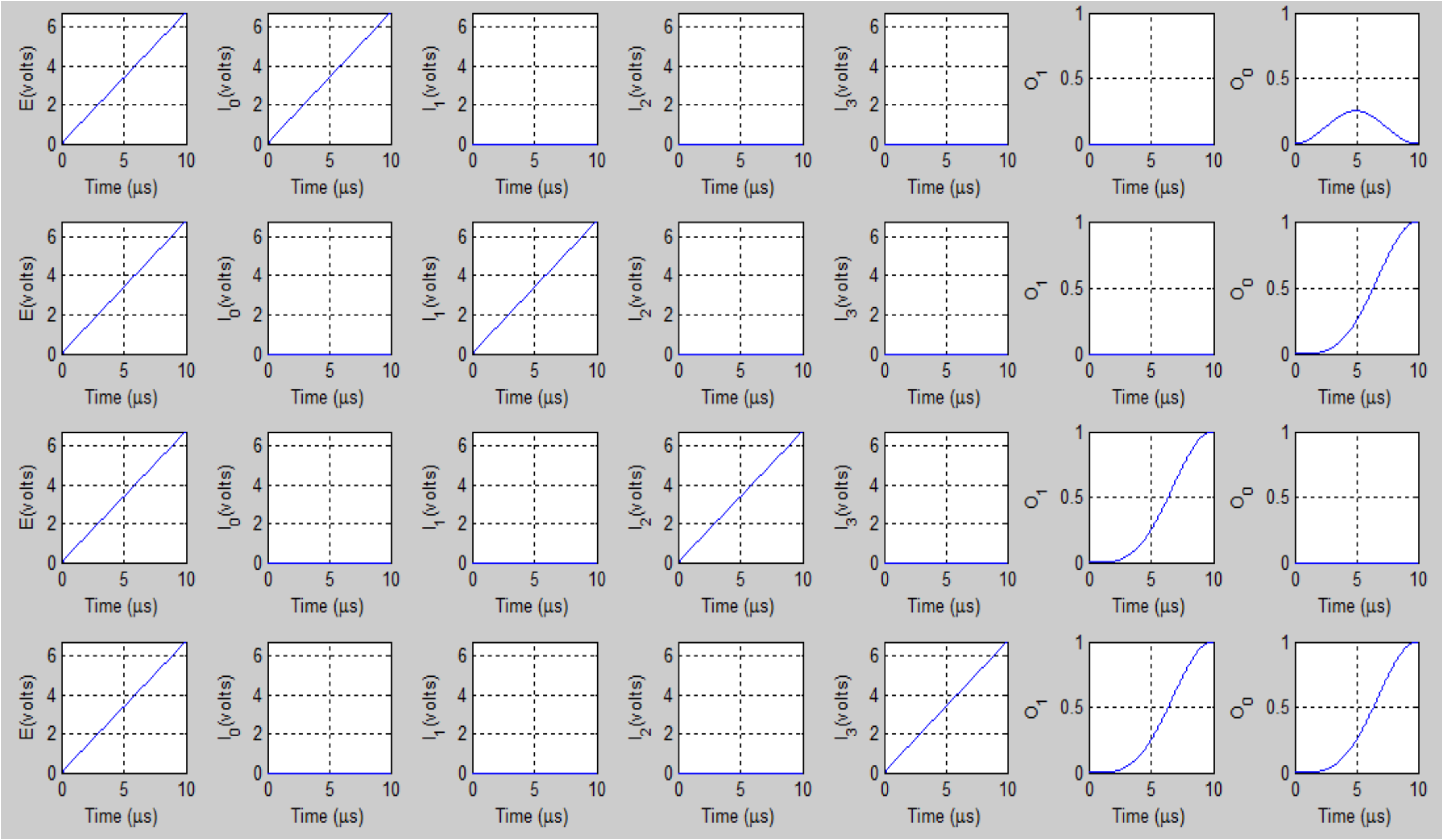

Figure 13: MATLAB simulation result of 4 to 2 Line Encoder

BPM layout and results of 4 to 2 Line Encoder

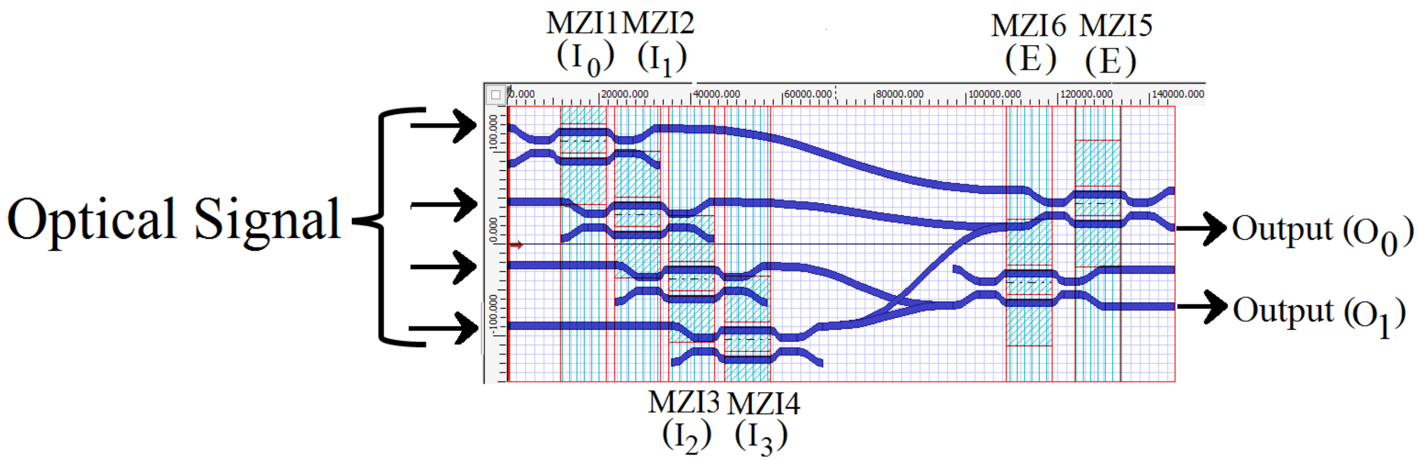

Figure 14 (a): OptiBPM layout diagram of 4 to 2 Line Encoder

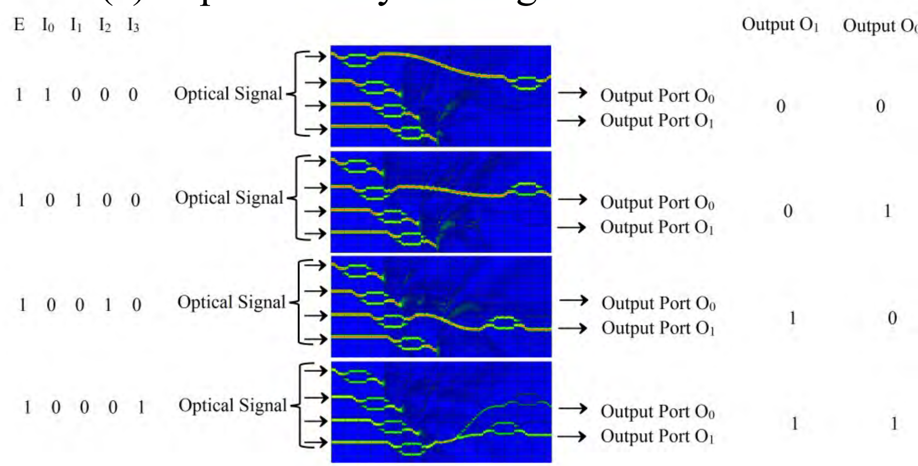

Figure 14 (b): OptiBPM simulation results for 4 to 2 Line Encoder

Design of Four-Bit Priority Encoder using MZIs

<u>Santosh Kumar</u>, et. al., IEEE/Workshop on Recent Advances in Photonics 2015, Indian Institute of Science, Bangalore, India, 16-17 Dec., 2015 (IEEE Xplore).

Design of Four-Bit Priority Encoder using MZIs

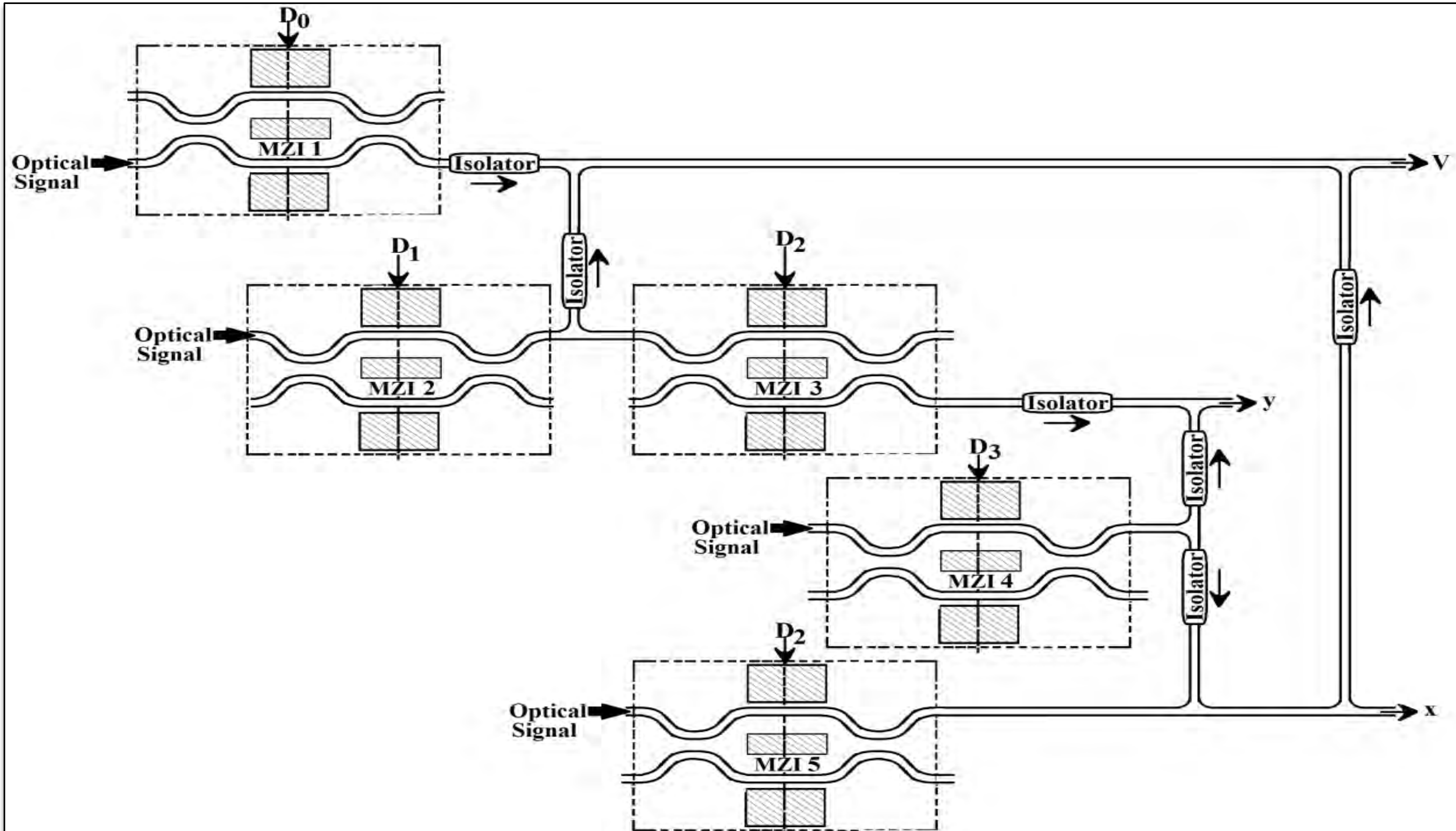

Figure 22: Schematic diagram of 4-bit priority encoder using MZIs

Mathematical expression of Four-Bit Priority Encoder

The proper combination of minterms provides the expression for the output of the priority encoder. The expression for valid-bit (V) can be written as

$$V = \sin^2\left(\frac{\Delta\varphi_{MZI\,1}}{2}\right) + \sin^2\left(\frac{\Delta\varphi_{MZI\,2}}{2}\right) + \sin^2\left(\frac{\Delta\varphi_{MZI\,4}}{2}\right) + \sin^2\left(\frac{\Delta\varphi_{MZI\,5}}{2}\right) \qquad (30)$$

Similarly x and y can be represented as

$$x = \sin^2\left(\frac{\Delta\varphi_{MZI\,4}}{2}\right) + \sin^2\left(\frac{\Delta\varphi_{MZI\,5}}{2}\right) \qquad (31)$$

$$y = \sin^2\left(\frac{\Delta\varphi_{MZI\,4}}{2}\right) + \sin^2\left(\frac{\Delta\varphi_{MZI\,2}}{2}\right)\cos^2\left(\frac{\Delta\varphi_{MZI\,3}}{2}\right) \qquad (32)$$

Where,

$$\left.\begin{aligned}
\varphi_{0MZI\,1} &= \frac{\varphi_{1MZI\,1} + \varphi_{2MZI\,1}}{2}\\
\varphi_{0MZI\,2} &= \frac{\varphi_{1MZI\,2} + \varphi_{2MZI\,2}}{2}\\
\varphi_{0MZI\,3} &= \frac{\varphi_{1MZI\,3} + \varphi_{2MZI\,3}}{2}\\
\varphi_{0MZI\,4} &= \frac{\varphi_{1MZI\,4} + \varphi_{2MZI\,4}}{2}\\
\varphi_{0MZI\,5} &= \frac{\varphi_{1MZI\,5} + \varphi_{2MZI\,5}}{2}
\end{aligned}\right\}
\qquad
\left.\begin{aligned}
\Delta\varphi_{MZI\,1} &= \varphi_{1MZI\,1} - \varphi_{2MZI\,1} = \frac{\pi}{V_\pi}D_0\\
\Delta\varphi_{MZI\,2} &= \varphi_{1MZI\,2} - \varphi_{2MZI\,2} = \frac{\pi}{V_\pi}D_1\\
\Delta\varphi_{MZI\,3} &= \varphi_{1MZI\,3} - \varphi_{2MZI\,3} = \frac{\pi}{V_\pi}D_2\\
\Delta\varphi_{MZI\,4} &= \varphi_{1MZI\,4} - \varphi_{2MZI\,4} = \frac{\pi}{V_\pi}D_3\\
\Delta\varphi_{MZI\,5} &= \varphi_{1MZI\,5} - \varphi_{2MZI\,5} = \frac{\pi}{V_\pi}D_2
\end{aligned}\right\}$$

MATLAB Result of Four-Bit Priority Encoder

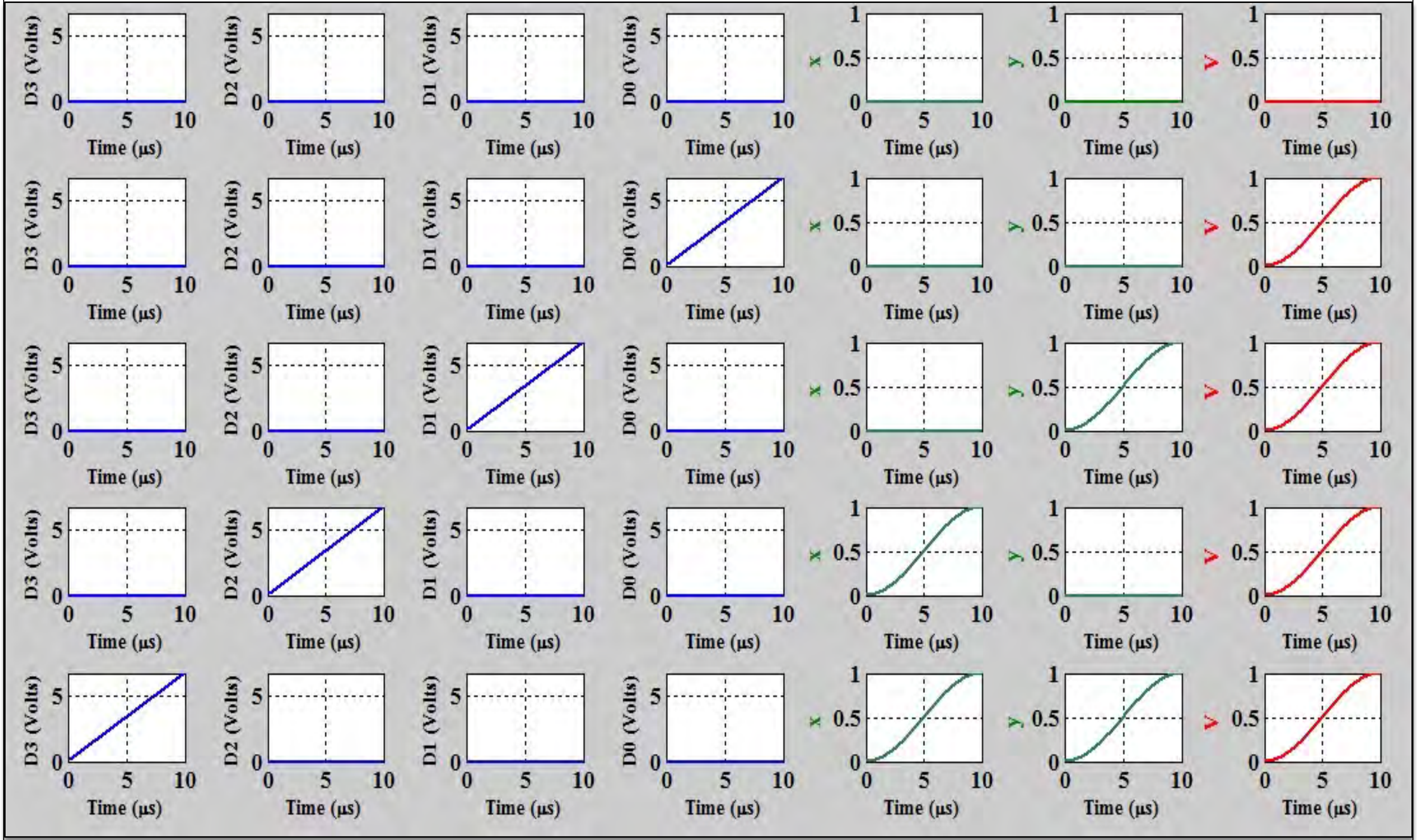

Figure 23: MATLAB Simulation results of four-bit priority encoder for different combinations of data signals.

Dr. Santosh Kumar

BPM Result of Four-Bit Priority Encoder

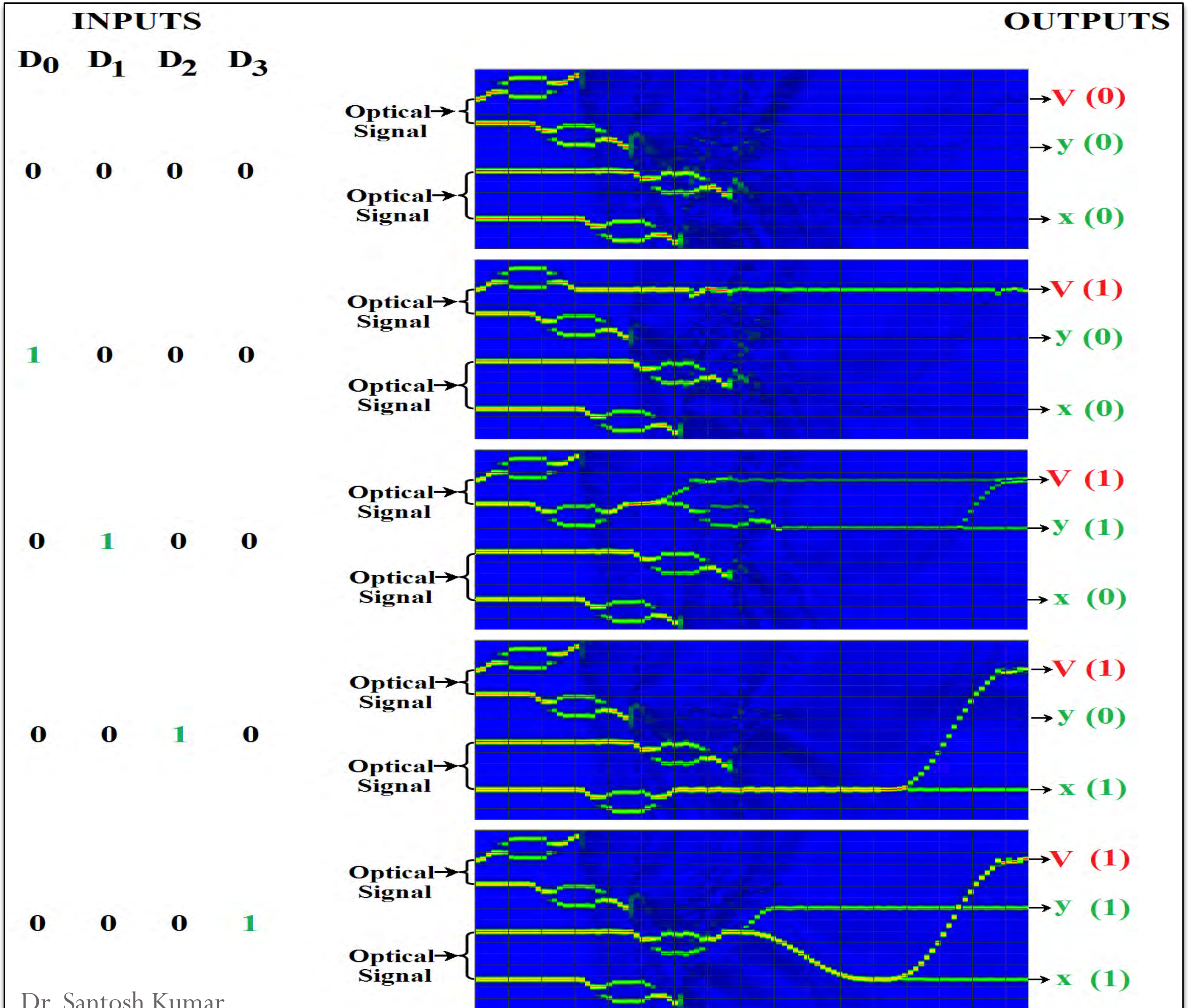

Dr. Santosh Kumar

Figure 24: Results of four-bit priority encoder for different combinations of data signals obtained through BPM.

Design of Optical seven segment decoder

Santosh Kumar et. al., Optical Engineering (SPIE), Vol. 56, Issue 1, pp. 017103 (Jan 06, 2017).

Design of Seven Segment Decoder

- Seven segment decoder is a device that allows placing digital information from many inputs to many outputs optically.

- Conventional seven segment decoder having seven LED for showing the decimal digit 0 to 9. Each LED require around 20mA current for their operation, so one seven segment decoder requires 140mA current.

Cont….

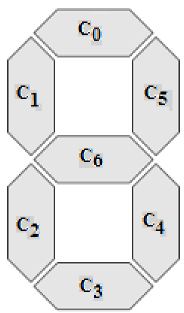

Figure 35: structure of seven segment display

Table 10: Truth table for seven segment decoder

A	B	C	D	C_0	C_1	C_2	C_3	C_4	C_5	C_6
0	0	0	0	1	1	1	1	1	1	0
0	0	0	1	0	1	1	0	0	0	0
0	0	1	0	1	1	0	1	1	0	1
0	0	1	1	1	1	1	1	0	0	1
0	1	0	0	0	1	1	0	0	1	1
0	1	0	1	1	0	1	1	0	1	1
0	1	1	0	1	0	1	1	1	1	1
0	1	1	1	1	1	1	0	0	0	0
1	0	0	0	1	1	1	1	1	1	1
1	0	0	1	1	1	1	1	0	1	1

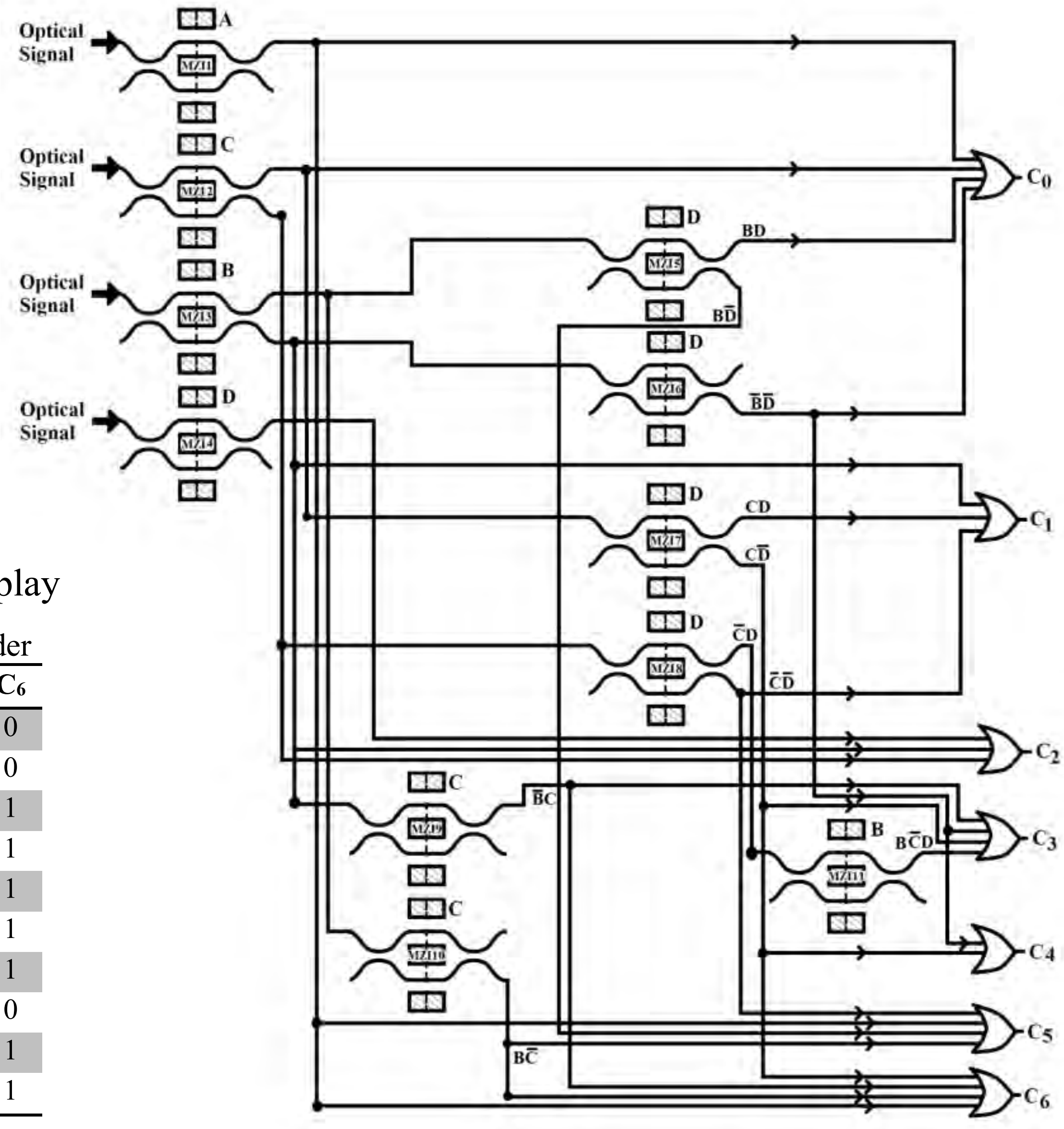

Figure 36: Schematic layout diagram of seven segment decoder

Cont….

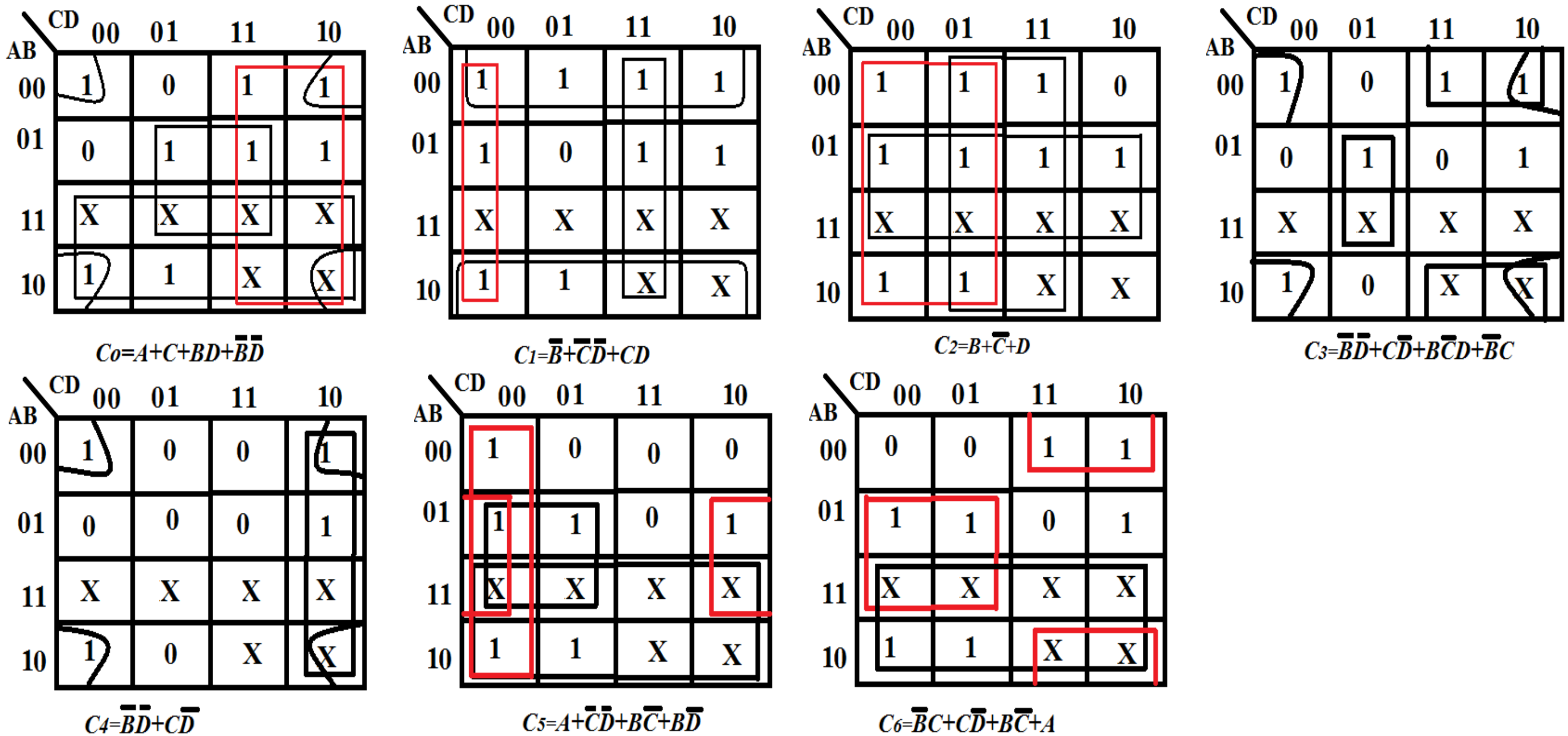

Figure 37: K Map for seven segment decoder

Mathematical Expression for Seven Segment Device

Normalized power at output port C_0 can be given as:

$$C_0 = sin^2\left(\frac{\Delta\emptyset_{MZI1}}{2}\right) + sin^2\left(\frac{\Delta\emptyset_{MZI2}}{2}\right) + sin^2\left(\frac{\Delta\emptyset_{MZI3}}{2}\right) \times sin^2\left(\frac{\Delta\emptyset_{MZI5}}{2}\right) + cos^2\left(\frac{\Delta\emptyset_{MZI3}}{2}\right) \times cos^2\left(\frac{\Delta\emptyset_{MZI6}}{2}\right) \quad (43)$$

Normalized power at output port C_1 is given as

$$C_1 = cos^2\left(\frac{\Delta\emptyset_{MZI3}}{2}\right) + sin^2\left(\frac{\Delta\emptyset_{MZI2}}{2}\right) \times sin^2\left(\frac{\Delta\emptyset_{MZI7}}{2}\right) + cos^2\left(\frac{\Delta\emptyset_{MZI2}}{2}\right) \times cos^2\left(\frac{\Delta\emptyset_{MZI8}}{2}\right) \quad (44)$$

Normalized power at output port C_2 is given as

$$C_2 = cos^2\left(\frac{\Delta\emptyset_{MZI2}}{2}\right) + cos^2\left(\frac{\Delta\emptyset_{MZI3}}{2}\right) + sin^2\left(\frac{\Delta\emptyset_{MZI4}}{2}\right) \quad (45)$$

Cont….

Normalized power at output port C_3 is given as

$$C_3 = cos^2\left(\frac{\Delta\emptyset_{MZI3}}{2}\right) \times sin^2\left(\frac{\Delta\emptyset_{MZI9}}{2}\right) + sin^2\left(\frac{\Delta\emptyset_{MZI2}}{2}\right) \times cos^2\left(\frac{\Delta\emptyset_{MZI7}}{2}\right) + cos^2\left(\frac{\Delta\emptyset_{MZI3}}{2}\right) \times cos^2\left(\frac{\Delta\emptyset_{MZI6}}{2}\right) + cos^2\left(\frac{\Delta\emptyset_{MZI2}}{2}\right) \times sin^2\left(\frac{\Delta\emptyset_{MZI8}}{2}\right) \quad (46)$$

Normalized power at output port C_4 is given as

$$C_4 = sin^2\left(\frac{\Delta\emptyset_{MZI2}}{2}\right) \times cos^2\left(\frac{\Delta\emptyset_{MZI7}}{2}\right) + cos^2\left(\frac{\Delta\emptyset_{MZI3}}{2}\right) \times cos^2\left(\frac{\Delta\emptyset_{MZI6}}{2}\right) \quad (47)$$

Normalized power at output port C_5 is given as

$$C_5 = sin^2\left(\frac{\Delta\emptyset_{MZI1}}{2}\right) + cos^2\left(\frac{\Delta\emptyset_{MZI2}}{2}\right) \times cos^2\left(\frac{\Delta\emptyset_{MZI8}}{2}\right) + sin^2\left(\frac{\Delta\emptyset_{MZI3}}{2}\right) \times cos^2\left(\frac{\Delta\emptyset_{MZI5}}{2}\right) + cos^2\left(\frac{\Delta\emptyset_{MZI10}}{2}\right) \times sin^2\left(\frac{\Delta\emptyset_{MZI3}}{2}\right) \quad (48)$$

Normalized power at output port C_6 is given as

$$C_6 = sin^2\left(\frac{\Delta\emptyset_{MZI1}}{2}\right) + cos^2\left(\frac{\Delta\emptyset_{MZI3}}{2}\right) \times sin^2\left(\frac{\Delta\emptyset_{MZI9}}{2}\right) + sin^2\left(\frac{\Delta\emptyset_{MZI2}}{2}\right) \times cos^2\left(\frac{\Delta\emptyset_{MZI7}}{2}\right) + cos^2\left(\frac{\Delta\emptyset_{MZI10}}{2}\right) \times sin^2\left(\frac{\Delta\emptyset_{MZI3}}{2}\right) \quad (49)$$

BPM layout of Seven Segment device

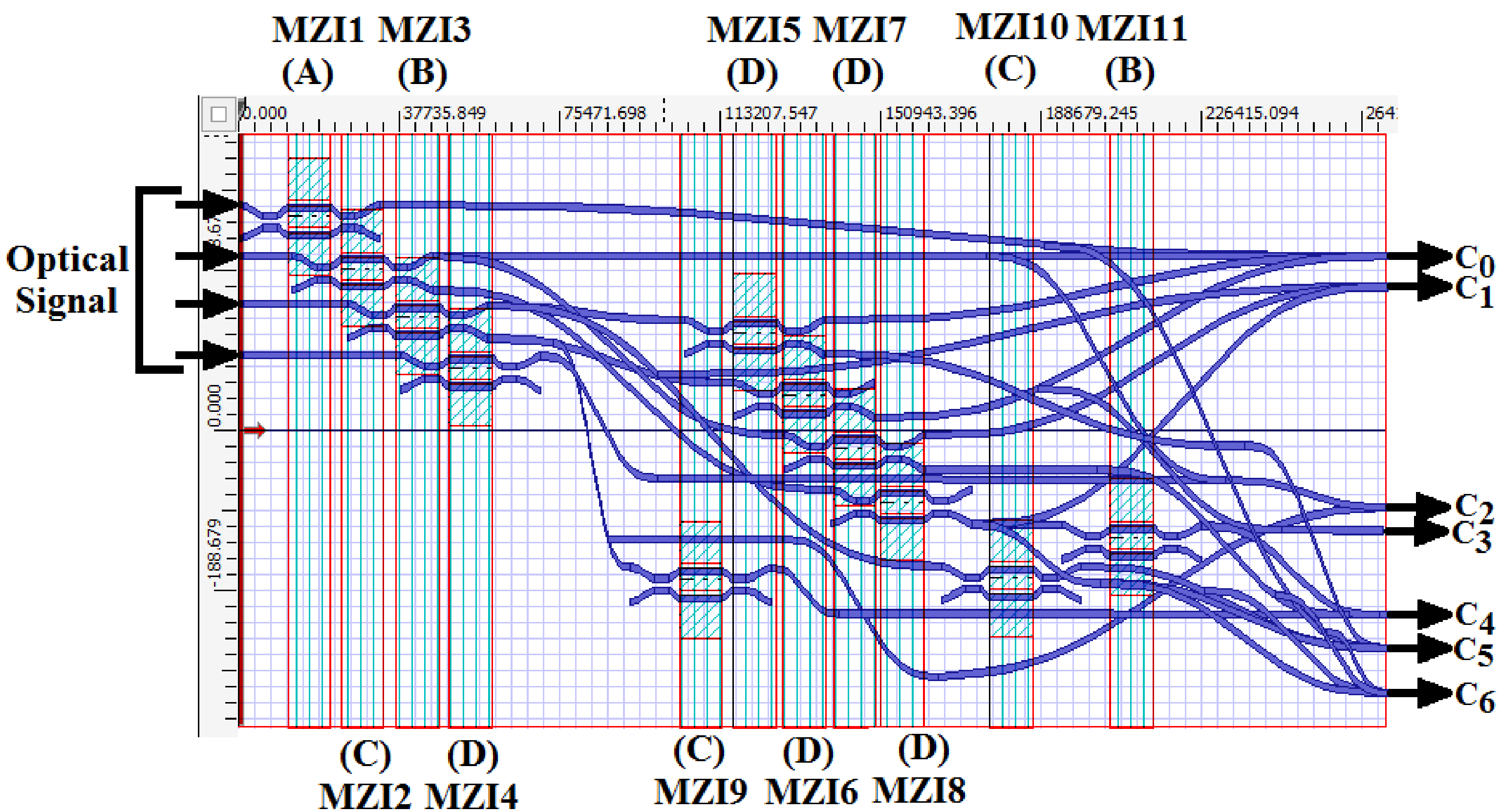

Figure 38: BPM layout of seven segment decoder

BPM results of Seven Segment Device

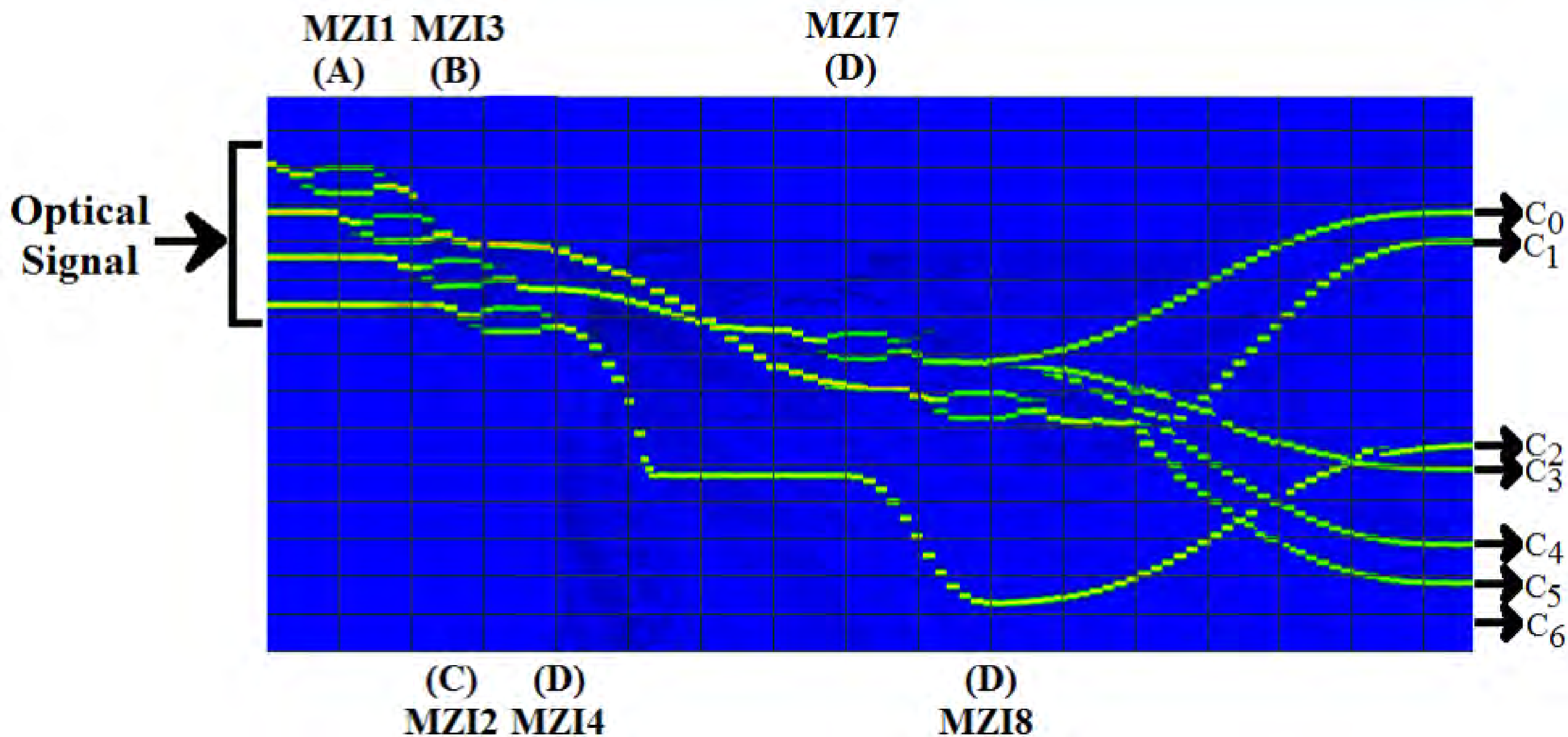

Figure 39: Results of seven segment decoder for different combinations of control signals ($ABCD = 0000$)obtained through beam propagation method

Design of Optical SR latch and flip flop

Santosh Kumar et. al., Journal of Optical Communications (2017).

Design of SR Latch and Flip-Flop

- SR latch or flip flop can maintain a binary state indefinitely until directed by an input signal to switch state.

- Any application of sequential logic circuit can be implemented by using SR flip flop and external gates. Flip flop have two stable states.

- It is also called binary or one bit storage memory element.

Cont….

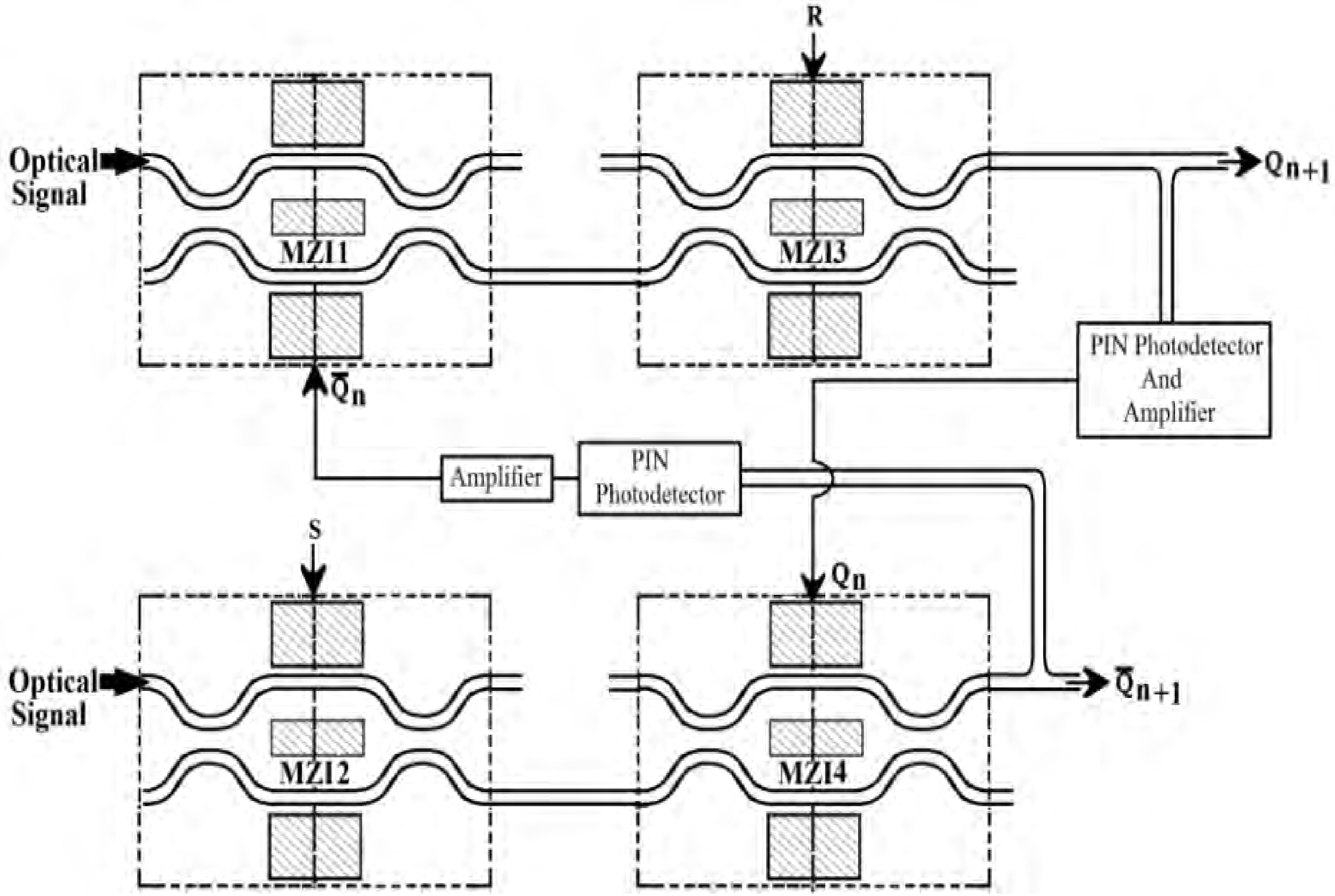

Figure 40: Schematic diagram of SR latch

Cont….

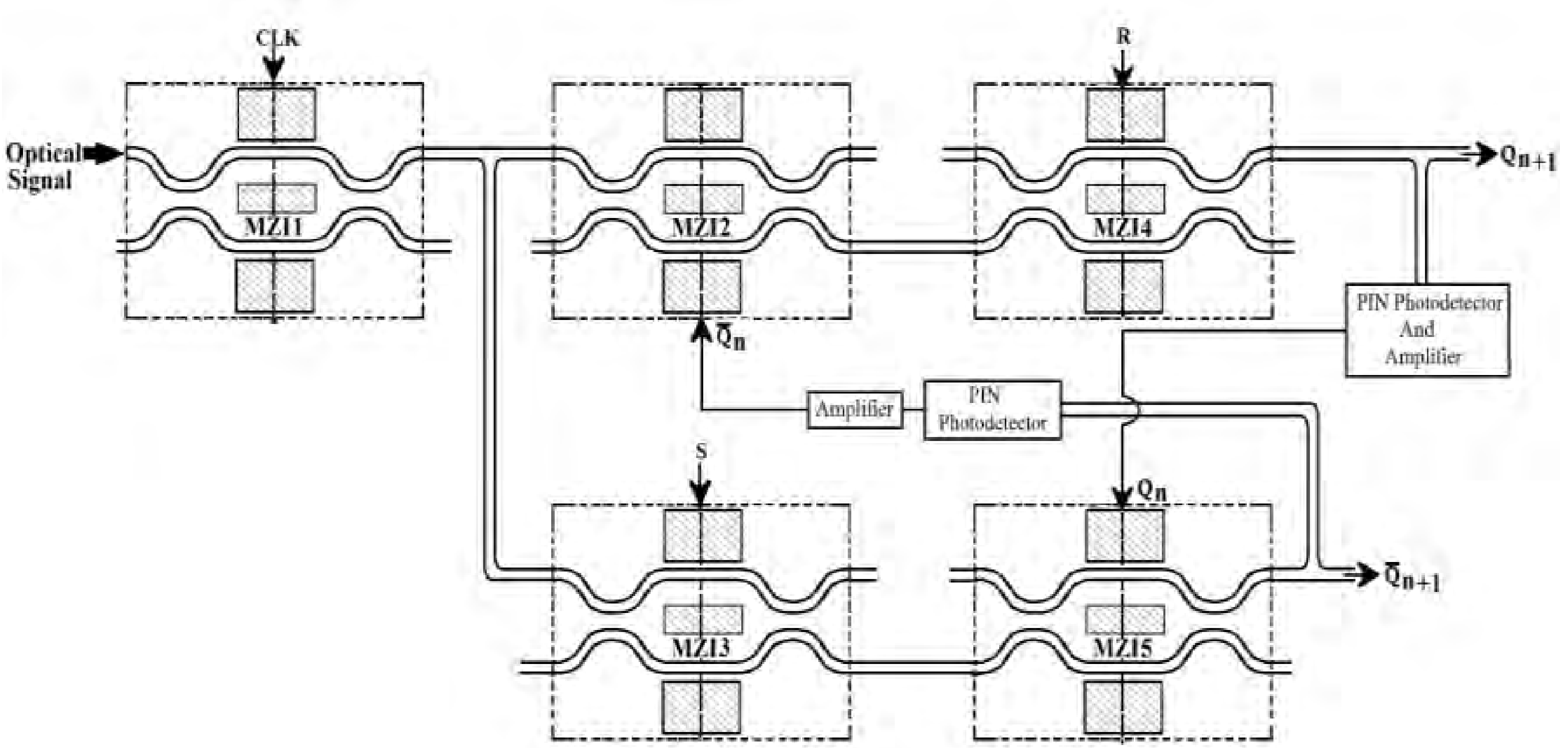

Figure 41: Schematic diagram of SR Flip Flop

Table 11: Functional table of SR latch

S	R	Q_{n+1}	$\bar{Q}_{n+1}$	States
0	0	Q_n	$\bar{Q}_n$	Previous State
0	1	0	1	Reset
1	0	1	0	Set
1	1	0	0	Invalid State

Mathematical Expression for SR Flip Flop

we can write the output Q_{n+1} at first output port of MZI4 as;

$$Q_{n+1} = \left|\frac{Q_{n+1_{\mathrm{MZI4}}}}{\mathrm{E_{in}}}\right|^2 = sin^2\left(\frac{\Delta\varphi_{MZI1}}{2}\right)cos^2\left(\frac{\Delta\varphi_{MZI2}}{2}\right)cos^2\left(\frac{\Delta\varphi_{MZI4}}{2}\right) \qquad (50)$$

The output$\bar{Q}_{n+1}$ at the first output port of MZI5 as:

$$\bar{Q}_{n+1} = \left|\frac{\bar{Q}_{n+1_{\mathrm{MZI5}}}}{\mathrm{E_{in}}}\right|^2 = sin^2\left(\frac{\Delta\varphi_{MZI1}}{2}\right)cos^2\left(\frac{\Delta\varphi_{MZI3}}{2}\right)cos^2\left(\frac{\Delta\varphi_{MZI5}}{2}\right) \qquad (51)$$

MATLAB simulation Results of SR Flip-Flop

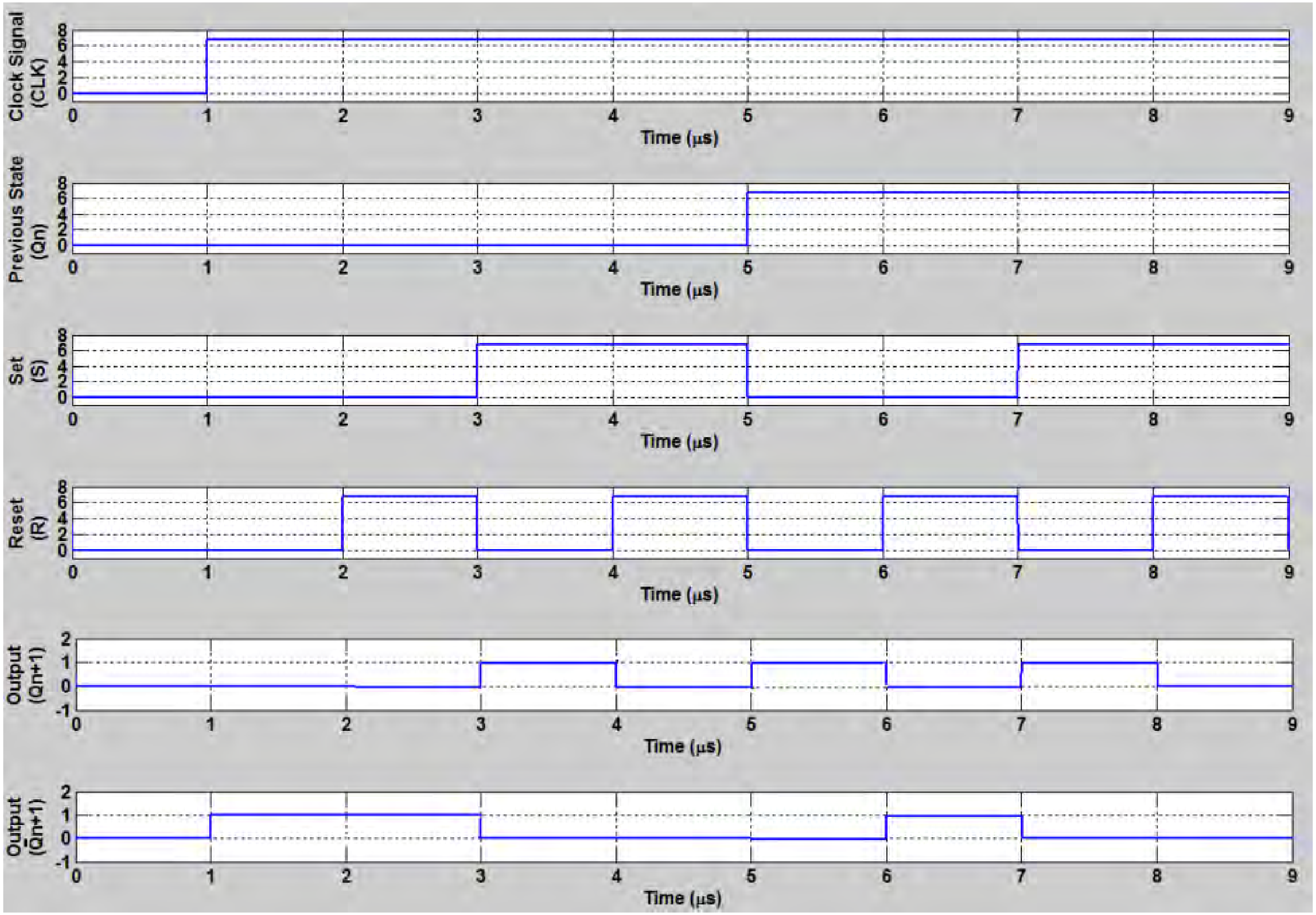

Figure 42: Timing diagram of SR flip flop

BPM Layout of SR latch

- Depending upon the values of SR and CLK signals at electrode of five MZIs, output optical signals (Q_{n+1} and $\bar{Q}_{n+1}$) can varies.

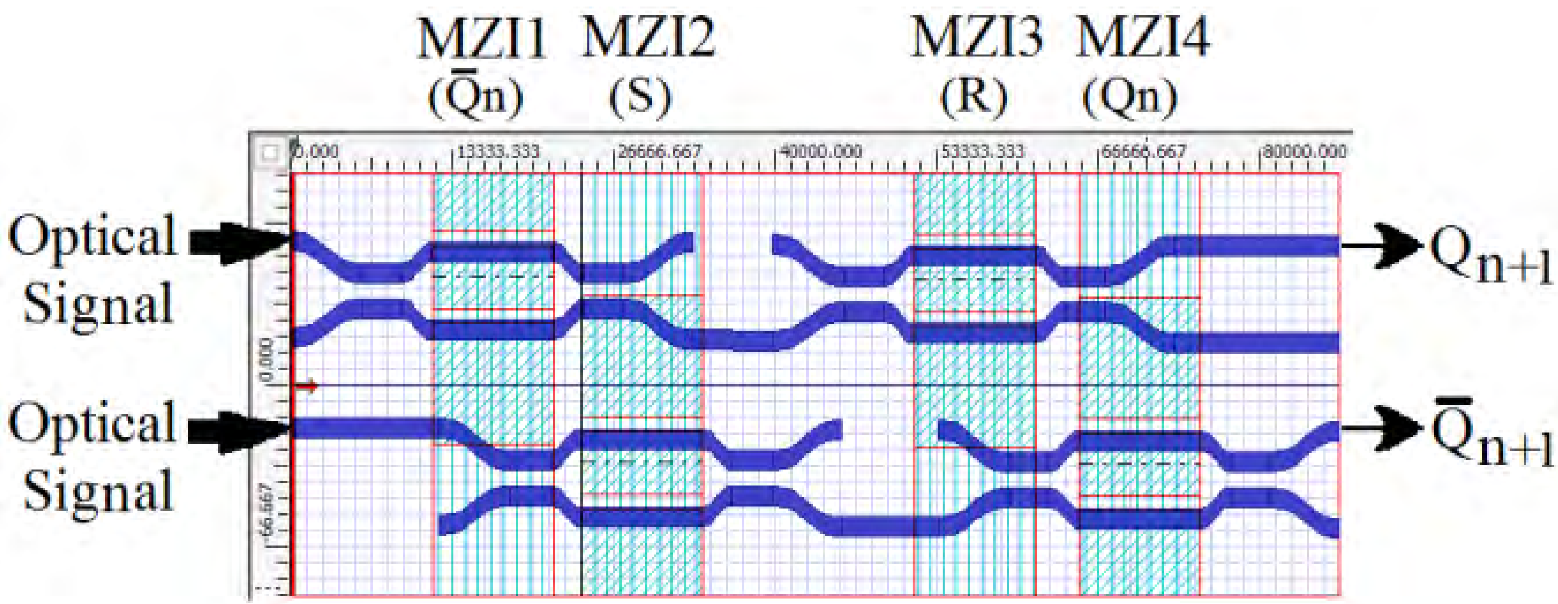

Figure 43: BPM layout of SR latch

BPM Layout of SR Flip-Flop

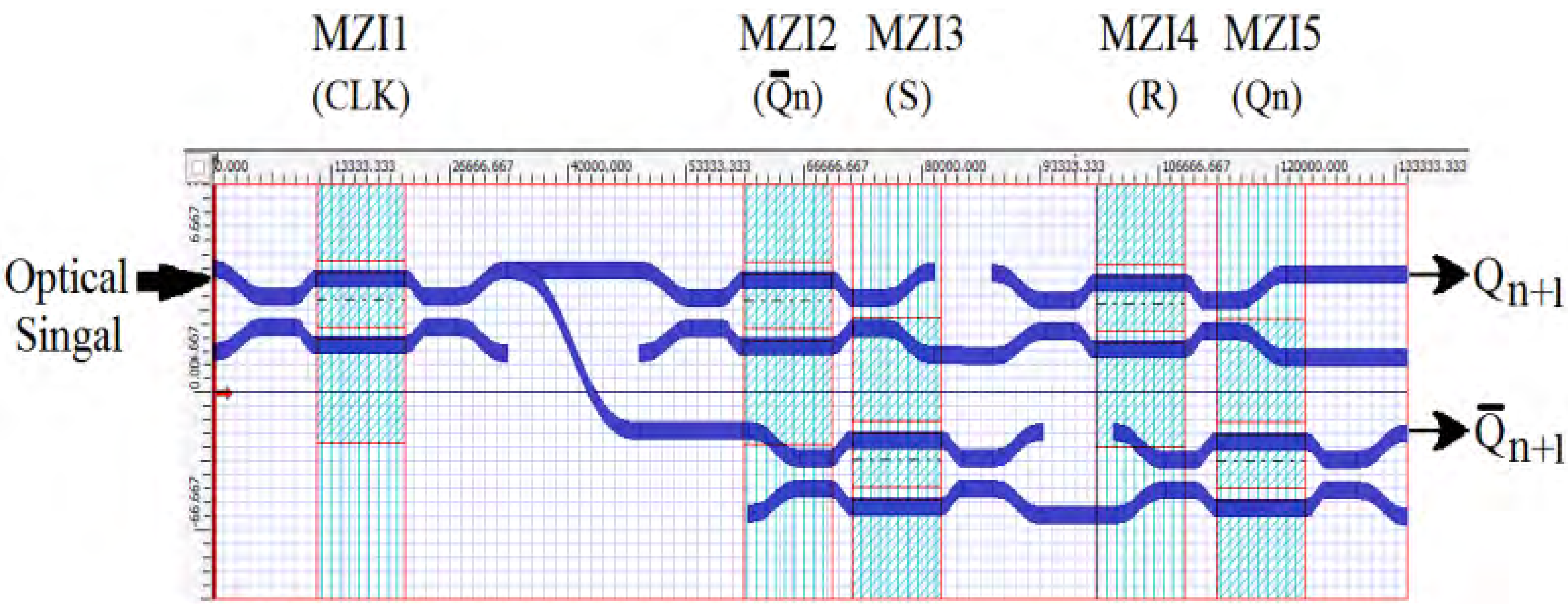

Figure 44: BPM layout of SR flip-flop

BPM results of SR Flip-Flop

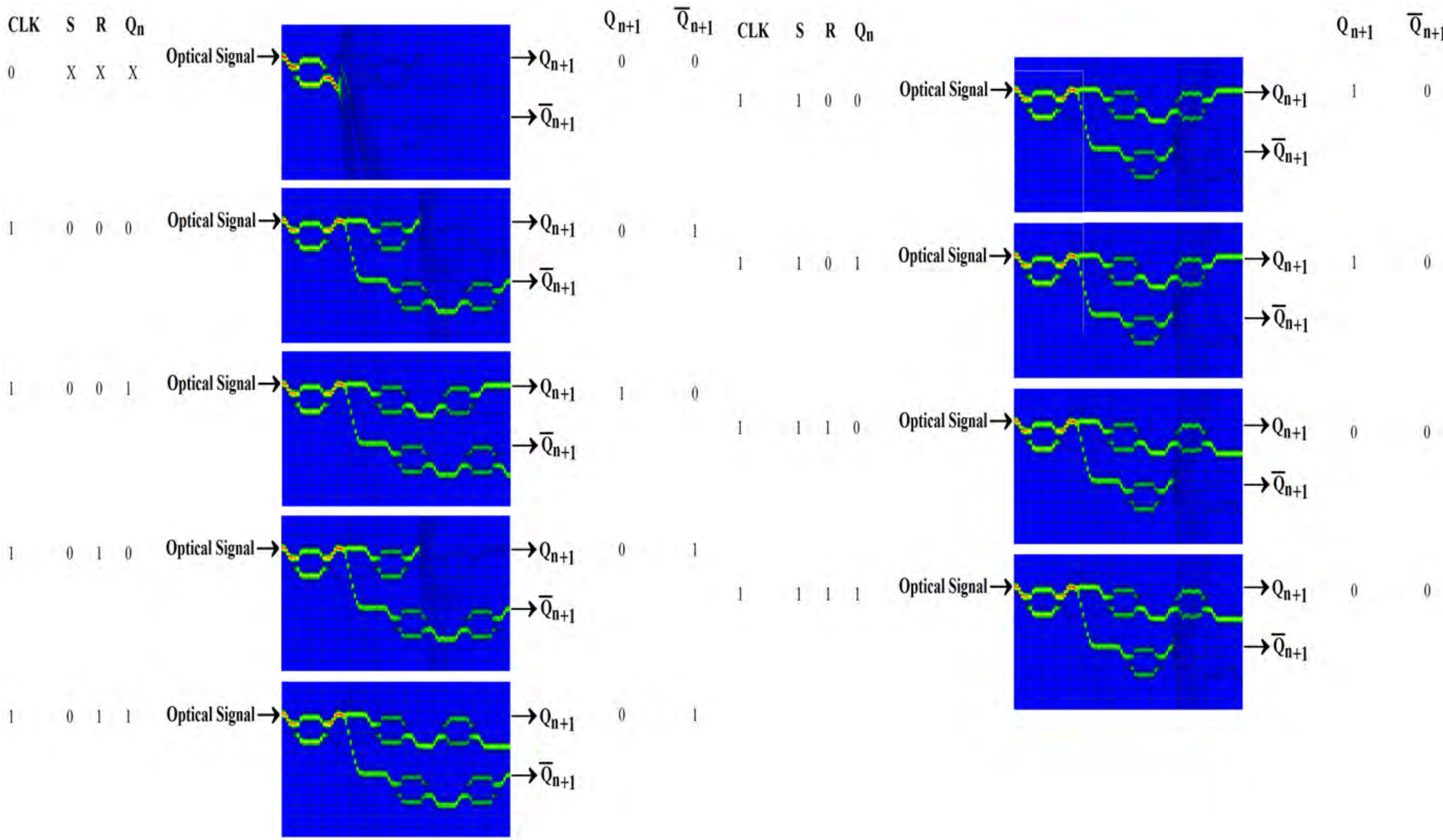

Figure 45 : Simulation results of SR flip flop for different combinations of SR control signals and $Q_n = 0$ and $Q_{n+1} = 0$

Design of D and T Flip-flops

Santosh Kumar et. al., Applied Optics (OSA), Vol. 54, Issue 21, PP. 6397-6405 (July 20, 2015)

Design of D and T Flip-flops

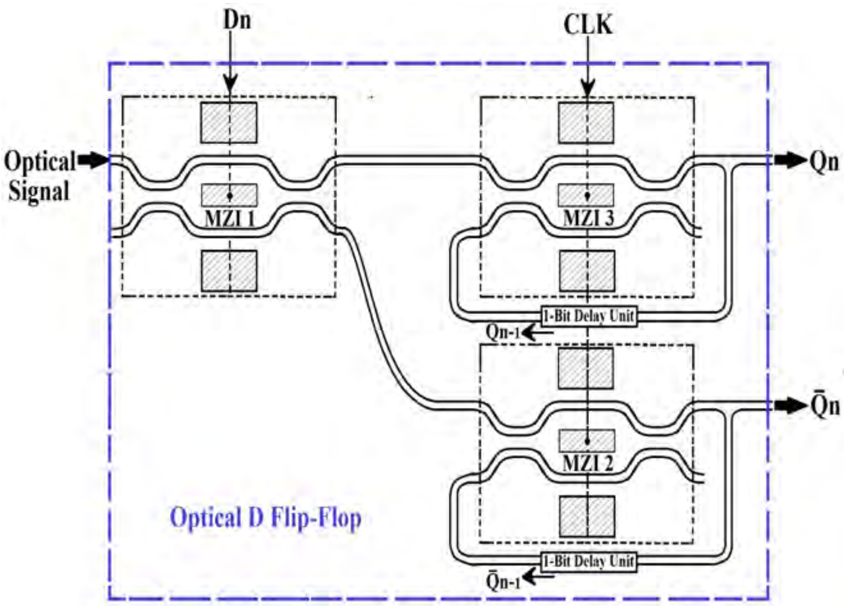

Fig. 15: Schematic diagram of D flip-flop.

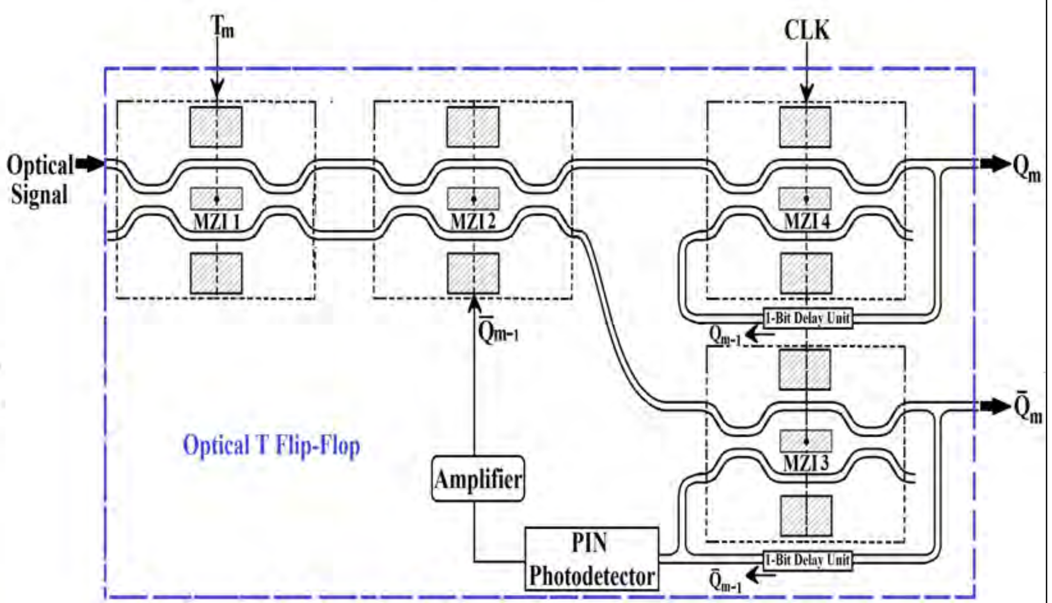

Fig. 16: Schematic diagram of T flip-flop.

Table 4: Function table of D flip-flop.

D_n	CLK	Q_n	$\bar{Q}_n$
0	1	0	1
1	1	1	0
×	0	Last Q_n	Last $\bar{Q}_n$

Table 5: Function table of T flip-flop.

T_m	Q_m	Q_{m+1}	$\bar{Q}_m$	$\bar{Q}_{m+1}$
0	0	0	1	1
0	1	1	0	0
1	0	1	1	0
1	1	0	0	1

Cont …

$$|Q_n|^2 = \sin^2\left(\frac{\Delta\varphi}{2}\right)|D_n|^2 + \cos^2\left(\frac{\Delta\varphi}{2}\right)|Q_{n-1}|^2 + |D_n|\,|Q_{n-1}|\,\sin\Delta\varphi \qquad (17)$$

Similarly for $\bar{Q}_n$ we can write,

$$|\bar{Q}_n|^2 = \sin^2\left(\frac{\Delta\varphi}{2}\right)|\bar{D}_n|^2 + \cos^2\left(\frac{\Delta\varphi}{2}\right)|\bar{Q}_{n-1}|^2 + |\bar{D}_n|\,|\bar{Q}_{n-1}|\,\sin(\Delta\varphi) \qquad (18)$$

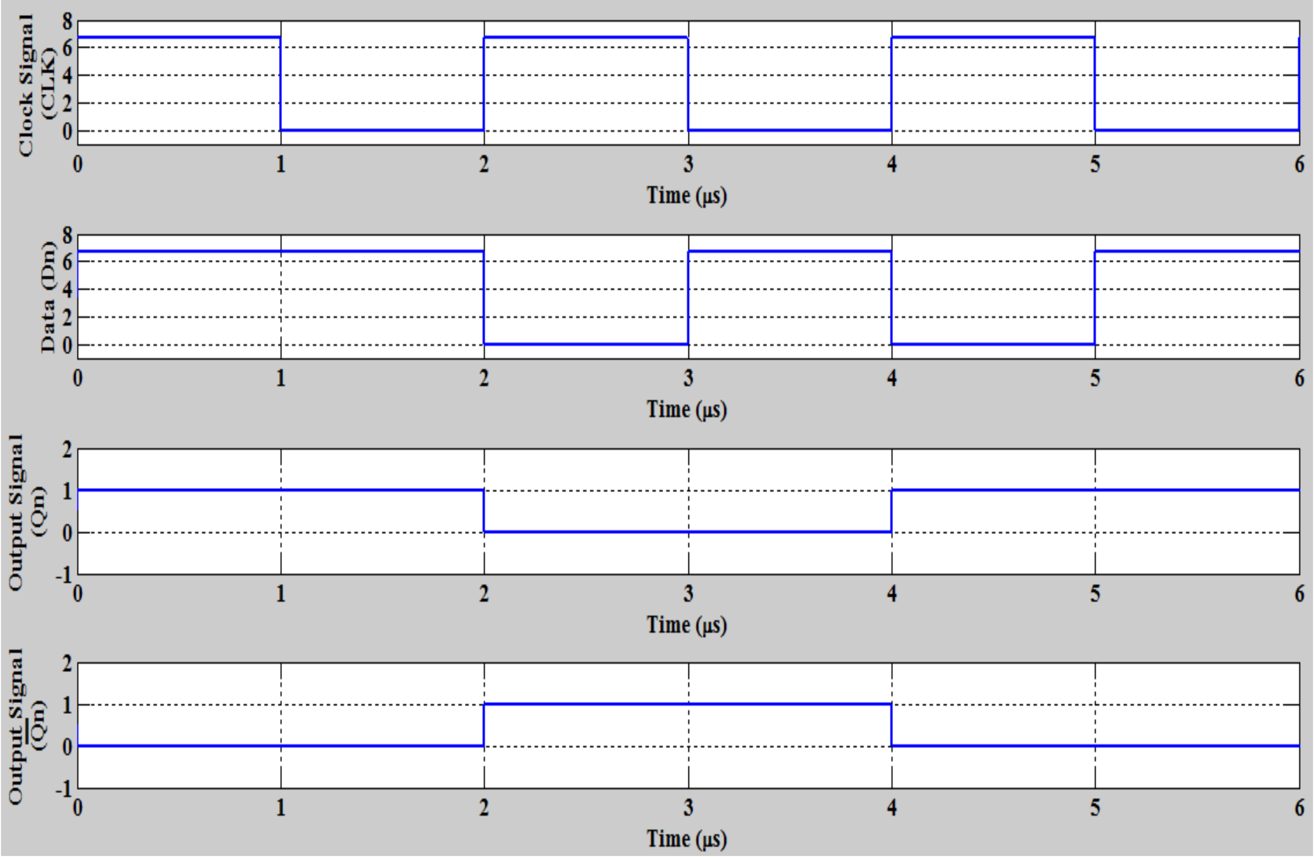

Fig. 17: MATLAB simulation result of D flip-flop.

Cont …

$$|Q_m|^2 = \sin^2\left(\frac{\Delta\varphi}{2}\right)|T_0|^2 + \cos^2\left(\frac{\Delta\varphi}{2}\right)|Q_{m-1}|^2 + |T_0|\,|Q_{m-1}|\,\sin(\Delta\varphi) \qquad (19)$$

Similarly for $\bar{Q}_n$ we can write,

$$|\bar{Q}_m|^2 = \sin^2\left(\frac{\Delta\varphi}{2}\right)|\bar{T}_0|^2 + \cos^2\left(\frac{\Delta\varphi}{2}\right)|\bar{Q}_{m-1}|^2 + |\bar{T}_0|\,|\bar{Q}_{m-1}|\,\sin(\Delta\varphi) \qquad (20)$$

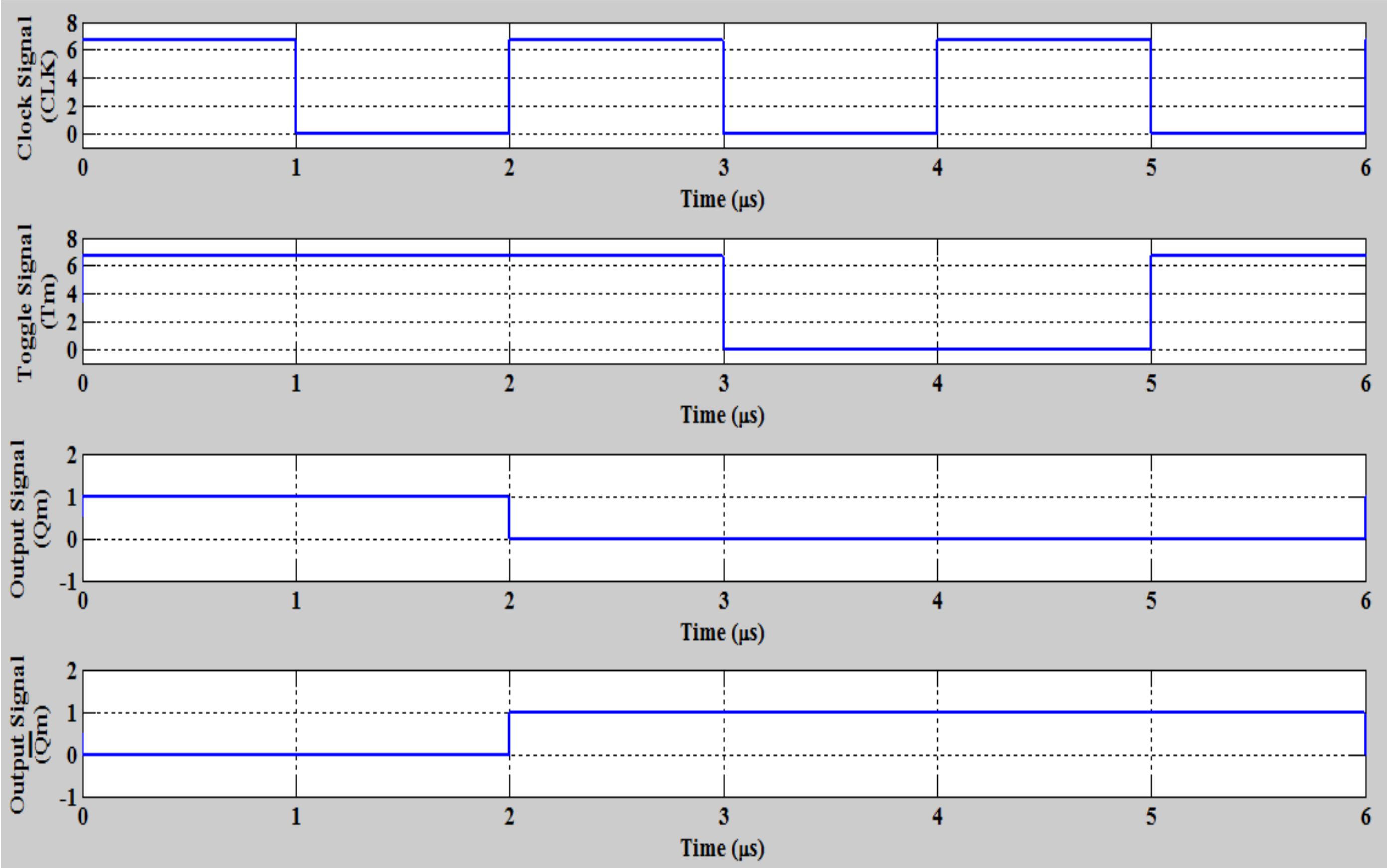

Fig. 18: MATLAB simulation result of T flip-flop.

Cont …

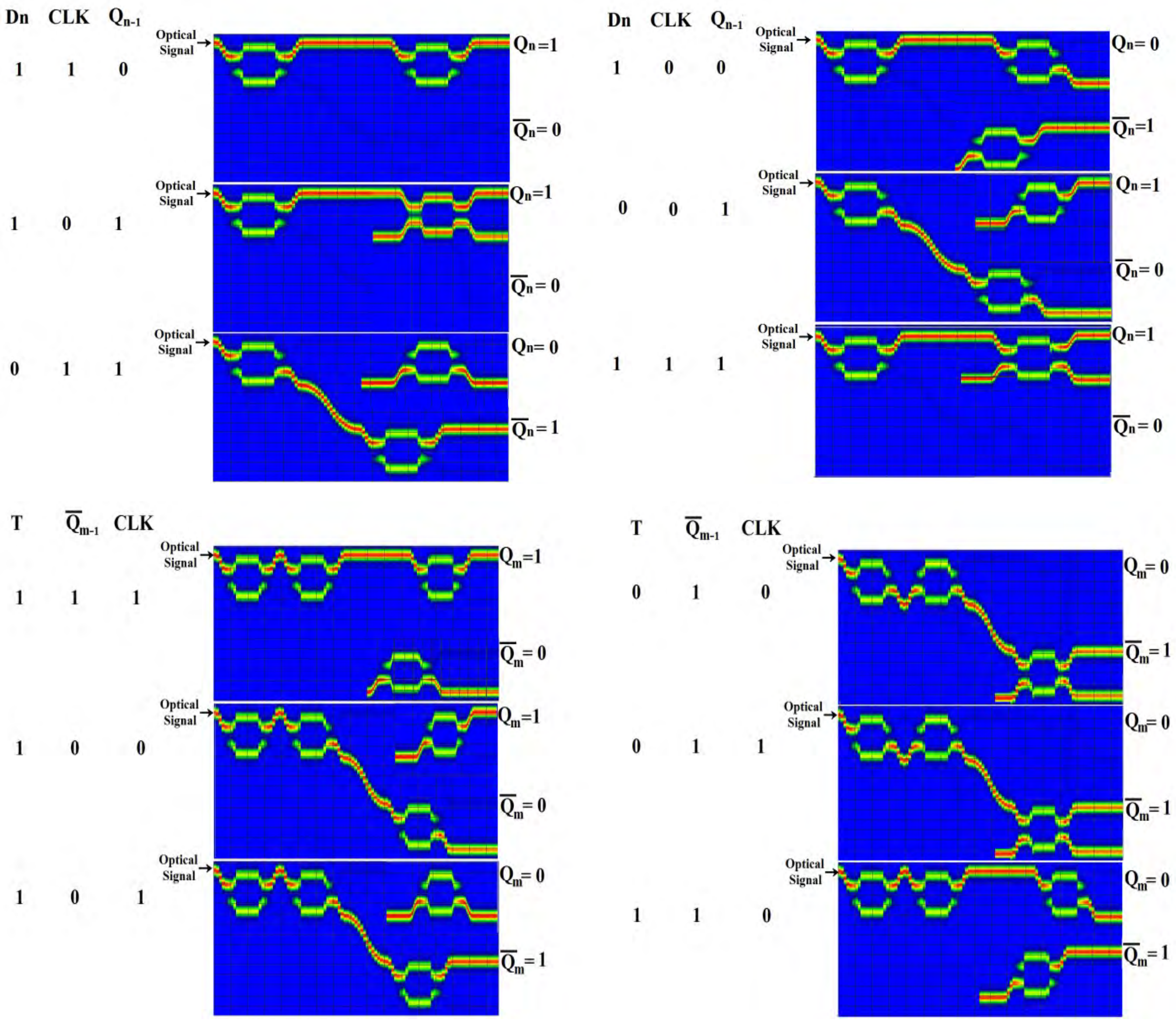

Fig. 19: Results of the D flip-flop for different combinations of control signals obtained through the BPM.

Design of Optical Synchronous Counter

Santosh Kumar, et. al., Optical & Quantum Electronics (Springer), Vol. 47, No. 6, (July 26, 2015).

Design of Optical Synchronous Counter

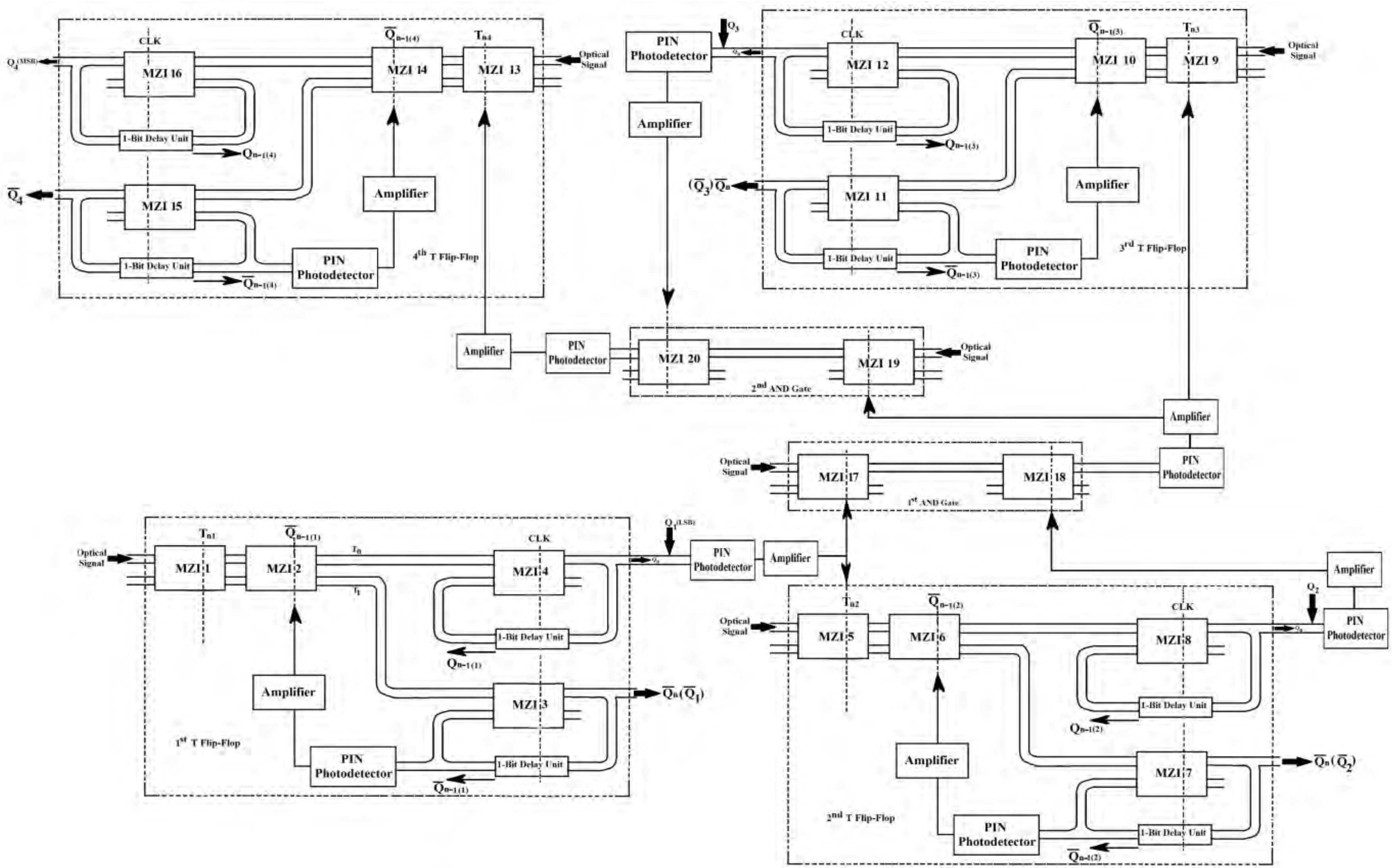

Fig. 20: Schematic diagram of a 4-bit synchronous up counter.

Cont …

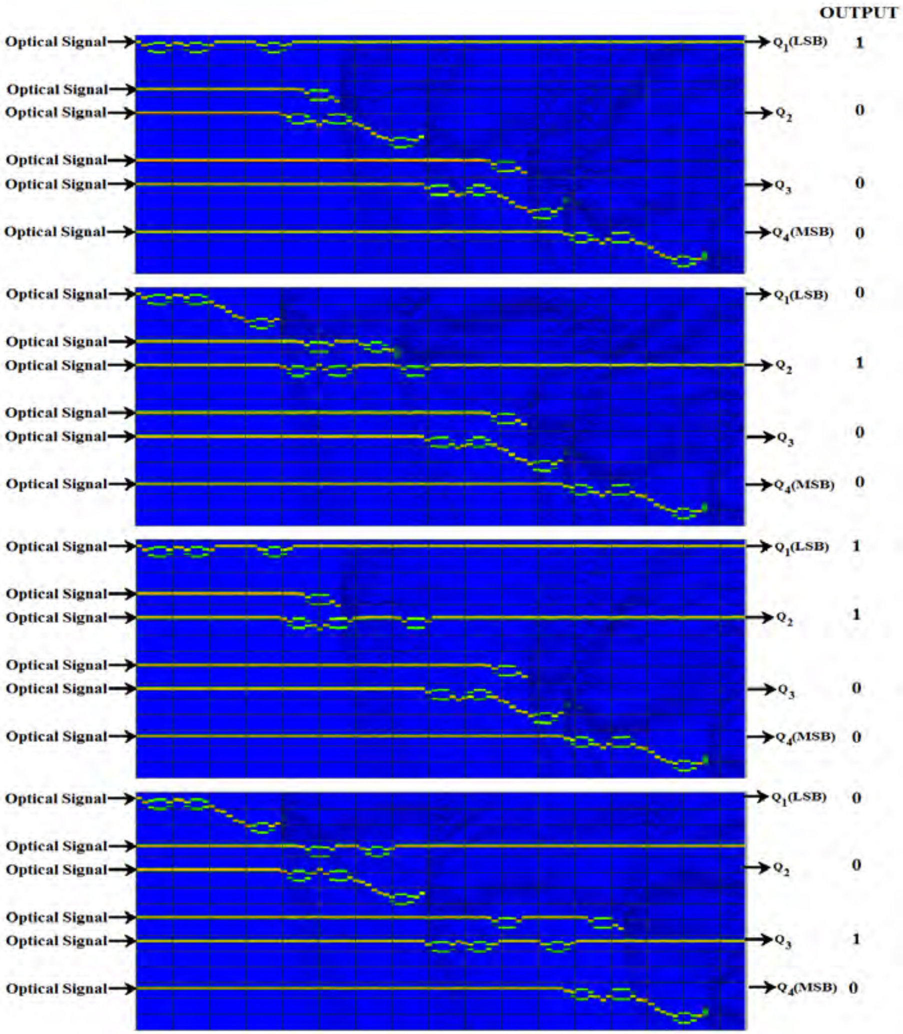

Fig. 21: Simulation result of proposed 4-bit synchronous up counter using BPM for different outputs (1000 to 0010).

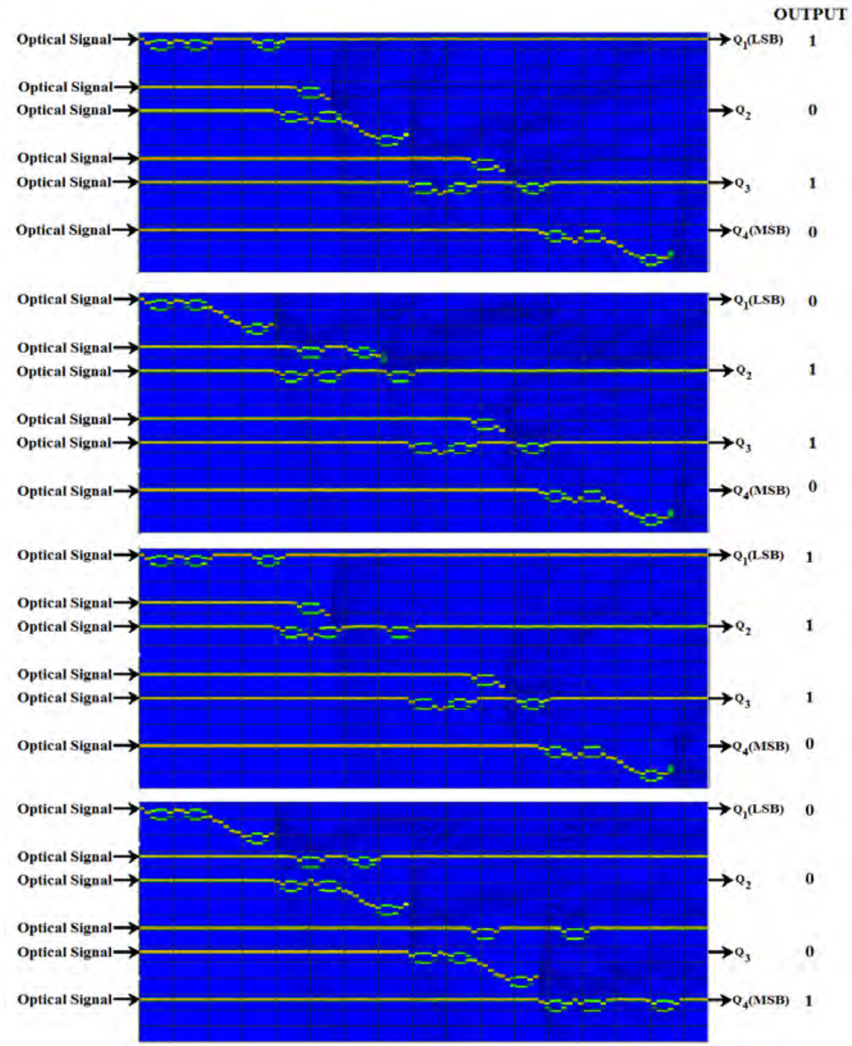

Fig. 22: Simulation result of proposed 4-bit synchronous up counter using BPM for different outputs (1010 to 0001).

Design of Programmable Logic Device

Santosh Kumar et. al., Photonic Network communications (Springer), Vol. 33, Issue 3, PP. 356-370 (June 2017).

Programmable Logic Device

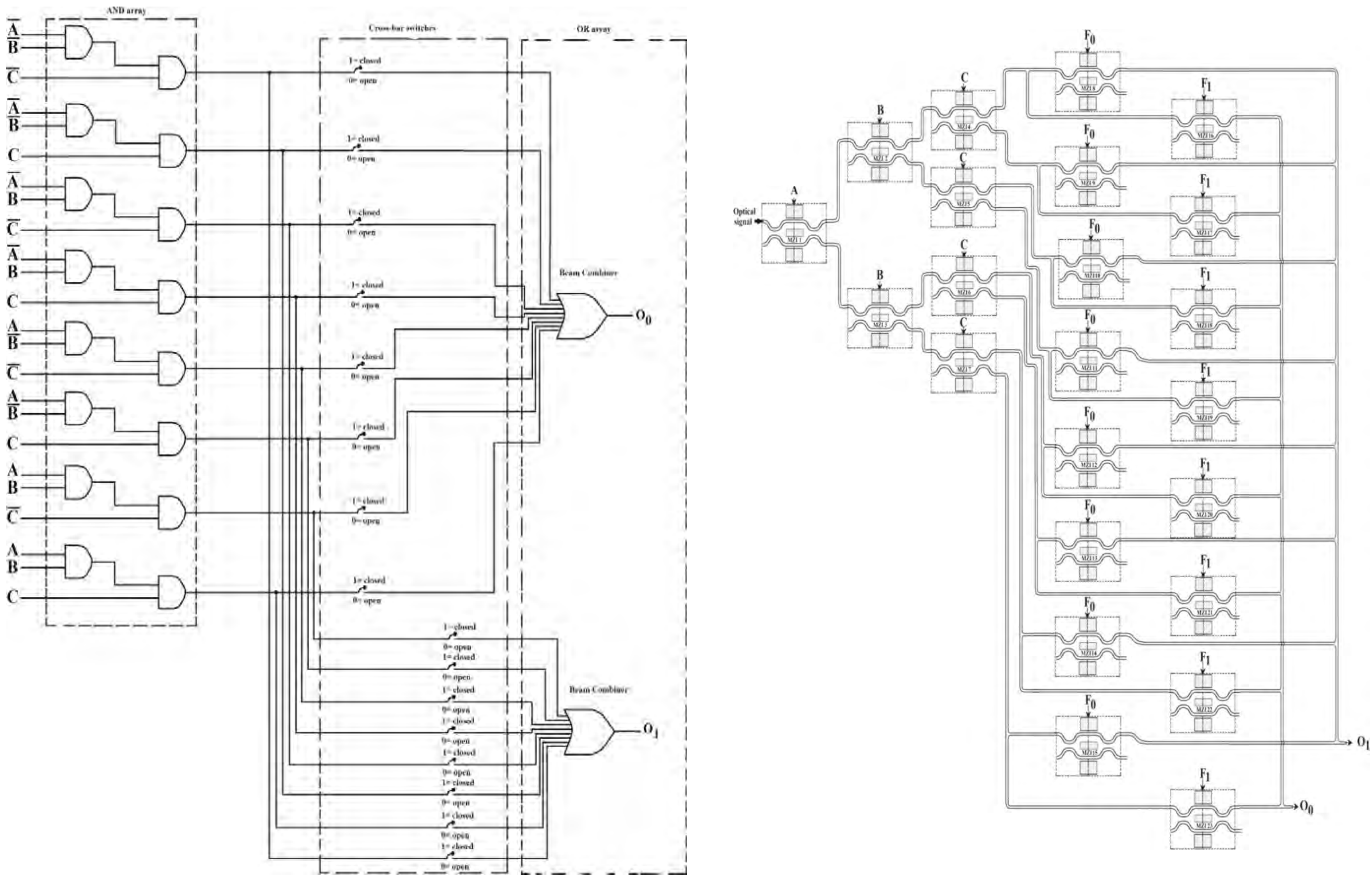

Figure: (a) Digital circuit of programmable logic device (b) Schematic diagram of using Mach–Zehnder interferometers

Mathematical Expression for Programmable logic device

$$O_0 = cos^2\left(\frac{\Delta\emptyset_{MZI1}}{2}\right) cos^2\left(\frac{\Delta\emptyset_{MZI3}}{2}\right) sin^2\left(\frac{\Delta\emptyset_{MZI7}}{2}\right) sin^2\left(\frac{\Delta\emptyset_{MZI22}}{2}\right)$$
$$+ cos^2\left(\frac{\Delta\emptyset_{MZI1}}{2}\right) sin^2\left(\frac{\Delta\emptyset_{MZI3}}{2}\right) cos^2\left(\frac{\Delta\emptyset_{MZI6}}{2}\right) sin^2\left(\frac{\Delta\emptyset_{MZI21}}{2}\right)$$
$$+ sin^2\left(\frac{\Delta\emptyset_{MZI1}}{2}\right) cos^2\left(\frac{\Delta\emptyset_{MZI2}}{2}\right) cos^2\left(\frac{\Delta\emptyset_{MZI5}}{2}\right) sin^2\left(\frac{\Delta\emptyset_{MZI19}}{2}\right)$$
$$+ sin^2\left(\frac{\Delta\emptyset_{MZI1}}{2}\right) sin^2\left(\frac{\Delta\emptyset_{MZI2}}{2}\right) sin^2\left(\frac{\Delta\emptyset_{MZI4}}{2}\right) sin^2\left(\frac{\Delta\emptyset_{MZI16}}{2}\right) \qquad (9)$$

$$O_1 = cos^2\left(\frac{\Delta\emptyset_{MZI1}}{2}\right) sin^2\left(\frac{\Delta\emptyset_{MZI3}}{2}\right) sin^2\left(\frac{\Delta\emptyset_{MZI6}}{2}\right) sin^2\left(\frac{\Delta\emptyset_{MZI12}}{2}\right)$$
$$+ sin^2\left(\frac{\Delta\emptyset_{MZI1}}{2}\right) cos^2\left(\frac{\Delta\emptyset_{MZI2}}{2}\right) sin^2\left(\frac{\Delta\emptyset_{MZI5}}{2}\right) sin^2\left(\frac{\Delta\emptyset_{MZI10}}{2}\right)$$
$$+ sin^2\left(\frac{\Delta\emptyset_{MZI1}}{2}\right) sin^2\left(\frac{\Delta\emptyset_{MZI2}}{2}\right) cos^2\left(\frac{\Delta\emptyset_{MZI4}}{2}\right) sin^2\left(\frac{\Delta\emptyset_{MZI9}}{2}\right)$$
$$+ sin^2\left(\frac{\Delta\emptyset_{MZI1}}{2}\right) sin^2\left(\frac{\Delta\emptyset_{MZI2}}{2}\right) sin^2\left(\frac{\Delta\emptyset_{MZI4}}{2}\right) sin^2\left(\frac{\Delta\emptyset_{MZI8}}{2}\right) \qquad (10)$$

MATLAB Results for Full Adder

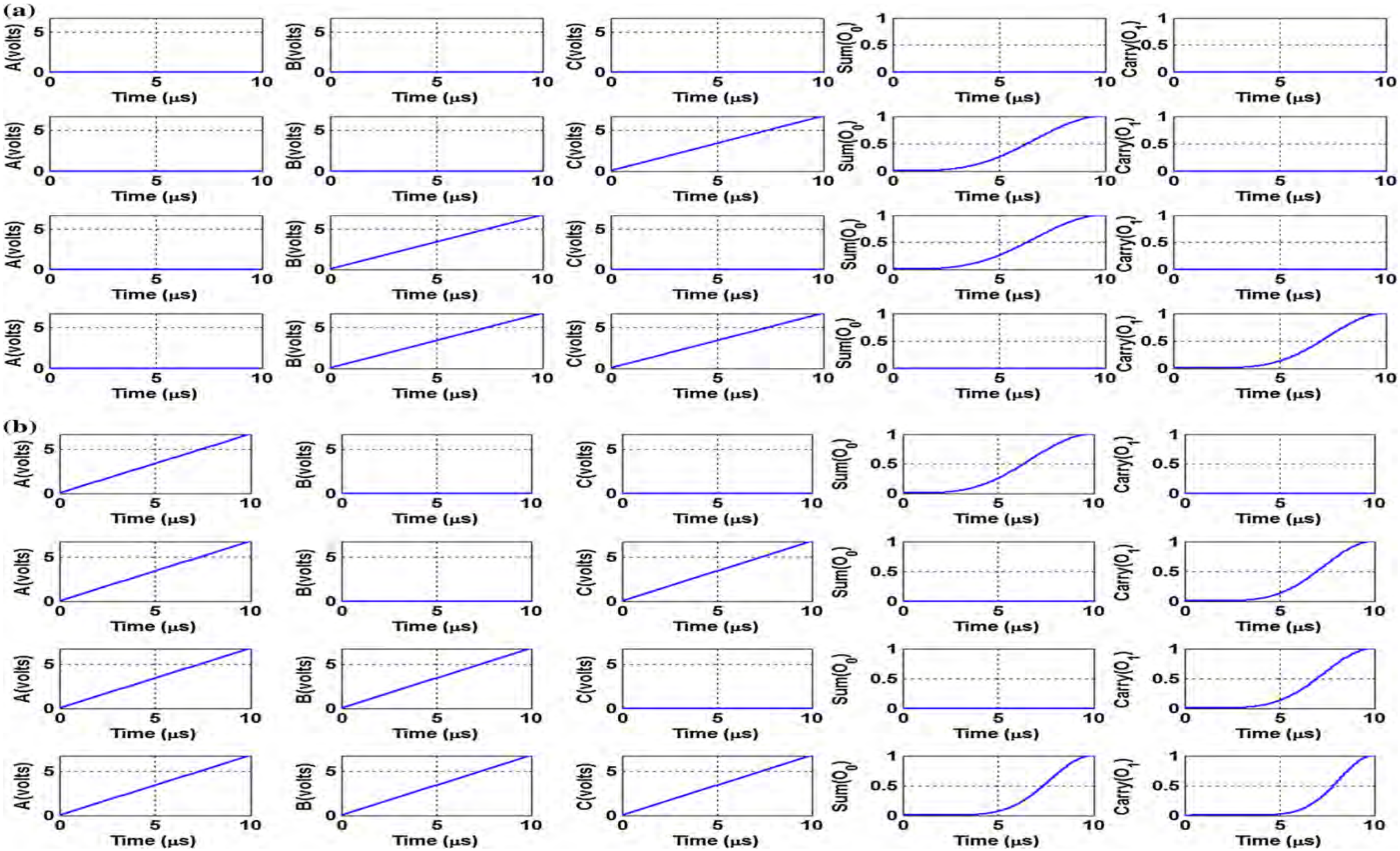

Figure: MATLAB simulation result of PLD (Full Adder) where A,B,C varies from 000 to 111

MATLAB Results for Full Subtractor

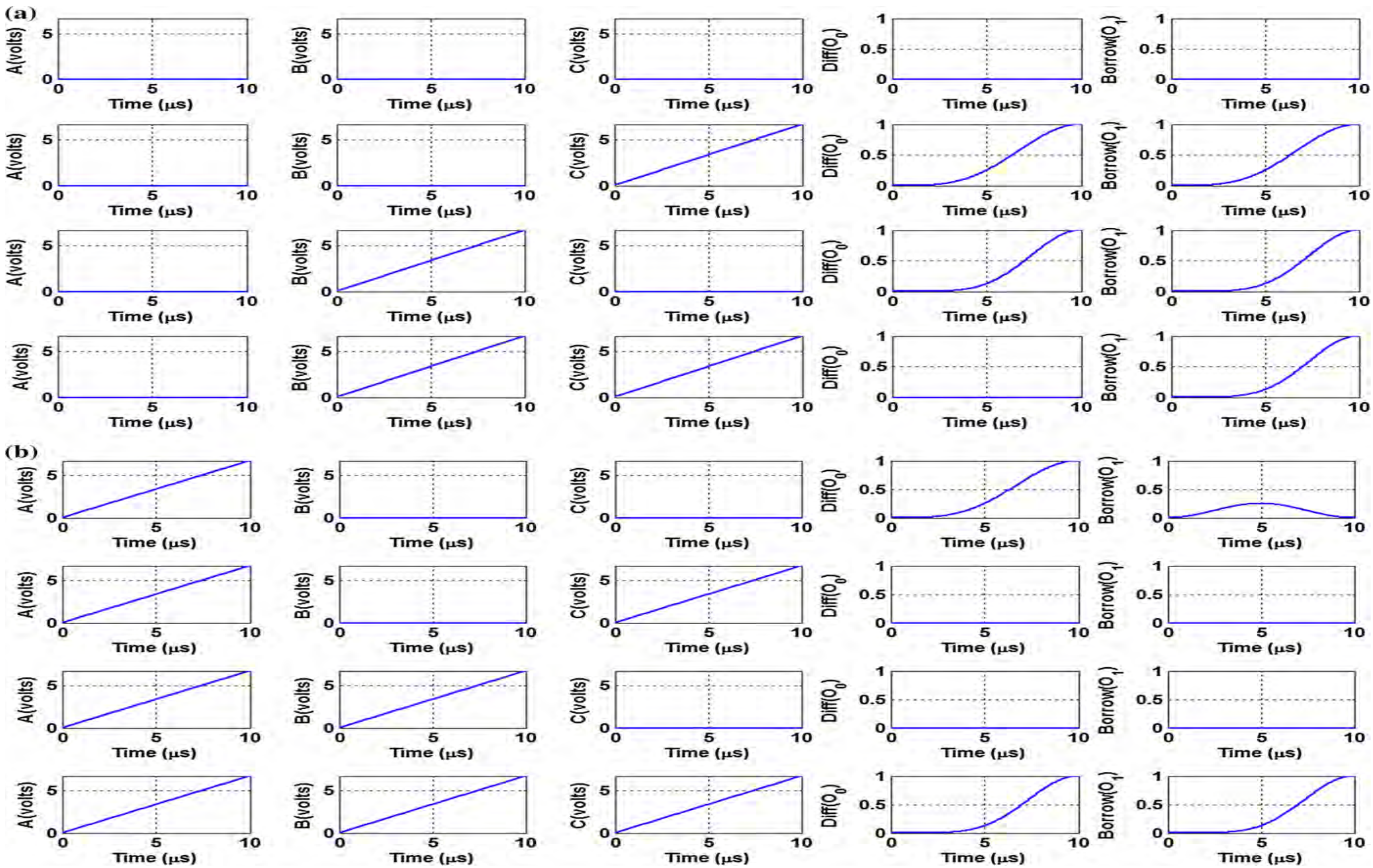

Figure: MATLAB simulation result of PLD (Full Subtractor) where A,B,C varies from 000 to 111

MATLAB Results for 2x1 Multiplexer

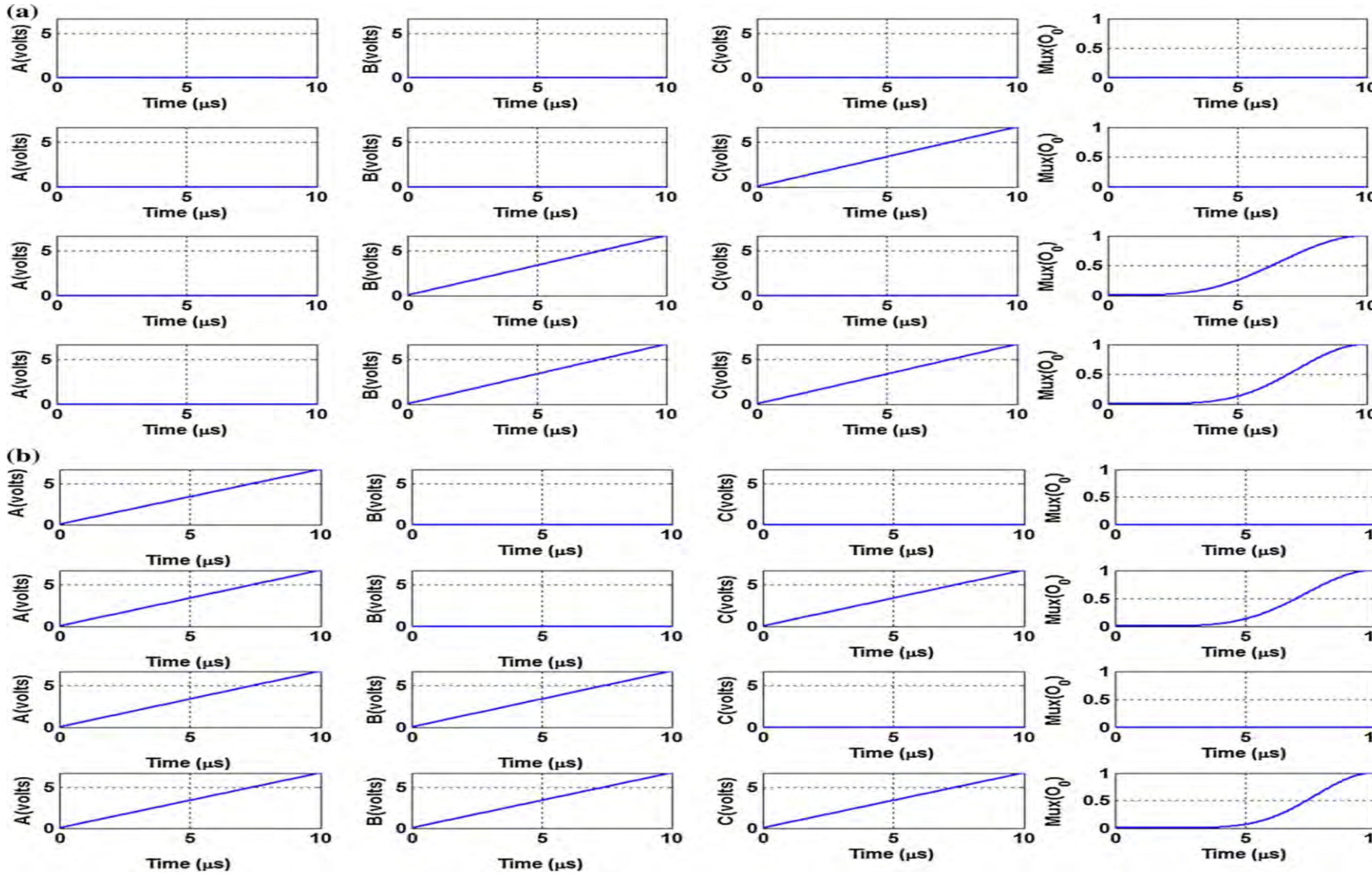

Figure: MATLAB simulation result of PLD (2x 1 Multiplexer) where A,B,C varies from 000 to 111

BPM Layout of Programmable Logic device

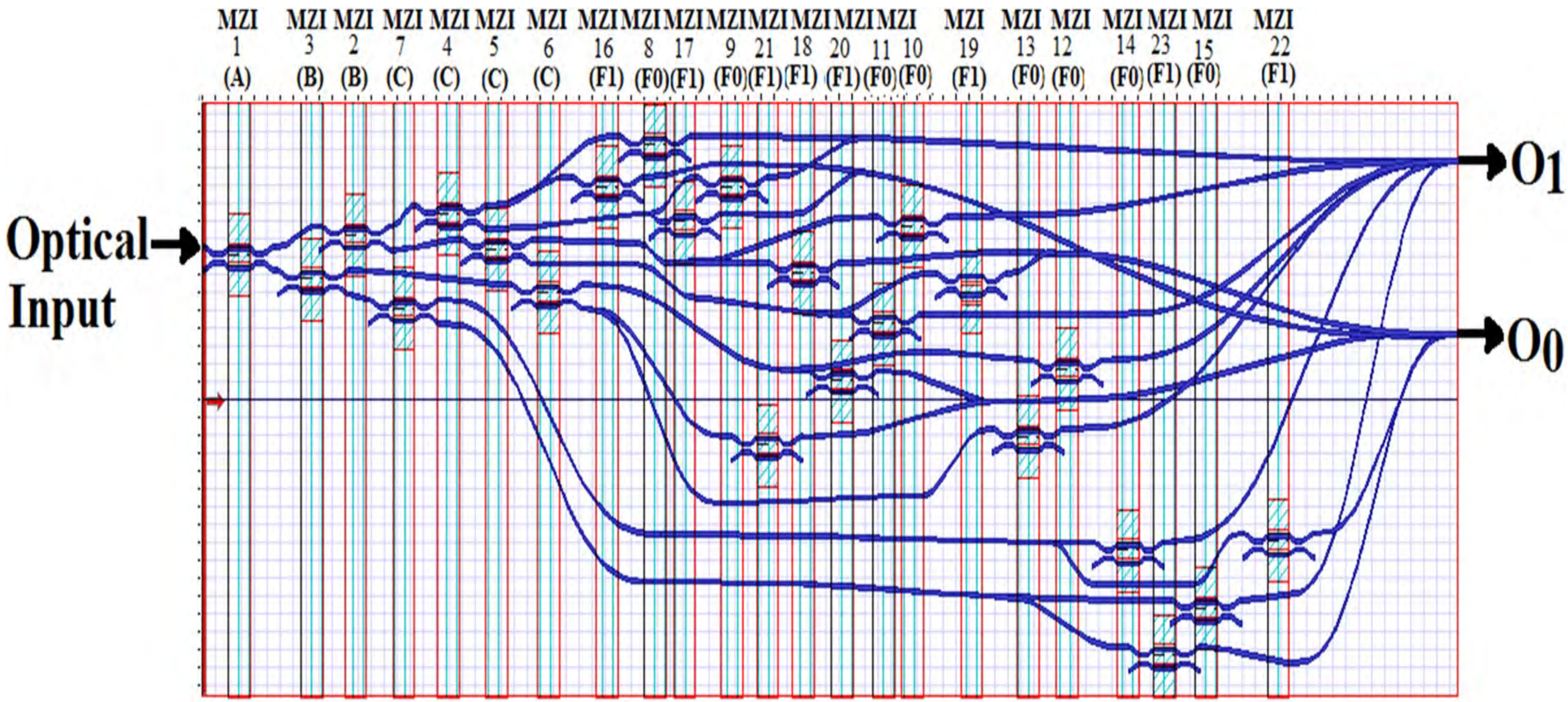

Figure: BPM layout of PLD

Simulation Result from BPM Layout (Full Adder)

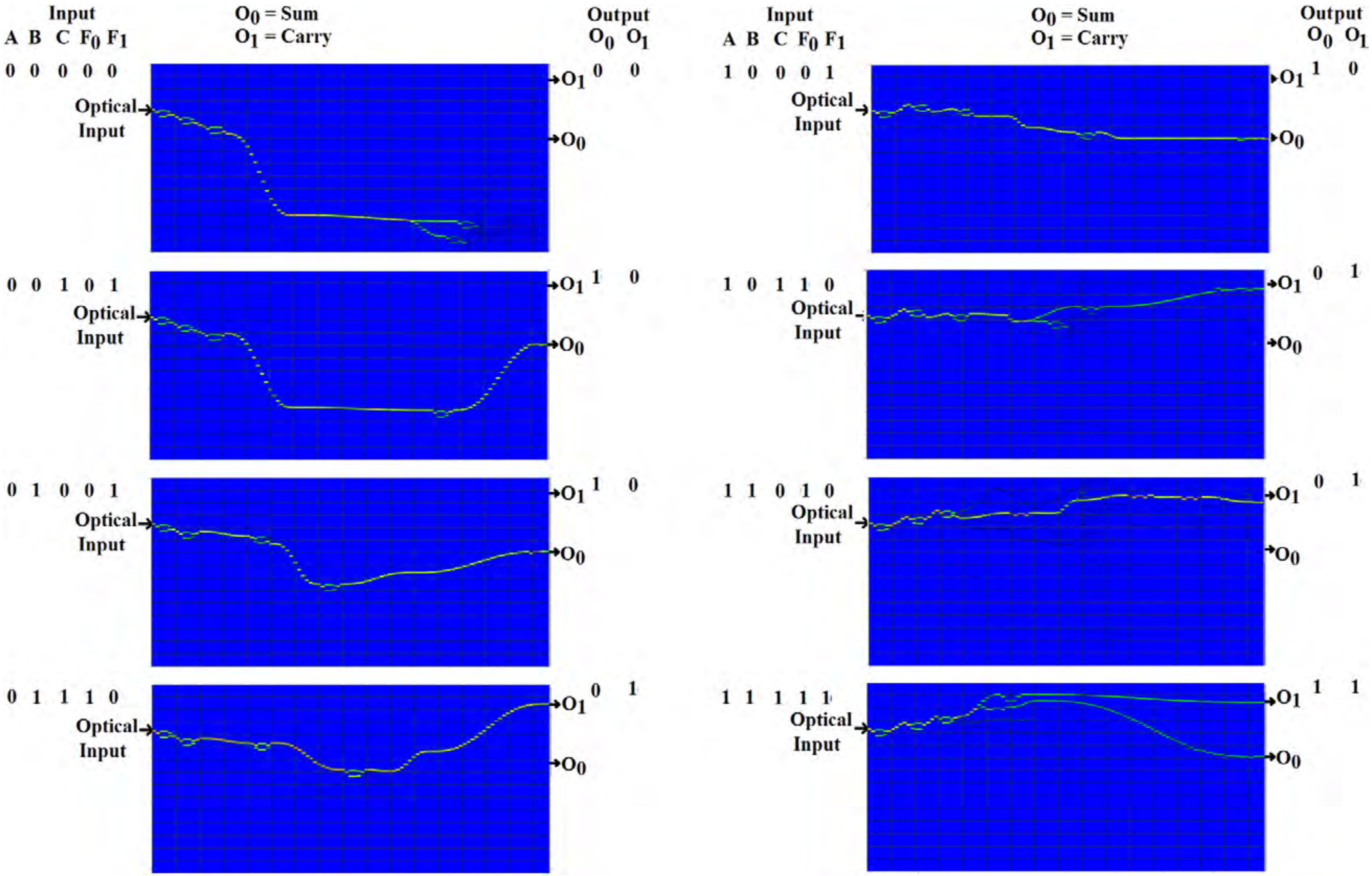

Figure: BPM simulation result of PLD (Full adder) where A,B,C varies from 000 to 111

Simulation Result from BPM Layout (Full Subtractor)

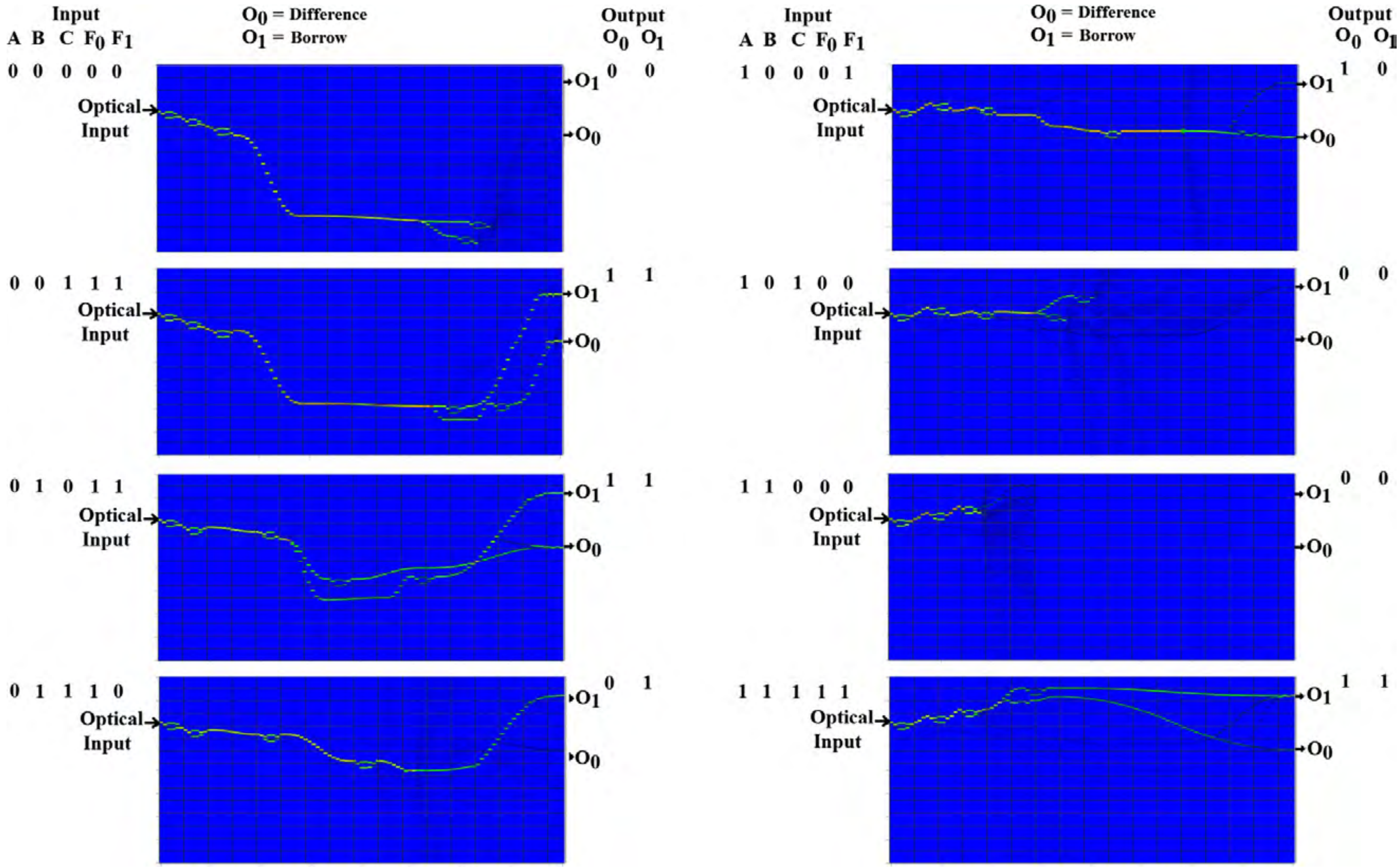

Figure: BPM simulation result of PLD (Full Subtractor) where A,B,C varies from 000 to 111

Simulation Result from BPM Layout (2x1 Multiplexer)

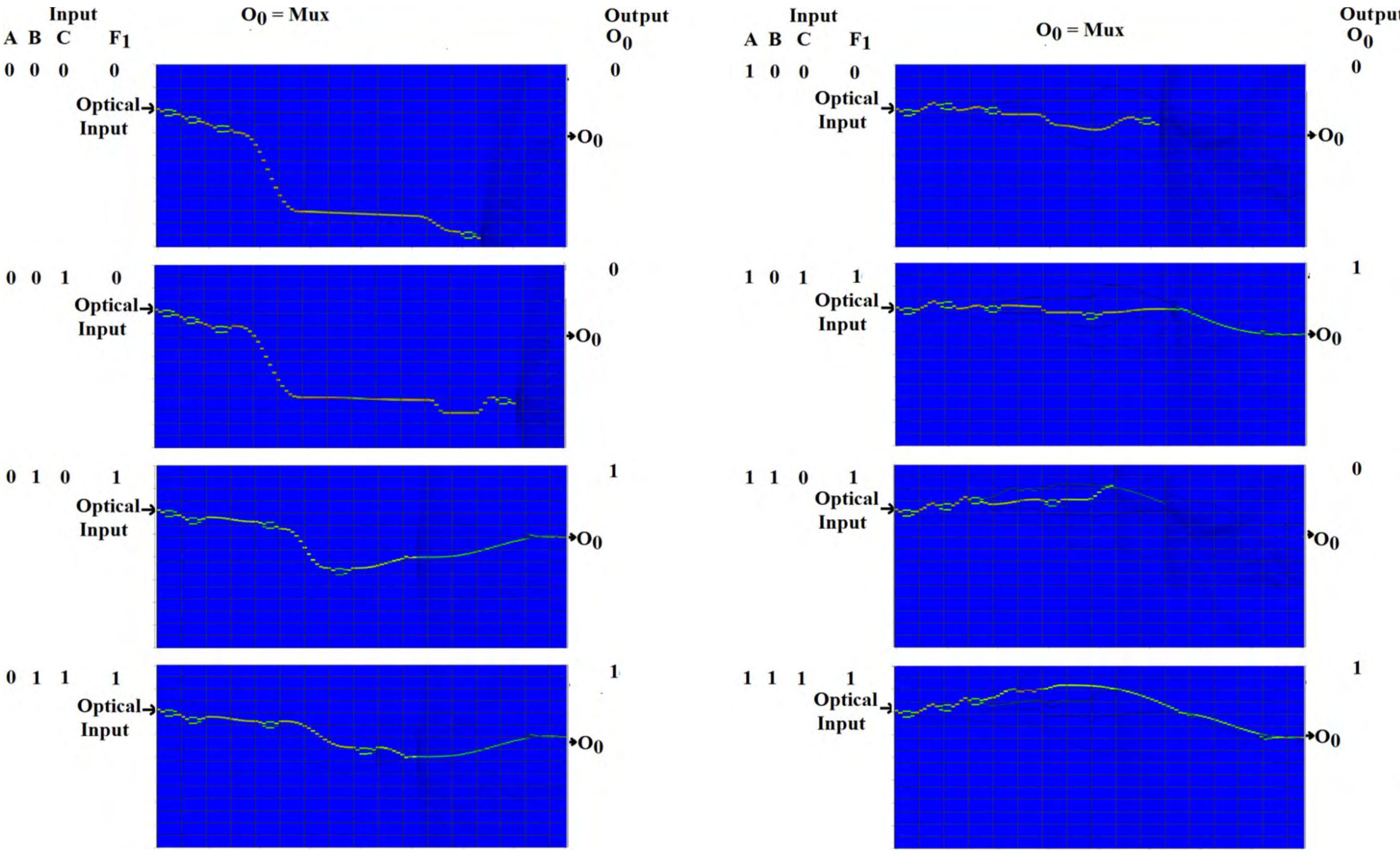

Figure: BPM simulation result of PLD (2x1 Multiplexer) where A,B,C varies from 000 to 111

Design of 1 x 4 Signal Router

Santosh Kumar et. al., *Optical Engineering (SPIE)*, vol. 52, no. 03, pp. 035002 (March 04, 2013)

1 x 4 Signal Router

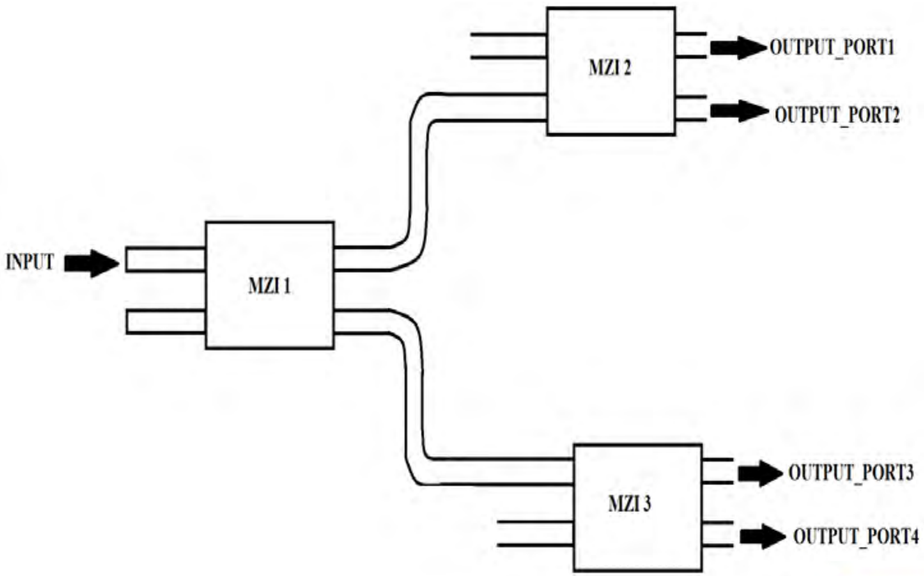

Figure 3.12: 1 x 4 signal router

Table 3.3: The output power at the 4 output port on the basis of control signal .

S_1	S_2	S_3	Output port1	Output port2	Output port3	Output port4
6.75V	0 V	‘X’	1	0	0	0
6.75V	6.75 V	‘X’	0	1	0	0
0 V	‘X’	6.75 V	0	0	1	0
0 V	‘X’	0 V	0	0	0	1

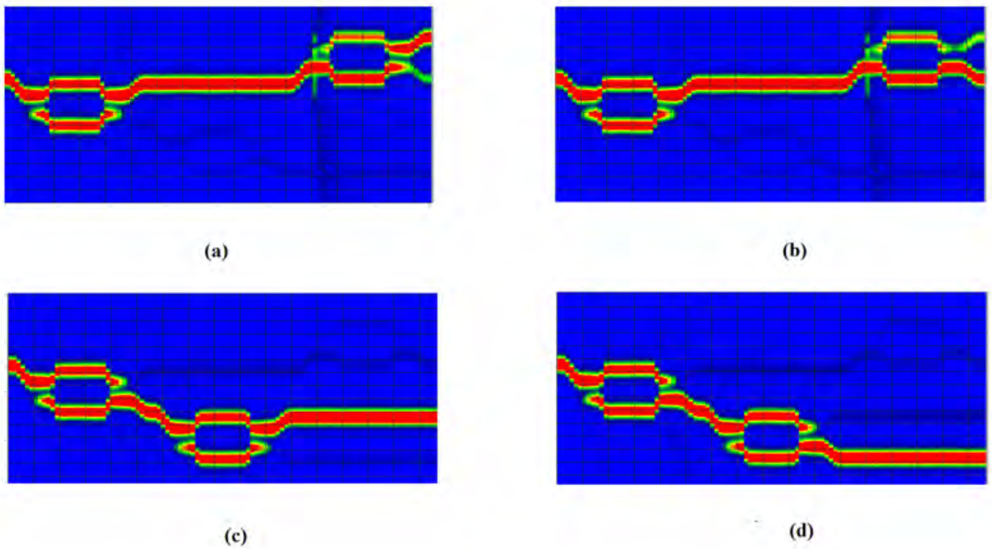

Figure 3.13: Optical field propagation at various output port depending upon the control signal .

Mathematical expression of 1x4 Signal Router

The mathematical expression for the normalized output power at the port 1, 2, 3 and 4 as follow;

$$P_{out\,1} = sin^2\left(\frac{\Delta\varphi_1}{2}\right) cos^2\left(\frac{\Delta\varphi_2}{2}\right) \quad when\ s_1 = 6.75V, s_2 = 0V\ and\ s_3 = {}'X' \qquad (3.8)$$

$$P_{out\,2} = sin^2\left(\frac{\Delta\varphi_1}{2}\right).sin^2\left(\frac{\Delta\varphi_2}{2}\right) \quad when\ s_1 = 6.75V, s_2 = 6.75V\ and\ s_3 = {}'X' \qquad (3.9)$$

$$P_{out\,3} = cos^2\left(\frac{\Delta\varphi_1}{2}\right) sin^2\left(\frac{\Delta\varphi_3}{2}\right) \quad when\ s_1 = 0V, s_2 = {}'X'\ and\ s_3 = 6.75V \qquad (3.10)$$

$$P_{out\,4} = cos^2\left(\frac{\Delta\varphi_1}{2}\right) cos^2\left(\frac{\Delta\varphi_3}{2}\right) \quad when\ s_1 = 0V, s_2 = {}'X'\ and\ s_3 = 0V \qquad (3.11)$$

Matlab Output at port 1 and 2

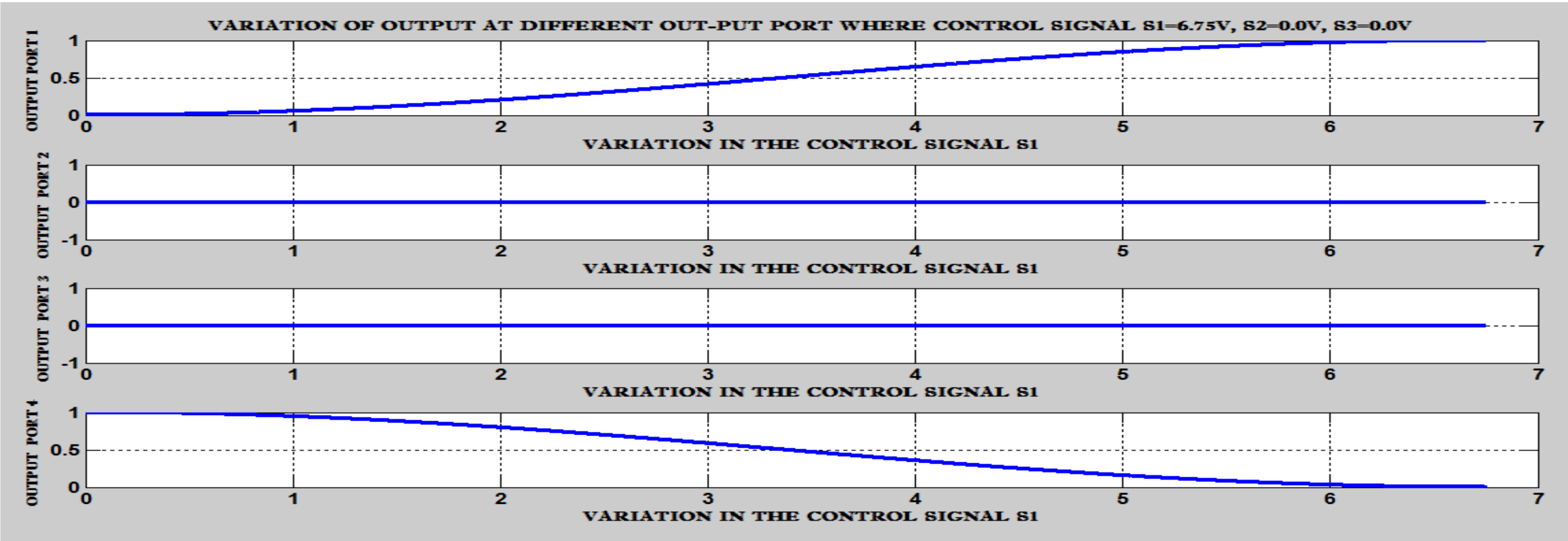

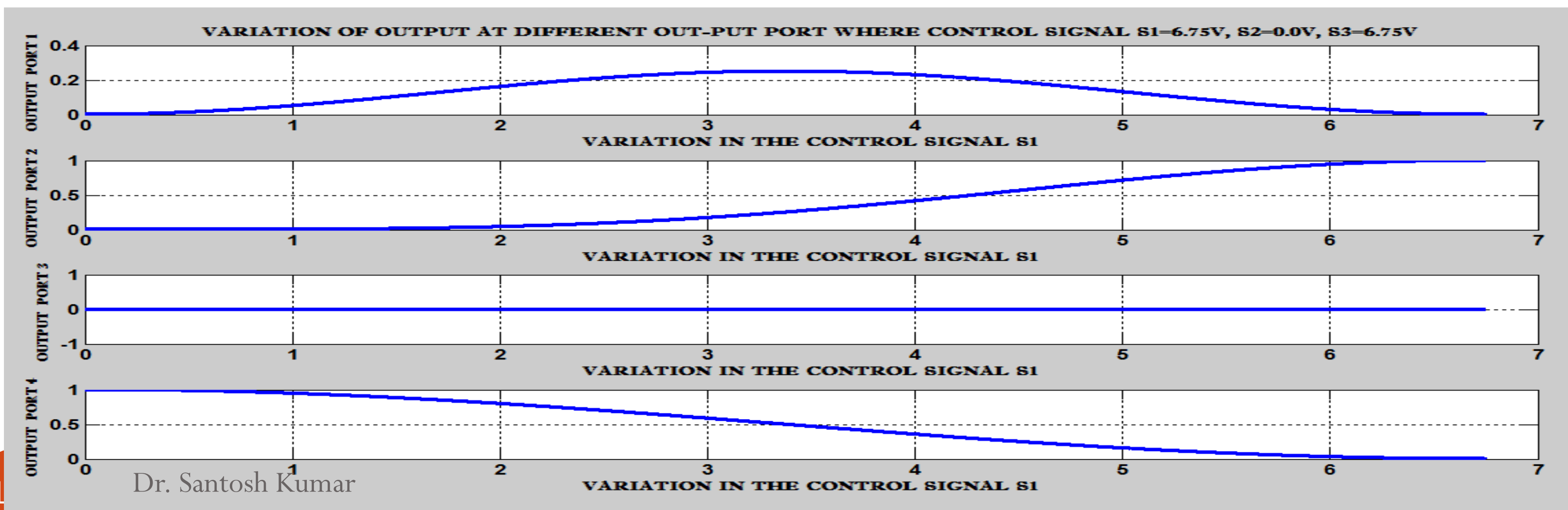

Matlab Output at port 3 and 4

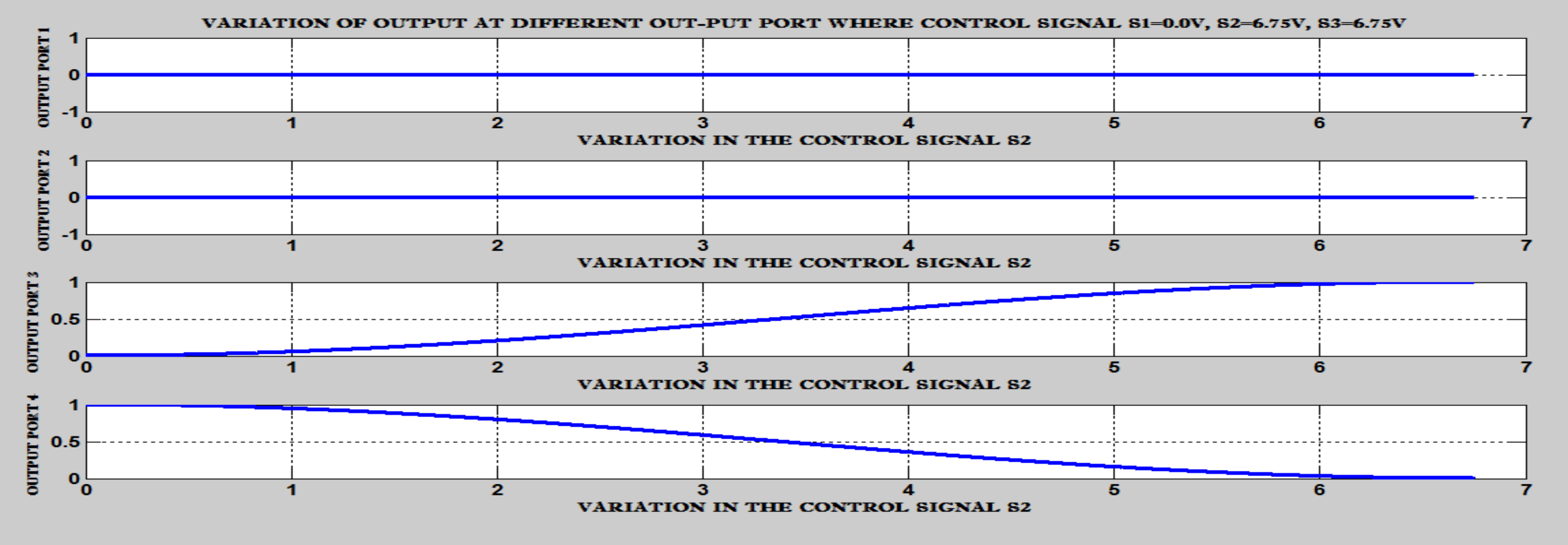

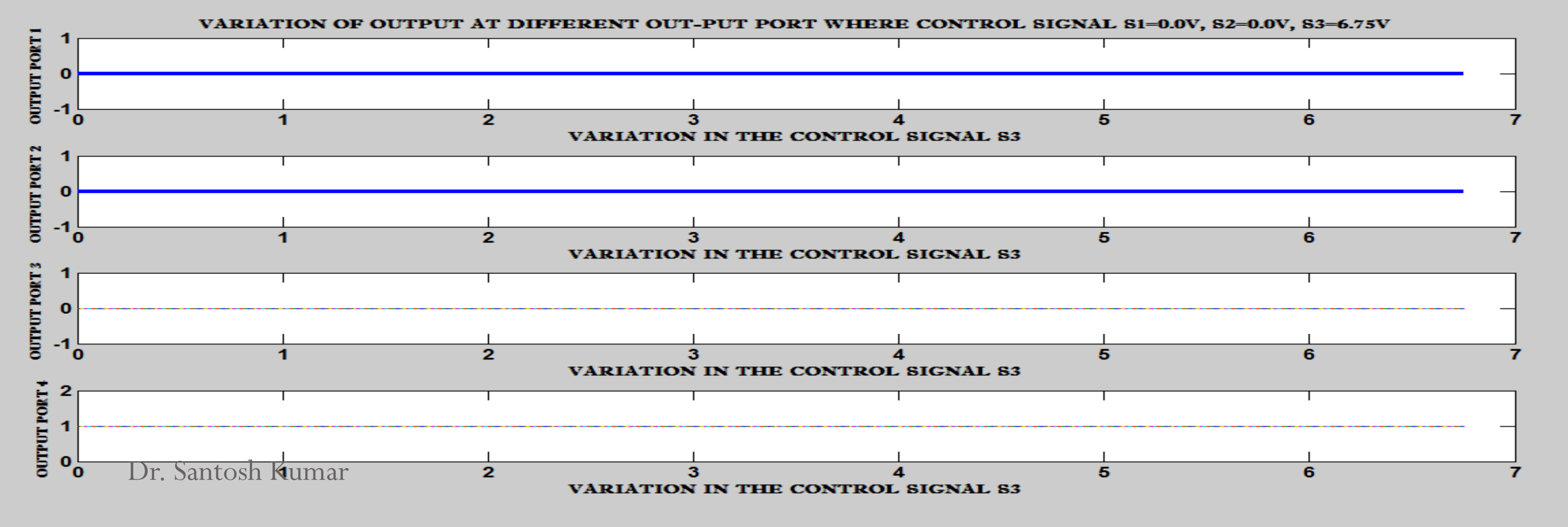

Design of 1 x 8 Signal Router

Santosh Kumar et. Al., *6th IEEE/International Conference on Advanced Infocomm Technology (IEEE/ICAIT-2013)*, Hsinchu, **Taiwan**, July 2013, *IEEE Xplore*.

1 x 8 Signal Router

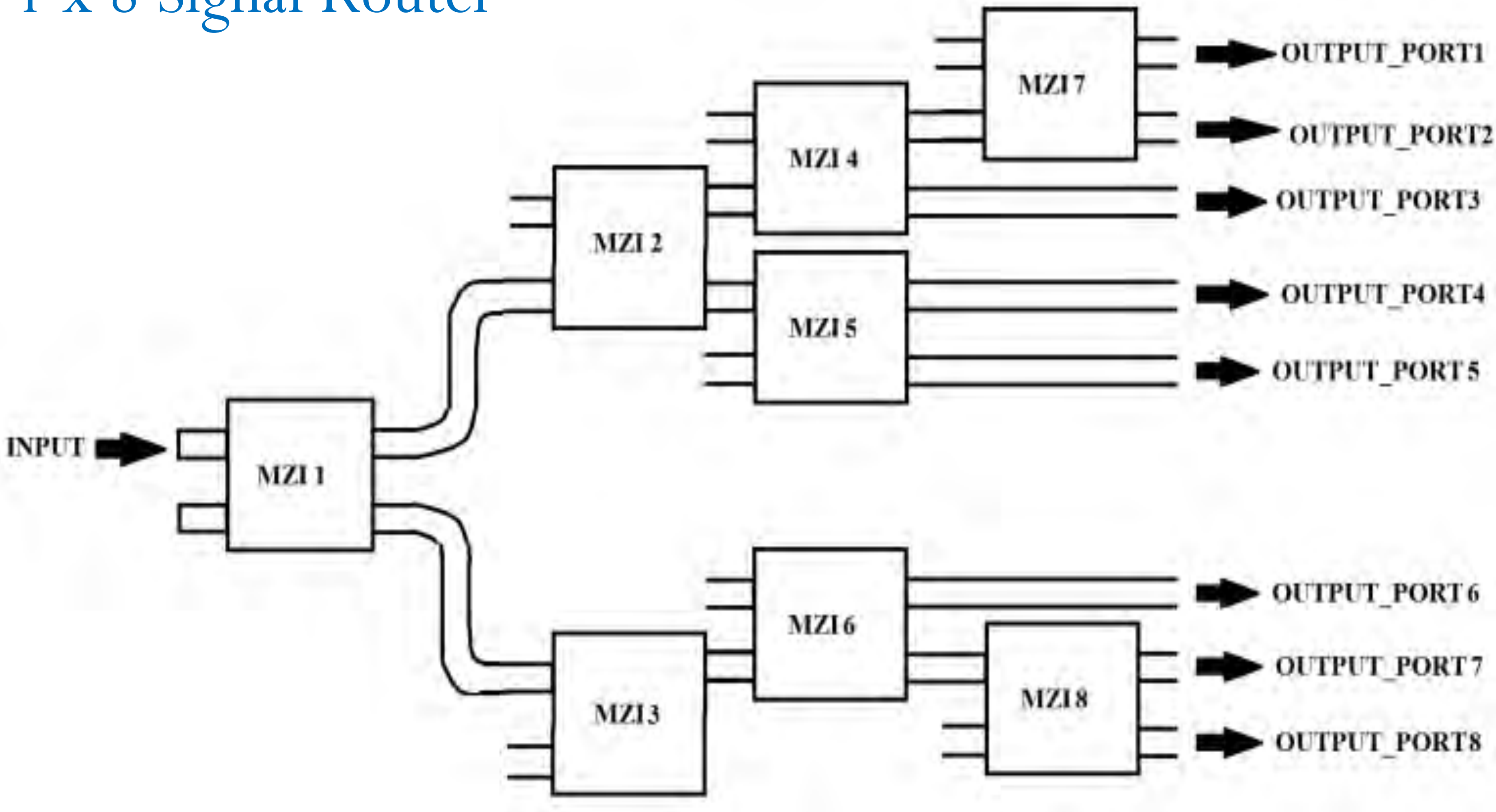

Figure 3.16: 1 x 8 signal router

Contd….

Output	S_1 (V)	S_2 (V)	S_3 (V)	S_4 (V)	S_5 (V)	S_6 (V)	S_7 (V)	S_8 (V)
port1	6.75	0.0	X	0.0	X	X	0.0	X
port2	6.75	0.0	X	0.0	X	X	6.75	X
port3	6.75	0.0	X	6.75	X	X	X	X
port4	6.75	6.75	X	X	6.75	X	X	X
port5	6.75	6.75	X	X	0.0	X	X	X
port6	0.0	X	6.75	X	X	0.0	X	X
port7	0.0	X	6.75	X	X	6.75	X	6.75
port8	0.0	X	6.75	X	X	6.75	X	0.0

Table 3.3: Different combination of control signal for 1 × 8 Signal router.

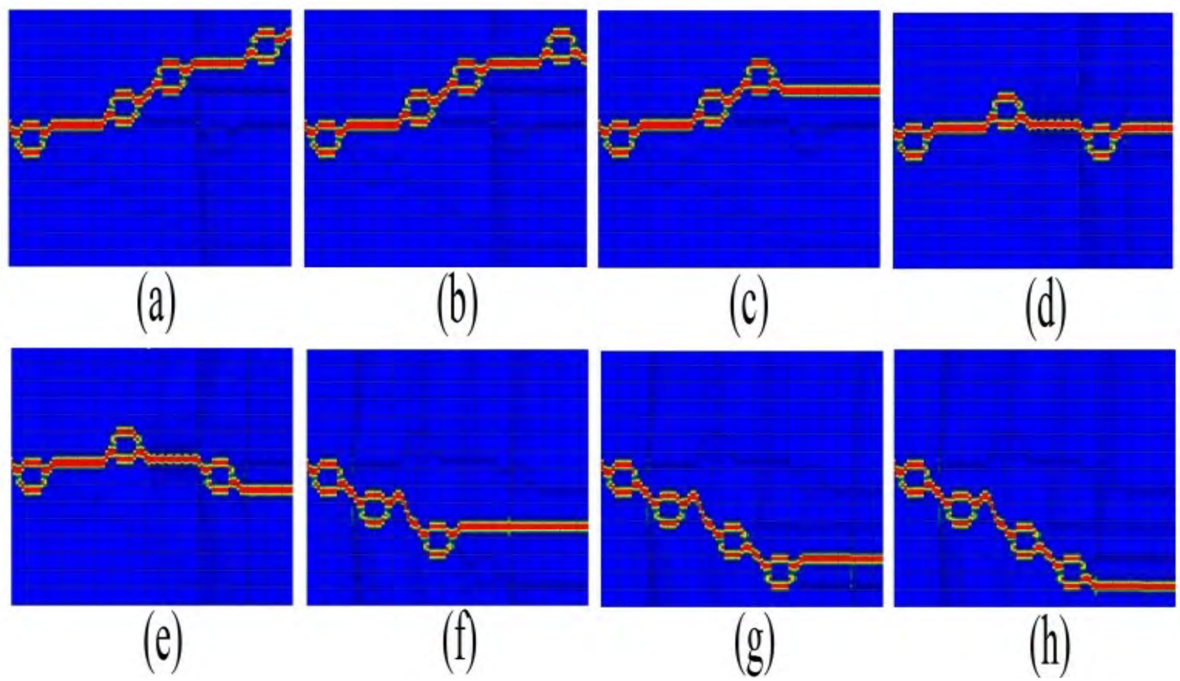

Figure 3.17: Optical field propagation at (a) port 1, (b) port 2, (c) port 3, (d) port 4, (e) port 5 (f) port 6, (g) port 7, (h) port 8.

Design of 4x4 signal router using MZIs

Santosh Kumar et. al., Optics Communication (Elsevier), Vol. 353, PP. 17-26, (May 8, 2015).

Design of 4x4 signal router using MZIs

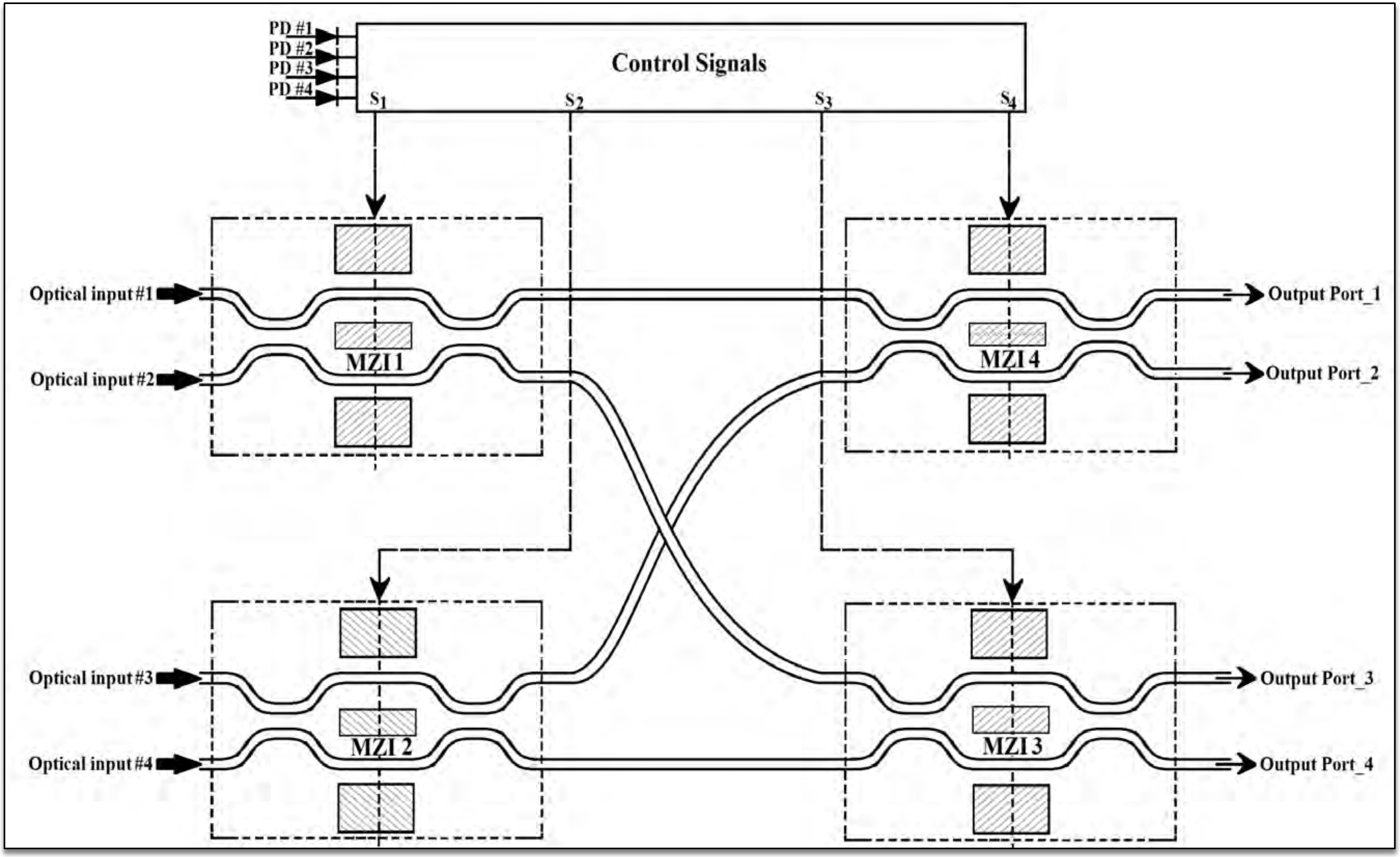

Figure 8: Schematic diagram of 4x4 signal router using MZIs.

Mathematical description of 4×4 Signal Router

Depending upon the control signals, the optical power from different input ports can be routed to any one of the four output ports. is calculated as follows;

For output port 1:

$$\mathrm{OUT1} = \left[\sin^2\left(\frac{\Delta\varphi_{\mathrm{MZI}\,1}}{2}\right)\sin^2\left(\frac{\Delta\varphi_{\mathrm{MZI}\,4}}{2}\right) + \cos^2\left(\frac{\Delta\varphi_{\mathrm{MZI}\,1}}{2}\right)\sin^2\left(\frac{\Delta\varphi_{\mathrm{MZI}\,4}}{2}\right) + \sin^2\left(\frac{\Delta\varphi_{\mathrm{MZI}\,2}}{2}\right)\cos^2\left(\frac{\Delta\varphi_{\mathrm{MZI}\,4}}{2}\right)\right] \quad (10)$$

For output port 2:

$$\mathrm{OUT2} = \left[\sin^2\left(\frac{\Delta\varphi_{\mathrm{MZI}\,1}}{2}\right)\cos^2\left(\frac{\Delta\varphi_{\mathrm{MZI}\,4}}{2}\right) + \cos^2\left(\frac{\Delta\varphi_{\mathrm{MZI}\,1}}{2}\right)\cos^2\left(\frac{\Delta\varphi_{\mathrm{MZI}\,4}}{2}\right) + \sin^2\left(\frac{\Delta\varphi_{\mathrm{MZI}\,2}}{2}\right)\sin^2\left(\frac{\Delta\varphi_{\mathrm{MZI}\,4}}{2}\right) + \cos^2\left(\frac{\Delta\varphi_{\mathrm{MZI}\,2}}{2}\right)\sin^2\left(\frac{\Delta\varphi_{\mathrm{MZI}\,4}}{2}\right)\right] \quad (11)$$

For output port 3:

$$\mathrm{OUT3} = \left[\cos^2\left(\frac{\Delta\varphi_{\mathrm{MZI}\,1}}{2}\right)\sin^2\left(\frac{\Delta\varphi_{\mathrm{MZI}\,3}}{2}\right) + \sin^2\left(\frac{\Delta\varphi_{\mathrm{MZI}\,1}}{2}\right)\sin^2\left(\frac{\Delta\varphi_{\mathrm{MZI}\,3}}{2}\right) + \cos^2\left(\frac{\Delta\varphi_{\mathrm{MZI}\,2}}{2}\right)\cos^2\left(\frac{\Delta\varphi_{\mathrm{MZI}\,3}}{2}\right) + \sin^2\left(\frac{\Delta\varphi_{\mathrm{MZI}\,2}}{2}\right)\cos^2\left(\frac{\Delta\varphi_{\mathrm{MZI}\,3}}{2}\right)\right] \quad (12)$$

For output port 4:

$$\mathrm{OUT4} = \left[\sin^2\left(\frac{\Delta\varphi_{\mathrm{MZI}\,1}}{2}\right)\sin^2\left(\frac{\Delta\varphi_{\mathrm{MZI}\,3}}{2}\right) + \cos^2\left(\frac{\Delta\varphi_{\mathrm{MZI}\,1}}{2}\right)\sin^2\left(\frac{\Delta\varphi_{\mathrm{MZI}\,3}}{2}\right) + \cos^2\left(\frac{\Delta\varphi_{\mathrm{MZI}\,2}}{2}\right)\cos^2\left(\frac{\Delta\varphi_{\mathrm{MZI}\,3}}{2}\right) + \sin^2\left(\frac{\Delta\varphi_{\mathrm{MZI}\,2}}{2}\right)\cos^2\left(\frac{\Delta\varphi_{\mathrm{MZI}\,3}}{2}\right)\right] \quad (13)$$

BPM Results of 4x4 Signal Router

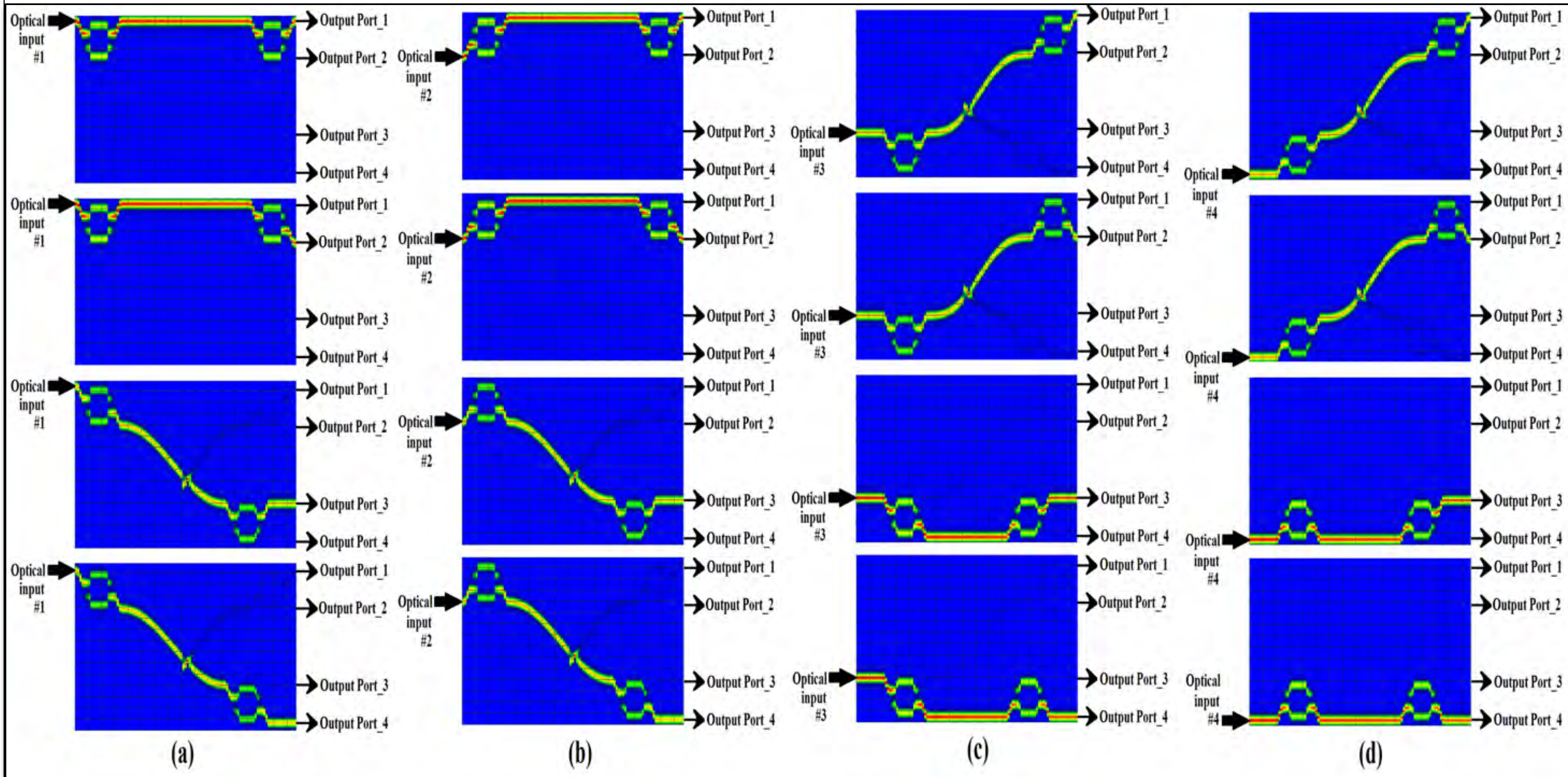

Figure 9: Routing of optical input signal to the four output ports from (a) first input port, (b) second input port , (c) third input port , (d) fourth input port.

Design of Wavelength Selectors Device

Santosh Kumar et. al., Optics Communications (Elsevier), Vol. 350, PP. 108-118 (April 4, 2015).

Design of Wavelength selectors using MZIs

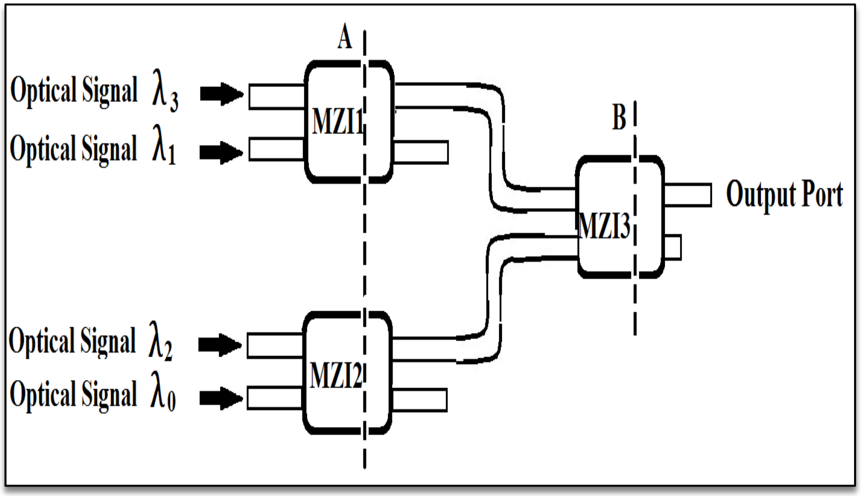

Figure 10: Schematic diagram of 4 × 1 wavelength selector device using the MZIs

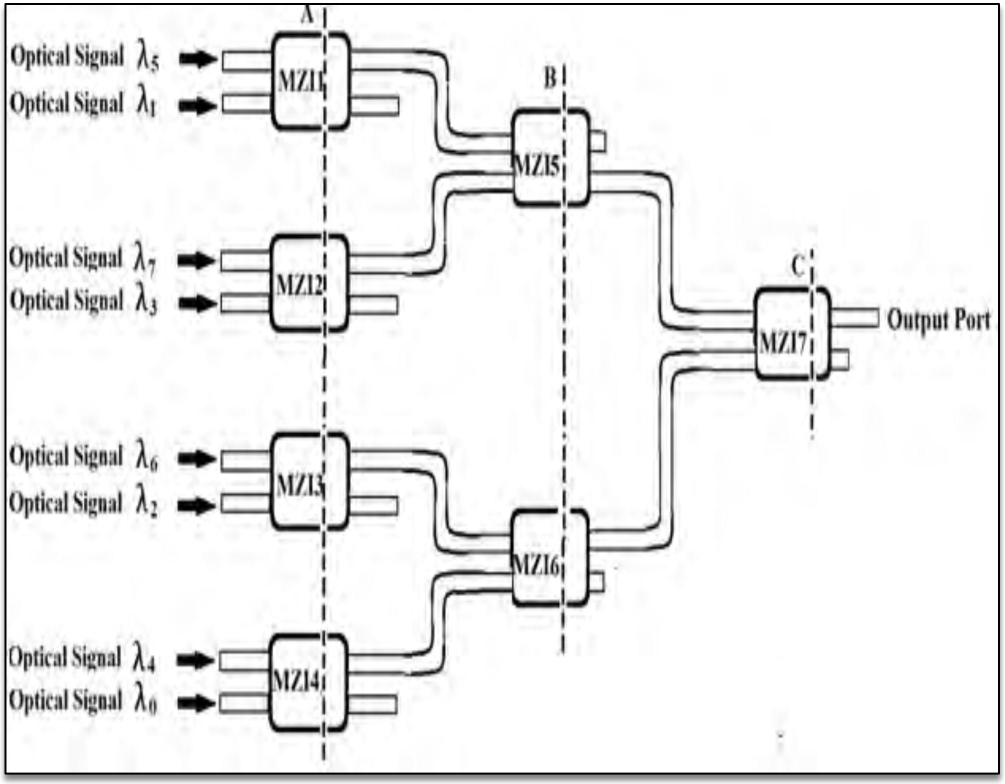

Figure 11: Schematic diagram of 8 × 1 wavelength selector using MZIs

Mathematical expression of 4x1 Wavelength Selector

The normalized output power for different control signals can be calculated as follows;

$$\mathrm{OUT1} = \left|\frac{\mathrm{OUT1}_{\mathrm{MZI}\,3_1}}{E_{in}}\right|^2 = \cos^2\left(\frac{\Delta\varphi_{\mathrm{MZI}\,1}}{2}\right)\cos^2\left(\frac{\Delta\varphi_{\mathrm{MZI}\,2}}{2}\right)\cos^2\left(\frac{\Delta\varphi_{\mathrm{MZI}\,3}}{2}\right) \quad (14)$$

$$\mathrm{OUT2} = \left|\frac{\mathrm{OUT1}_{\mathrm{MZI}\,3_2}}{E_{in}}\right|^2 = \cos^2\left(\frac{\Delta\varphi_{\mathrm{MZI}\,1}}{2}\right)\cos^2\left(\frac{\Delta\varphi_{\mathrm{MZI}\,2}}{2}\right)\sin^2\left(\frac{\Delta\varphi_{\mathrm{MZI}\,3}}{2}\right) \quad (15)$$

$$\mathrm{OUT3} = \left|\frac{\mathrm{OUT1}_{\mathrm{MZI}\,3_3}}{E_{in}}\right|^2 = \sin^2\left(\frac{\Delta\varphi_{\mathrm{MZI}\,1}}{2}\right)\sin^2\left(\frac{\Delta\varphi_{\mathrm{MZI}\,2}}{2}\right)\cos^2\left(\frac{\Delta\varphi_{\mathrm{MZI}\,3}}{2}\right) \quad (16)$$

$$\mathrm{OUT4} = \left|\frac{\mathrm{OUT1}_{\mathrm{MZI}\,3_4}}{E_{in}}\right|^2 = \sin^2\left(\frac{\Delta\varphi_{\mathrm{MZI}\,1}}{2}\right)\sin^2\left(\frac{\Delta\varphi_{\mathrm{MZI}\,2}}{2}\right)\sin^2\left(\frac{\Delta\varphi_{\mathrm{MZI}\,3}}{2}\right) \quad (17)$$

MATLAB Result of 4x1 Wavelength Selector

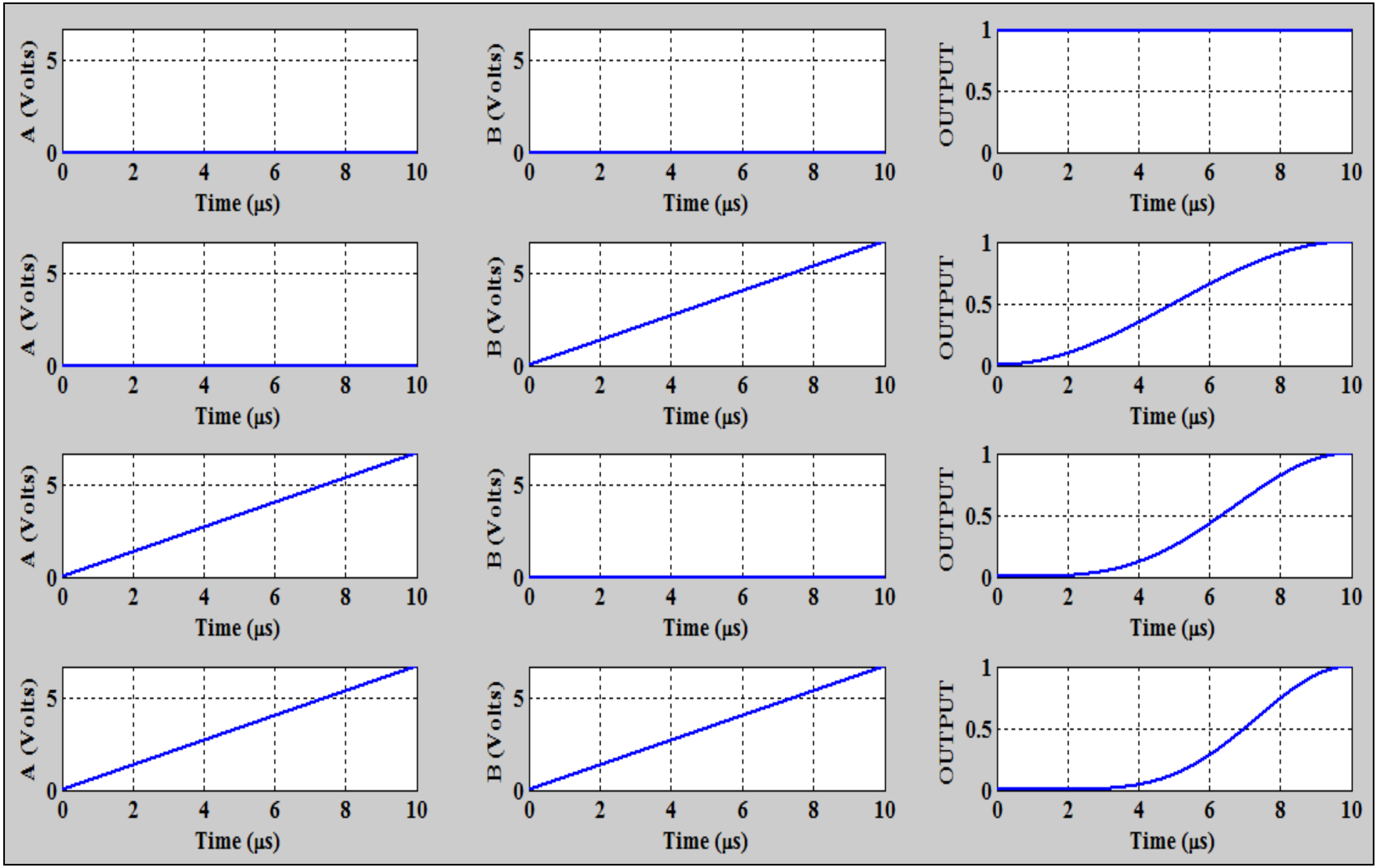

Figure 12: MATLAB simulation result of 4×1 wavelength selector, when $\lambda_0 - \lambda_3$ is transmitted individually at output port.

BPM Result of 4x1 Wavelength Selector

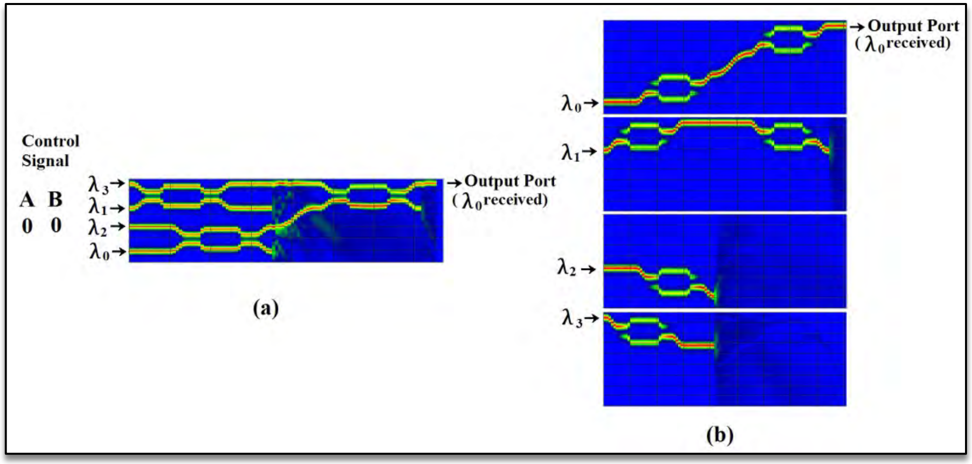

Fig.13: Simulation result of (a) 4 × 1 wavelength selector, when (b) only λ_0 is transmitted at output port for control signal $A = 0$ and $B = 0$

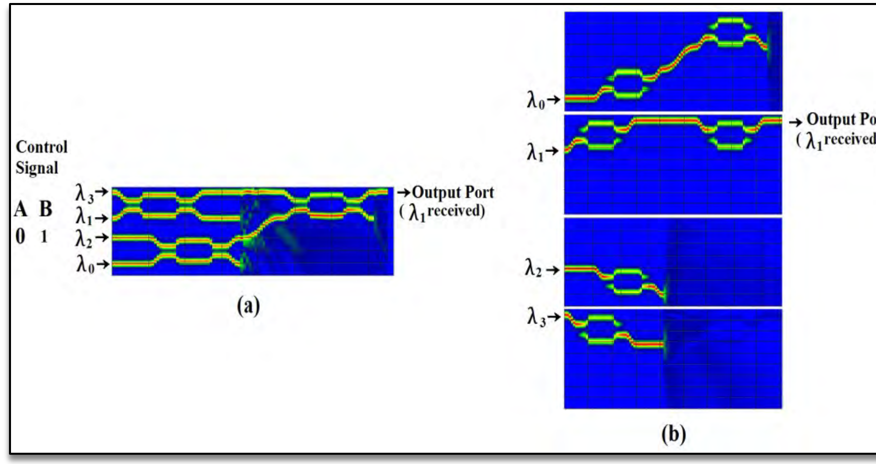

Fig.14: Simulation result of (a) 4 × 1 wavelength selector, when (b) only λ_1 is transmitted at output port for control signal $A = 0$ and $B = 1$

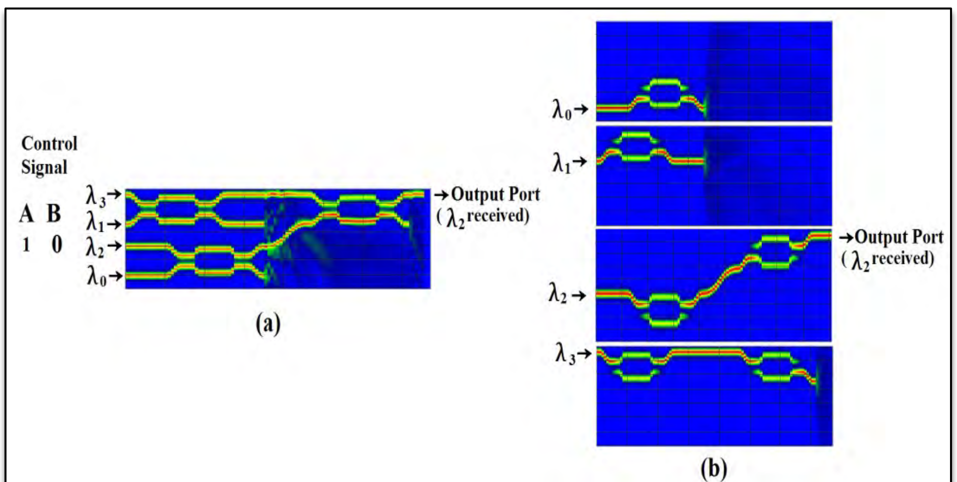

Fig.15: Simulation result of (a) 4 × 1 wavelength selector, when (b) only λ_2 is transmitted at output port for control signal $A = 1$ and $B = 0$

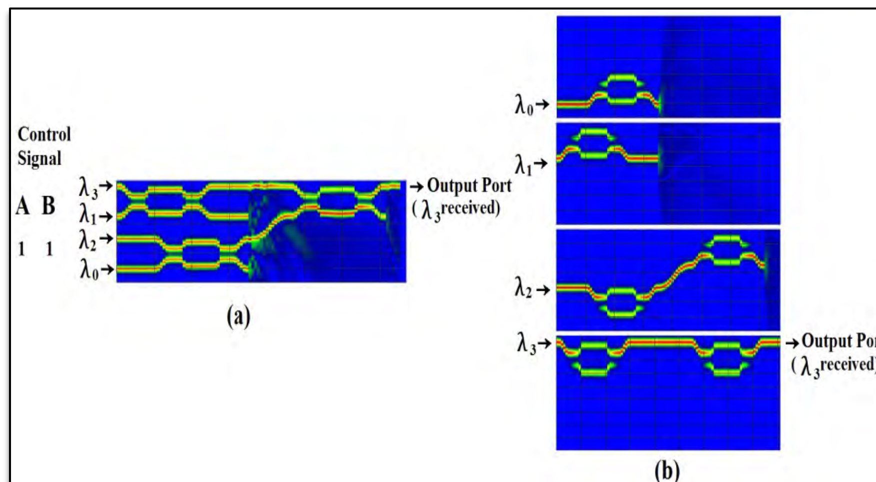

Fig.16: Simulation result of (a) 4 × 1 wavelength selector, when (b) only λ_3 is transmitted at output port for control signal $A = 1$ and $B = 1$

Mathematical expression of 8x1 Wavelength Selector

The normalized output power for different control signals can be represented by the following equations;

$$OUT1 = \left|\frac{OUT1_{MZI\,7_1}}{E_{in}}\right|^2 = \cos^2\left(\frac{\Delta\varphi_{MZI\,4}}{2}\right)\cos^2\left(\frac{\Delta\varphi_{MZI\,6}}{2}\right)\cos^2\left(\frac{\Delta\varphi_{MZI\,7}}{2}\right) \quad (18)$$

$$OUT2 = \left|\frac{OUT1_{MZI\,7_2}}{E_{in}}\right|^2 = \cos^2\left(\frac{\Delta\varphi_{MZI\,1}}{2}\right)\cos^2\left(\frac{\Delta\varphi_{MZI\,5}}{2}\right)\sin^2\left(\frac{\Delta\varphi_{MZI\,7}}{2}\right) \quad (19)$$

$$OUT3 = \left|\frac{OUT1_{MZI\,7_3}}{E_{in}}\right|^2 = \cos^2\left(\frac{\Delta\varphi_{MZI\,3}}{2}\right)\sin^2\left(\frac{\Delta\varphi_{MZI\,6}}{2}\right)\cos^2\left(\frac{\Delta\varphi_{MZI\,7}}{2}\right) \quad (20)$$

$$OUT4 = \left|\frac{OUT1_{MZI\,7_4}}{E_{in}}\right|^2 = \cos^2\left(\frac{\Delta\varphi_{MZI\,2}}{2}\right)\sin^2\left(\frac{\Delta\varphi_{MZI\,5}}{2}\right)\sin^2\left(\frac{\Delta\varphi_{MZI\,7}}{2}\right) \quad (21)$$

$$OUT5 = \left|\frac{OUT1_{MZI\,7_5}}{E_{in}}\right|^2 = \sin^2\left(\frac{\Delta\varphi_{MZI\,4}}{2}\right)\cos^2\left(\frac{\Delta\varphi_{MZI\,6}}{2}\right)\cos^2\left(\frac{\Delta\varphi_{MZI\,7}}{2}\right) \quad (22)$$

$$OUT6 = \left|\frac{OUT1_{MZI\,7_1}}{E_{in}}\right|^2 = \sin^2\left(\frac{\Delta\varphi_{MZI\,1}}{2}\right)\cos^2\left(\frac{\Delta\varphi_{MZI\,5}}{2}\right)\sin^2\left(\frac{\Delta\varphi_{MZI\,7}}{2}\right) \quad (23)$$

$$OUT7 = \left|\frac{OUT1_{MZI\,7_3}}{E_{in}}\right|^2 = \sin^2\left(\frac{\Delta\varphi_{MZI\,3}}{2}\right)\sin^2\left(\frac{\Delta\varphi_{MZI\,6}}{2}\right)\cos^2\left(\frac{\Delta\varphi_{MZI\,7}}{2}\right) \quad (24)$$

$$OUT8 = \left|\frac{OUT1_{MZI\,7_4}}{E_{in}}\right|^2 = \sin^2\left(\frac{\Delta\varphi_{MZI\,2}}{2}\right)\sin^2\left(\frac{\Delta\varphi_{MZI\,5}}{2}\right)\sin^2\left(\frac{\Delta\varphi_{MZI\,7}}{2}\right) \quad (25)$$

MATLAB Result of 8x1 Wavelength Selector

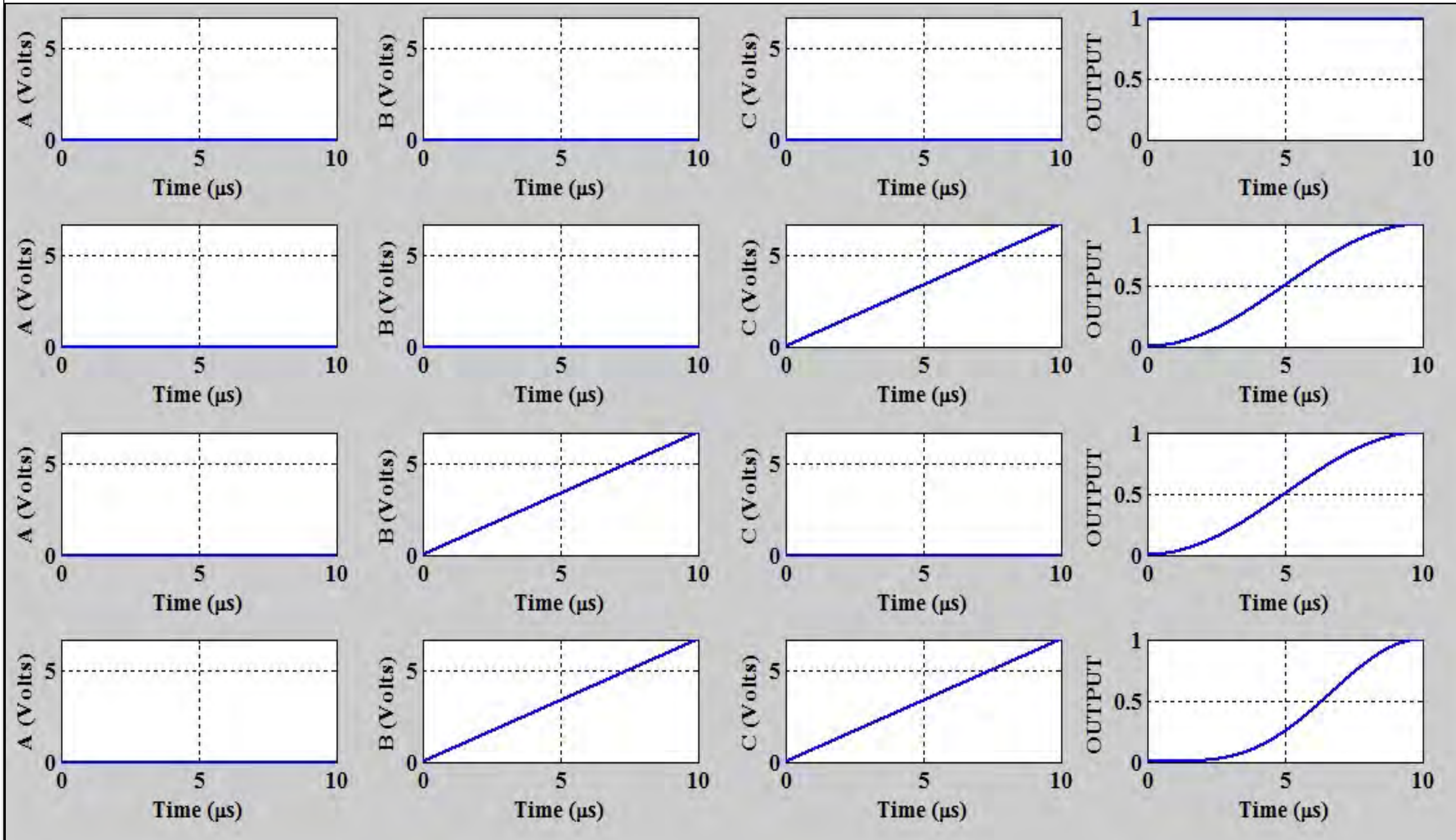

Figure 17(a): MATLAB simulation result of 8× 1 wavelength selector, when $\lambda_0 - \lambda_3$ is transmitted individually at output port.

Cont…

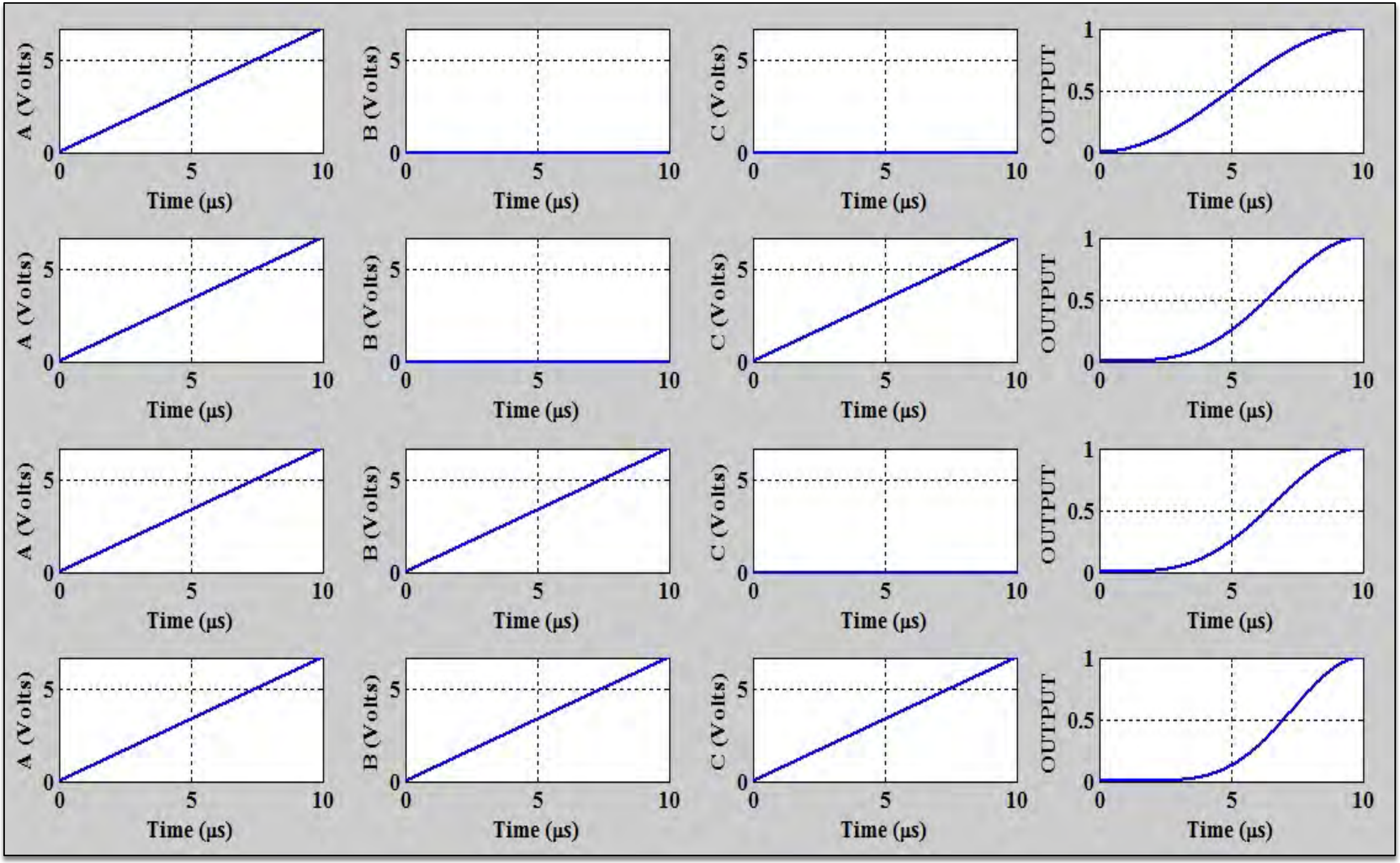

Figure 17(b): MATLAB simulation result of 8× 1 wavelength selector, when $\lambda_4 - \lambda_7$ is transmitted individually at output port.

BPM Result of 8x1 Wavelength Selector

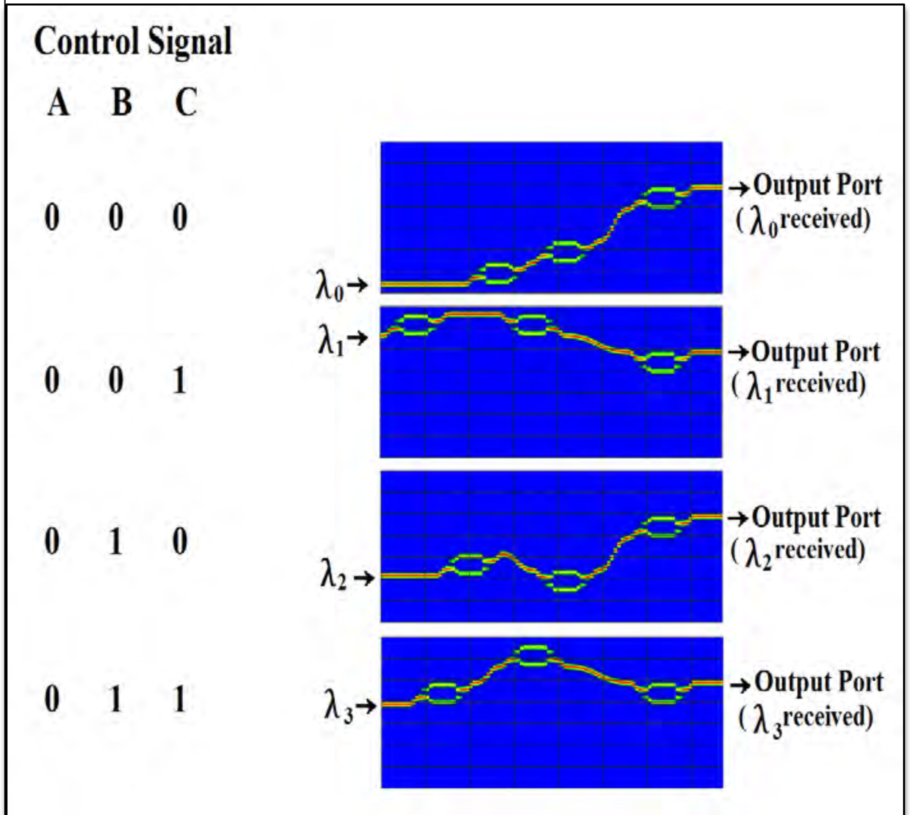

Figure 18(a): Simulation results of 8×1 wavelength selector, when wavelengths $(\lambda_0-\lambda_3)$ are transmitted at output port by applying different control signals

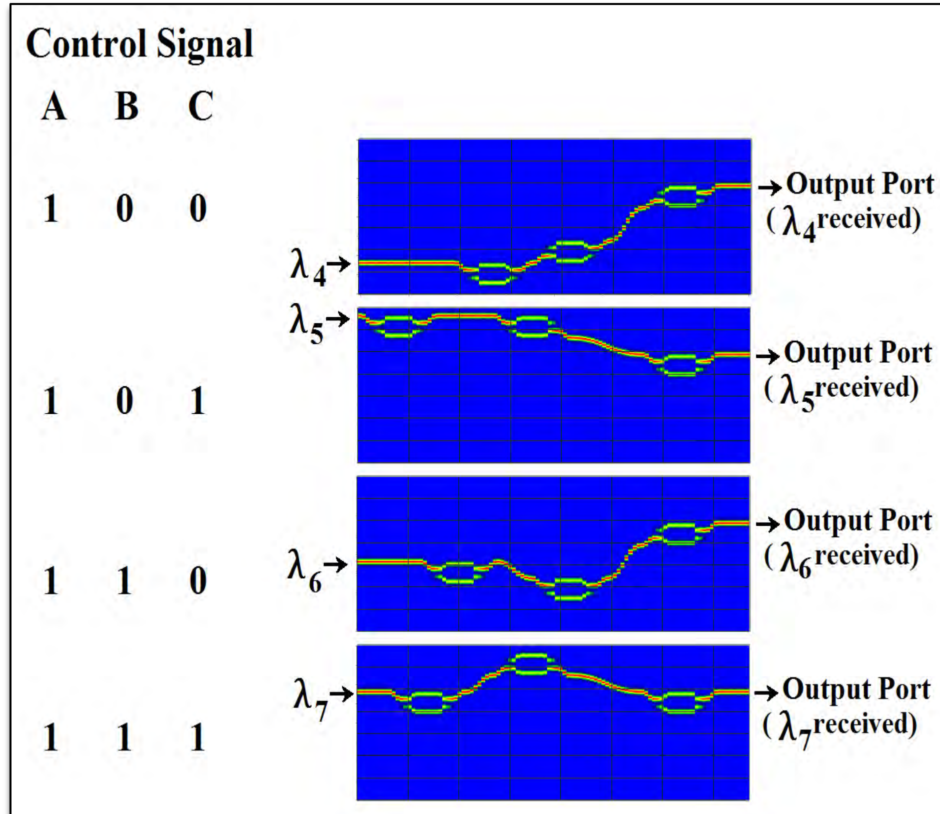

Figure 18(b): Simulation results of 8×1 wavelength selector, when wavelengths $(\lambda_4-\lambda_7)$ are transmitted at output port by applying different control signals

Design of Reversible gates

Santosh Kumar et al., Applied optics, Vol. 55. PP.-5693-5701 (OSA) (July,2016).

Reversible Logic Gates (Feynman gate)

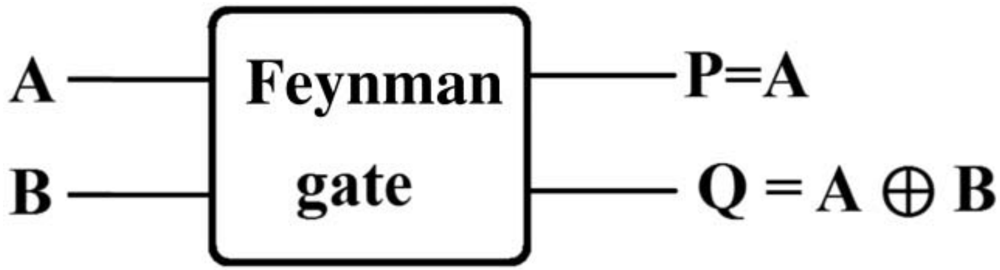

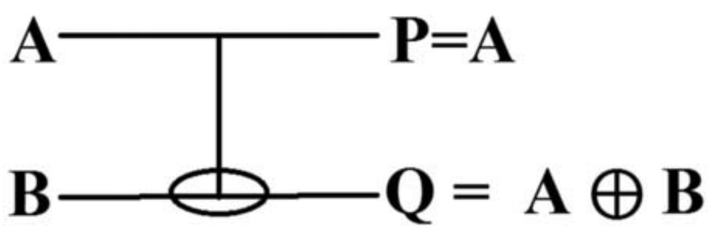

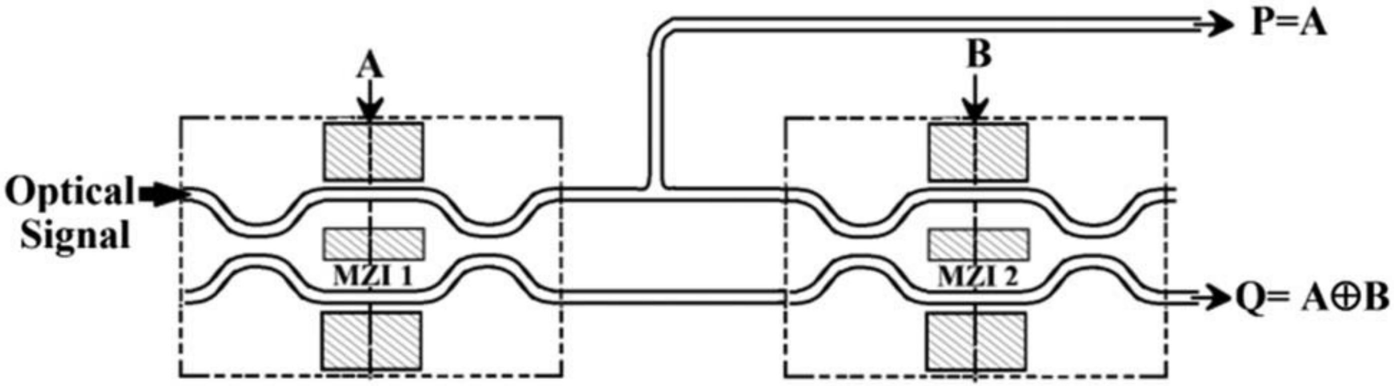

Figure: Logic symbol and Schematic diagram of Feynman gate using MZIs.

Mathematical Expression for Reversible gates

Mathematical formulation for Feynman gate

$$\mathrm{P} = \sin^2\left(\frac{\Delta\emptyset_{\mathrm{MZI1}}}{2}\right)$$

$$\mathrm{Q} = \sin^2\left(\frac{\Delta\emptyset_{\mathrm{MZI1}}}{2}\right)\cos^2\left(\frac{\Delta\emptyset_{\mathrm{MZI2}}}{2}\right) + \cos^2\left(\frac{\Delta\emptyset_{\mathrm{MZI1}}}{2}\right)\sin^2\left(\frac{\Delta\emptyset_{\mathrm{MZI2}}}{2}\right)$$

MATLAB Results for Feynman gate

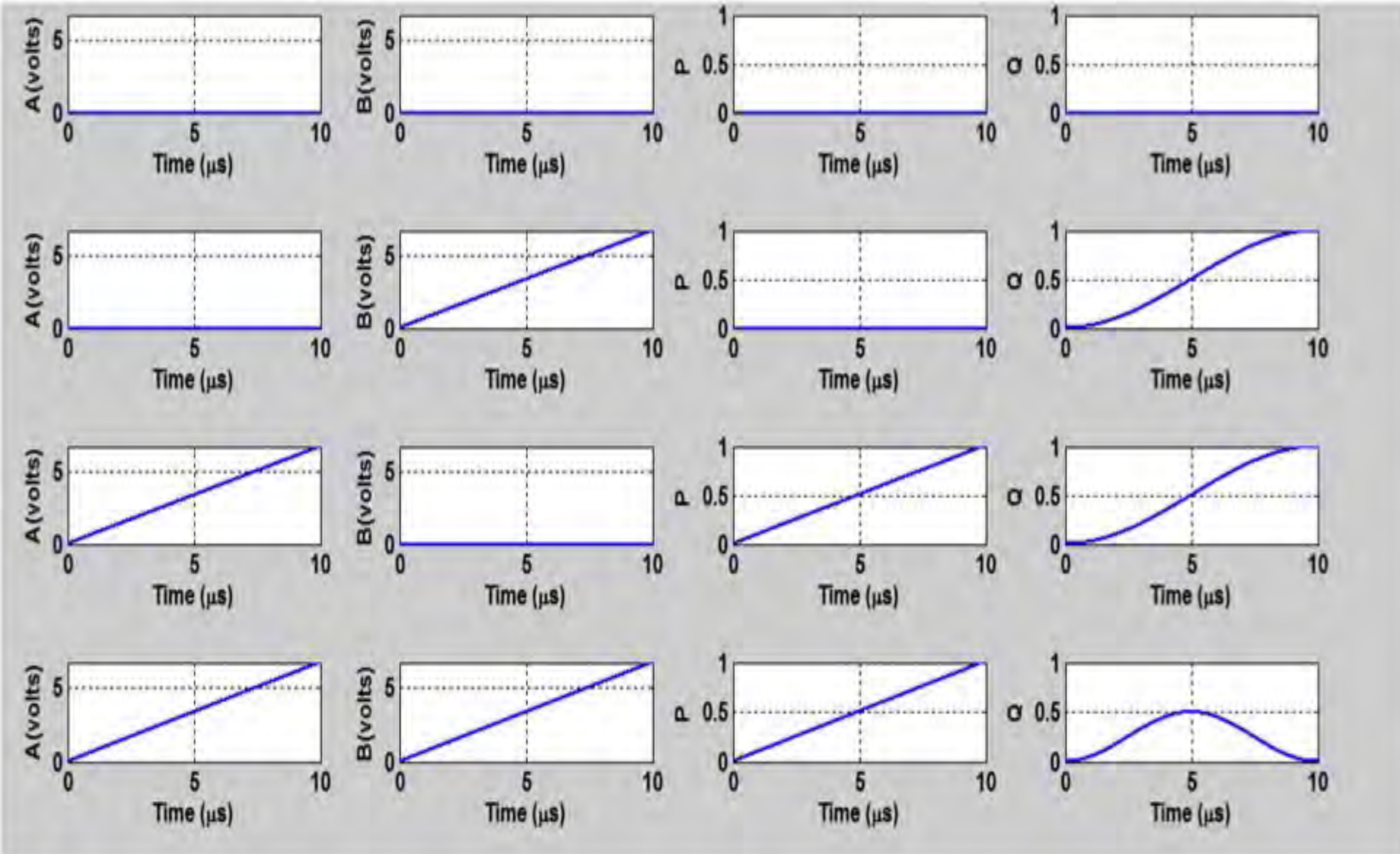

Figure: MATLAB simulation result of Feynman gate where A,B varies from 00 to 11

BPM Layout of Feynman gate

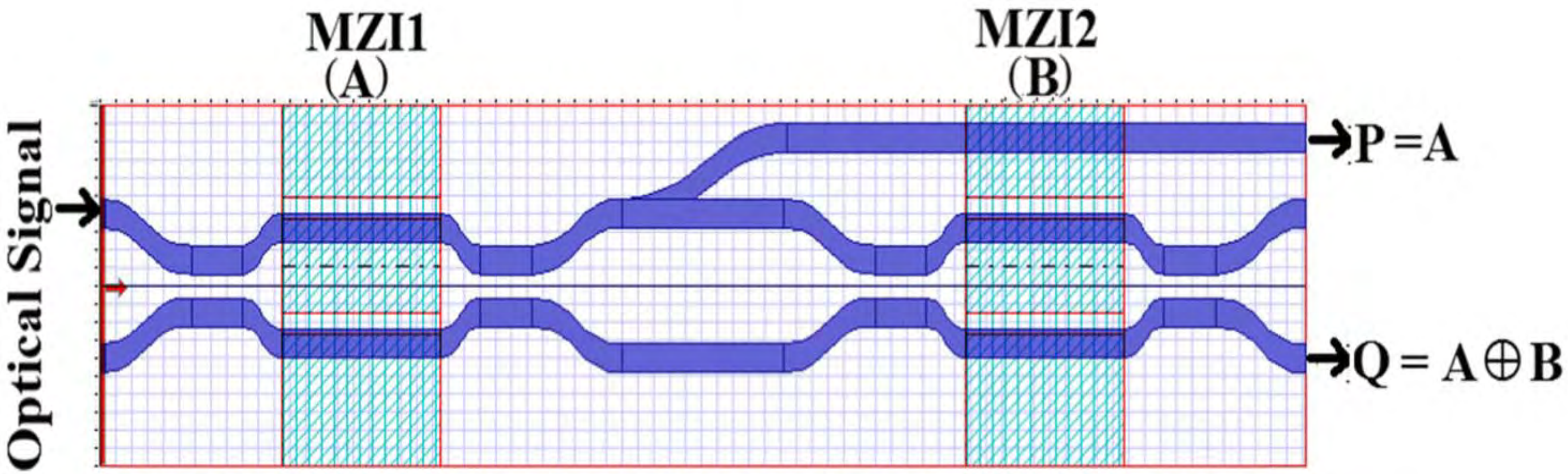

Figure: BPM layout of Feynman gate

Simulation Result from BPM (Feynman gate)

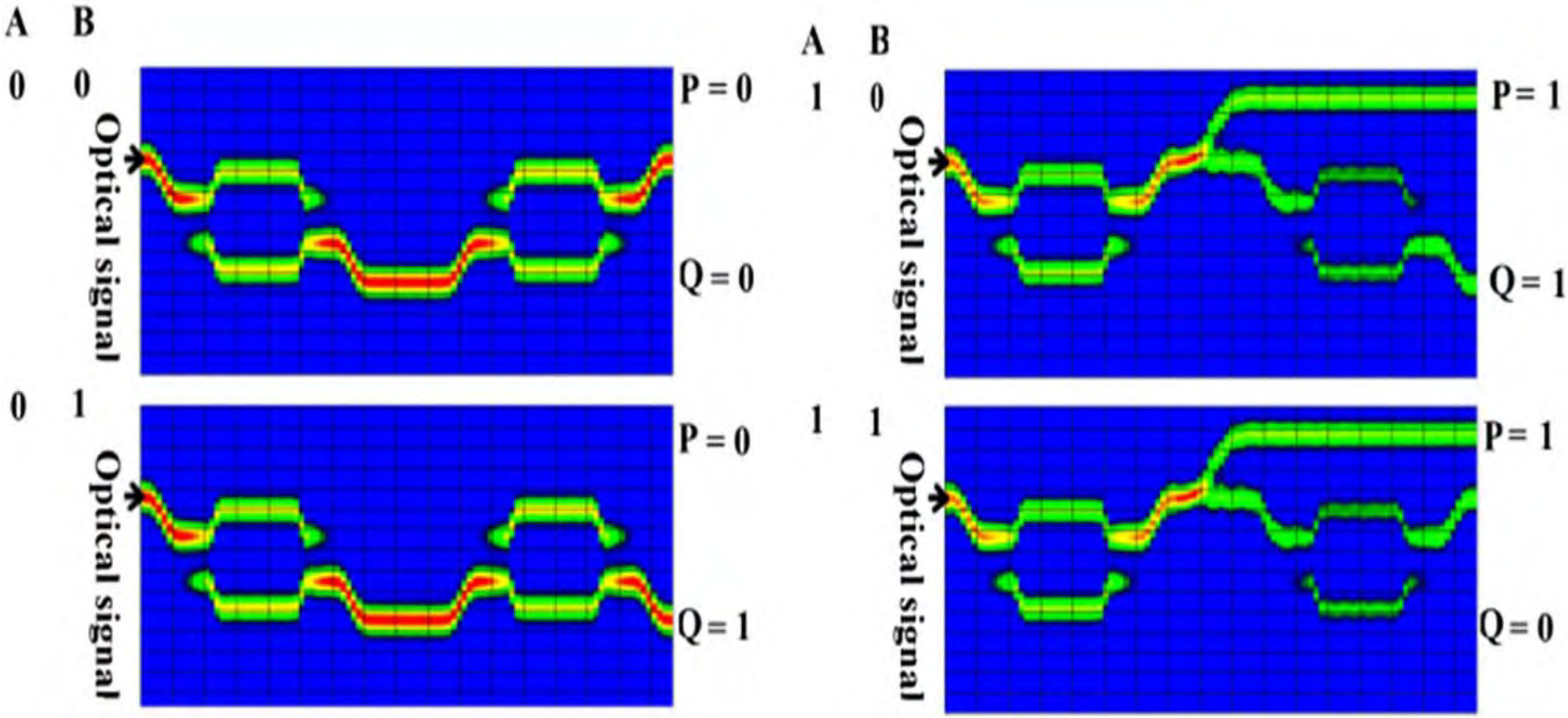

Figure: BPM result of Feynman gate where A, B varies from 00 to 11

Application Example (Feynman gate as D-flip flop)

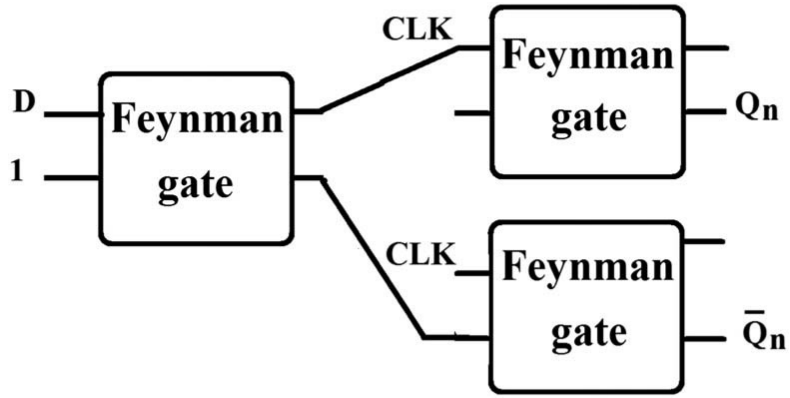

Figure: Application of Feynman gate as D flip flop

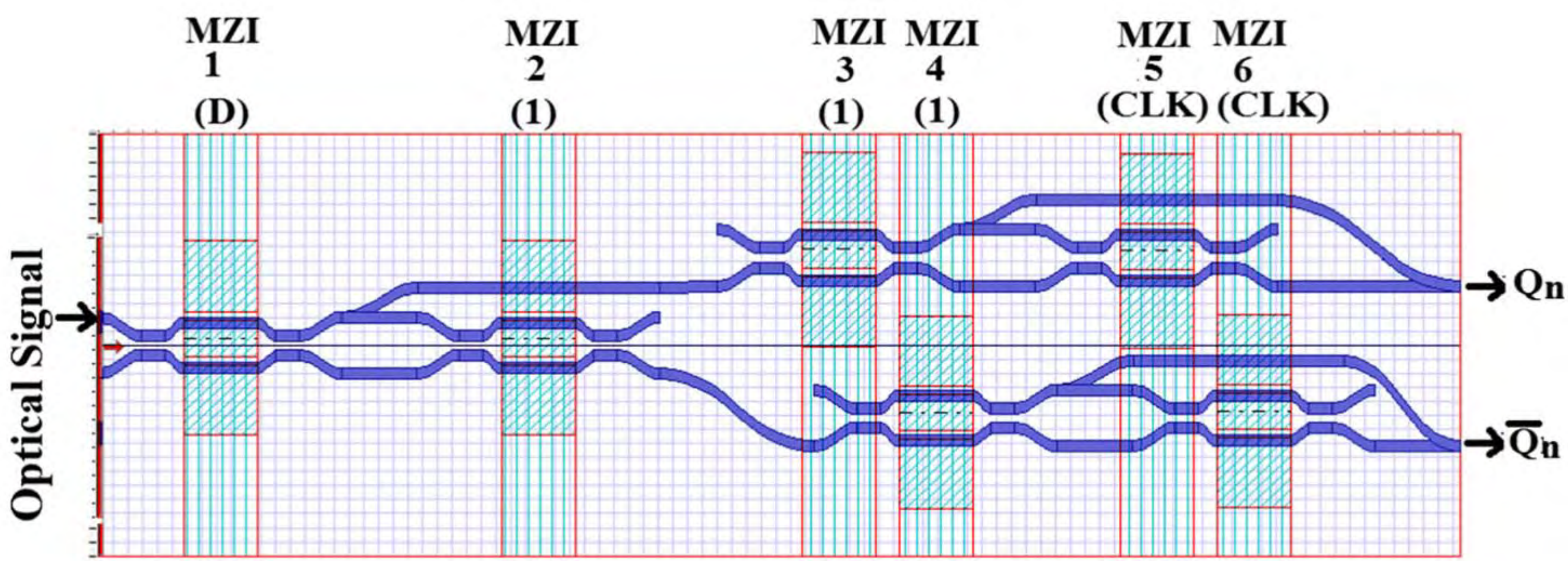

Dr. Santosh Kumar

Figure: BPM layout of D Flip-flop using Feynman gate

Simulation Result (Feynman as D flip flop)

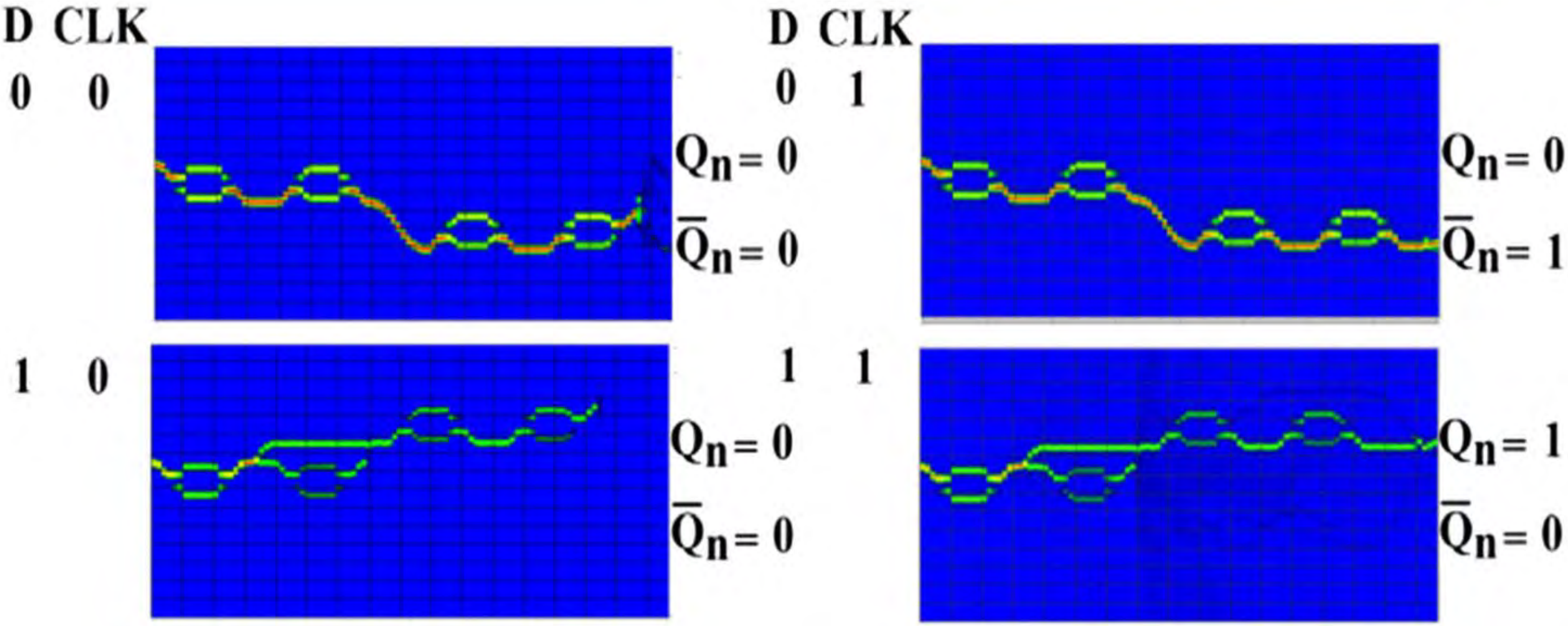

Figure: BPM results of D flip flop

Reversible Logic Gates (Fredkin)

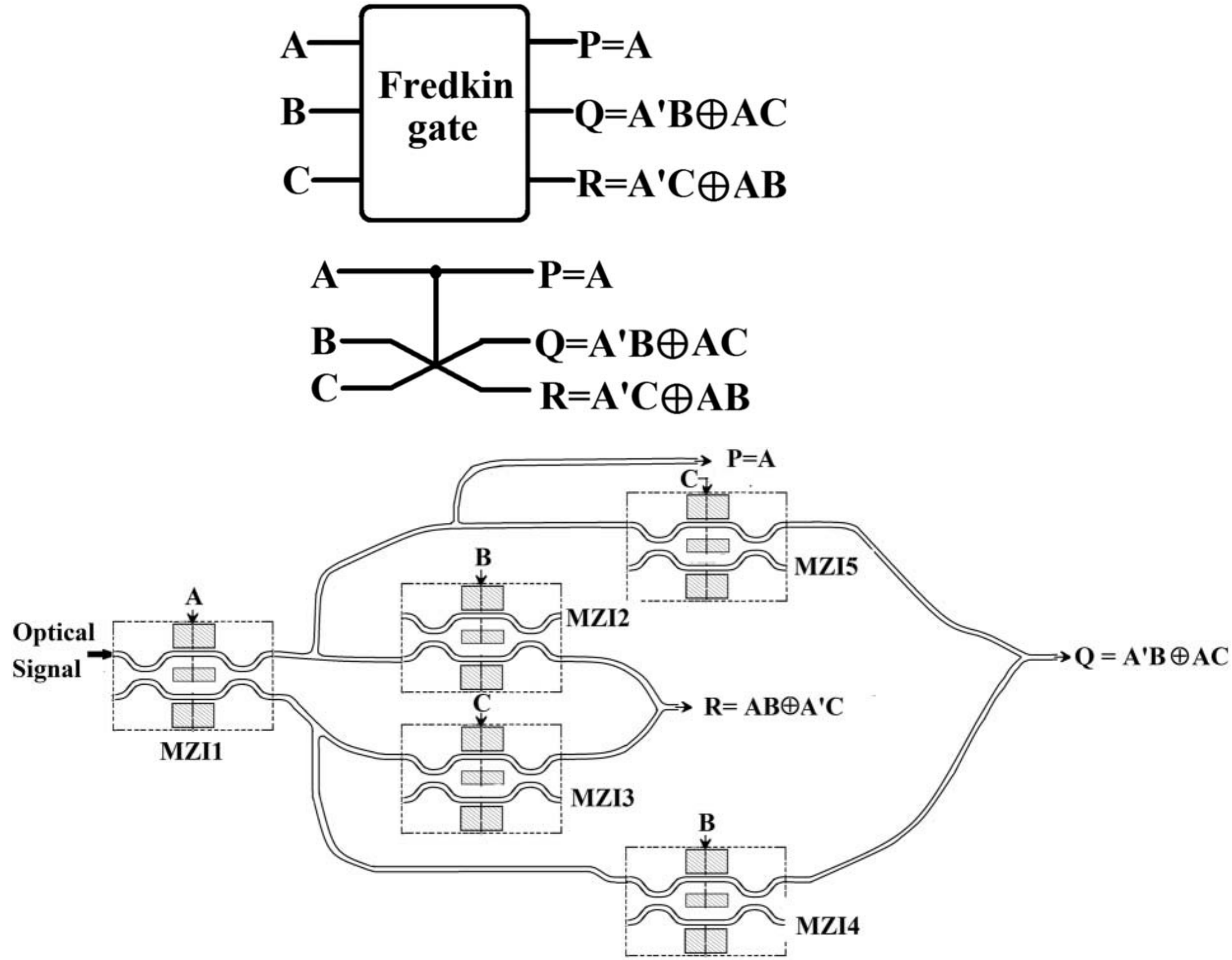

Figure: Logic symbol and Schematic diagram of Fredkin gate using MZIs.

Mathematical Expression for Reversible gates

Mathematical formulation for Fredkin gate

$$P = \sin^2\left(\frac{\Delta\emptyset_{\mathrm{MZI1}}}{2}\right)$$

$$Q = \sin^2\left(\frac{\Delta\emptyset_{\mathrm{MZI1}}}{2}\right)\sin^2\left(\frac{\Delta\emptyset_{\mathrm{MZI5}}}{2}\right) + \cos^2\left(\frac{\Delta\emptyset_{\mathrm{MZI1}}}{2}\right)\sin^2\left(\frac{\Delta\emptyset_{\mathrm{MZI4}}}{2}\right)$$

$$R = \sin^2\left(\frac{\Delta\emptyset_{\mathrm{MZI1}}}{2}\right)\sin^2\left(\frac{\Delta\emptyset_{\mathrm{MZI2}}}{2}\right) + \cos^2\left(\frac{\Delta\emptyset_{\mathrm{MZI1}}}{2}\right)\sin^2\left(\frac{\Delta\emptyset_{\mathrm{MZI3}}}{2}\right)$$

MATLAB Results for Fredkin gate

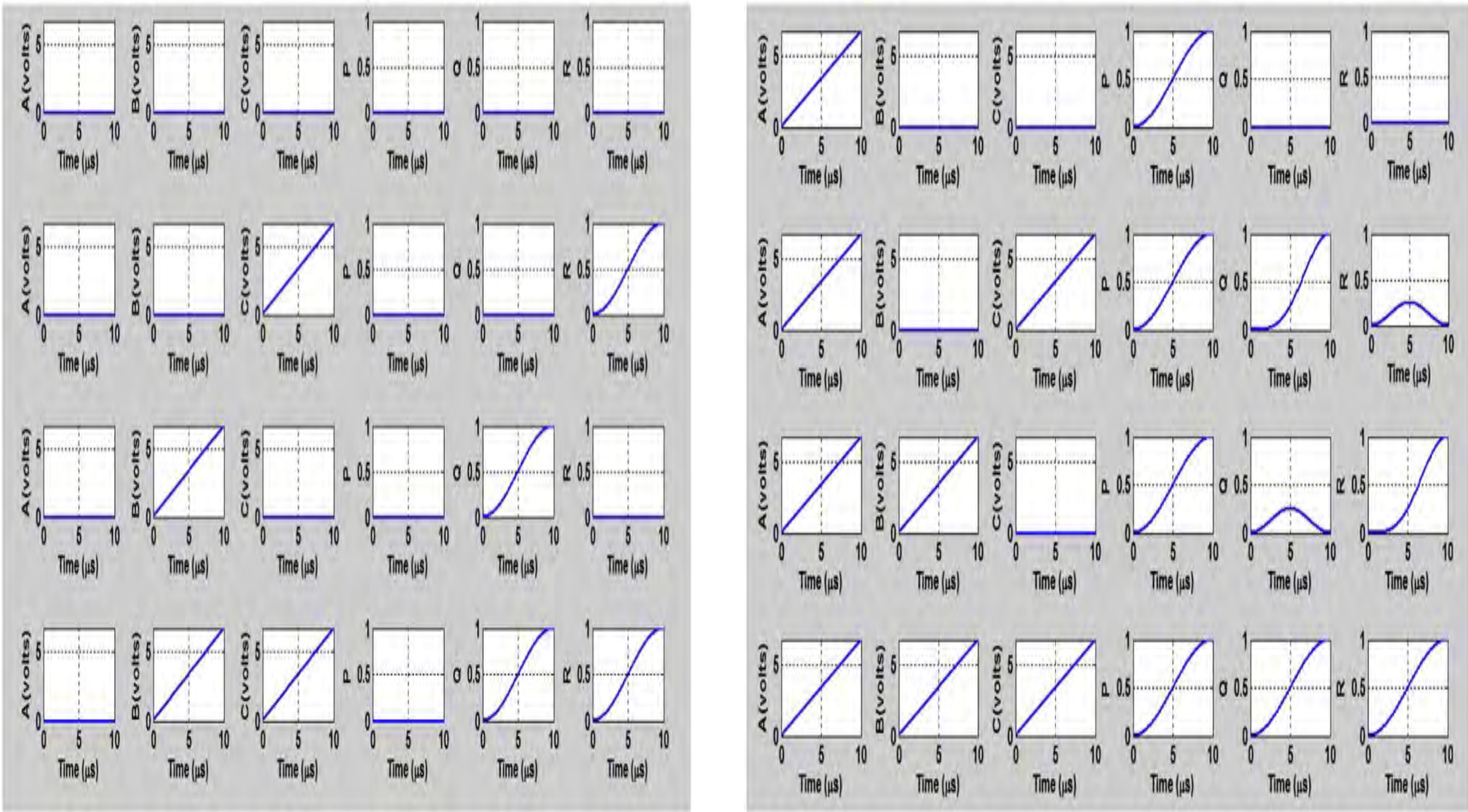

Figure: MATLAB simulation result of Fredkin Gate where A,B,C varies from 000 to 111

BPM Layout of Fredkin gate

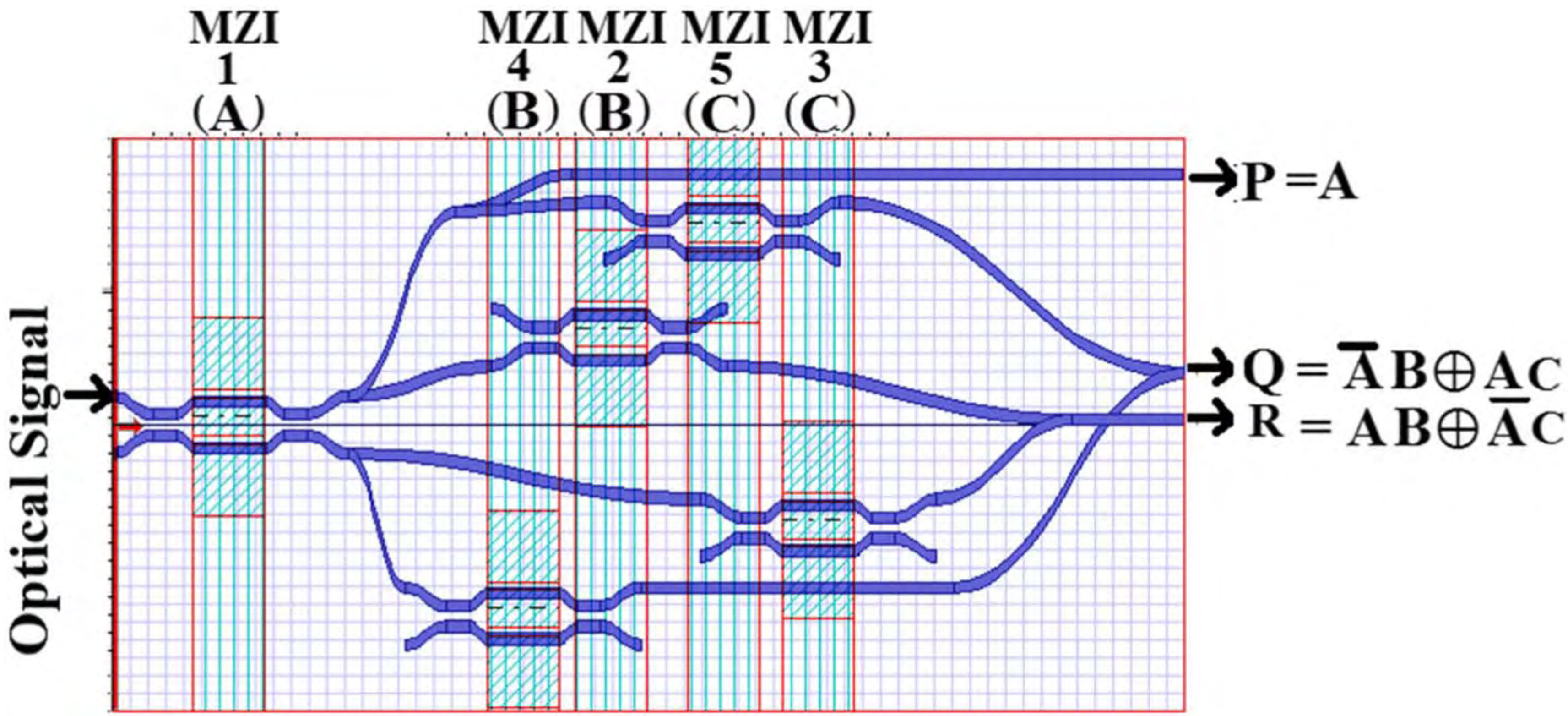

Figure: BPM layout of Fredkin gate

Simulation Result from BPM (Fredkin gate)

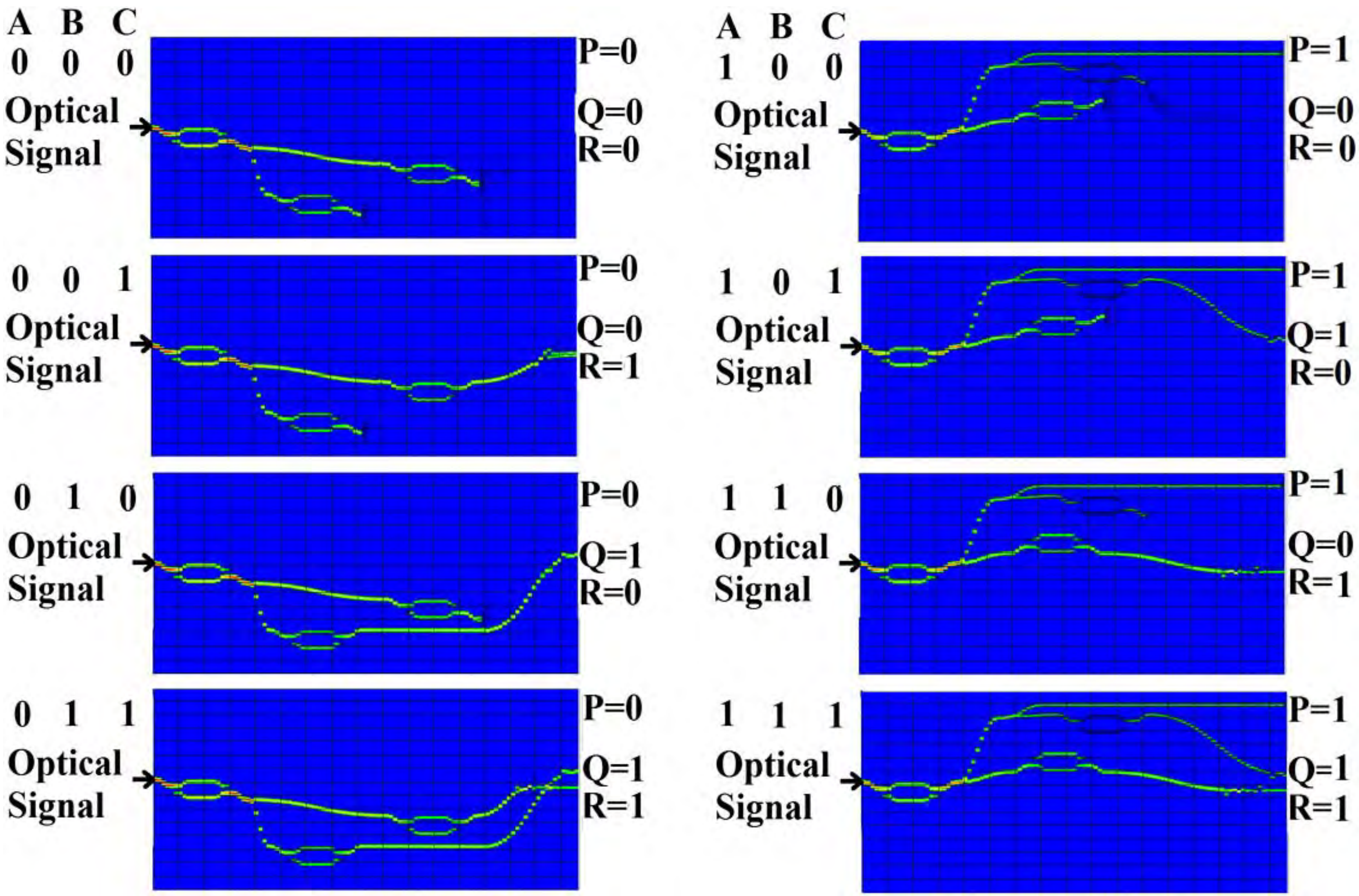

Figure: BPM result of Fredkin gate where A,B,C varies from 000 to 111

Application Example (Fredkin gate)

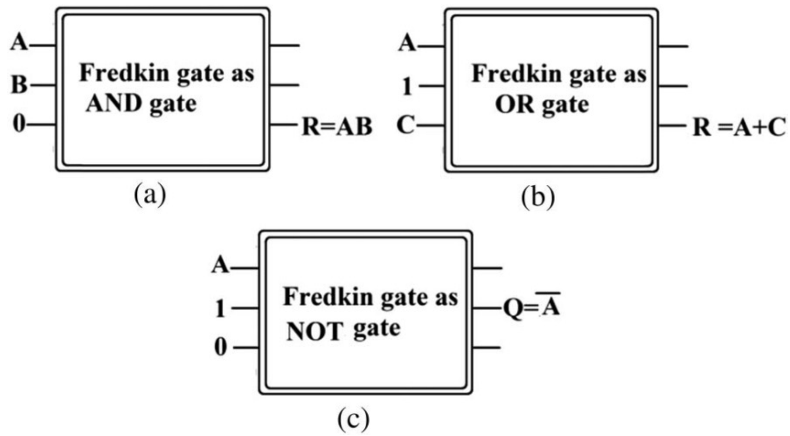

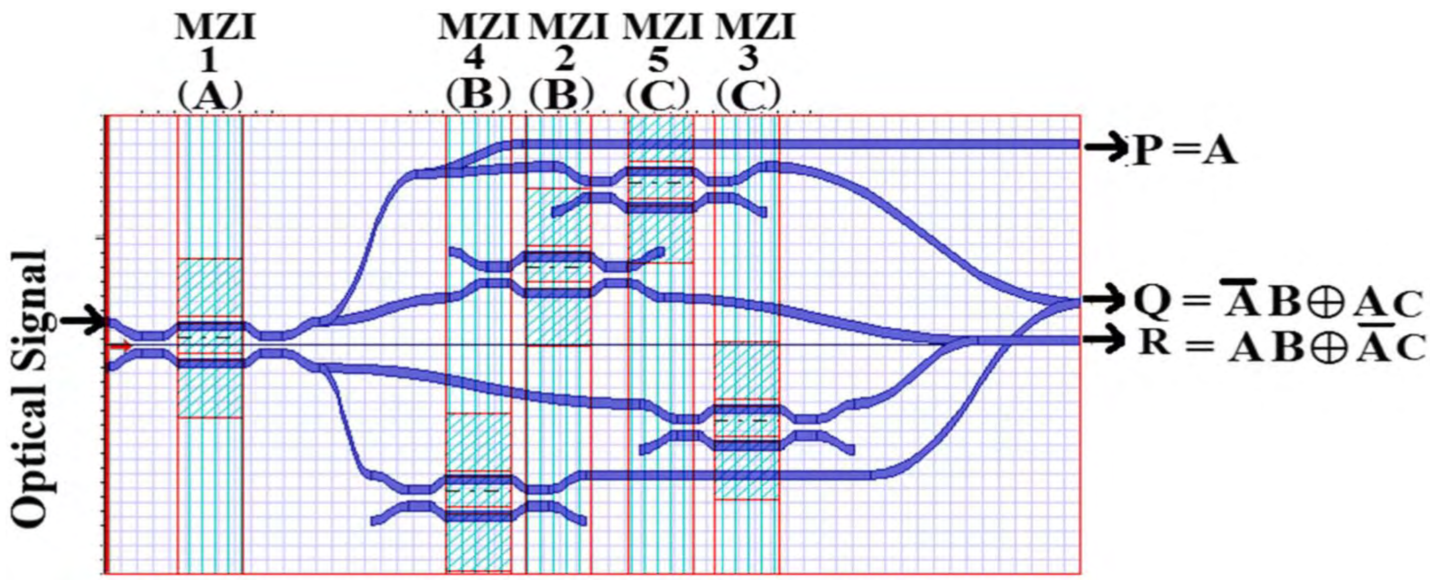

Figure: Application example and BPM layout of Fredkin gate

Simulation Result (Fredkin gate application)

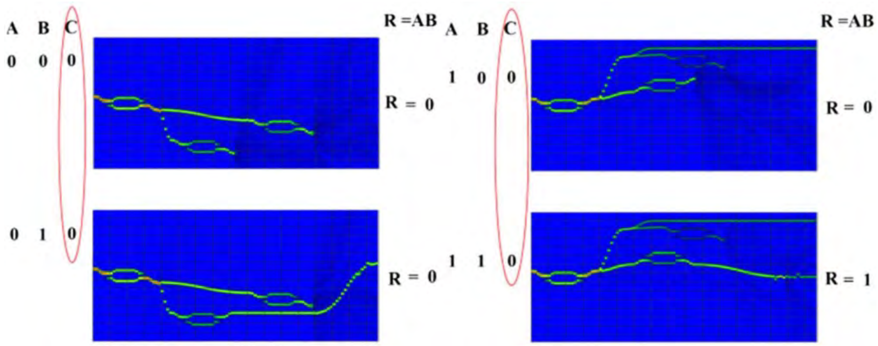

As AND Gate

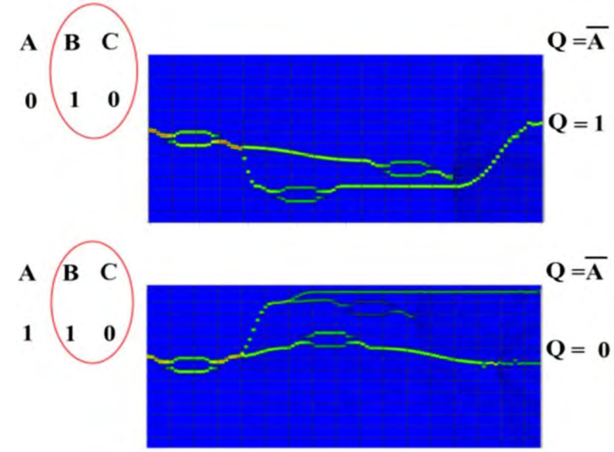

As NOT Gate

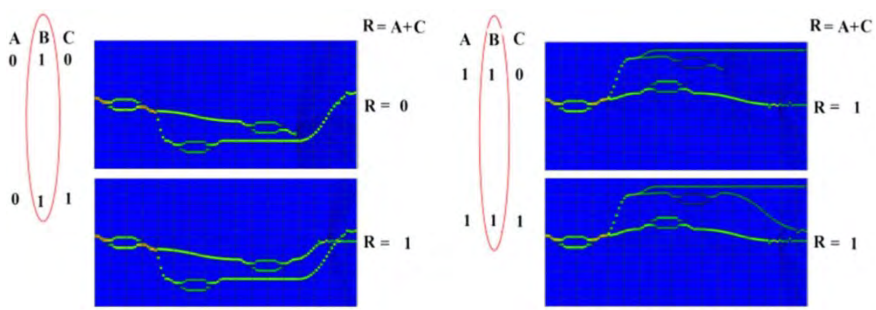

As OR Gate

Figure: BPM result of Fredkin gate used as different applications

Design of reversible multiplexer

Santosh Kumar et al., Optical Engineering (SPIE) 55(11), 115101 (2016)

2x1 Reversible Multiplexer

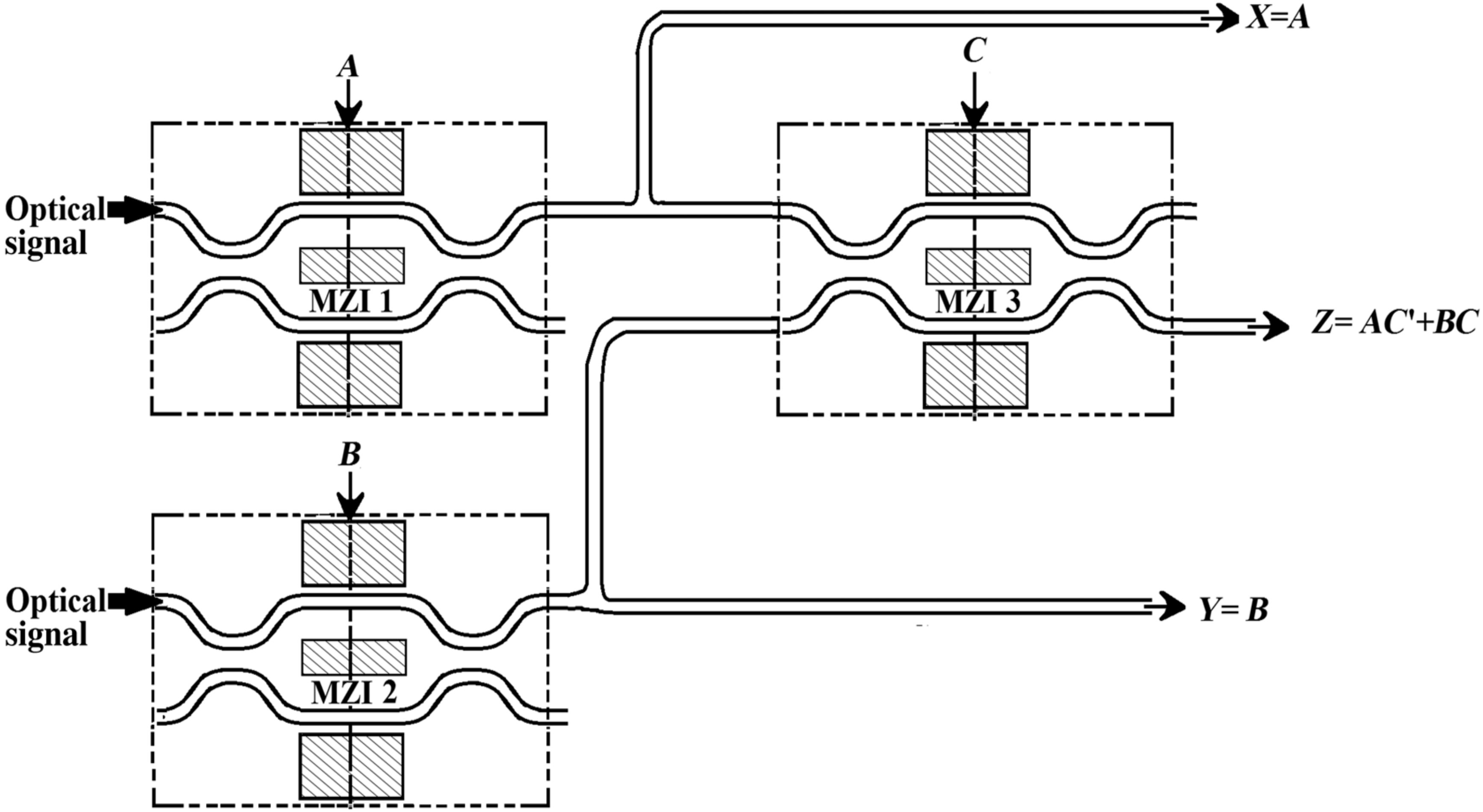

Figure: Reversible 2 × 1 multiplexer using MZI.

Mathematical Expression for 2x1Multiplexer

X,Y,Z is output power calculated for A,B,C respectively.

$$X = \left[\sin^2\left(\frac{\Delta\varphi_{MZI1}}{2}\right)\right]$$

$$Y = \left[\sin^2\left(\frac{\Delta\varphi_{MZI2}}{2}\right)\right]$$

$$Z = \left[\sin^2\left(\frac{\Delta\varphi_{MZI1}}{2}\right)\cos^2\left(\frac{\Delta\varphi_{MZI3}}{2}\right)\right] + \left[\sin^2\left(\frac{\Delta\varphi_{MZI2}}{2}\right)\sin^2\left(\frac{\Delta\varphi_{MZI3}}{2}\right)\right]$$

MATLAB Results for 2x1 Multiplexer

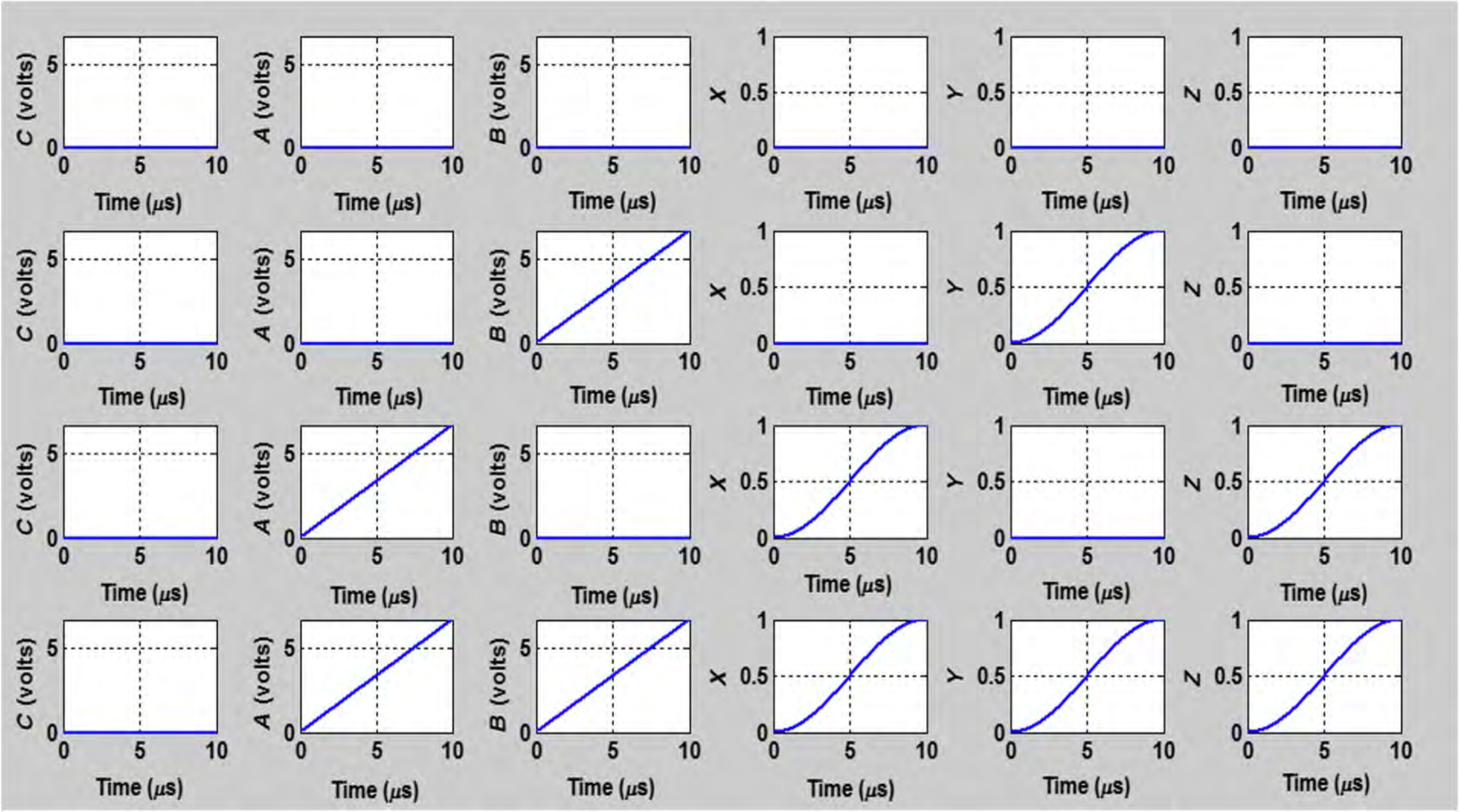

Figure: MATLAB simulations results of reversible 2x1 multiplexer where C, A, B varies from 000 to 011

Contd..

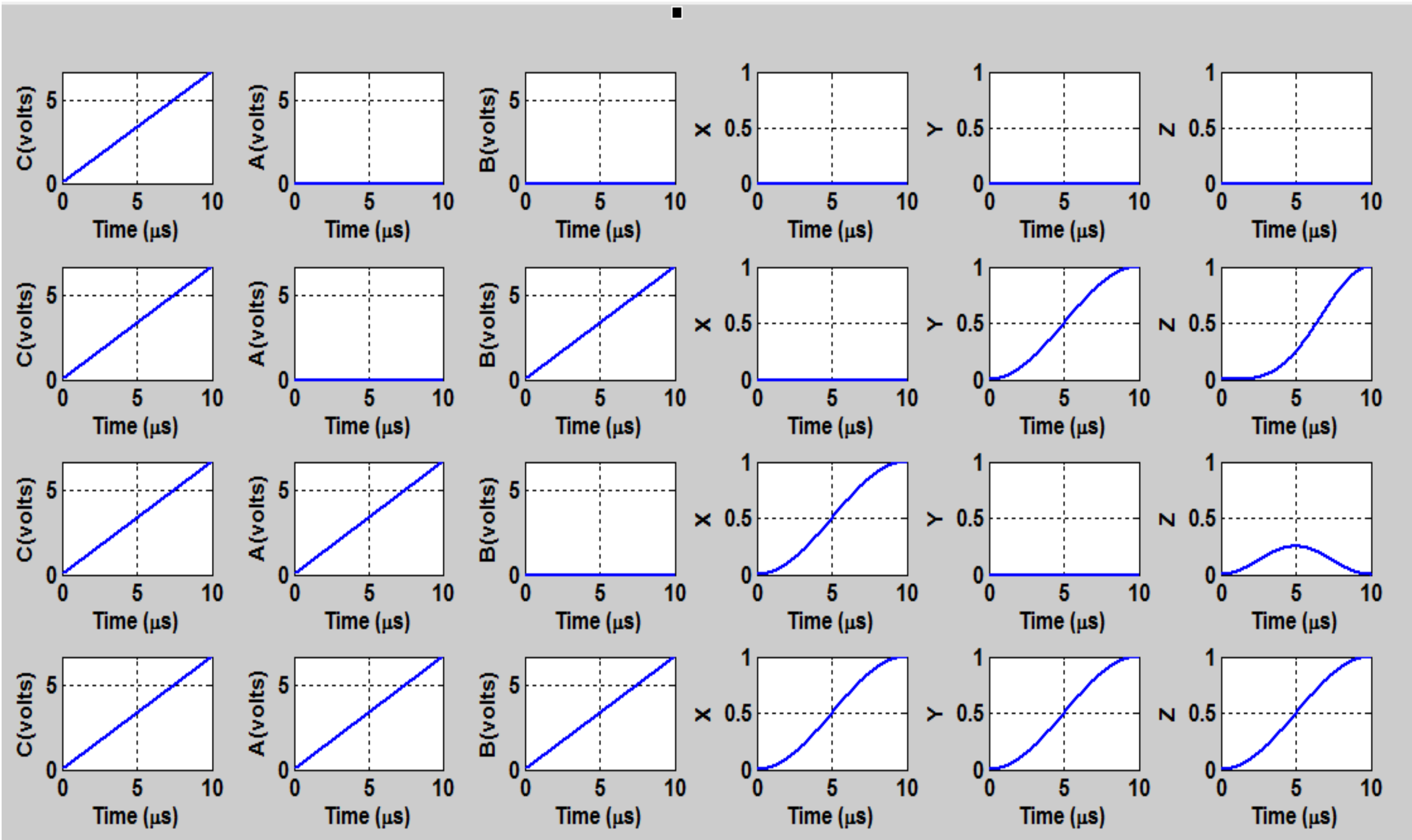

Figure: MATLAB simulations results of reversible 2x1 multiplexer where C, A, B varies from 100 to 111

BPM Layout of 2x1Multiplexer

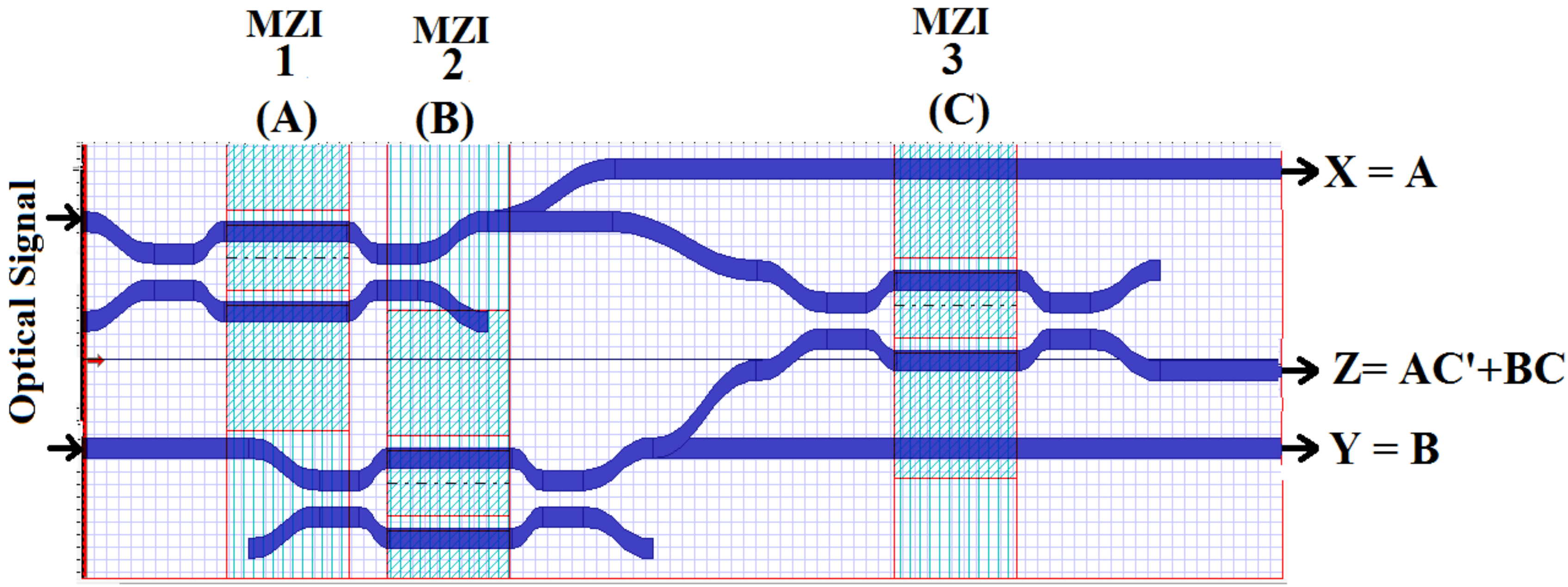

Figure: BPM layout of reversible 2x1 multiplexer

Simulation Result from BPM for 2x1 Multiplexer

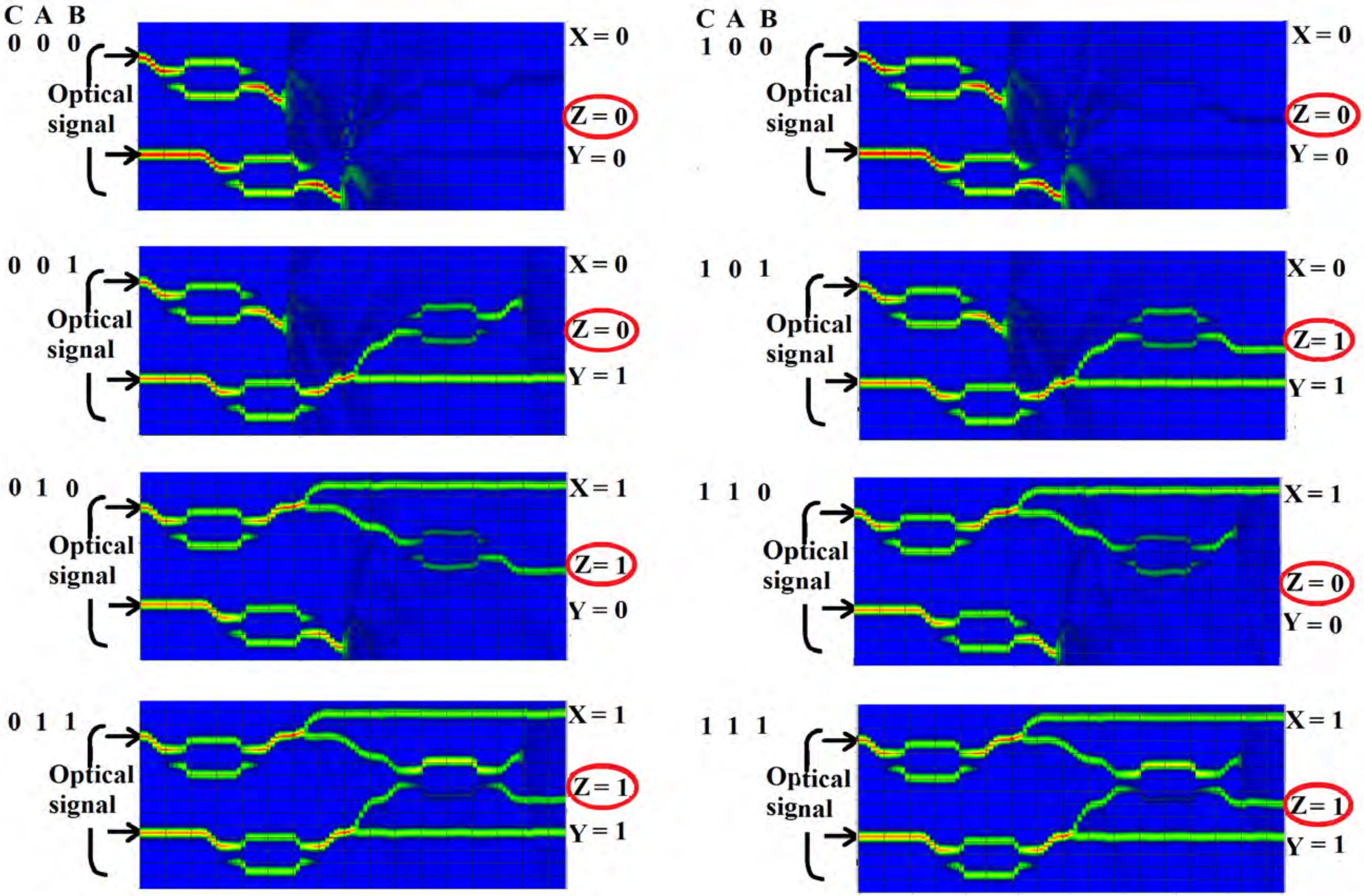

Figure: BPM results of reversible 2x1 multiplexer where C, A, B varies from 000 to 111

4x1 Multiplexer

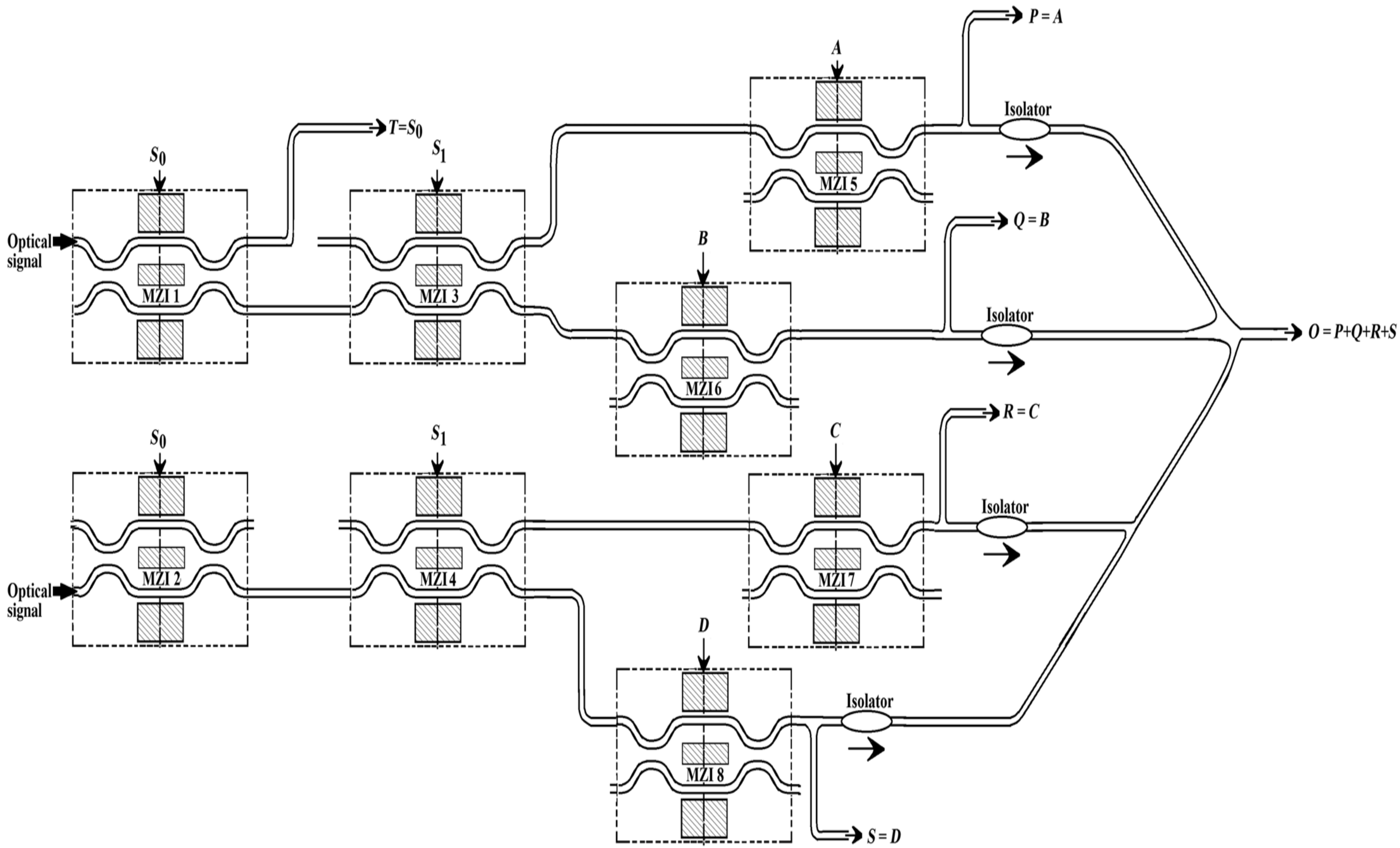

Figure: Reversible 4 × 1 multiplexer using MZI

Mathematical Expression for 4x1Multiplexer

$$P = \left[\cos^2\left(\frac{\Delta\varphi_{MZI1}}{2}\right)\cos^2\left(\frac{\Delta\varphi_{MZI3}}{2}\right)\sin^2\left(\frac{\Delta\varphi_{MZI5}}{2}\right)\right]$$

$$Q = \left[\cos^2\left(\frac{\Delta\varphi_{MZI1}}{2}\right)\sin^2\left(\frac{\Delta\varphi_{MZI3}}{2}\right)\sin^2\left(\frac{\Delta\varphi_{MZI6}}{2}\right)\right]$$

$$R = \left[\sin^2\left(\frac{\Delta\varphi_{MZI2}}{2}\right)\cos^2\left(\frac{\Delta\varphi_{MZI4}}{2}\right)\sin^2\left(\frac{\Delta\varphi_{MZI7}}{2}\right)\right]$$

$$S = \left[\sin^2\left(\frac{\Delta\varphi_{MZI2}}{2}\right)\sin^2\left(\frac{\Delta\varphi_{MZI4}}{2}\right)\cos^2\left(\frac{\Delta\varphi_{MZI8}}{2}\right)\right]$$

$$T = \left[\sin^2\left(\frac{\Delta\varphi_{MZI1}}{2}\right)\right]$$

$$O = \left[\begin{array}{l} \left\{ \cos^2\left(\frac{\Delta\varphi_{MZI1}}{2}\right)\cos^2\left(\frac{\Delta\varphi_{MZI3}}{2}\right)\sin^2\left(\frac{\Delta\varphi_{MZI5}}{2}\right)\right\} + \left\{ \cos^2\left(\frac{\Delta\varphi_{MZI1}}{2}\right)\sin^2\left(\frac{\Delta\varphi_{MZI3}}{2}\right)\sin^2\left(\frac{\Delta\varphi_{MZI6}}{2}\right)\right\} + \\ \left\{ \sin^2\left(\frac{\Delta\varphi_{MZI2}}{2}\right)\cos^2\left(\frac{\Delta\varphi_{MZI4}}{2}\right)\sin^2\left(\frac{\Delta\varphi_{MZI7}}{2}\right)\right\} + \left\{ \sin^2\left(\frac{\Delta\varphi_{MZI2}}{2}\right)\sin^2\left(\frac{\Delta\varphi_{MZI4}}{2}\right)\cos^2\left(\frac{\Delta\varphi_{MZI8}}{2}\right)\right\} \end{array} \right.$$

MATLAB Results for 4x1 Multiplexer

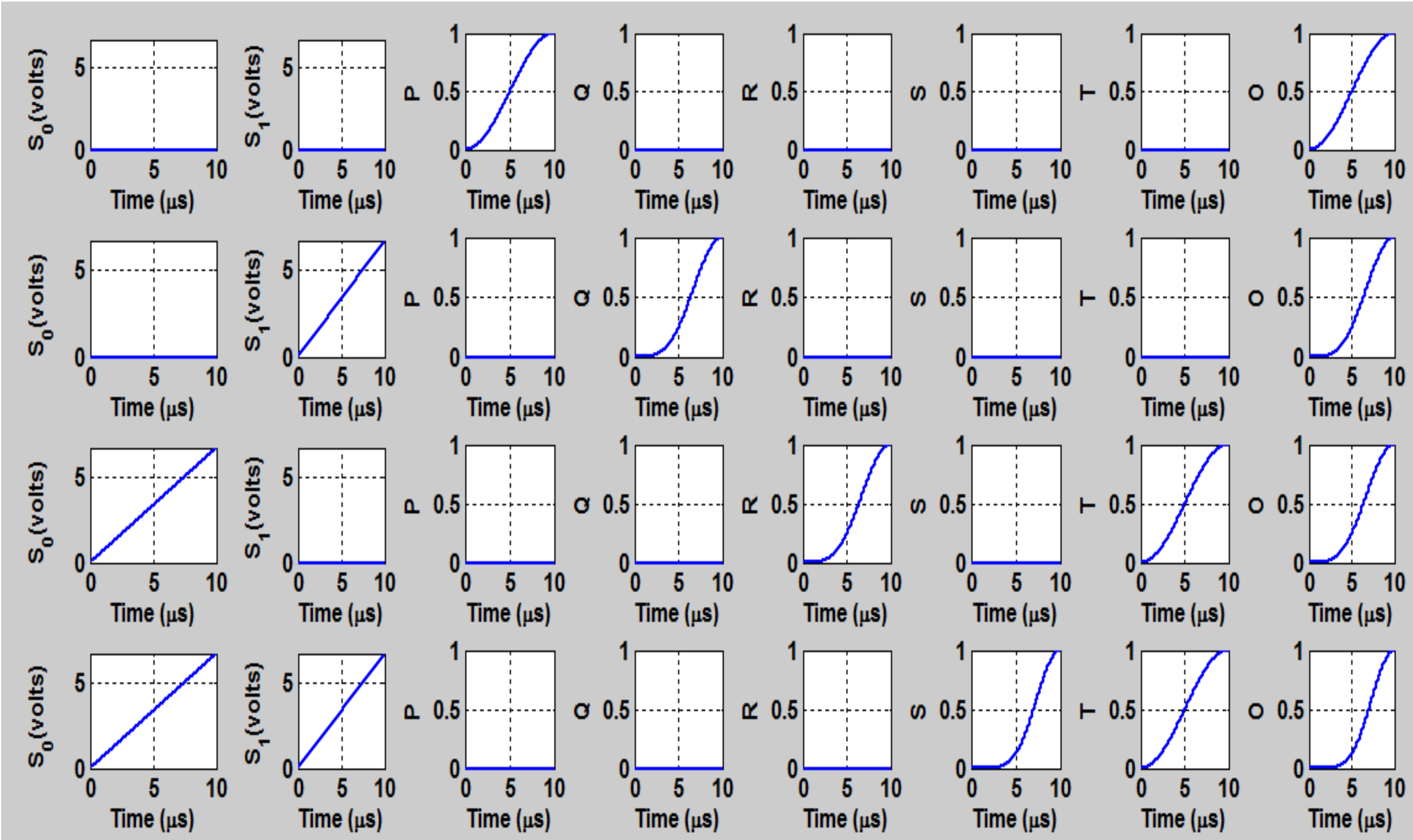

Figure: MATLAB simulations results of reversible 4x1 multiplexer where varies from 00 to 11

BPM Layout of 4x1Multiplexer

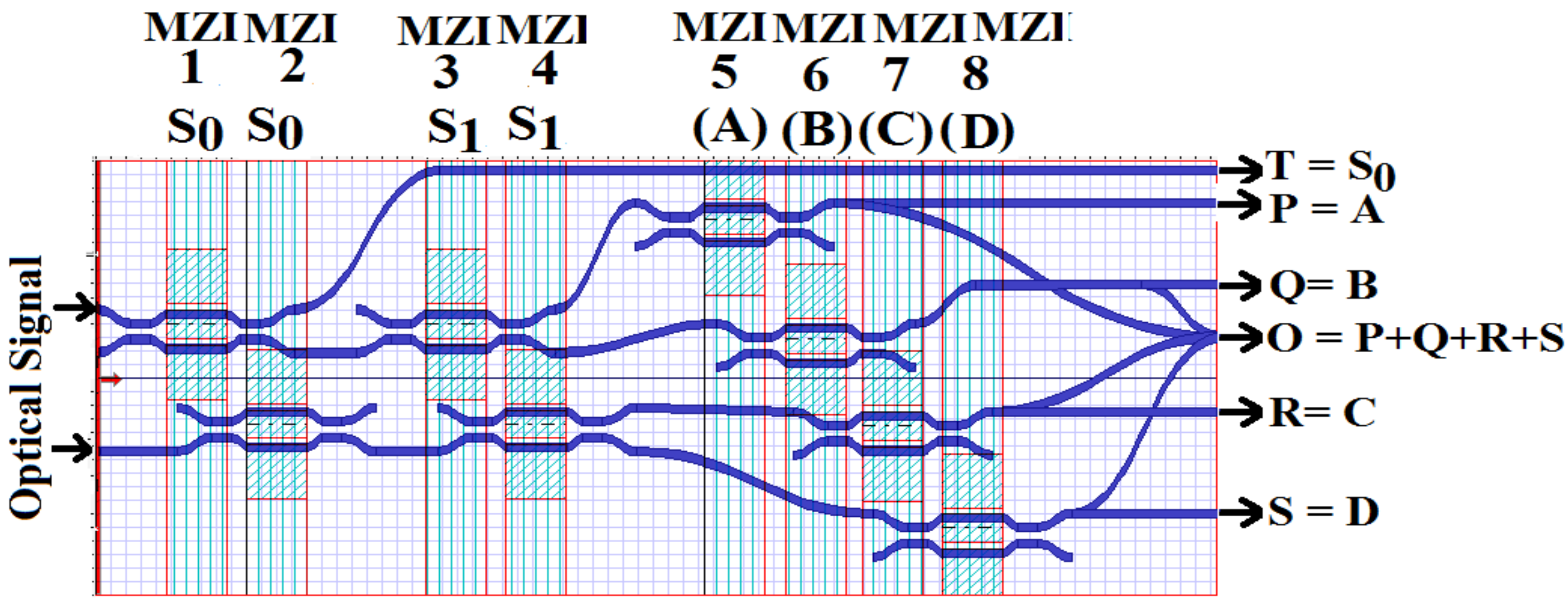

Figure: BPM layout of reversible 2x1 multiplexer

Simulation Result from BPM for 4x1 Multiplexer

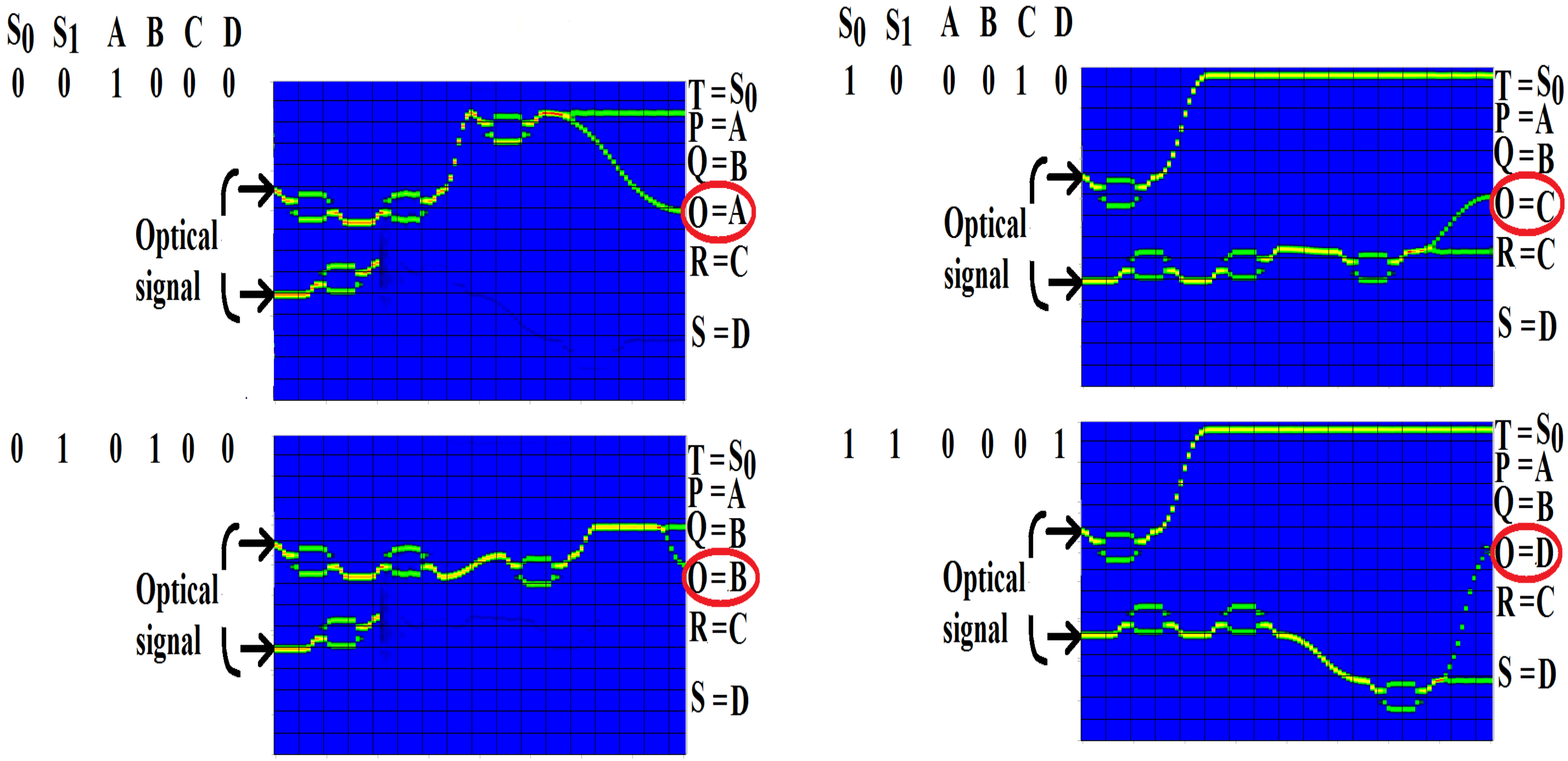

Figure: BPM results for 4x1 Multiplexer

Design of Reversible Sequential Circuits

<u>Santosh Kumar</u> et. al., Optical Engineering (SPIE) 55(12),125105 (2016).

Logic Diagram of different sequential circuits

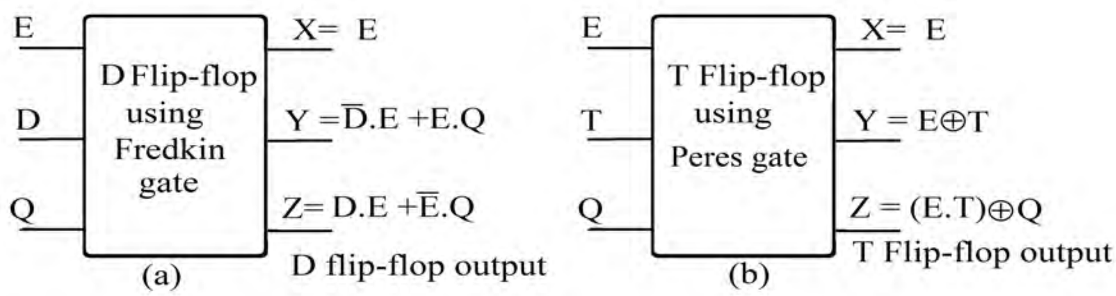

Figure: (a) D Flip-flop using Fredkin gate (b) T Flip-flop using Peres gate

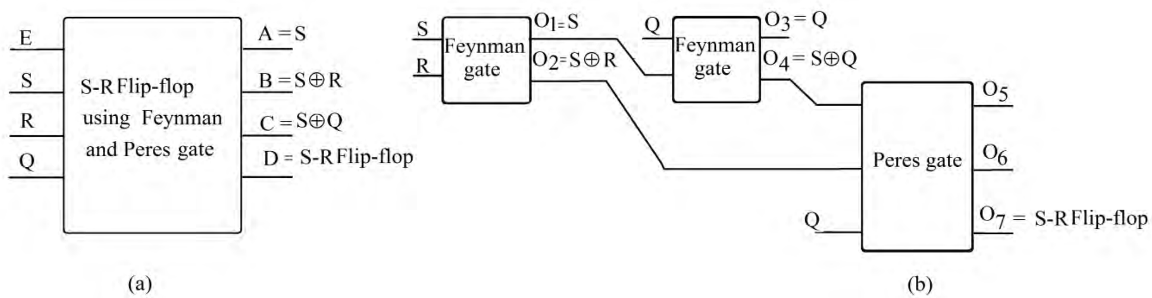

Figure: S-R Flip-flop using Feynman and Peres gate (a) block level design (b) gate level design

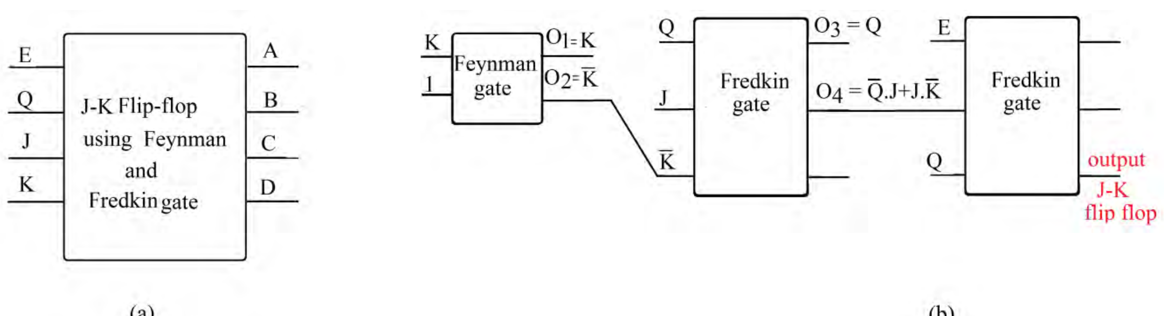

Figure: J-K Flip-flop using Feynman and Fredkin gate (a) block level design (b) gate level design

D Flip-flop

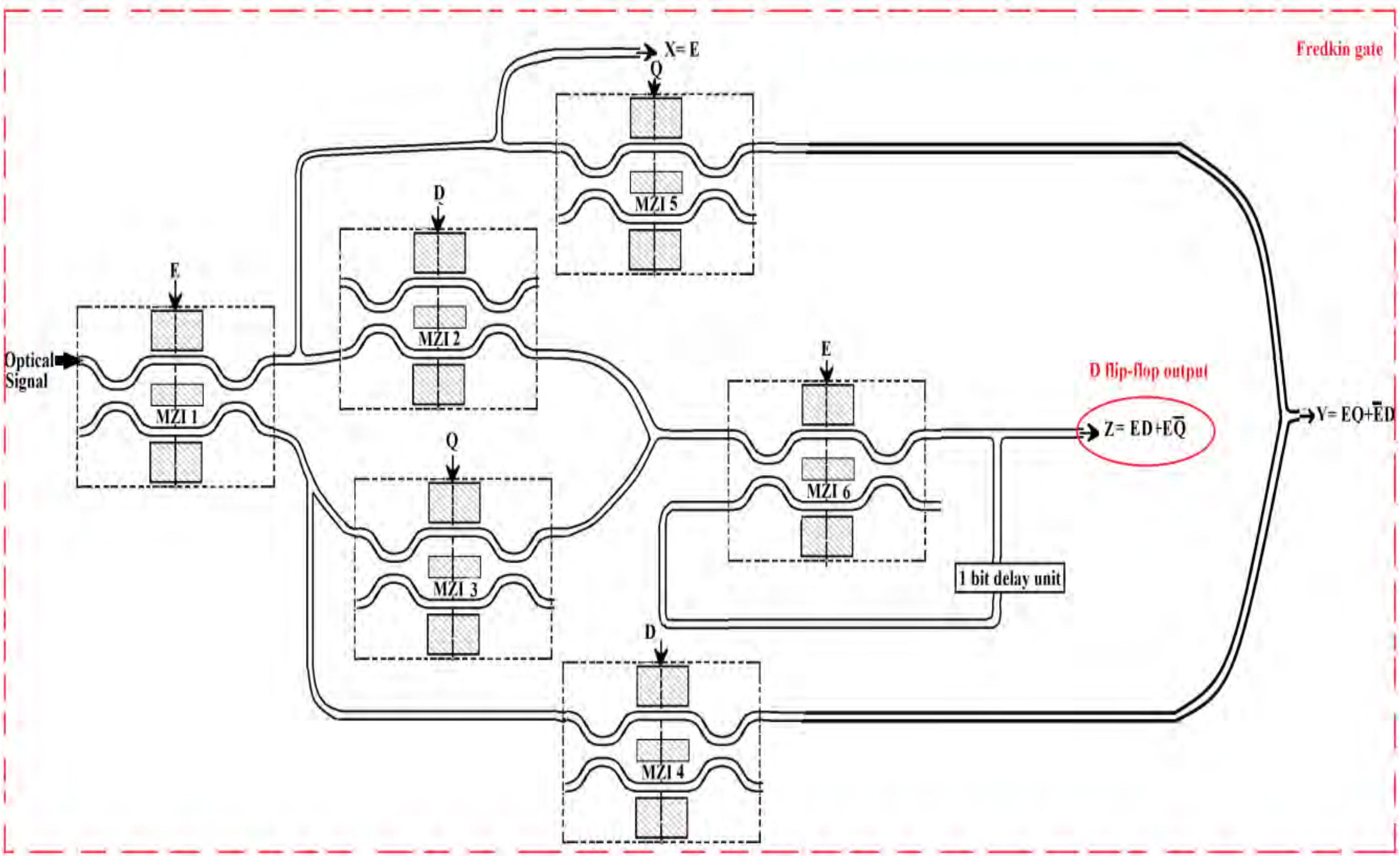

Figure: D Flip-flop using Feynman

Mathematical Expression for D flip-flop

Mathematical formulation for D flip-flop can be calculated as:

$$\begin{aligned} Z = \; & \sin^2\left(\frac{\Delta\phi_{\mathrm{MZI1}}}{2}\right)\sin^2\left(\frac{\Delta\phi_{\mathrm{MZI2}}}{2}\right)\sin^2\left(\frac{\Delta\phi_{\mathrm{MZI6}}}{2}\right) \\ & + \cos^2\left(\frac{\Delta\phi_{\mathrm{MZI1}}}{2}\right)\sin^2\left(\frac{\Delta\phi_{\mathrm{MZI3}}}{2}\right)\sin^2\left(\frac{\Delta\phi_{\mathrm{MZI6}}}{2}\right) \end{aligned}$$

MATLAB Results for D flip-flop

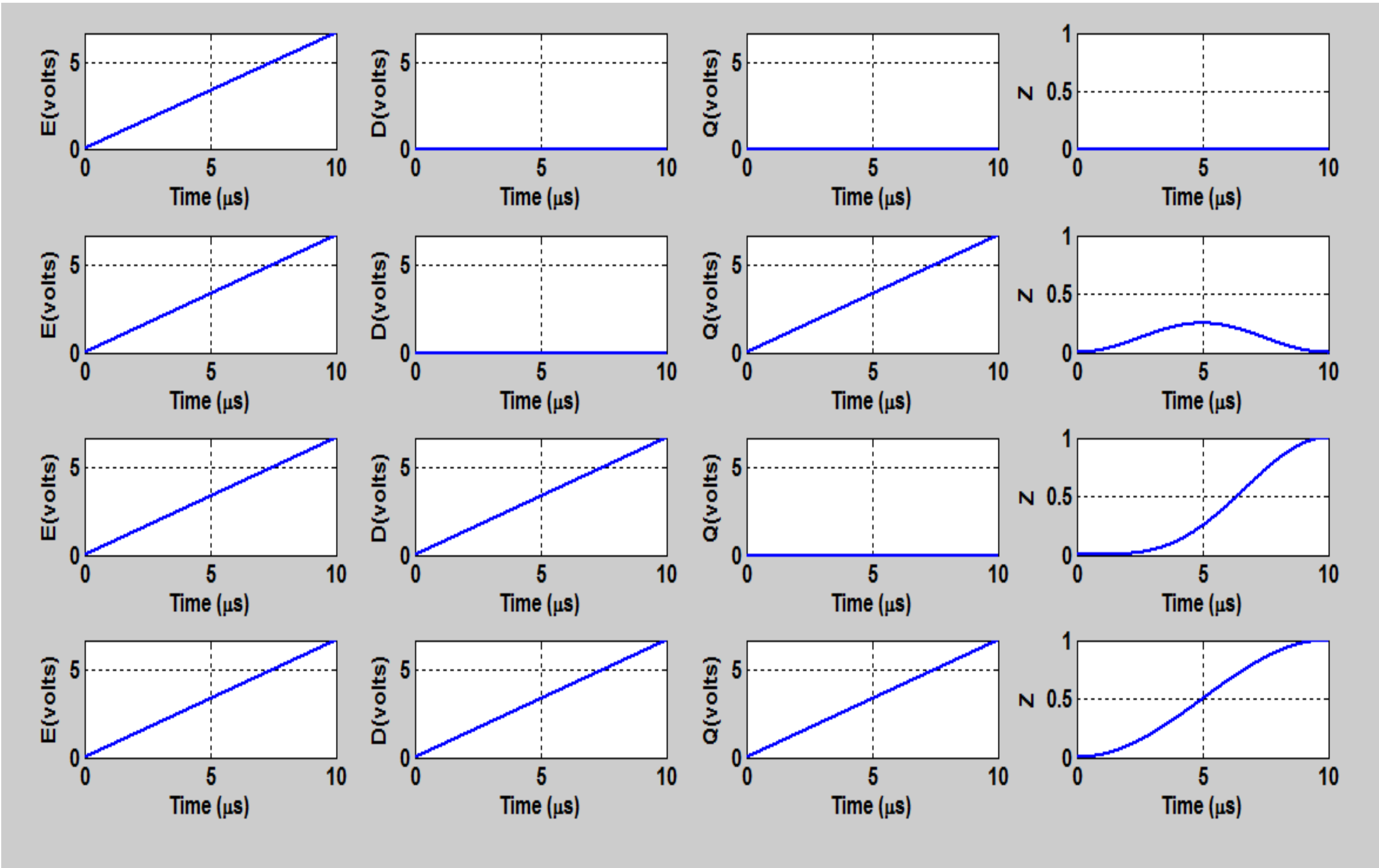

Figure: MATLAB simulation results of D flip-flop using Fredkin gate where input signal E, D, Q varies from 100 to 111

BPM Layout and Simulation result of D Flip-flop

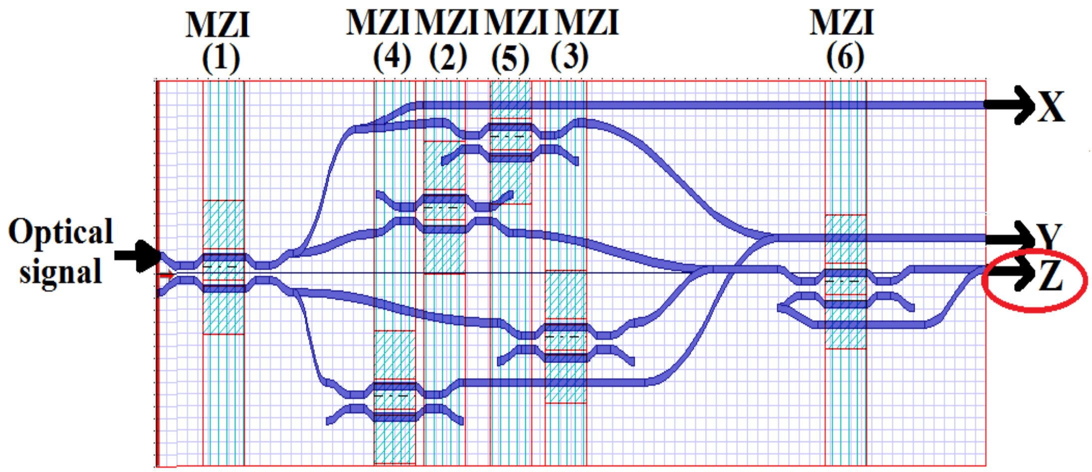

Figure: BPM layout of D Flip-flop using Fredkin gate

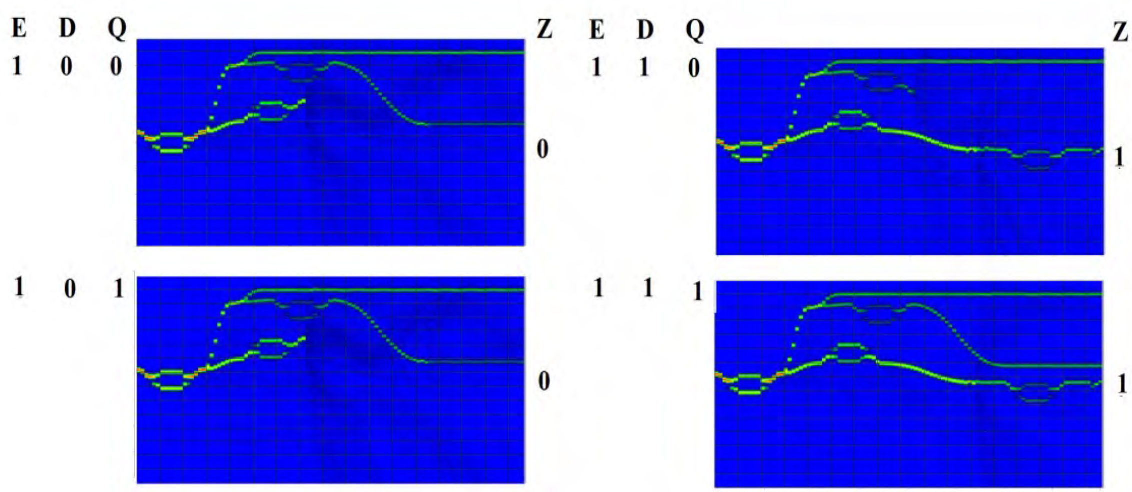

Figure: BPM simulation results for D flip-flop

T Flip-flop

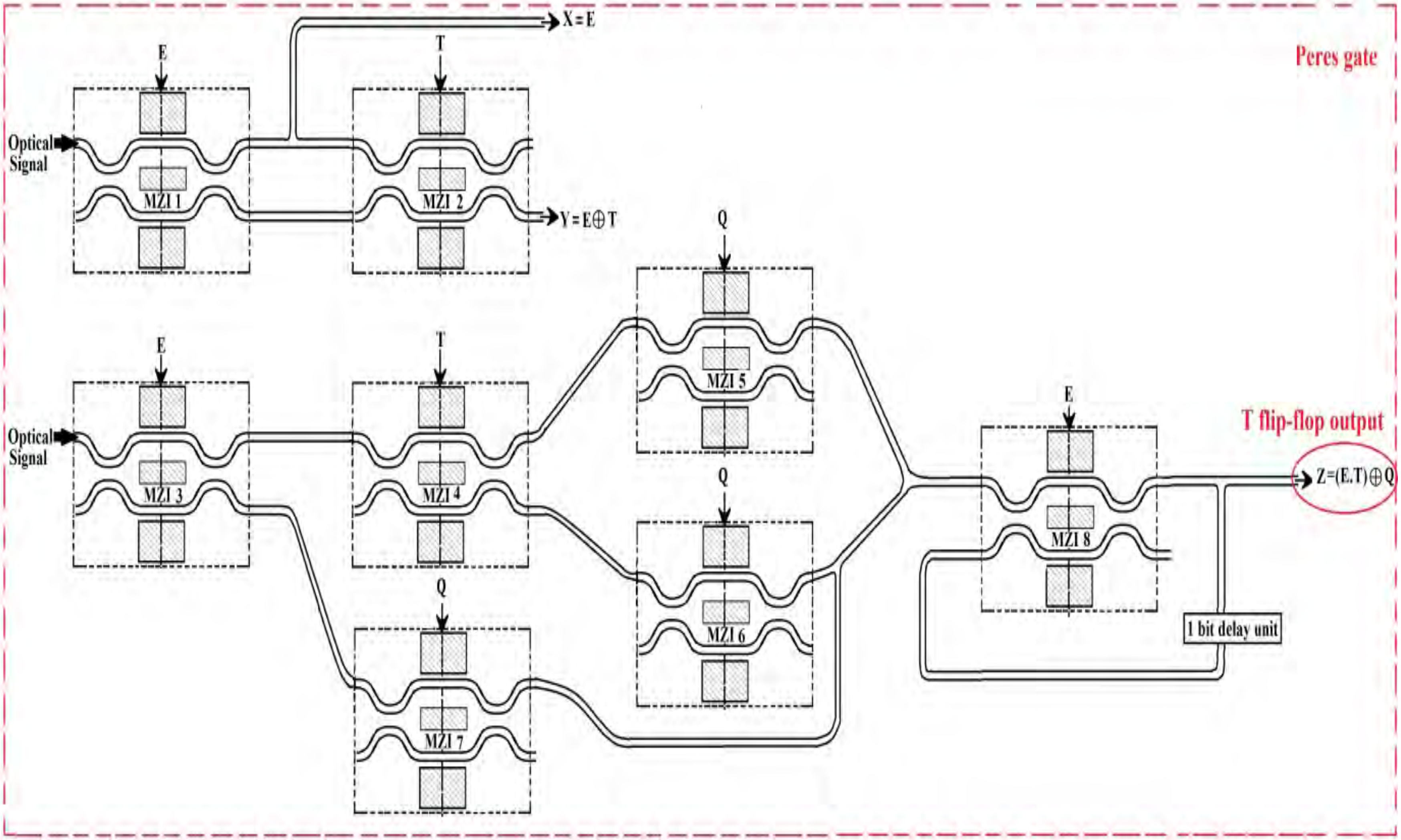

Figure: T Flip-flop using Peres gate

Mathematical Expression for T flip-flop

Mathematical formulation for T flip-flop can be calculated as:

$$\begin{aligned} Z = \; & \sin^2\left(\frac{\Delta\emptyset_{\mathrm{MZI3}}}{2}\right)\sin^2\left(\frac{\Delta\emptyset_{\mathrm{MZI4}}}{2}\right)\sin^2\left(\frac{\Delta\emptyset_{\mathrm{MZI5}}}{2}\right)\sin^2\left(\frac{\Delta\emptyset_{\mathrm{MZI8}}}{2}\right) \\ & + \sin^2\left(\frac{\Delta\emptyset_{\mathrm{MZI3}}}{2}\right)\cos^2\left(\frac{\Delta\emptyset_{\mathrm{MZI4}}}{2}\right)\sin^2\left(\frac{\Delta\emptyset_{\mathrm{MZI5}}}{2}\right)\sin^2\left(\frac{\Delta\emptyset_{\mathrm{MZI8}}}{2}\right) \\ & + \cos^2\left(\frac{\Delta\emptyset_{\mathrm{MZI3}}}{2}\right)\sin^2\left(\frac{\Delta\emptyset_{\mathrm{MZI7}}}{2}\right)\sin^2\left(\frac{\Delta\emptyset_{\mathrm{MZI8}}}{2}\right) \end{aligned}$$

MATLAB Results for T flip-flop

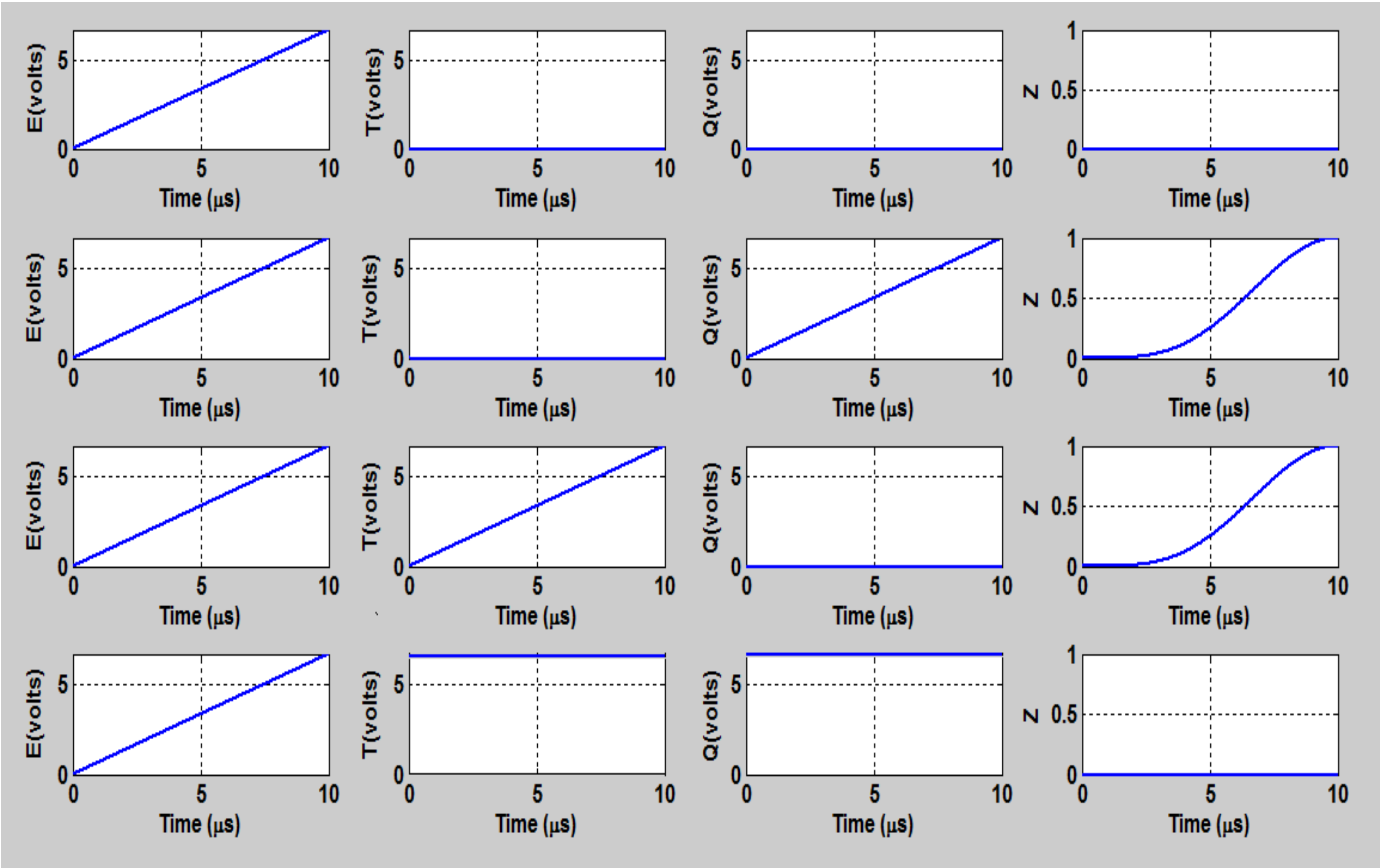

Figure: MATLAB simulation results of D flip-flop using Fredkin gate where input signal E, D, Q varies from 100 to 111

BPM Layout of T Flip-flop

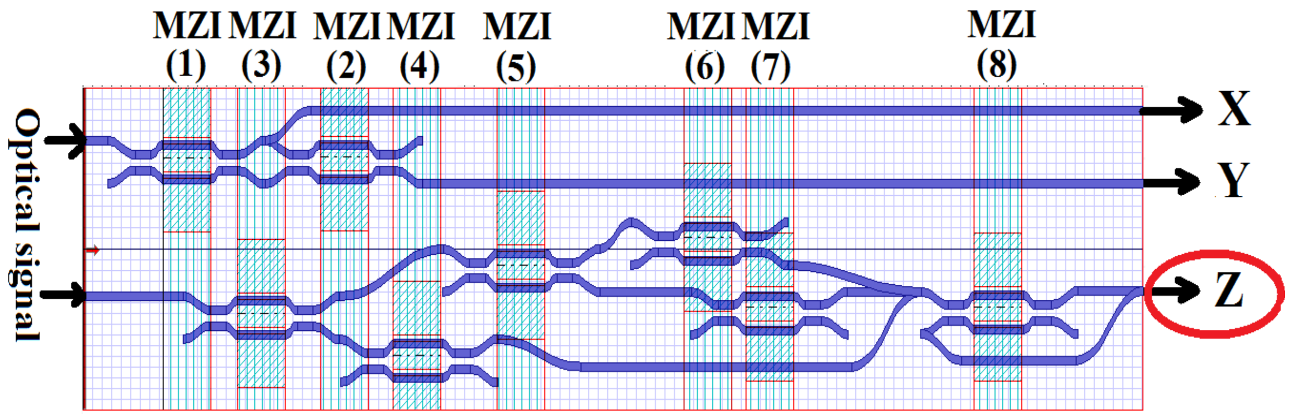

Figure: BPM layout of T Flip-flop using Peres gate

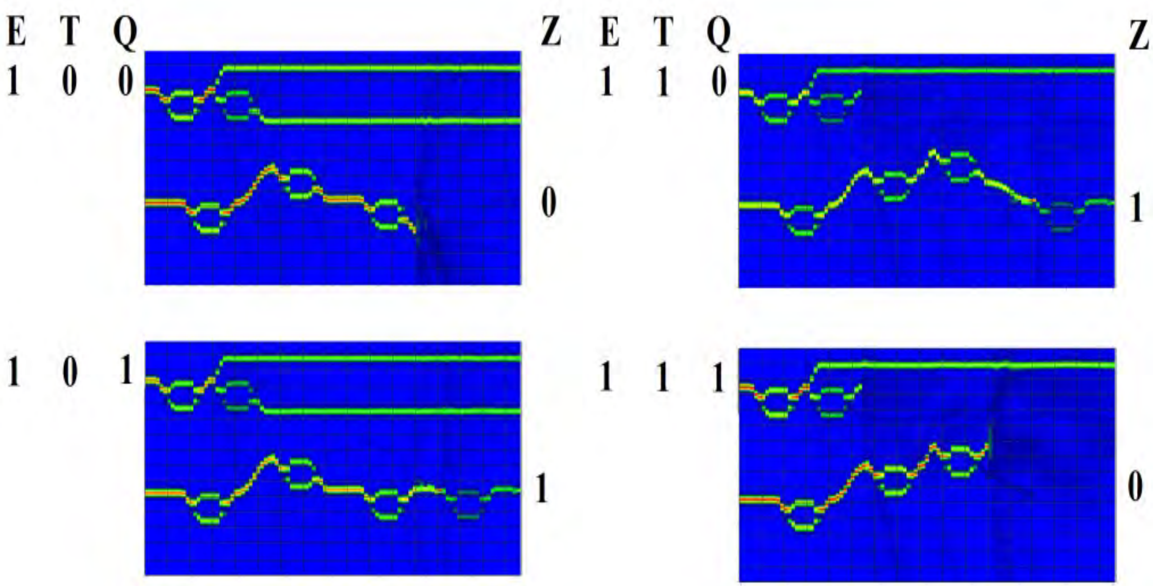

Figure: BPM simulation results for T flip-flop

S-R Flip-flop

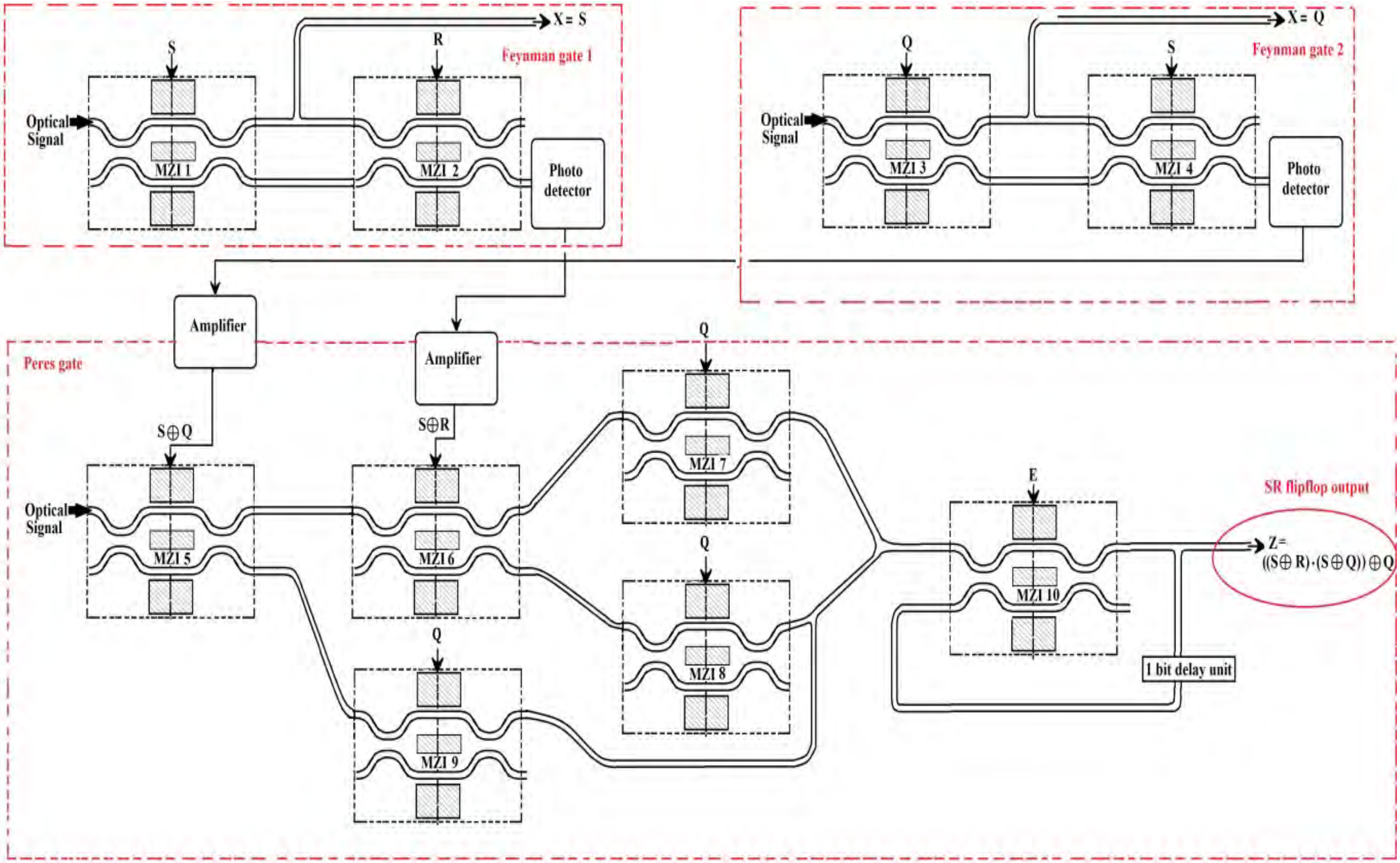

Figure: S-R flip-flop using Peres gate and Feynman gate

Mathematical Expression for S-R code converter

Mathematical formulation for S-R flip-flop can be calculated as:

$$D = \sin^2\left(\frac{\Delta\emptyset_{\mathrm{MZI5}}}{2}\right)\sin^2\left(\frac{\Delta\emptyset_{\mathrm{MZI6}}}{2}\right)\sin^2\left(\frac{\Delta\emptyset_{\mathrm{MZI7}}}{2}\right)\sin^2\left(\frac{\Delta\emptyset_{\mathrm{MZI10}}}{2}\right)$$
$$+\sin^2\left(\frac{\Delta\emptyset_{\mathrm{MZI5}}}{2}\right)\cos^2\left(\frac{\Delta\emptyset_{\mathrm{MZI6}}}{2}\right)\sin^2\left(\frac{\Delta\emptyset_{\mathrm{MZI8}}}{2}\right)\sin^2\left(\frac{\Delta\emptyset_{\mathrm{MZI10}}}{2}\right)$$
$$+\cos^2\left(\frac{\Delta\emptyset_{\mathrm{MZI5}}}{2}\right)\sin^2\left(\frac{\Delta\emptyset_{\mathrm{MZI9}}}{2}\right)\sin^2\left(\frac{\Delta\emptyset_{\mathrm{MZI10}}}{2}\right)$$

MATLAB Results for S-R flip-flop

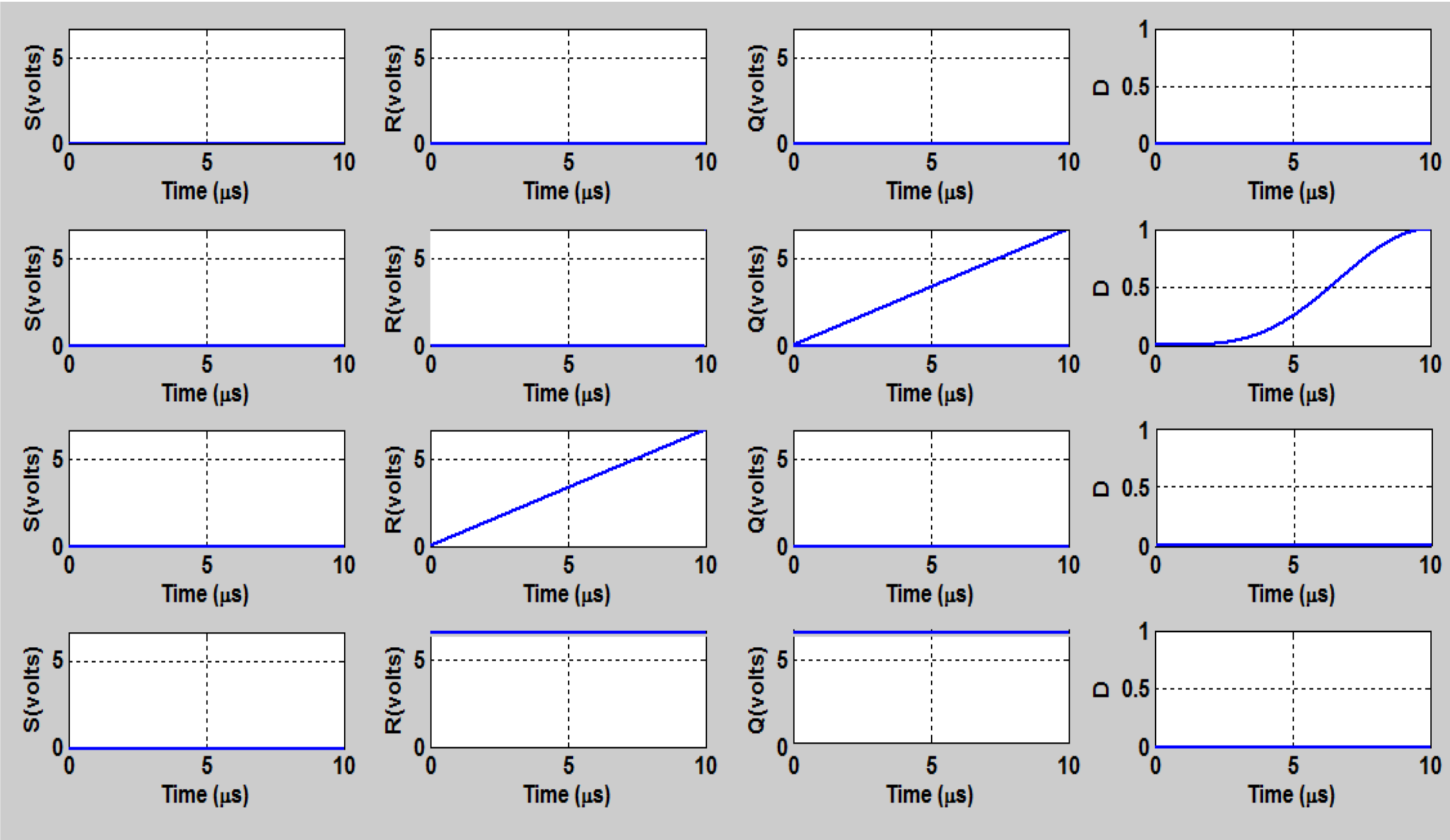

Figure: MATLAB simulation results of S-R flip-flop using Feynman gate and Peres gate where input signal S, R, Q varies from 000 to 011

Contd..

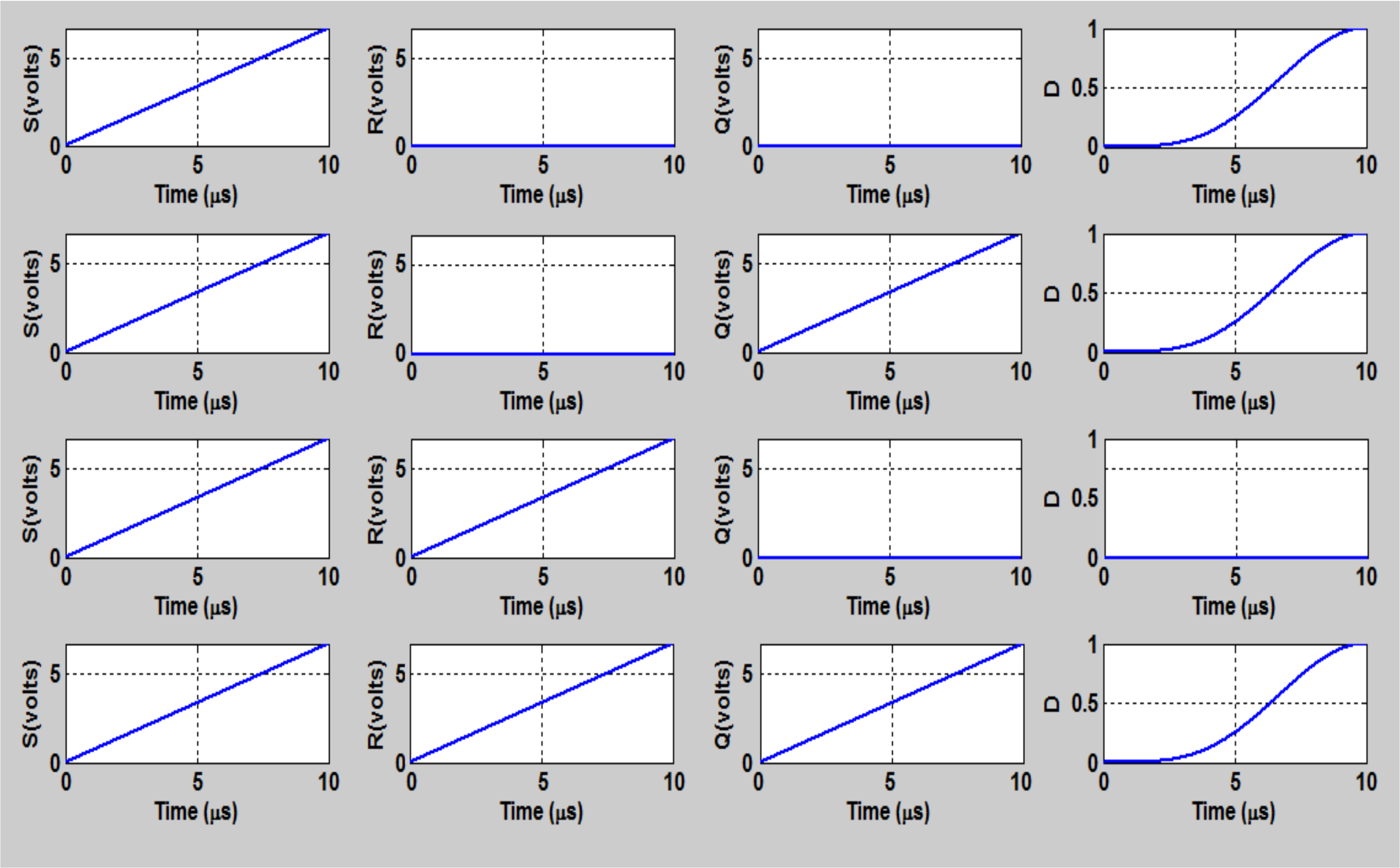

Figure: MATLAB simulation results of S-R flip-flop using Feynman gate and Peres gate where input signal S, R, Q varies from 100 to 111

BPM Layout of R-S Flip-flop

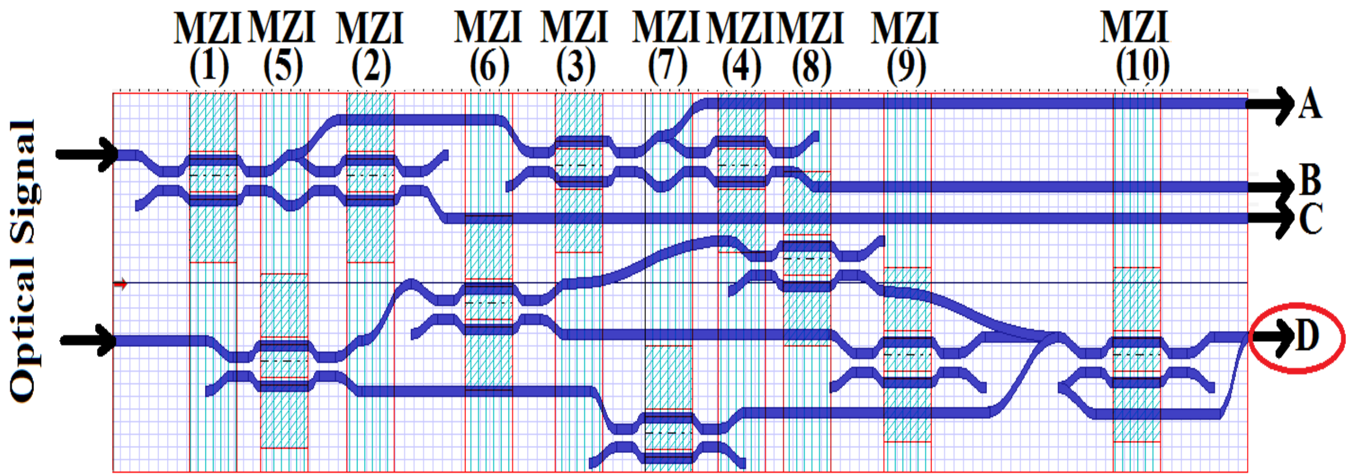

Figure: BPM layout of S-R Flip-flop using Feynman and Peres gate

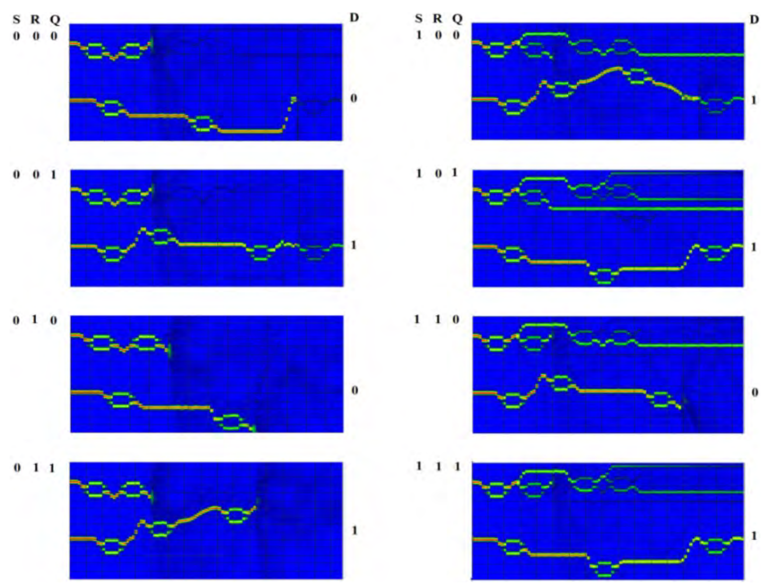

Figure: BPM simulation results for S-R flip-flop

J-K Flip-flop

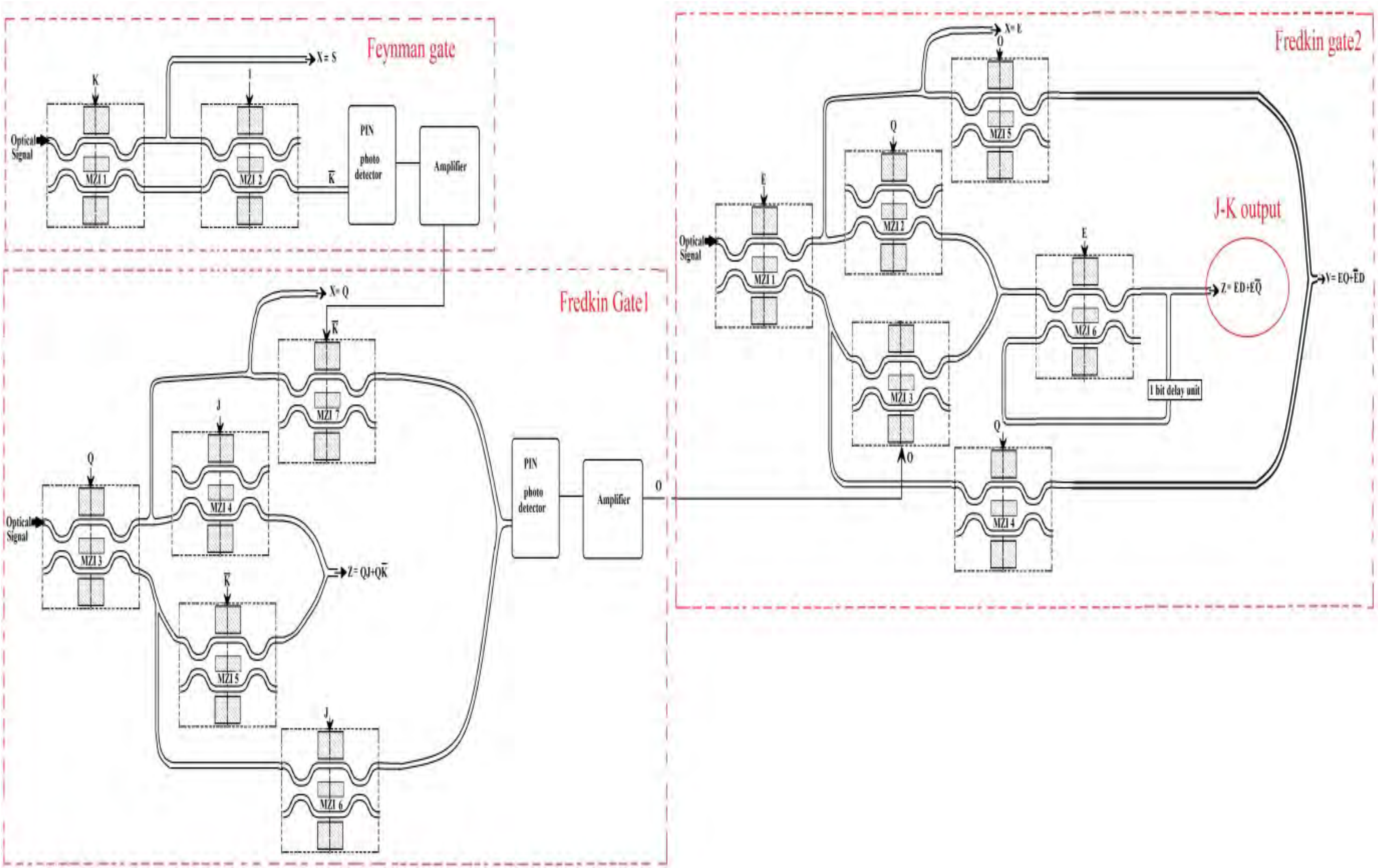

Figure: J-K flip-flop using Fredkin and Feynman gate

Mathematical Expression for J-K flip flop

Mathematical formulation for J-K flip-flop can be calculated as:

$$\begin{aligned} \mathrm{D} = \; & \sin^2\left(\frac{\Delta\phi_{\mathrm{MZI8}}}{2}\right)\sin^2\left(\frac{\Delta\phi_{\mathrm{MZI9}}}{2}\right)\sin^2\left(\frac{\Delta\phi_{\mathrm{MZI10}}}{2}\right) \\ & + \cos^2\left(\frac{\Delta\phi_{\mathrm{MZI8}}}{2}\right)\sin^2\left(\frac{\Delta\phi_{\mathrm{MZI9}}}{2}\right)\sin^2\left(\frac{\Delta\phi_{\mathrm{MZI10}}}{2}\right) \end{aligned}$$

MATLAB Results for J-K flip-flop

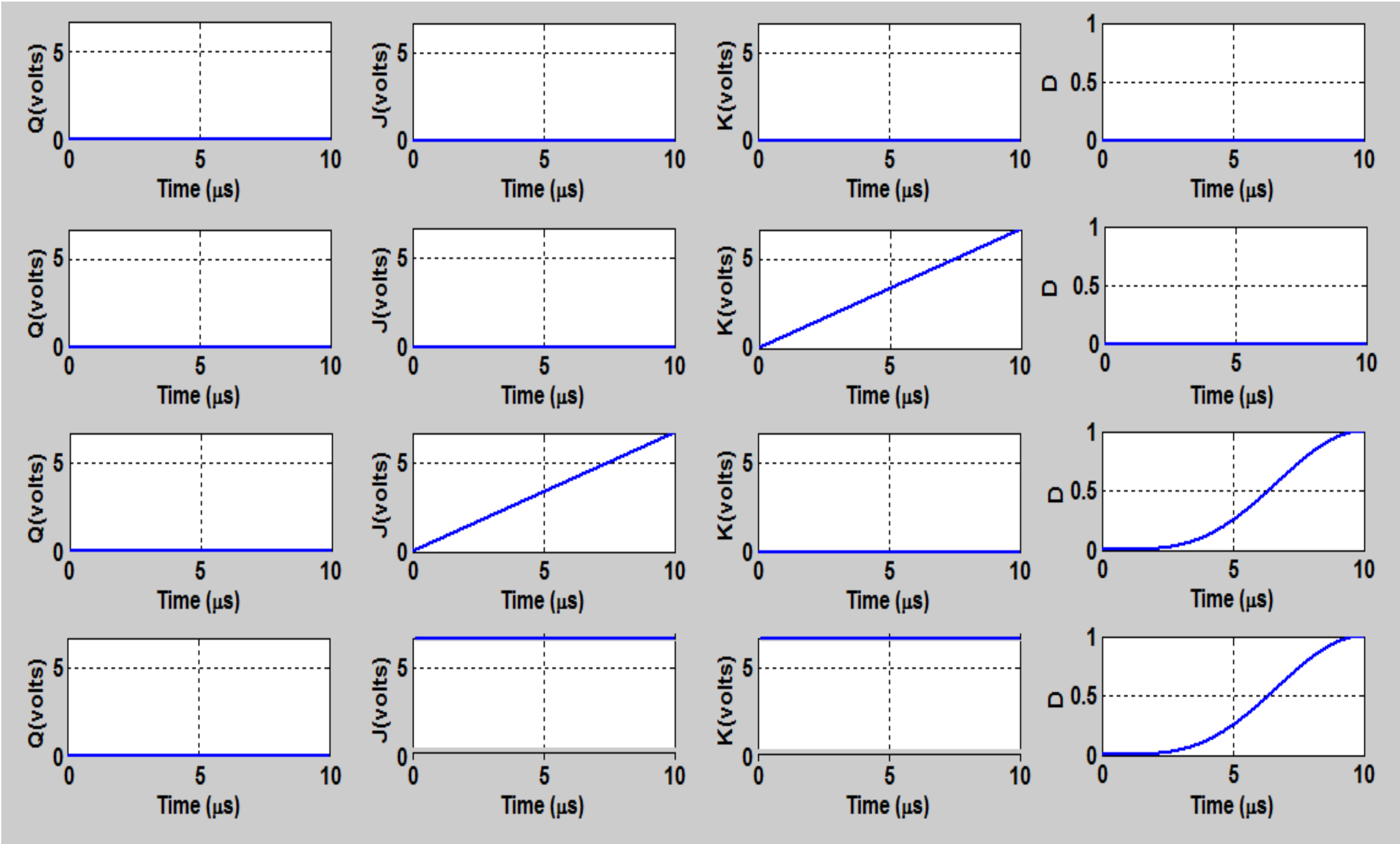

Figure: MATLAB simulation results of J-K flip-flop using Feynman gate and Fredkin gate where input signal Q, J, K varies from 000 to 011

Contd..

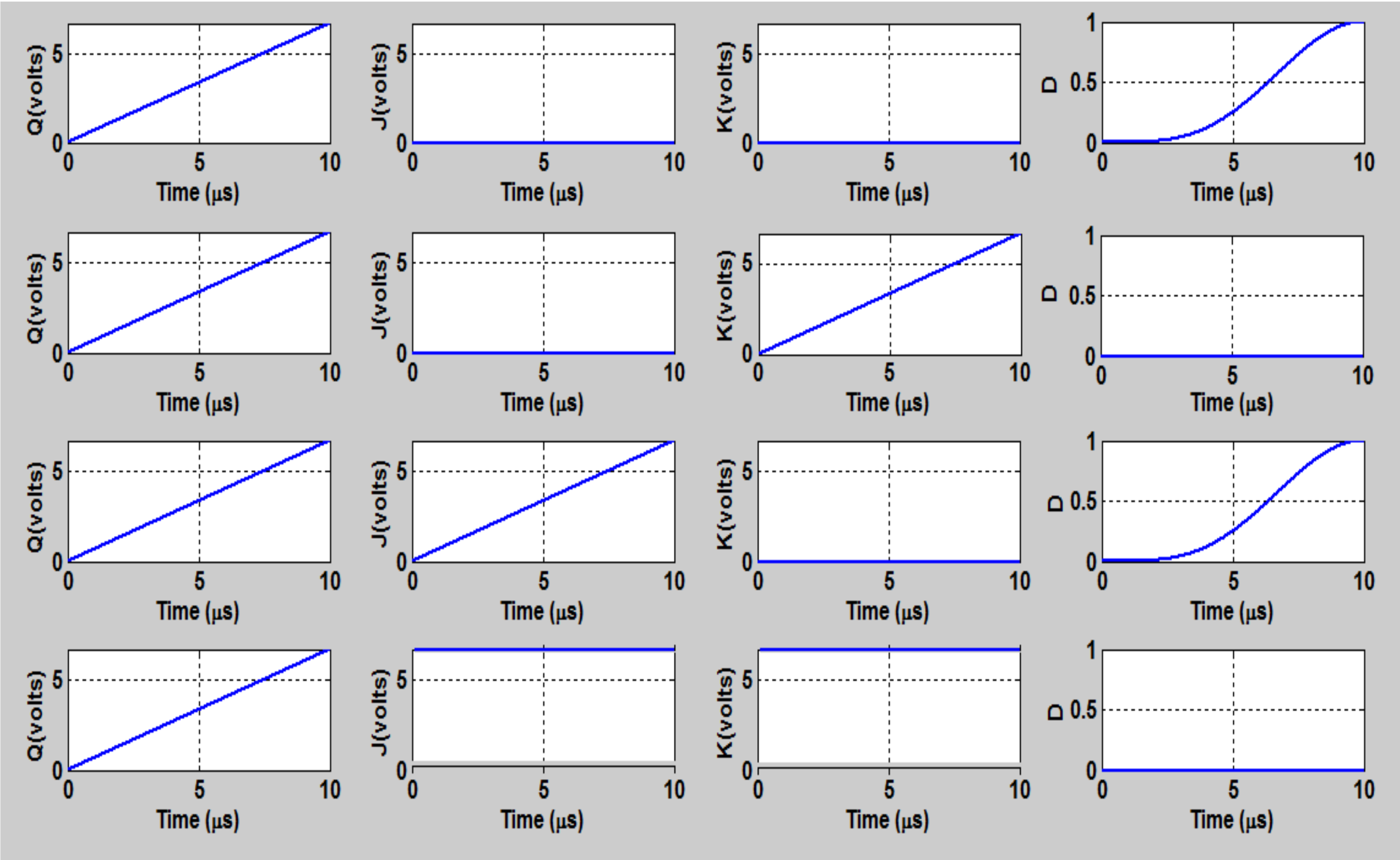

Figure: MATLAB simulation results of J-K flip-flop using Feynman gate and Fredkin gate where input signal Q, J, K varies from 100 to 111

BPM Layout of J-K Flip-flop

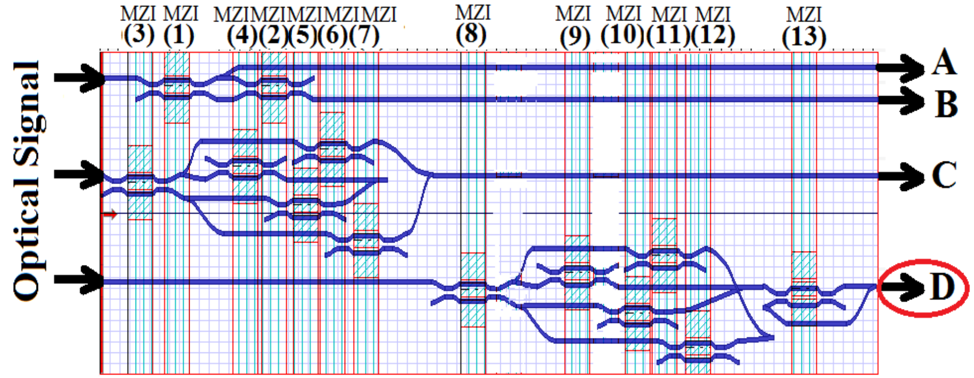

Figure: BPM layout of J-K Flip-flop using Feynman and Fredkin gate

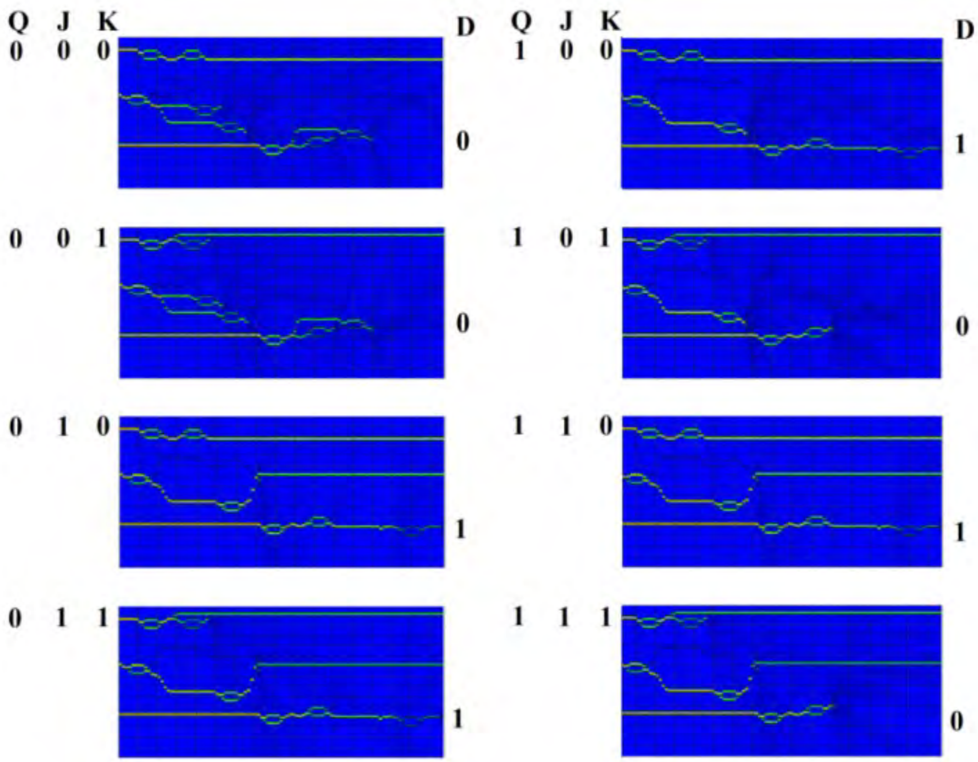

Figure: BPM simulation results for J-K flip-flop

Design of Optical Reversible gate (Peres Gate)

Santosh Kumar et. al., OSA Fio2016, Rochester, New York, USA. (Oct 17-21,2016)

Reversible Optical gate (Peres gate)

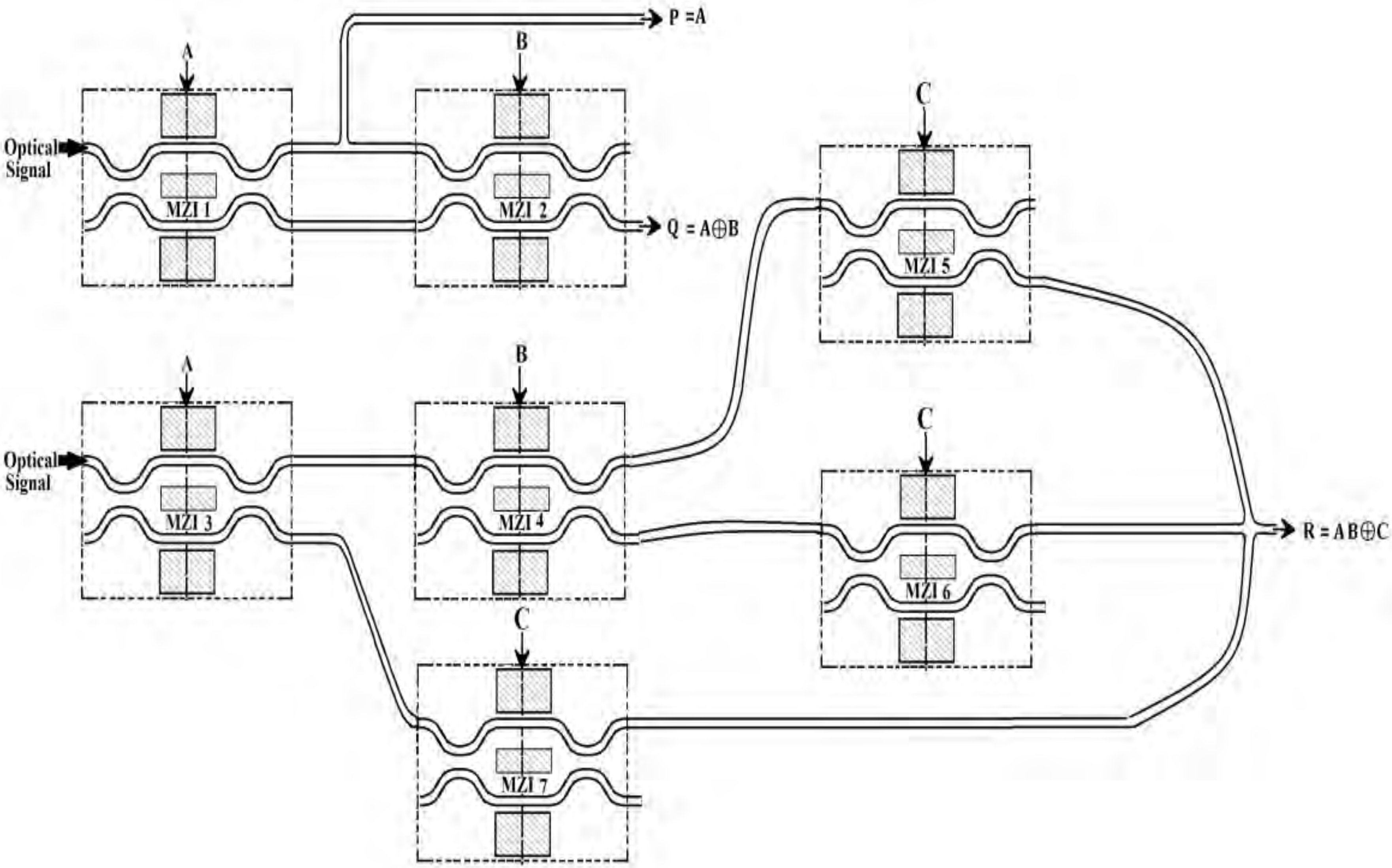

Figure: Schematic diagram of Peres gate using MZIs

MATLAB Results for Reversible gate

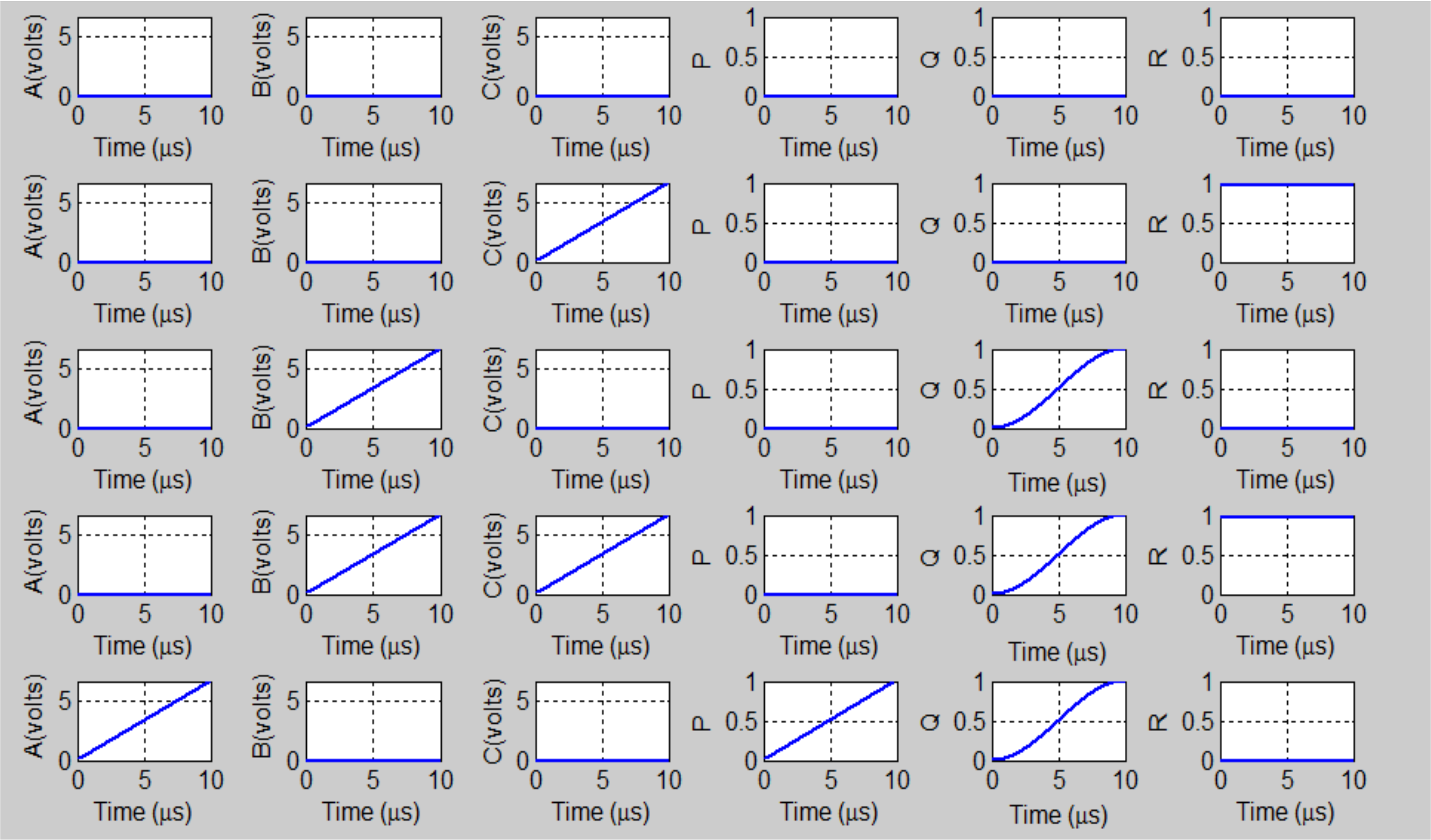

Figure: MATLAB Simulation result of proposed Peres gate where input A, B, C varies from 000 to 100

Simulation Result from BPM

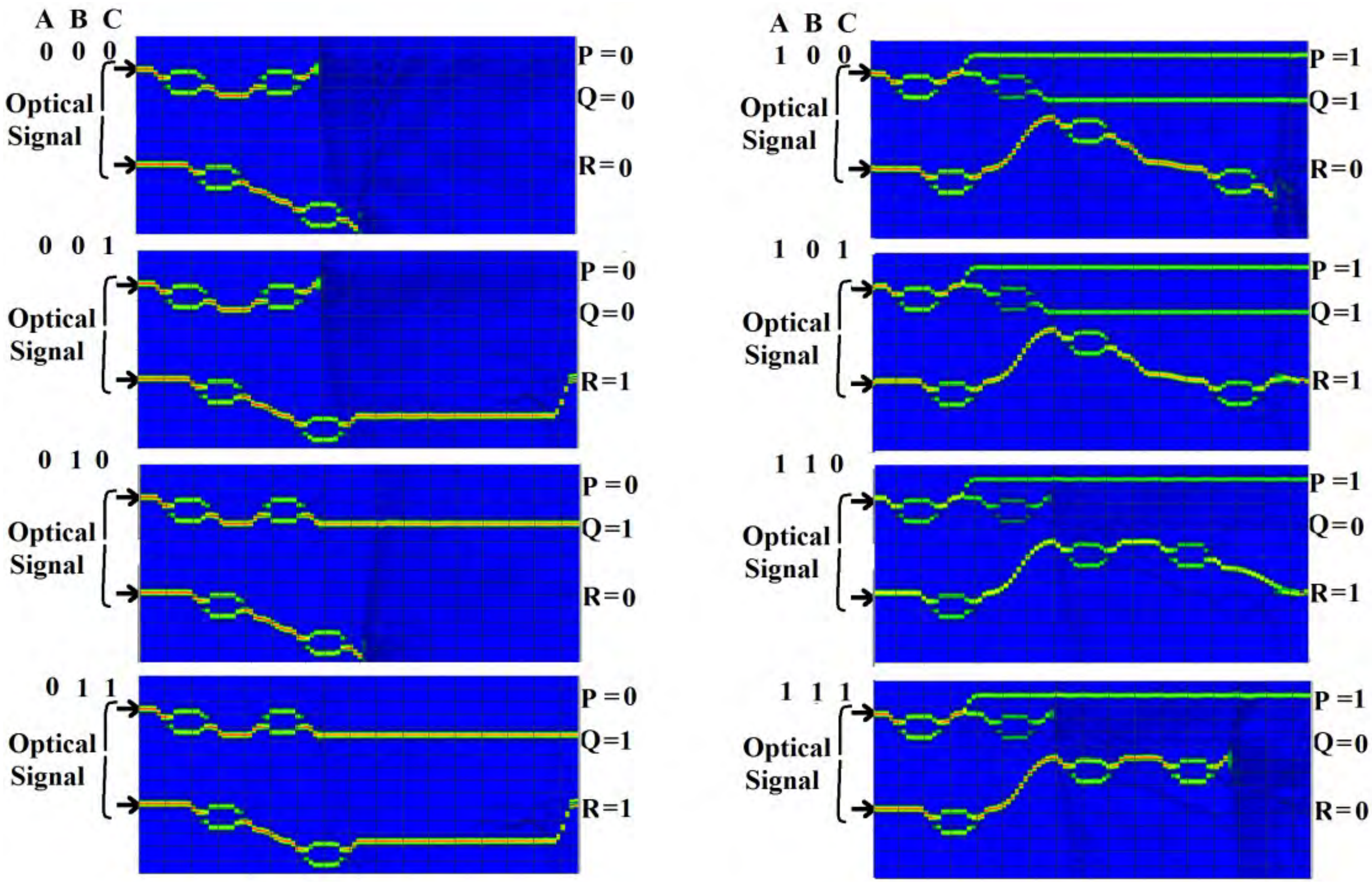

Figure: BPM result of proposed Peres gate where input A, B, C varies from 000 to 111

Ultrafast Optical Reversible Double Feynman logic gate

<u>Santosh Kumar</u> et al., Proc. SPIE 10105, Oxide-based Materials and Devices VIII, SPIE Photonics West - 2017, **San Francisco, California, USA**, PP. 1010520 (28 Jan. - 2 Feb. 2017).

Schematic diagram double Feynman gate using MZI

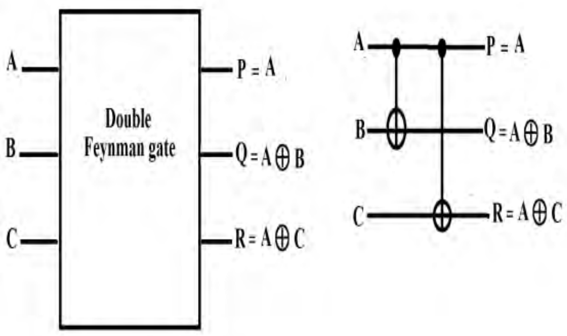

Figure: Logic diagram

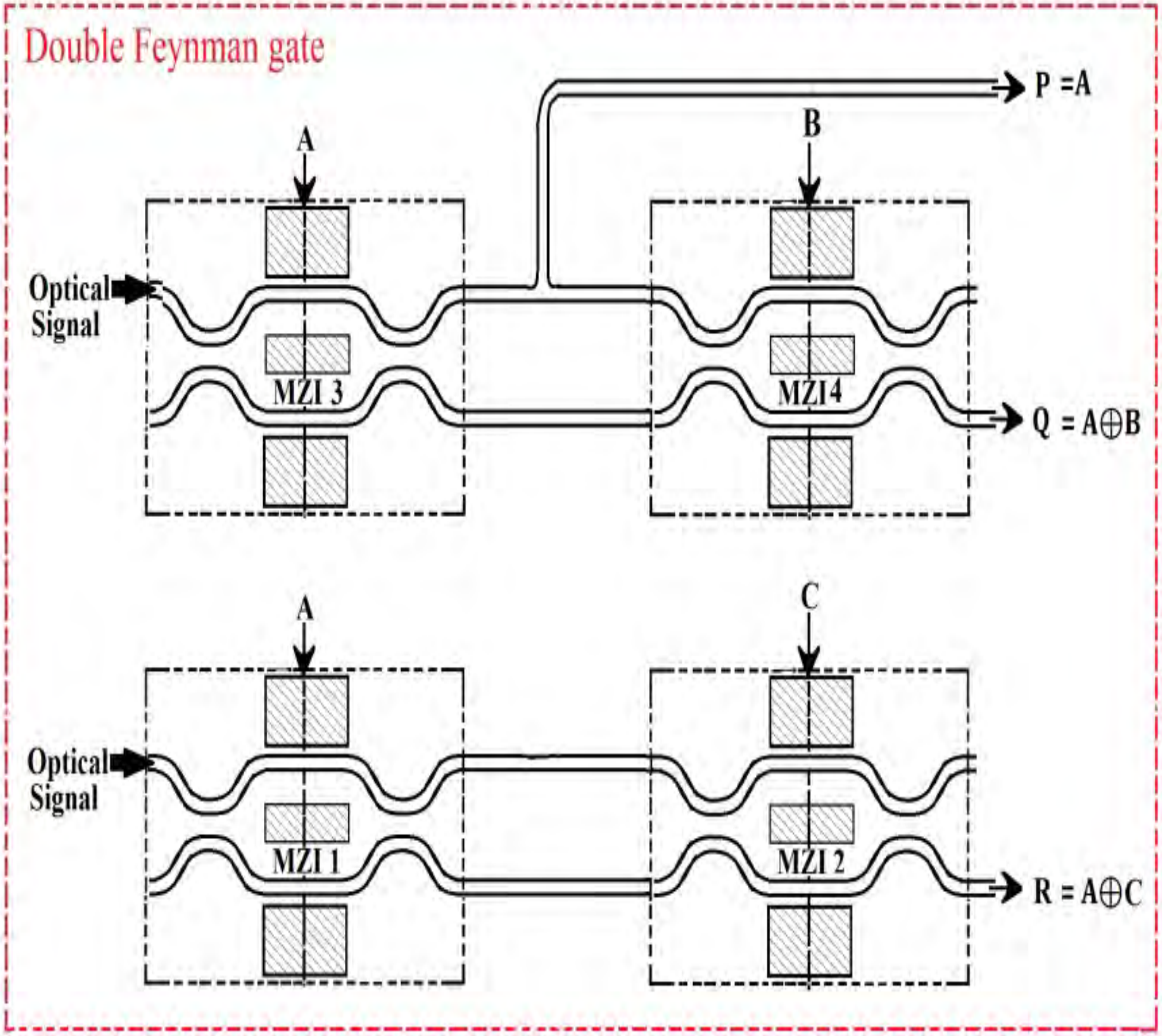

Figure: Schematic diagram of double Feynman gate using Mach-Zehnder interferometer

Truth table and mathematical expression for double Feynman gate

$$P = \sin^2\left(\frac{\Delta\emptyset_{MZI3}}{2}\right)$$

$$Q = \sin^2\left(\frac{\Delta\emptyset_{MZI3}}{2}\right)\cos^2\left(\frac{\Delta\emptyset_{MZI4}}{2}\right) + \cos^2\left(\frac{\Delta\emptyset_{MZI3}}{2}\right)\sin^2\left(\frac{\Delta\emptyset_{MZI4}}{2}\right)$$

$$R = \sin^2\left(\frac{\Delta\emptyset_{MZI1}}{2}\right)\cos^2\left(\frac{\Delta\emptyset_{MZI2}}{2}\right) + \cos^2\left(\frac{\Delta\emptyset_{MZI1}}{2}\right)\sin^2\left(\frac{\Delta\emptyset_{MZI2}}{2}\right)$$

Input			**output**		
A	**B**	**C**	**P**	**Q**	**R**
0	0	0	0	0	0
0	0	1	0	0	1
0	1	0	0	1	0
0	1	1	0	1	1
1	0	0	1	1	1
1	0	1	1	1	0
1	1	0	1	0	1
1	1	1	1	0	0

MATLAB simulation results

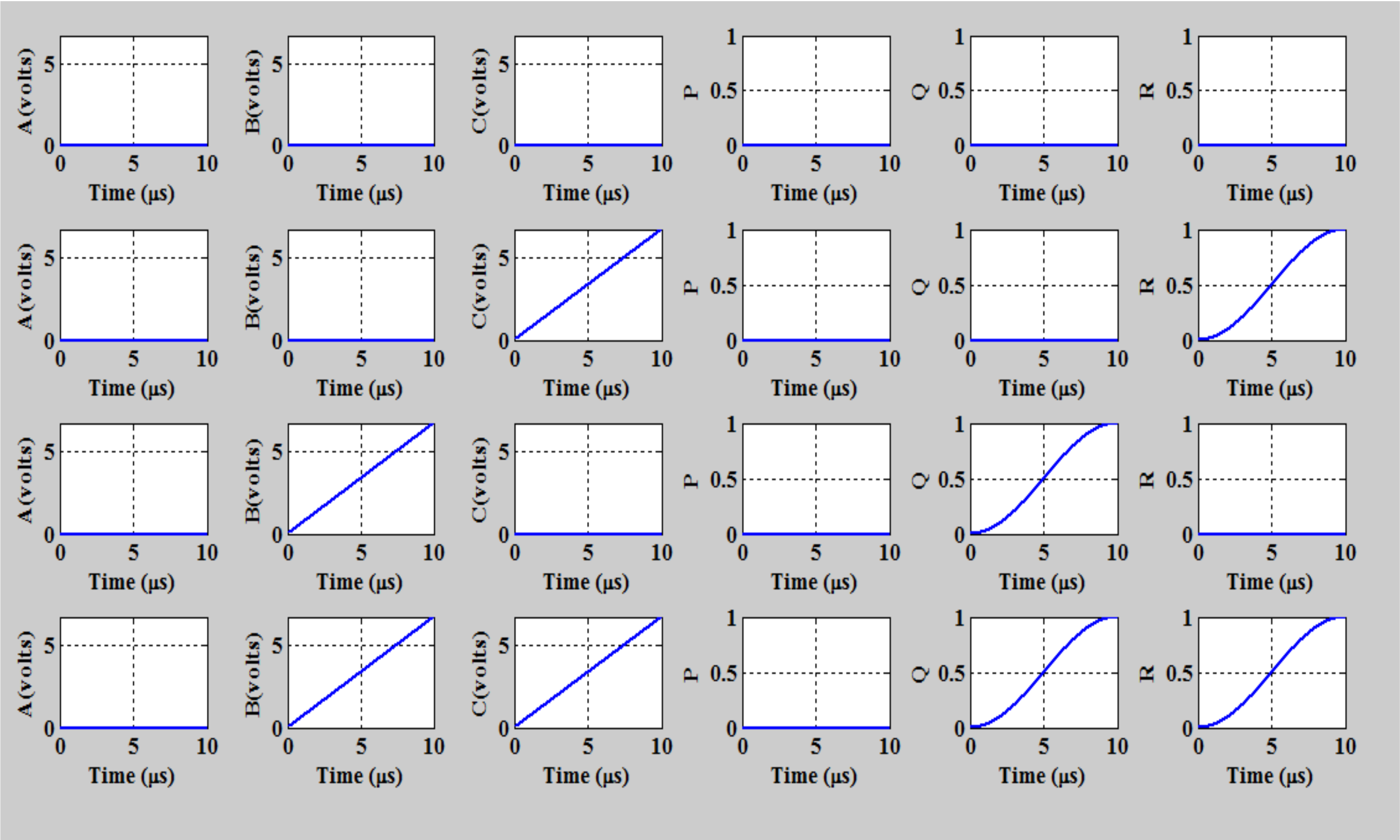

Figure: MATLAB simulation results where input signal A; B and C varies from 000 to 011

Contd..

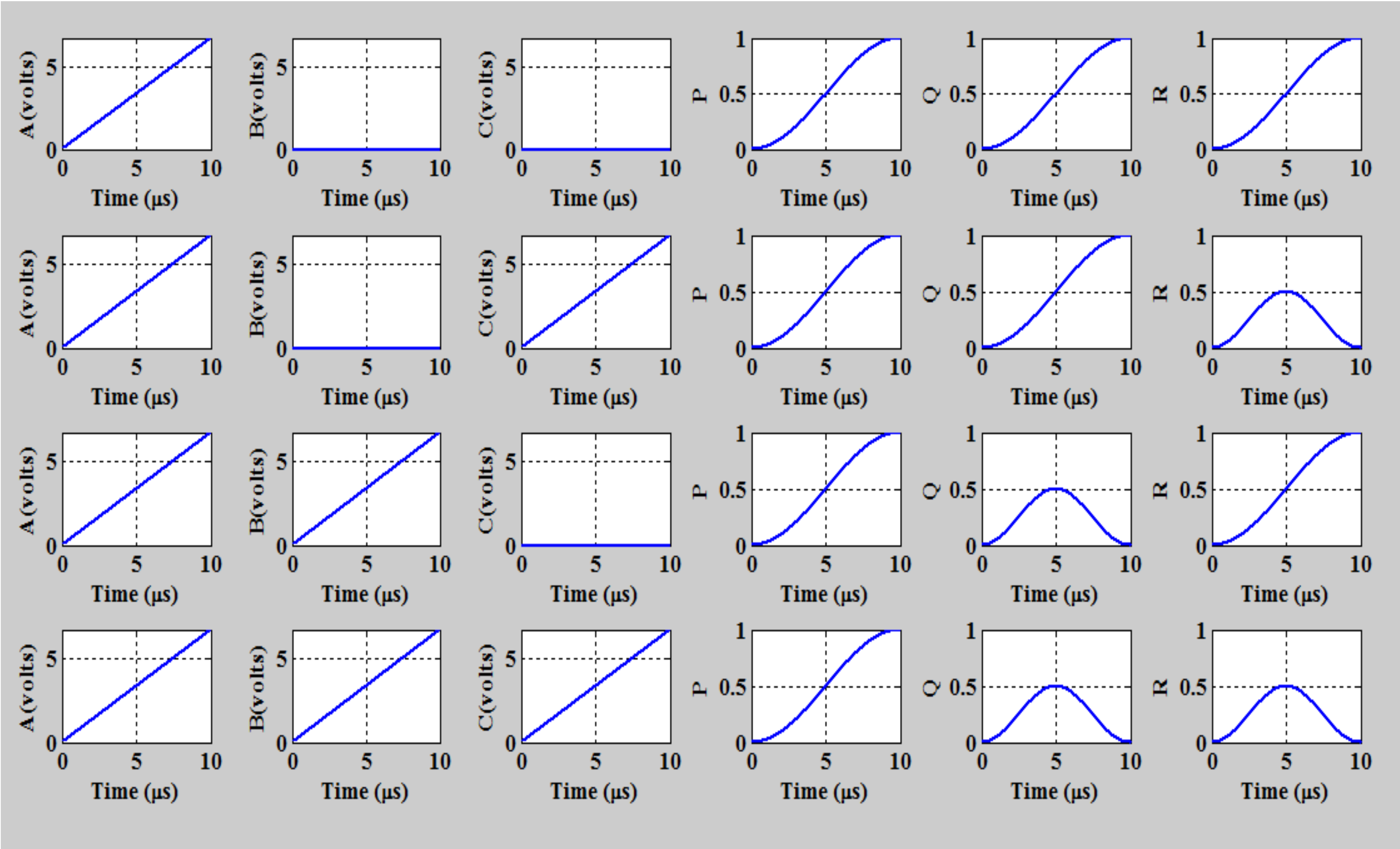

Figure: MATLAB simulation results where input signal A; B and C varies from 100 to 111

BPM simulation results

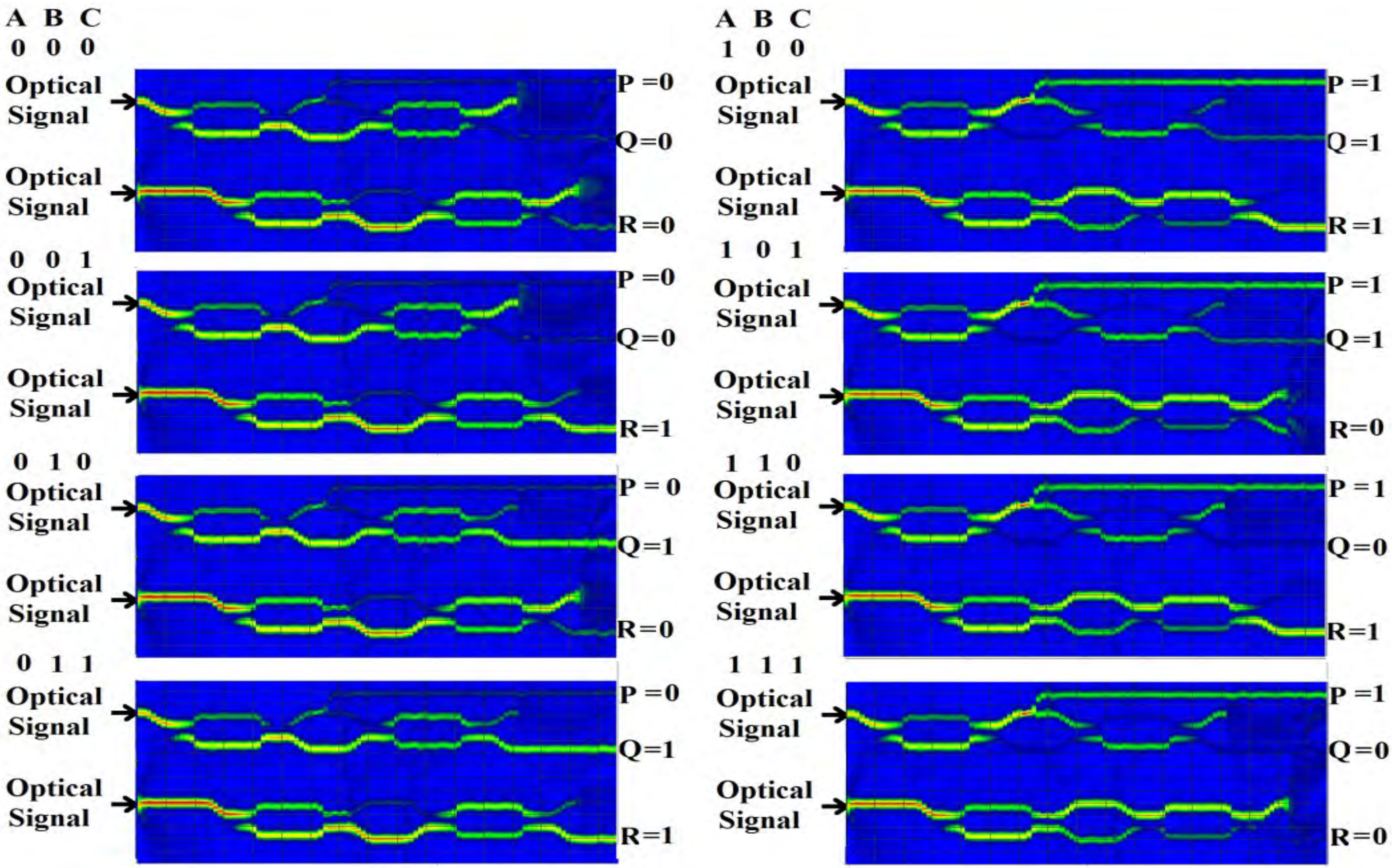

Figure: BPM simulation results of double Feynman gate where input signal varies from 000 to 111

Design of Peres gate and its applications

Peres gate and its applications

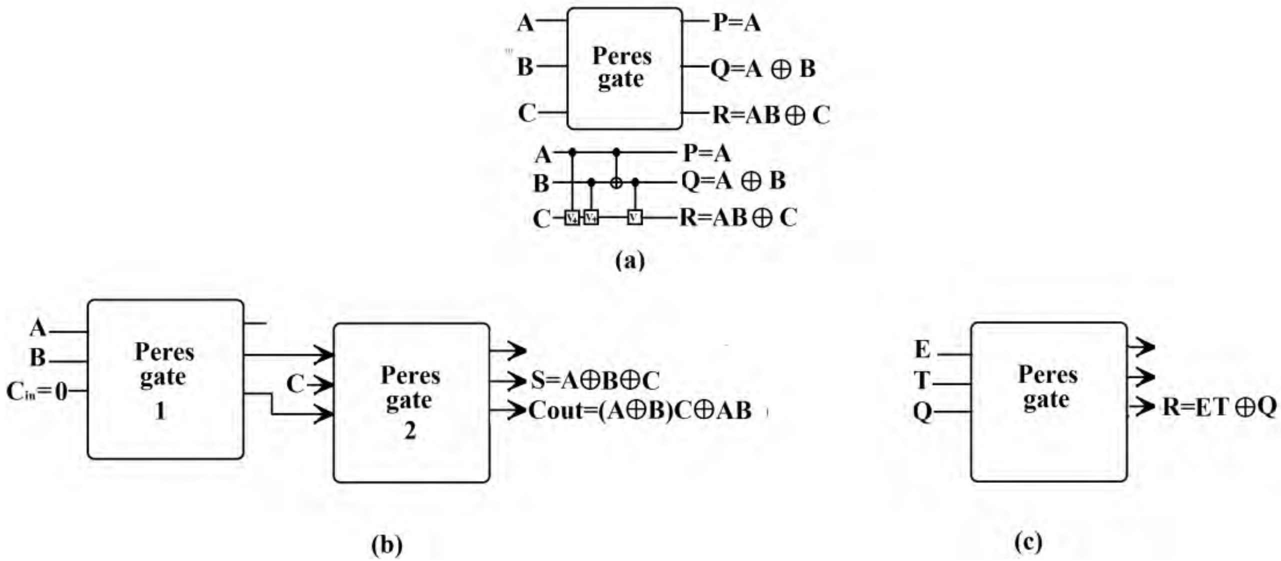

Figure: Logic design of Peres gate and its application as full-adder and T flip-flop

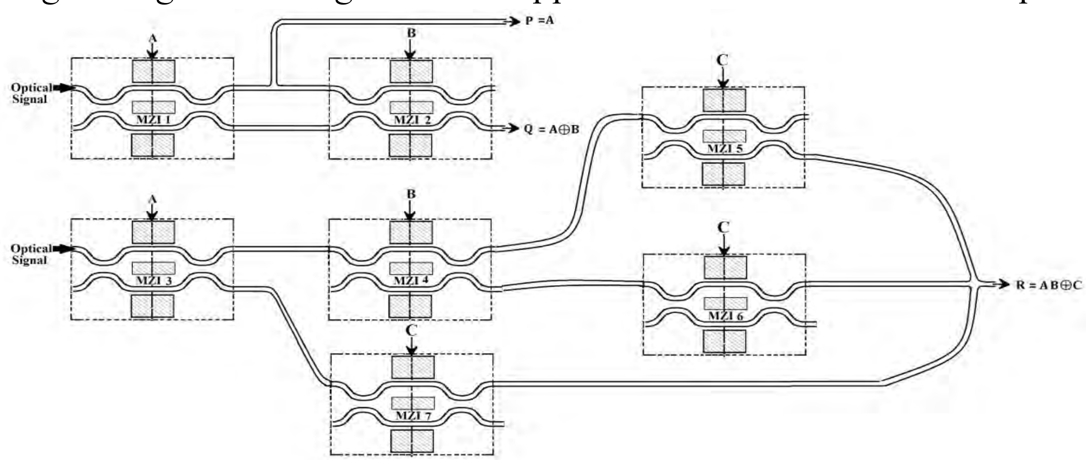

Figure: Schematic of Peres gate using Mach-Zehnder interferometer

Dr. Santosh Kumar

Mathematical expression for Peres gate

$$P = \sin^2\left(\frac{\Delta\emptyset_{\mathrm{MZI1}}}{2}\right)$$

$$Q = \sin^2\left(\frac{\Delta\emptyset_{\mathrm{MZI1}}}{2}\right)\cos^2\left(\frac{\Delta\emptyset_{\mathrm{MZI2}}}{2}\right) + \cos^2\left(\frac{\Delta\emptyset_{\mathrm{MZI1}}}{2}\right)\sin^2\left(\frac{\Delta\emptyset_{\mathrm{MZI2}}}{2}\right)$$

$$\begin{aligned} R = {} & \sin^2\left(\frac{\Delta\emptyset_{\mathrm{MZI3}}}{2}\right)\sin^2\left(\frac{\Delta\emptyset_{\mathrm{MZI4}}}{2}\right)\cos^2\left(\frac{\Delta\emptyset_{\mathrm{MZI5}}}{2}\right) \\ & + \sin^2\left(\frac{\Delta\emptyset_{\mathrm{MZI3}}}{2}\right)\cos^2\left(\frac{\Delta\emptyset_{\mathrm{MZI4}}}{2}\right)\sin^2\left(\frac{\Delta\emptyset_{\mathrm{MZI6}}}{2}\right) \\ & + \cos^2\left(\frac{\Delta\emptyset_{\mathrm{MZI3}}}{2}\right)\sin^2\left(\frac{\Delta\emptyset_{\mathrm{MZI7}}}{2}\right) \end{aligned}$$

MATLAB Simulation Results

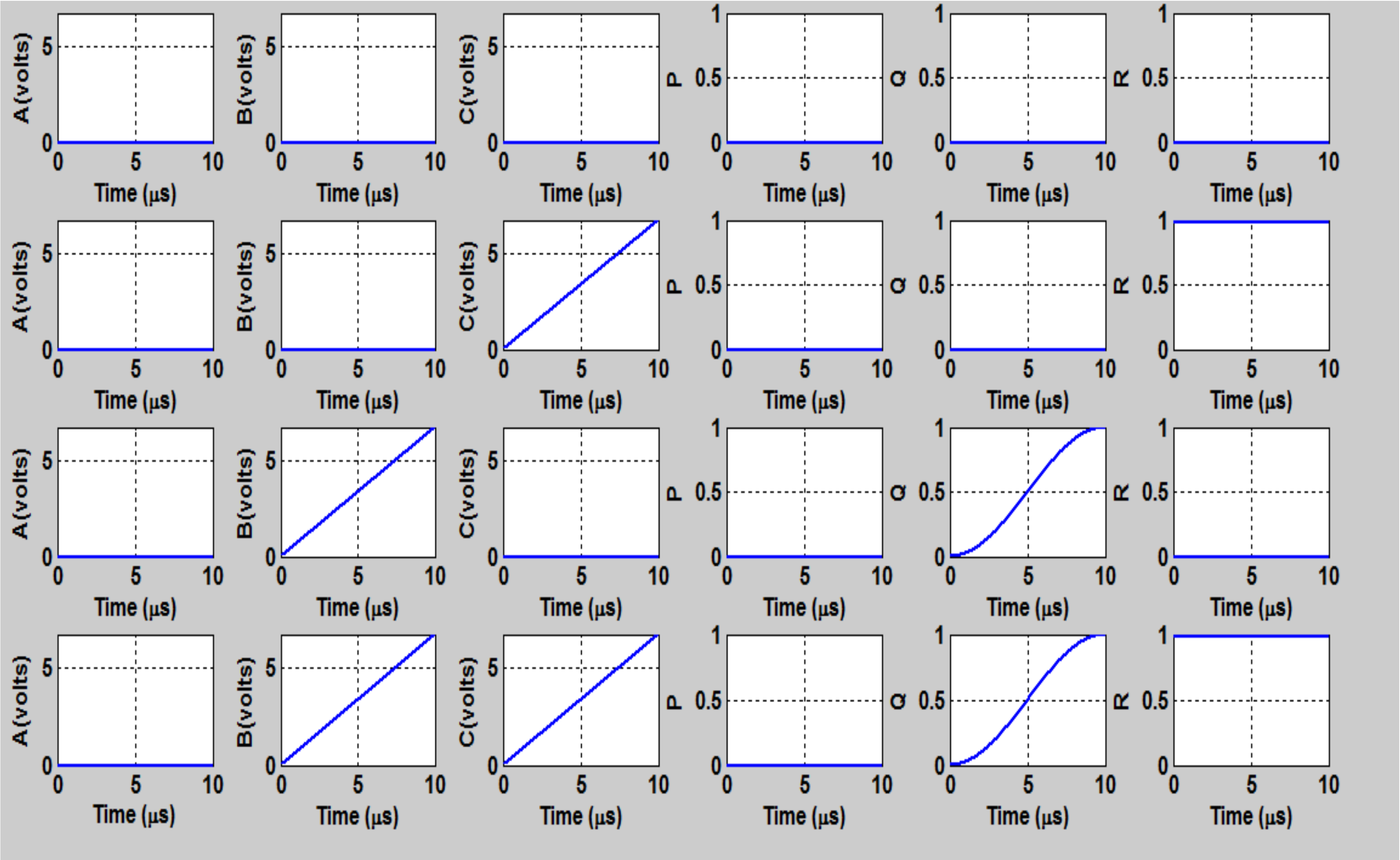

Figure: MATLAB simulation results of Peres gate where A, B, C varies from 000 to 011

MATLAB Simulation Results

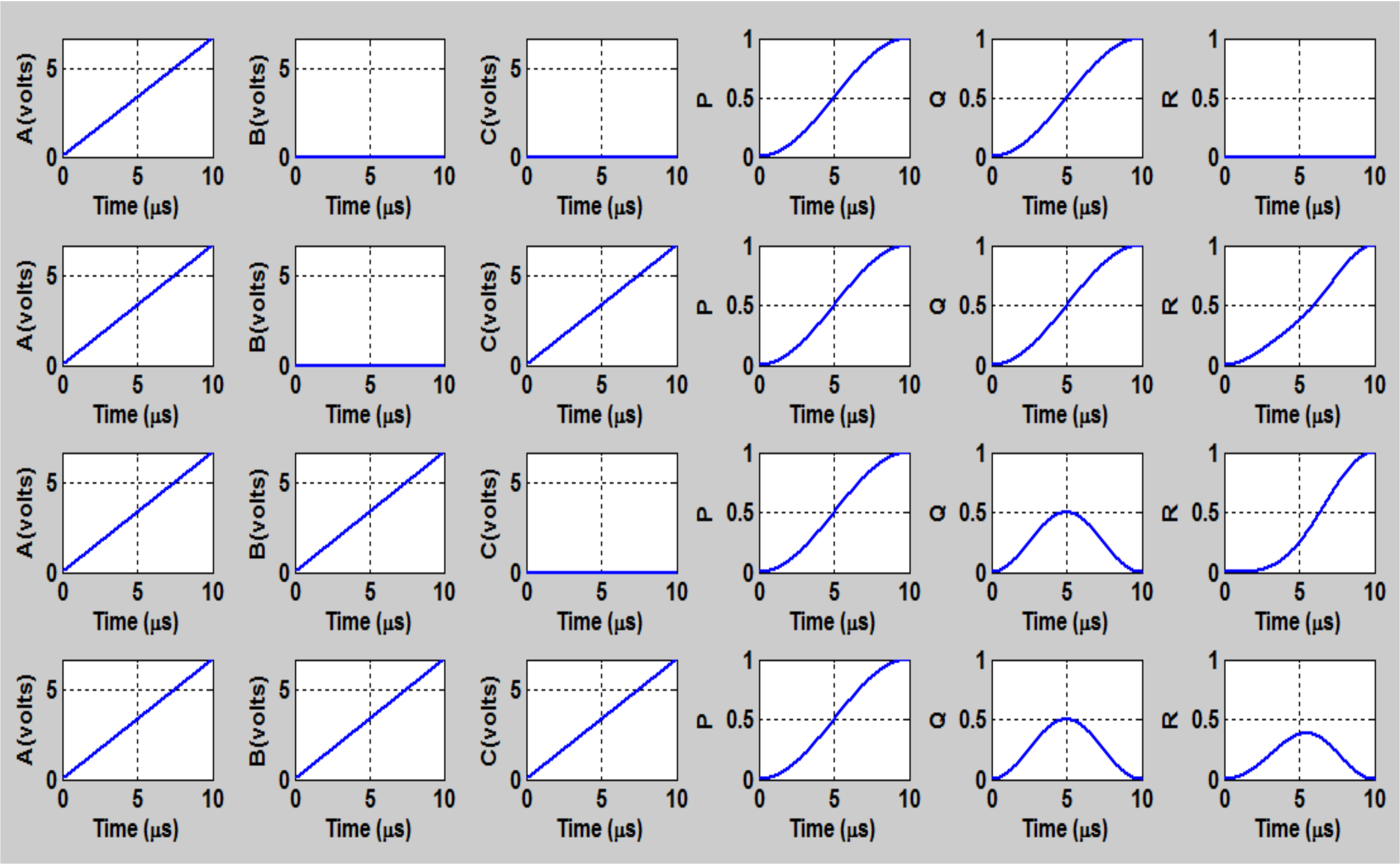

Figure: MATLAB simulation results of Peres gate where A, B, C varies from 100 to 111

Full Adder using Peres gate

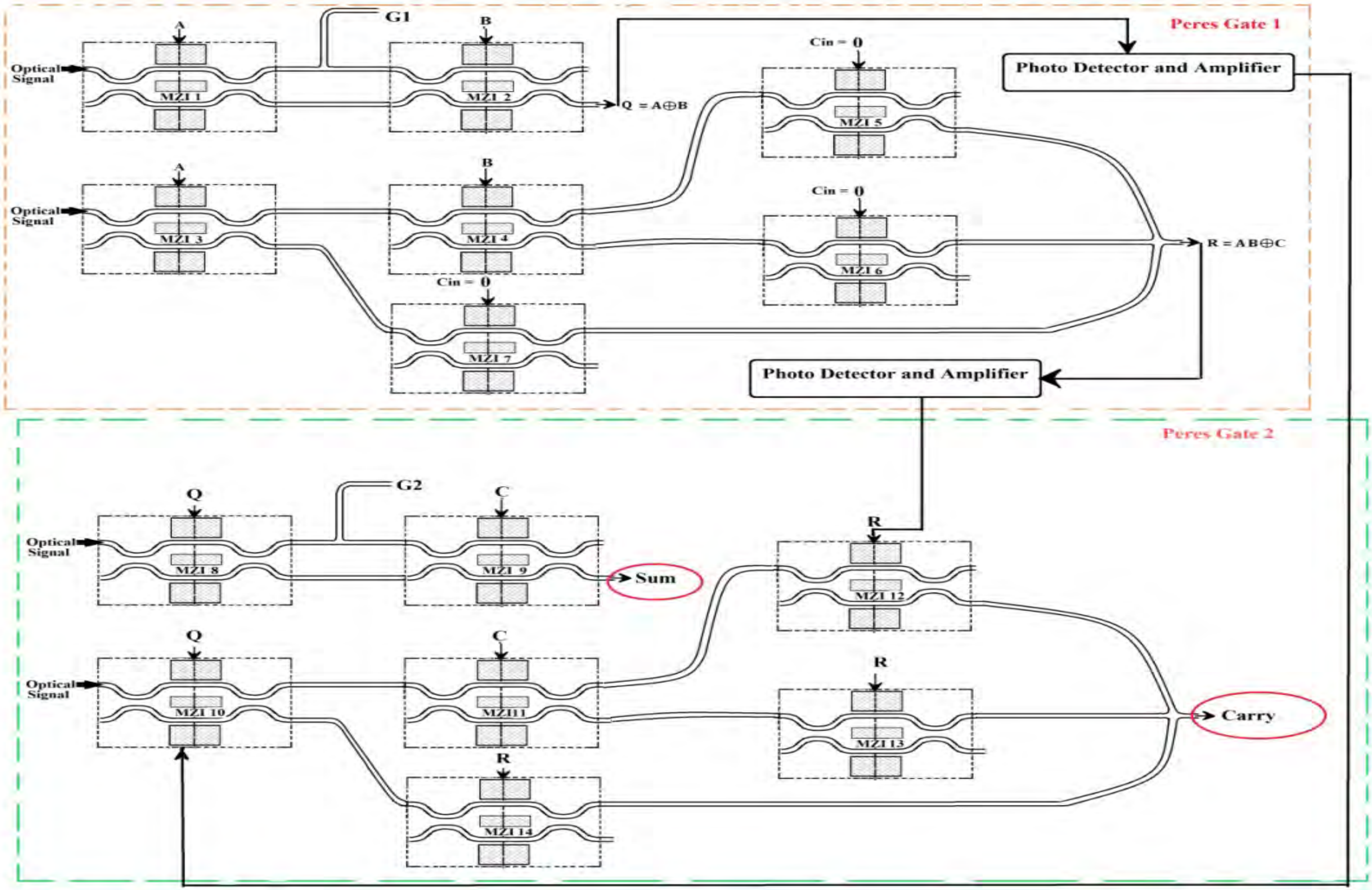

Figure: Schematic of full-adder using MZI based Peres gate

Mathematical expression for Full adder using Peres gate

$$Q = \sin^2\left(\frac{\Delta\emptyset_{\mathrm{MZI1}}}{2}\right)\cos^2\left(\frac{\Delta\emptyset_{\mathrm{MZI2}}}{2}\right) + \cos^2\left(\frac{\Delta\emptyset_{\mathrm{MZI1}}}{2}\right)\sin^2\left(\frac{\Delta\emptyset_{\mathrm{MZI2}}}{2}\right)$$

$$R = \sin^2\left(\frac{\Delta\emptyset_{\mathrm{MZI3}}}{2}\right)\sin^2\left(\frac{\Delta\emptyset_{\mathrm{MZI4}}}{2}\right)\cos^2\left(\frac{\Delta\emptyset_{\mathrm{MZI5}}}{2}\right)$$
$$+ \sin^2\left(\frac{\Delta\emptyset_{\mathrm{MZI3}}}{2}\right)\cos^2\left(\frac{\Delta\emptyset_{\mathrm{MZI4}}}{2}\right)\sin^2\left(\frac{\Delta\emptyset_{\mathrm{MZI6}}}{2}\right) + \cos^2\left(\frac{\Delta\emptyset_{\mathrm{MZI3}}}{2}\right)\sin^2\left(\frac{\Delta\emptyset_{\mathrm{MZI7}}}{2}\right)$$

$$\mathrm{Sum} = \sin^2\left(\frac{\Delta\emptyset_{\mathrm{MZI8}}}{2}\right)\cos^2\left(\frac{\Delta\emptyset_{\mathrm{MZI9}}}{2}\right) + \cos^2\left(\frac{\Delta\emptyset_{\mathrm{MZI8}}}{2}\right)\sin^2\left(\frac{\Delta\emptyset_{\mathrm{MZI9}}}{2}\right)$$

$$\mathrm{Carry} = \sin^2\left(\frac{\Delta\emptyset_{\mathrm{MZI10}}}{2}\right)\sin^2\left(\frac{\Delta\emptyset_{\mathrm{MZI11}}}{2}\right)\cos^2\left(\frac{\Delta\emptyset_{\mathrm{MZI12}}}{2}\right)$$
$$+ \sin^2\left(\frac{\Delta\emptyset_{\mathrm{MZI10}}}{2}\right)\cos^2\left(\frac{\Delta\emptyset_{\mathrm{MZI11}}}{2}\right)\sin^2\left(\frac{\Delta\emptyset_{\mathrm{MZI13}}}{2}\right) + \cos^2\left(\frac{\Delta\emptyset_{\mathrm{MZI10}}}{2}\right)\sin^2\left(\frac{\Delta\emptyset_{\mathrm{MZI14}}}{2}\right)$$

MATLAB Simulation Results of Full adder

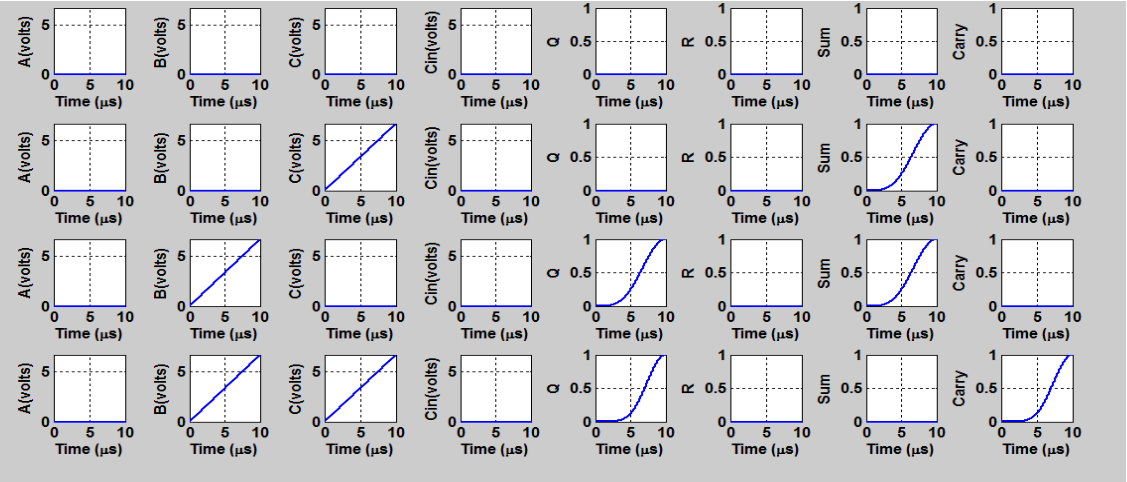

Figure: MATLAB simulation results of full-adder using Peres gate where A, B, C varies from 000 to 011

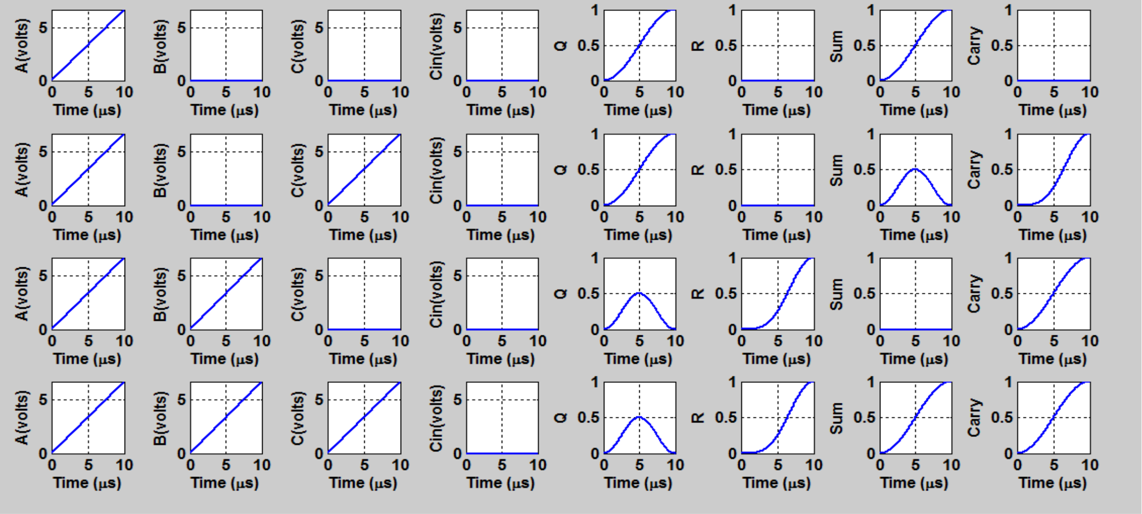

Figure: MATLAB simulation results of full-adder using Peres gate where A, B, C varies from 100 to 111

T Flip-flop using Peres gate and its mathematical expression

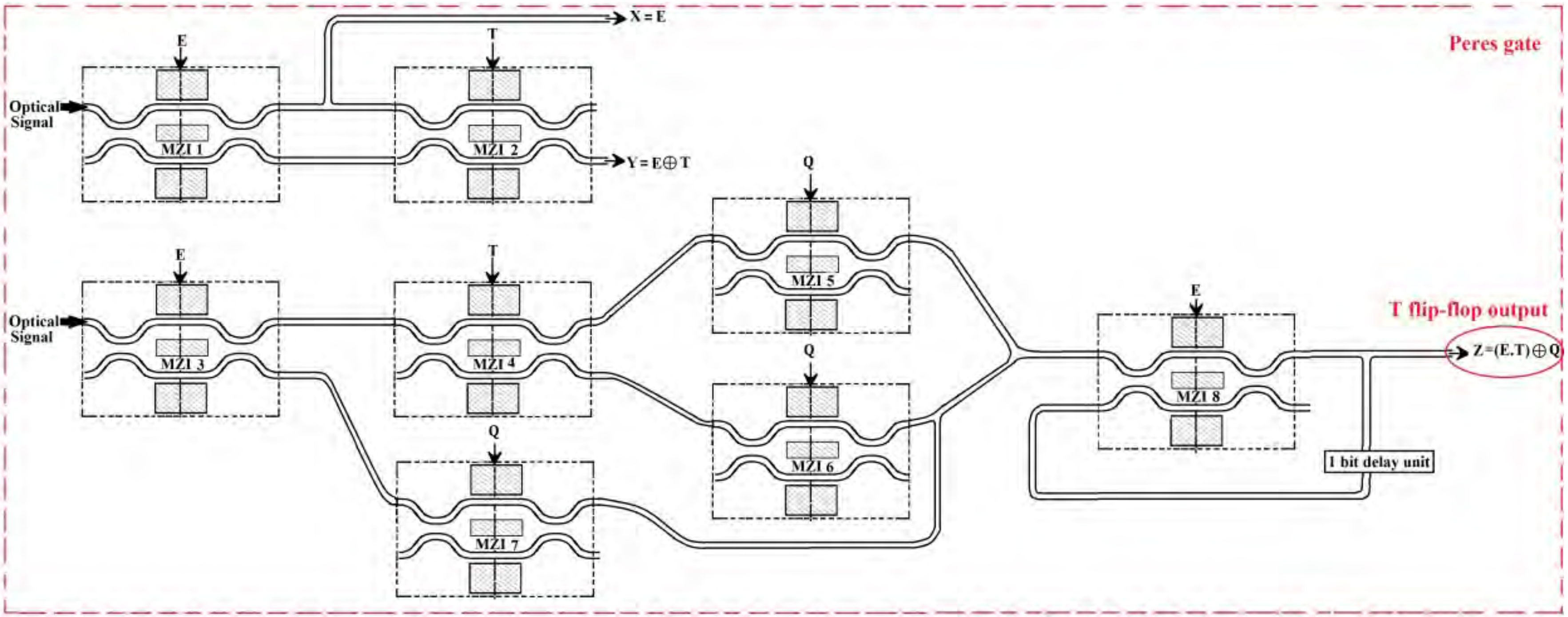

Figure: Schematic of T Flip-flop using Peres gate

$$Z = \sin^2\left(\frac{\Delta\emptyset_{MZI3}}{2}\right)\sin^2\left(\frac{\Delta\emptyset_{MZI4}}{2}\right)\sin^2\left(\frac{\Delta\emptyset_{MZI5}}{2}\right)\sin^2\left(\frac{\Delta\emptyset_{MZI8}}{2}\right)$$

$$+\sin^2\left(\frac{\Delta\emptyset_{MZI3}}{2}\right)\cos^2\left(\frac{\Delta\emptyset_{MZI4}}{2}\right)\sin^2\left(\frac{\Delta\emptyset_{MZI6}}{2}\right)\sin^2\left(\frac{\Delta\emptyset_{MZI8}}{2}\right)$$

$$+\cos^2\left(\frac{\Delta\emptyset_{MZI3}}{2}\right)\sin^2\left(\frac{\Delta\emptyset_{MZI7}}{2}\right)\sin^2\left(\frac{\Delta\emptyset_{MZI8}}{2}\right)$$

MATLAB Simulation Results of T-Flip flop

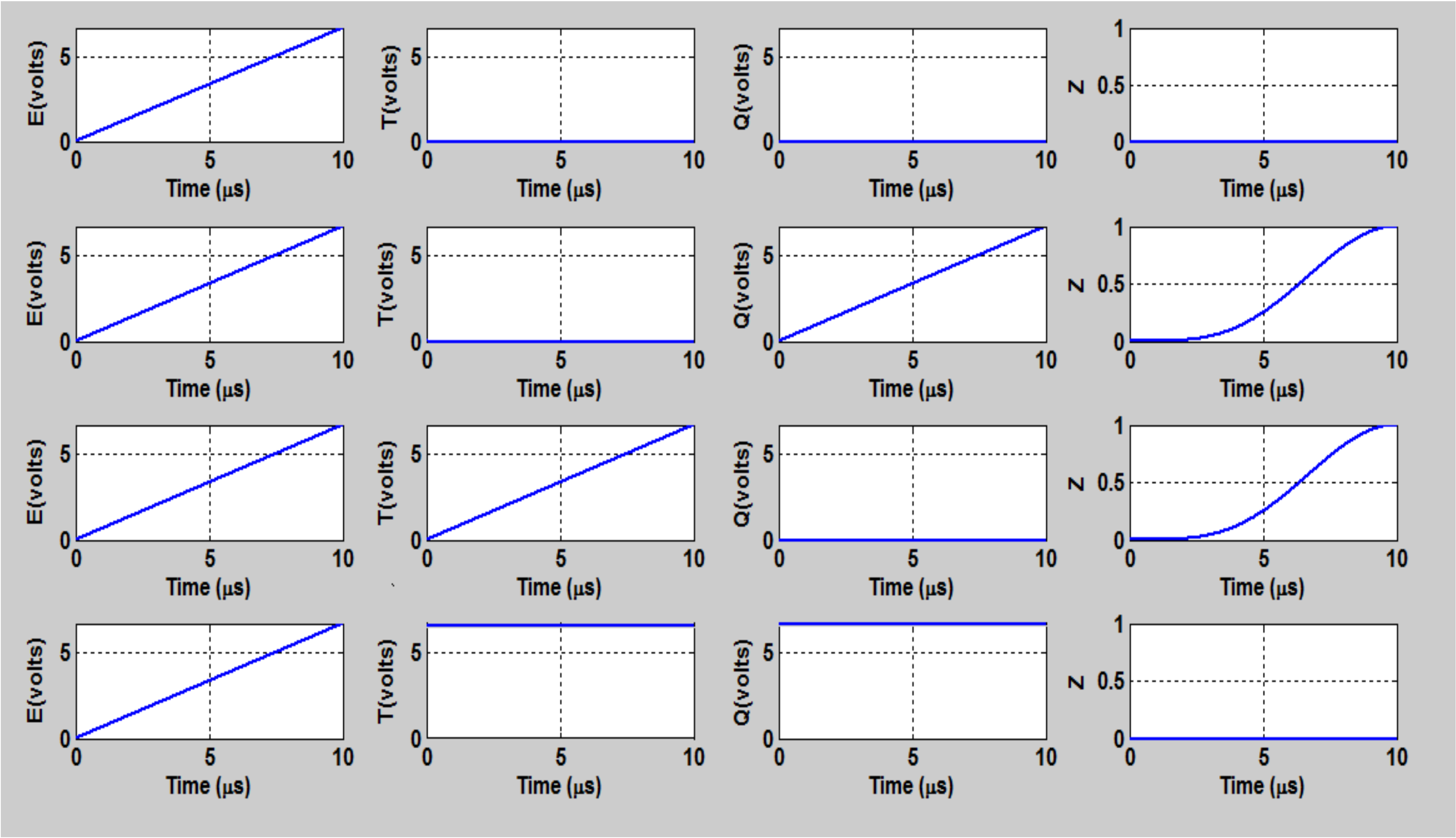

Figure: MATLAB simulation results of T- flip-flop using Peres gate where input signal E, T, Q varies from 100 to 111

BPM layout of Peres gate

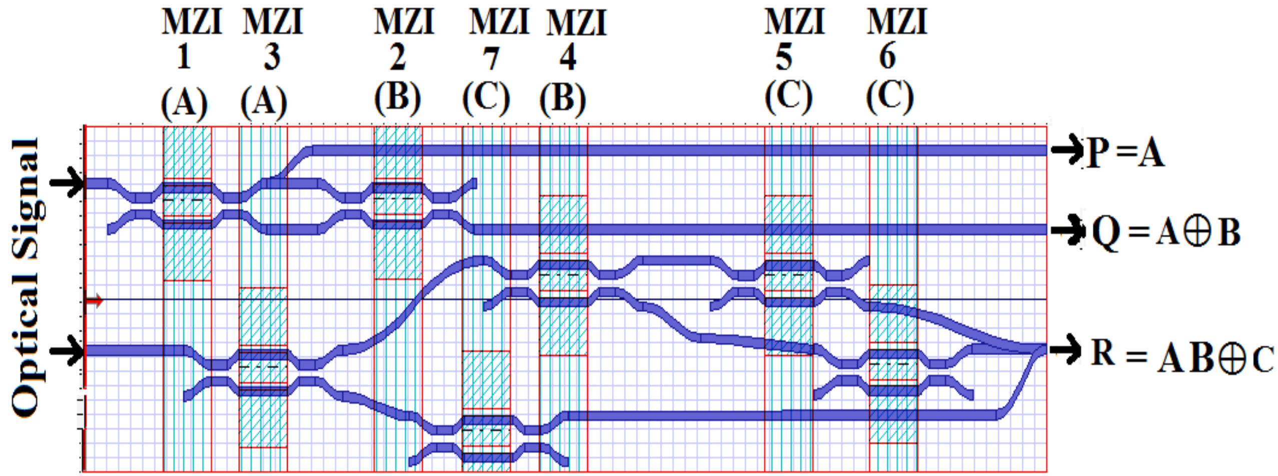

Figure: BPM layout of reversible Peres gate using MZI

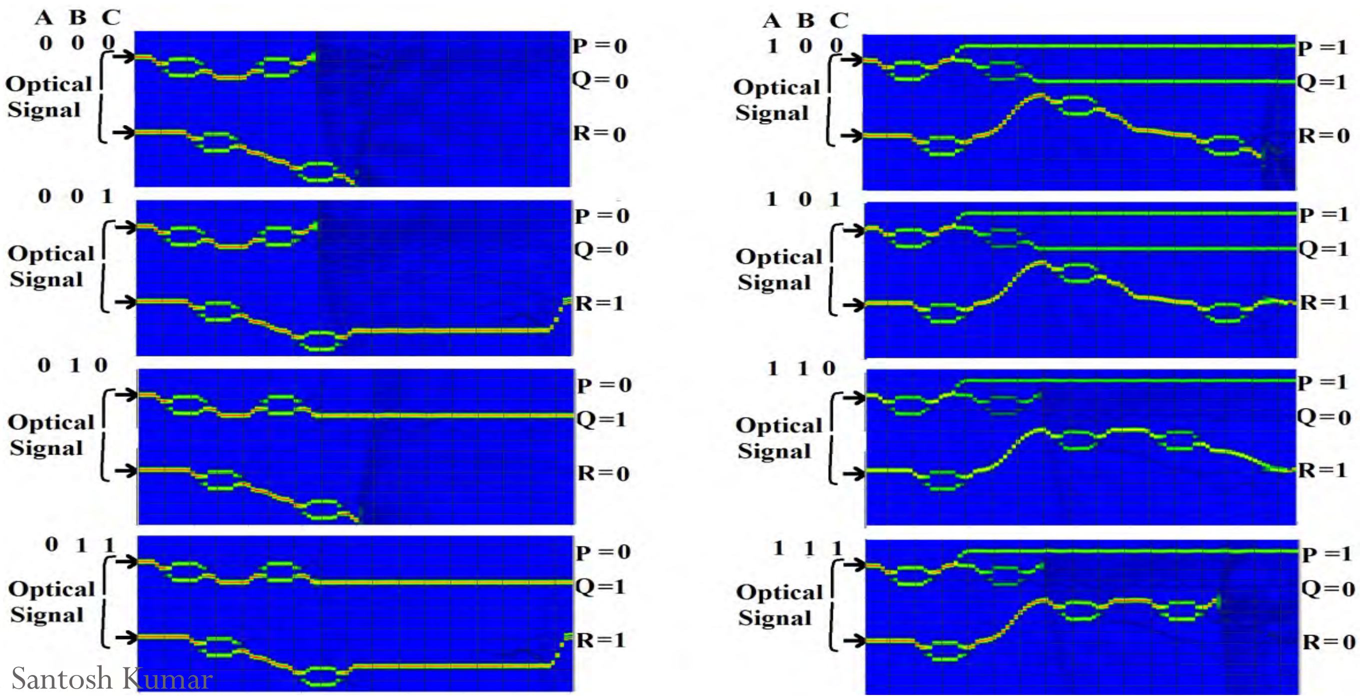

Figure: BPM simulation result of reversible Peres gate using MZI

BPM layout of Full adder using Peres gate

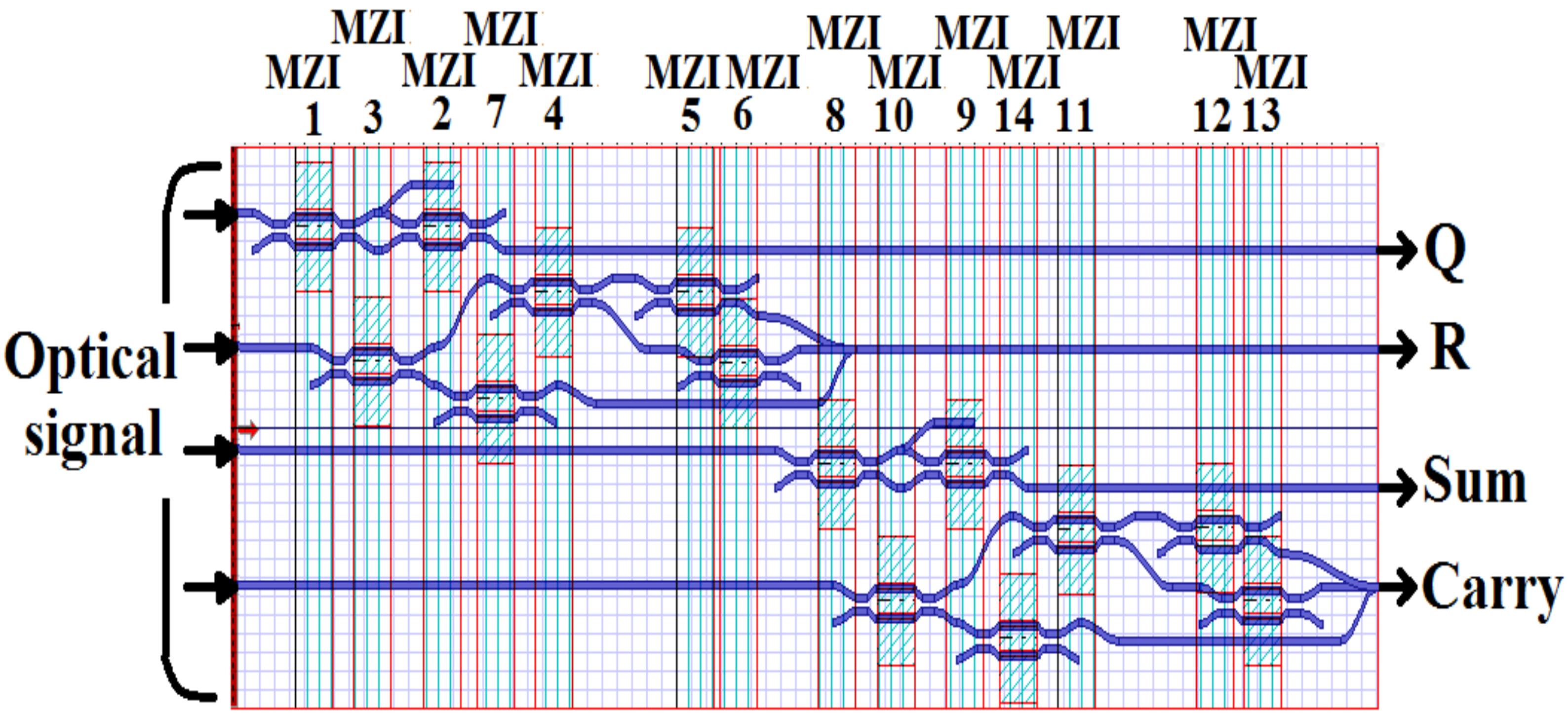

Figure: BPM layout of reversible Full adder using MZI based Peres gate.

Simulation Result of Full adder

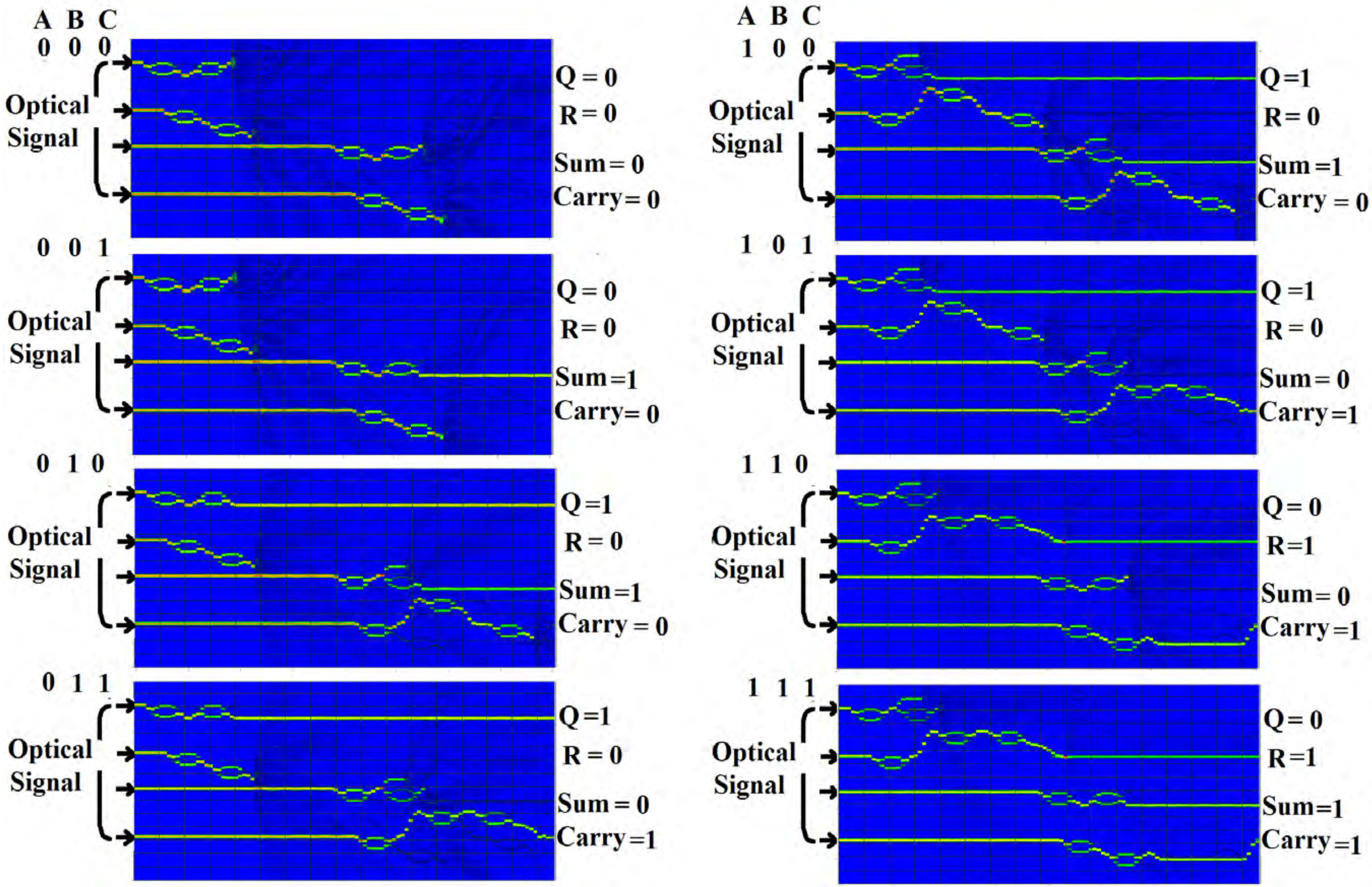

Figure: BPM simulation result of reversible full adder using MZI based Peres gate

BPM layout of T-Flip flop using Peres gate

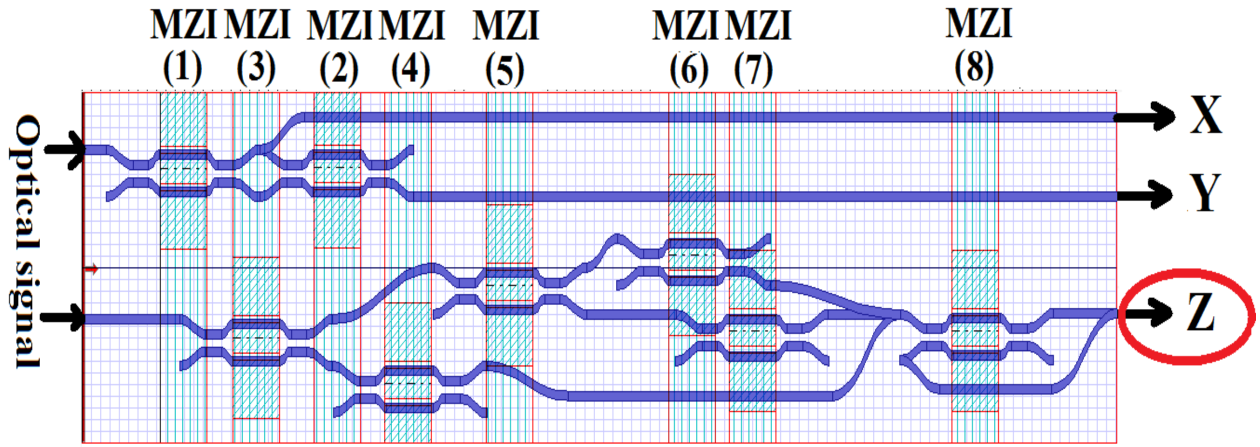

Figure: BPM layout of reversible T- flip-flop using MZI based Peres gate

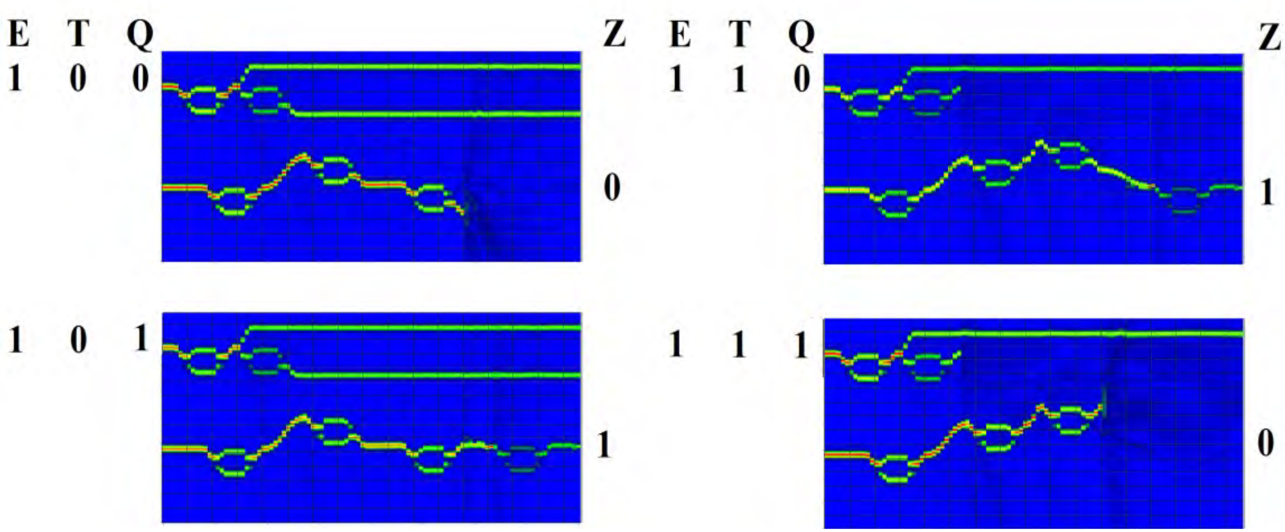

Figure: BPM simulation result of reversible T- flip-flop using MZI based Peres gate

Design of Reversible Full adder using Peres gate

- Figure 10 shows the logic diagram of full adder using Peres gate.
- As shown in Fig.10 (a), Peres gate is having 3 outputs which equals to $P = A, Q = A \oplus B \ and \ R = (A.B) \oplus C$ respectively.
- In Fig. 10 (b), it is shown that by using two Peres gate in cascading, one can design reversible full-adder circuit.
- The third input of first Peres gate is ancilla input C_{in} , which is equals to 0 and first output is garbage output.
- By cascading second and third output of first gate as inputs to second Peres gate, sum and carry output of full adder circuit will be available at second and third output port of second Peres gate respectively.

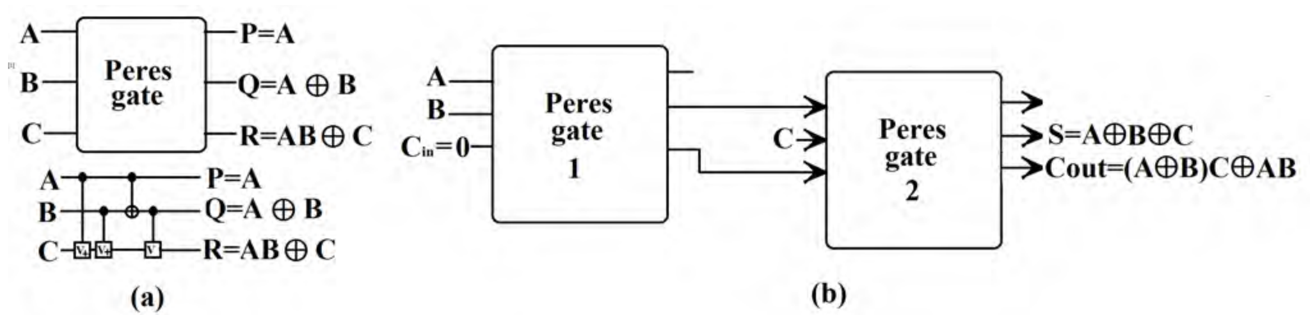

Figure 10: Logic design of reversible full-adder using Peres gate

cont…

- Figure 11 shows the equivalent MZI diagram of the circuit.
- Photo detector and amplifier is used to convert optical signal to electrical form to control the electrode voltage.

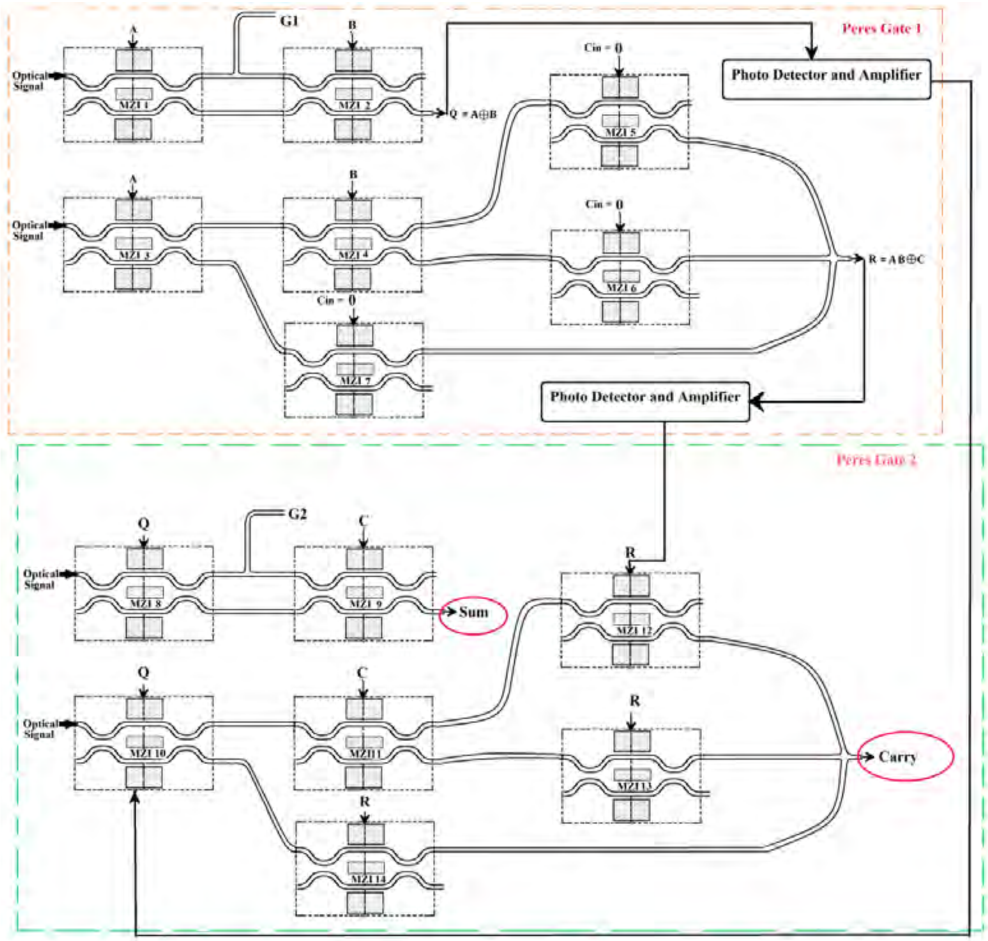

Figure 11: Schematic of full-adder using MZI based Peres gate

BPM Layout of Reversible Full Adder

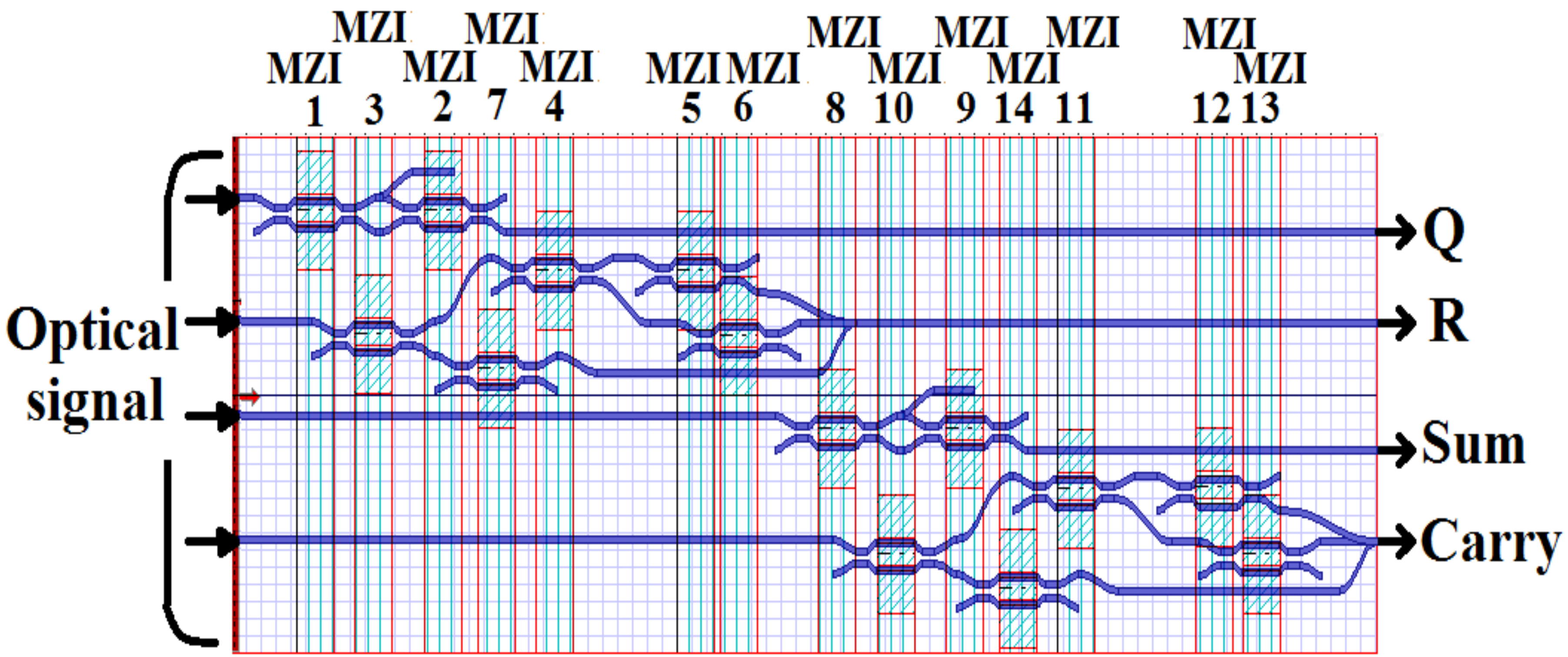

Figure: Layout diagram of Reversible Full Adder using MZIs

MATLAB Simulation results

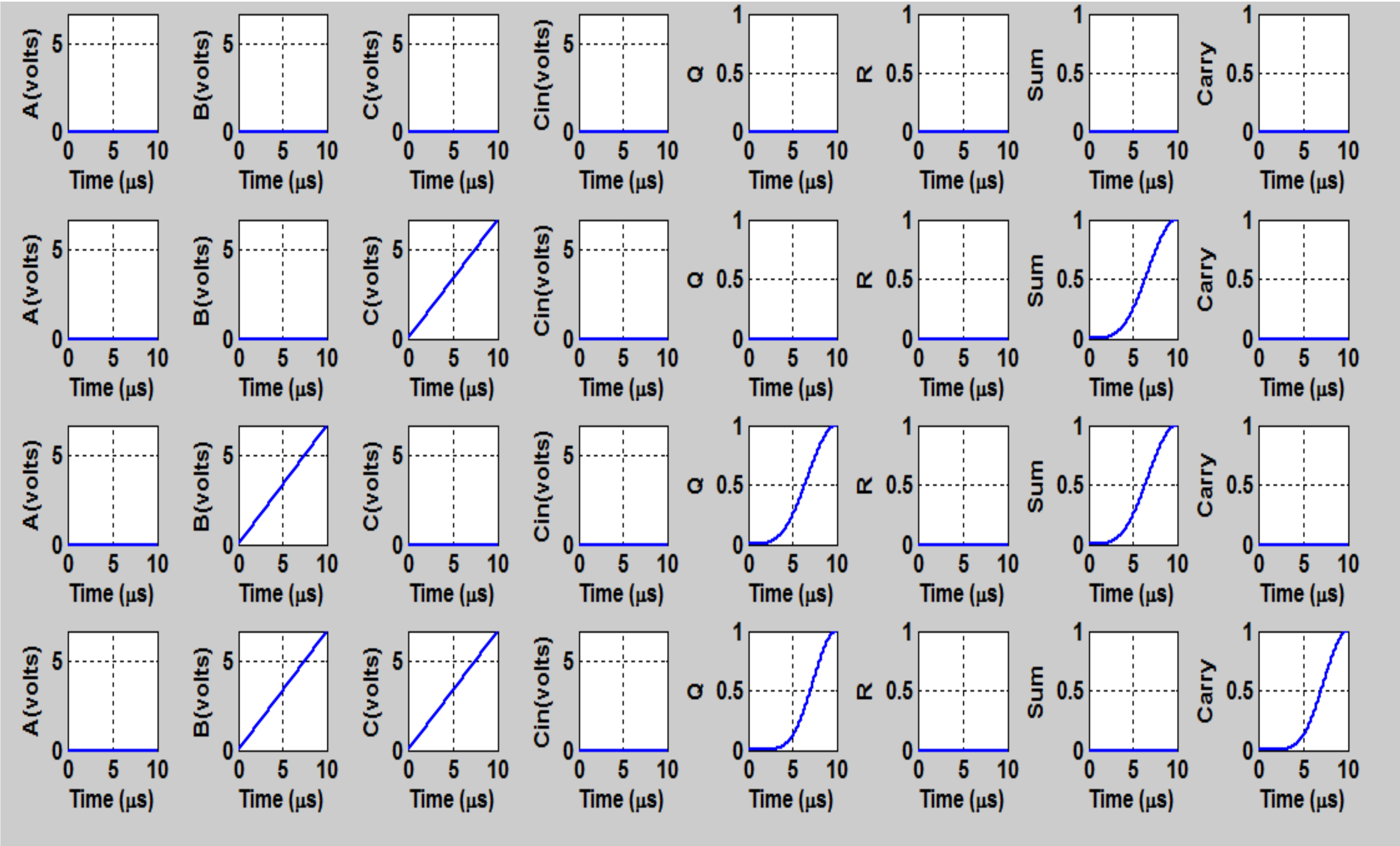

Figure: MATLAB simulation results where input(A,B,C) varies from 000 to 011

Opti-BPM Simulation results

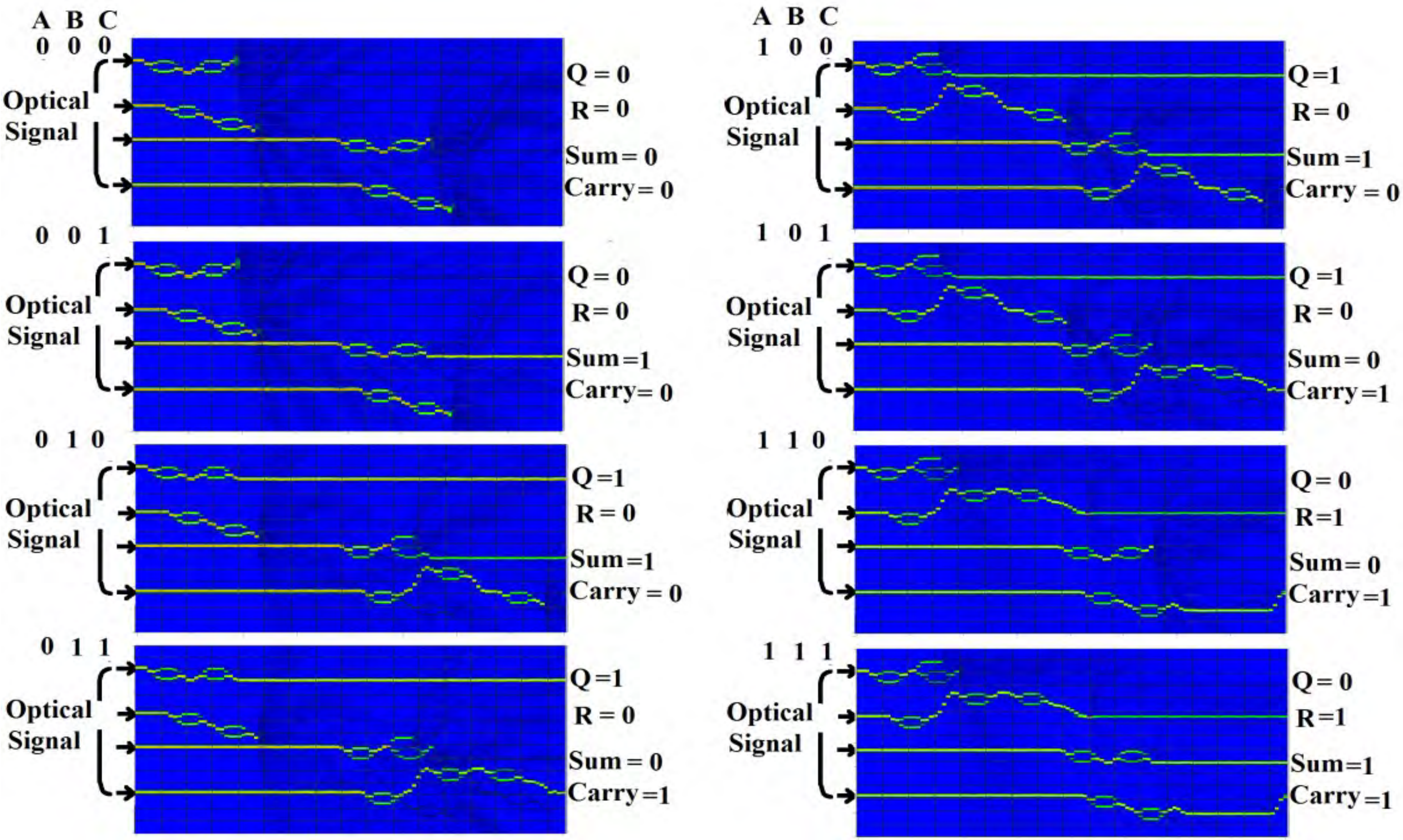

Figure: OptiBPM simulation results for Reversible Full Adder

Optical reversible hybrid Adder/Subtractor

Reversible Adder/Subtractor using Feynman gate and TR gate

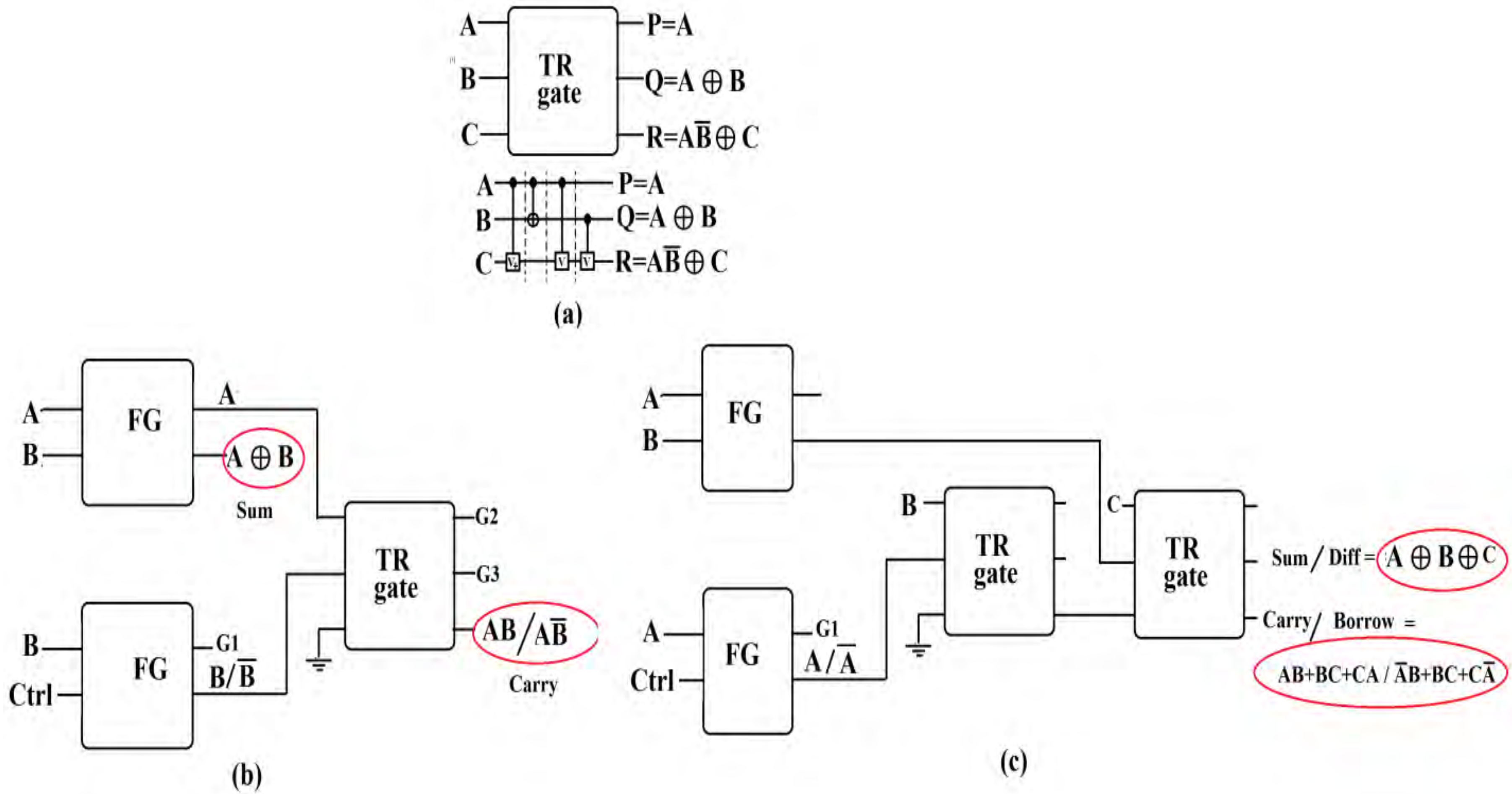

Figure: Logic Diagram of Adder-Subtractor using Feynman and TR gate(a) TR gate representation (b) Half adder-subtractor (c) Full adder-subtractor.

MZI diagram of Reversible Adder/Subtractor

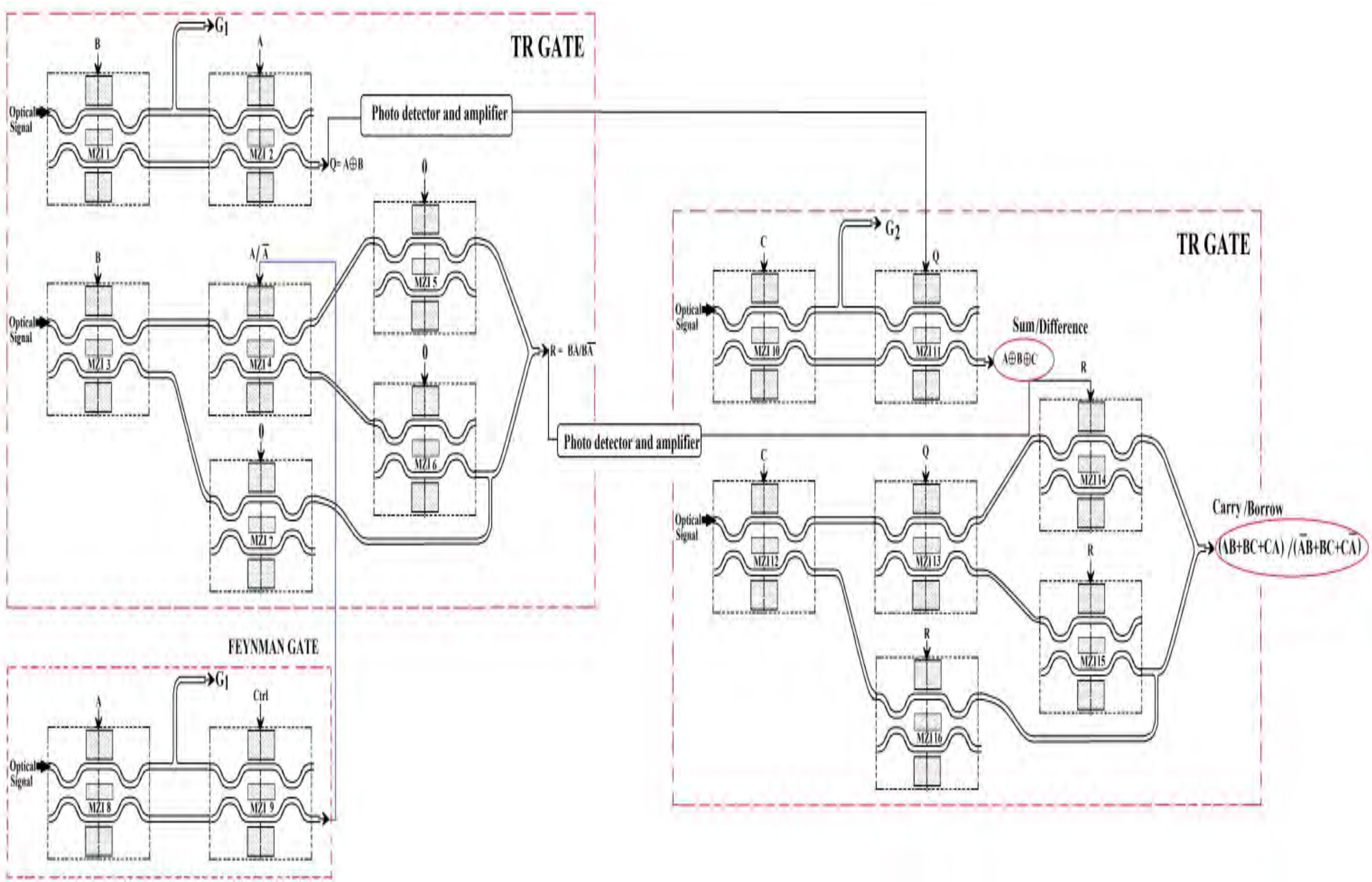

Figure: MZI diagram of Full adder subtractor

Mathematical expression for reversible adder-subtractor

$$\text{Sum/Difference} = \sin^2\left(\frac{\Delta\varnothing_{\text{MZI10}}}{2}\right)\cos^2\left(\frac{\Delta\varnothing_{\text{MZI11}}}{2}\right) + \cos^2\left(\frac{\Delta\varnothing_{\text{MZI10}}}{2}\right)\sin^2\left(\frac{\Delta\varnothing_{\text{MZI11}}}{2}\right)$$

$$\begin{aligned}\text{Carry/Borrow} &= \sin^2\left(\frac{\Delta\varnothing_{\text{MZI12}}}{2}\right)\sin^2\left(\frac{\Delta\varnothing_{\text{MZI13}}}{2}\right)\sin^2\left(\frac{\Delta\varnothing_{\text{MZI14}}}{2}\right)\\ &+ \sin^2\left(\frac{\Delta\varnothing_{\text{MZI12}}}{2}\right)\cos^2\left(\frac{\Delta\varnothing_{\text{MZI13}}}{2}\right)\cos^2\left(\frac{\Delta\varnothing_{\text{MZI15}}}{2}\right)\\ &+ \cos^2\left(\frac{\Delta\varnothing_{\text{MZI12}}}{2}\right)\sin^2\left(\frac{\Delta\varnothing_{\text{MZI15}}}{2}\right)\end{aligned}$$

MATLAB simulation results

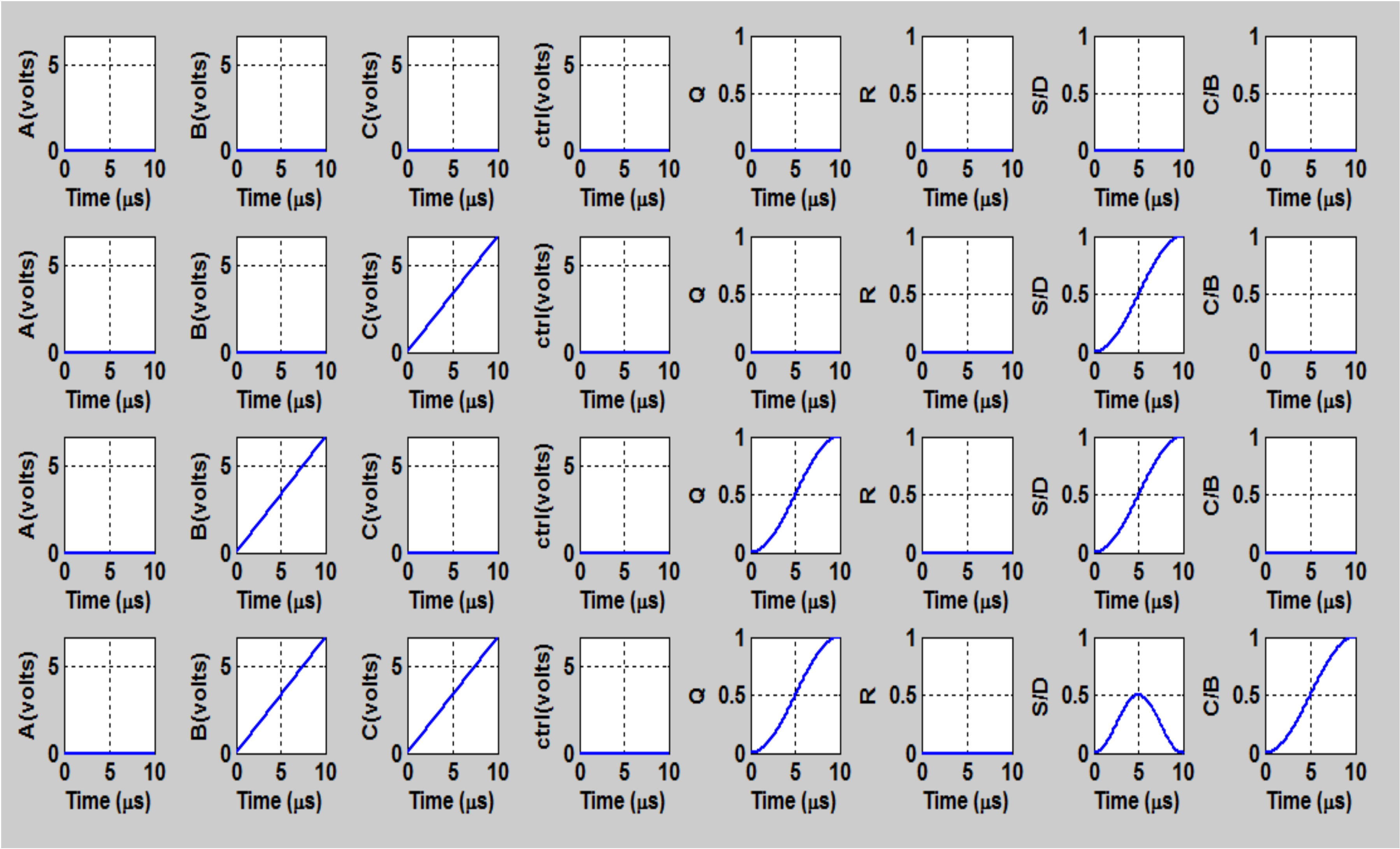

Figure: MATLAB simulation results of proposed device as Full adder where A, B, C varies from 000 to 011

MATLAB simulation results

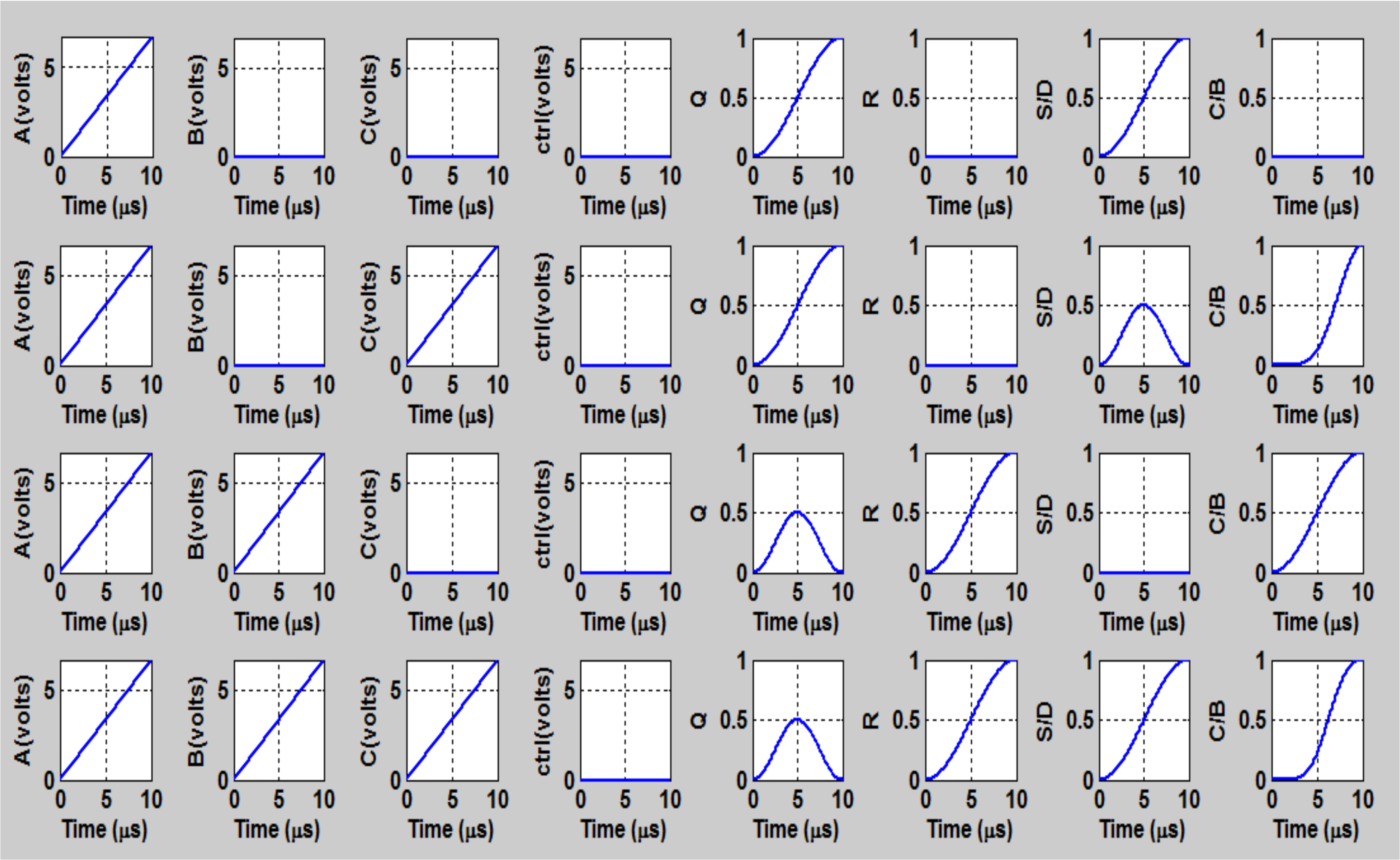

Figure: MATLAB simulation results of proposed device as Full adder where A, B, C varies from 100 to 111.

MATLAB simulation results

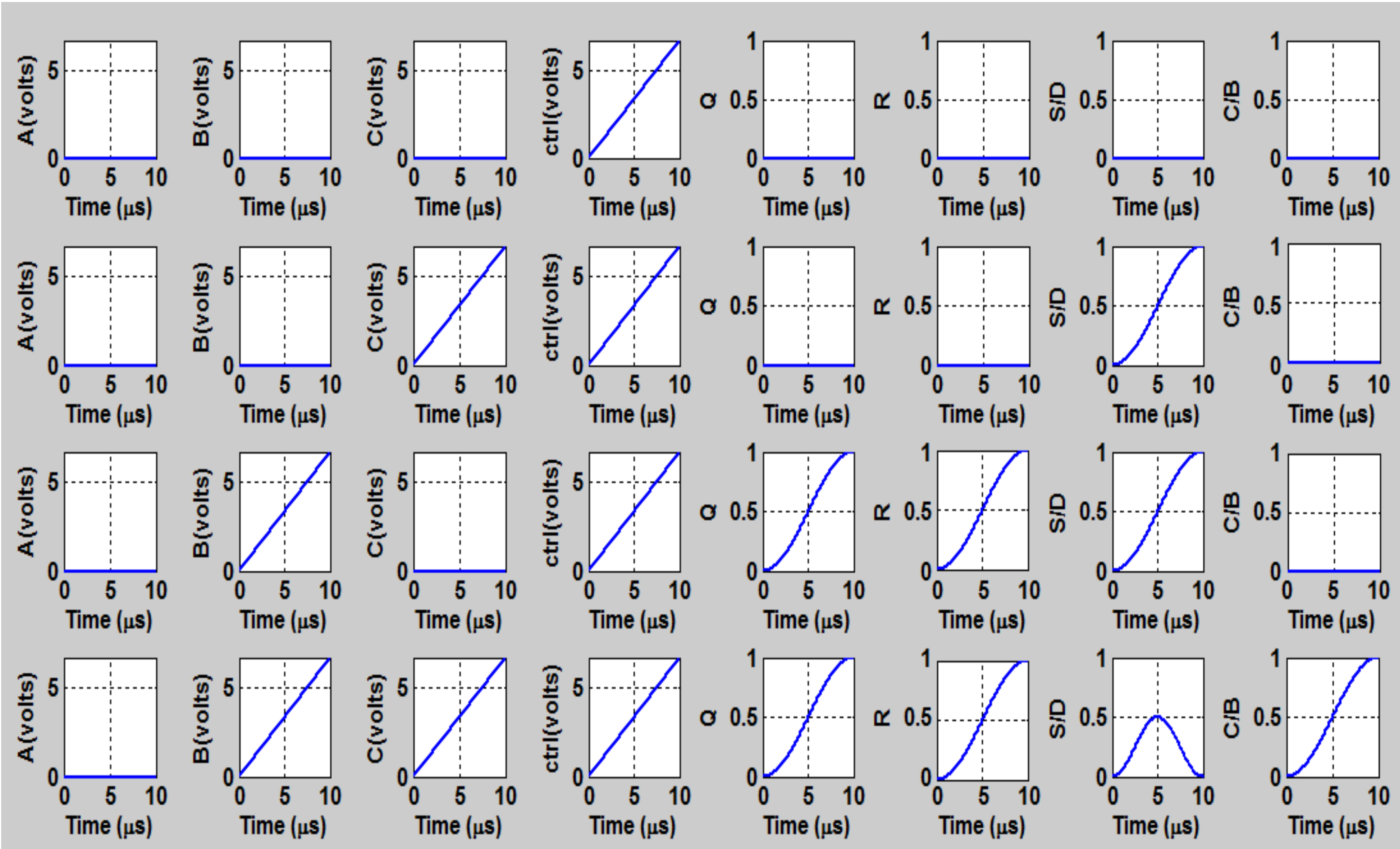

Figure: MATLAB simulation results of proposed device as Full subtractor where A, B, C varies from 000 to 011.

MATLAB simulation results

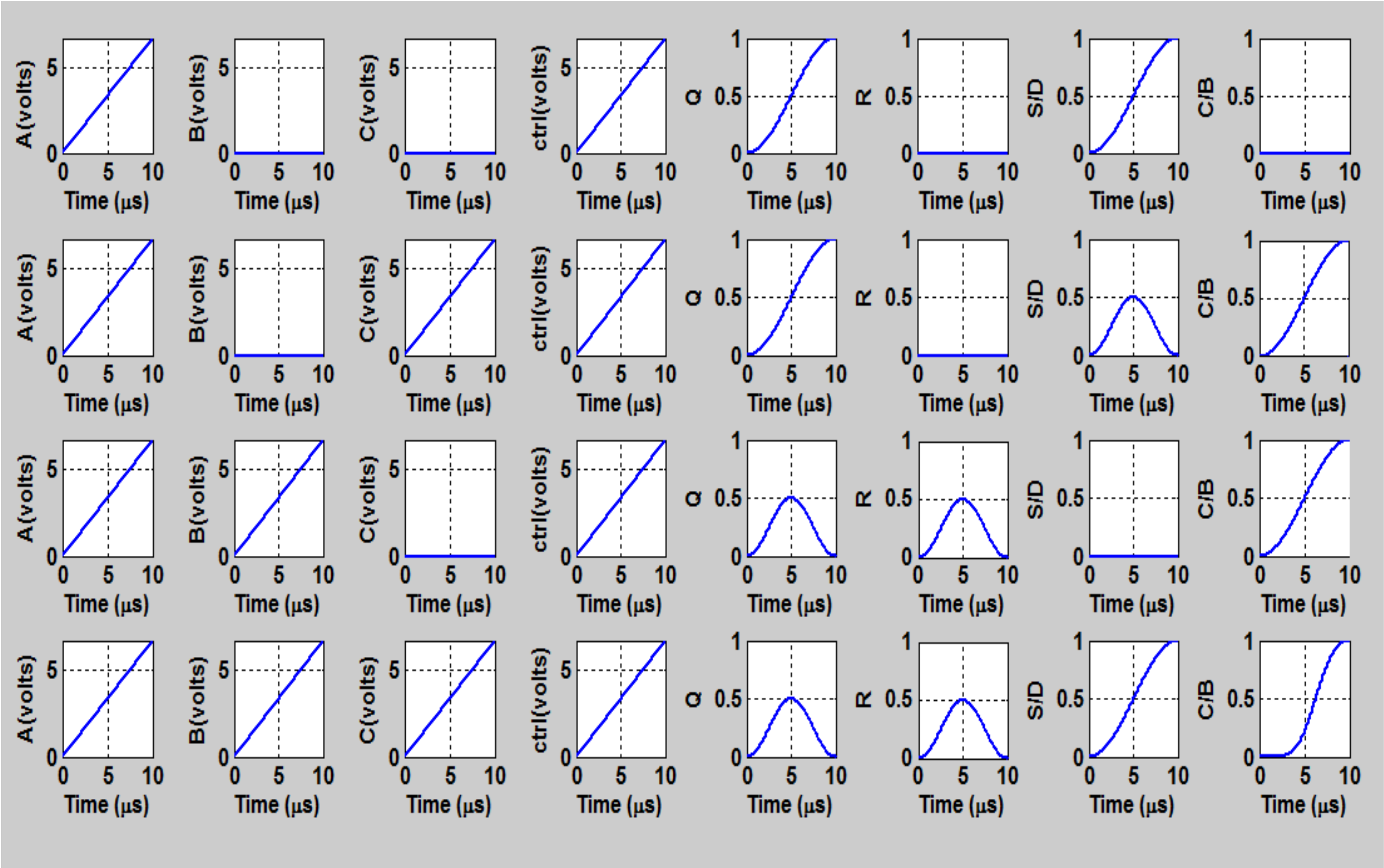

Figure: MATLAB simulation results of proposed device as Full subtractor where A, B, C varies from 100 to 111

BPM Layout of Reversible Full Adder-subtractor

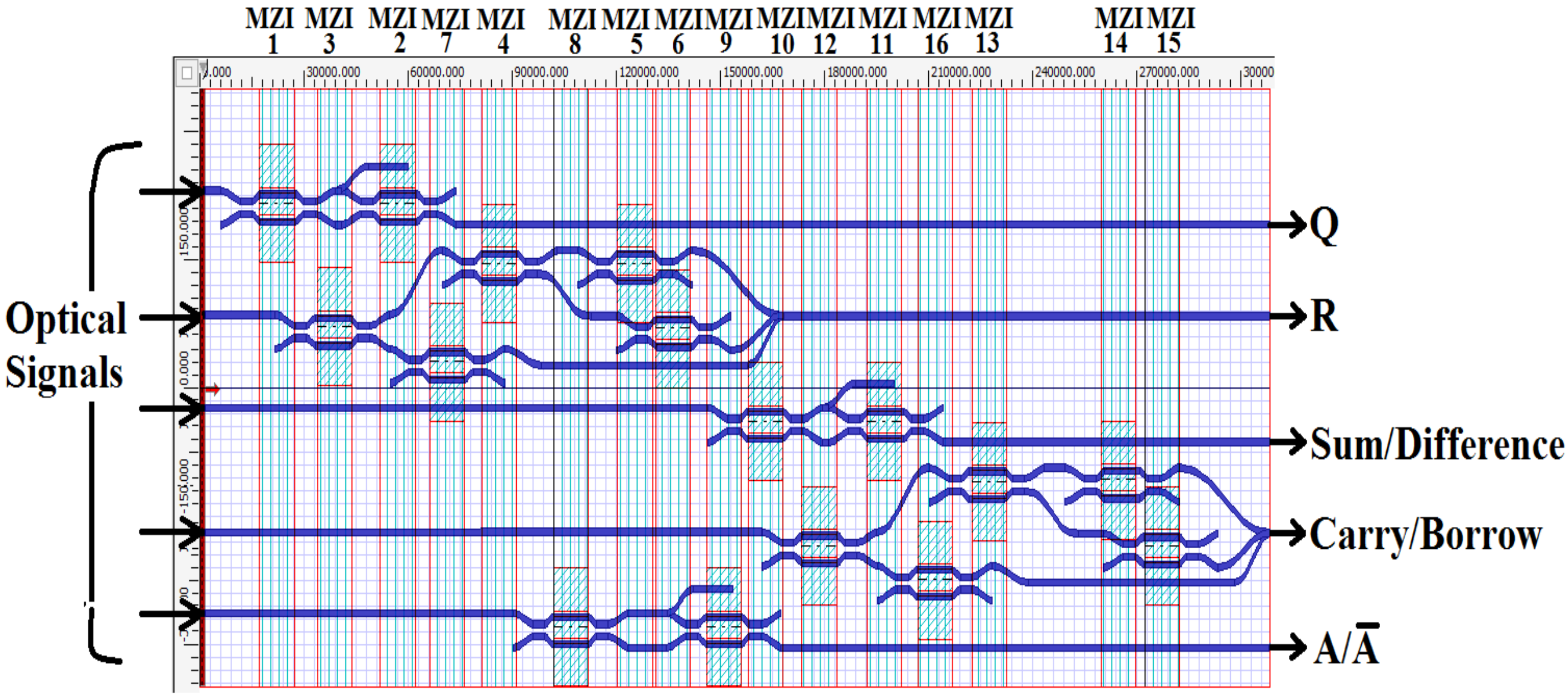

Figure: BPM layout of Hybrid Full adder/subtractor using TR gate

BPM Simulation Result

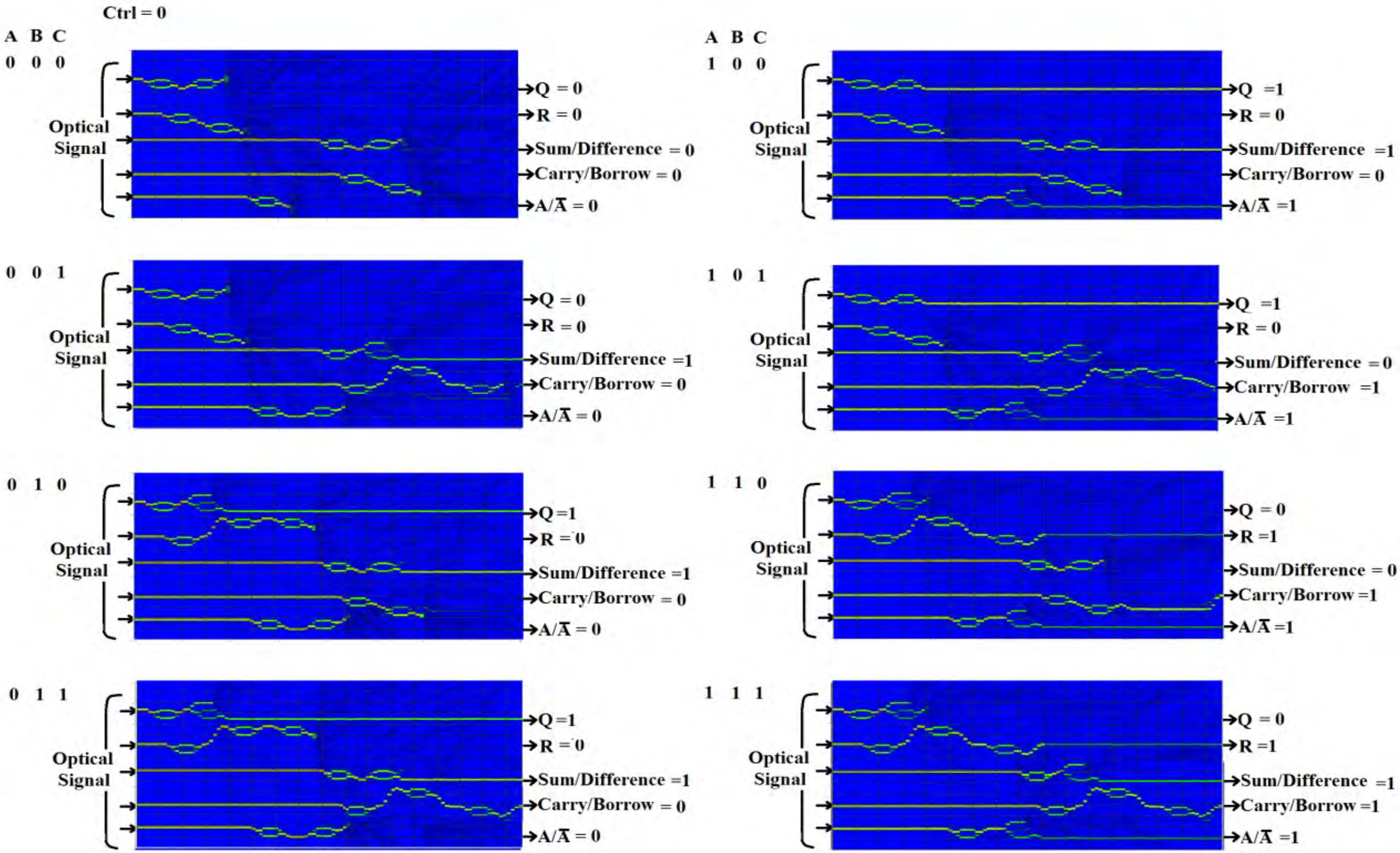

Figure: Optical field pattern of proposed device as full adder using BPM while input signal A, B, C varies from 000 to 111

BPM Simulation Result

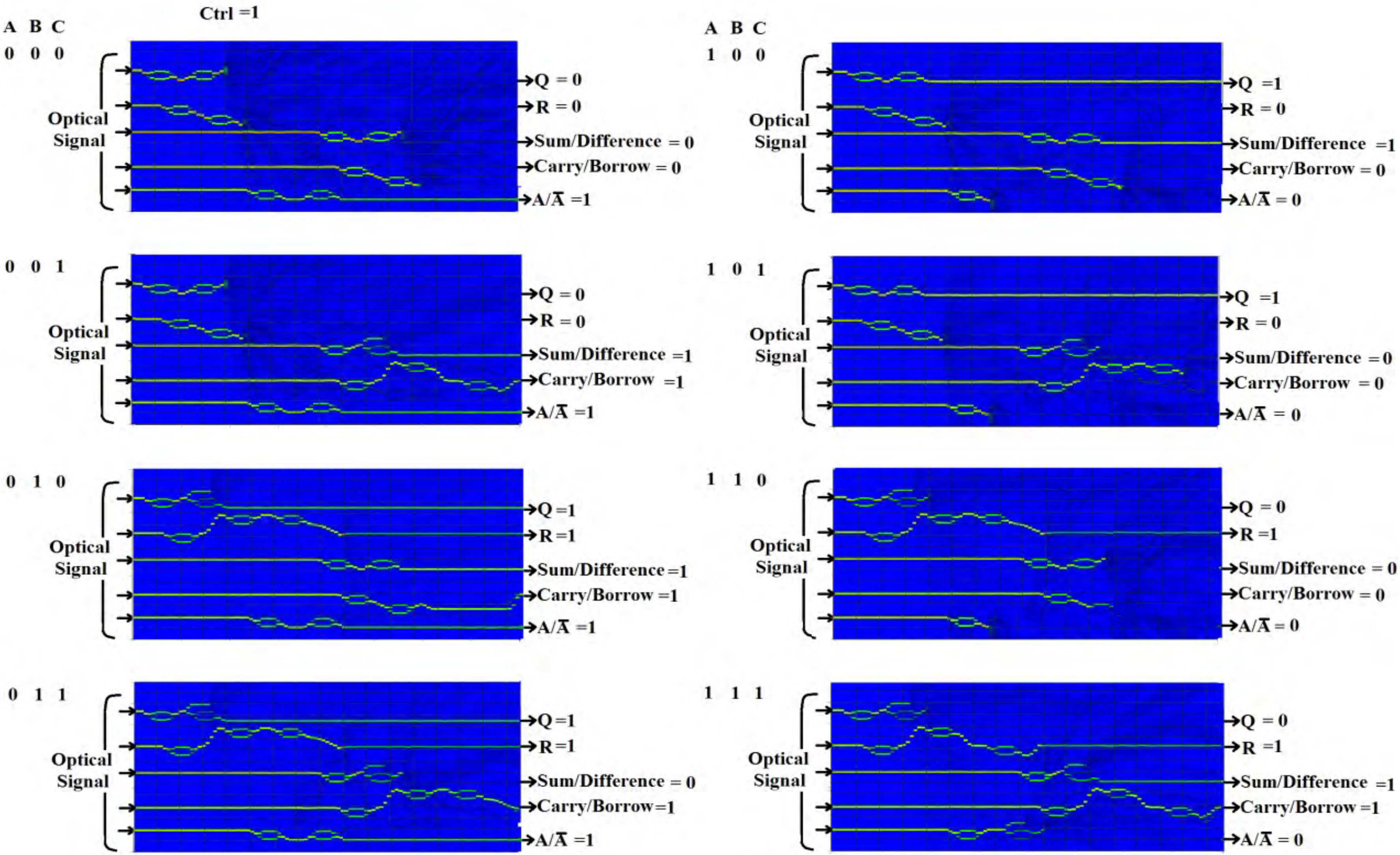

Figure: Optical field pattern of proposed device as full subtarctor using BPM while inputs signal A, B, C varies from 000 to 111

Design of Reversible TR gate

Santosh Kumar et al, OSA FiO-2017, Washington D.C, USA. (Sept 16-22, 2017)

Schematic diagram using MZI

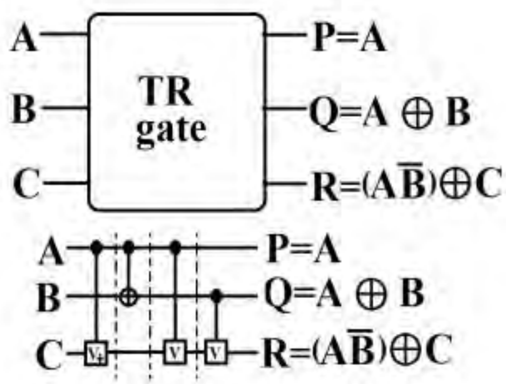

Figure: Logic diagram of TR gate

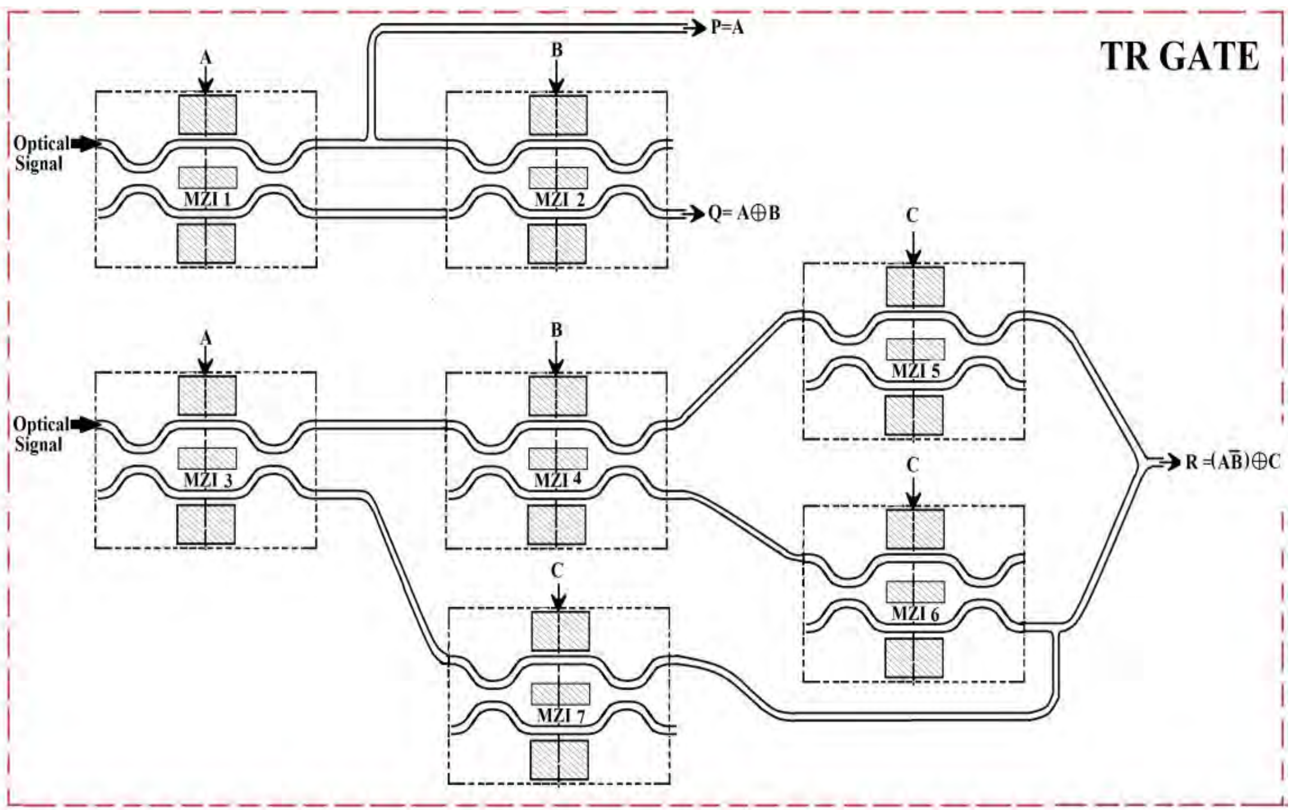

Figure: Schematic diagram of TR gate using lithium niobate based MZI

BPM Layout for TR gate

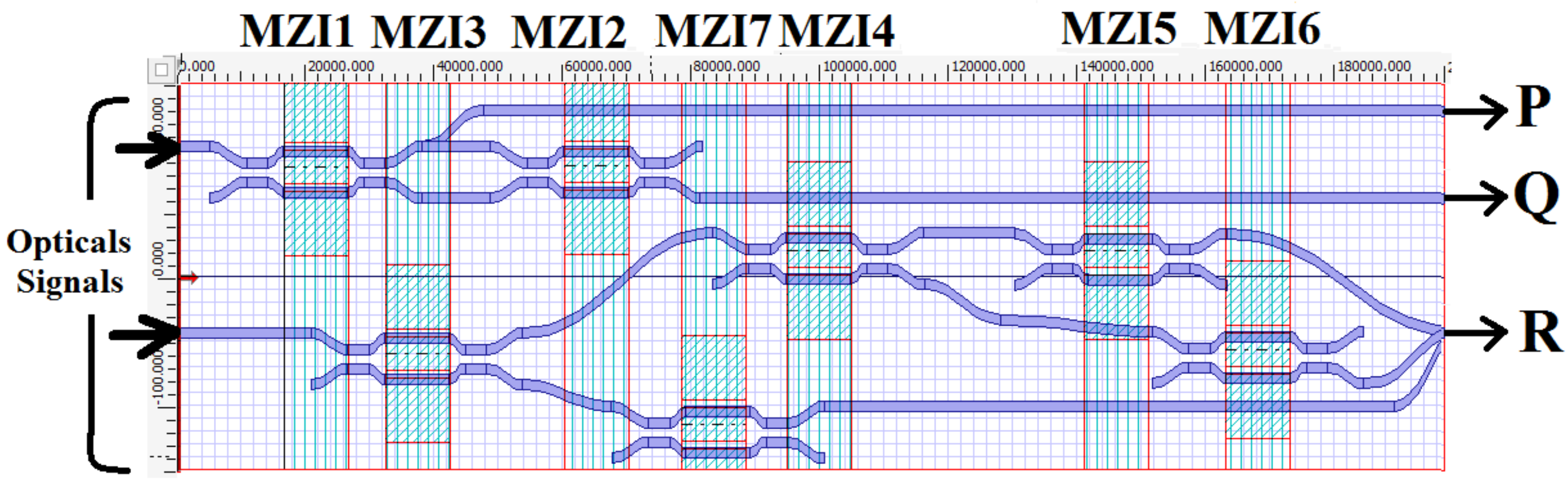

Figure: BPM layout of TR gate using MZI

MATLAB simulation results

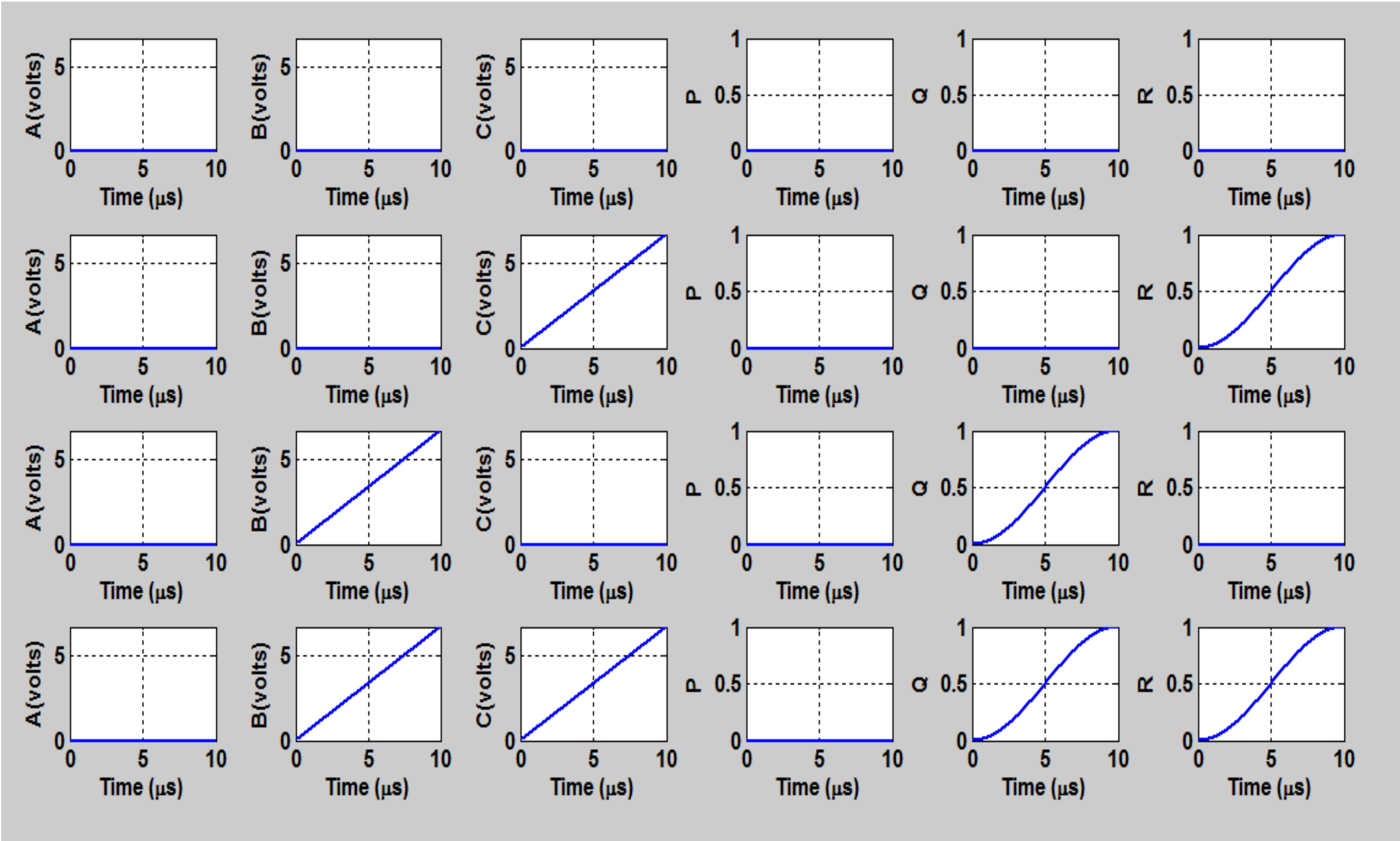

Figure: MATLAB simulation results where A, B, C varies from 000 to 011.

BPM simulation results

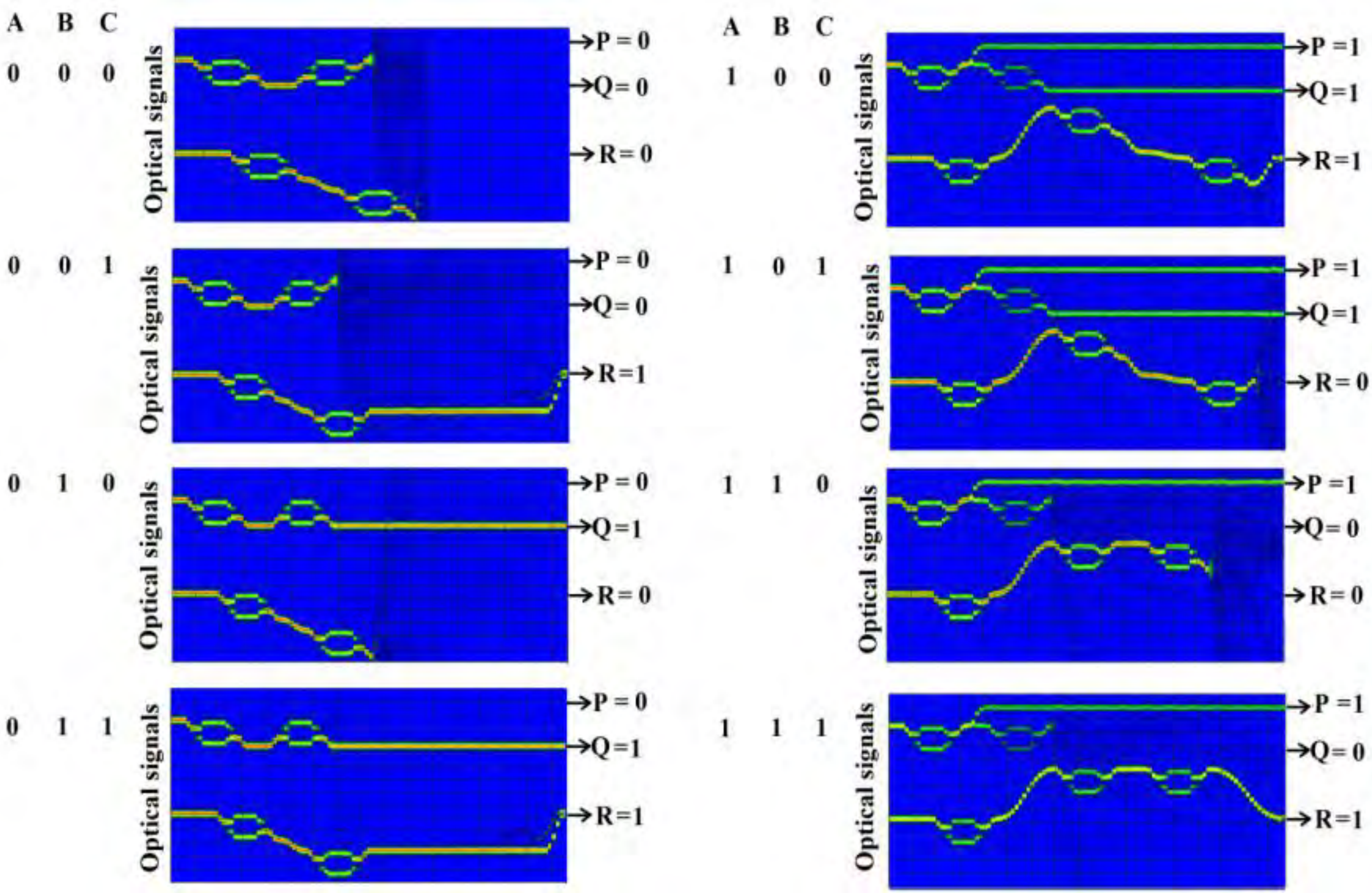

Figure: BPM simulation results where Inputs A, B, C varies from 000 to 111.

Study and analysis of some factors influencing the performances of proposed devices

Performance parameters

- The factors which influences the performance of the devices are
  - transmission loss
  - cross talk
  - extinction ratio
  - variation of bit rate

Variation of transition loss

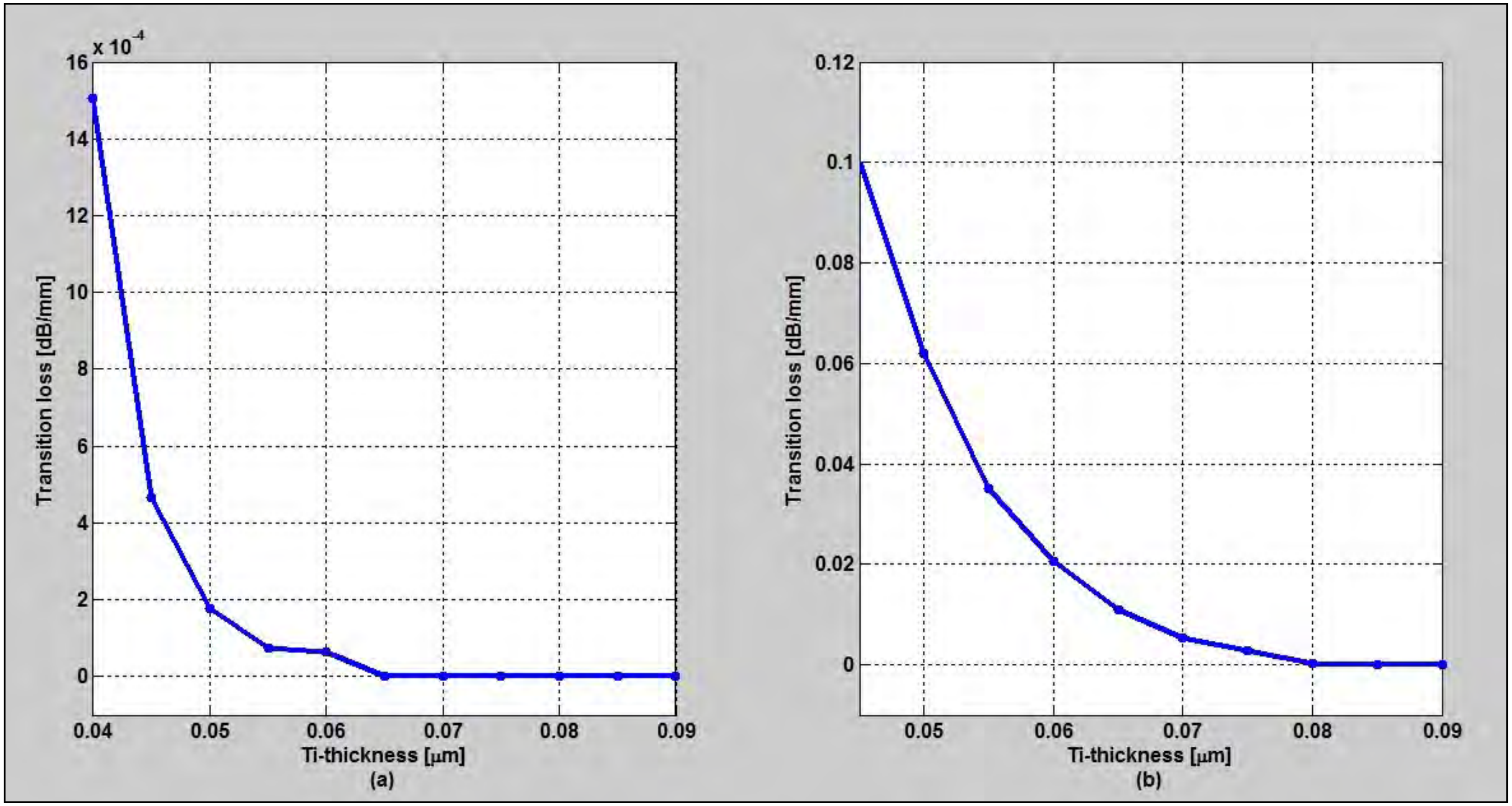

Figure: Variation of loss with respect to Ti- thickness (t_s) for (a) straight waveguide and (b) curved (S-bend) waveguide for operating wavelength 1.3 μm.

Crosstalk

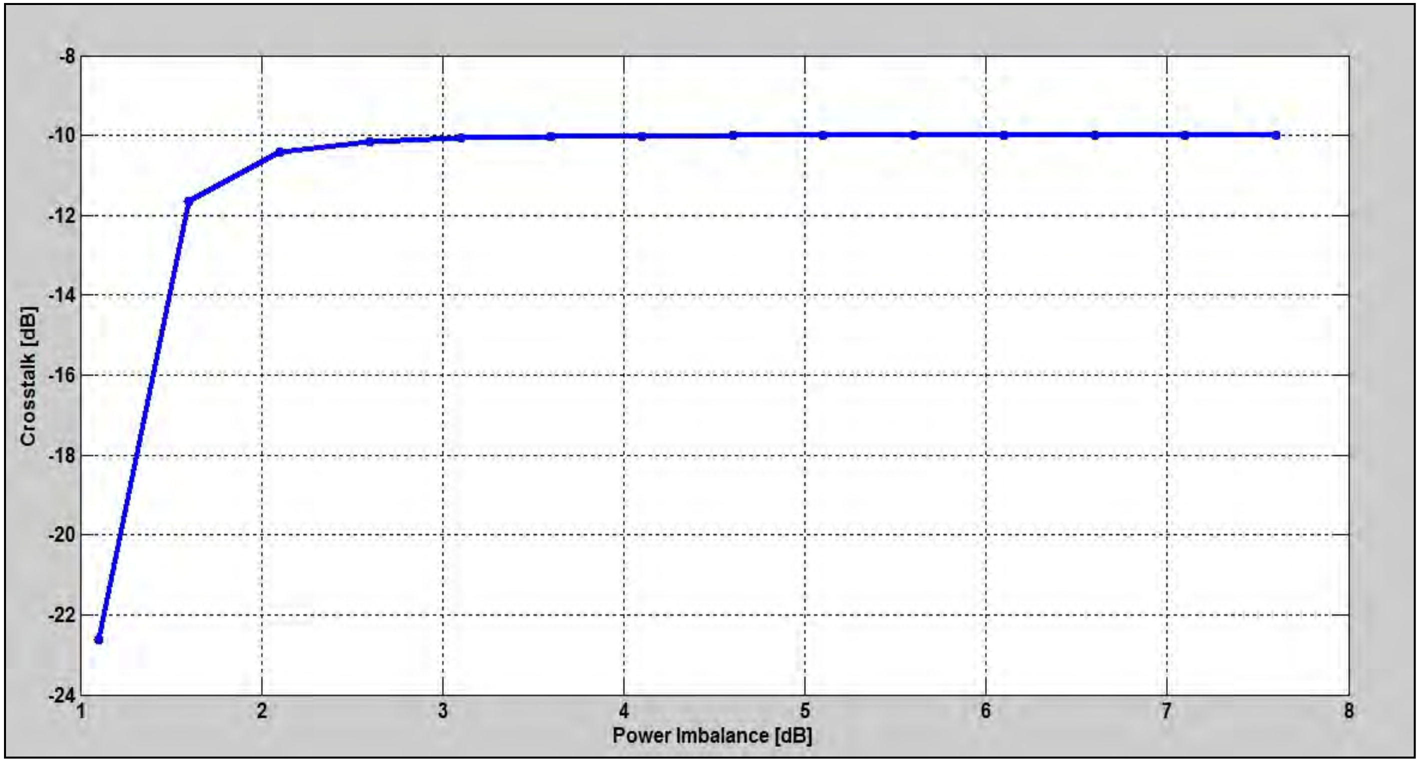

Figure: Representation of crosstalk level with variation of power imbalance (Switch state : Cross) for operating wavelength 1.3 µm.

Cont…..

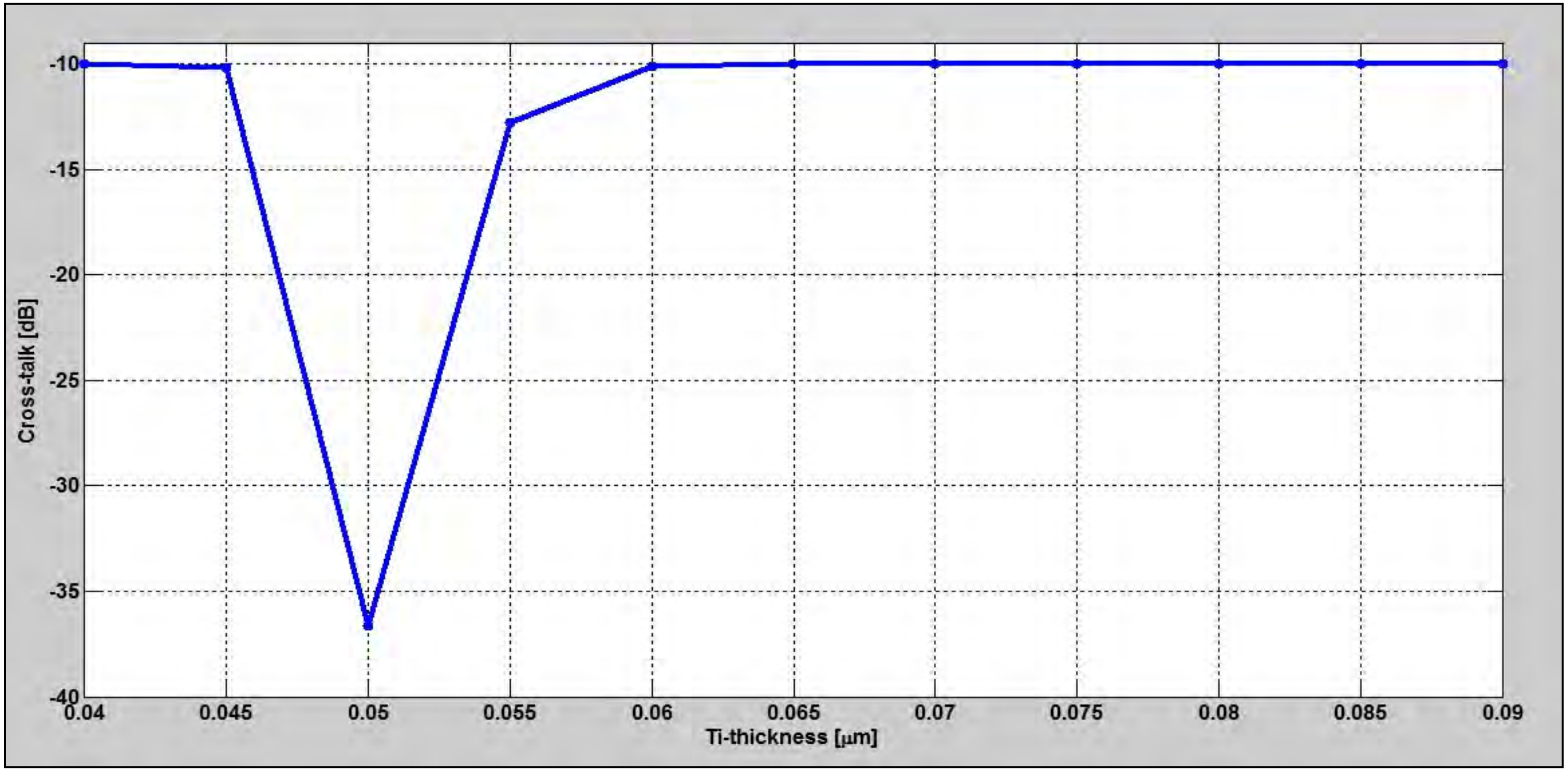

Figure: Calculated cross-talk levels due to variation in Ti-thickness for operating wavelength 1.3 µm; (switch state: Cross).

Variation of extinction ratio

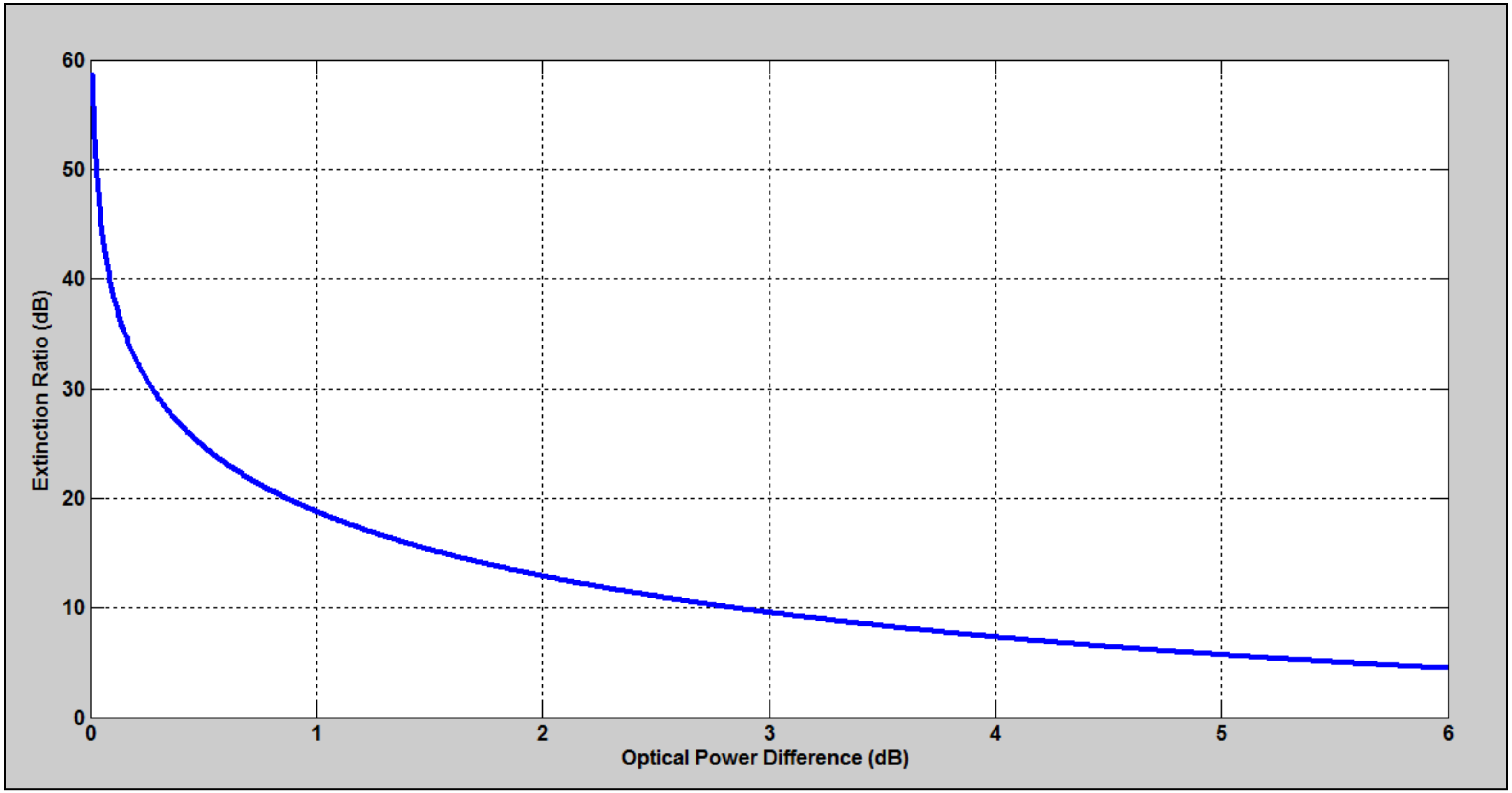

Figure: Extinction ratio for an modulator versus the optical power difference between its two arms

Variation of bit rate

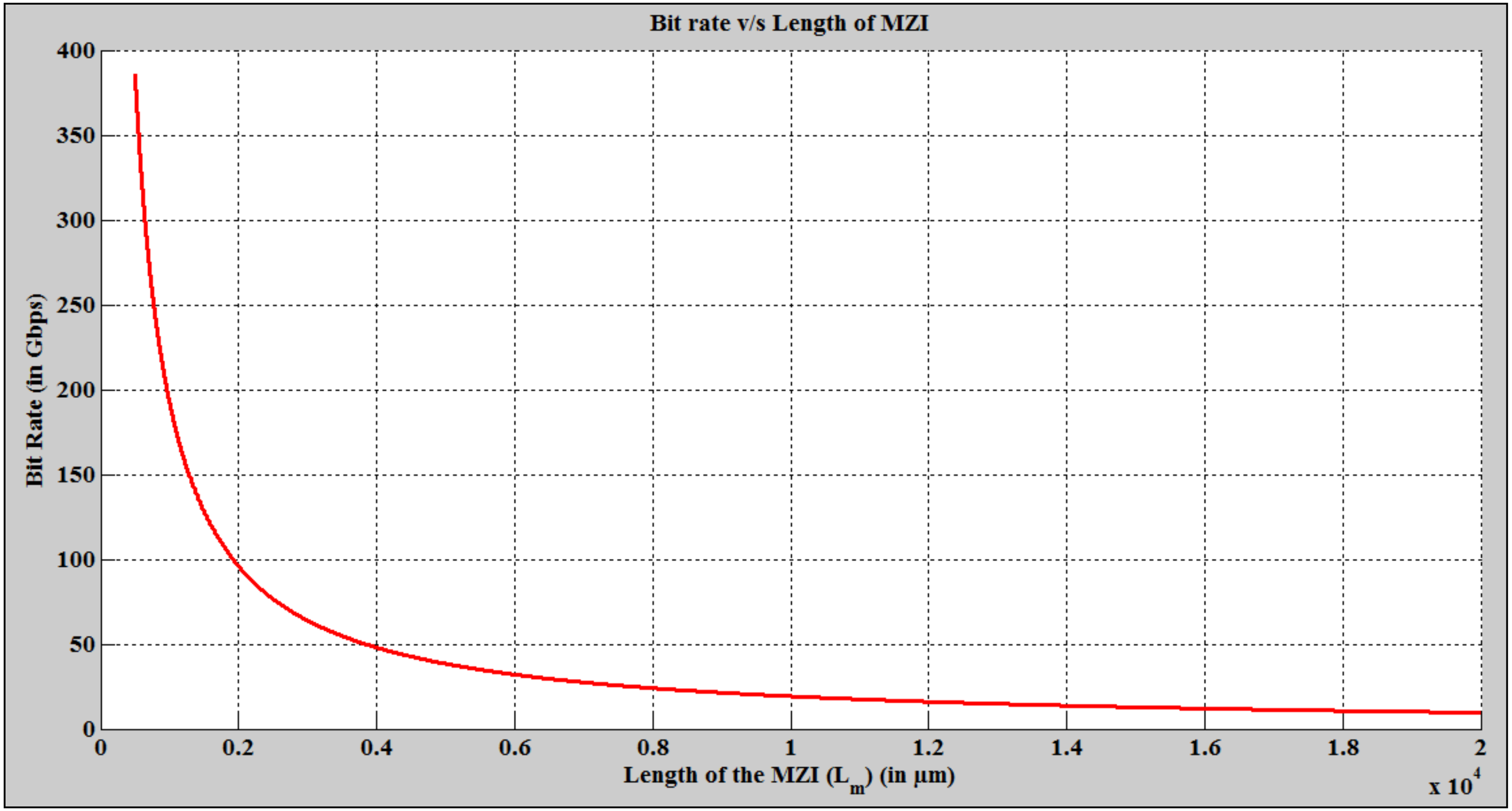

Figure: Variation of bit rate with respect to length of MZI.

Variation of chromatic dispersion and modal dispersion

The chromatic dispersion of a single $LiNbO_3$ based MZI is given by (Raghavendra and Prasad 2010);

$$D_c = -\left(\frac{L_m.\Delta\lambda.\lambda}{c}\right).\left(\frac{d^2 n_e}{d\lambda^2}\right)$$

Where

$L_m \rightarrow$ the length of a single MZI.

$\lambda \rightarrow$ the operating wavelength.

$\Delta\lambda \rightarrow$ the spectral line width of optical source.

$n_e \rightarrow$ the effective refractive index of the material ($LiNbO_3$).

The modal dispersion, D_{modal} for a multimode step-index electro-optic device with length L_m is given by

$$D_m = \frac{L_m n_e \Delta n_e}{c}$$

Δn_e is the relative refractive index difference.

The total dispersion coefficient D_{total} is given by

$$D_{total} = D_m + D_c$$

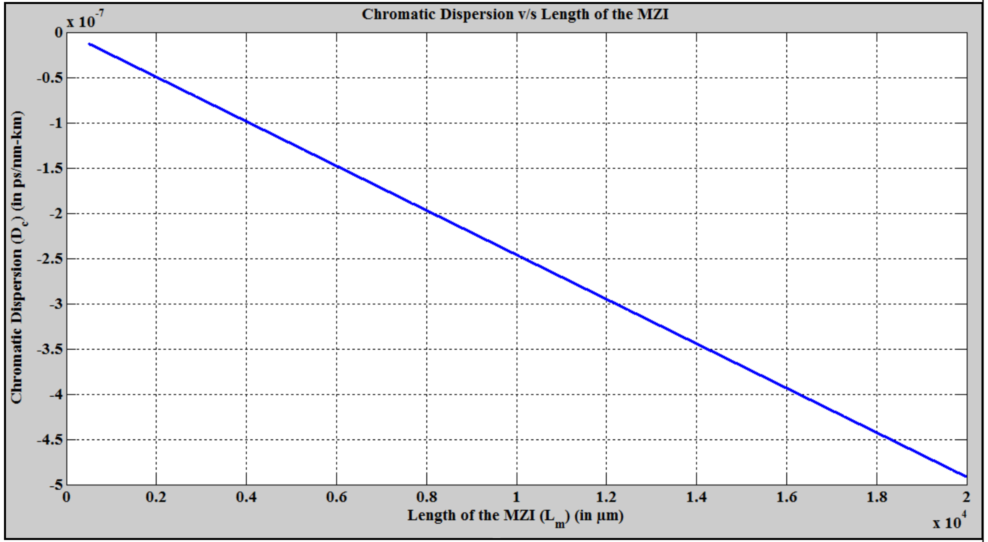

Figure: Variation of chromatic dispersion with respect to length of MZI.

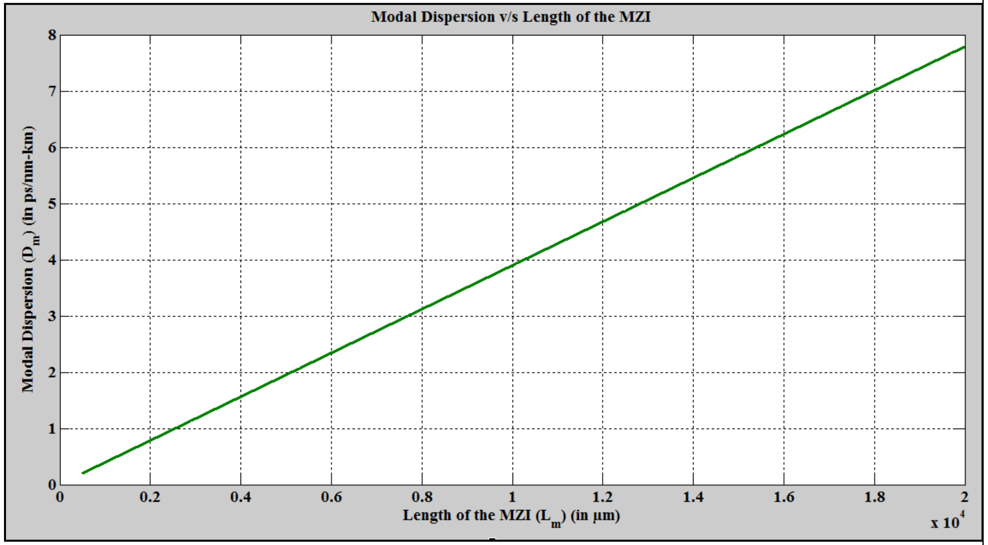

Figure: Variation of modal dispersion with increase in length of MZI.

Future scope

- In this study, a thorough study of $LiNbO_3$ based MZIs is performed to design various optical signal processing devices. However, more compact devices having less complexity may be proposed further to get better performance.

- By using the applied electrode voltage and some of the sensing material in one arm of MZI, it can be used for designing the ultra-efficient optical modulator and sensors.

- On the basis of the simulation results; a 3-dB coupler, Mach-Zehnder interferometer and other optical integrated devices can be fabricated.

References

- Besse, P.A., Melchior, H., "All-optical switches based on Mach-Zehnder configuration with improved extinction ratios", IEEE Photo. Technol. Lett., Vol 9, pp.55-57, 1997.
- Cotter, D., Manning, R.J., Blow, K.J., Ellis, A.D., Kelly, A.E., Nesset, D., Phillips, I.D., Poustie, A.J., Rogers, D.C., "Nonlinear optics for high-speed digital information processing Science", Vol 286, pp.1523 1999.
- Dimitriadou, E., Zoiros, K.E., "On the design of reconfigurable ultrafast all-optical NOR and NAND gates using a single quantum-dot semiconductor optical amplifier-based Mach-Zehnder interferometer", J. Opt., Vol 14, pp.105401, 2012a.
- Dimitriadou, E., Zoiros, K.E., "On the feasibility of ultrafast all optical NAND gate using single quantum-dot semiconductor optical amplifier-based Mach-Zehnder interferometer"' Opt. Laser Technol., Vol 44, pp.1971–1981, 2012b.
- Dimitriadou, E., Zoiros, K.E., "Proposal for all-optical NOR gate using single quantum-dot semiconductor optical amplifier-based Mach-Zehnder interferometer", Opt. Commun, Vol 285, pp.1710–1716, 2012c.
- Dimitriadou, E., Zoiros, K.E., "Proposal for ultrafast all-optical XNOR gate using single quantum-dot semiconductor optical amplifier-based Mach-Zehnder interferometer", Opt. Laser Technol., Vol 45, pp.79–88, 2013.
- Gayen, D.K., Chattopadhyay, T., Pal, R.K., Roy, J.N., "All-optical multiplication with the help of semiconductor optical amplifier-assisted Sagnac switch", Opt. Commun., Vol 9, No. 2, pp.57-67, 2010.
- Han, H., Zhang, M., Ye, P., Zhang, F., "Parameter design and performance analysis of an ultrafast all-optical XOR gate based on quantum dot semiconductor optical amplifiers in nonlinear mach–zehnder interferometer", Opt. Commun., Vol 281, pp.5140–5145, 2008.
- Hill, M.T., "A fast low-power optical memory based on coupled micro-ring lasers", Nature, Vol 432, pp.206-209, 2004.
- Jackson, K.P., Xiao, G., Shaw, H.J., "Coherent optical fibre delay-line processor", Electron. Lett., Vol 22, pp.1335–1337, 1986.
- Kaur, S., "All optical data comparator and decoder using SOA-based Mach–Zehnder interferometer, Vol 124, pp.2650-2653, 2011.
- Keiser, G., "Optical Fiber Communication", New York: McGraw-HILL; 2nd Edition, 2000.

References

- **Kumar, S., Bisht, A., Amphawan, A., "Four bit priority encoder using lithium niobate based mach-zehnder interferometers", IEEE Workshop on Recent Advances in Photonics, Indian Institute of Science, Bangalore, IEEE Xplore, 2015f.**

- **Kumar, S., Bisht, A., Singh, G., Amphawan, A, "Implementation of 2-bit multiplier based on electro-optic effect in Mach-Zehnder interferometers", Optical and Quantum Electronics, Vol 47, No. 7, pp.3677-3688, 2015e.**

- **Kumar, S., Bisht, A., Singh, G., Choudhary, K., Sharma, D., "Implementation of wavelength selector based on electro-optic effect in Mach-Zehnder interferometers for high speed communications", Opt. Comm., Vol 350, pp.108-118, 2015a.**

- Kumar, S., Raghuwanshi, S.K., Kumar, A., "Implementation of optical switches by using mach-zehnder interferometer", Opt. Engg., Vol 52, No. 9, pp.097106, 2013.

- Kumar, S., Raghuwanshi, S.K., Rahman, B.M.A., "Design of universal shift register based on electro-optic effect of LiNbO3 in Mach–Zehnder interferometer for high speed communication", Opt. Quant. Electron., Vol 47, No. 11, pp.3509-3524, 2015d.

- **Kumar, S., Singh, G., Bisht, A., "4x4 signal router based on electro-optic effect of mach-zehnder interferometer for wavelength division multiplexing applications", Opt. Comm., Vol 353, pp.17-26, 2015b.**

- Kumar, S., Singh, G., Bisht, A., Sharma, S., Amphawan, A., "Proposed new approach to the design of universal logic gates using the electro-optic effect in Mach–Zehnder interferometers", Appl. Optics, Vol 54, No. 28, pp.8479–8484, 2015c.

- L., Lei, Dong, J., Y., Zhang, He, H., Yu, Y., Zhang, X., "Reconfigurable photonic full-adder and full-subtractor based on three-input XOR gate and logic minterms", Electron. Lett., Vol 48, No. 7, pp.399–400, 2012.

- Li, G.L., Yu, P.K.L., "Optical intensity modulators for digital and analog applications", J. Lightwave Technol., Vol 21, No. 9, pp.2010-2030, 2003.

- Li, Q., Zhu, M., Li, D., Zhang, Z., Wei, Y., Hu, M., Zhou, X., Tang, X., "Optical logic gates based on electro-optic modulation with Sagnac interferometer", Appl. Opt., Vol 53, No. 21, pp.4708-4715, 2014.

- Liu, L., Kumar, R., Huybrechts, K., Spuesens, T., Roelkens, G., Geluk, E.J., Vries, T.de, Regreny, P., Thourhout, D.V., Baets, R., Morthier, G., "An ultra-small, low-power, all-optical flip flop memory on a silicon chip", Nature, Vol 268, pp.1-6, 2010.

- Maeda, Y., "All-optical NAND logic device operating at 1.51-1.55 μm in Er-doped aluminosilicate glass",

References

- Raghuwanshi, S.K., Kumar, A., Chen, N.K., “Implementation of sequential logic circuits using the Mach–Zehnder interferometer structure based on electro-optic effect”, Opt. Comm., Vol 333, pp.193-208, 2014.
- Raghuwanshi, S.K., Kumar, A., Kumar, S., “1×4 signal router using 3-Mach-Zhender interferometers”, Opt. Engg., Vol 52, No. 3, pp.035002, 2013.
- Raghuwanshi, S.K., Kumar, S., Kumar, V., Chack, D., “Propagation study of Y-branch having inbuilt optical splitters and combiner using beam propagation method”, Progress In Electromagnetics Research Symposium Proceedings”, pp. 720-724, 2012.
- Shen, Z.Y.,Wu,L.L., “Reconfigurable optical logic unit with a terahertz optical asymmetric demultiplexer and electro-opticswitches”, Appl. Opt., pp.47, No. 21, pp.3737–3742, 2008.
- Singh, G., Janyani, V., Yadav, R.P., “Modeling of a high performance Mach–Zehnder interferometer all optical switch”, Optica Applicata, Vol 42, pp.613-625, 2012.
- Stokes, L.F., Chodorow, M., Shaw, H.J., “All-single-mode fiber resonator”, Opt. Lett., 5, Vol 7, pp.288–290. 1982.
- Stubkjaer, K.E., “Semiconductor optical amplifier-based all-optical gates for high-speed optical processing”, IEEE J. Sel. Top. Quantum Electron., Vol 6, No. 6, pp.1428–1435, 2000.
- Sun, H., Wang, Q., Dong, H., Dutta, N.K., “XOR performance of a quantum-dot semiconductor optical amplifier based Mach-Zender interferometer”, Opt. Exp., Vol 136, pp.1892–1899, 2005.
- Tazawa, H., Steier, W.H., “Analysis of ring resonator-based traveling-wave modulators”, IEEE Photon. Technol. Lett., Vol 18, pp.211–213, 2006.
- Vikram, C.S., Caulfield, H.J., “Position-sensing detector for logical operations using incoherent light”, Opt. Eng., Vol 44, pp.115201-115204, 2005.
- Wang, J., Meloni, G., Berrettini, G., Poti, L., Bogoni, A., “All-optical clocked flip-flops and binary counting operation using SOA-based SR latch and logic gates”, IEEE J. Sel. Topics Quantum Electron., Vol 16, No. 5, pp.1486–1494, 2010.

THANK YOU